Title

THE MOLECULAR STRUCTURE OF ORGANIC OVERLAYERS ON PALLADIUM SINGLE CRYSTAL SURFACES: A LEED AND HREELS STUDY

Author

Ohtani, H.

Publication Date

1988-11-01

LBL-26938

Center for Advanced Materials

CAM

The Molecular Structure of Organic Overlayers on Palladium Single Crystal Surfaces: A LEED and HREELS Study

H. Ohtani
(Ph.D. Thesis)

November 1988

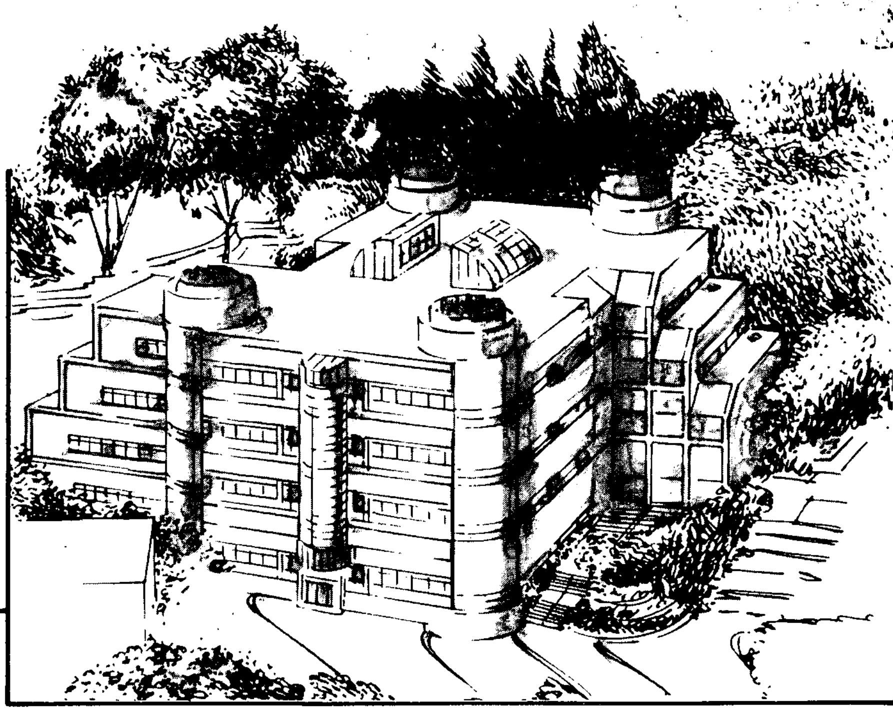

Materials and Chemical Sciences Division

Lawrence Berkeley Laboratory • University of California
ONE CYCLOTRON ROAD, BERKELEY, CA 94720 • (415) 486-4755

Prepared for the U.S. Department of Energy under Contract DE-AC03-76SF00098

LBL-26938

THE MOLECULAR STRUCTURE OF ORGANIC OVERLAYERS ON PALLADIUM SINGLE CRYSTAL SURFACES: A LEED AND HREELS STUDY

Hiroko Ohtani
Ph.D. Thesis

Department of Chemistry
University of California at Berkeley
and
Center for Advanced Materials
Materials and Chemical Sciences Division
Lawrence Berkeley Laboratory
1 Cyclotron Road
Berkeley, California 94720

November 1988

This work was supported by the Director, Office of Energy Research, Office of Basic Energy Sciences, Chemical Sciences Division, of the U.S. Department of Energy under Contract No. DE-AC03-76SF00098.

The Molecular Structure of Organic Overlayers on Palladium Single Crystal Surfaces: A LEED and HREELS Study

Hiroko Ohtani

ABSTRACT

The surface structures of molecular overlayers on palladium single crystal surfaces have been determined by dynamical low energy electron diffraction (LEED) and by a combination of LEED and high resolution electron energy-loss spectroscopy (HREELS).

An ion-pumped multi-technique UHV apparatus equipped with a computer-controlled video LEED system and a HREEL spectrometer has been designed and constructed for this thesis project.

The surface structure of the clean Pd(111) is confirmed to be close to the ideal bulk structure. Slight deviations, possibly hydrogen-induced, are obtained for the interlayer spacings down to the fifth layer: $\Delta d_{12} = +0.03 \pm 0.03$Å, $\Delta d_{23} = -0.03 \pm 0.03$Å, and $\Delta d_{34} = \Delta d_{45} = +0.05 \pm 0.03$Å (positive values indicate expansion from the bulk spacing value).

The CO molecules adsorbed on Pd(111) with a $(\sqrt{3} \times \sqrt{3})R30^\circ$ periodicity at one-third monolayer coverage are found to be preferentially adsorbed at fcc-type hollow sites with the C-O axis perpendicular to the surface. The optimal carbon-oxygen and metal-carbon bond lengths are 1.15 ± 0.05Å and 2.05 ± 0.04Å, respectively. This is the first LEED structure analysis of CO adsorbed at a hollow site on a clean metal surface without the presence of a coadsorbate.

The molecular structure of the ordered (3x3) superlattice of coadsorbed C_6H_6 and CO on the Pd(111) crystal face has been investigated. The benzene molecules are found to be oriented with their carbon rings parallel to the surface, centered over fcc-type 3-fold hollow sites. The C-C bond lengths in the benzene ring skeleton are found to be either 1.40±0.10Å or 1.46±0.10Å depending on the position of the C-C bonds relative to the underlying Pd atoms. These bond lengths are very close to the corresponding gas phase value of 1.397Å. This contrasts with similar coadsorbate systems of benzene and CO on Rh(111) or Pt(111), where significant in-plane distortions and enlargements of the benzene ring have been detected. A trend toward more distortion and increasing average C-C bond length has been found in changing substrates from Pd to Rh to Pt, while the metal-carbon bond lengths decrease in that same sequence. This is interpreted to indicate that the metal-carbon bond becomes shorter, while the C-C bonds weaken from Pd to Rh to Pt, which is further supported by HREELS data.

Coadsorbed CO molecules are necessary to form an ordered benzene overlayer on Pd(111). They occupy fcc-hollow sites surrounding the benzene molecules. The C-O axis is perpendicular to the surface, and the carbon-oxygen and palladium-carbon bond lengths are found to be 1.17±0.05Å and 2.05±0.04Å, respectively.

Similar coadsorption structures of C_6H_6 and CO have been produced on a Rh(111) crystal surface, and the overlayer structures have been imaged with scanning tunneling microscopy (STM). The images show that the coadsorbed structures are well ordered and that the molecular arrangement in the unit cell is consistent with LEED results. Images further show translational domain boundaries, step-edge structures, and evidence for surface diffusion. LEED crystallography, by determining the position of the nuclei, detects an in-plane distortion of the benzene molecules with 3-fold symmetrical features in the benzene ring. STM, which depends more on the density of states, also shows 3-fold symmetrical features in the benzene ring. These observations are interpreted in the framework of molecular-orbital theory.

A tabulation is compiled of the ordering characteristics of clean and adsorbate-covered single crystal surfaces based on diffraction patterns observed with LEED. Over 3000 structures are classified by rotational symmetry of the substrate surfaces and by type of sub-class: alloy surfaces, organic overlayers, coadsorbed overlayers, physisorbed overlayers, and high-Miller-index (stepped) surfaces. The important characteristics of each sub-class are reviewed and future directions of LEED investigations are proposed.

Acknowledgements

At long last, I am finishing my Ph.D. work. My life in Berkeley was enjoyable, overall, because of very friendly coworkers and an excellent research environment. I would like to especially acknowledge the following people.

Prof. Gabor A. Somorjai, my research director, assigned me the surface crystallography project. The idea of combining HREELS and LEED crystallography to solve the structure of organic overlayers came from him. He spent a lot of time discussing the progress of the research with me, as well as on life in general.

Dr. Michel A. Van Hove of LBL introduced and taught me surface crystallography by LEED. In most cases Prof. Somorjai, Dr. Van Hove and myself set up the short range goals together. Dr. Van Hove helped me in evaluating the experimental LEED I-V curves; He also conducted the dynamical LEED calculations discussed in chapters 4, 5, and 6.

Drs Miquel Salmeron, Te-Hua Lin, Mathew Mate, Greg Blackman, Vicki Grassian, and Dave Kelly introduced me to surface science instrumentation, and helped me to start the project. Dr. Frank Ogletree was always ready to answer "correctly" the questions I had about instrumentation.

The construction of a new UHV apparatus has been facilitated by the support staff of the Materials and Chemical Sciences Division. Bob McAllister built the HREEL spectrometer which finally showed great performance several months before I left Berkeley. Weyland Wong and Dan Coulomb skillfully built many parts of the apparatus including the modified sample manipulator. Bob Wright helped to maintain the vacuum system.

Much of the scientific work described here was performed in collaboration. In addition to the people previously mentioned, my coworkers in Berkeley have included Brian Bent, Chi-tzu Kao, Bruno Marchon, Morgan Edwards, and Pedro Nascente. While in IBM Almaden I was assisted by Robert Wilson and Shirly Chiang.

Prof. Somorjai's group, consisting of about 30 graduate students, visiting scientists and postdocs from all over the world, provided many friendly and stimulating relationships, as well as help for each other whenever necessary. Ken Lewis, Ted Oyama, Peter McAnally, Istvan Boszormenyi, and David Jentz were on campus sharing the joys and the disappointments of the research work.

I also enjoyed scientific discussions with former group members over the phone, particularly with Prof. Eric Garfunkel and Prof. Bruce Koel.

My parents encouraged me throughout this work. Music, especially by Mozart, brought me happiness and retrieved my motivation towards working hard.

This work was supported by the Director, Office of Basic Energy Science, Materials Science Division of the U.S. Department of Energy under Contract No. DE-AC03-76SF00098. An IBM Japan overseas scholarship also supported this graduate research work.

Table of Contents

1. Introduction

"Surface science", which deals with the physics and chemistry of the outermost part of matter (usually within several atomic layers), is currently growing towards more complex and diverse systems. Among these, the importance of the study of organic monolayers on surfaces cannot be overemphasized, not only because of scientific importance, but also technological importance. For example chemisorption and reaction of reactant molecules on catalyst surfaces are crucial steps for heterogeneous catalysis, and surface science has given considerable insight to the molecular level understanding of these phenomena.[1] The molecular level understanding of interactions between organic lubricants and the substrate surfaces is expected to become more and more important in the are a of tribology.

Keeping such future applications in mind, we have studied the surface structure of organic monolayers on well-defined single crystal surfaces under an ultrahigh vacuum environment, since it is true not only for molecules and solids, but also for surfaces, that "structure (or atomic arrangement)" is a key fundamental physical parameter from which other chemical or electronic properties can be derived.

About 30 years ago people were very impressed and surprised when Eischens et al. showed the existence of CO molecules chemisorbed on surfaces using transmission infrared spectroscopy,[2,3] since it had been extremely difficult to find surface analytical methods sensitive enough to study molecular overlayers. Since then many surface science techniques have been developed and we can now determine the bond lengths and bond angles of CO molecules on surfaces quite accurately within ~0.1Å using dynamical LEED analysis as shown in Chapter 5. More complicated coadsorption structures of benzene and CO can be also determined by combining high resolution electron energy loss spectroscopy(HREELS) and LEED, and we have verified the distortion of chemisorbed benzene molecules due to substrate-adsorbate and adsorbate-adsorbate interactions (Chapter 6). Furthermore, we have succeeded in imaging molecular orbitals of benzene and CO molecules on surfaces in real space using the recently developed scanning tunneling microscope. This work not only confirmed the LEED results, but also showed possible application of STM for studying more diverse organic overlayers with various defects (steps, kinks, domain boundaries, etc.), and even for surface dynamics (nucleation, ordering, surface reactions, etc.).

I am more than happy if the readers feel that surface science is moving towards more matured stages through this thesis.

Hiroko Ohtani

Berkeley 1988

References

1. G. A. Somorjai, *Chemistry in Two Dimensions: Surfaces,* Cornell University Press, Ithaca, New York, 1981.

2. R. P. Eischens, W. A. Pliskin, and S. A. Francis, *J. Chem. Phys.*, vol. 22, p. 1786, 1954.

3. R. P. Eischens and W. A. Pliskin, *Advances in Catalysis*, vol. 10, p. 1, 1958.

2. Surface Science Techniques

In this chapter, we describe several surface science techniques in order to give the minimum knowledge necessary to follow this thesis for those who are not familier with UHV (Ultra High Vacuum) surface science.*

2.1. Single Crystal Metal Surfaces

In order to study the structure of molecular overlayers, the atomic arrangement of the substrate has to be known. Therefore, we used well-defined single crystals of palladium and rhodium as substrates. These crystals were oriented and spark cut to the (111) plane, then polished with a sequence of finer emery grits and finally with a 0.5 μm diamond paste. The accuracy of the orientation was verified to be within $\pm 0.5^\circ$ with Laue backscattered X-ray diffraction. The model of the (111) face is shown in Fig. 2-1.

2.2. Ultra High Vacuum Chamber

We have examined the clean surfaces and adsorbate-covered surfaces in ultra high vacuum (UHV) conditions less than 5×10^{-10} torr produced by either sputter-ion pumps or oil diffusion pumps.[1] The UHV condition was necessary in order to keep the sample surface away from any contaminant gases during the

Part of this chapter has been published in the following article:
H. Ohtani, C. -T. Kao, M.A. Van Hove, and G.A. Somorjai, Progress in Surface Science, **23**, 155 (1986).

experiments. Using the basic kinetic gas theory, it is shown that under ordinary vacuum conditions of $\sim 10^{-6}$ torr, the whole surface could be covered in a second; whereas with base pressures in the range of 10^{-10} it is possible to keep the surface clean for ~1hr. (Of course this depends on the reactivity of the surface towards gas-adsorption.)[2]

2.3. Sample Preparation

When a single crystal sample is introduced into an UHV chamber, its surface is usually covered with various contaminants from the air. In the case of Pd(111) and Rh(111), the surface is almost completely covered with carbonaceous materials. We therefore have to clean the surface in the vacuum chamber. We can chemically clean these surfaces by heating in oxygen, but when the surface is very dirty, sputtering off the topmost atomic layers by noble gas (typically Ar) ions is more effective. After the chemically pure surface is prepared, we heat the crystal at higher temperatures (anneal) in order to retrieve an atomically smooth surface.

In order to put molecular species onto the clean surfaces, various gas reagents have been introduced into the vacuum chamber through variable leak valves. As long as the base pressure is maintained at less than $\sim 10^{-6}$ torr, this method will not damage pumps, ion gages, or other surface science instruments.

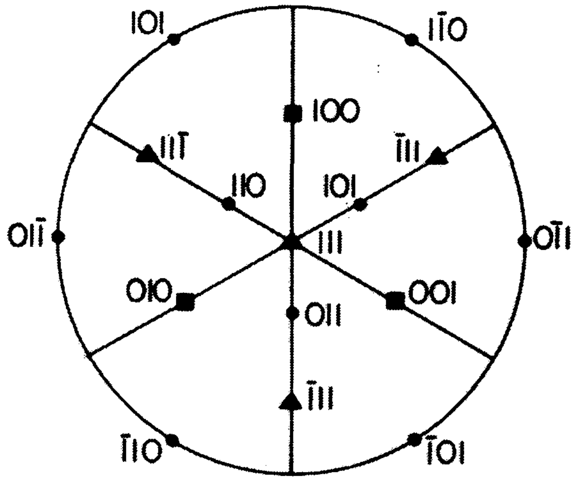

Standard Cubic (111) Projection

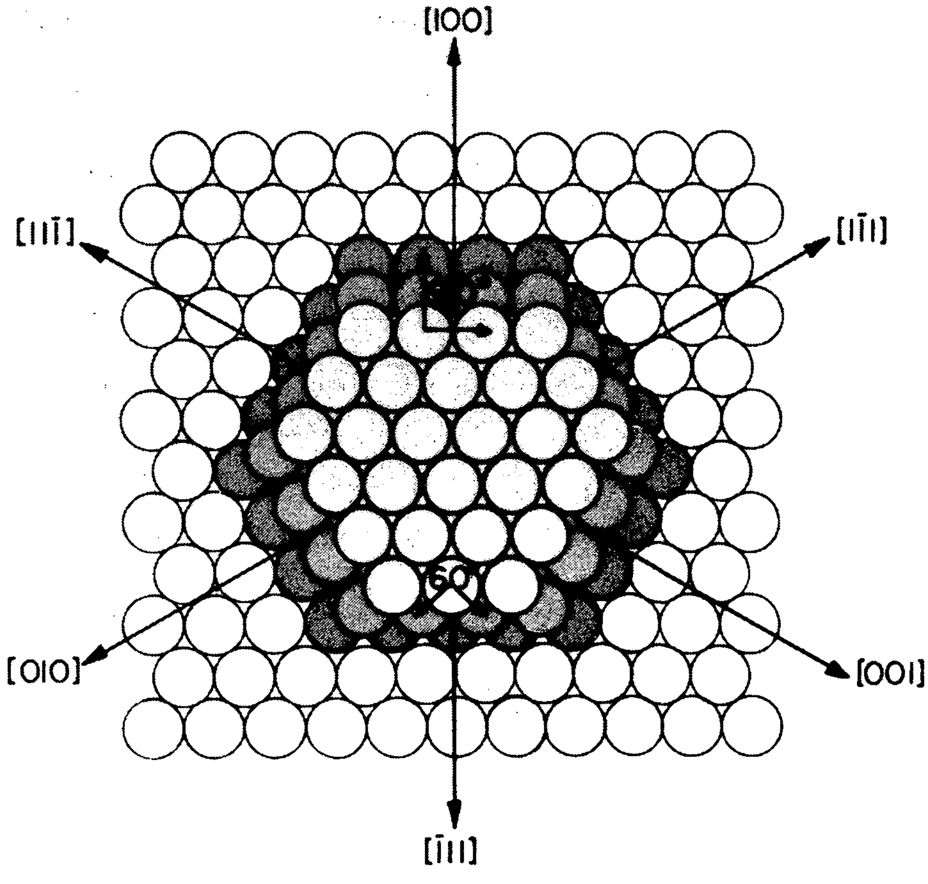

XBB 861-655

[Fig. 2-1] The (111) face of a face centered cubic crystal. The structure of various steps are also shown.

2.4. Use of Low-Energy Electrons for Probing Surfaces

Low-energy electrons ($10<E<1000eV$) interact with matter much more strongly than photons and their mean free path in solids is of the order of several atomic layers, giving rise to very surface sensitive probes (Fig. 2-2). Auger electron spectroscopy, low-energy electron diffraction, and high-resolution electron energy loss spectroscopy described in the following sections utilize such slow electrons.

2.5. Auger Electron Spectroscopy

Auger Electron Spectroscopy is one of the most common techniques for identifying surface chemical composition. Its sensitivity is about 1% of a monolayer, and we have used this technique to verify the purity of the clean surfaces.

The Auger precess occurs in the following manner. [Fig. 2-3] First, an energetic beam of electrons (2-5keV) or an X-ray strikes the material, ionizing a core electron in an atom. The atom can then relax to the ground state through two processes: emission of an X-ray as a valence shell electron falls to the core, or radiationless relaxation. The latter case is called the "Auger process", and the atom relaxes by having a valence shell electron fall to the core, and then evolving another valence shell electron with a well defined kinetic energy (Auger electron) by electrostatic interaction. To a first approximation the energy of the Auger electron depicted in Fig. 2-3 is given by

$$E_{Auger} = E_k - E_{LI} - E_{LIII} \tag{2.1}$$

and is independent of the energy of the incident electron. Thus Anger electron spectroscopy is widely used for identifying the surface chemical composition.

In this study a glancing angle primary electron gun is used to excite the surface atoms and a retarding field analyzer[2] (RFA) is used to analyze the kinetic energy of the Auger electrons. (RFA uses the same electron optics of LEED, thus LEED and AES can be performed using the same apparatus.)

2.6. Low Energy Electron Diffraction

2.6.1. Apparatus

A schematical LEED experiment is shown in Fig. 2-4. A monoenergetic beam of electrons (10 eV to 300 eV) is directed at the surface of a single crystal which backscatters a portion of the incoming electrons. A set of hemispherical grids is used to remove the inelastically backscattered electrons while the elastically backscattered electrons are post-accelerated onto a phosphorous screen for viewing of the diffraction pattern. The crystal and the detection system are enclosed in a ultrahigh vacuum (UHV) chamber in order to attain and maintain a clean surface. The diffraction pattern on the phosphorous screen can be viewed and photographed from outside the UHV chamber. A polaroid camera is commonly used for photographing the diffraction pattern and the published LEED patterns are from such photographs.

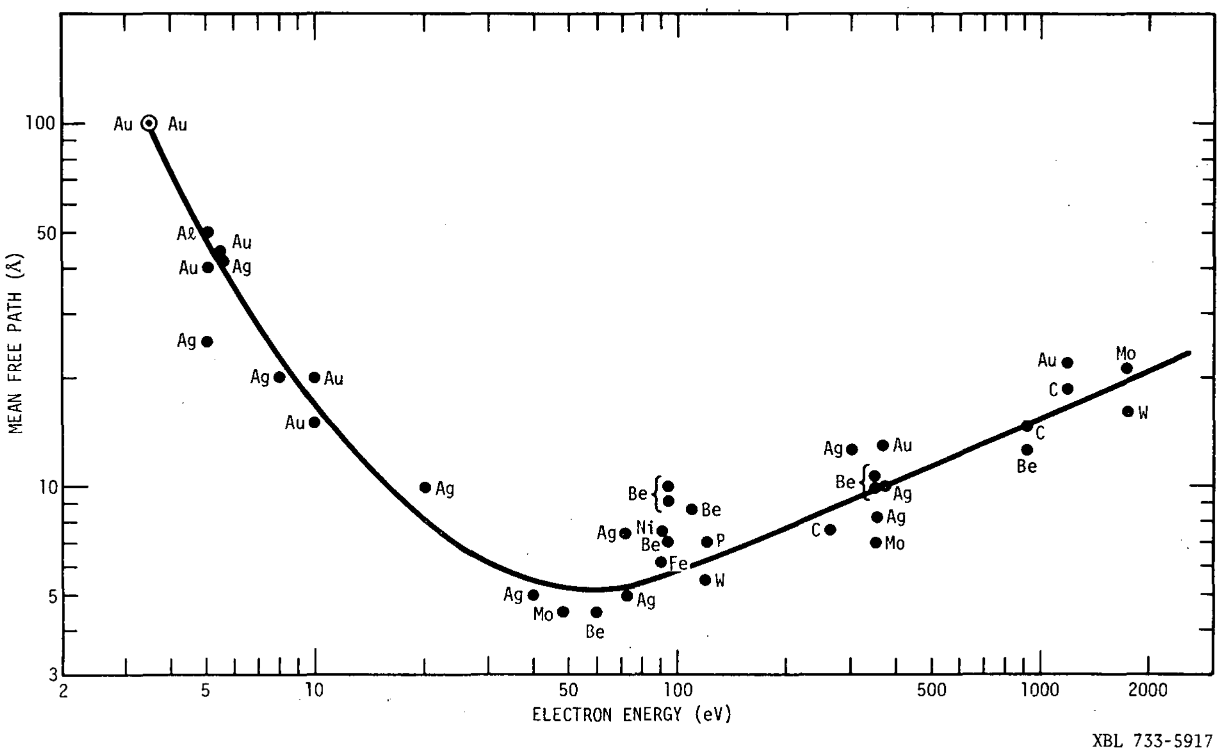

[Fig. 2-2] Electron mean free path as a function of electron kinetic energy.

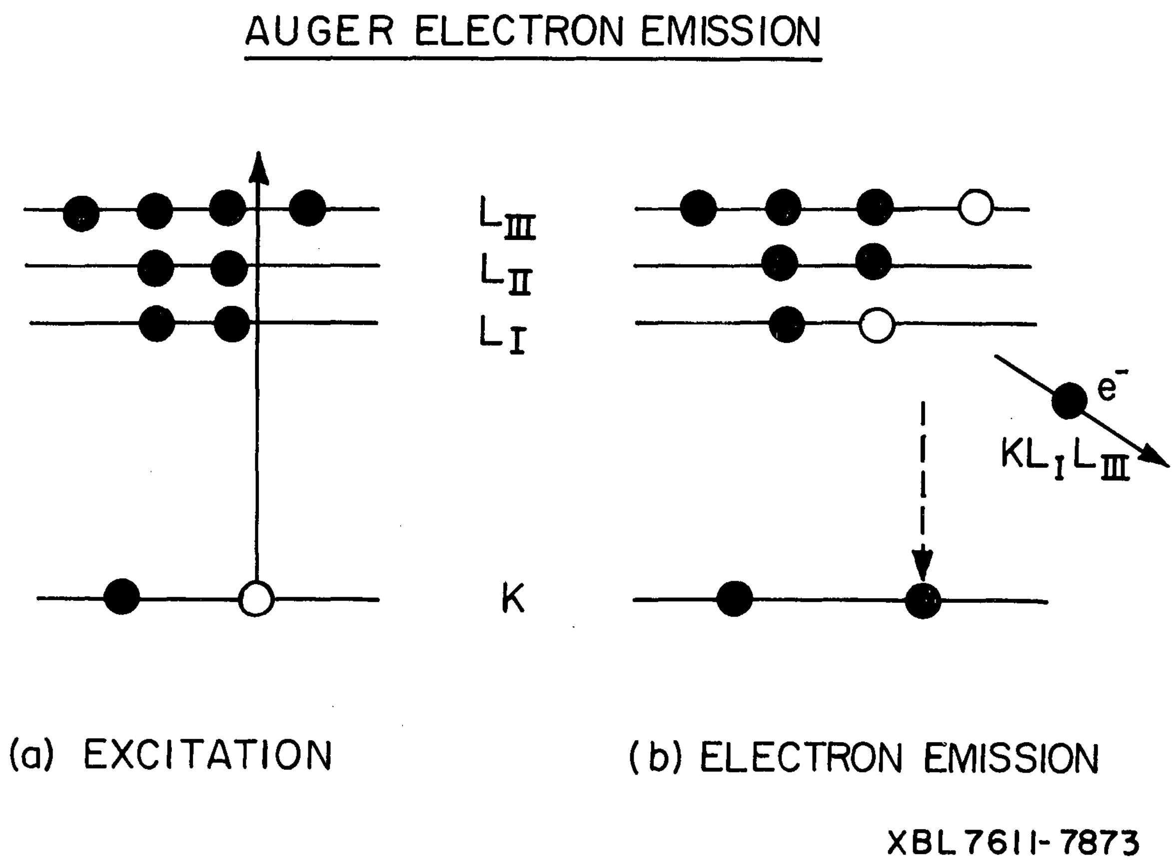

[Fig. 2-3] Scheme of the Auger electron emission process.

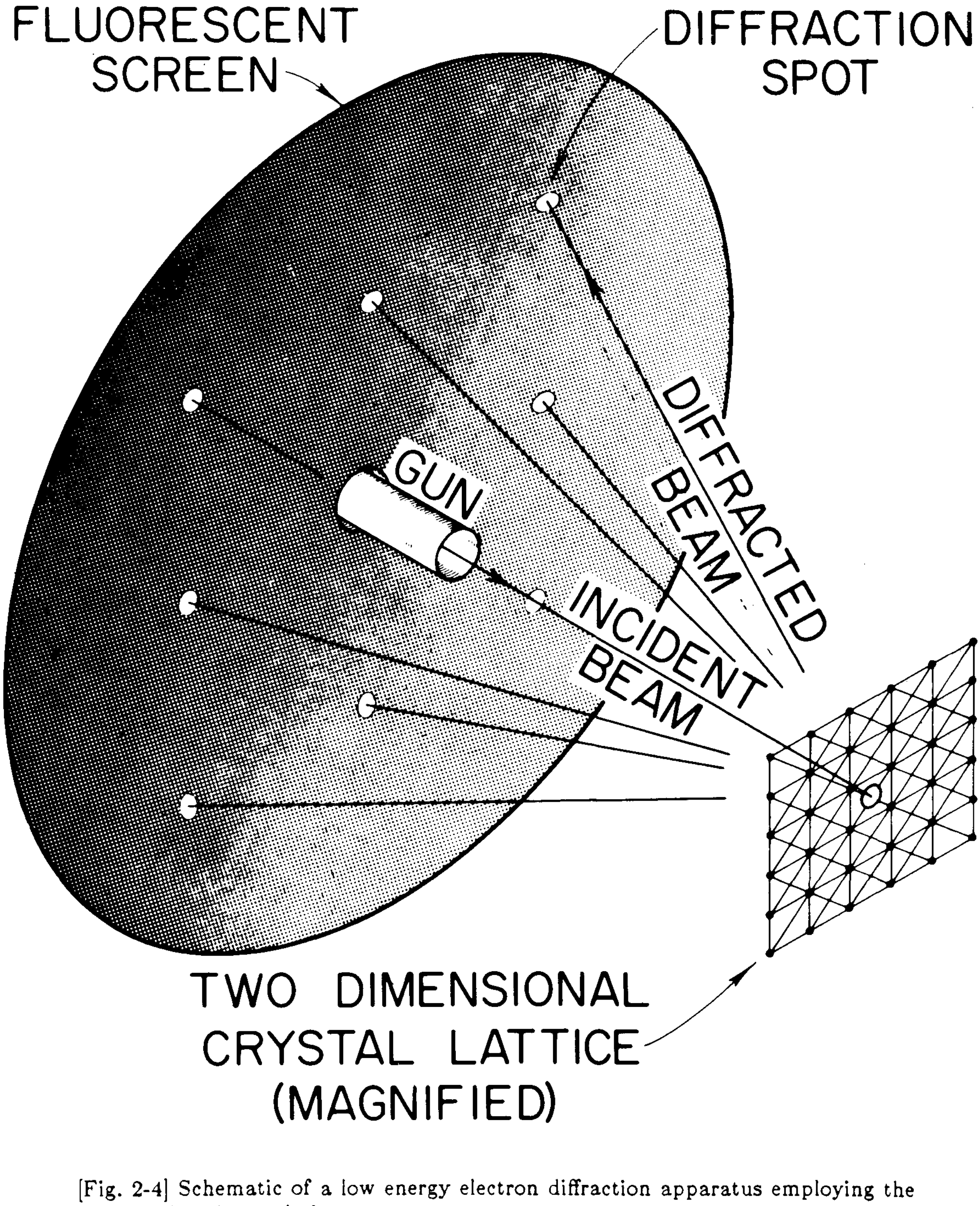

[Fig. 2-4] Schematic of a low energy electron diffraction apparatus employing the post-acceleration technique.

A well ordered crystal surface will yield a diffraction pattern consisting of bright, well defined spots with very low background intensity. The sharpness and overall intensity of the spots depend on the degree of order of the surface. Although the surface may be somewhat irregular on the scale of a micron or more, the presence of sharp diffraction features indicates that the surface is ordered on an atomic scale, i.e., most of the surface atoms are located in a two-dimensional lattice structure.

The electron beam source commonly used yields an instrumental response width of about 100Å. This means that sharp diffraction features are obtained only if the regions of well-ordered atoms ("domains") have an area of $(100\text{Å})^2$ or larger. Diffractions from smaller domains give rise to beam broadening.[3,4,5] Any random defects in the periodic array of atoms (including point defects and steps) gives rise to "diffuse intensity" in all directions.

2.6.2. Interpretation of the LEED Pattern and Notation for Surface Structures

2.6.2.1. General Case

LEED spot patterns represent the reciprocal lattice of the surface. The diffraction pattern must be inverted to real space in order to obtain the real-space periodicity. In this section we describe how this conversion is performed. First, the relationship between the reciprocal and real-space lattices of the substrate will be given. Then the determination of the surface periodicity from the LEED patterns will be discussed.

The pattern of spots has two-dimensional translational periodicity which is given by the vector $\vec{T}^*$, which has the form

$$\vec{T}^* = m^*\vec{a}^* + n^*\vec{b}^* \tag{2.2}$$

where m* and n* are integers and $\vec{a}^*$ and $\vec{b}^*$ are the basis vectors of the reciprocal unit cell. The reciprocal lattice, T*, is related to the real-space lattice, $\vec{T}$,

$$\vec{T} = m\vec{a} + n\vec{b} \tag{2.3}$$

where m and n are integers and $\vec{a}$ and $\vec{b}$ are the basis vectors of the primitive surface lattice. The reciprocal unit cell vectors $\vec{a}^*$ and $\vec{b}^*$ are related to the real-space unit-cell vectors $\vec{a}$ and $\vec{b}$ by the following equations:

$$\vec{a}^* = \frac{\vec{b} \times \vec{z}}{\vec{a} \cdot (\vec{b} \times \vec{z})} \tag{2.4a}$$

$$\vec{b}^* = \frac{\vec{z} \times \vec{a}}{\vec{a} \cdot (\vec{b} \times \vec{z})} \tag{2.4b}$$

where $\vec{z}$ is normal to the surface. The relationship between the reciprocal and real-space vectors for a two-dimensional hexagonal lattice is shown in Fig. 2-5.

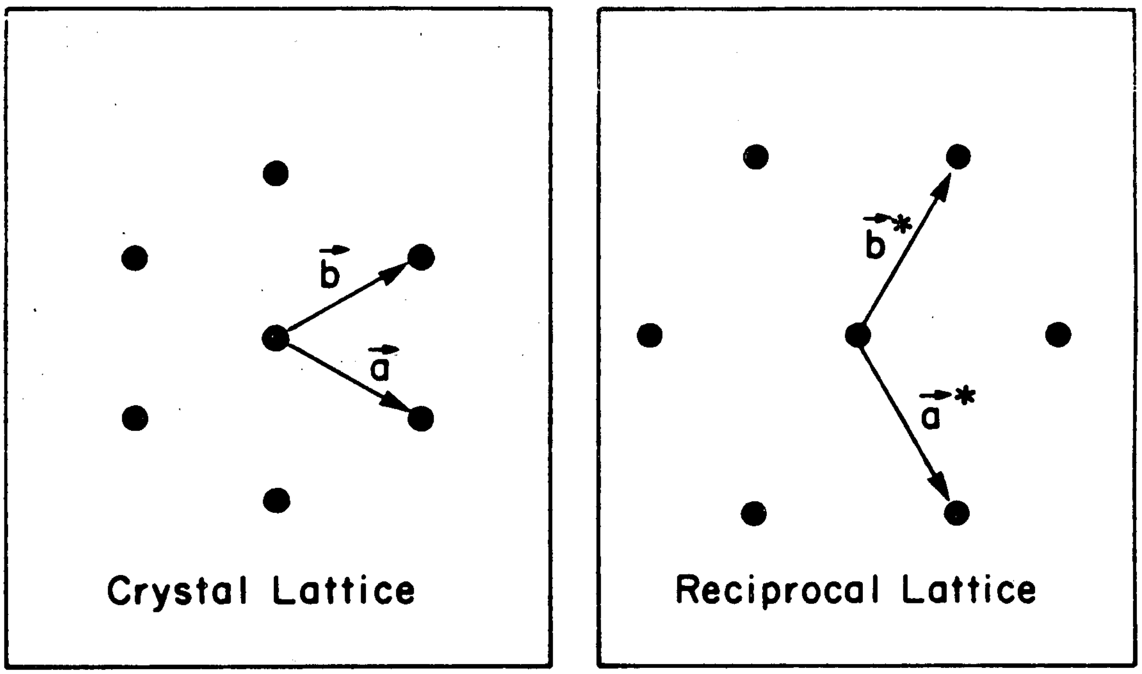

XBL 787-9590

[Fig. 2-5] Real-space vectors $\vec{a}$ and $\vec{b}$ and reciprocal-space vectors $\vec{a}^*$ and $\vec{b}^*$ of a two-dimensional hexagonal lattice.

Reconstruction of the clean surface or adsorption of a gas on a surface usually results in a change in the diffraction pattern corresponding to the appearance of a new surface periodicity; the new lattice is called a superlattice. This is illustrated in Fig. 2-6, which shows a diffraction pattern of a clean Pt(111) surface and the diffraction pattern formed after the adsorption of an ordered layer of acetylene. Figure 2-7 shows the unit cells responsible for the diffraction patterns in Fig. 2-6 superimposed on a model of the Pt(111) surface. No information concerning the location of the adsorbate species within this unit cell (the location relative to the substrate atom positions) is indicated. This information can be obtained only from analysis of the diffraction spot intensities.

To make the transition from the diffraction pattern in Fig. 2-6 to the surface structure in Fig. 2-7, we need to reference the reciprocal superlattice to the reciprocal substrate lattice defined by the vectors $\vec{a}^*$ and $\vec{b}^*$. This is carried out by a visual inspection of the diffraction pattern, in which the differences in spot intensities are neglected and only the positions of the diffraction beams are considered.

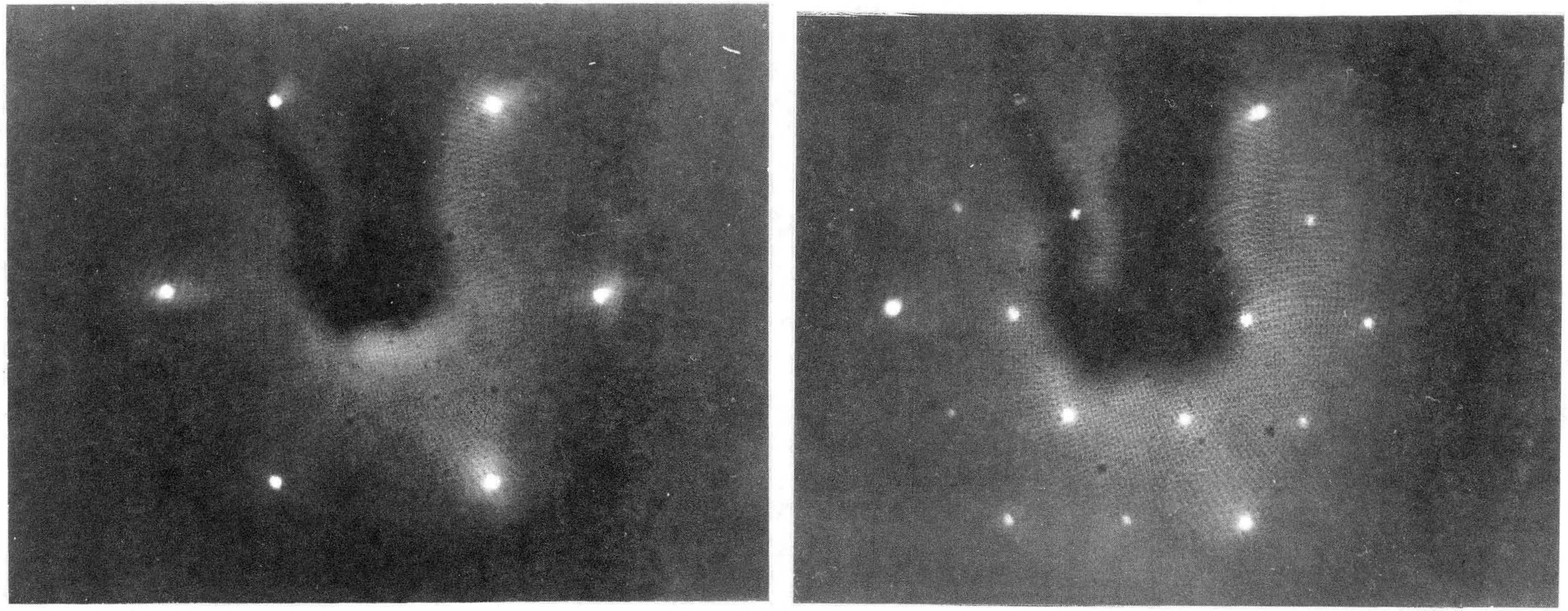

[Fig. 2-6] LEED patterns of a clean Pt(111) (left) surface and the same surface with an ordered overlayer of acetylene (right). For both diffraction patterns, the incident beam energy is 68 eV. A spot of the center of the pattern and several other spots on the right in the patterns are invisible due to obstruction by the sample manipulator.

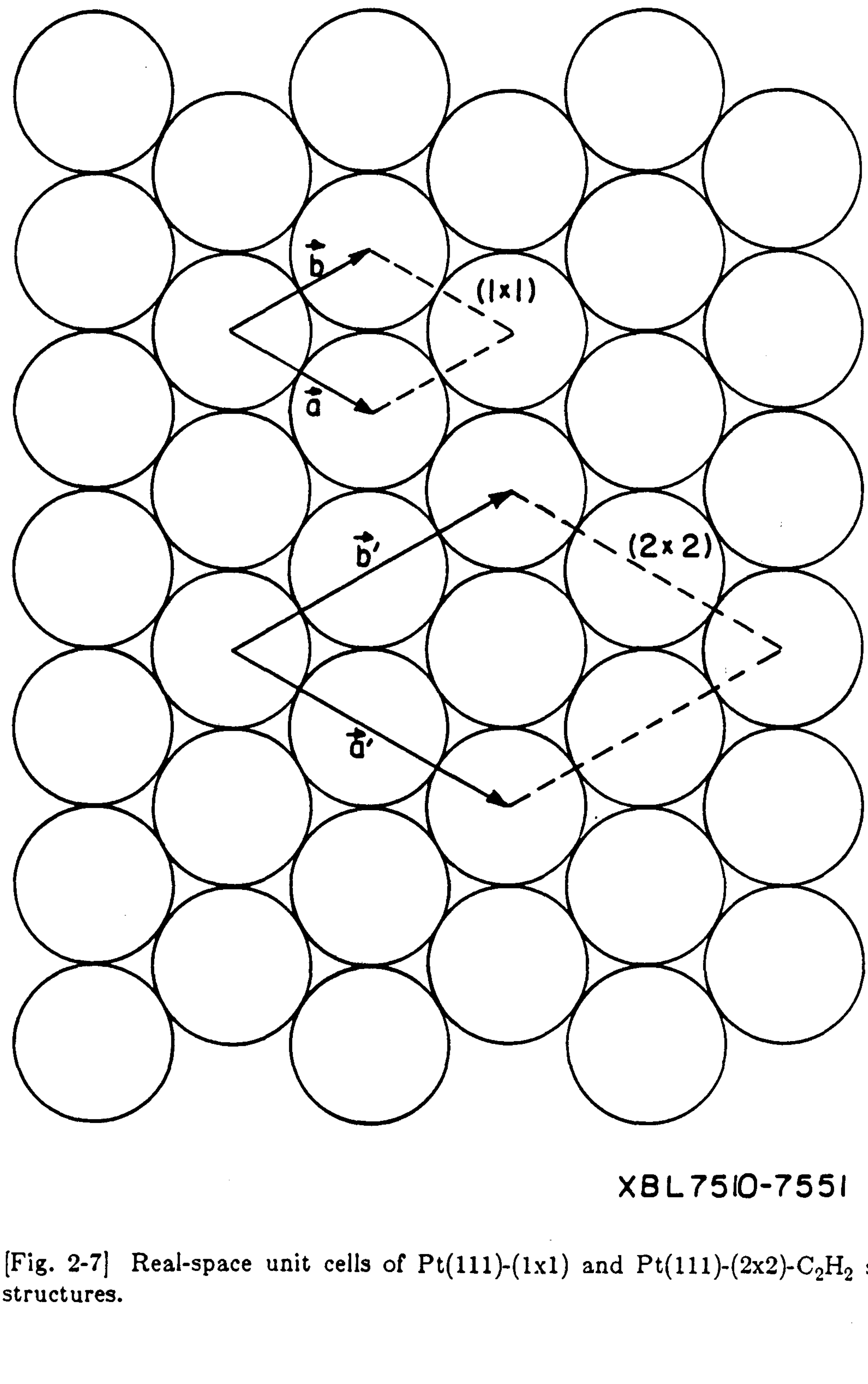

[Fig. 2-7] Real-space unit cells of Pt(111)-(1x1) and Pt(111)-(2x2)-C_2H_2 surface structures.

For the general case, the relationship of reciprocal substrate lattice to the reciprocal superlattice is given by the equations

$$\vec{a}^* = m_{11}^* \, \vec{a}^{*\prime} + m_{12}^* \, \vec{b}^{*\prime} \qquad (2.5a)$$

$$\vec{b}^* = m_{12}^* \, \vec{a}^{*\prime} + m_{22}^* \, \vec{b}^{*\prime} \qquad (2.5b)$$

where $\vec{a}^{*\prime}$ and $\vec{b}^{*\prime}$ are the basis vectors of the reciprocal superlattice and the coefficients m_{11}^*, m_{12}^*, m_{21}^*, and m_{22}^* define the matrix

$$M^* = \begin{pmatrix} m_{11}^* & m_{12}^* \\ m_{21}^* & m_{22}^* \end{pmatrix} \qquad (2.6)$$

In real space the superlattice is related to the substrate lattice by the equations

$$\vec{a}^{\prime} = m_{11} \, \vec{a} + m_{12} \, \vec{b} \qquad (2.7a)$$

$$\vec{b}^{\prime} = m_{21} \, \vec{a} + m_{22} \, \vec{b} \qquad (2.7b)$$

where $\vec{a}'$ and $\vec{b}'$ are the basis vectors of the primitive superlattice and the coefficients m_{11}, m_{12}, m_{21}, and m_{22} define the matrix

$$M = \begin{pmatrix} m_{11} & m_{12} \\ m_{21} & m_{22} \end{pmatrix} \qquad (2.8)$$

The coefficients of the two matrices M and M^* are related by the following equations:

$$m_{11} = m_{11}^* \quad , \qquad (2.9a)$$

$$m_{12} = m_{21}^* \quad , \qquad (2.9b)$$

$$m_{21} = m^*_{12} \quad , \tag{2.9c}$$

$$m_{22} = m^*_{22} \quad , \tag{2.9d}$$

so that if either M or M^* is known, the other may be very easily obtained. In LEED experiments, M^* is determined by visual inspection of the diffraction pattern and then transformed to give M, which defines the surface structure in real space.

For the case of ordered adsorption on Pt(111), visual inspection of the LEED patterns in Fig. 2-6 gives

$$M^* = \begin{pmatrix} 2 & 0 \\ 0 & 2 \end{pmatrix}$$

The matrix M thus becomes

$$\begin{pmatrix} 2 & 0 \\ 0 & 2 \end{pmatrix}$$

so that $\vec{a}' = 2\vec{a}$ and $\vec{b}' = 2\vec{b}$, as depicted in Fig. 2-7.

A superlattice is termed commensurate when all matrix elements M_{ij} (i,j = 1,2) are integers. If at least one matrix element M_{ij} is an irrational number, then the superstructure is termed incommensurate. Superlattices can be incommensurate in one surface dimension or in both surface dimensions.

Alternatively to the matrix method of denoting surface structures, another system, originally proposed by Wood, is more commonly used. Whereas the matrix notation can be applied to any system, Wood's notation can only be used when the angle between the superlattcie vectors $\vec{a}'$ and $\vec{b}'$ is equal to the angle between the substrate vectors $\vec{a}$ and $\vec{b}$. If this condition is met, the surface structure is labeled using the general form

$$p(u \times v)R\Phi^\circ \quad or \quad c(u \times v)R\Phi^\circ \quad , \tag{2.10}$$

depending on whether the unit cell is primitive or centered (the prefix p is often dropped). In Wood's notation the adsorbate unit cell is related to the substrate unit mesh by the scale factors u and v, where

$$|\vec{a}'| = u|\vec{a}| \quad , \tag{2.11a}$$

$$|\vec{b}'| = v|\vec{b}| \quad . \tag{2.11b}$$

The label RΦ° indicates a rotation of the superlattice by Φ° from the substrate lattice. For $\Phi = 0$, the RΦ° label is omitted, so the surface structure in Fig. 2-7 is labeled as p(2 × 2) or simply (2 × 2). The label for the total system refers to the type of substrate, the superlattice periodicity, and the surface species. The platinum-acetylene adsorbate system shown in Fig. 2-7 would be labeled Pt(111)–$\begin{pmatrix} 2 & 0 \\ 0 & 2 \end{pmatrix}$–$C_2H_2$ in matrix notation and as Pt(111)–p(2 × 2)–C_2H_2 in Wood's notation. Wood's notation is more commonly used, and the matrix notation is usually applied only to systems to which Wood's notation does not apply, namely for which the angle between the superlattice vectors differs from the angle between substrate vectors.

An example of an adsorbate that produces a centered unit cell is shown in Figs. 2-8 and 2-9. In Fig. 2-8 diffraction patterns are shown from a clean Rh(100) surface and from a Rh(100) surface after exposure to one half monolayer of oxygen. By visual inspection it can be seen that

$$M^* = \begin{pmatrix} 1 & -1 \\ 1 & 1 \end{pmatrix}$$

so Eqs. (2-9a—d) yield

$$M = \begin{pmatrix} 1 & 1 \\ -1 & 1 \end{pmatrix}$$

M defines the primitive unit cell of the adsorbate, which is drawn with solid lines in Fig. 2-9. This unit cell is labeled $(\sqrt{2}\times\sqrt{2})R45°$ in Wood's notation. Since the centered unit cell drawn in with dotted lines in Fig. 2-9 also describes the adsorbate unit cell, another way of labeling this structure would be c(2 × 2). The total system is labeled as Rh(100)—$\begin{pmatrix} 1 & 1 \\ -1 & 1 \end{pmatrix}$—O, Rh(100)—$(\sqrt{2}\times\sqrt{2})R45°$—O, or Rh(100)—c(2 × 2)—O.

Unreconstructed surfaces of some common face-centered cubic (fcc), body-centered cubic (bcc), and hexagonal close-packed (hcp) crystal structures are shown in Fig. 2-10. The unreconstructed surface has a surface unit cell that is predicted by the projection of the bulk X-ray unit cell onto that surface. That unit cell is denoted as p(1 × 1) or (1 × 1) by Wood's notation: The same surface unit lattice is denoted by $\begin{pmatrix} 1 & 0 \\ 0 & 1 \end{pmatrix}$ in the more general matrix notation. In Table 2-

1 several superlattices that are commonly detected on low-Miller-index surfaces are listed both by their matrix and by their Wood notations.

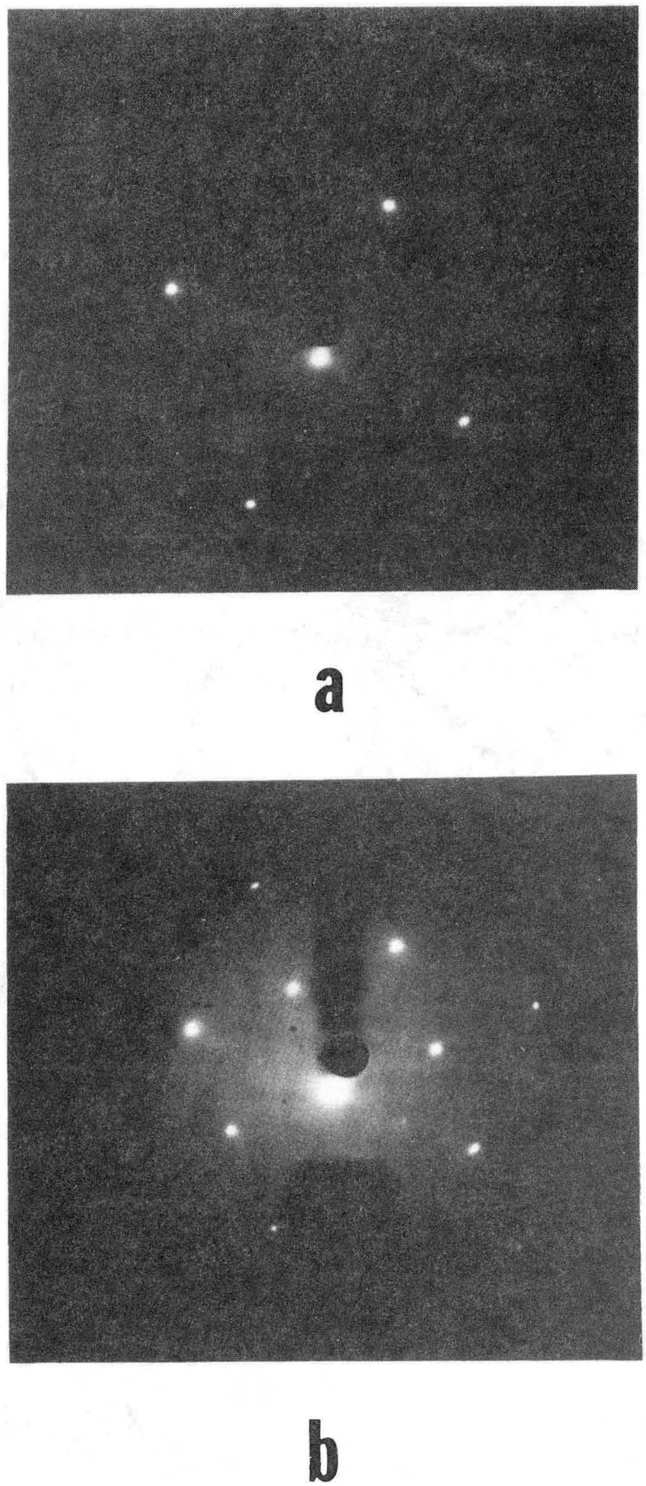

[Fig. 2-8] LEED patterns of (a) clean Rh(100) at 74 eV, and (b) oxygen-covered Rh(100) at 85 eV.

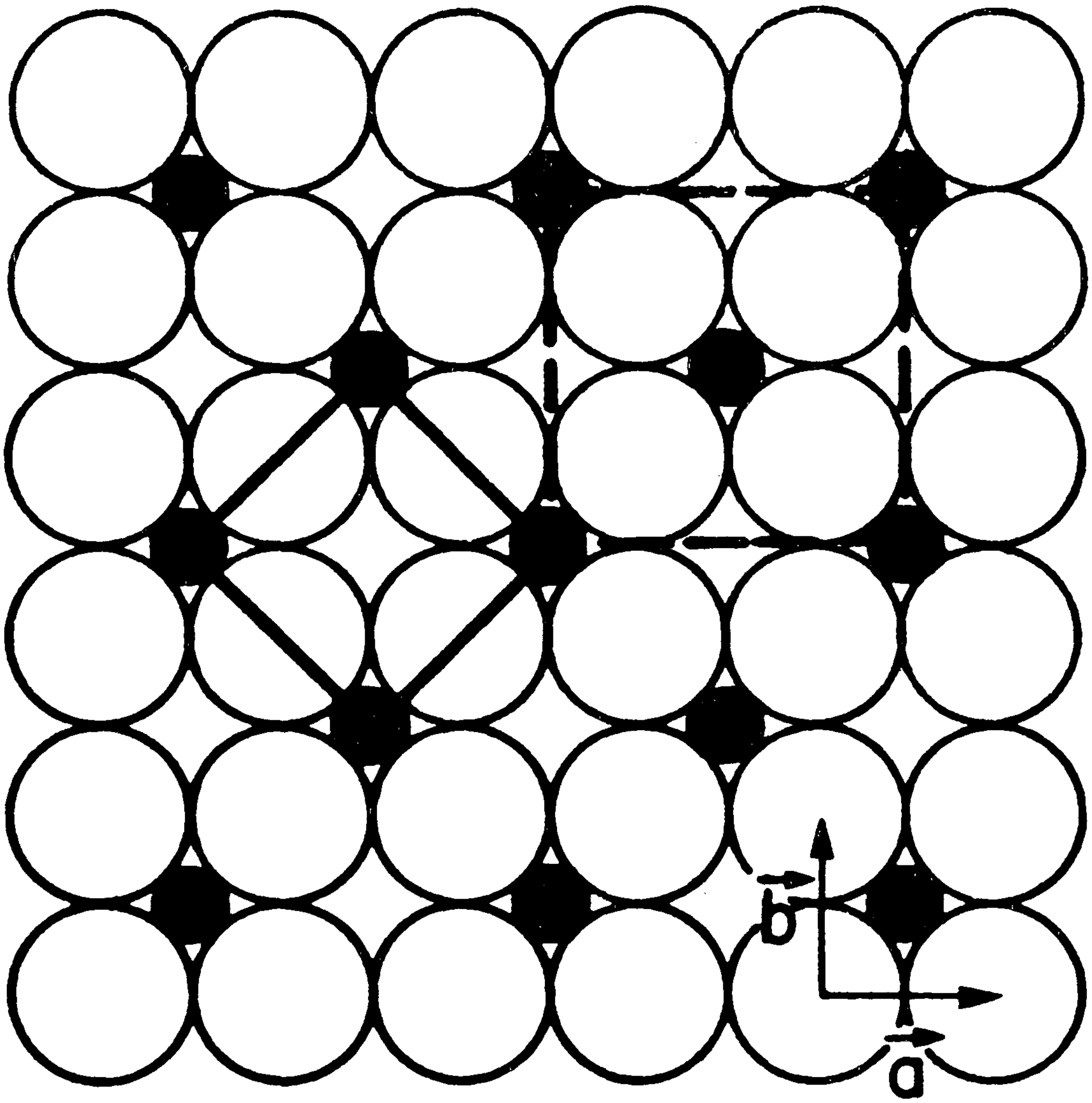

XBL 787-9589

[Fig. 2-9] Real-space unit cells for the two notations $(\sqrt{2}\times\sqrt{2})R45^\circ$ (solid lines) and c(2x2) (dashed lines) for an oxygen structure on the Rh(100) surface.

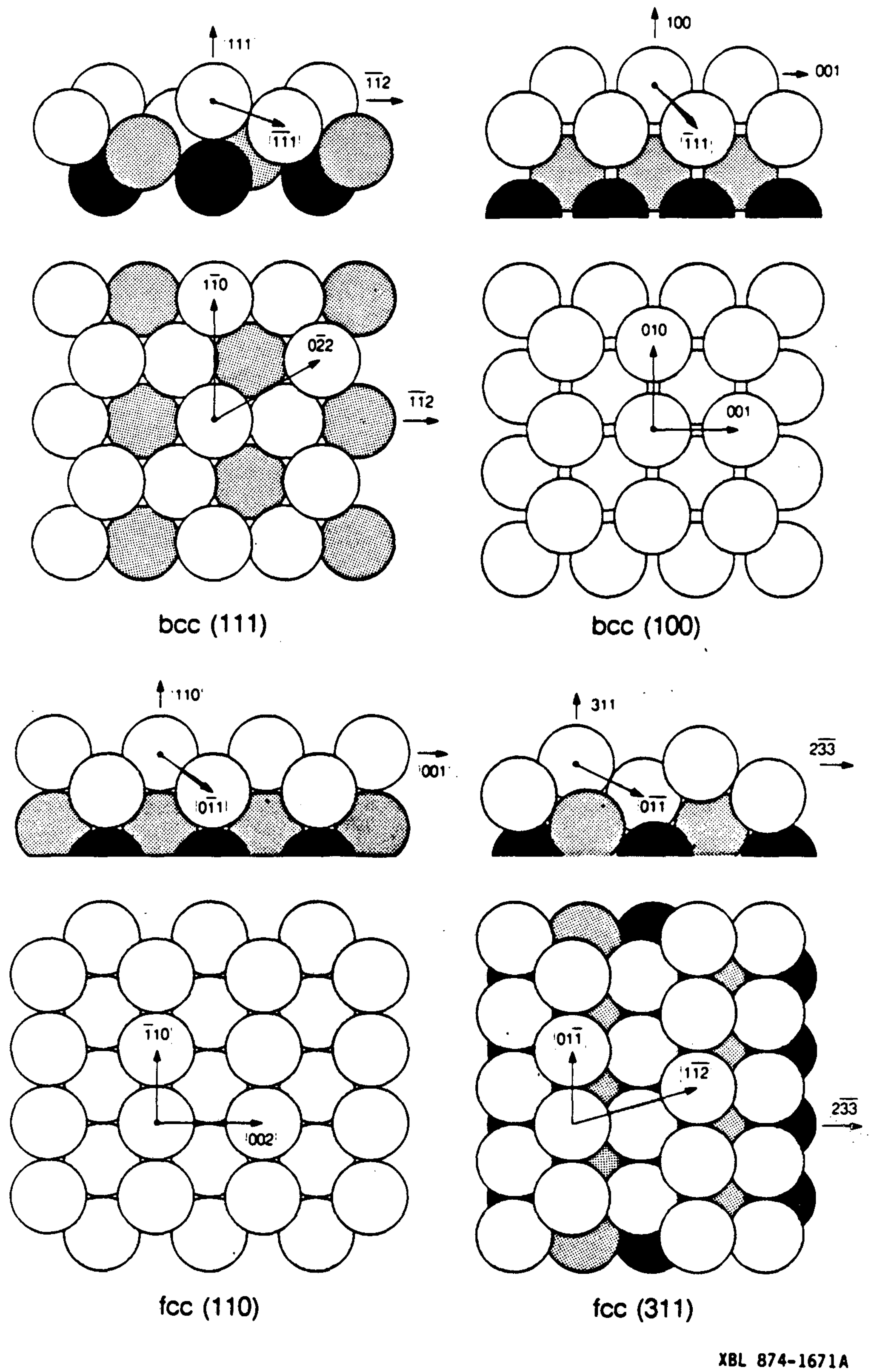

[Fig. 2-10] Atomic arrangement in various unreconstructed, unrelaxed clean metal surfaces. In each panel, the top and bottom sketches give top and side views, respectively.[6]

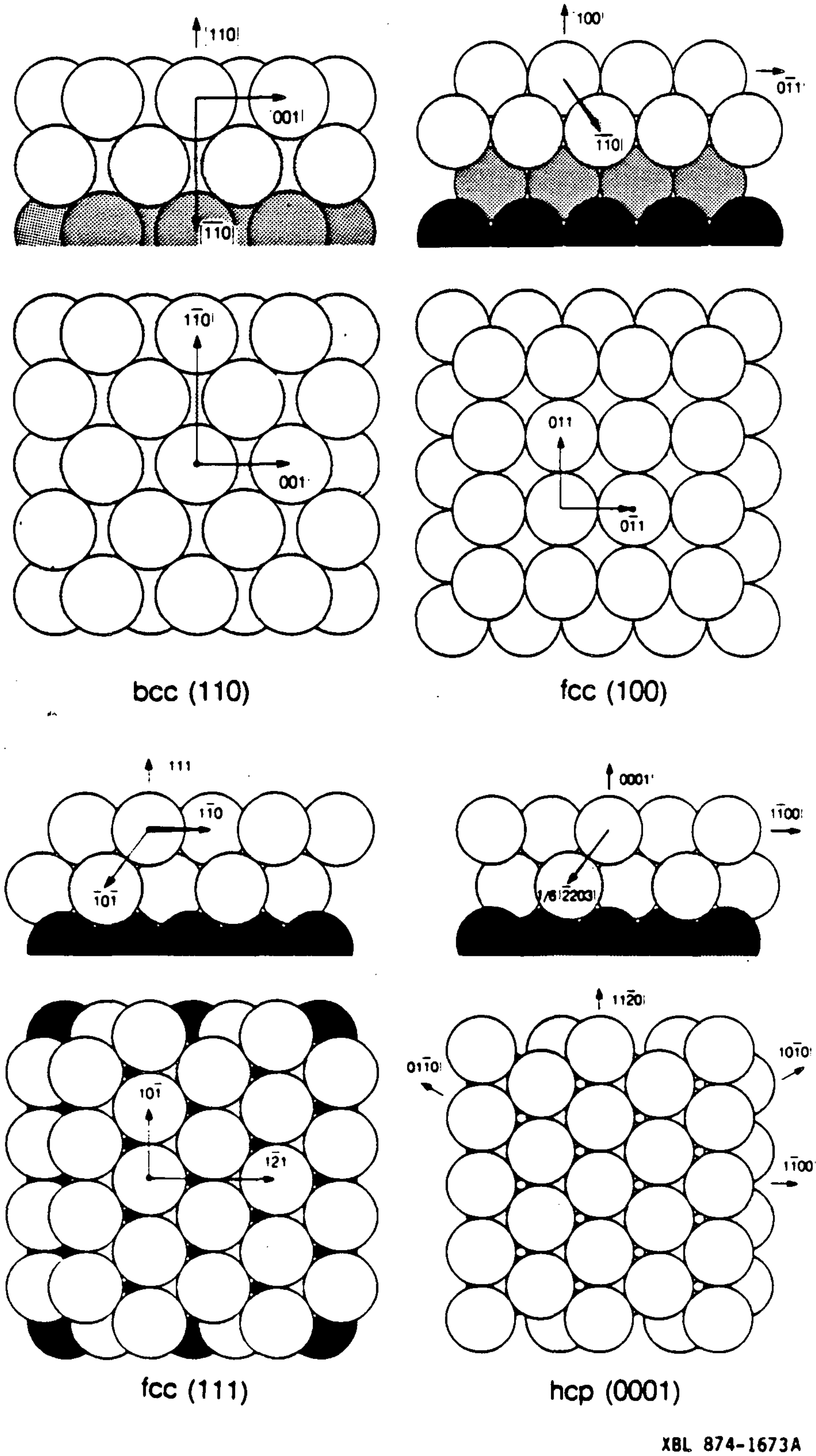

[Fig. 2-10] (continued)

Table 2-1. Wood and matrix notations for a variety of superlattices on low-Miller-index crystal surfaces.

	Superlattice unit cell	
Substrate	Wood notation	Matrix notation
fcc(100), bcc(100)	p(1×1)	$\begin{pmatrix}1 & 0\\0 & 1\end{pmatrix}$
	$c(2\times2) = (\sqrt{2}\times\sqrt{2})R45^\circ$	$\begin{pmatrix}1 & -1\\1 & 1\end{pmatrix}$
	p(2×1)	$\begin{pmatrix}2 & 0\\0 & 1\end{pmatrix}$
	p(1×2)	$\begin{pmatrix}1 & 0\\0 & 2\end{pmatrix}$
	p(2×2)	$\begin{pmatrix}2 & 0\\0 & 2\end{pmatrix}$
	$(2\sqrt{2}\times\sqrt{2})R45^\circ$	$\begin{pmatrix}2 & 2\\-1 & 1\end{pmatrix}$
fcc(111) (60° between basis vectors)	p(2×1)	$\begin{pmatrix}2 & 0\\0 & 1\end{pmatrix}$
	p(2×2)	$\begin{pmatrix}2 & 0\\0 & 2\end{pmatrix}$
	$(\sqrt{3}\times\sqrt{3})R30^\circ$	$\begin{pmatrix}1 & 1\\-1 & 2\end{pmatrix}$
fcc(110)	p(2×1)	$\begin{pmatrix}2 & 0\\0 & 1\end{pmatrix}$
	p(3×1)	$\begin{pmatrix}3 & 0\\0 & 1\end{pmatrix}$
	c(2×2)	$\begin{pmatrix}1 & -1\\1 & 1\end{pmatrix}$
bcc(110)	p(2×1)	$\begin{pmatrix}2 & 0\\0 & 1\end{pmatrix}$

2.6.2.2. High-Miller-Index (Stepped) Surfaces

The atomic structures of high-Miller-index surfaces are composed of terraces, separated by steps, which may have kinks in them. For example, the (775) surface of an fcc crystal consists of (111) terraces, six atoms wide, separated by steps of $(11\bar{1})$ orientation and single-atom height.

The step notation devised by Lang and Somorjai[7] compacts this type of information into the general form

$$w(h_t k_t l_t) \times (h_s k_s l_s) \tag{2.12}$$

where $(h_t k_t l_t)$ and $(h_s k_s l_s)$ are the Miller indices of the terrace plane and the step plane, respectively, while w is the number of atoms that are counted in the width of the terrace, including the step-edge atom and the in-step atom. Thus, the fcc(775) surface is denoted by $7(111) \times (11\bar{1})$, or also by $7(111) \times (111)$ for simplicity. A stepped surface which has steps that are themselves high-Miller-index faces is termed a kinked surface. For example, the fcc(10,8,7) = $7(111) \times (310)$ surface is a kinked surface. The step notation is, of course, equally applicable to surfaces of bcc, hcp, and other crystals, in addition to surfaces of fcc crystals. However, the overwhelming majority of experimental research on high-Miller-index surfaces has utilized fcc crystals.

There is another notation called microfacet notation developed by Van Hove and Somorjai.[8] This notation is based on the idea that any Miller-index-vector (hkl) which specifies a certain crystal face can be decomposed in terms of three linearly independent vectors such as (111), (110), and (100). For example the fcc(10,8,7) kinked surface has the microfacet notation, fcc[$7_{14}(111)+1_1(110)+2_2(100)$]. By using this notation, we can easily recognize that the (10,8,7) unit cell contains fourteen unit cells of the (111) microfacet, one unit cell of the (110) microfacet, and two unit cells of the (100) microfacet.

The surface structures observed on stepped surfaces are listed in Table 2-2. Here the crystal faces are denoted either by their Miller indices or by their stepped surface notation, depending on which system was used by the original authors. Table 2-2 describes the correlation between these two notations for fcc crystals. Using this table, one may convert back and forth between the two notations.

Table 2-2. Correspondence between the Miller-Index Notation and Stepped Surface Notation

Miller Index	Stepped Surface Designation	Angle Between the Macroscopic Surface and Terrace (degrees)
(544)	(S)–[9(111)×(100)]	6.2
(755)	(S)–[6(111)×(100)]	9.5
(533)	(S)–[4(111)×(100)]	14.4
(211)	(S)–[3(111)×(100)]	19.5
(311)	(S)–[2(111)×(100)]	29.5
	(S)–[2(100)×(111)]	25.2
(511)	(S)–[3(100)×(111)]	15.8
(711)	(S)–[4(100)×(111)]	11.4
(665)	(S)–[12(111)×(111)]	4.8
(997)	(S)–[9(111)×(111)]	6.5
(332)	(S)–[6(111)×(111)]	10.0
(221)	(S)–[4(111)×(111)]	15.8
(331)	(S)–[3(111)×(111)]	22.0
	(S)–[2(110)×(111)]	13.3
(771)	(S)–[4(110)×(111)]	5.8
(610)	(S)–[6(100)×(110)]	9.5
(410)	(S)–[4(100)×(110)]	14.0
H310)	(S)–[3(100)×(110)]	18.4
(210)	(S)–[2(100)×(110)]	26.6
	(S)–[2(110)×(100)]	18.4
(430)	(S)–[4(110)×(100)]	8.1
(10,8,7)	(S)–[7(111)×(310)]	8.5

2.7. Surface Structure Determination with LEED

2.7.1. Physical Basis

As shown in the previous section, one can determine the size, shape, and orientation of the surface unit cells by "LEED pattern analysis". However if one wants to obtain the complete surface structure, the intensity of the LEED spots should be analyzed.

Let's summarize first how we determine the crystal structures with X-ray crystallography, since the basic idea of the LEED surface crystallography is analogous to X-ray crystallography. An ideal crystal is constructed by the infinite repetition of identical structural units in space.[9] In the simplest crystals the structural unit is a single atom, but the smallest structural unit may comprise many atoms or molecules. Thus the structure of all crystals can be described in terms of a lattice, with a group of atoms attached to every lattice point. The group of atoms is called basis; when repeated in space it forms the crystal structure (Fig. 2.11) This relation is described as follows:

$$lattice + basis = crystal\ structure \qquad (2.13)$$

When an X-ray beam with a wavelength comparable with the lattice constant hits a crystal, the reflected beams undergo constructive and destructive interference due to the periodicity of the lattice, and forms a diffraction pattern. The diffraction pattern of a crystal is a map of the reciprocal lattice of the crystal. This means that the direction of the diffraction beams tells us the shape, size and orientation of the unit cell (this is called "lattice" in equation (2.13)) and the relative intensity of the diffraction beams determines the composition of the "basis", which is the arrangement of atoms within a unit cell.

In the case of a "surface", the surface structure is described in the similar way:

$$2 \ dimensional \ lattice + basis = surface \ structure \tag{2.14}$$

The de Broglie wavelength of electrons, λ, is given by the formula

$$\lambda \ (in \ \AA) = \sqrt{\frac{150}{E(in \ eV)}} \tag{2.15}$$

Therefore a low-energy electron with the energy range of 10 to 500eV has a wavelength of 3.9Å to 0.64Å (note that these values are comparable to interatomic distances of the solid surface). When such low-energy electrons hit an ordered surface, a LEED pattern which corresponds to the reciprocal lattice of the surface is produced. Thus the "2 dimensional lattice" (or the size, shape, and orientation of the surface unit cell) can be deduced from the LEED pattern, and the "basis" (the arrangement of atoms within a unit cell) can be deduced by the relative intensity of the LEED spots.

We have measured the intensity of the LEED spots at various energies and various angles of incidence in order to increase the accuracy of the LEED structure analysis. The plot of the intensity of each LEED spot against the energy of incident electrons is called an I-V curve, and the surface structure is obtained by comparing the experimental I-V curves with the theoretical I-V curves calculated for many plausible surface configurations.

2.7.2. Calculation of LEED I-V curves

The I-V curve calculation normally must include the multiple scattering of the electrons in the surface region, resulting in so-called "dynamical" calculations. The scattering potential of the surface atomic lattice is represented by the muffin-tin model: it assumes spherically-symmetrical ion-core potentials, surrounded by a constant muffin-tin level (Fig. 2-12). Then the LEED electrons are expressed as linear combinations of either plane waves or spherical waves. The spherical waves are used for describing the scattering by the ion cores and the multiple scattering between atoms in individual layers. The plane waves are used for describing the wavefunction between the successive atomic layers.

The LEED I-V curves are calculated in the following sequence:[10] (1) computation of the single-atom scattering amplitudes; (2) computation of all scattering within a single layer of atoms; (3) computation of all scattering between the various atomic layers in the surface region.

In order to reduce the computational effort, various approximations are used as shown in chapter 4 (clean Pd(111)), in chapter 5 (CO on Pd(111)) , and in chapter 6 (benzene and CO on Pd(111)). More detailed treatments of the calculation of LEED I-V curves are available in the literature.[11,10,12]

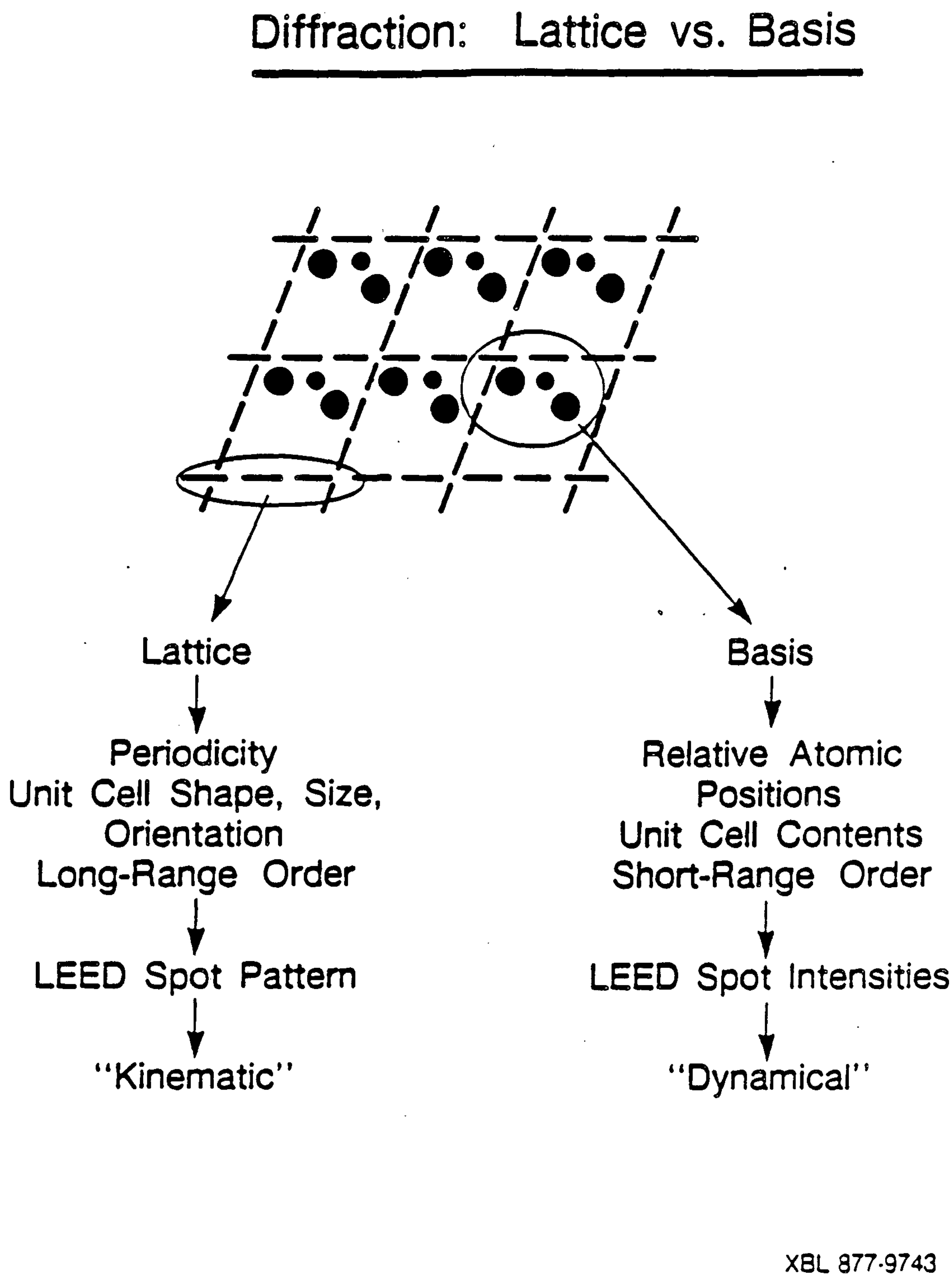

[Fig. 2-11] Representation of periodic crystal structure.[13]

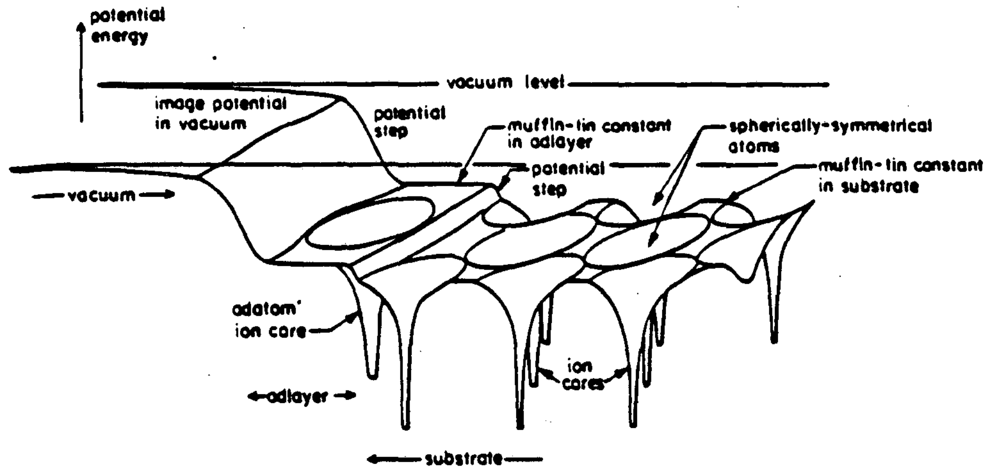

[Fig. 2-12] Sketch of muffin-tin potential at a surface.[11]

2.7.3. R-factor Analysis

An R-factor (reliability factor) is used as an objective measure of the agreement between experiment and calculated I-V curves. Structure determination involves a search through various model geometries to minimize the value of the R-factors. In our study, theory and experiment are compared through a set of R-factors(ROS, R1, R2, RRZJ, and RPE) and their average (R_{VHT}). They are:[14]

$$ROS = \textit{fraction of energy range with slopes of opposite signs in the experimental and theoretical } I-V \textit{ curves,} \tag{2.16}$$

$$R1 = 0.75\int | I_e - cI_t | \, dE \, / \int | I_e | \, dE, \tag{2.17}$$

$$R2 = 0.5\int (I_e - cI_t)^2 dE \, / \int I_e{}^2 dE, \tag{2.18}$$

$$RRZJ = 0.5\int \left[| I_e'' - cI_t'' | \; | I_e' - cI_t' | /(| I_e' | + \max | I_e' |) \right] dE / (0.027\int | I_e | \, dE), \tag{2.19}$$

$$RPE = 0.5\int (Y_e - Y_t)^2 / \int (Y_2{}^2 + Y_t{}^{2)}, \quad Y(E) = L/(1 + V_{0i}{}^2 L^2), \quad L = I'/I \tag{2.20}$$

Here $c = \int | I_e | \, dE / \int | I_t | \, dE$; the apostrophe designates differentiation with respect to the energy. RRZJ is the reduced Zanazzi-Jona R-factor,[15] while RPE is Pendry's R-factor,[16] both renormalized with a factor 0.5 to match the scale of the other R-factors. The 5-average R-factor (R_{VHT}) is:

$$R_{VHT} = \frac{1}{5}(ROS + R1 + R2 + RRZJ + RPE) \tag{2.21}$$

2.7.4. LEED Intensity Measurement

2.7.4. LEED Intensity Measurement

We used a Video LEED data-acquisition system similar to the one developed by Heilman et al.[17,18] Our system is shown schematically in Fig. 2-13.[19] After the surface structure to be investigated is produced in the vacuum chamber, the image of the entire LEED screen is taken with a high-sensitivity vidicon tube camera. The incident electron energy is changed stepwise by a computer, and the video signal is recorded by a video cassette recorder for each energy. The intensity of each diffracted beam is then digitized for entire energy range with 256 gray levels by means of digital video processor. Thus a complete set of I-V curves can be generated in about 3 minutes. with 256 gray levels by means of digital video processor.

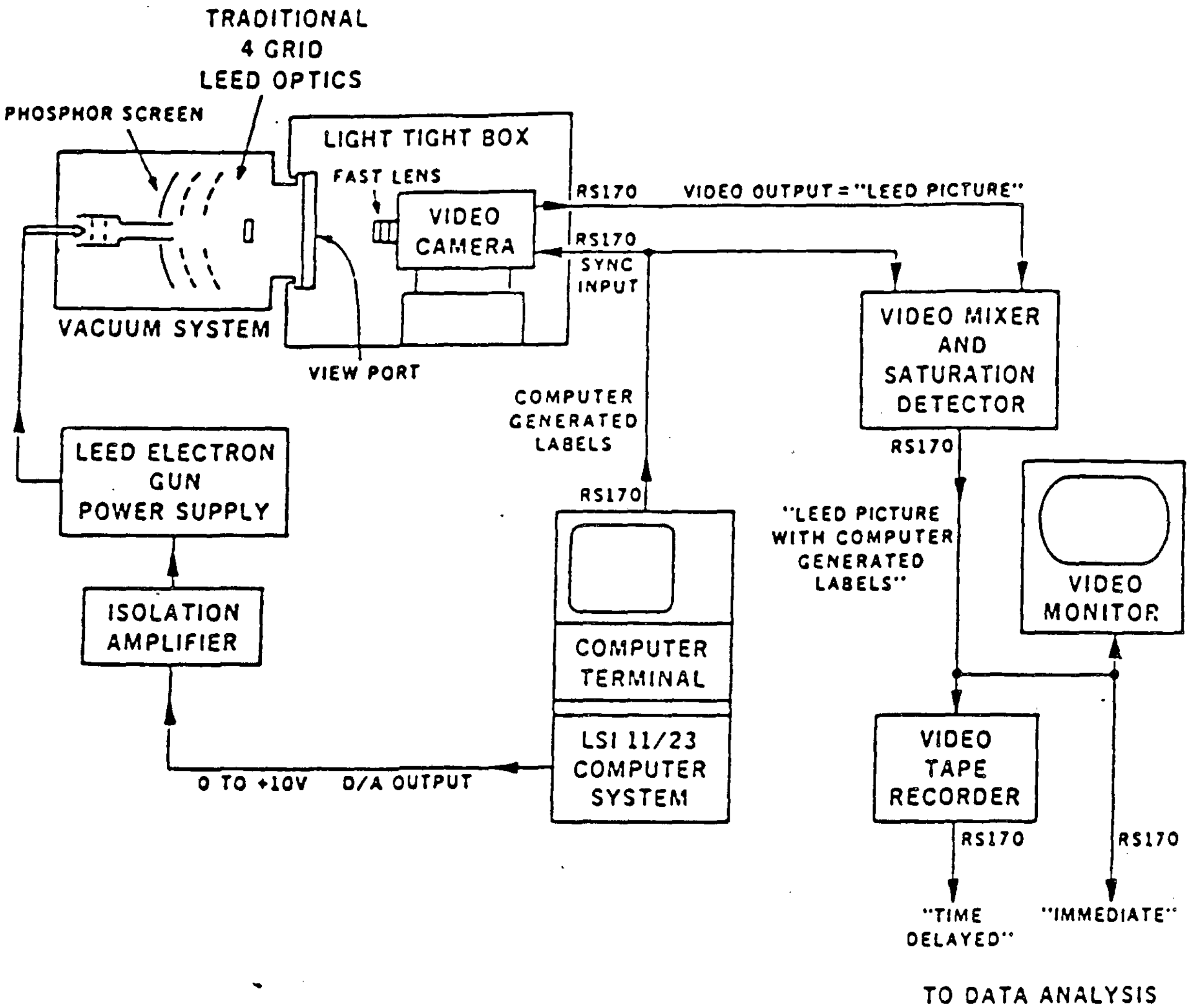

VIDEO RESOLUTION 512 x 480 pixels
typical spot fwhm 6 to 20 pixels

INTENSITY RESOLUTION 256 grey levels

RATE 30 full frames / second
the Video Digitizer can acquire and
integrate video images in real time

IV Curves for all beams in a LEED pattern
may be recorded in 1 to 3 minutes

[Fig. 2-13] Video LEED data-acquisition system.

2.8. Thermal Desorption Spectroscopy

Thermal desorption spectroscopy (TDS) can provide information on adsorption states, population, energetics of bonding, chemical reactions on surfaces, and adsorbate-adsorbate interactions.

In a typical TDS experiment, a clean sample is exposed to gaseous reagents to produce an adsorbate-covered surface. Then while the sample is heated at a constant rate, the partial pressure of each desorbed gas is monitored using a mass spectrometer. The resulting partial pressure versus temperature plot is analyzed using the Redhead method:[20]

$$E_{des}/(RT_p{}^2) = (\nu_1/\beta)\exp\left[-E_{des}/RT_p\right] \ (1st\ order) \tag{2.22}$$

$$E_{des}/(RT_p{}^2) = (\nu_2/\beta)\theta_0\exp\left[-E_{des}/RT_p\right] \ (2st\ order) \tag{2.23}$$

where T_p is the peak temperature, β, the (linear) heating rate, ν_1 and ν_2, preexponential factors, and θ_0, the initial coverage. Therefore, by comparing the experimental thermal desorption spectra with these formula, one could obtain the order of desorption and the heat of desorption of various adsorbates. One should remember however that these formula are based on the assumption that the preexponential factor and the heat of desorption are coverage independent, which may not be very realistic. Even though the TDS experiments are very easy, their quantitative interpretation is not straightforward since we have to make several assumptions such as uniformity of the adsorption sites.

In this thesis, TDS is used primarily to determine the surface coverage of adsorbate by measuring the peak area.

2.9. High Resolution Electron Energy Loss Spectroscopy

2.9.1. Basic Description

High-resolution electron energy loss spectroscopy (HREELS) is based on detection of energy losses in a monoenergetic electron beam scattered from a surface. The losses result from surface phonons or vibrations of adsorbed surface atoms or molecules. The technique offers high surface sensitivity (0.001 monolayer in ideal cases).[21]

The design of our spectrometer is very similar to that of Froitzeim et al as shown in Fig. 2-14, 2-15. [22] The spectrometer was built by Bob McAllister of McAllister Technical Services (Berkeley, California). The spectrometer basically consists of two sectors: one is an electron gun, and the other one is an electron energy analyzer. Electrons are emitted by a hot tungsten filament and focused onto the slit of monochromator by a negatively biased repeller and a three element asymmetric electrostatic lens systems (A1 A2, A3). A1, A2, and A3 are all split in a vertical plane to allow deflection of the beam in a horizontal direction. Then the electrons are monochromized by passing through 127° cylindrical monochromator. After exiting the monochromator the electrons are directed at the sample face by lenses B1 and B2. Typically, an incident electron energy of 2 to

10 eV is used. After scattering from the sample, the electrons are introduced to the 127 ° analyzer through lenses B3, B4, and analyzer slit. After energy analysis, the electrons are detected by a channeltron. The typical energy resolution is ~2.5 to 10meV (20 to 80 wave numbers).

2.9.2. Initial Tuning of the HREEL Spectrometer

When a new HREEL spectrometer is installed, we have to experimentally determine the optimal operating conditions. In short, we want to obtain the optimal voltage settings for each parts of HREEL spectrometer and the optimal position of the sample. This is done as follows:

(1) Place the sample in cavity at the focal point of the spectrometer.

(2) Connect a fast picoammeter, such as Keithley Electrometer, to monochromator collimator. Turn on the filament with the filament current of ~ 2A, and maximize the current to the monochromator collimator by adjusting the voltages applied to A1, A2, A3 lenses, and repeller. (~$3x10^{-5}$A has been detected for our spectrometer)

(3) Connect a fast picoammeter to monochromator slit (MS). Maximize the current to MS by adjusting the voltages applied to A1, A2, A3, repeller, and collimator. (~$1x10^{-5}$A has been detected for our spectrometer)

(4) Connect a fast picoammeter to the sample. Maximize the current to the sample by adjusting the voltages applied to A1, A2, A3, repeller, collimator, monochromator sectors, B1, B2, and the sample position.

(5) The beam energy and the filament current should be optimized at this stage. It is important that the sample current has a maximum as a function of filament current (~ 2.1 amps). This insures that the monochromator is functioning properly. Avoid increasing the filament current over 2.2 amps. This may overload the monochromator and possibly burn out the filament. (The sample current of $\sim 5 \times 10^{-10}$A has been detected for our spectrometer)

(6) Disconnect the picoammeter from the crystal, and the observe elastic peak. Copy voltages from B1 and B2 to B4 and B3, respectively. Maximize and sharpen the elastic peak by adjusting all the parameters. The elastic peak is extremely sensitive to any movement of the crystal particularly to the distance in our out from the focal point of the spectrometer, and the angle of incidence. There is also a strong interaction between the beam energy, the crystal position, and the voltages applied to the crystal and B2 and B3 lenses.

The examples of HREELS are shown in Fig. 16, and Fig. 17. Complete results and interpretation will appear elsewhere.

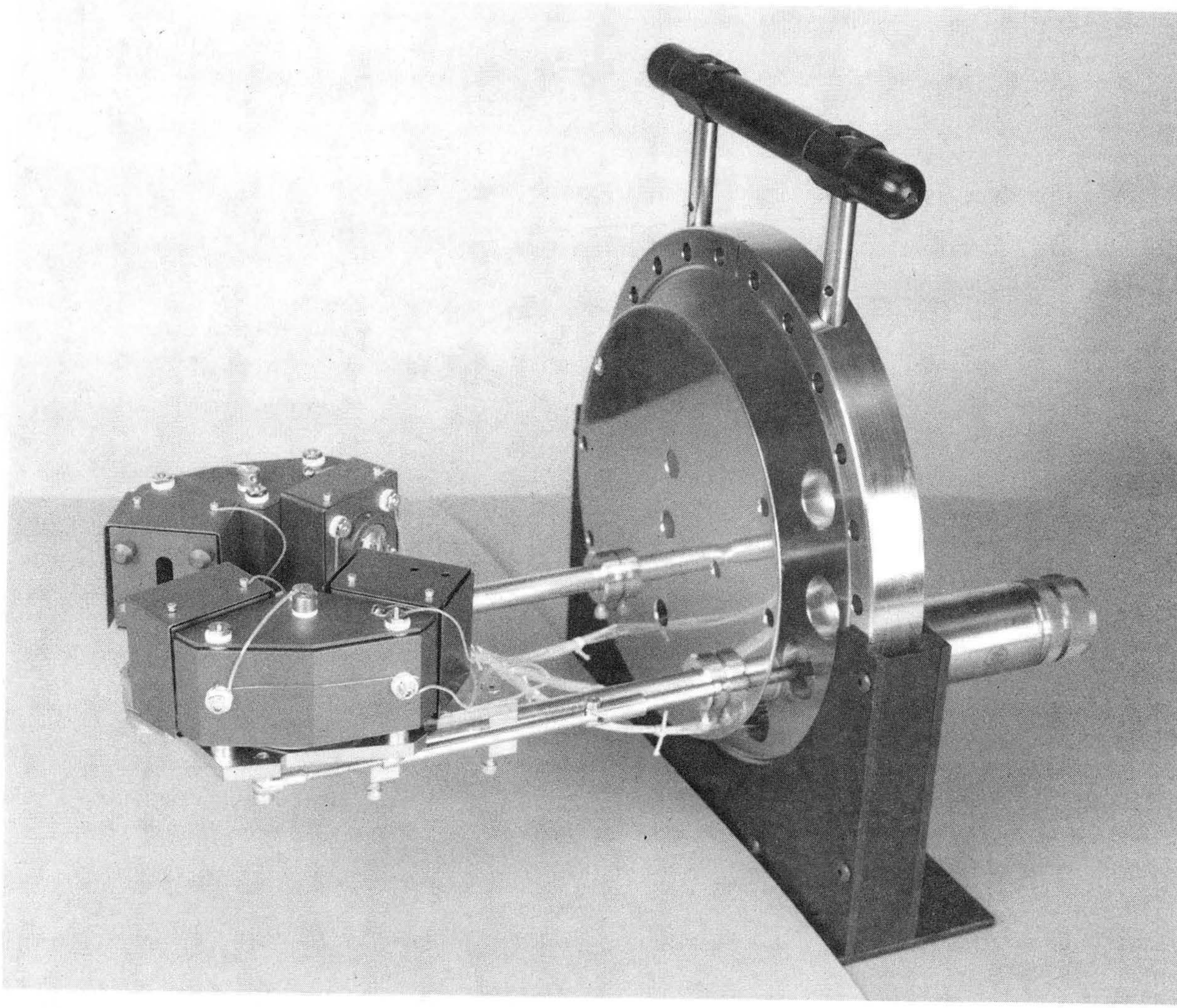

[Fig. 2-14] Photograph of new HREEL Spectrometer with a rotatable analyzer.

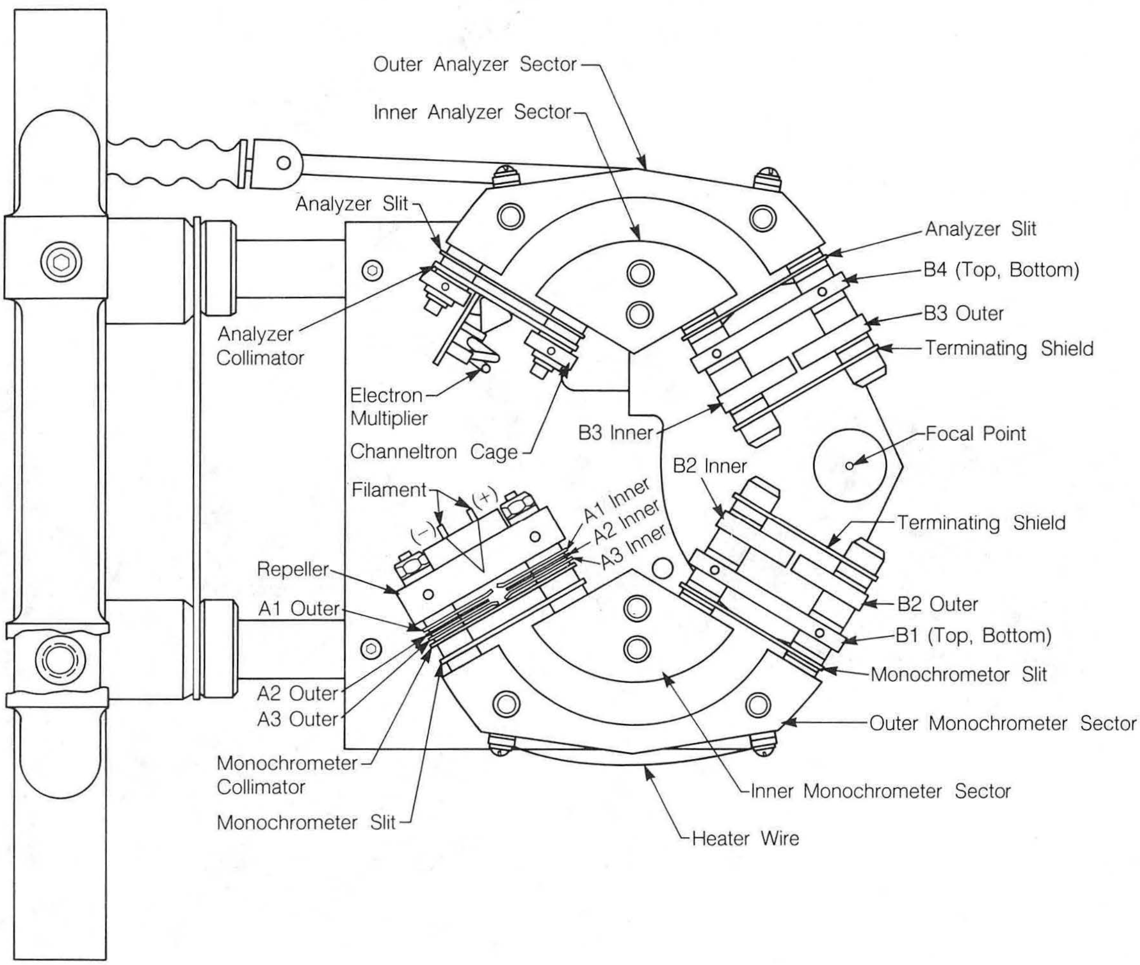

[Fig. 2-15] Schematic of the new HREEL Spectrometer.

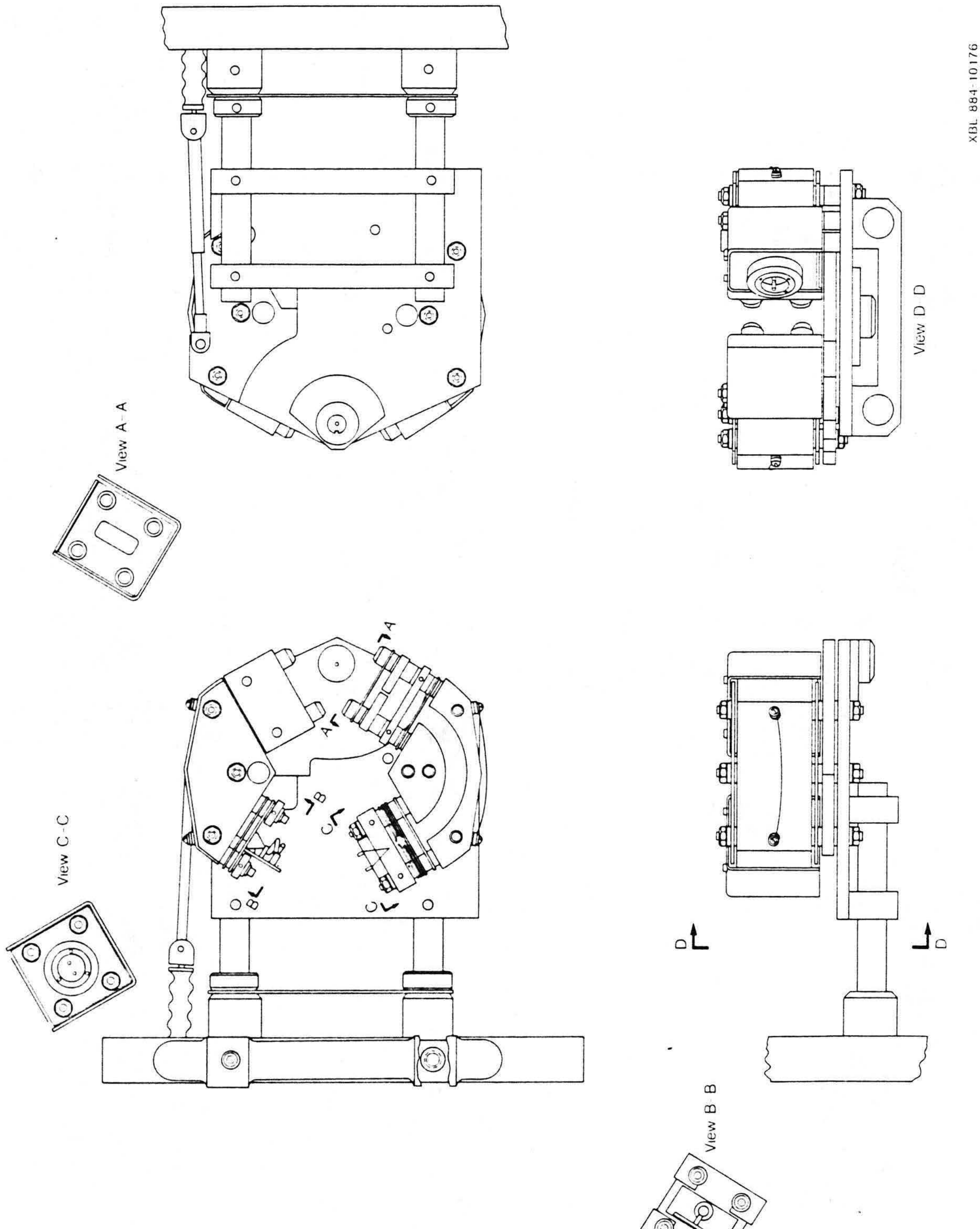

[Fig. 2-15] (continued)

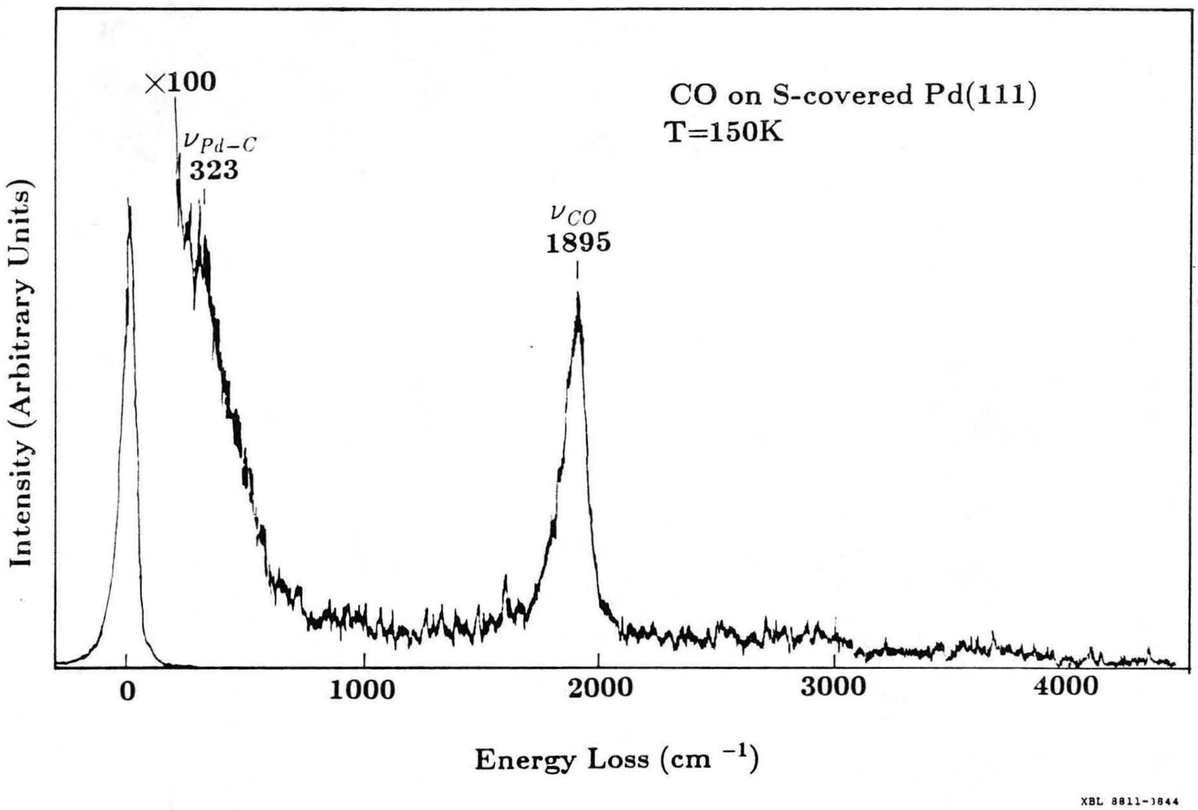

[Fig. 2-16] HREELS of CO on S-covered Pd(111) at 150K.

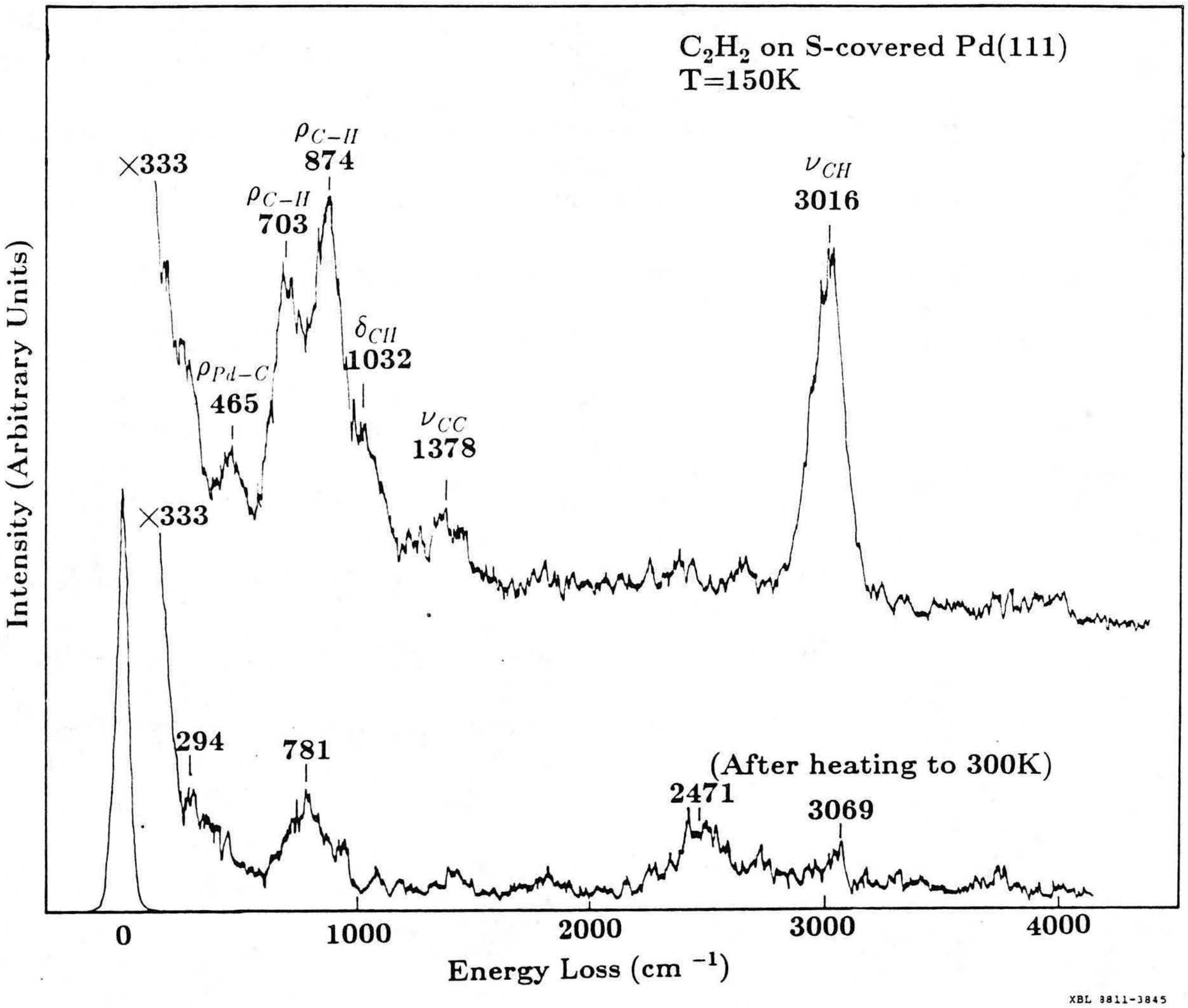

[Fig. 2-17] HREELS of C_2H_2 on S-covered Pd(111) at ~ 150K.

2.9.3. Scattering Mechanism

The energy losses observed in HREELS can be classified into two categories depending on the kind of interaction between the incident electrons and the surfaces. One is is called "long-range inelastic scattering" or "dipole-scattering" mechanism. The dipole-scattering mechanism is described as follows: The oscillating component of the electric dipole moment sets up electric fields in the vacuum above the crystal, and these oscillating electric fields (~.surface vibrational mode) scatter the incoming electron inelastically, in such way similar to the interaction experienced by phonons in IR reflection absorption spectroscopy. This interaction involves only those vibration modes that have a net dynamical dipole moment perpendicular to the surface.(Surface dipole selection rule),[23] since the dipole moment parallel to the surface is cancelled due to the image dipole moment in the metal. This effect (surface dipole selection rule) is shown in Fig. 2-18. A point charge above the surface induces an opposite charge at the image point at the near surface region of the metal surface, as shown on the left. The same argument holds for the interaction between a dipole and a metal, which is shown in the center and on the right. The relationship of the potential (Φ) for dipole moments parallel ($P_{||}$) and perpendicular ($P_{\perp}$) to the surface is also given in terms of the dielectric constant (ϵ). In metals, $|\epsilon|$ is large and thus $\Phi(P_{||})$ is small. The dipole scattering mechanism produces an intense lobe of inelastically scattered electrons centered on the specular beam. This selection rule allows the intensity of energy loss peaks in specular HREEL spectra to be used to determine the symmetry and orientation of the adsorbed species.

The other interaction mechanism is "short-range inelastic scattering". This is commonly separated into two categories: impact scattering and inelastic scattering via an intermediate negative ion resonance. Impact scattering induces polarization of the charge density of the adsorbate-substrate system, while resonance scattering involves temporary trapping of the electron within the molecule. In these cases, the angular distribution of the scattered electrons is much broader than that is observed for dipole scattered electrons. The data from "short-range inelastic scattering" is a very useful complement to the specularly measured data, since their selection rules are different. Very rigorous theoretical treatment including the multiple scattering effect has been developed for the "short-range inelastic scattering", which is direct to the surface structure determination of the adsorbate-covered surfaces with HREELS.[24,25,26,27]

DIPOLE SELECTION RULE

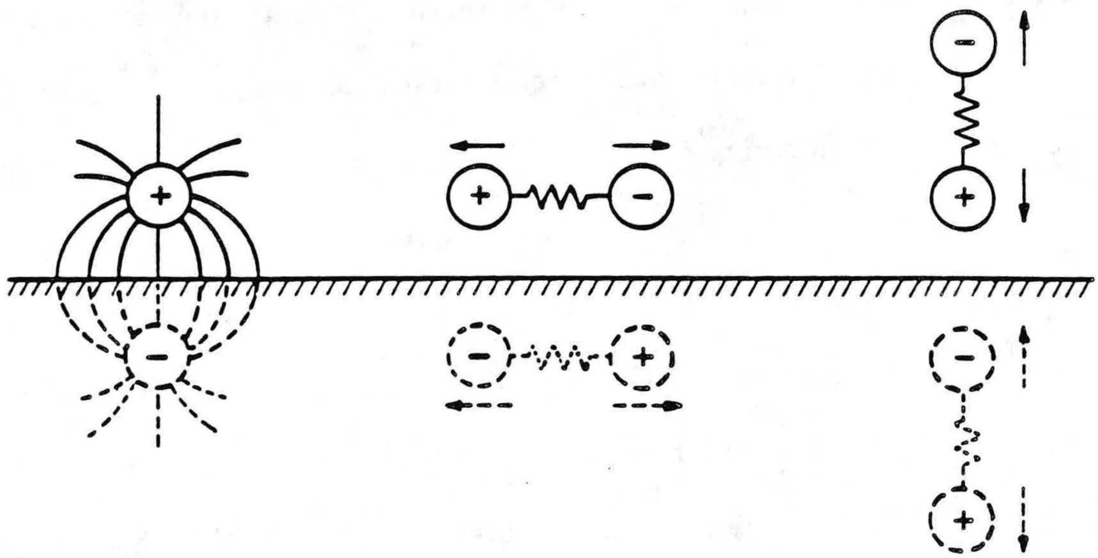

$$\Phi(P_{\parallel}) = P_{\parallel} - \left(\frac{\varepsilon - 1}{\varepsilon + 1}\right) P_{\parallel} = \frac{2}{\varepsilon + 1} P_{\parallel}$$

$$\Phi(P_{\perp}) = P_{\perp} - \left(\frac{\varepsilon - 1}{\varepsilon + 1}\right) P_{\perp} = \frac{2\varepsilon}{\varepsilon + 1} P_{\perp}$$

XBL781-4415

[Fig. 2-18] Physical basis for the dipole selection rule for metal surfaces.

2.10. Scanning Tunneling Microscopy

The Scanning Tunneling Microscope (STM) is a device capable of imaging solid surfaces with atomic resolution. The instrument was invented in 1981 by Gerd Binnig and Heinrich Rohrer.[28,29,30] The underlying physical basis of the STM is electron tunneling. The microscope uses a metal tip with an extremely small radius of curvature that is brought to within about 10Å of the surface of the material to be imaged. A voltage is applied to the tip, and a small tunnel current passes between the tip and the sample material. This tunnel current is proportional to the local density of states of the surface, at the position of the tip.[31] The effective lateral resolution is related to the tip radius R and the vacuum gap distance d approximately as $[(2Å)(R+d)]^{1/2}$.[31] Therefore by scanning the tip across the surface of the sample, while the distance between the tip and surface is adjusted to maintain a constant tunneling current, a contour map of the electronic density of the surface, which resembles the topography of the surface, is obtained.

Many other applications of the STM are bing investigated, including electronic and vibrational spectroscopy of the surfaces and surface modification, etc.

References

1. J. F. O'Hanlon, *A User's Guide to Vacuum Technology,* Wiley-Interscience, New York, 1980.

2. G. Ertl and J. Küppers, *Low Energy Electrons and Surface Chemistry,* p. 53, Verlag Chemie, Weinheim, 1974.

3. L. L. Kesmodel and G. A. Somorjai, *Acc. Chem. Res.*, vol. 9, p. 392, 1976.

4. G. A. Somorjai, in *Principles of Surface Chemistry*, Prentice-Hall, Englewood Cliffs, N. J., 1972.

5. G. Ertl and J. Küppers, in *Low Energy Electrons and Surface Chemistry*, Verlag Chemie, Weinheim, 1979.

6. J.M. MacLaren, J.B. Pendry, R.J. Rous, D.K. Saldin, G.A. Somorjai, M.A. Van Hove, and D.D. Vvedensky, in *Surface Crystallographic Information Services: A Handbook of Surface Structures*, Reidel, Dordrecht, 1987.

7. B. Lang, R. W. Joyner, and G. A. Somorjai, *Surf. Sci.*, vol. 30, p. 454, 1972.

8. M. A. Van Hove and G. A. Somorjai, *Surf. Sci.*, vol. 92, p. 489, 1980.

9. C. Kittel, in *Introduction to Solic State Physics, 6th edition*, John Wiley & Sons, N. Y., 1986.

10. M. A. Van Hove and S. Y. Tong, *Surface Crystallography by LEED,* Springer Verlag, Berlin, 1979.

11. J. B. Pendry, *Low Energy Electron Diffraction,* Academic Press, London, 1974.

12. M. A. Van Hove, W. H. Weinberg, and C.-M. Chan, *Low Energy Electron Diffraction: Experiment, Theory and Structural Determination.*, Springer Verlag, Heidelberg, 1986.

13. M. A. Van Hove, *Proc. 8th Int. Summer Institute in Surface Science, Milwaukee*, 1987.

14. R. J. Koestner, M. A. Van Hove, and G. A. Somorjai, *Surface Science*, vol. 107, p. 439, 1981.

15. E. Zanazzi and F. Jona, *Surface Sci.*, vol. 62, p. 61, 1977.

16. J. B. Pendry, *J. Phys.*, vol. C13, p. 937, 1980.

17. P. Heilmann, E. Lang, K. Heinz, and K. Müller, *Applied Physics*, vol. 9, p. 247, 1976.

18. E. Lang, P. Heilmann, G. Hanke, K. Heinz, and K. Müller, *Applied Physics*, vol. 19, p. 287, 1979.

19. D. F. Ogletree, G. A. Somorjai, and J. E. Katz, *Review of Scientific Instruments*, vol. 57, p. 3012, 1986.

20. P. A. Readhead, *Vacuum*, vol. 12, p. 203, 1962.

21. J. L. Erskine, *Proc. Workshop High-Energy Excitations Condens. Matter.*, vol. 2, p. 577, 1984.

22. H. Froitzheim, H. Hopster, H. Ibach, and S. Lehwald, *Applied Physics*, vol. 13, p. 147, 1977.

23. H. Ibach and D. L. Mills, *Electron Energy Loss Spectroscopy and Surface Vibrations*, Academic Press, New York, 1982.

24. C. H. Li, S. Y. Tong, and D. L. Mills, *Physical Review B*, vol. 21, p. 3057, 1980.

25. S. Y. Tong, C. H. Li, and D. L. Mills, *Phys. Rev. Lett.*, vol. 44, p. 407, 1980.

26. R. E. Palmer, P. J. Rous, J. L. Wilkes, and R. F. Willis, *Phys. Rev. Lett.*, vol. 60, p. 329, 1988.

27. R. J. Rous, P. E. Palmer, and R. F. Willis, *Phys. Rev. B*, vol. in preparation.

28. G. Binnig, H. Rohrer, Ch. Gerber, and H. Weibel, *Appl. Phys. Lett.*, vol. 40, p. 178, 1981.

29. G. Binnig, H. Rohrer, Ch. Gerber, and H. Weibel, *Physica (Utrecht)*, vol. 107B+C, p. 1335, 1981.

30. G. Binnig, H. Rohrer, Ch. Gerber, and H. Weibel, *Proc. 6th Int. Conf. on Low-Temperature Physics*, 1981.

31. J. Tersoff and D. R. Hamann, *Physical Review B*, vol. 31, p. 805, 1985.

3. Design and Construction of Ultrahigh Vacuum System for Surface Crystallography with LEED and HREELS

3.1. Introduction

The structure determination of molecular overlayers is a crucial step in understanding important surface phenomena such as heterogeneous catalysis, corrosion, and friction. To date the most widely used technique for this purpose is low energy electron diffraction (LEED): more than 20 molecular overlayer structures have been already determined.[1] LEED crystallography determines surface structures by comparing experimental LEED intensities with theoretical ones. This can be done systematically with established multiple scattering calculation along with R-factor analysis.[2] Usually LEED crystallography requires enormous computational effort, since one has to search through all the probable trial structures.

Vibrational spectroscopy is very useful for experimentally reducing such computational effort, especially in the case of molecular overlayers, by eliminating some classes of trial structures. (Vibrational spectroscopy estimates approximate orientation of molecular species.) In this chapter, we describe a design of ultrahigh vacuum system for both LEED crystallography and HREELS vibrational spectroscopy.

3.2. UHV vessel

I designed an UHV apparatus where the LEED optics and the HREEL spectrometer are located at same level, as opposed to the two level design previously used in Somorjai's research group.[3] In this UHV apparatus a 2.5" off axis manipulator positions the sample on a circle in a horizontal plane. The focal points of the HREEL spectrometer, the LEED optics, the glancing incidence electron gun for Auger electron spectroscopy, and the ion sputtering gun all lie on this circle. The sample can be moved from one instrument focus to another with great reproducibility by just rotating the sample manipulator. Also this one level design allows us to utilize high-precision sample manipulator with relatively short shaft length. This is crucial for LEED crystallography (not LEED pattern observation). The UHV chamber consists of a 12"O.D. bell jar with 27 ports specified in Table 3-1.

The UHV vessel has been fabricated by the Kurt J. Lesker co. The material used was 304 series stainless steel. The side view and the top view are shown in Figure 3-1 and 3-2. The 127° cylindrical deflector HREEL spectrometer[4] is attached to the 10" flange at the same level as the LEED optics. The analyzer of this spectrometer is rotatable around sample position in order to detect the off-specularly scattered electrons as well as the specularly scattered electrons. This is very important to understand the nature of the loss peaks. (See section 2.9.3)

The design of the vessel is shown in Figure 3-3 and 3-4. A primary vacuum pump (Varian 240 l/s diode ion pump) is located just below the vessel through a 8" gate valve for effective pumping. After a careful bakeout for several days at about 160 C, a base pressure of $3x10^{-11}$ torr has been obtained.

Table 3-1. Orientation of the ports for LEED/HREELS UHV vessel (1)

	FLG O.D.	TUBE O.D.	ROT	Z	R	θ	L	∡	↺	
#1	6"	4"	NO	0.0	-	-	-	-	-	sample manipulator
#2	8"	6"	NO	7.75	8.00	0°	-	-	-	viewport
#3	8"	6"	NO	7.75	12.50	180°	-	-	-	LEED optics (Varian 981-0127)
#4	2-3/4"	1-3/4"	NO	7.75	2.50	180°	9.75	79°	32°	AUGER gun (Varian 981-2545)
#5	2-3/4"	1-3/4"	NO	7.75	2.50	180°	9.25	79°	340.3°	ion gun (Varian 981-2043)
#6	8"	6"	NO	7.75	8.00	252.5°	-	-	-	CMA (Varian 981-2707)
#7	2-3/4"	1-3/4"	NO	7.75	2.50	252.5°	10.0	71°	0°	ion gun/ AES gun
#8	2-3/4"	1-3/4"	NO	7.75	2.50	252.5°	10.0	61°	123.7°	ion gun/ AES gun
#9	6"	4"	NO	7.75	9.50	306.25°	-	-	-	QMS
#10	2-3/4"	1-3/4"	NO	7.75	2.50	306.25°	8.0	60°	0°	ion gun
#11	10"	8"	NO	7.75	12.50	90°	-	-	-	HREELS
#12	2-3/4"	1-3/4"	NO	7.75	2.90	90°	7.0	60°	0°	view port
#13	4-1/2"	2-1/2"	NO	16.00	7.50	0°	-	-	-	
#14	2-3/4"	1-3/4"	NO	14.00	7.50	45°	-	-	-	leak valve(1)
#15	2-3/4"	1-3/4"	NO	18.00	7.50	45°	-	-	-	leak valve(2)
#16	4-1/2"	2-1/2"	NO	16.00	7.50	90°	-	-	-	cooling system
#17	2-3/4"	1-3/4"	NO	14.00	7.50	130°	-	-	-	leak valve(3)
#18	2-3/4"	1-3/4"	NO	18.00	7.50	130°	-	-	-	heating lamp
#19	6"	4-1/2"	NO	16.00	8.00	170°	-	-	-	T.S.P.
#20	2-3/4"	1-3/4"	NO	14.00	7.50	252.5°	-	-	-	ion gauge
#21	2-3/4"	1-3/4"	NO	18.00	7.50	252.5°	-	-	-	
#22	6"	4-1/2"	NO	16.00	8.00	306.25°	-	-	-	

Table 3-2. Orientation of the ports for LEED/HREELS UHV vessel (2)

	FLG O.D.	TUBE O.D.	ROT	Z	R	θ	L	α	φ	
#23	1-1/3"	3/4"	YES	7.75	2.10	90°	6.5	75°	90°	
#24	1-1/3"	3/4"	YES	7.75	2.10	90°	6.5	75°	270°	
#25	1-1/3"	3/4"	YES	8.75	2.50	0°	5.5	50°	90°	
#26	1-1/3"	3/4"	YES	8.75	2.50	0°	5.5	50°	270°	
#27	8"	6"	NO	23.5	-	-	-	-	-	gate valve

(unit: inch)

[Definition of parameters]

Z: distance along centerline from top flange face

R: distance from centerline to flange face (on axis focus)
or, to focus (for off axis focus)

θ: rotation of R around center line

L: distance from off axis focus to flange face

α: angle between R and L

φ: rotation of L around R at fixed α. φ =0° when L and the centerline are co-planer.

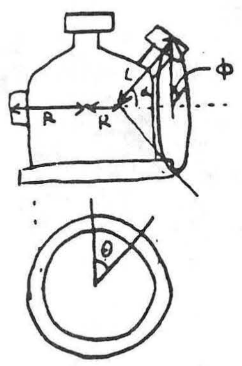

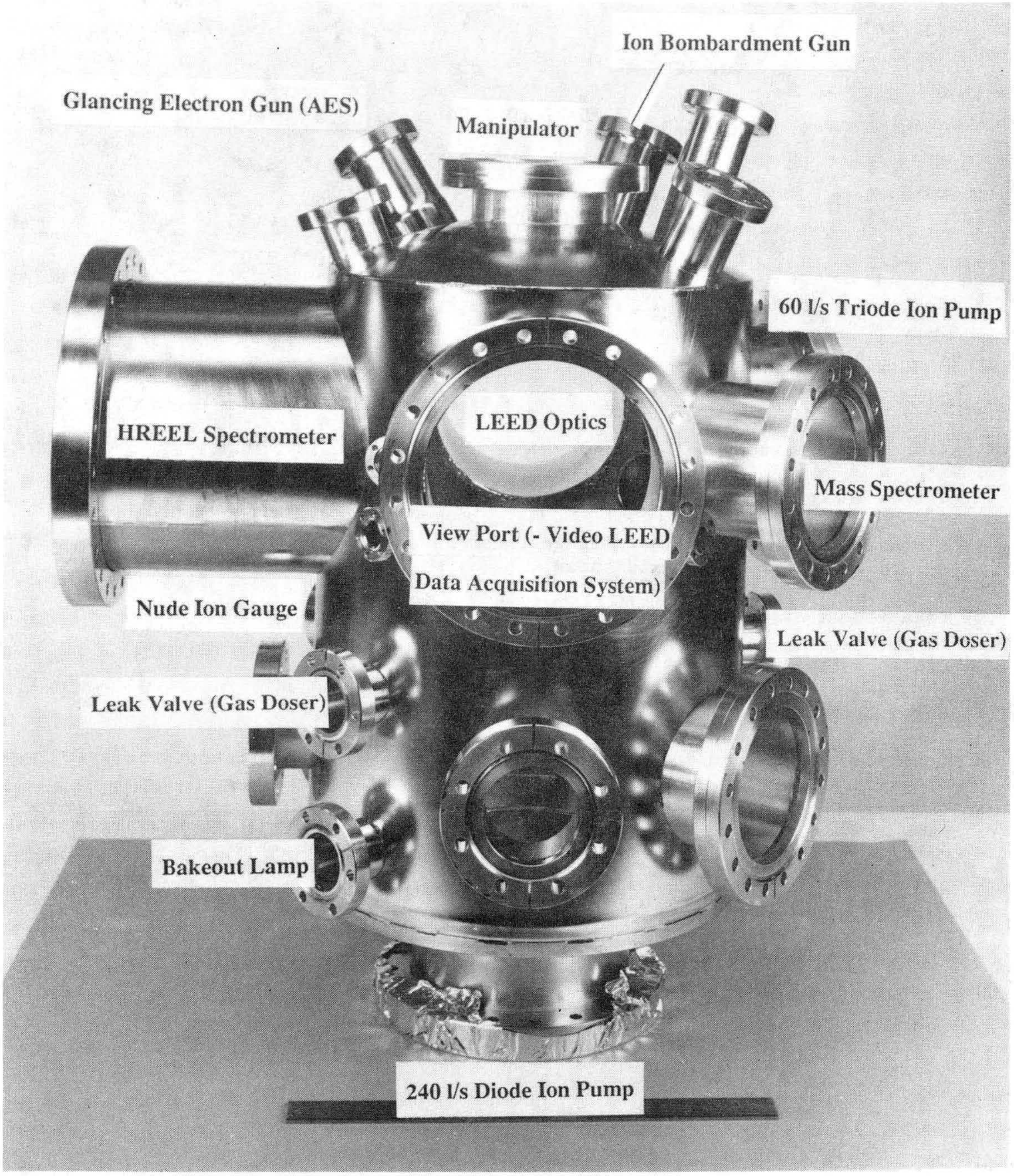

[Fig. 3-1] Photograph of UHV vessel for LEED/HREELS apparatus (side view)

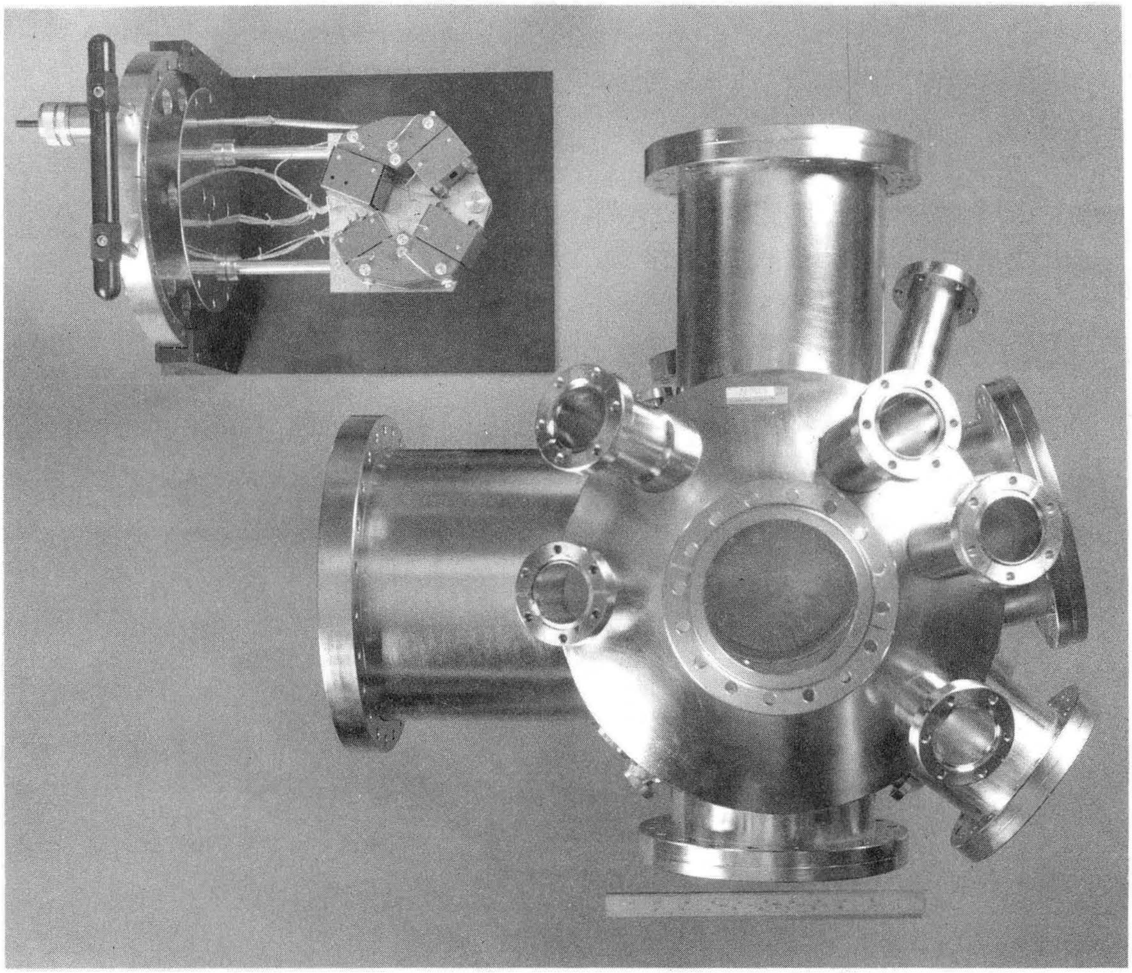

[Fig. 3-2] Photograph of UHV vessel for LEED/HREELS apparatus (top view)

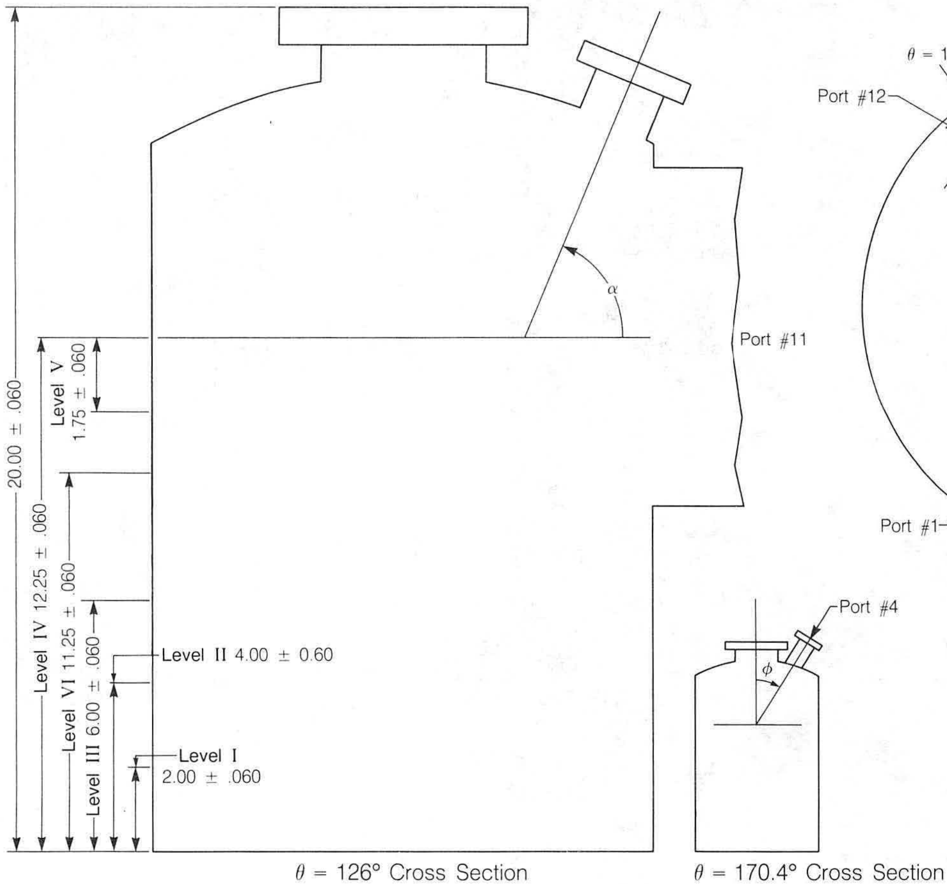

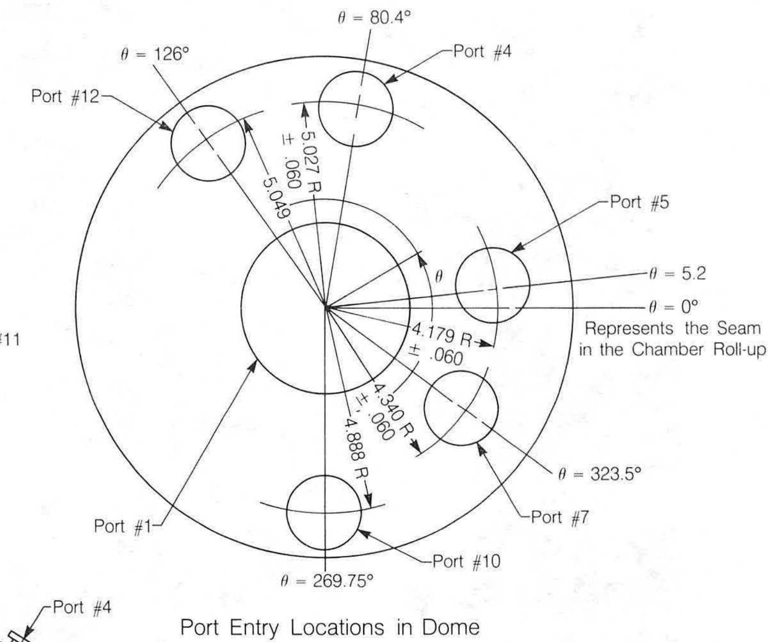

Port Entry Locations in Dome

Port No.	Angle α	Angle ϕ	Hole Size
1	90°	0°	4.00
4	79°	32°	1.75
5	79°	340.3°	1.75
7	71°	0°	1.75
10	65°	0°	1.75
12	67°	0°	1.75

XBL 883-10105

[Fig. 3-3] Design of UHV vessel for LEED/HREELS apparatus (1)

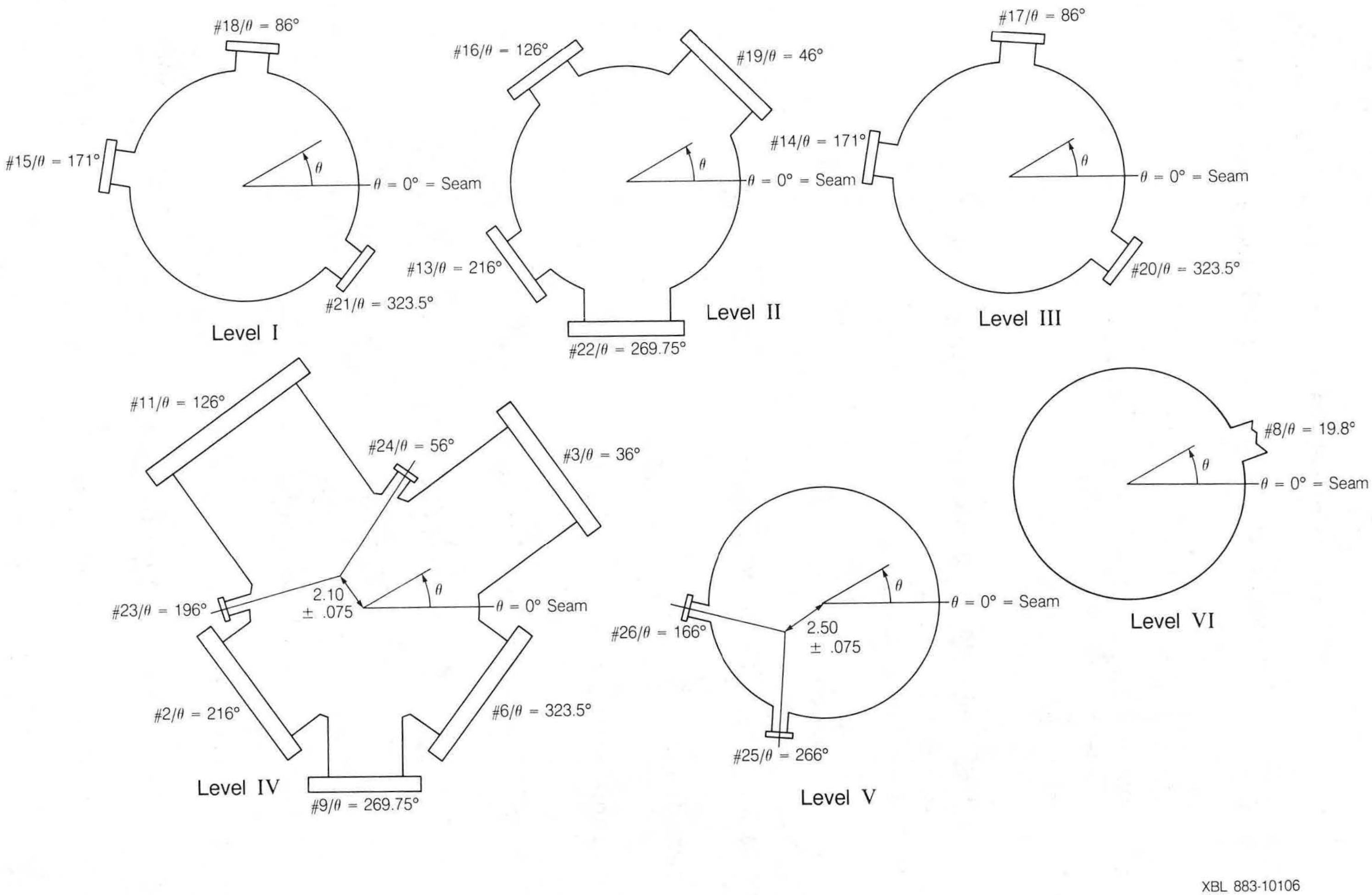

[Fig. 3-4] Design of UHV vessel for LEED/HREELS apparatus (2)

3.3. Sample Manipulator

A high precision sample manipulator is necessary for LEED crystallography, in order to precisely control the angle of incidence of the electron beam on the single crystal sample face. Our design of the sample manipulator has following capabilities.

1. The sample is mounted 2.5" away from the main shaft.
2. X, Y, and Z travel of the main shaft
3. Rotation of the sample around the main shaft (ω motion)
4. Adjusting the angle of the main shaft
5. Flip motion of the sample (θ motion)
6. Azimuthal rotation of the sample (ϕ motion)
7. Internal electron bombardment heating
8. Cooling of the sample with liquid. N_2 or liquid. H_e.
9. Sample temperature measurement with a thermocouple
10. Minimized volume of sample holder which allows easy observation of the LEED pattern

(The motion of the manipulator is defined in Fig. 3-5)

A photograph of the sample manipulator is shown in Fig. 3-6. The detailed design of the parts is shown in Fig. 3-7, Fig. 3-8, and Fig. 3-9. The complete blue prints are available. Request should be directed to:

H. Ohtani or

D. Coulomb

MCSD, Lawrence Berkeley Laboratory

Berkeley, CA 94720.

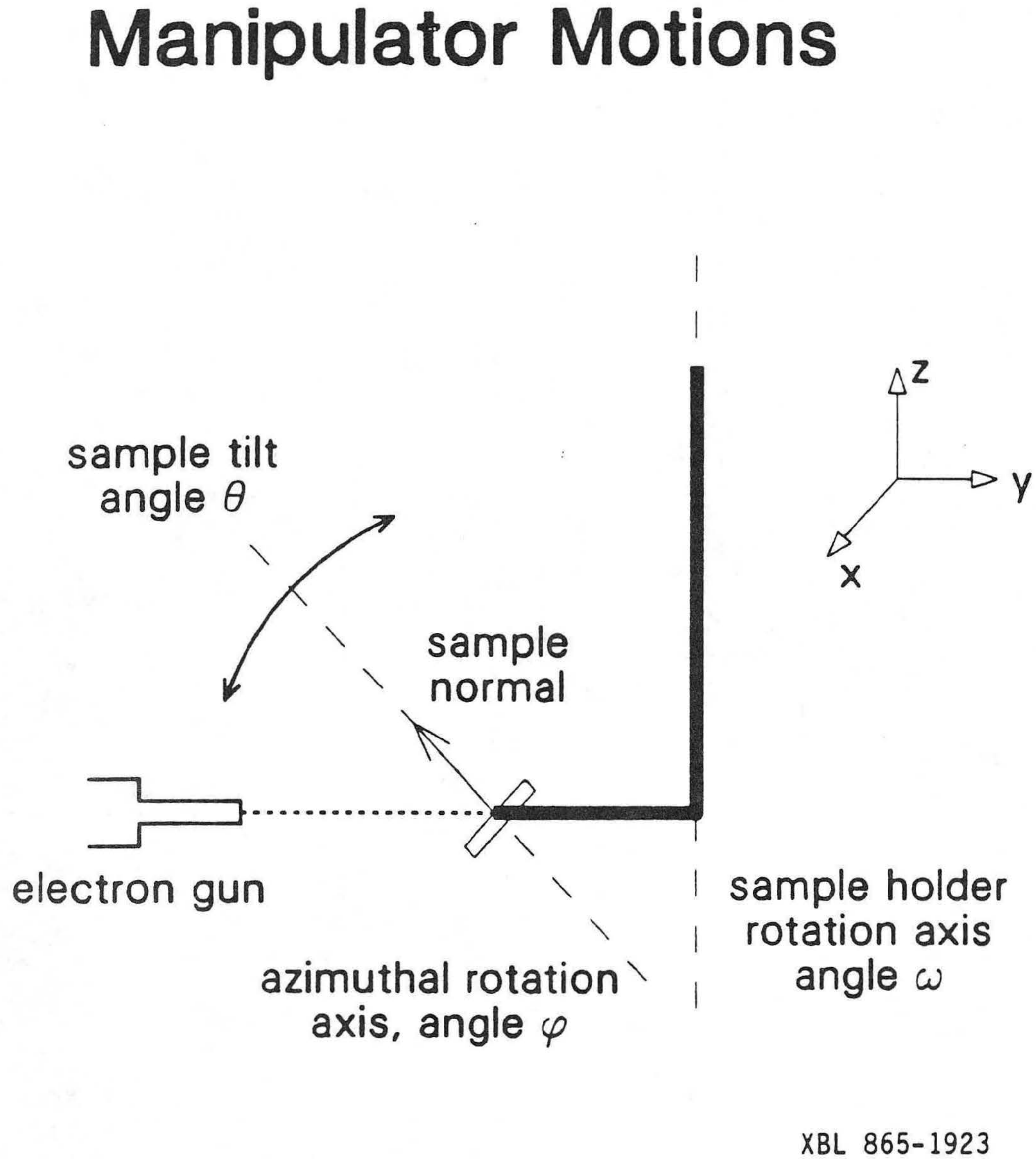

[Fig. 3-5] Manipulator motion definitions

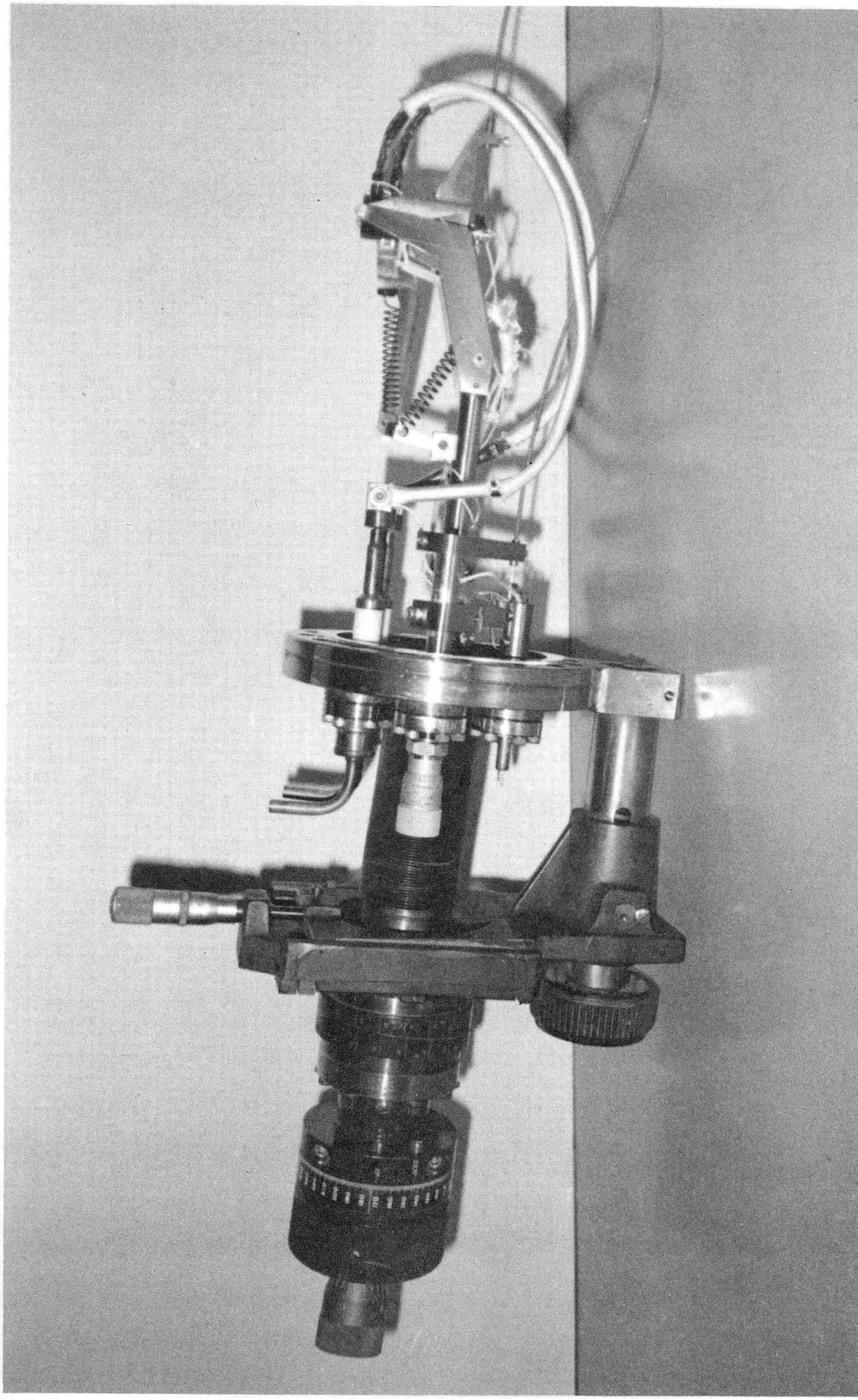

[Fig. 3-6] Photograph of high-precision manipulator for LEED and HREELS

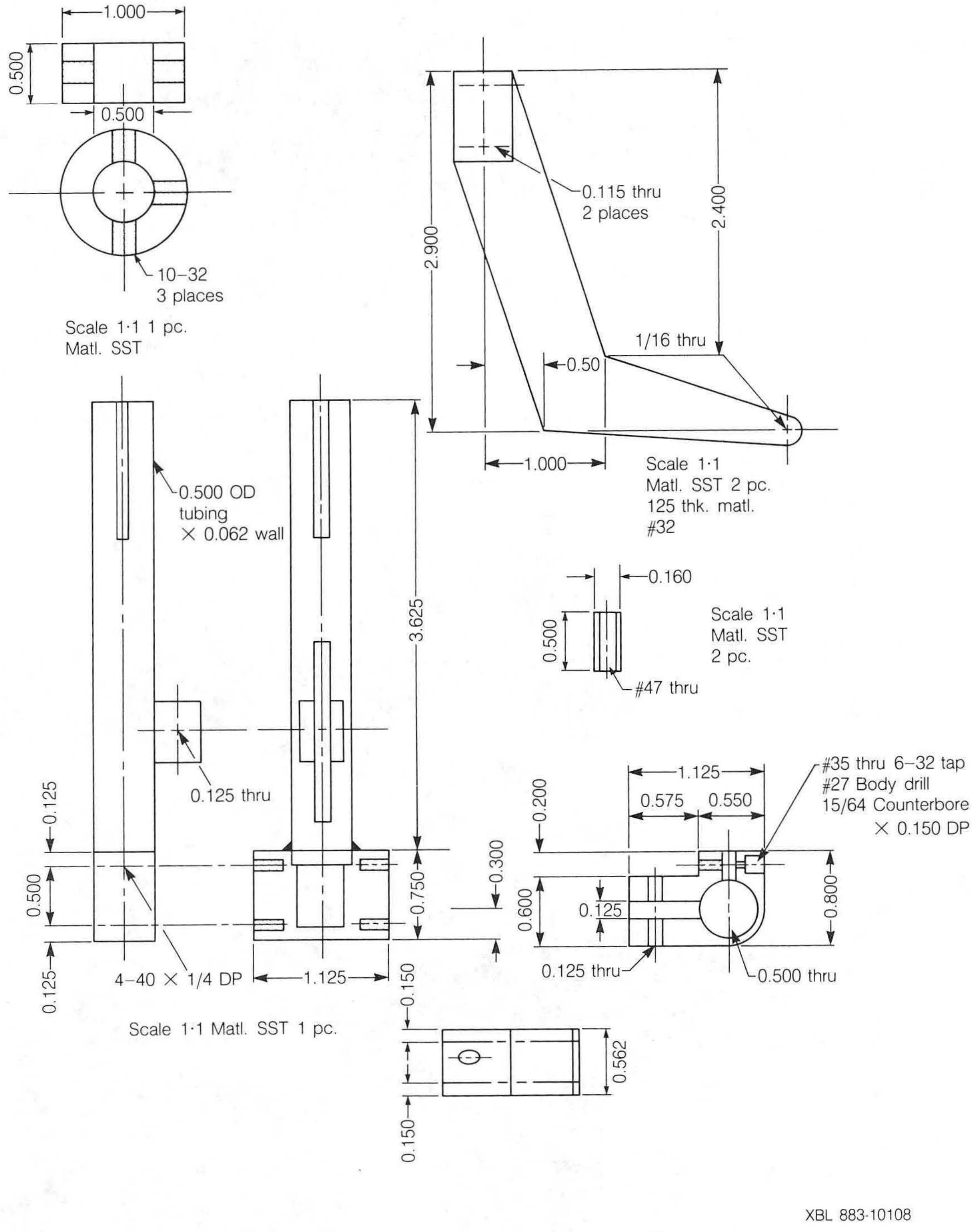

[Fig. 3-7] Parts of high-precision manipulator for LEED and HREELS (1)

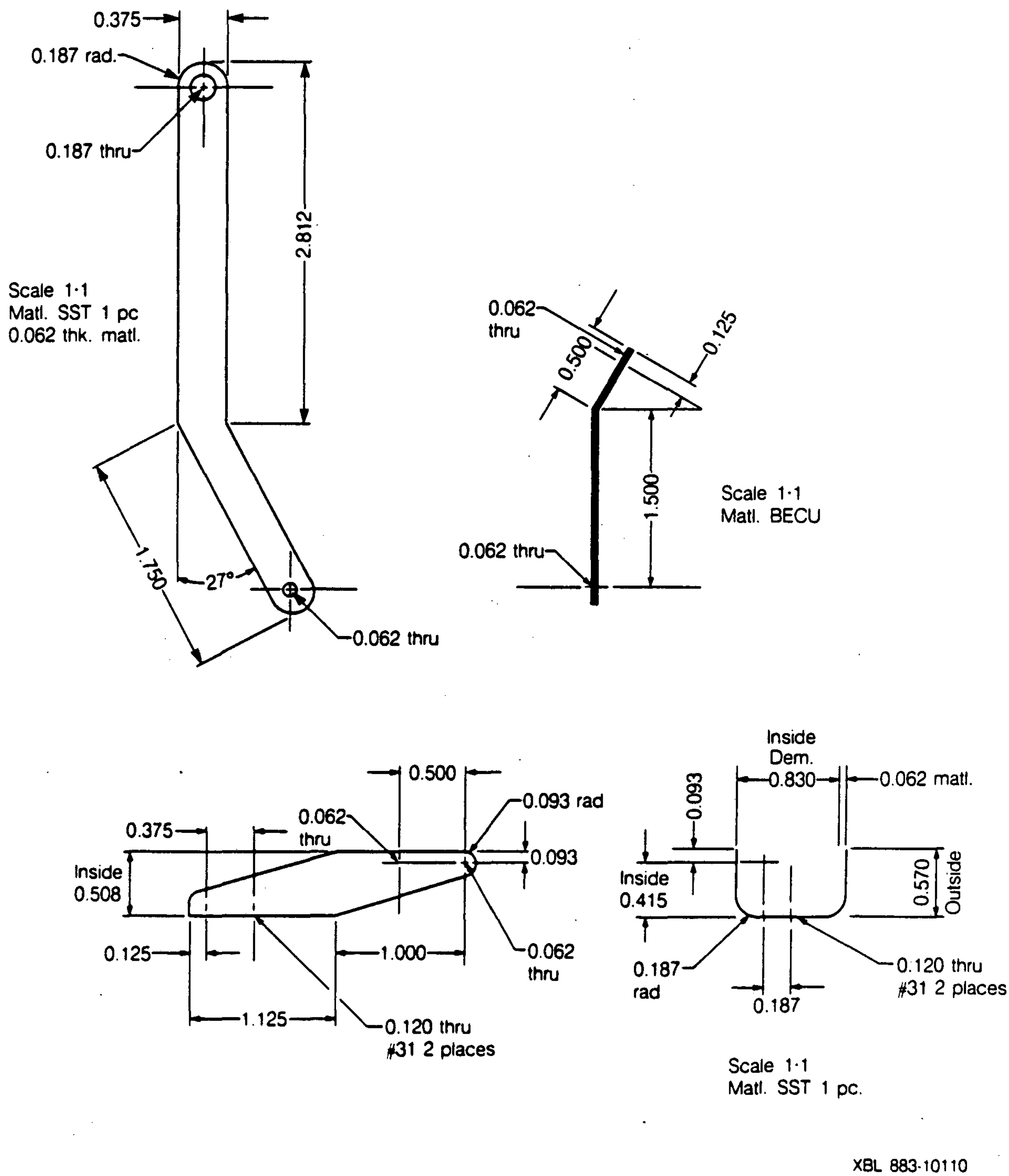

[Fig. 3-8] Parts of high-precision manipulator for LEED and HREELS (2)

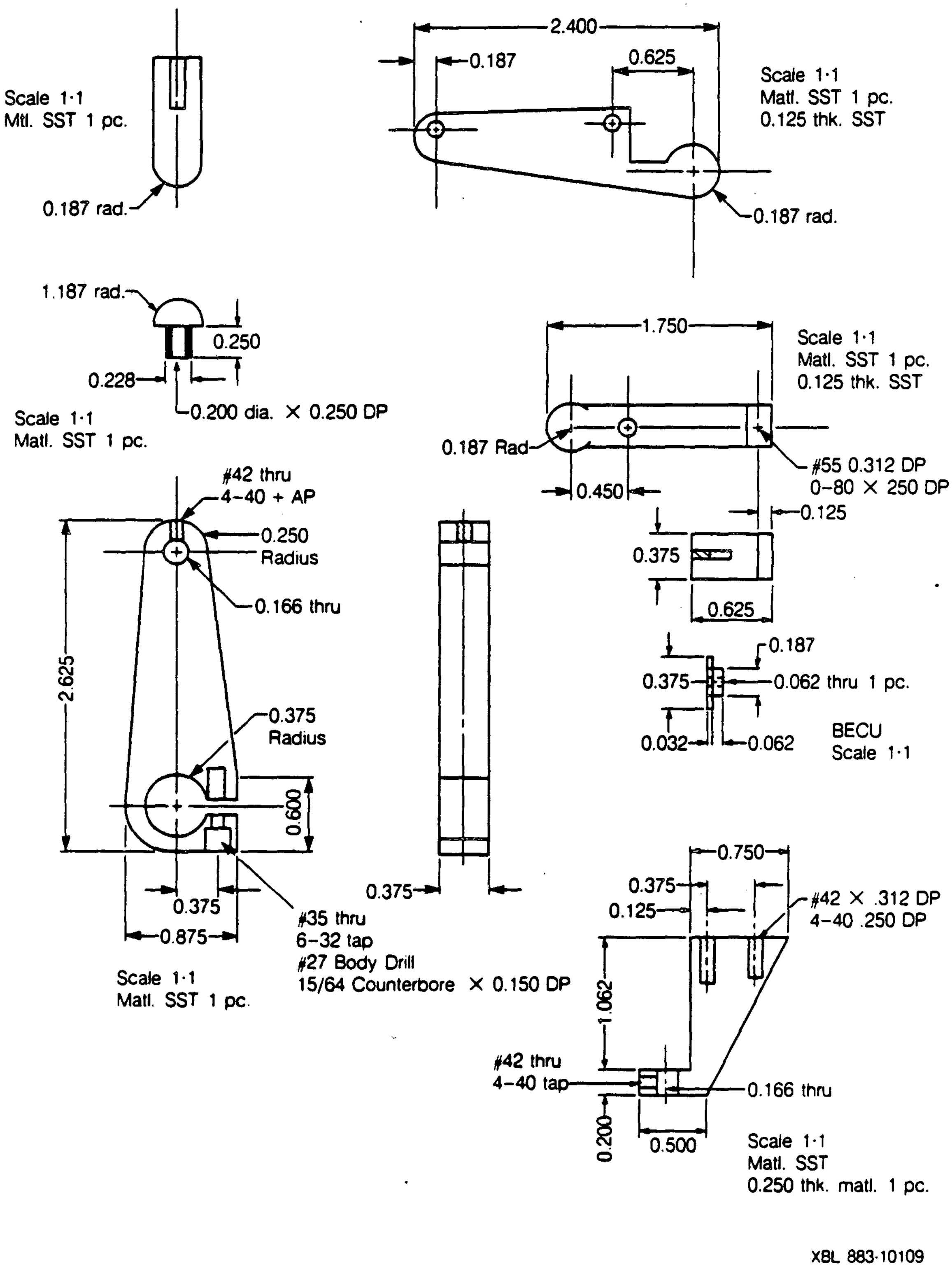

[Fig. 3-9] Parts of high-precision manipulator for LEED and HREELS (3)

The precise X,Y,Z and θ motion are obtained by using commercially available high precision XYZ translator (Varian model 981-2536). These motions are necessary to bring the crystal sample to the focal point of each surface examining apparatus. The angle of the main shaft can be adjusted using a special variable spacer (Huntington Precision Acu-Ports model VF-175-10) attached to the XYZ translator.

The mechanical design of the flip and azimuthal motions is similar to the one used previously for digital LEED apparatus.[5] **Flip motion (theta motion)** of the sample is necessary to obtain the desired angle of incidence of the electron beam on the sample for LEED I-V measurements. This motion is controlled by a lever-arm driven by the coaxial linear motion feedthrough, with a beryllium-copper spring to provide the return force.[5]

Azimuthal rotation of the sample is used to obtain a mirror plane of symmetry of the LEED pattern, which greatly simplifies LEED I-V calculations, when the electron beam is not normal to the crystal surface (off-normal measurements). The azimuthal rotation of the crystal is driven by a spring-loaded cable in a flexible sheath working against a beryllium-copper spring. The cable is 0.025" soft-temper 304 stainless steel wire and the cable sheath is a tightly coiled 0.075" diameter spring wound of 0.010" stainless steel wire. This cable can bend 360° on a 3cm radius, so it easily follows the x,y,z,θ, and ω motion of the manipulator. The desired azimuthal angle can be obtained by adjusting the cable with a micrometer-drive linear motion feed-through on the manipulator flange.

A schematic of the sample holder is shown in Fig. 3-10. A single crystal sample is spotwelded to Ta support wires or to a Ta film, and then attached to the Ta plate of the holder. The thermocouple is directly spotwelded to the sample. The filament for electron beam heating is made of 8 mil W wire. A palladium crystal of dimensions, $6mm \times 8mm \times 0.45mm$ can be heated to 600C with the filament current of 5A and the electron beam energy of 1.0keV.

The sample can also be cooled with liquid N_2 through a pair of copper braid which lead to a pair of liquid N_2 cold fingers. A sample temperature of about 120K can be obtained by this method. The sample can be also cooled with liquid He_e by simply connecting the two copper braids to a closed-cycle cryogenic refrigeration system. The detailed design of the parts of this sample holder is shown in Fig. 3-11.

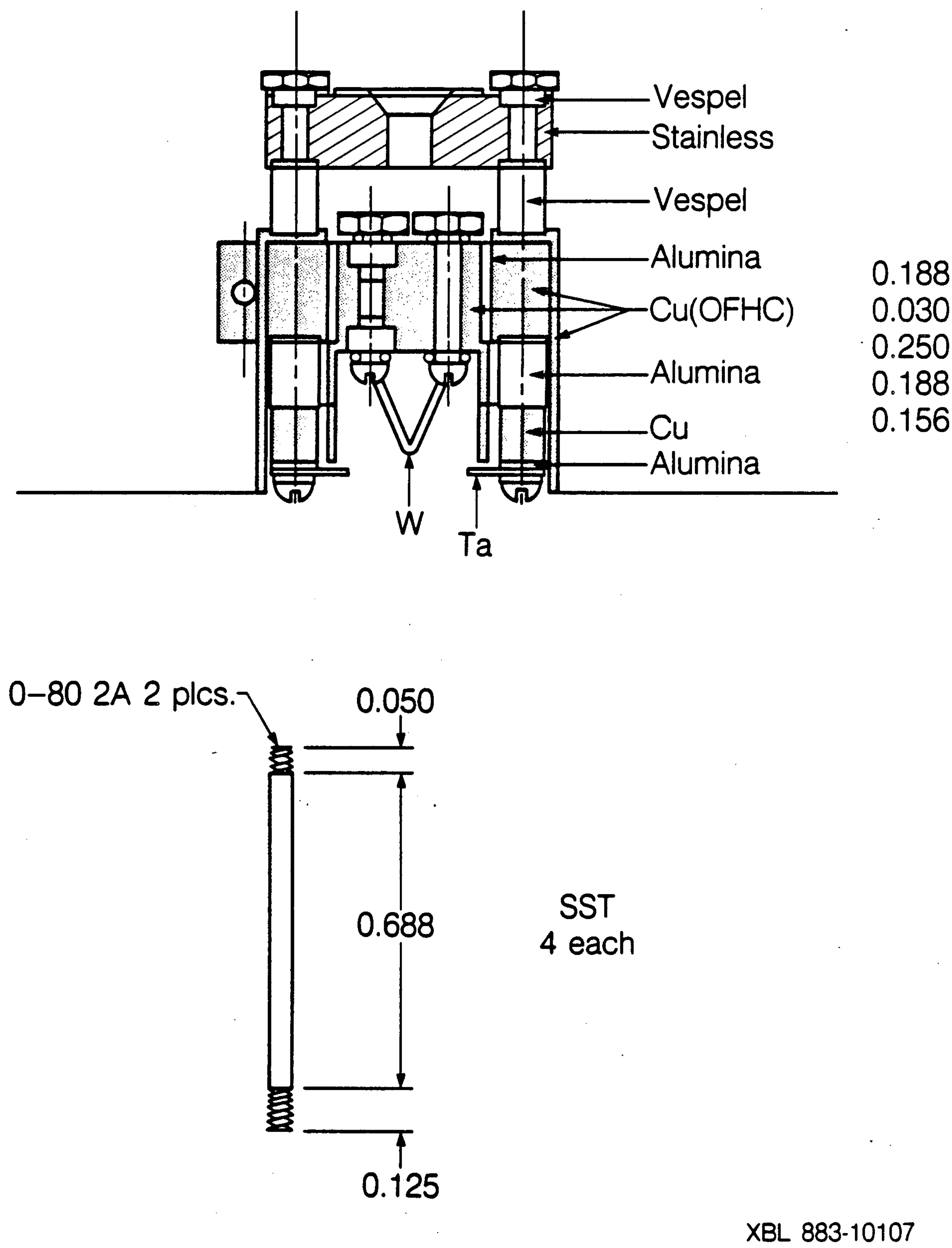

[Fig. 3-10] Schematic of sample holder

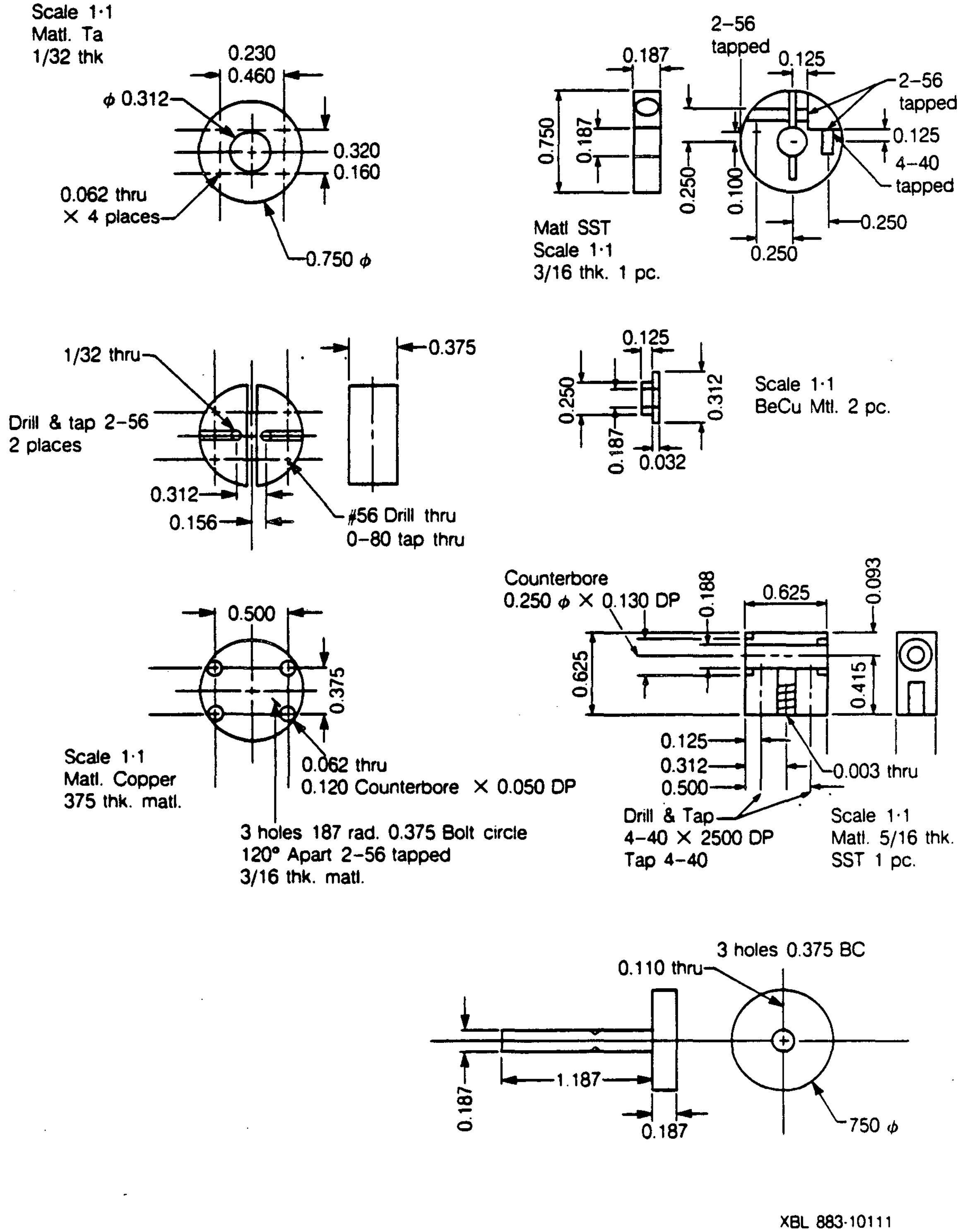

[Fig. 3-11] Parts for sample holder

References

1. J.M. MacLaren, J.B. Pendry, R.J. Rous, D.K. Saldin, G.A. Somorjai, M.A. Van Hove, and D.D. Vvedensky, in *Surface Crystallographic Information Services: A Handbook of Surface Structures*, Reidel, Dordrecht, 1987.

2. M. A. Van Hove and S. Y. Tong, *Surface Crystallography by LEED,* Springer Verlag, Berlin, 1979.

3. L. H. Dubois, *PhD Thesis*, Chemistry Department, University of California at Berkeley, 1980.

4. H. Ibach and D. L. Mills, *Electron Energy Loss Spectroscopy and Surface Vibrations,* Academic Press, New York, 1982.

5. D. F. Ogletree, *PhD Thesis*, Physics Department, University of California at Berkeley, 1986.

4. LEED Intensity Analysis of the Surface Structure of Pd(111)

4.1. Introduction

We report here a detailed dynamical LEED analysis of the clean Pd(111) surface.* This analysis is of value in various structural determinations involving a series of molecules adsorbed on this substrate, starting with the CO structure described in Chapter 5. The structure of clean Pd(111) has already been studied by LEED intensity analysis[1,2] and High-Energy Ion Scattering (HEIS).[3,4] All these studies have yielded the ideal structure of the truncated bulk. To our knowledge, however, no detailed structure determination to explore the surface relaxation has been performed on this surface.

4.2. Experiment

4.2.1. Experimental Apparatus

Experiments were performed in an ion-pumped, stainless steel UHV system, equipped with a quadrupole mass spectrometer, an ion bombardment gun, and a four-grid LEED optics. An off-axis electron gun, and the LEED optics were used

* Some part of this chapter has been published in the following journal:
H. Ohtani, M. A. Van Hove, and G. A. Somorjai, Surface Science, **187**, 372 (1987).

for Auger electron spectroscopy. We used a palladium crystal of dimension, 6mm x 8 mm x 0.45 mm, spot-welded to tantalum support wires. The crystal could be cooled to ~ 140 K by conduction from a pair of liquid nitrogen cold fingers or heated resistively to ~ 1500 K. Temperatures were measured by a 0.005" chromel-alumel thermocouple spot-welded to one edge of the palladium crystal. The system base pressure was in the 10^{-10} torr range. H_2 and CO were the main components of the residual gas.

The LEED optics and vacuum chamber were enclosed by two sets of Helmholtz coils to minimize the magnetic field near the crystal. These coils were adjusted until there was no significant deflection of the specularly-reflected beam over the 20 to 300 eV energy range used for LEED intensity vs. energy (I-V) measurements. There were no exposed insulators or ungrounded conductors in the vicinity of the crystal in order to minimize electrostatic fields. The LEED electron gun was operated in the space-charge limited mode, so that the beam current increased monotonically and approximately linearly over the voltage range used. At 200 eV the beam current was ~ 4.0μ-amps. The intensity-energy curves were normalized with respect to incident beam current. The crystal was mounted on a manipulator capable of independent azimuthal and co-latitude rotations. The crystal surface was oriented with the (111) face perpendicular to the azimuthal rotation axis as determined by visual comparison of the intensities of symmetry related substrate beams. It is possible to see deviations from normal incidence of less than 0.2° with this method. The accuracy of the orientation was confirmed by the close agreement of I-V curves for symmetry-related beams. The off-normal incidence angles were set by rotating the crystal away from the experimentally determined normal-incidence position using a scale inscribed on the manipulator.

LEED data were collected using a high-sensitivity vidicon TV camera with a f/.85 lens. The data were recorded on video tapes, and the diffraction patterns were analyzed using a real-time video digitizer interfaced to an LSI-11 microcomputer.[5] Sixteen consecutive video frames at constant energy were summed to improve the signal/noise ratio, and an image recorded at zero beam voltage was subtracted to correct for the camera dark current and stray light from the LEED screen or filament. After such analysis at each energy, I-V curves were generated by a data reduction program that locates diffraction spots in the digitized image, integrates the spot intensity, and makes local background corrections.[6]

4.2.2. Sample Preparation

The major impurities in the Pd(111) crystals were sulfur and carbon. These were removed by several cycles of oxidation ($P_{O2} = 5\times10^{-7}$torr, 400C) and 500 eV argon ion bombardment ($P_{Ar} = 5\times10^{-5}$torr, both at room temperature and at 600C) followed by annealing at 500C. Right before the experiment, the crystal was flashed to 600C to desorb adsorbed CO and H originating from the background gas in the UHV chamber and to remove any residual carbon by diffusion into the bulk.[7] The surface cleanliness was checked by AES [Fig 4-1]. The clean

Pd(111) surface showed a sharp (1x1) LEED pattern with very low background intensity [Fig 4-2]. Once the cleaning procedure was established, we no longer took Auger spectra before the LEED experiments so as to avoid possible contamination due to the electron-beam decomposition of residual gas on the surface.

4.2.3. I-V Curve Measurement

The I-V data were collected at normal incidence and with the incident electron beam rotated 5° from normal incidence toward both the $[1, 1, \bar{2}]$ and $[\bar{1}, \bar{1}, 2]$ directions, which can be labeled $(\theta, \phi) = (5°, 0°)$ and $(5°, 180°)$, respectively; these directions of tilt maintain one mirror plane of symmetry. The energy range used was 20-300eV. The normal-incidence data set has 5 independent beams over a cumulative energy range of 700eV. [Fig. 4-3] The (5°, 0°) and (5°, 180°) data sets have 11 and 10 independent beams respectively, and each has a cumulative energy range of 1300eV. [Fig. 4-4, 4-5] The final I-V curves were obtained by averaging symmetrically equivalent beams.

Comparison with theory was limited to energies below 200 eV. It covered cumulative energy ranges of 330 eV, 590 eV, and 630 eV for the data at $(\theta, \phi) =$ (0°, 0°), (5°, 0°), and (5°, 180°), respectively.

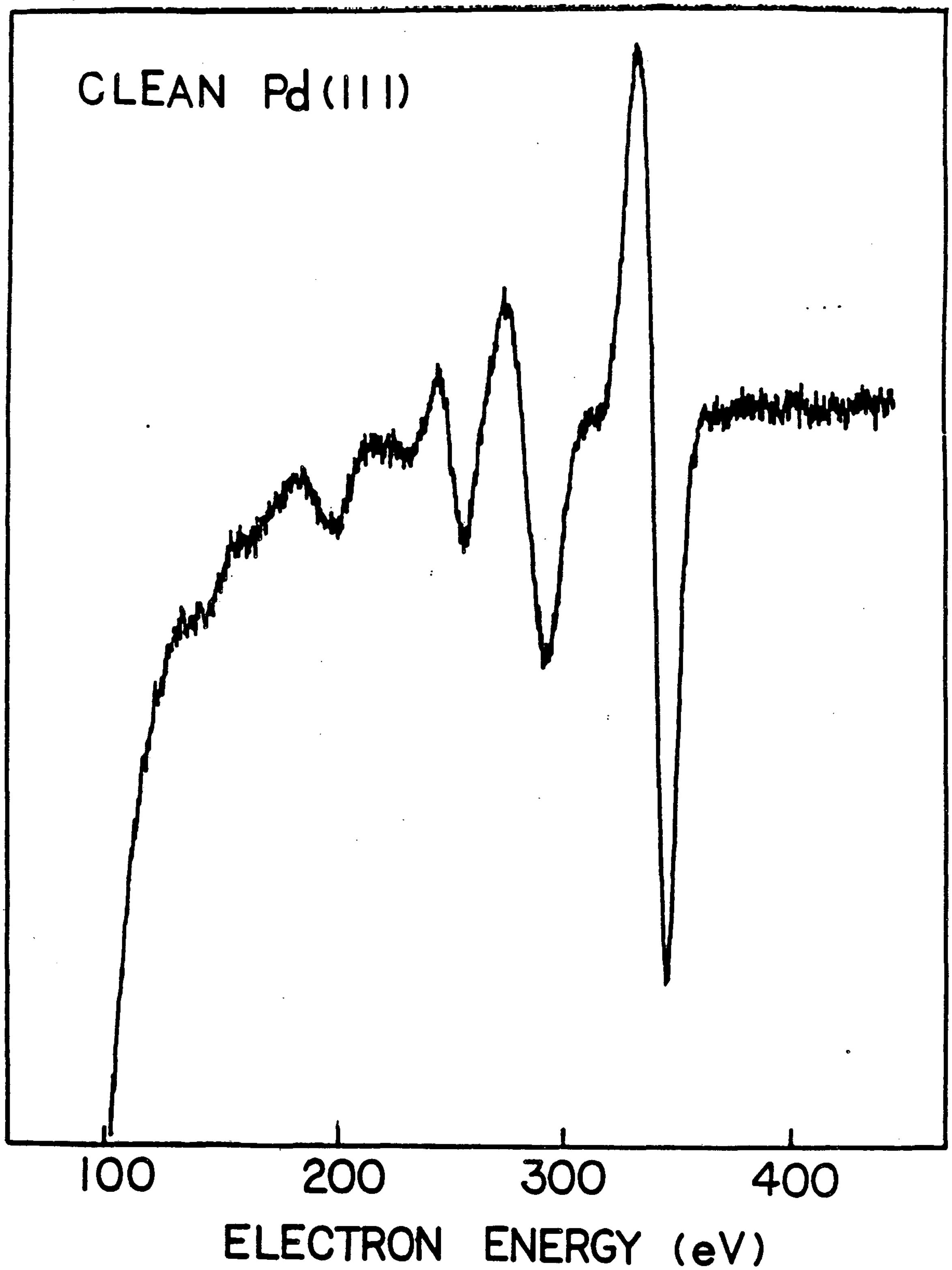

[Fig. 4-1] An Auger spectrum of the clean Pd(111) crystal surface. XBL 888-2883

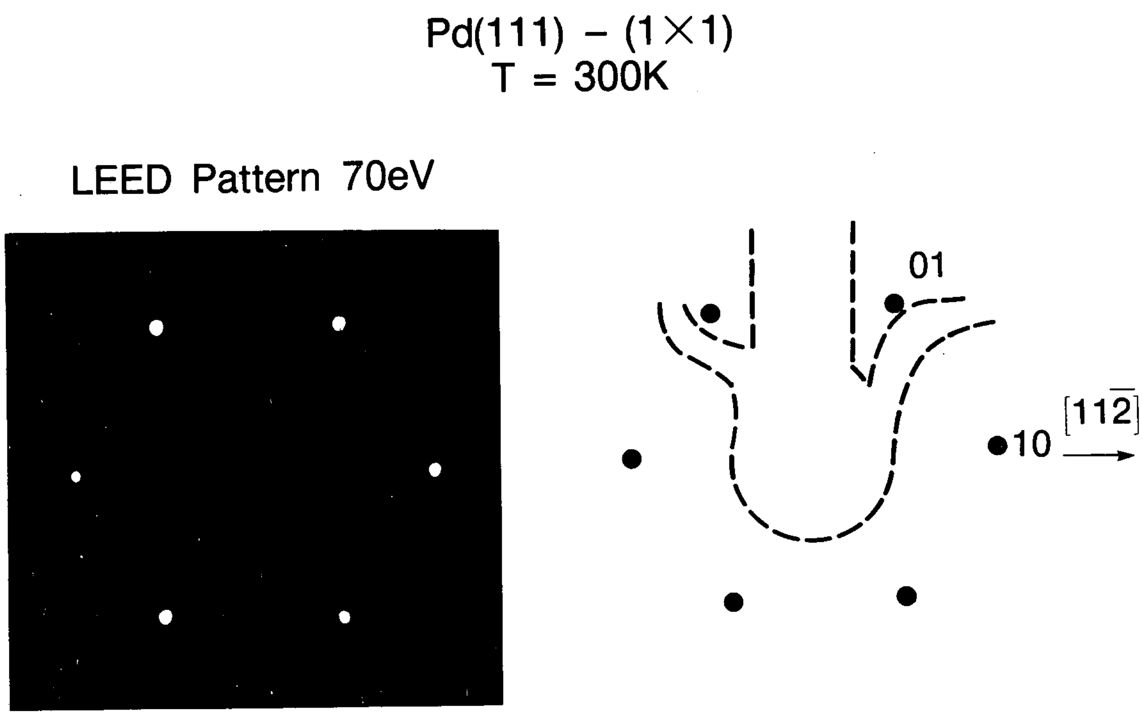

[Fig. 4-2] A photograph of the LEED pattern of the clean Pd(111) crystal surface. The incident electron energy is 70eV. Near-normal incidence is used.

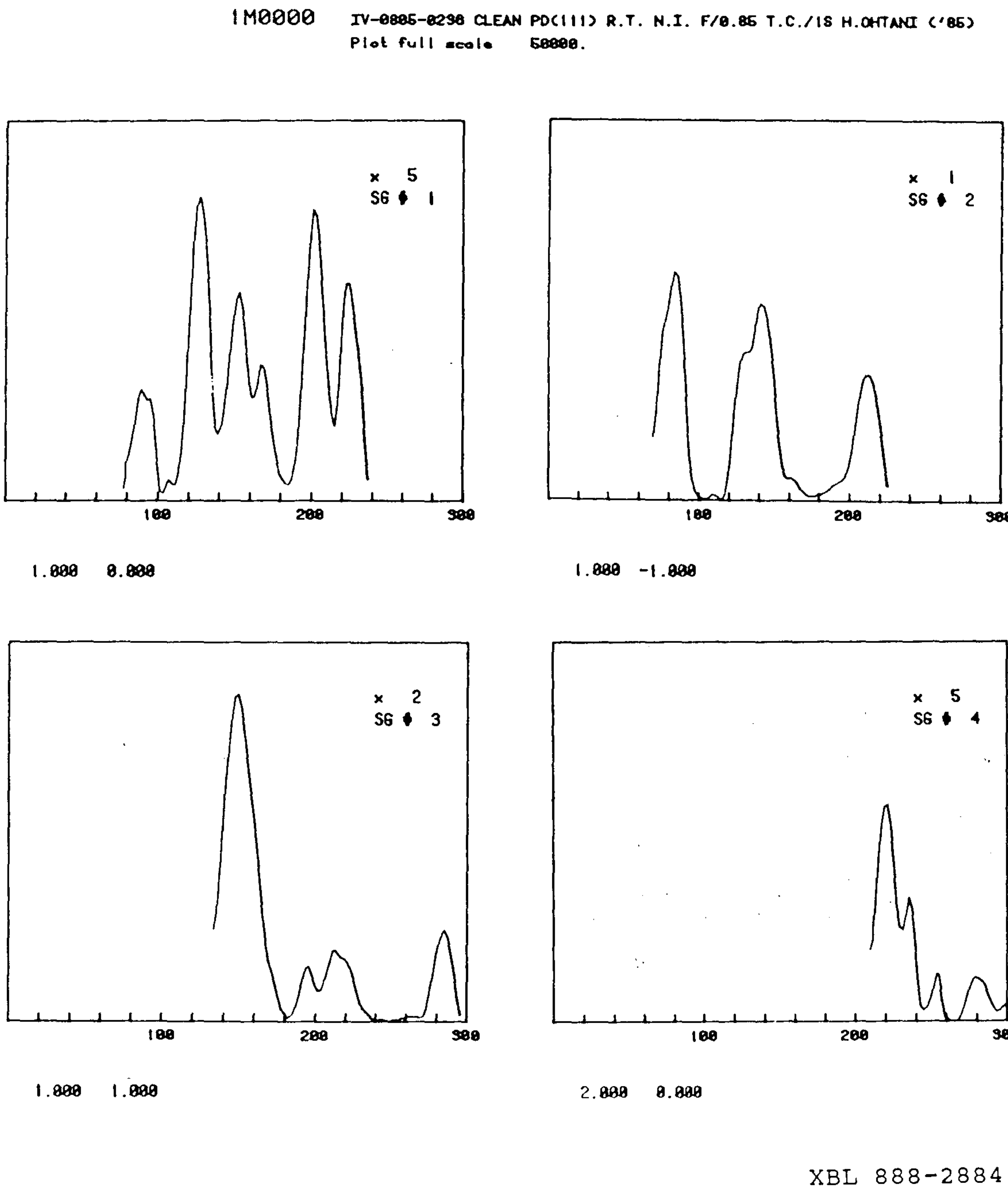

[Fig. 4-3] Experimental LEED I-V curves for clean Pd(111), recorded at 300K. $(\theta, \phi) = (0°, 0°)$.

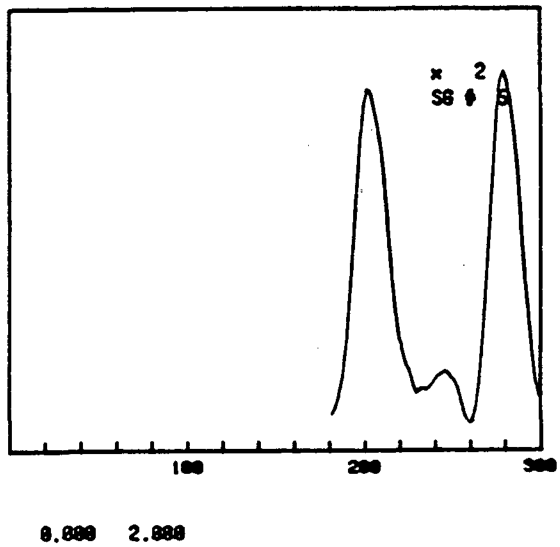

[Fig. 4-3] (continued)

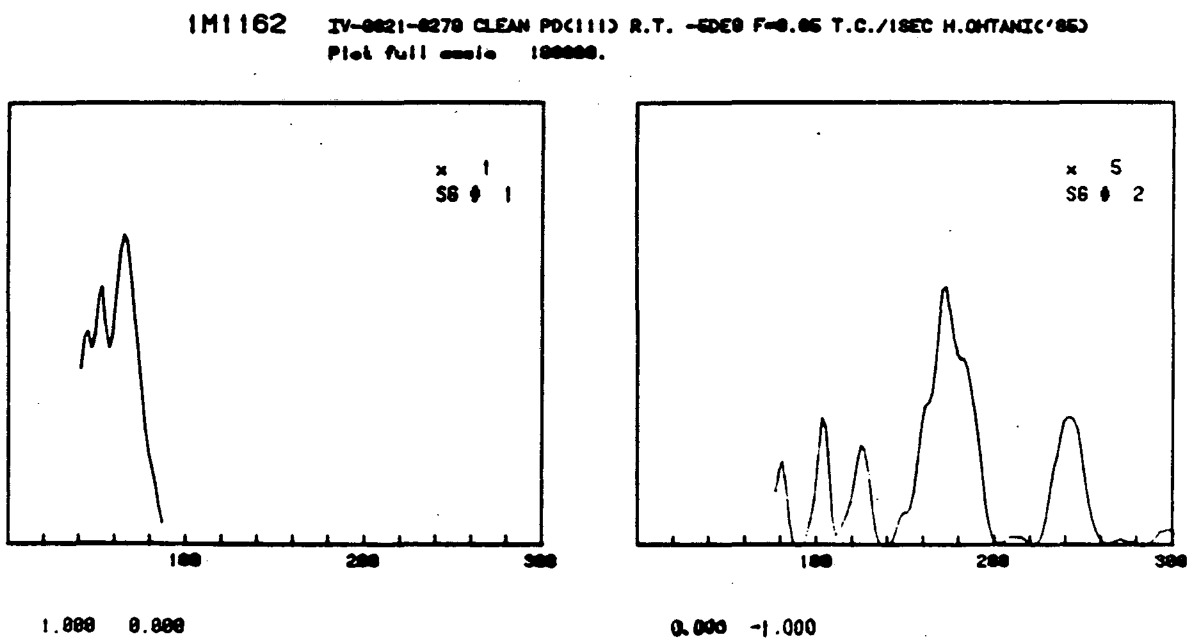

XBL 888-2885

[Fig. 4-4] Experimental LEED I-V curves for clean Pd(111), recorded at 300K. $(\theta, \phi) = (5°, 180°)$.

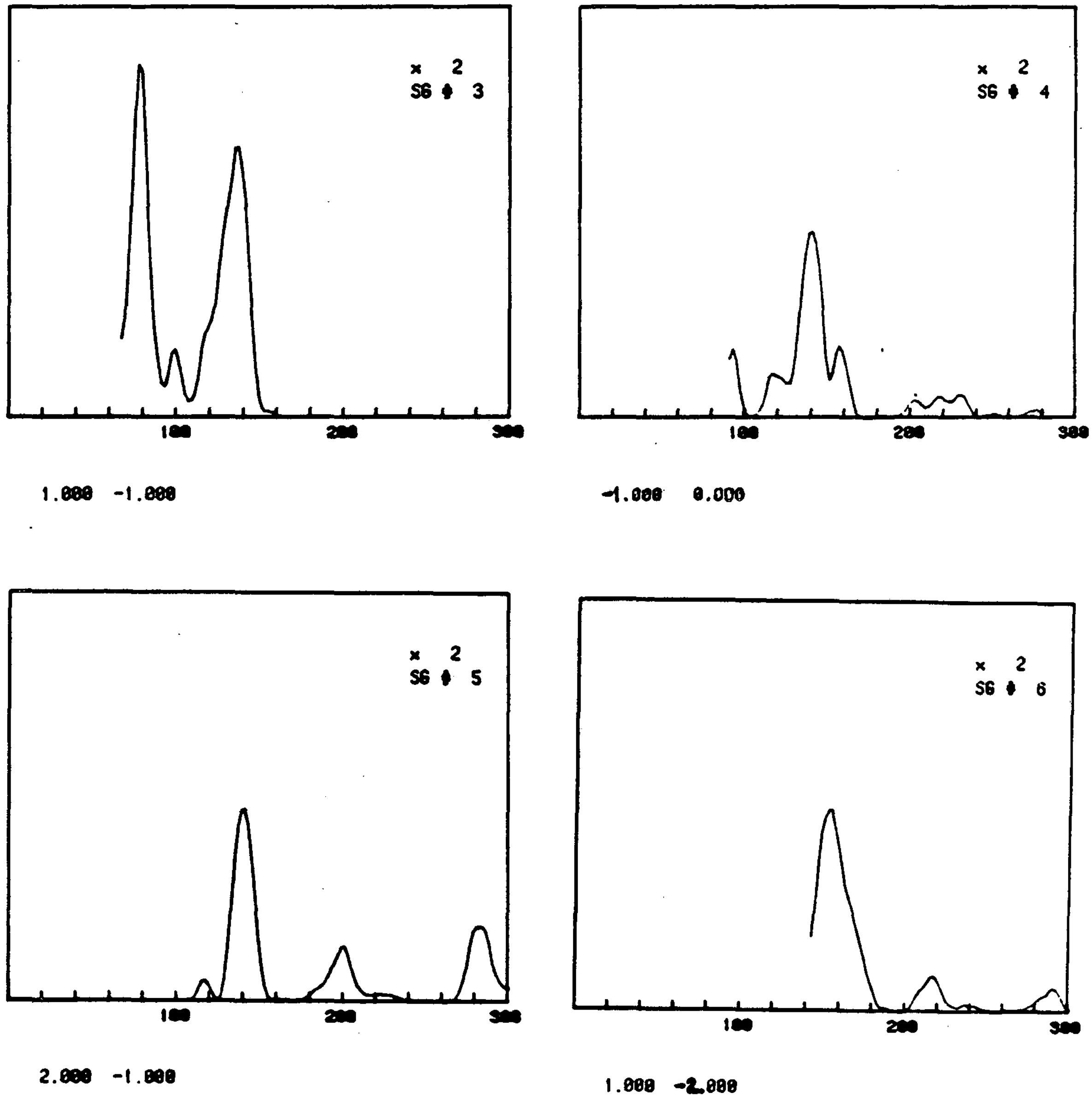

XBL 888-2886

[Fig. 4-4] (continued)

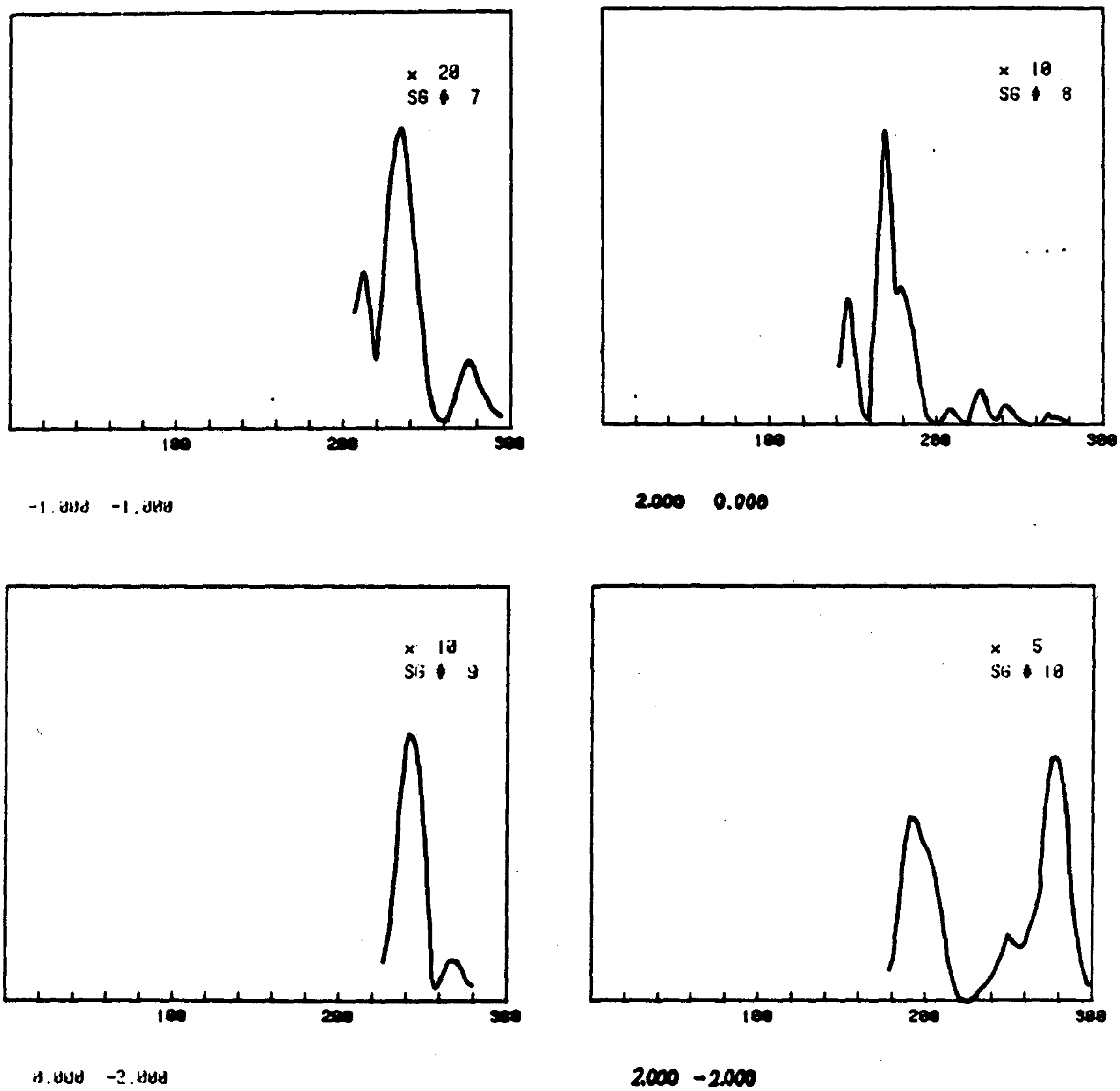

XBL 888-2887

[Fig. 4-4] (continued)

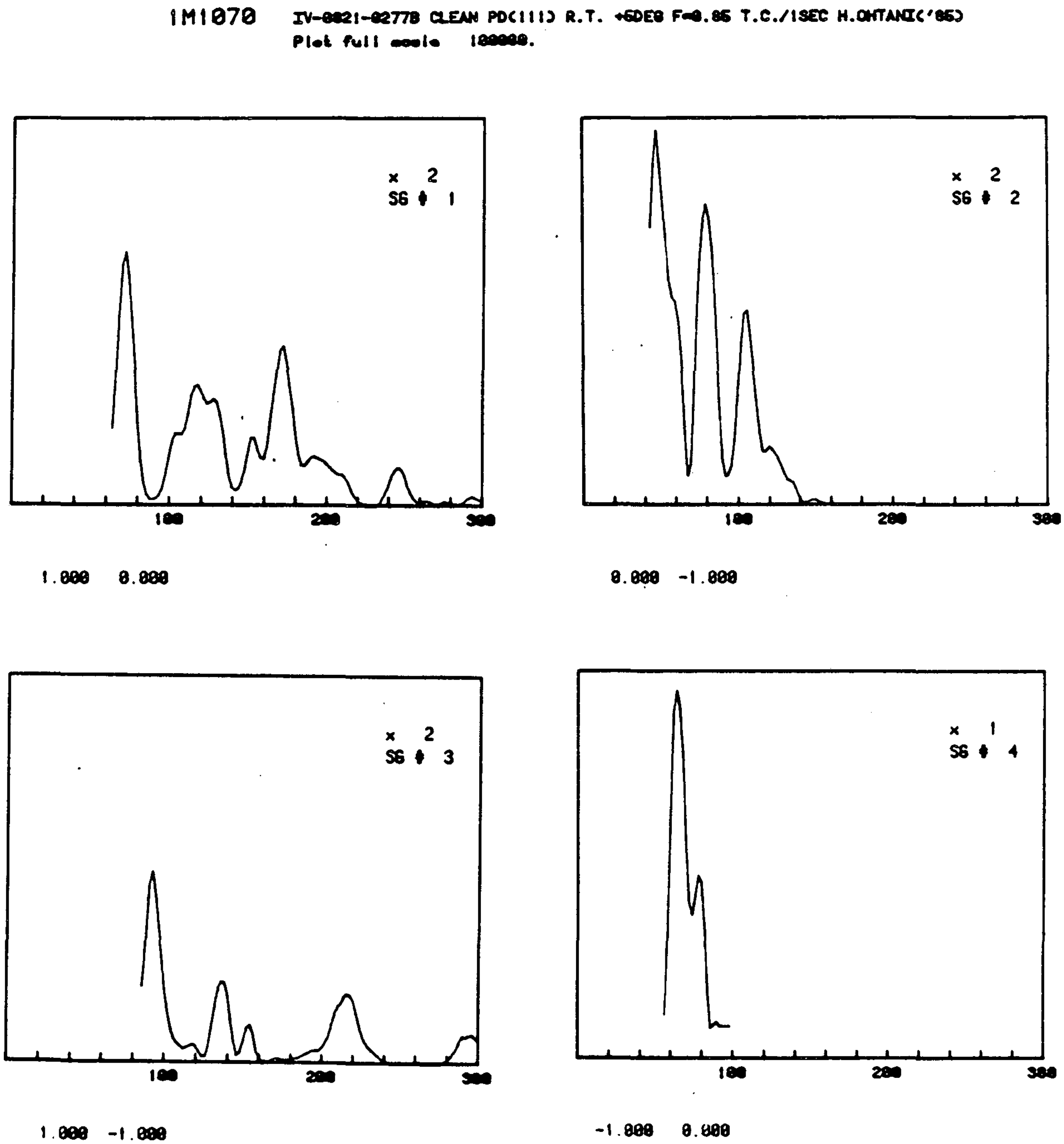

XBL 888-2888

[Fig. 4-5] Experimental LEED I-V curves for clean Pd(111), recorded at 300K. $(\theta, \phi) = (5°, 0°)$.

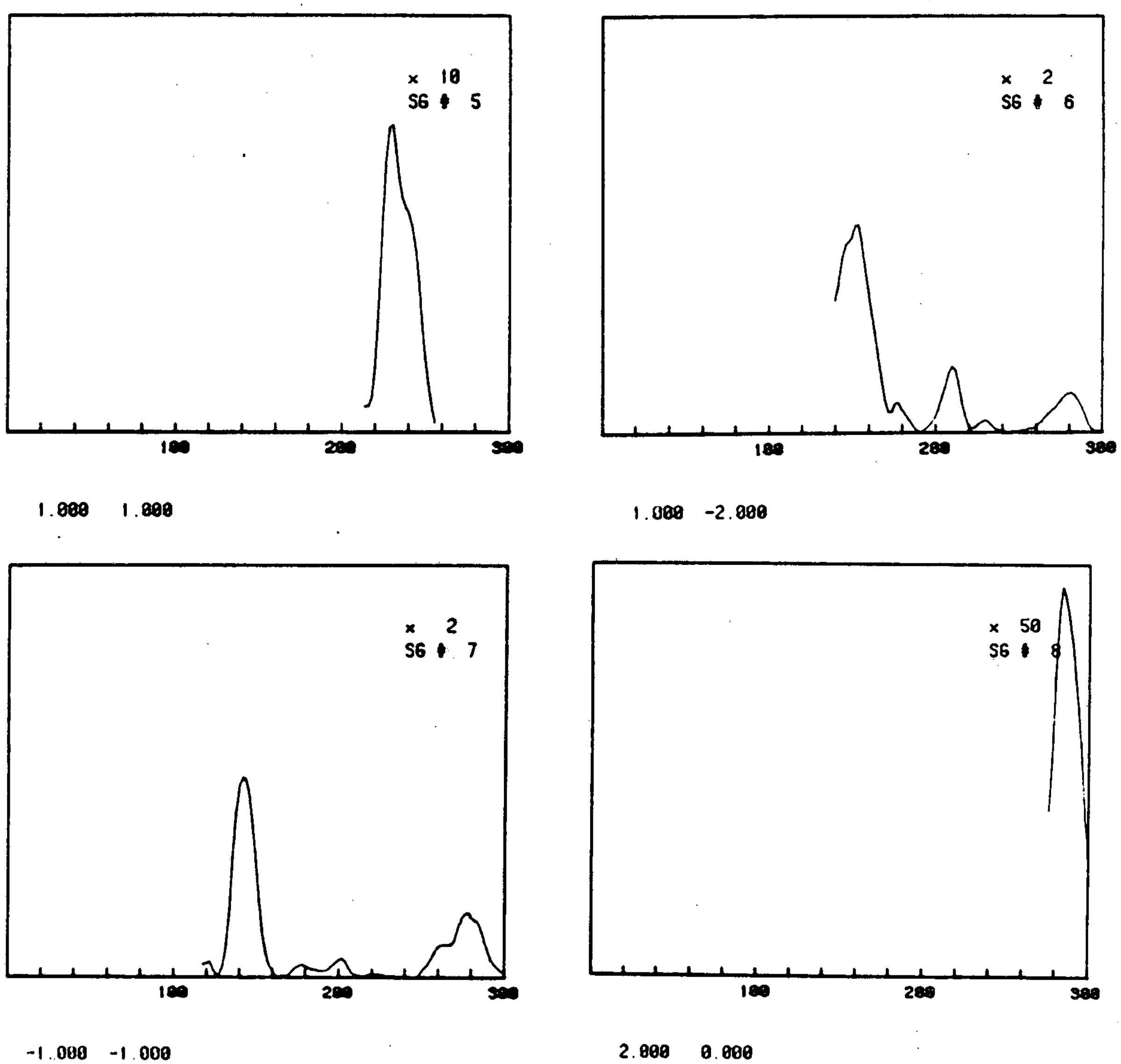

XBL 888-2889

[Fig. 4-5] (continued)

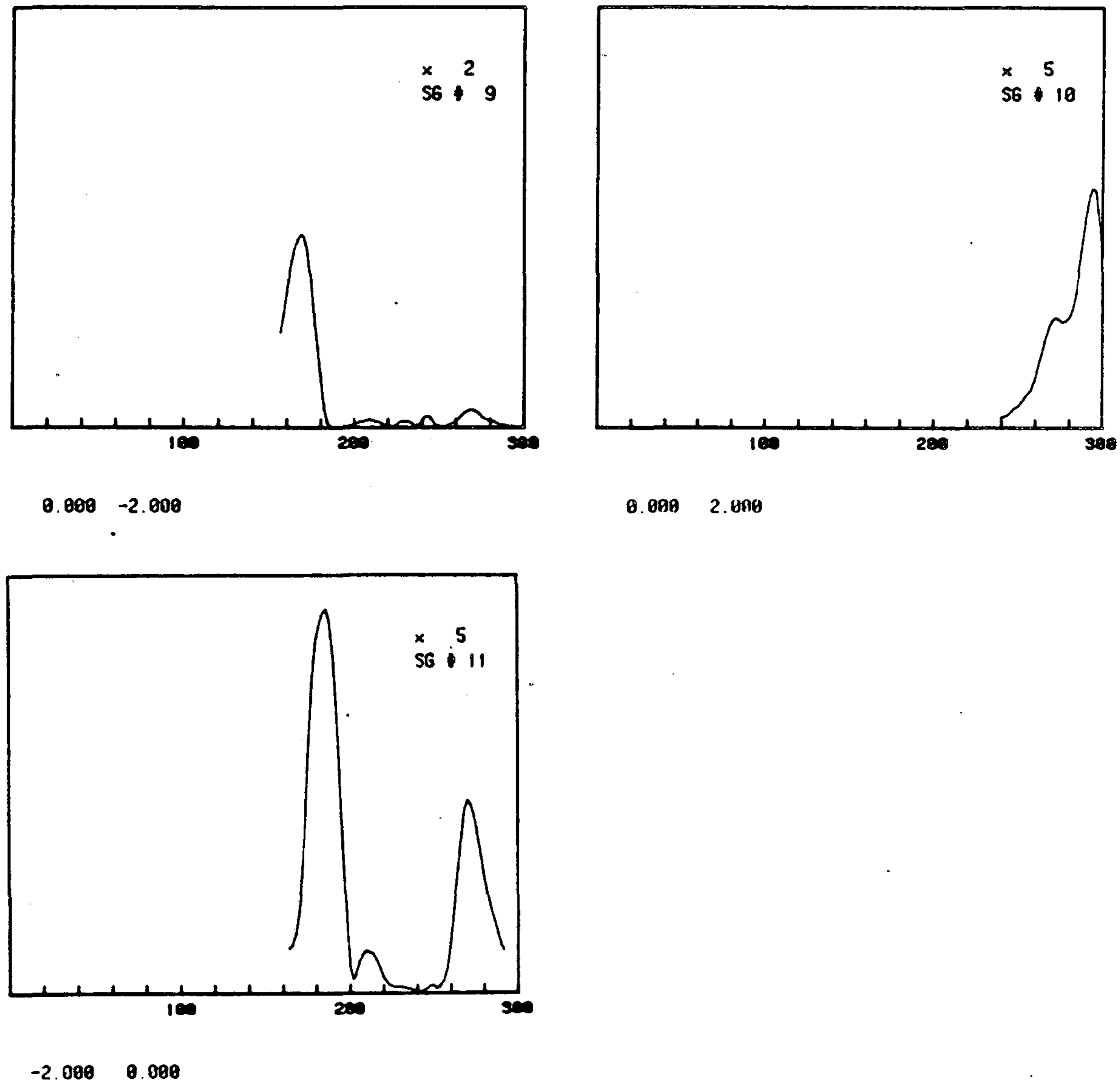

XBL 888-2890

[Fig. 4-5] (continued)

4.3. Theory

We have chosen established multiple-scattering methods to calculate LEED intensities.[8] For most trial structures Renormalized Forward Scattering was used to stack the metal layers.

The phase shifts describing the electron scattering by palladium atoms were obtained from a band-structure potential,[9] used previously for LEED studies of Pd(100) and CO on Pd(100).[10,11] The spherical-wave expansion was cut off at $l_{max}=7$. The imaginary part of the muffin-tin potential was held constant at 5eV. The metal Debye temperature was uniformly chosen as the bulk value (270K), divided by 1.2 to represent enhanced surface vibrations.

For the comparison between experiment and theory, a set of five R-factor formulas and their average was used, as described previously and used by us in many prior LEED analyses.[12,13,14]

4.4. Analysis and Results

In an initial analysis of the clean Pd(111) surface structure, we allowed the topmost layer spacing d_{12} to relax. We found it to expand by about 0.05Å using both the normal and the off-normal incidence data. This unexpected behavior prompted us to investigate a multilayer relaxation. To that end we allowed the two top spacings d_{12} and d_{23} to relax independently of each other and independently of the deeper spacings, which were all varied together ($d_{34}=d_{45}=$ ...). At our LEED energies, very little sensitivity to d_{45} and deeper spacings exists. The ranges of variation were as follows, where we refer the changes Δd_{mn} to the bulk value 2.2462Å, and use positive values for expansions:

$$-0.05 \leq \Delta d_{12} \leq 0.10Å \textit{ in steps of } 0.05Å$$

$$-0.20 \leq \Delta d_{23} \leq 0.10Å \textit{ in steps of } 0.05Å$$

$$0.0 \leq \Delta d_{34} = \Delta d_{45} = \Delta d_{56} = \cdots \leq 0.10Å \textit{ in steps of } 0.05Å$$

The comparison between the experimental and theoretical I-V curves is shown in Fig. 4-6 (normal incidence data) and in Fig. 4-7 (off-normal incidence data). In both cases, a slight expansion of the topmost layer-spacing improved the R-factor value as shown in Table 4-1. An R-factor contour plot for normal incidence data is presented in Fig. 4-8. Besides changes in interlayer spacing, we also investigated possible changes in layer stacking at the clean surface, allowing the stacking to change from face-center cubic (fcc) to hexagonal close-packed (hcp): (A) ideal fcc crystal structure in the surface region (ABCABC...stacking); (B) ideal hcp structure in the surface region (ABABA...stacking); (C) fcc monolayer on hcp structure (ABCBCB...stacking); and (D) hcp monolayer on fcc structure(ABACBAC...stacking).

We have found that the ideal fcc stacking sequence (A) is favored and that the optimal interlayer spacings are: Δd_{12}= +0.03±0.03Å, Δd_{23}= −0.03± 0.03Å, and Δd_{34}= Δd_{45} = +0.05±0.03 Å. The optimum muffin-tin zero level was V_0= 8.0±0.5 eV below vacuum. This structure yields a five-R-factor average of R=0.12 (using the normal-incidence data only, since the final optimization was not performed with off-normal data); the corresponding Zanazzi-Jona and Pendry R-factor values are approximately 0.09 and 0.22, respectively.

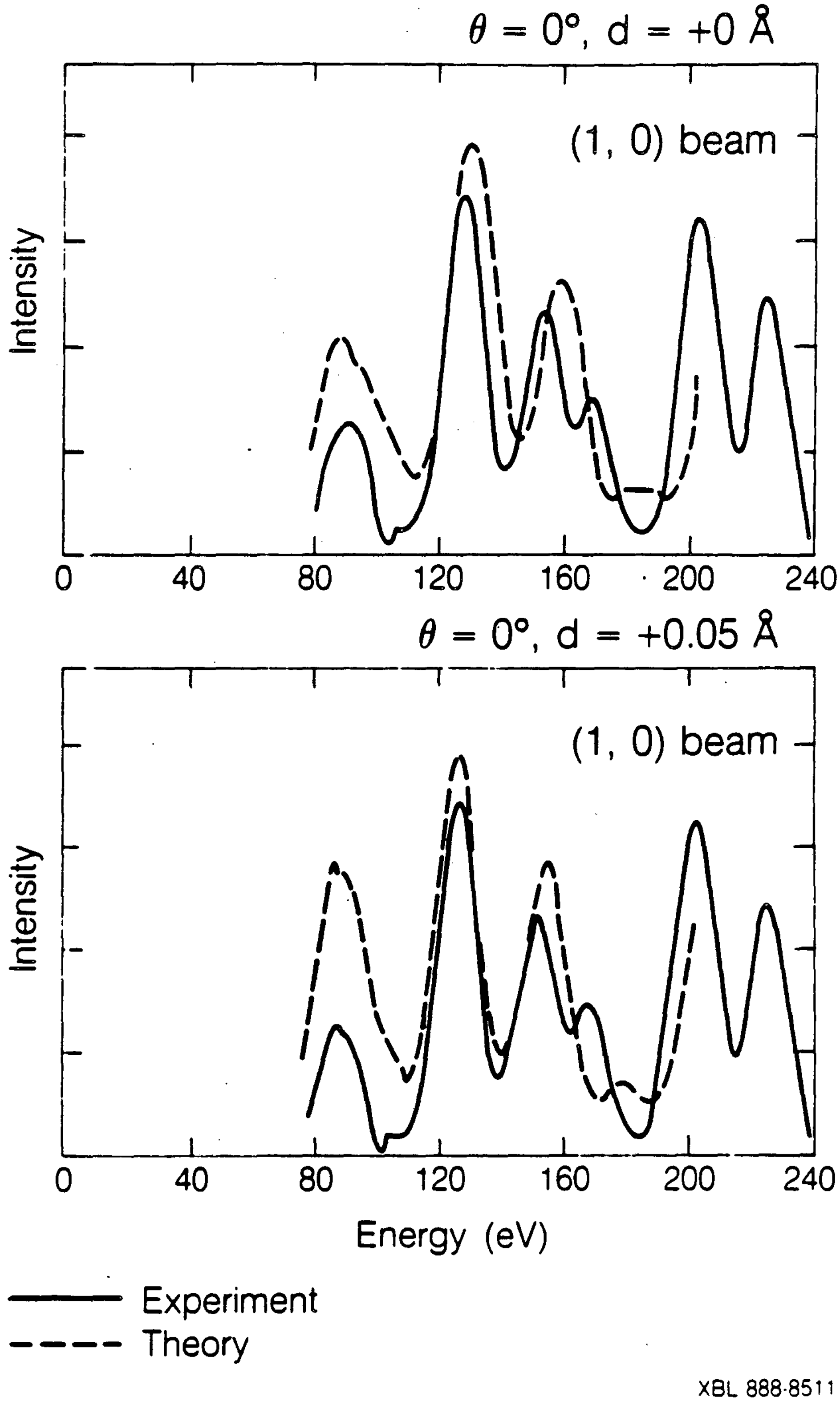

[Fig. 4-6] Comparison between the experimental I-V curves and the theoretical I-V curves for ideal bulk-terminated surface structure is shown in the upper column. The theoretical I-V curves in the lower column are based on the model with a slight expansion of the topmost interlayer spacing. (θ=0, ϕ=0)

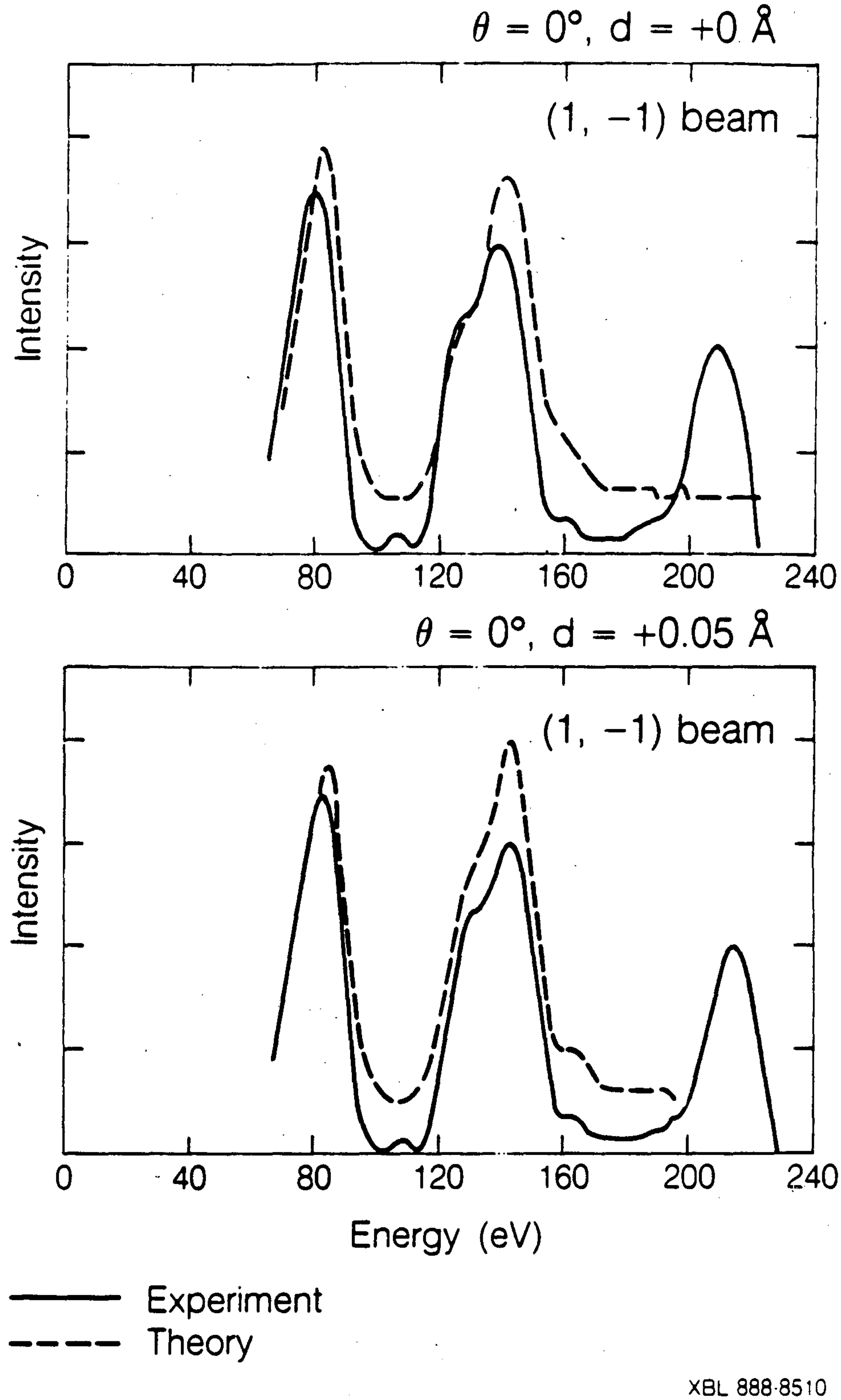

[Fig. 4-6] (continued)

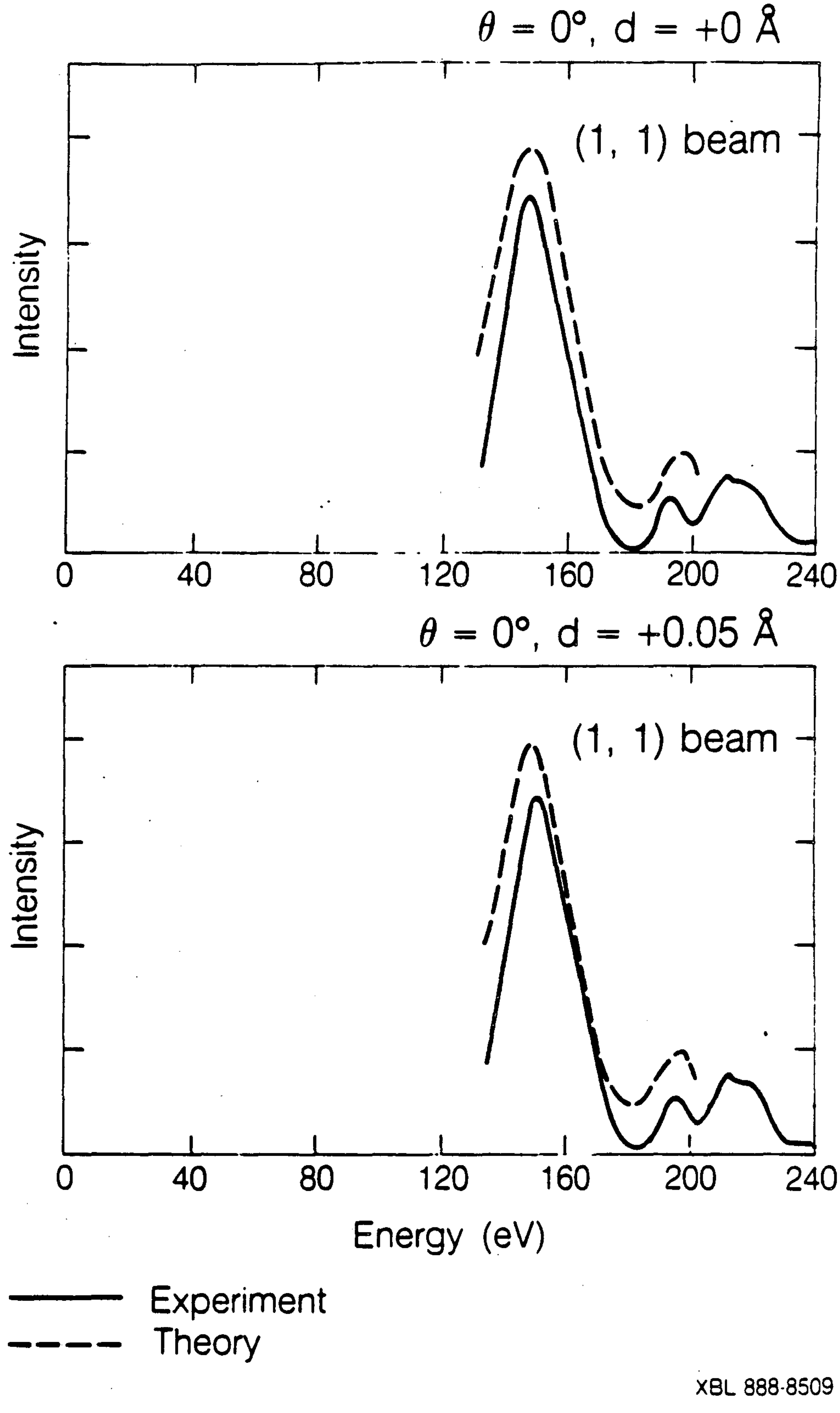

[Fig. 4-6] (continued)

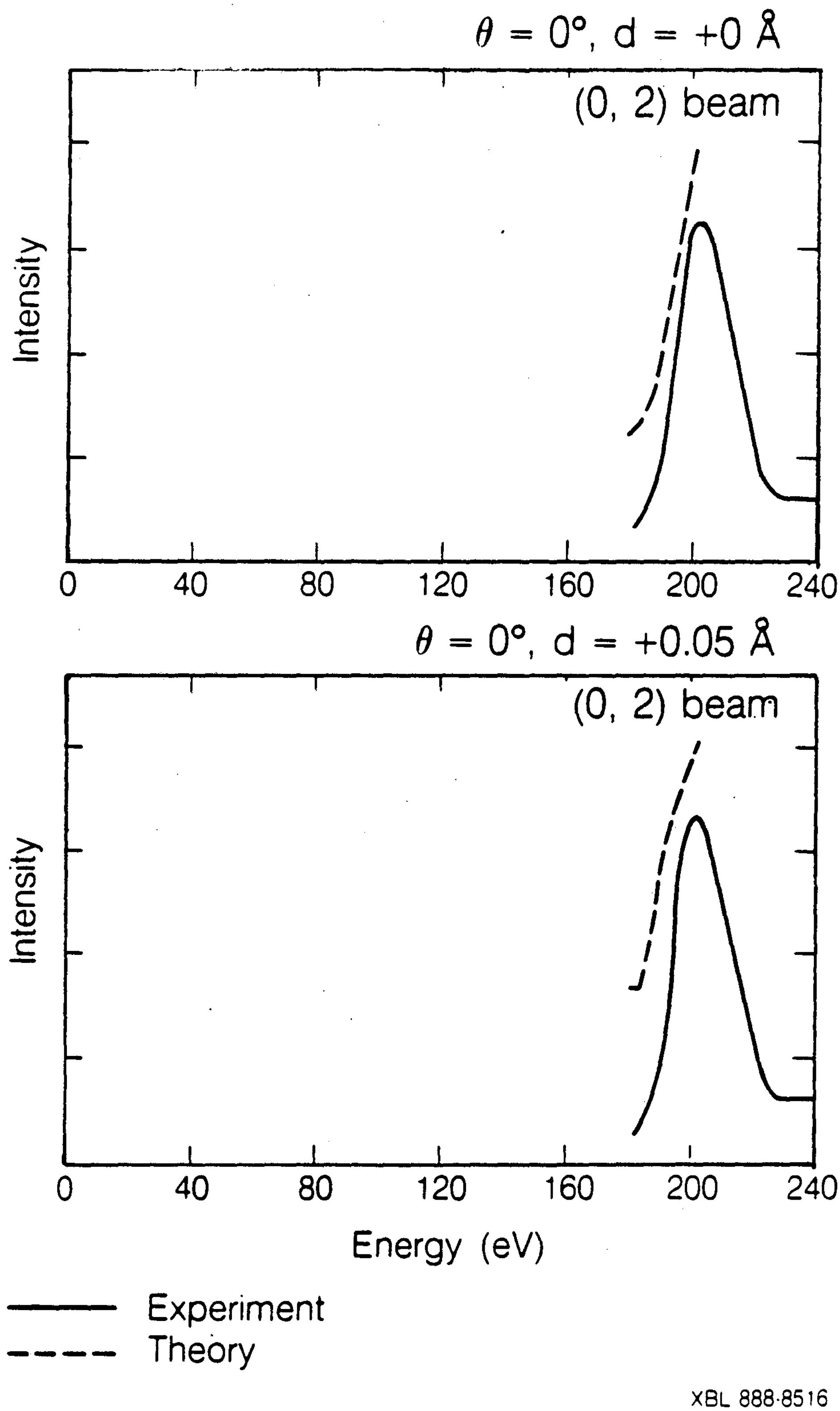

[Fig. 4-6] (continued)

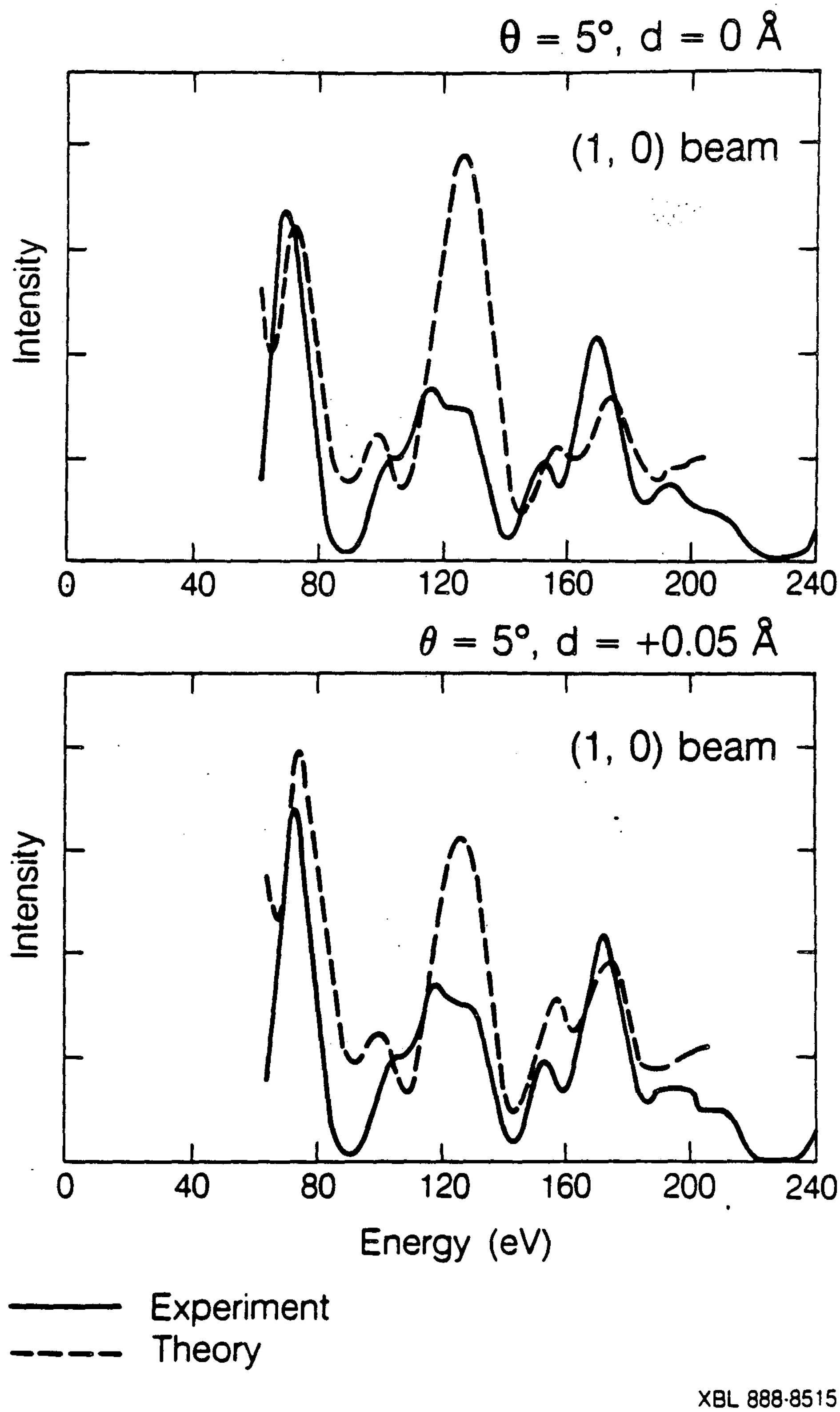

[Fig. 4-7] Comparison between the experimental I-V curves and the theoretical I-V curves for the ideal bulk-terminated surface structure is shown in the upper column. The theoretical I-V curves in the lower column are based on the model with a slight expansion of the topmost interlayer spacing. (θ=5, ϕ=0)

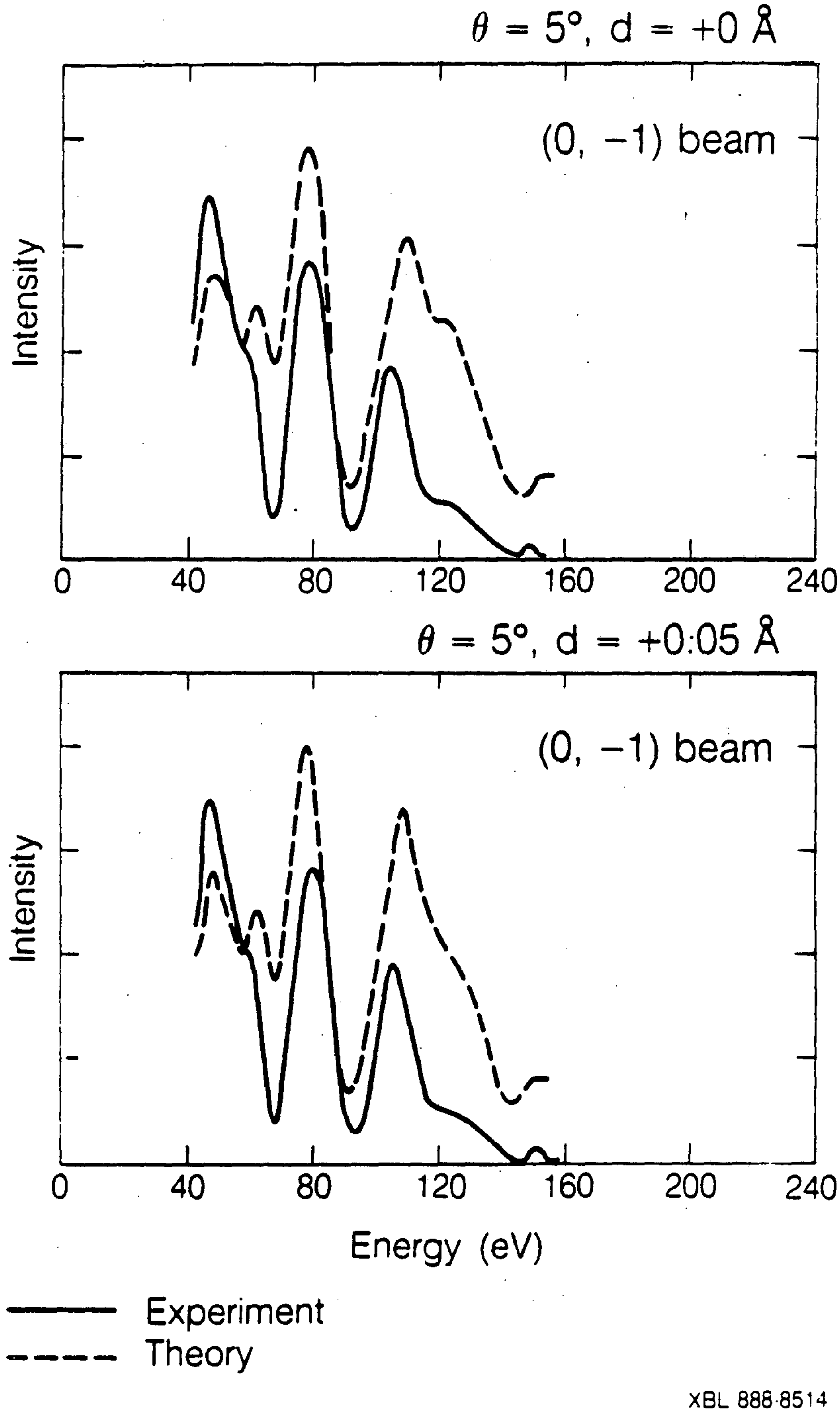

[Fig. 4-7] (continued)

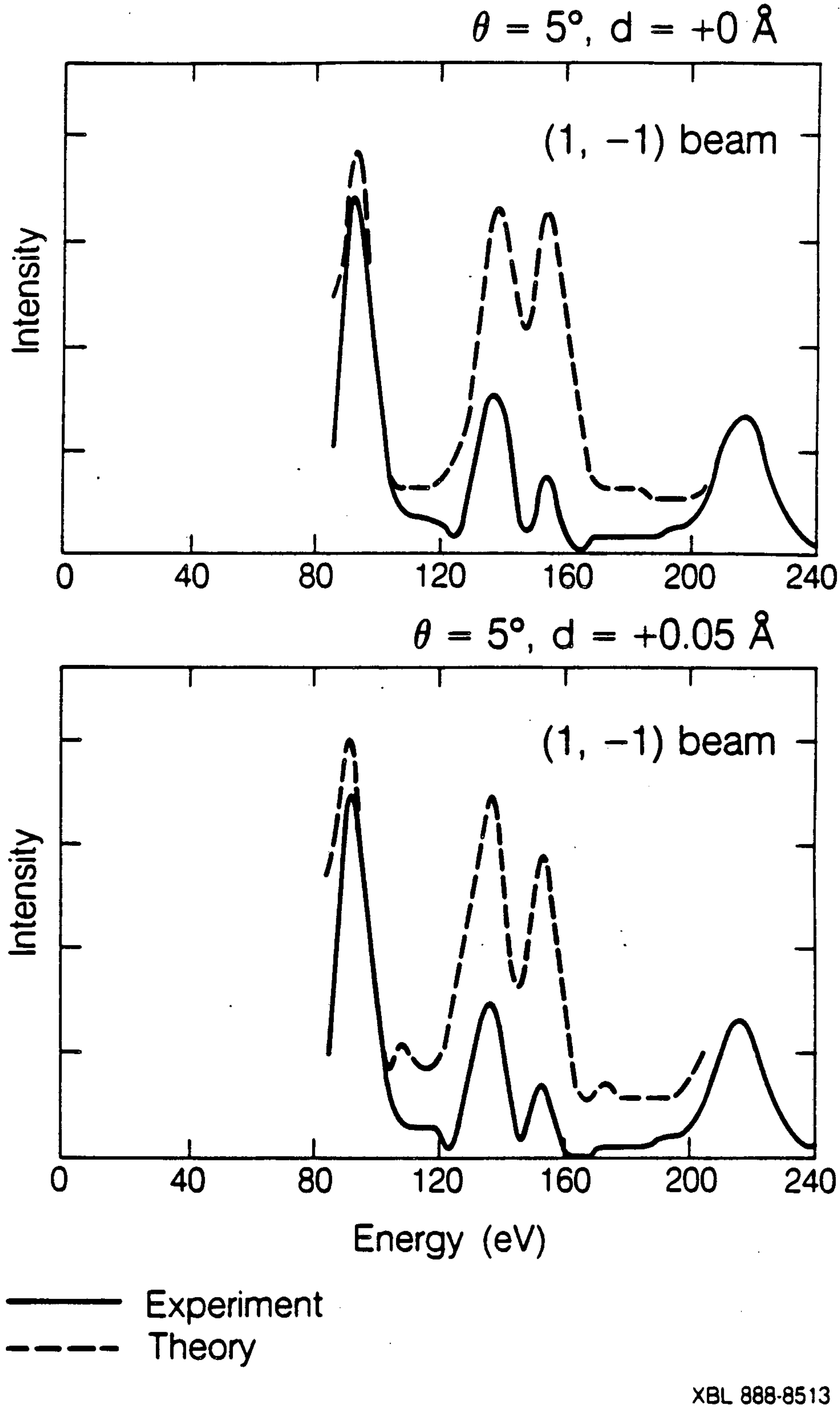

[Fig. 4-7] (continued)

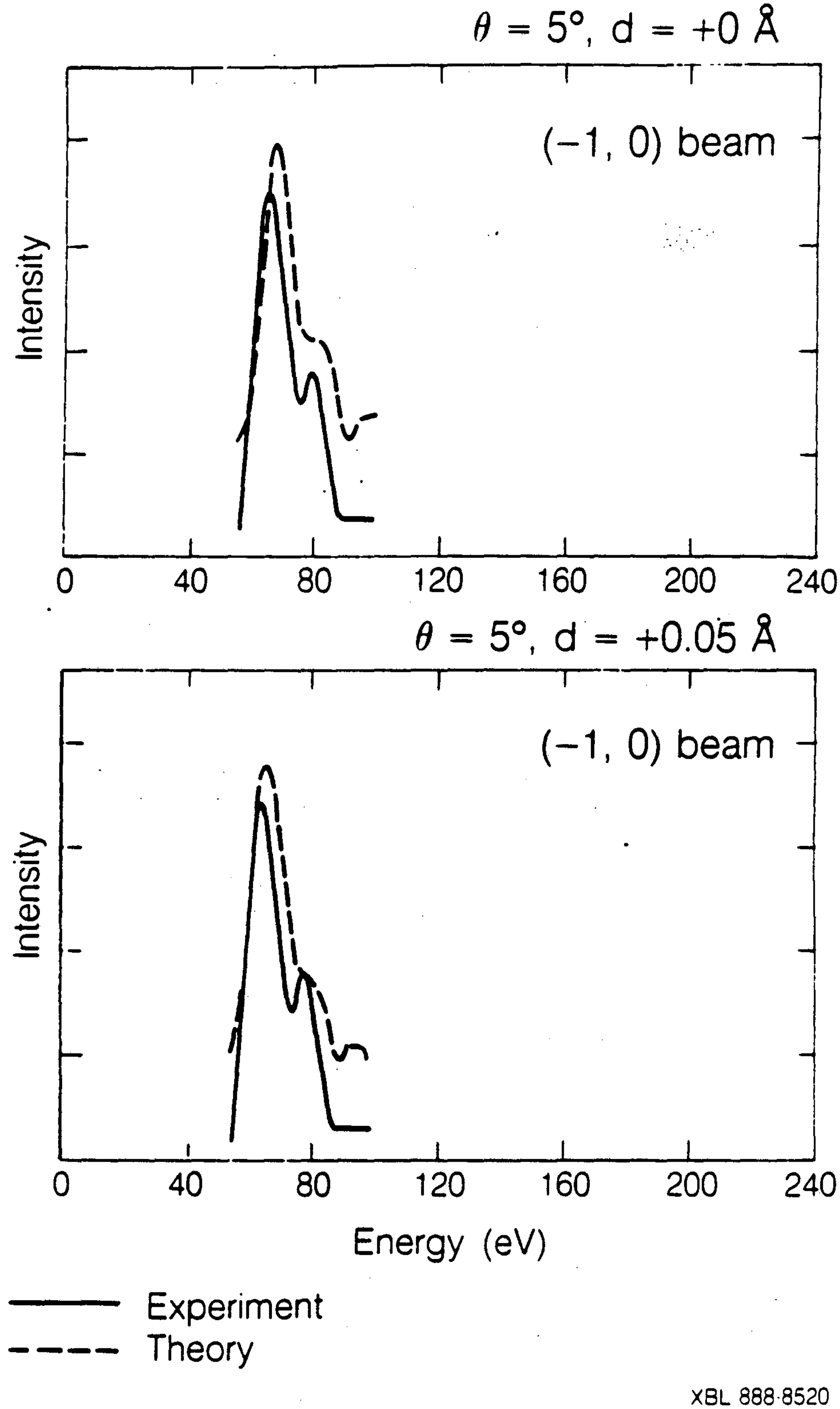

[Fig. 4-7] (continued)

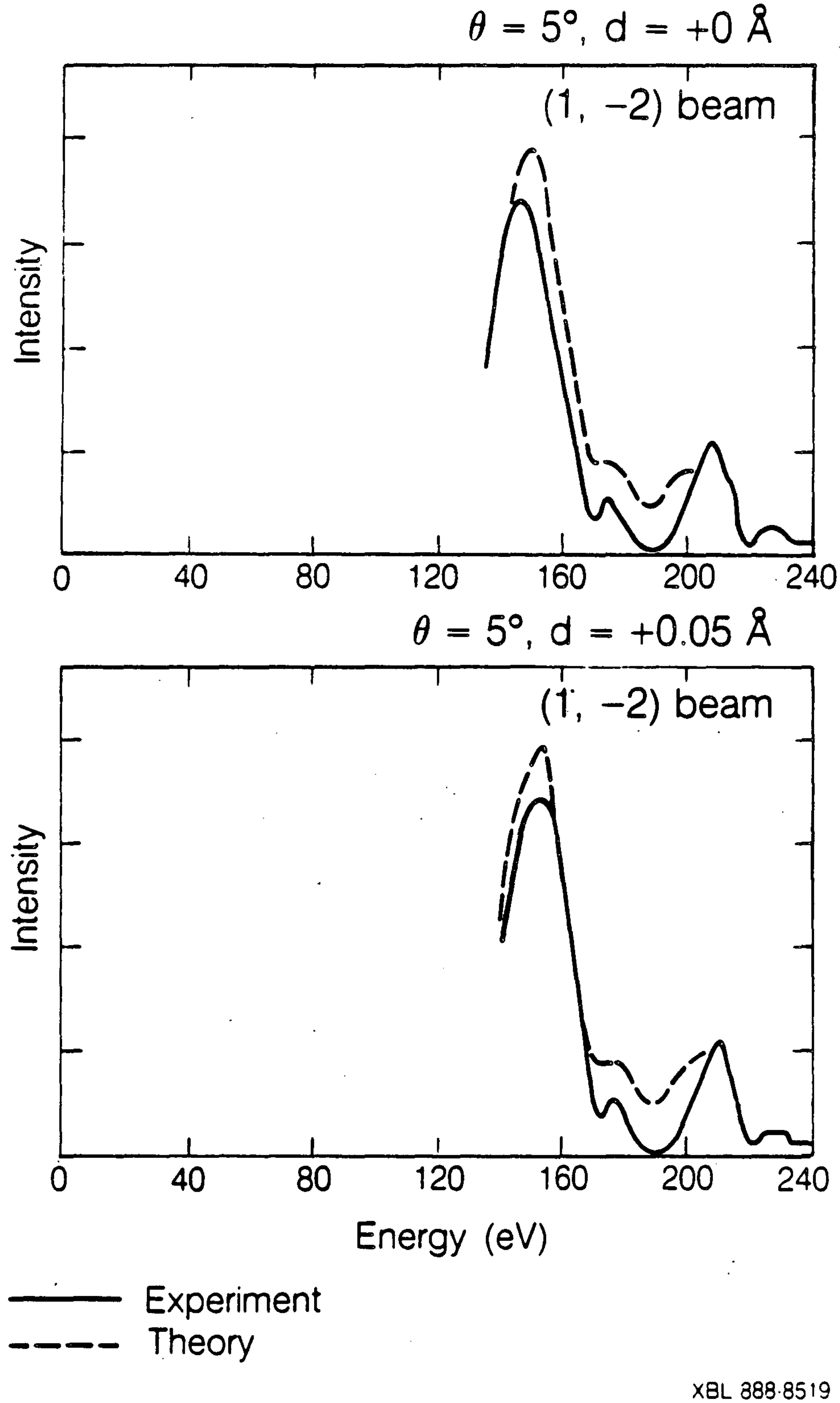

[Fig. 4-7] (continued)

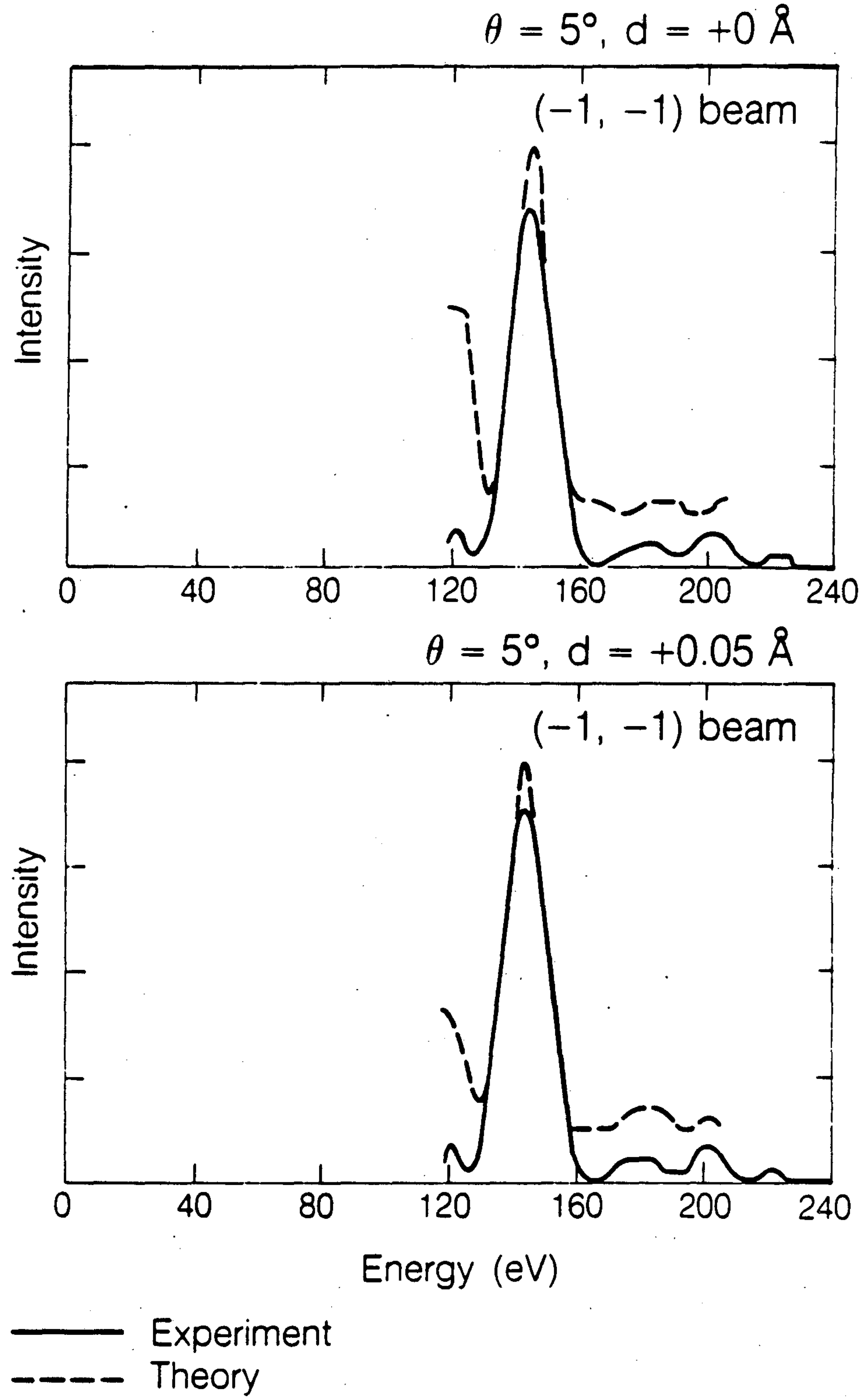

XBL 888-8518

[Fig. 4-7] (continued)

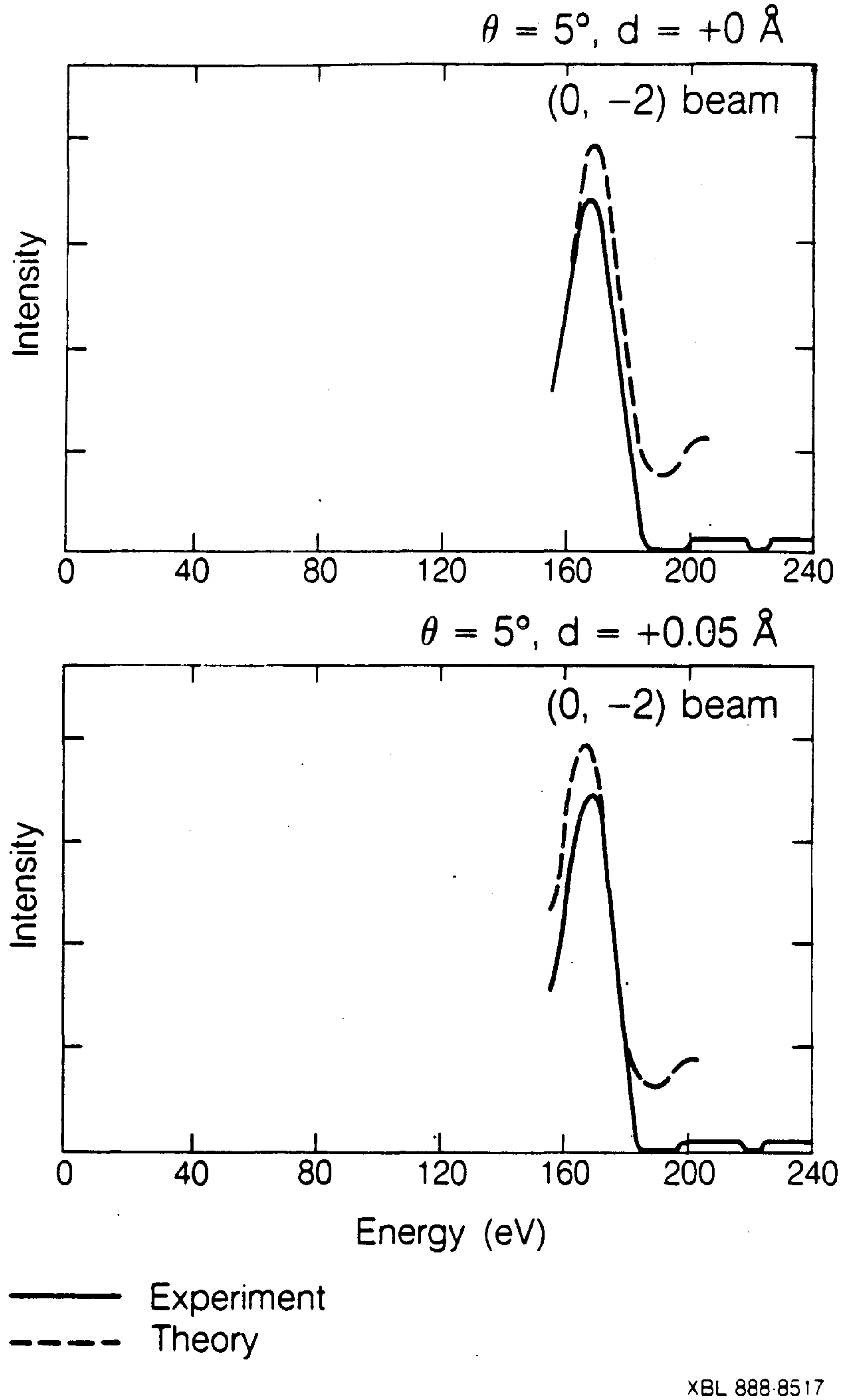

[Fig. 4-7] (continued)

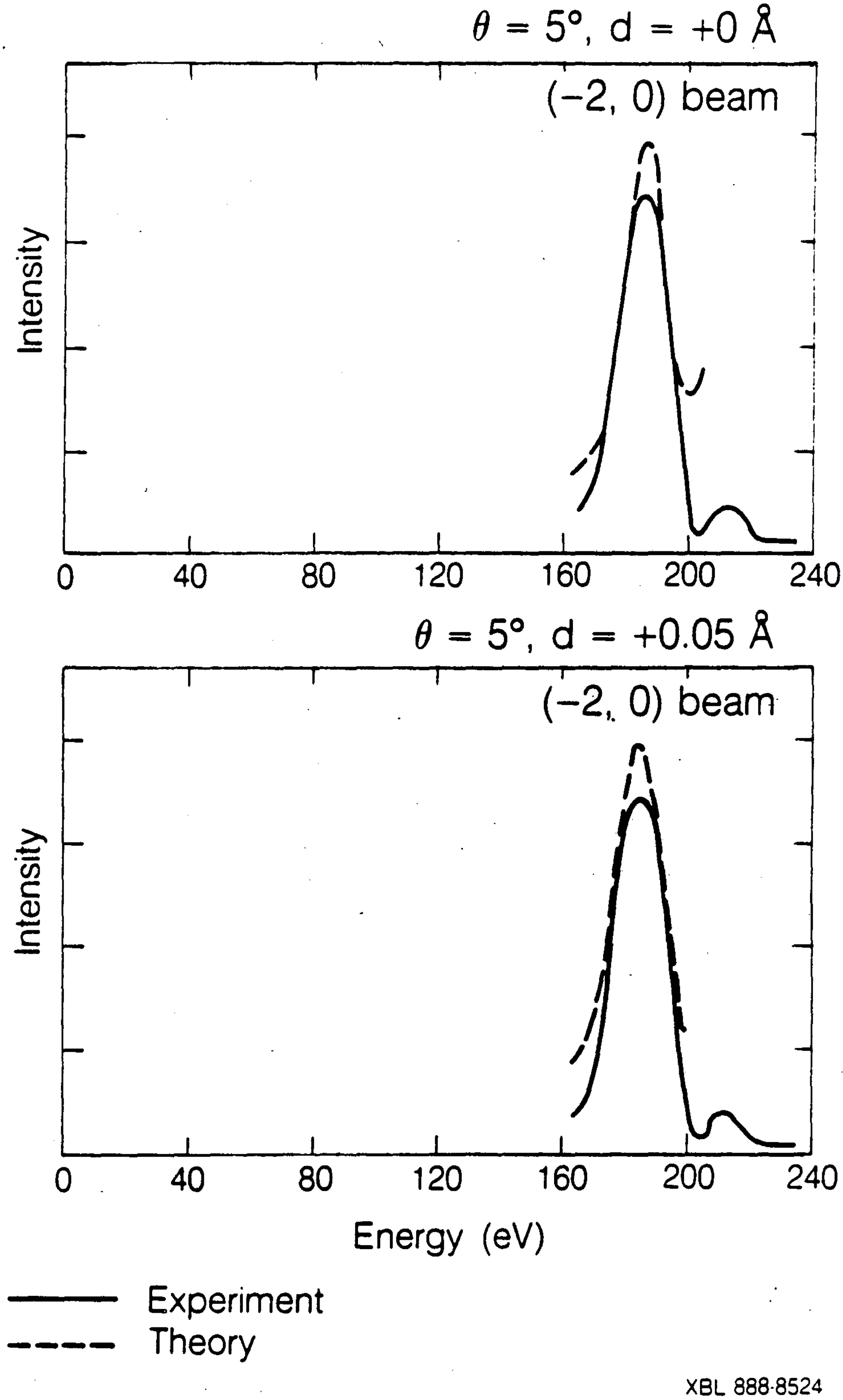

[Fig. 4-7] (continued)

[Table 4-1] R-factor comparison for Pd(111) with and without relaxation.

Angle of Incidence	Model	Muffin-tin zero	5-Average R-Factor
$\theta=0°$ [Fig. 4-6 (upper)]	$\Delta d_{12}=0Å$	$V_0=8eV$	0.1617
$\theta=0°$ [Fig. 4-6 (lower)]	$\Delta d_{12}=0.05Å$	$V_0=8eV$	0.1166
$\theta=5°$ [Fig. 4-7 (upper)]	$\Delta d_{12}=0Å$	$V_0=7eV$	0.1990
$\theta=5°$ [Fig. 4-7 (lower)]	$\Delta d_{12}=0.05Å$	$V_0=7eV$	0.1420

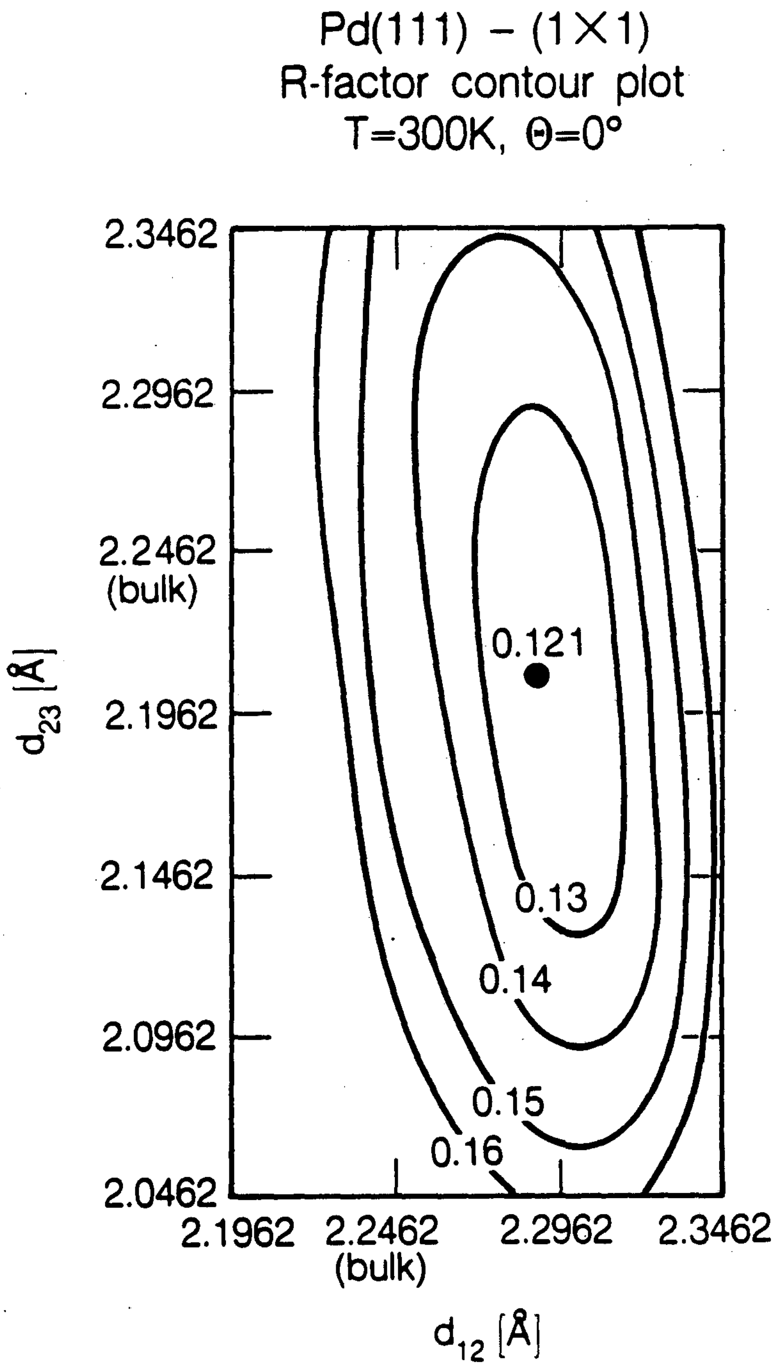

[Fig. 4-8] Contour plot of the five-R-factor average as a function of two of the structural parameters for clean Pd(111). The parameters used are the interlayer spacing between the 1st and 2nd Pd layers, d_{12}, and that between the 2nd and 3rd Pd layers, d_{23}. The bulk spacing is 2.2462Å. Δd_{34} and Δd_{45} were held at +0.05Å for this plot. Muffin-tin zero at V_0= 8eV.

4.5. Discussion

The structure of clean Pd(111) which we obtain has the ideal bulk structure within ~0.05Å. The 5 average R-factor value is small (0.12), indicating good agreement between theory and experiment. The small deviations of our optimal structural values for the interlayer spacings from the ideal structure are:

$$\Delta d_{12} = +0.03 \pm 0.03 \AA \quad [+1.3 \pm 1.3\%]$$

$$\Delta d_{23} = -0.03 \pm 0.03 \AA \quad [-1.3 \pm 1.3\%]$$

$$\Delta d_{34} = +0.05 \pm 0.03 \AA \quad [+2.2 \pm 1.3\%]$$

$$\Delta d_{45} = +0.05 \pm 0.03 \AA \quad [+2.2 \pm 1.3\%]$$

(positive/negative values correspond to expansion/contraction).

The average spacing expansion of the near surface region (from the 1st layer to the 5th layer) is ~1.1% with respect to the bulk value.

Since Pd(111) is a close-packed face, one may expect an ideal surface structure. Indeed, almost all the close-packed metal surfaces appear to have the ideal, unrelaxed structure or perhaps a slightly contracted structure. According to a recent surface structure tabulation,[15] possibly the only exceptions until now were the cases of Al(111) and Pt(111). For Al(111), there are contradictory results for the topmost interlayer spacing: Two results show expansions (+2.2%, +5%), two other results show contractions (–3%, –8%), and some show unrelaxed structures. For Pt(111), several results show expansions (+0.5%, +1%, +1.3%, +1.5%, +1.5%), and others show ideal structures.

In view of the easy absorption of hydrogen in bulk palladium and of the resulting difficulty of keeping the Pd(111) surface free of hydrogen, it is possible that the small relaxations seen at this surface are due to hydrogen in the surface region. It is well known that the Pd bulk lattice expands as the hydrogen concentration in the bulk increases.[16,17] For example, when the H/Pd ratio is ~0.6, where the α phase and the β phase coexist, the lattice expansion is ~3.5%. Most hydrogen is presumably located in the octahedral interstitial sites.[16,17] Regarding the surface properties of hydrided palladium, Christmann *et al.*[1] have exposed a Pd(111) crystal to more than 100L of hydrogen, and observed Bragg peak shifts corresponding to an average expansion of the interlayer spacings by ~ 2% in the surface region. The occupation of subsurface sites by hydrogen on Pd(111) has been suggested by W. Eberhardt *et al.*,[18] F.Greuter *et al.*,[19] T.E. Felter *et al.*,[20,21] and S.M. Foiles *et al.*.[22] These studies indicate that octahedral sites between the first and second layers could be the most favorable subsurface sites. This would be consistent with the small topmost spacing expansion which we see.

We should also mention here that a dynamical LEED analysis of clean Pd(100) has shown similar results.[10,11] The structure is close to ideal, but the optimal topmost spacing seems to be slightly expanded: $\Delta d_{12} = +2.5 \pm 2.5\%$.

4.6. Conclusions

The structure of Pd(111) surface is confirmed to be almost equal to that of the bulk structure, within ~ 0.05Å with good R-factor values. Small deviation from the ideal bulk value are found, which might indicate surface relaxations due to hydrogen in the near surface region. [Fig. 4-9, Table 4-2]

The Structure of Pd(111) Surface

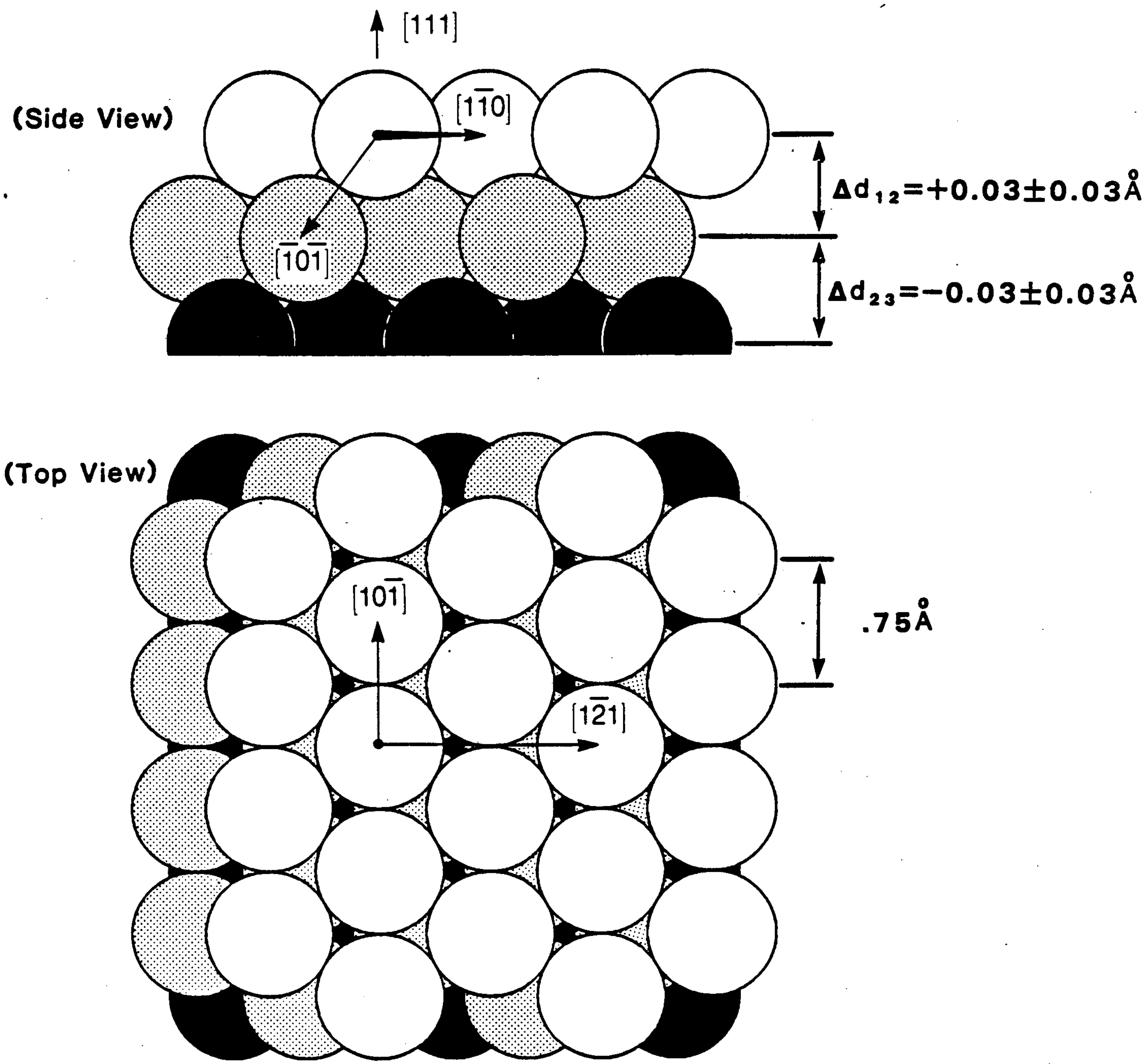

[Fig. 4-9] The optimum structure for the Pd(111) surface, as determined by dynamical LEED and R-factor analysis.

TABLE 4-2. Structure Result in Format of Surface Crystallographic Information Service (SCIS)[15]

SURFACE: Substrate Face: Pd(111)

Surface Pattern: (1x1), (1,0/0,1)

STRUCTURE: Bulk Structure: fcc; Temp: 300K

REFERENCE UNIT CELL: a=2.75Å; b=2.75Å; A(a,b)=60°

Layer	Atom	Atom Positions		Normal Layer Spacing
S1	Pd	0.0	0.0	2.28
S2	Pd	0.3333	0.3333	2.22
S3	Pd	0.6667	0.6667	2.30
S4	Pd	0.0	0.0	2.30

2D Symmetry: p3m1

Thermal Vibrations: Debye Temp=225K

R-factor: R_{VHT}=0.12 R_{ZJ}=0.09 R_P=0.22

References

1. K. Christmann, G. Ertl, and O. Schober, *Surf. Sci.*, vol. 40, p. 61, 1973.

2. F. Maca, M. Scheffler, and W. Berndt, *Surface Science*, vol. 160, p. 467, 1985.

3. Y. Kuk, L.C. Feldman, and P.J. Silverman, *J. Vac. Sci. Technol. A*, vol. 1, p. 1060, 1983.

4. Y. Kuk, L. C. Feldman, and P. J. Silverman, *Physical Review Letters*, vol. 50, p. 511, 1983.

5. D. F. Ogletree, G. A. Somorjai, and J. E. Katz, *Review of Scientific Instruments*, vol. 57, p. 3012, 1986.

6. L. L. Kesmodel and G. A. Somorjai, *Physical Review B*, vol. 11, p. 630, 1975.

7. T.M. Gentle, *Ph.D. Thesis*, Chemistry Department, University of California, Berkeley, 1984.

8. M. A. Van Hove and S. Y. Tong, *Surface Crystallography by LEED*, Springer Verlag, Berlin, 1979.

9. V.L. Moruzzi, J.F. Janak, and A.R. Williams, in *Calculated Electronic Properties of Metals*, Pergamon, New York, 1978.

10. R. J. Behm, K. Christmann, G. Ertl, M. A. Van Hove, P. A. Thiel, and W. H. Weinberg, *Surface Science*, vol. 88, p. L59, 1979.

11. R. J. Behm, K. Christmann, G. Ertl, and M. A. Van Hove, *Journal of Chemical Physics*, vol. 73, p. 2984, 1980.

12. D. F. Ogletree, M. A. Van Hove, and G. A. Somorjai, *Surface Science*, vol. 173, p. 351, 1986.

13. R. J. Koestner, M. A. Van Hove, and G. A. Somorjai, *Surface Science*, vol. 107, p. 439, 1981.

14. M. A. Van Hove, R. J. Koestner, J. C. Frost, and G. A. Somorjai, *Surface Science*, vol. 129, p. 482, 1983.

15. J.M. MacLaren, J.B. Pendry, R.J. Rous, D.K. Saldin, G.A. Somorjai, M.A. Van Hove, and D.D. Vvedensky, in *Surface Crystallographic Information Services: A Handbook of Surface Structures*, Reidel, Dordrecht, 1987.

16. F.A. Lewis, in *The Palladium Hydrogen System", Academic Press (1967)*, Academic Press, 1967.

17. E. Wicke, H. Brodowsky, and H. Zühner, in *Hydrogen in Metals II*, ed. J. Völkl, Springer-Verlag, Berlin, 1978.

18. W. Eberhardt, F. Greuter, and E.W. Plummer, *Phys. Rev. Lett.*, vol. 46, p. 1085, 1981.

19. F. Greuter, W. Eberhardt, J. DiNardo, and E.W. Plummer, *J. Vac. Sci. Tec.*, vol. 18, p. 433, 1981.

20. T.E. Felter, S.M. Foiles, M.S. Daw, and R.H. Stulen, *Surf. Sci.*, vol. 171, p. L379, 1986.

21. T.E. Felter and R.H. Stulen, *J. Vac. Sci. Tec.*, vol. A3, p. 1566, 1985.

22. S.M. Foiles and M.S. Daw, *J. Vac. Sci. Tec.*, vol. A3, p. 1565, 1985.

5. LEED Intensity Analysis of the Surface Structures of CO Adsorbed on Pd(111) in a $(\sqrt{3}x\sqrt{3})R30°$ Arrangement

5.1. Introduction

Following the structure determination of the clean Pd(111) surface, a molecular structure of carbon monoxide adsorbed on this surface has been analyzed*. Adsorption structures have already been determined for CO molecularly adsorbed on Pt(111)[1] Rh(111),[2,3] Ru(0001)[4] Ni(100)[5,6,7,8,9] Cu(100),[5,6] and Pd(100).[10,11] On these surfaces, the CO molecules have been confirmed to adsorb at 1-fold coordinated top sites or 2-fold coordinated bridge sites. Three-fold coordinated hollow sites occur less frequently: CO on Pd(111) is the only ordered case in which vibrational spectroscopy indicates[12,13] hollow sites (coadsorption also induces hollow sites for CO, as we have found with coadsorbed benzene).[14,15,16] For this reason and in preparation for other adsorbate studies on Pd(111), we have analyzed the structures of CO-covered Pd(111).

The CO/Pd(111) system has been extensively studied in the past with a variety of techniques, including Thermal Desorption Spectroscopy

* Some part of this chapter has been published in the following article:
H. Ohtani, M. A. Van Hove, and G. A. Somorjai, Surface Science, **187**, 372 (1987).

(TDS),[17,18,19,20,21,22] work-function measurements,[17,18] adsorption isotherms,[17,18] LEED pattern analysis,[12,13,17,18,19,23,24,25] molecular beam experiments,[26] Ultraviolet Photoelectron Spectroscopy (UPS),[19,27] Angle-Resolved Photoelectron Emission Spectroscopy (ARPES),[28,25] Infrared Reflection Absorption Spectroscopy (IRAS),[12,13] Electron Energy Loss Spectroscopy (EELS),[23] Penning-Ionization Electron Spectroscopy (PIES),[27] and Secondary Ion Mass Spectroscopy (SIMS).[20]

These investigations have shown that CO is molecularly bonded to the Pd(111) surface through the carbon atom. The IRAS studies have shown the following dependence of the CO stretching frequency on the CO coverage(θ): At low coverages a band appears at ~1820 cm^{-1}. This band gradually shifts up to ~1840 cm^{-1}, when a $(\sqrt{3}x\sqrt{3})R30°$ LEED pattern is observed at θ=1/3. Then this band moves quickly to ~1920 cm^{-1} by θ=0.4. For θ=0.5, the frequency is ~1940cm^{-1}. At higher coverages, a second band appears above 2000 cm^{-1}. According to the site assignments used in metal-carbonyl clusters, these results suggest that CO molecules are adsorbed on hollow sites up to θ=1/3, on bridge sites at θ=1/2, and on both bridge and top sites at higher coverages.

However, since the CO stretching frequency is affected by intermolecular interactions and the interaction between CO and metal, one cannot infer definitively from the C-O stretching frequency (1840cm^{-1}) whether CO molecules are adsorbed at hollow sites or at bridge sites. LEED can independently verify the site assignment. Furthermore, two inequivalent hollow sites are available on the Pd(111) surface, namely the fcc hollow site and the hcp hollow site (a hcp hollow site has a 2nd layer atom at the bottom of the hollow, while a fcc hollow site does not have one). Vibrational spectroscopy can not distinguish CO molecules adsorbed at these two different hollow sites, whereas LEED can. In addition, LEED can yield bond lengths and bond angles.

We report here the first study of the structure of Pd(111)-($\sqrt{3}$x$\sqrt{3}$)R30°-CO by dynamical LEED analysis. We not only verify the CO adsorption site, but also analyze the detailed bond lengths. These results can be useful for interpreting various kinds of spectroscopic data, such as IRAS, UPS, ARPES, EELS, and for better understanding of CO chemisorption on transition metals in general.

5.2. Experimental

Experiments were performed in an ion-pumped, stainless steel UHV system, equipped with a quadrupole mass spectrometer, an ion bombardment gun, and a four-grid LEED optics as described in detail in Chapter 4.

5.2.1. Sample Preparation

The ($\sqrt{3}$x$\sqrt{3}$)R30°-CO pattern was produced by exposing the clean Pd(111) to a nominal 8x10^{-9} torr of CO for 100 sec at room temperature. The crystal was located 10 cm away from a stainless steel doser tube 0.15 cm in diameter. A bright ($\sqrt{3}$x$\sqrt{3}$)R30° pattern was obtained reproducibly [Fig. 5-1]. The TDS (at mass 28) showed a single peak at 480K with heating rate ~15K/s [Fig.

5-2]. This implies that most of the CO molecules adsorb at one kind of site at this coverage. At higher coverages, a second peak appears at lower temperature, as reported before.[27,20,21,22]

5.2.2. I-V Curve Measurement

The I-V data were collected with the same incident electron angles as used for clean Pd(111). The energy range used was 20-200eV. The normal-incidence data set has I-V curves for 8 independent beams over a cumulative energy range of 700 eV. The (5°, 0°) and the (5°, 180°) data sets have 17 and 12 independent beams and cumulative energy ranges of 1350 and 1200 eV, respectively. Both the normal-incidence data and the (5°, 0°) data are averages of two independent experiments.

The final I-V curves were obtained by averaging symmetrically equivalent beams. The cumulative energy ranges compared with theory were 610 eV, 1170 eV, and 1080 eV for (θ, ϕ) = (0°, 0°), (5°, 0°), and (5°, 180°), respectively. Some of these I-V curves are plotted in Fig. 5-3 and Fig. 5-4.

Pd(111) – ($\sqrt{3} \times \sqrt{3}$)R30° – CO
T = 300K

LEED Pattern 65eV

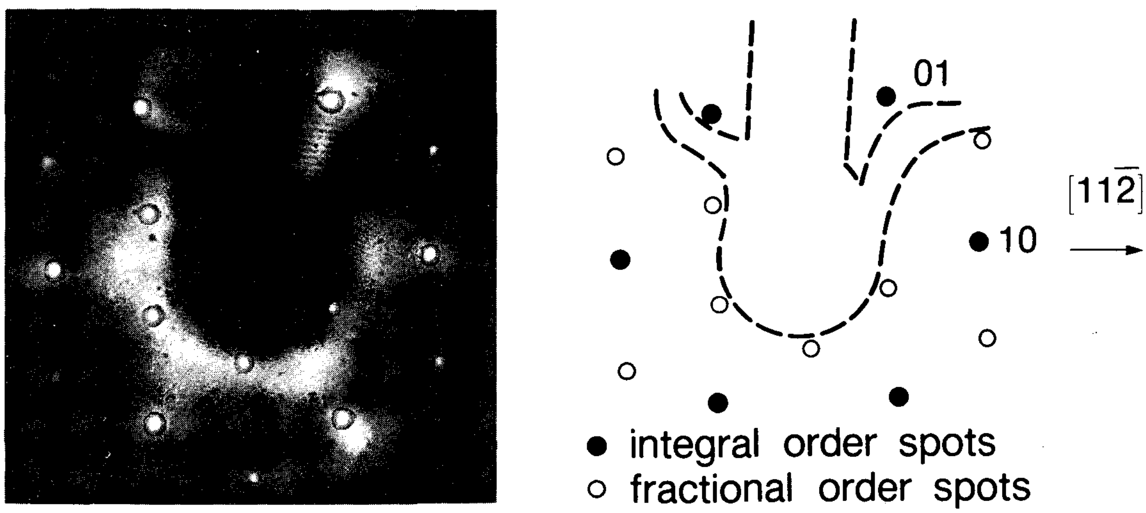

[Fig. 5-1] A photograph of the LEED pattern of the ($\sqrt{3}$x$\sqrt{3}$)R30° structure formed when 1/3 monolayer of CO is adsorbed at room temperature on Pd(111). The incident electron energy is 65eV. Near-normal incidence is used.

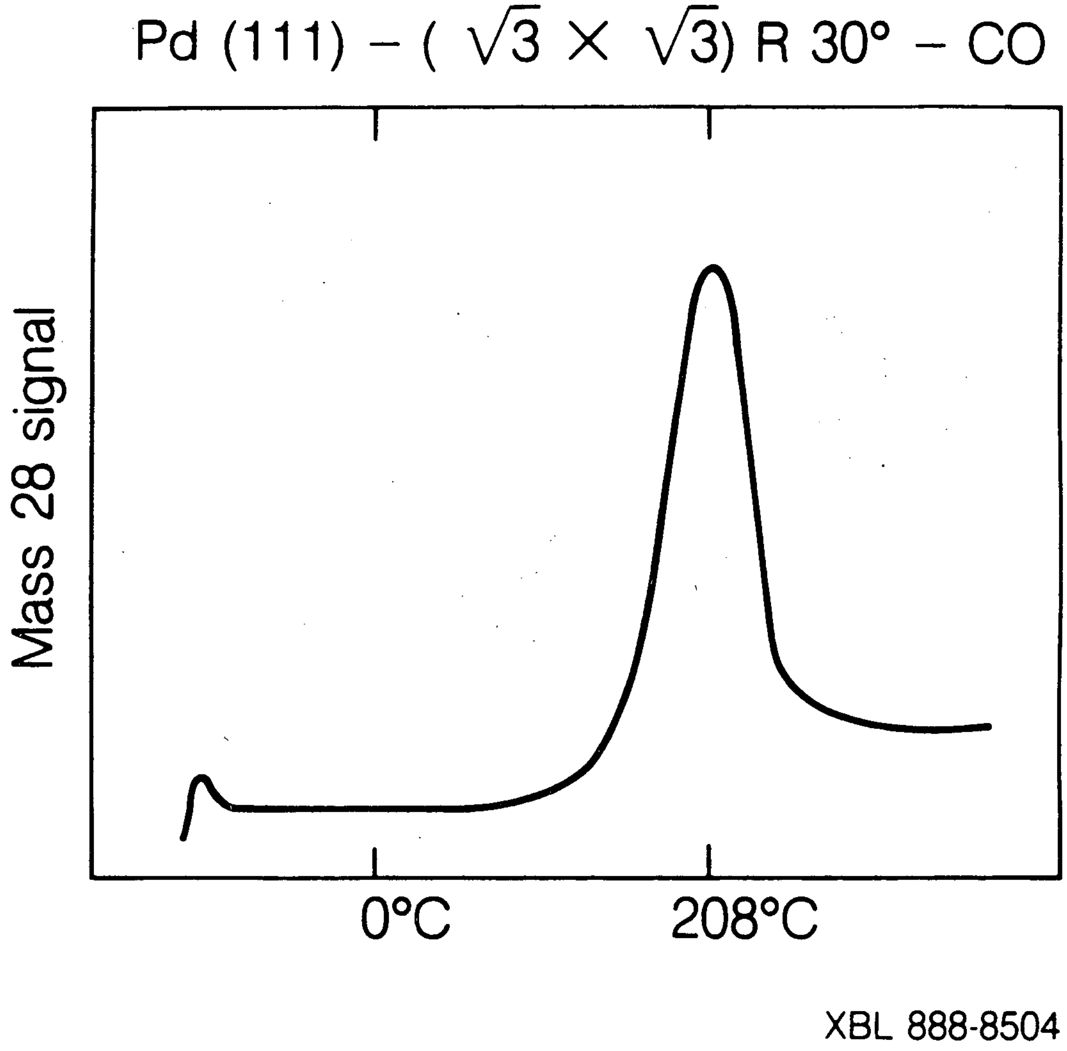

[Fig. 5-2] The TDS (mass=28) of the Pd(111)-($\sqrt{3}$x$\sqrt{3}$)R30°-CO

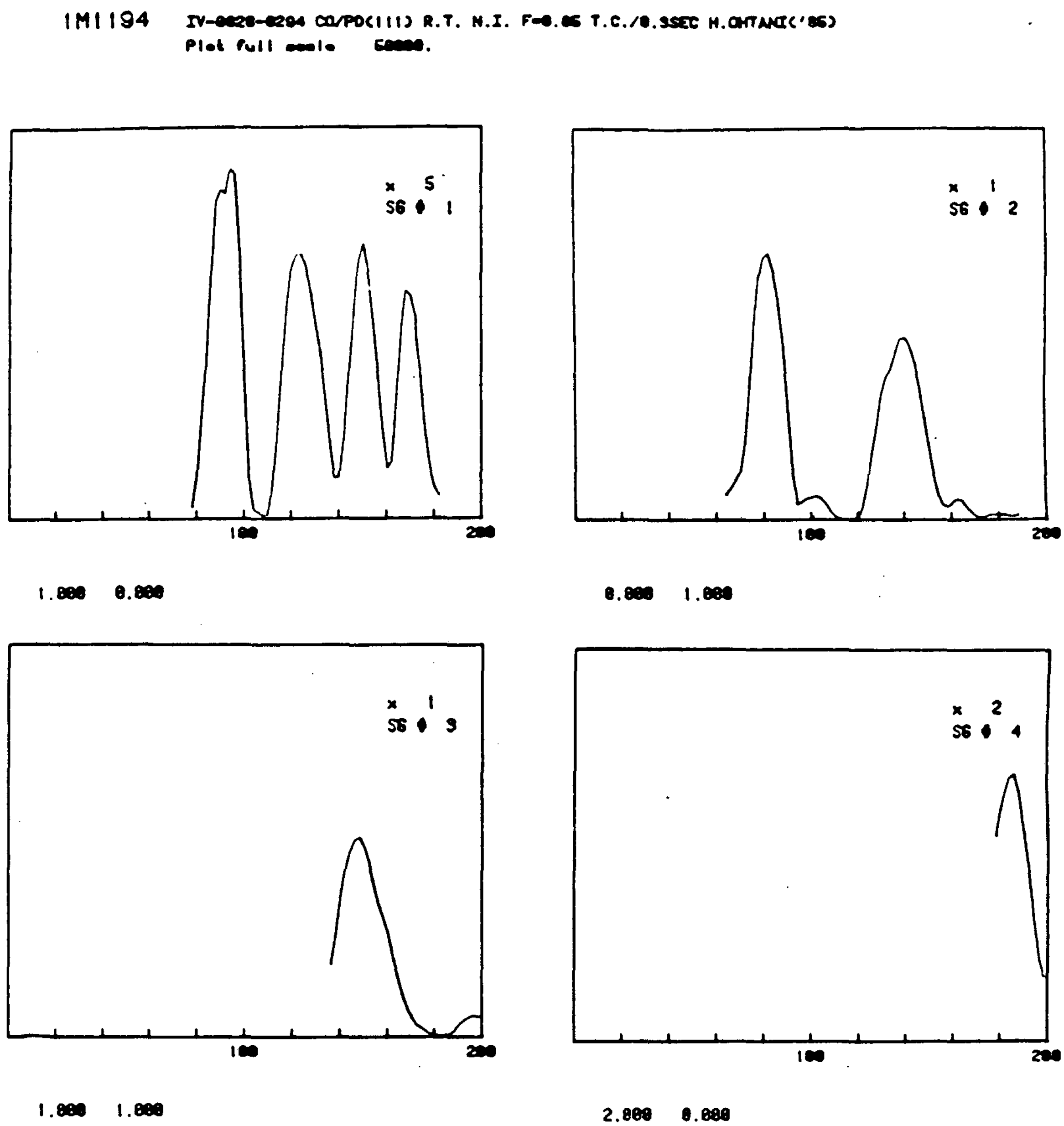

XBL 888-2891

[Fig. 5-3] Experimental I-V curves for Pd(111)-($\sqrt{3}$x$\sqrt{3}$)R30°-CO, recorded at 300K. $(\theta,\phi)=(0°, 0°)$.

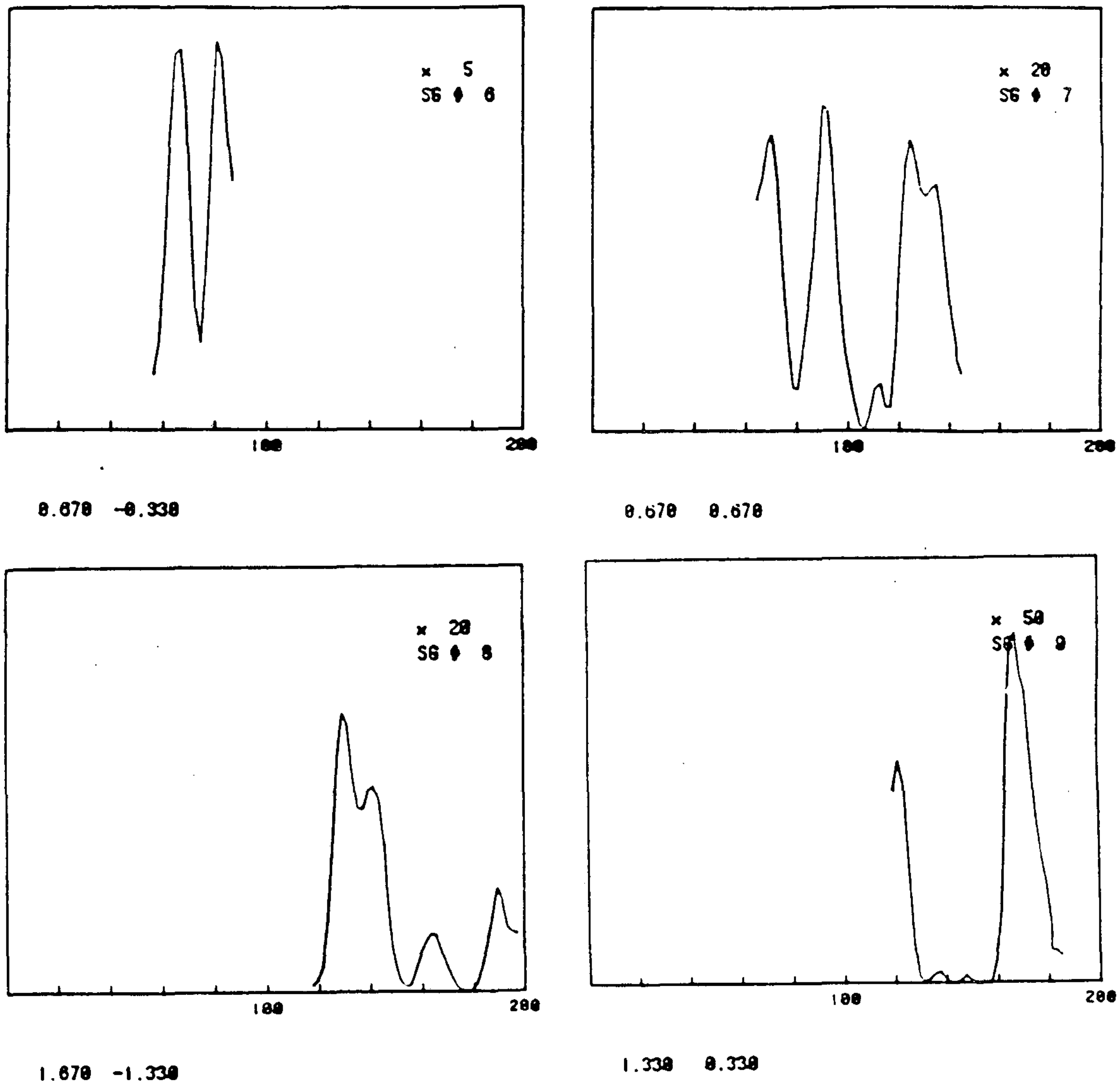

XBL 888-2892

[Fig. 5-3] (continued)

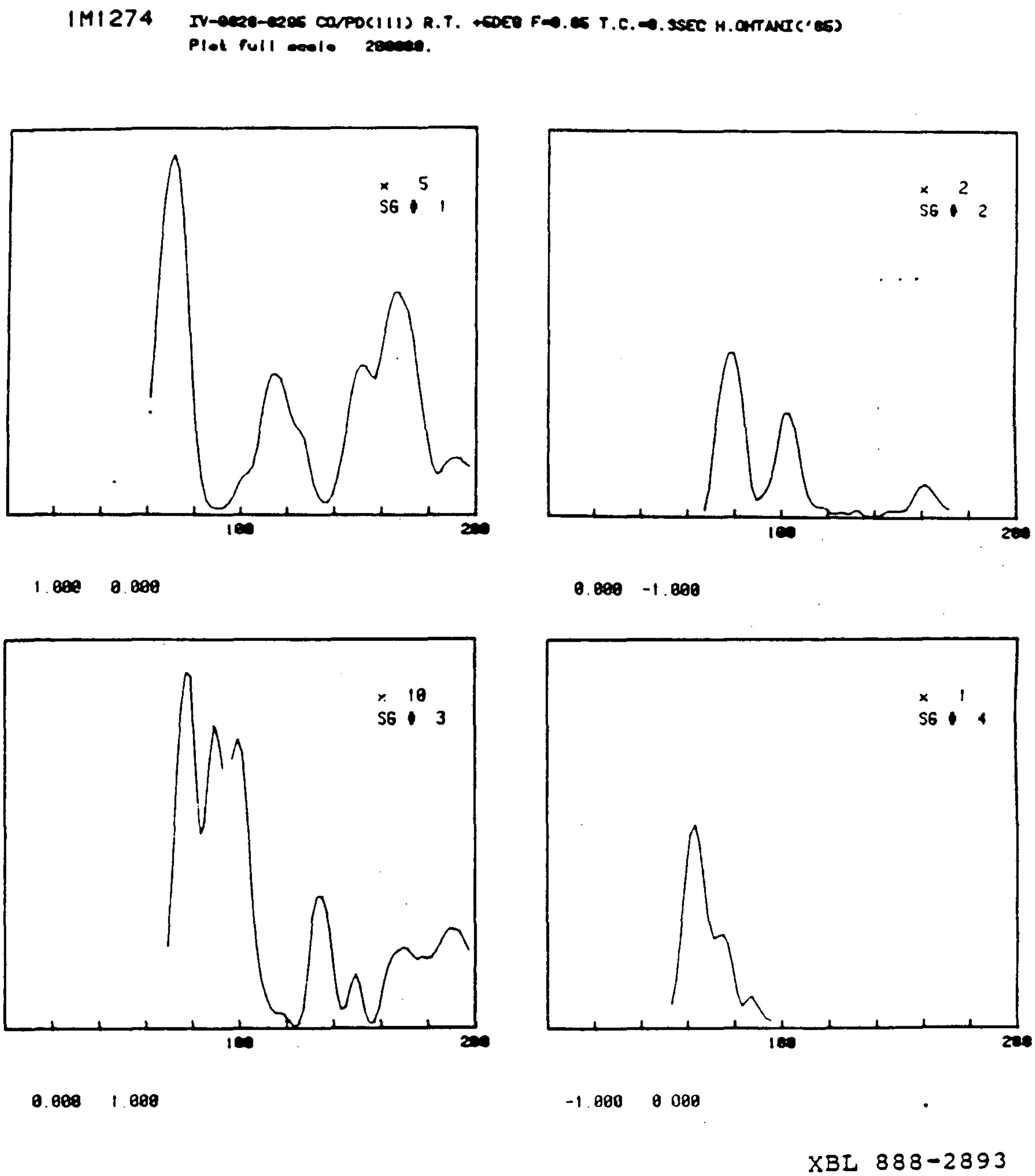

[Fig. 5-4] Experimental I-V curves for Pd(111)-($\sqrt{3}$x$\sqrt{3}$)R30°-CO, recorded at 300K. (θ,ϕ)=(5°, 0°).

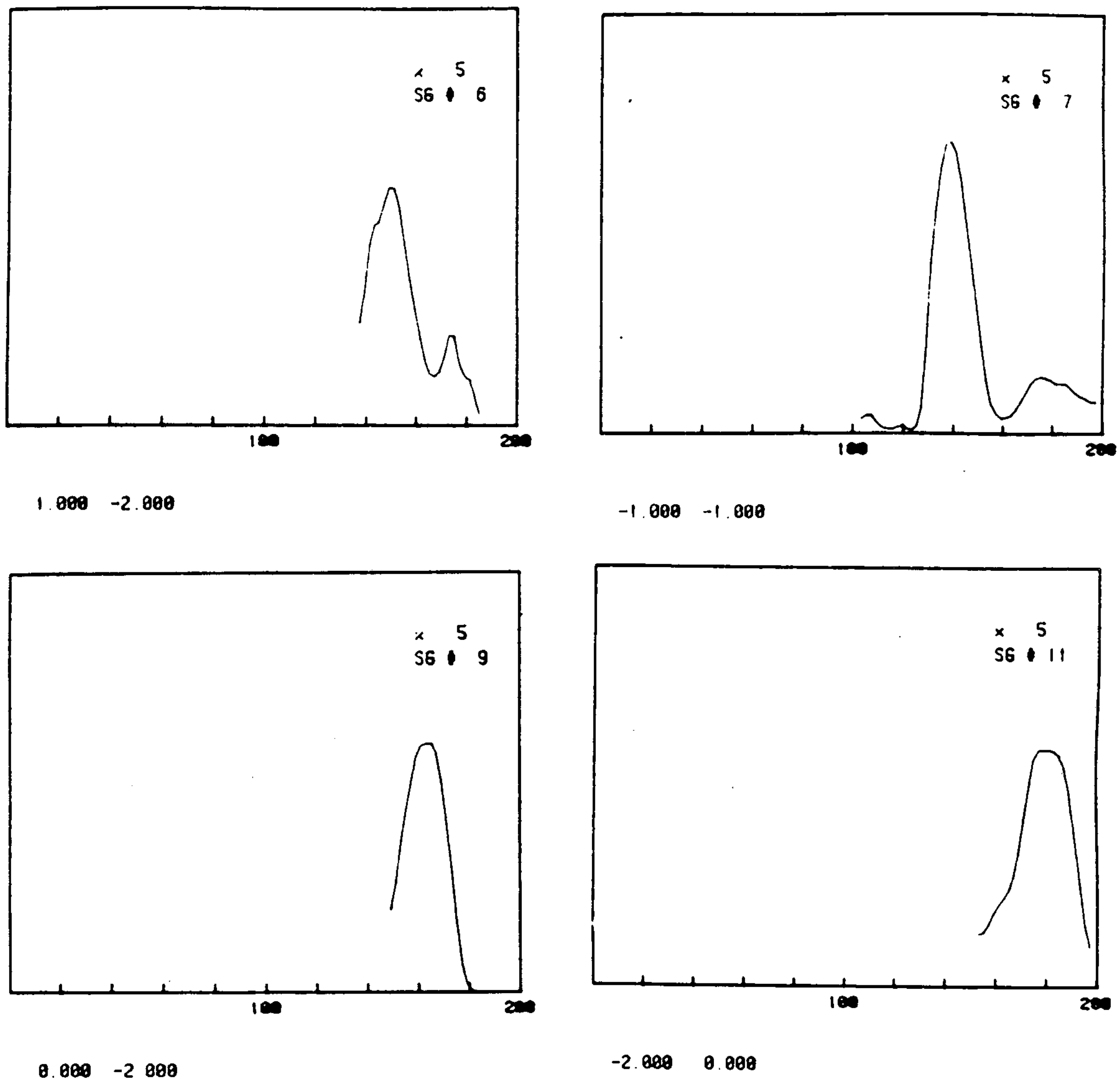

XBL 888-2894

[Fig. 5-4] (continued)

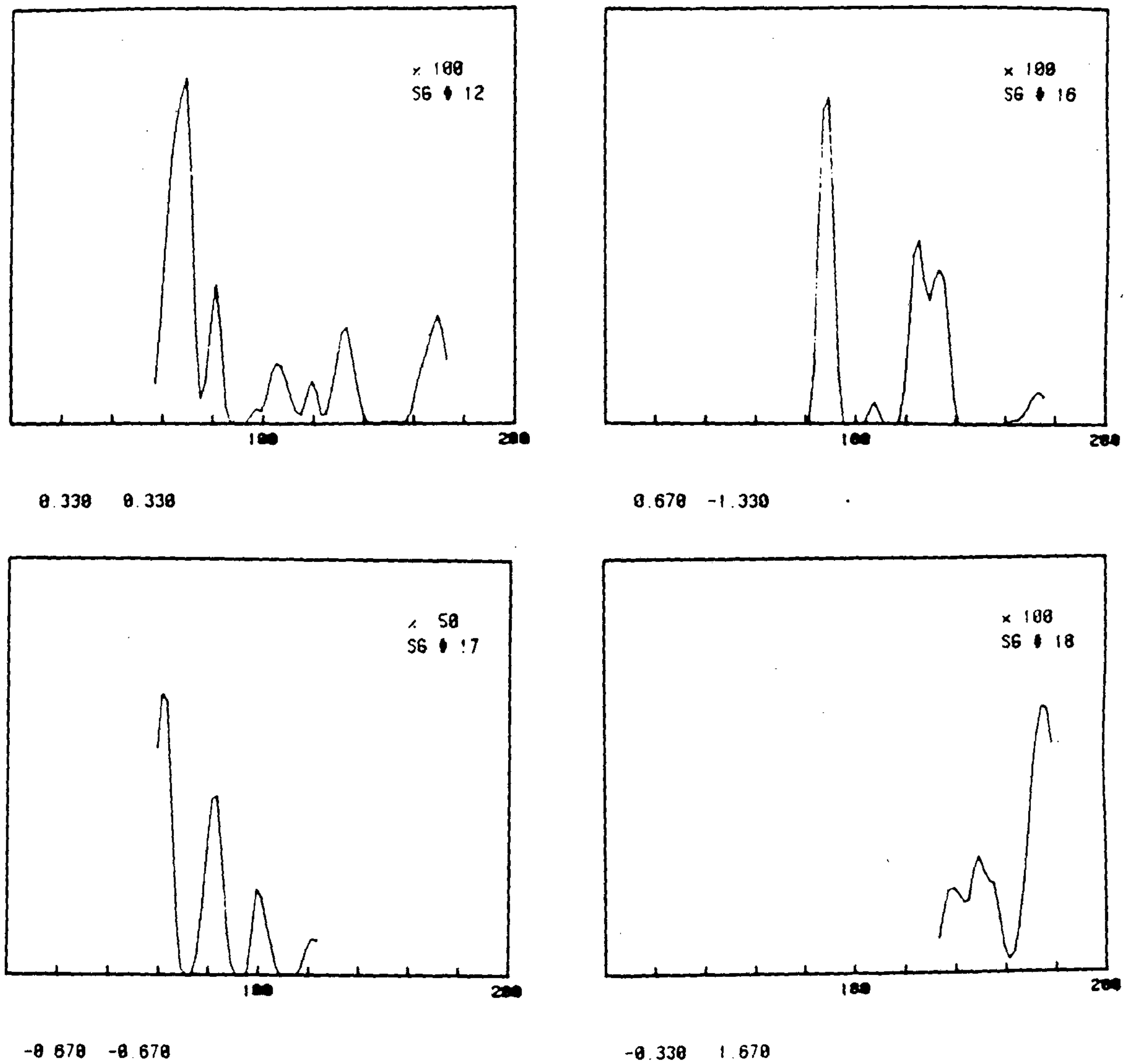

XBL 888-2895

[Fig. 5-4] (continued)

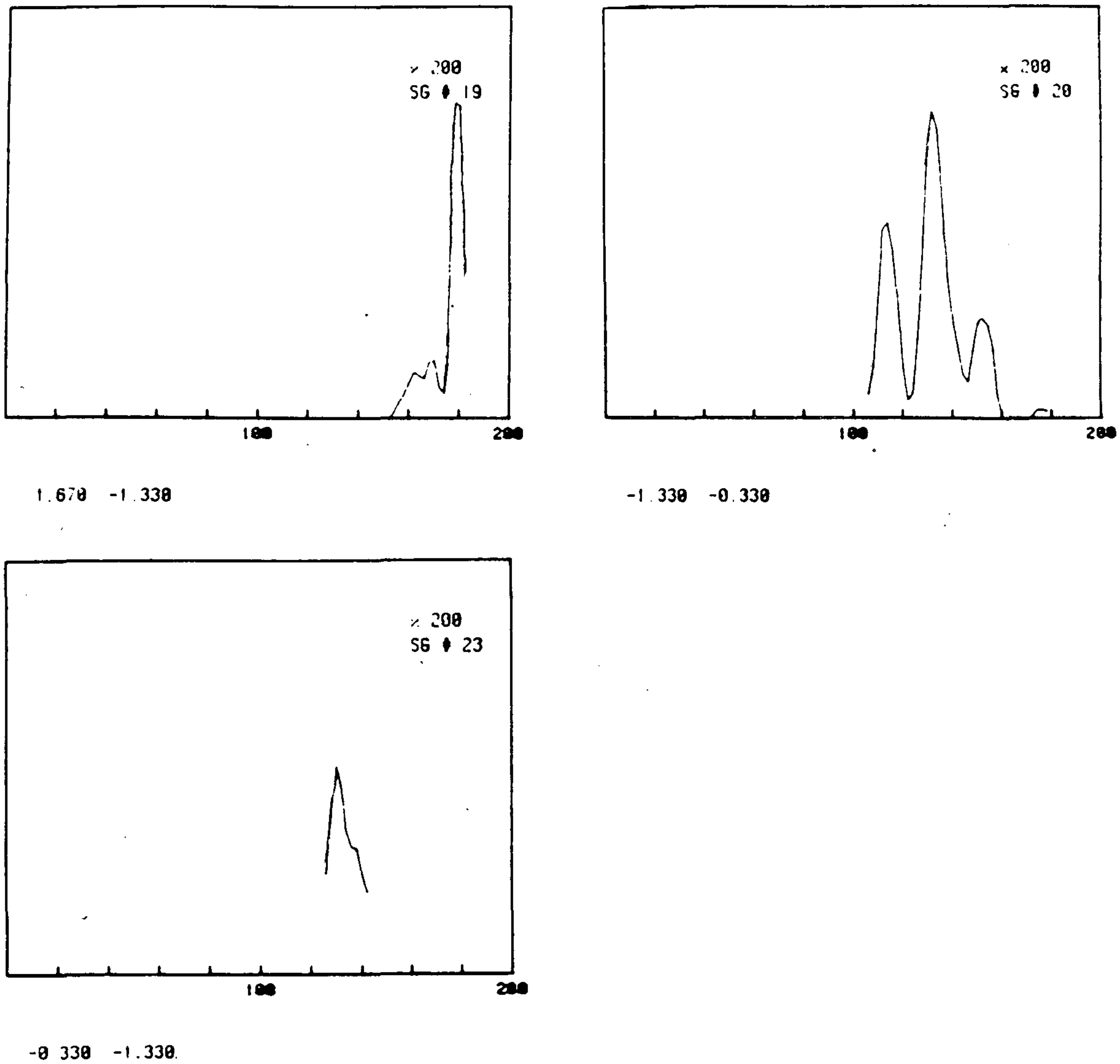

XBL 888-2896

[Fig. 5-4] (continued)

5.3. Theory

We have chosen established multiple-scattering methods to calculate LEED intensities.[29] For most trial structures Renormalized Forward Scattering was used to stack the metal layers and the separate C and O overlayers. To investigate possible CO-induced lateral distortions of the topmost metal layer as well as short C-O distances, the Combined Space Method was applied. The C, O, and topmost metal atoms were treated as a single composite layer with Matrix Inversion.

The phase shifts describing the electron scattering by palladium atoms were obtained from a band-structure potential,[30] used previously for LEED studies of Pd(100) and CO on Pd(100).[10,11] The CO scattering phase shifts are the same as used previously in studies of CO adsorbed on various metal surfaces.[1,2,3,9,10,11] The spherical-wave expansion was cut off at l_{max}=7, with the exception of the case of lateral substrate distortions, for which l_{max}=6 was used. The imaginary part of the muffin-tin potential was held constant at 5eV. The metal Debye temperature was uniformly chosen as the bulk value (270K), divided by 1.2 to represent enhanced surface vibrations. The C and O atoms were given the mean square vibration amplitudes of the bulk Pd atoms, multiplied by 2 to take a probable surface enhancement into account.

For the comparison between experiment and theory, a set of five R-factor formulas and their average was used, as described previously and used by us in many prior LEED analyses.[1,2,3]

5.4. Analysis and Results

We have examined a variety of adsorbed structures for CO in the $(\sqrt{3}x\sqrt{3})R30°$ unit cell as listed in Table 5-1 (additionally an hcp-terminated substrate was tested).

[Table 5-1] Test structures for Pd(111)-$(\sqrt{3}x\sqrt{3})R30°$-CO (the notation $x_1(\Delta x)x_2$ indicates a variation range x_1 to x_2 and a step Δx)

	Adsorption site	d_{C-O}(Å)	d_{Pd-C}(Å)	Δd_{12}(Å)	Δd_{23}(Å)	Δr^*(Å)
A	top	1.1(.1)1.4	1.7(.1)2.2	0.0	0.0	0.0
B	fcc-hollow	1.1(.1)1.4	1.2(.1)1.7	0.0	0.0	0.0
C	bridge	1.1(.1)1.4	1.3(.1)1.8	0.0	0.0	0.0
D	hcp-hollow	1.1(.1)1.4	1.2(.1)1.7	0.0	0.0	0.0
E	fcc-hollow	1.15	1.1(.1)1.4	−.2(.1).3	−.3(.1).1	0.0
F	fcc-hollow	1.15	1.1(.1)1.4	−.3(.1).2	−.4(.1)0.0	0.1,−0.1

* lateral displacement in the 1st layer Pd atoms (See Fig.5-7), including either expansion away from CO ($\Delta r>0$) or contraction toward CO ($\Delta r<0$)

They all assume one CO molecule per unit cell with C-O axis perpendicular to the surface. For the first set of analyses (A,B,C,D), the ideal substrate structure was assumed and the CO adsorption sites, the carbon-oxygen bond length, and the perpendicular metal-carbon distance were varied independently. The favored structure among these has CO at a fcc hollow site with a carbon-oxygen bond length of ~1.1Å and a perpendicular metal-carbon distance of ~1.3Å; this was found with both the normal-incidence data and the off-normal-incidence data. The results of these analyses are shown in Table 5-2.

[Table 5-2] R-factor comparison for CO adsorbed at different sites, keeping the substrate bulk-like. (the best geometry here is not interpolated between calculated grid points)

model		Best geometry		5-Average R-Factor
		d_{C-O}(Å)	d_{Pd-C}(Å)	
A	top	1.4	2.0	0.4123
B	fcc-hollow	1.1	1.3	0.3004
C	bridge	1.1	1.7	0.3771
D	hcp-hollow	1.2	1.6	0.4127

Finally, in trial(F), we allowed a lateral displacement of the atoms in the 1st substrate layer to investigate the possibility of a CO-induced metal reconstruction. The displacements were made compatible with the $(\sqrt{3}x\sqrt{3})R30°$ unit cell and kept of the highest symmetry, as illustrated in Fig. 5-7. Such displacements, however, worsened the R-factor ($\Delta R \sim 0.1$ for a displacement of $\Delta r = 0.1$Å). After settling the CO adsorption site to fcc-hollow, we used the normal incidence data to examine possible substrate relaxations, since we had observed a slight relaxation for the clean Pd(111) surface. The theoretical I-V curves near the optimal structure are plotted against experimental I-V curves in Fig. 5-5. The theoretical curves at the upper column are based on the model of CO on ideal Pd(111), and the theoretical curves at the lower column are based on the model of CO on the slightly relaxed Pd(111) [See Table 5-3]. The changes of the perpendicular interlayer spacings of the Pd(111) substrate improved the R-factor. R-factor contour plots for these analyses (trial E) are presented in Fig. 5-6. (The minimum R-factor values in these contour plots are higher than ones shown in Table. 5-2, since a different approximation scheme has been employed.)

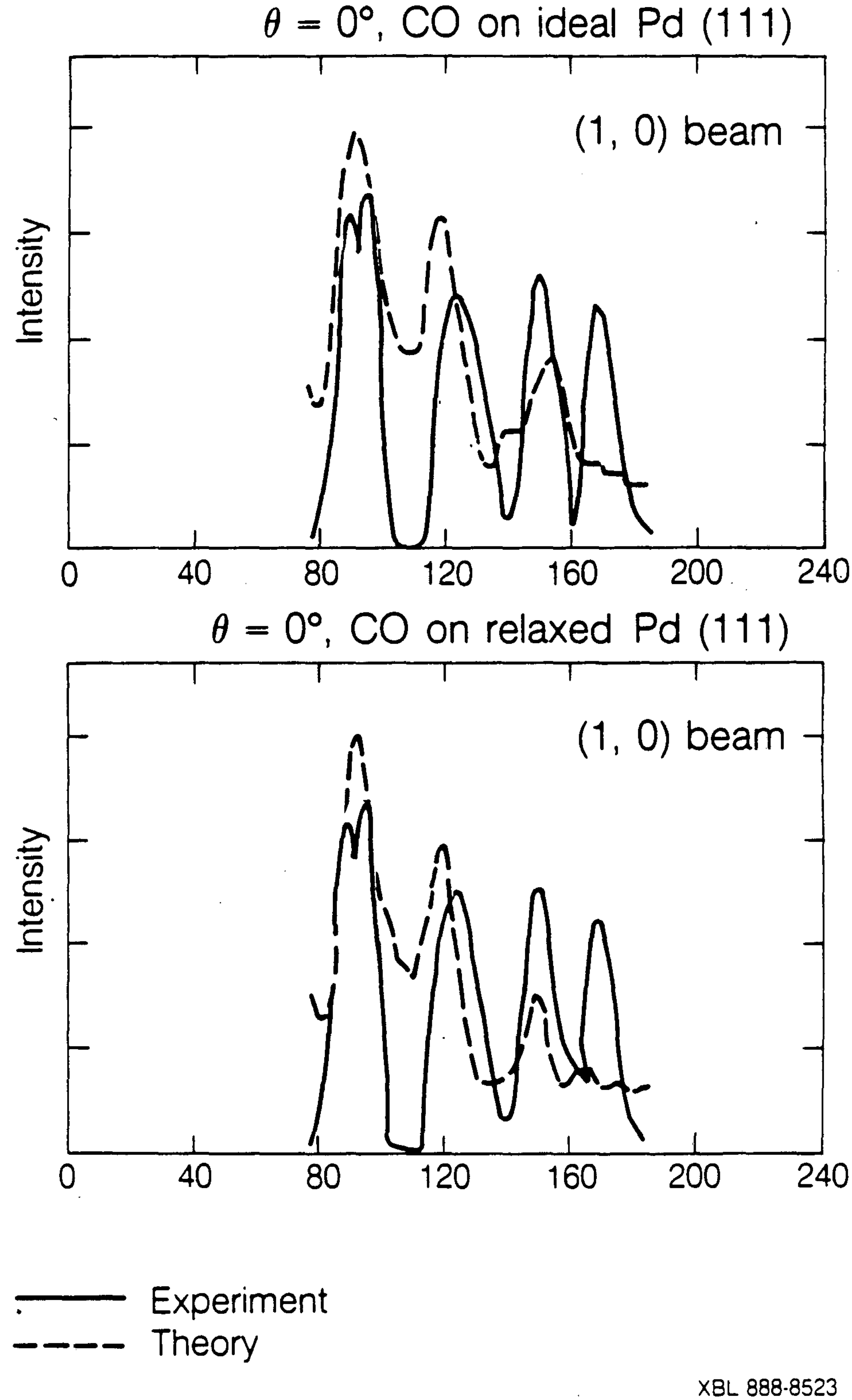

[Fig. 5-5] Selected calculated LEED I-V curves at normal incidence for Pd(111)-($\sqrt{3}$x$\sqrt{3}$)R30°-CO for a structure near the minimum R-Factor, together with experimental I-V curves.

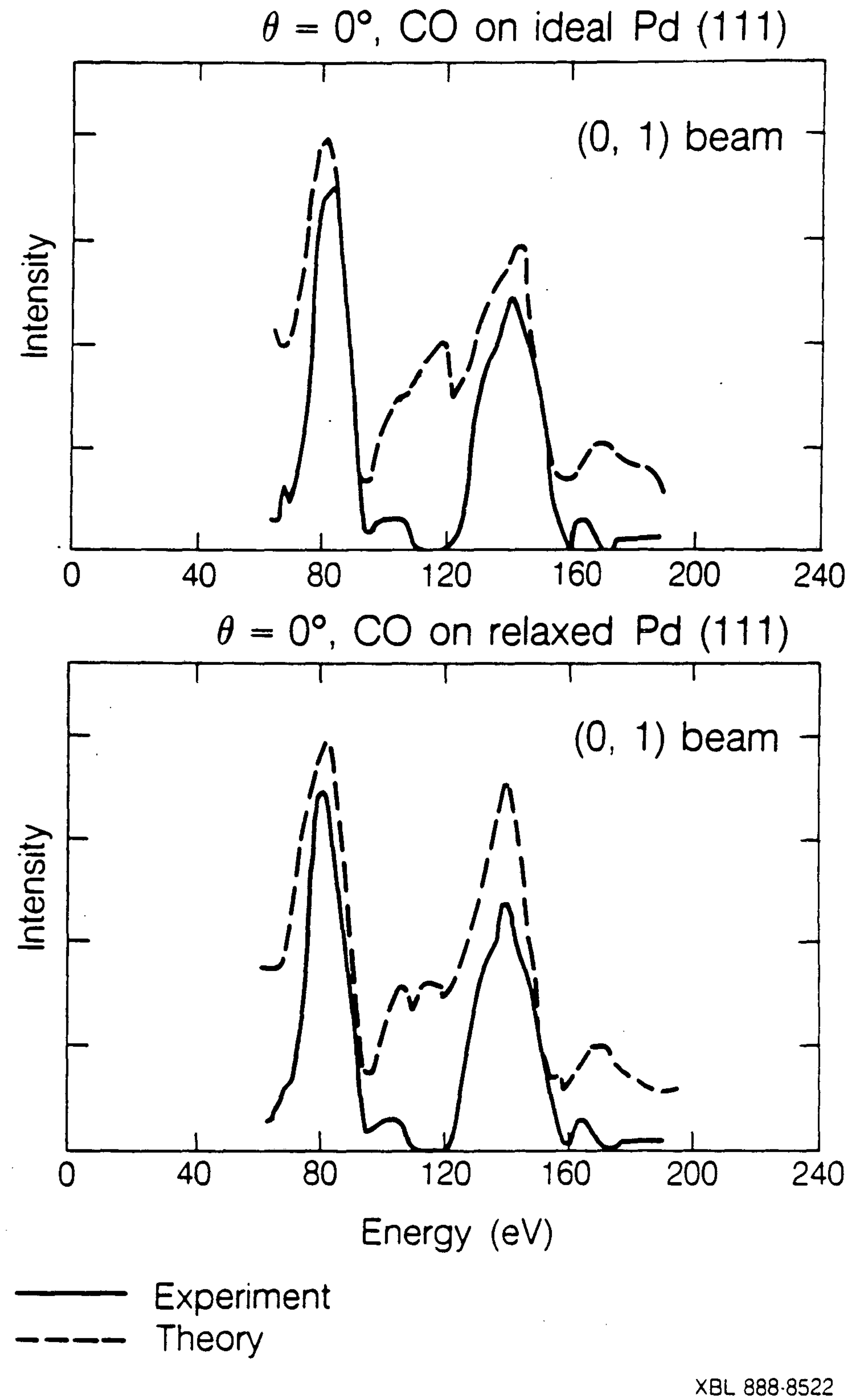

[Fig. 5-5] (continued)

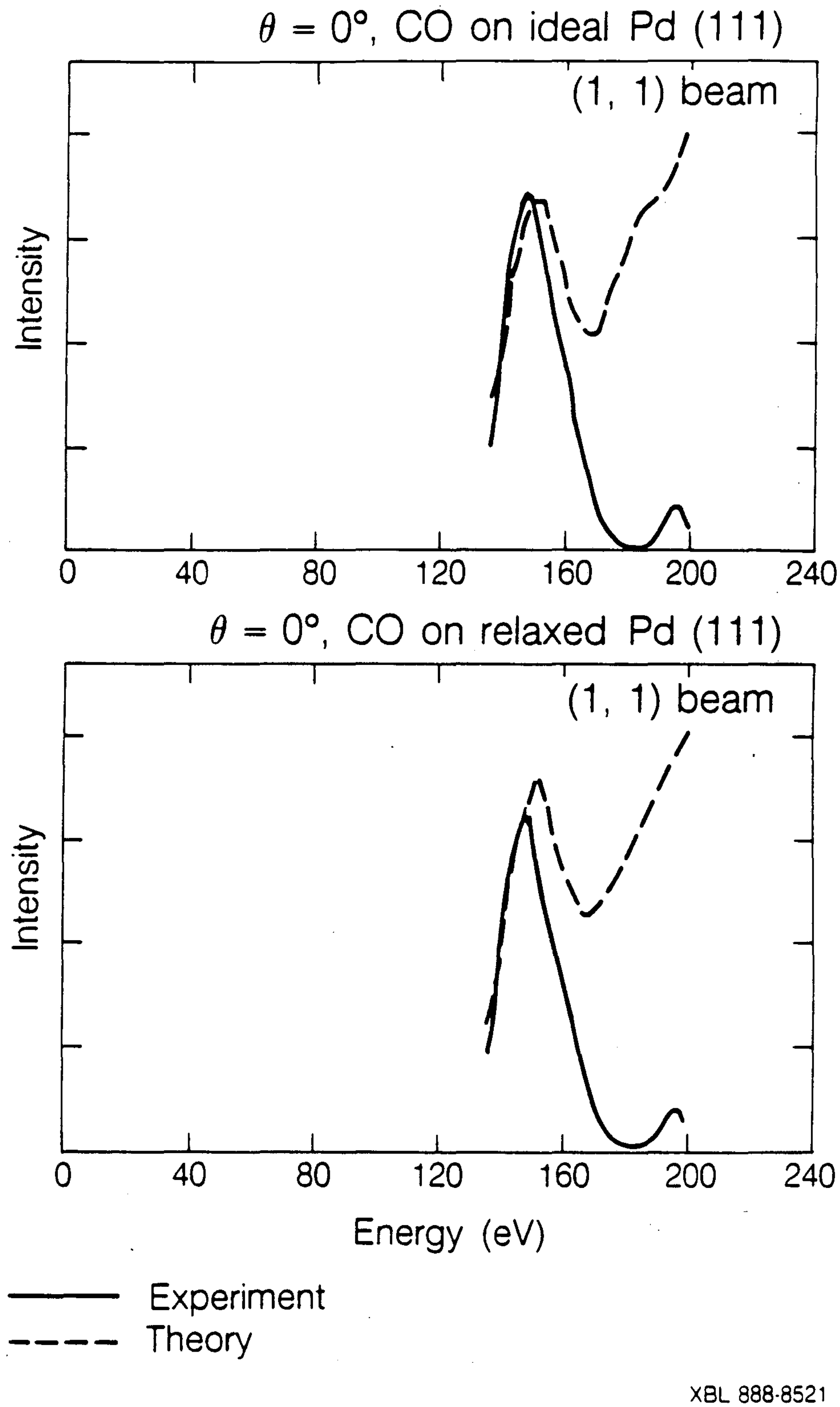

[Fig. 5-5] (continued)

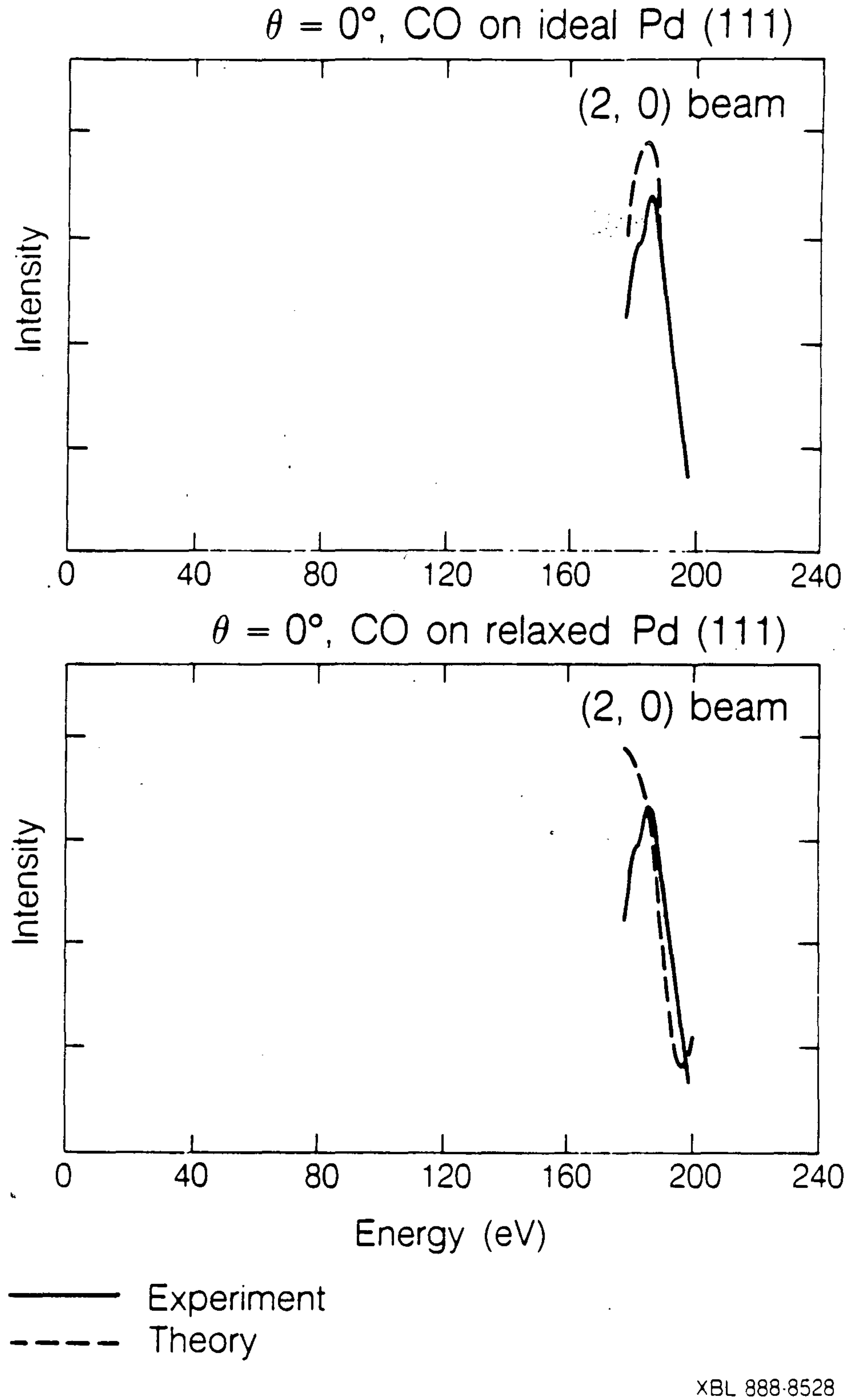

[Fig. 5-5] (continued)

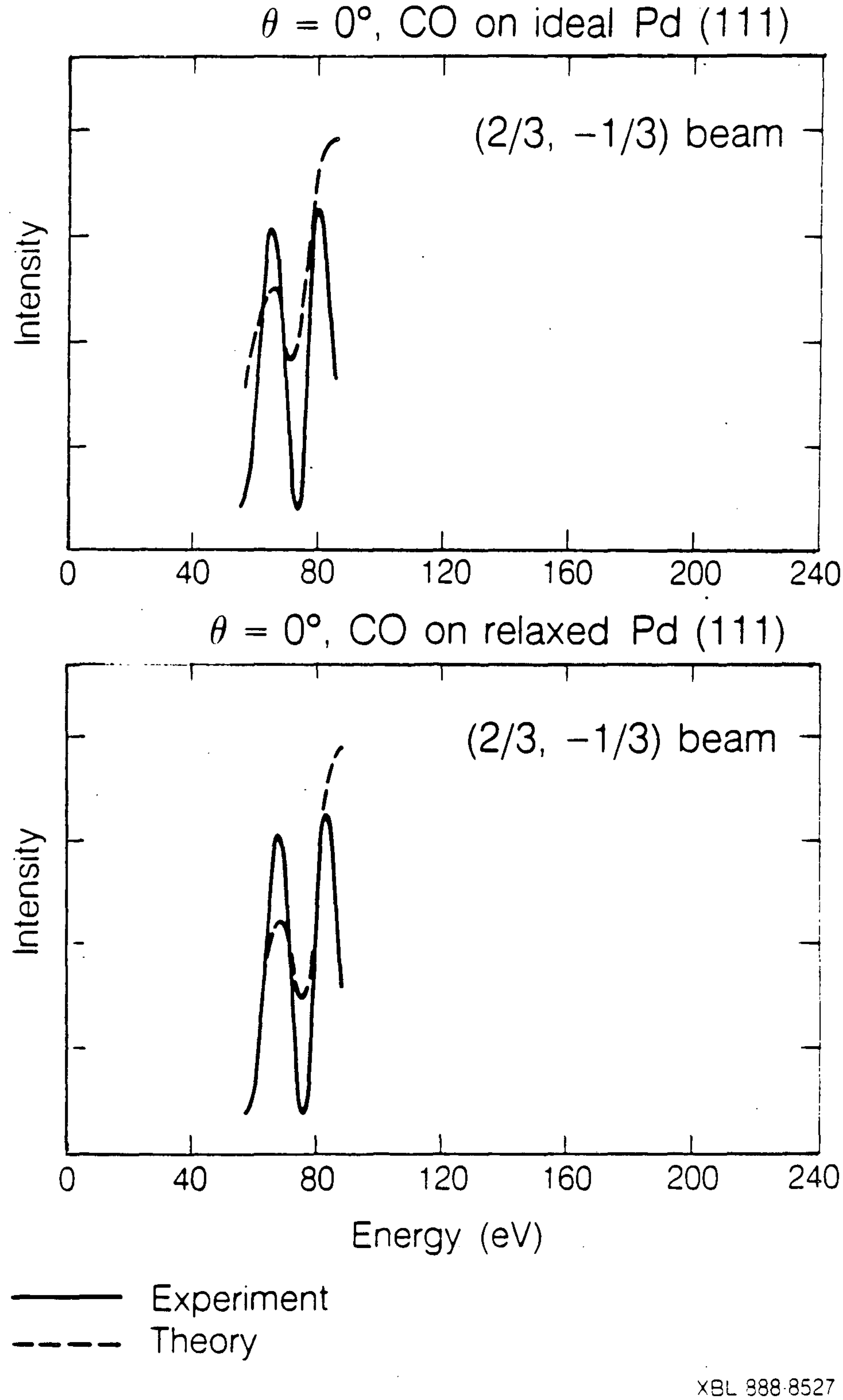

[Fig. 5-5] (continued)

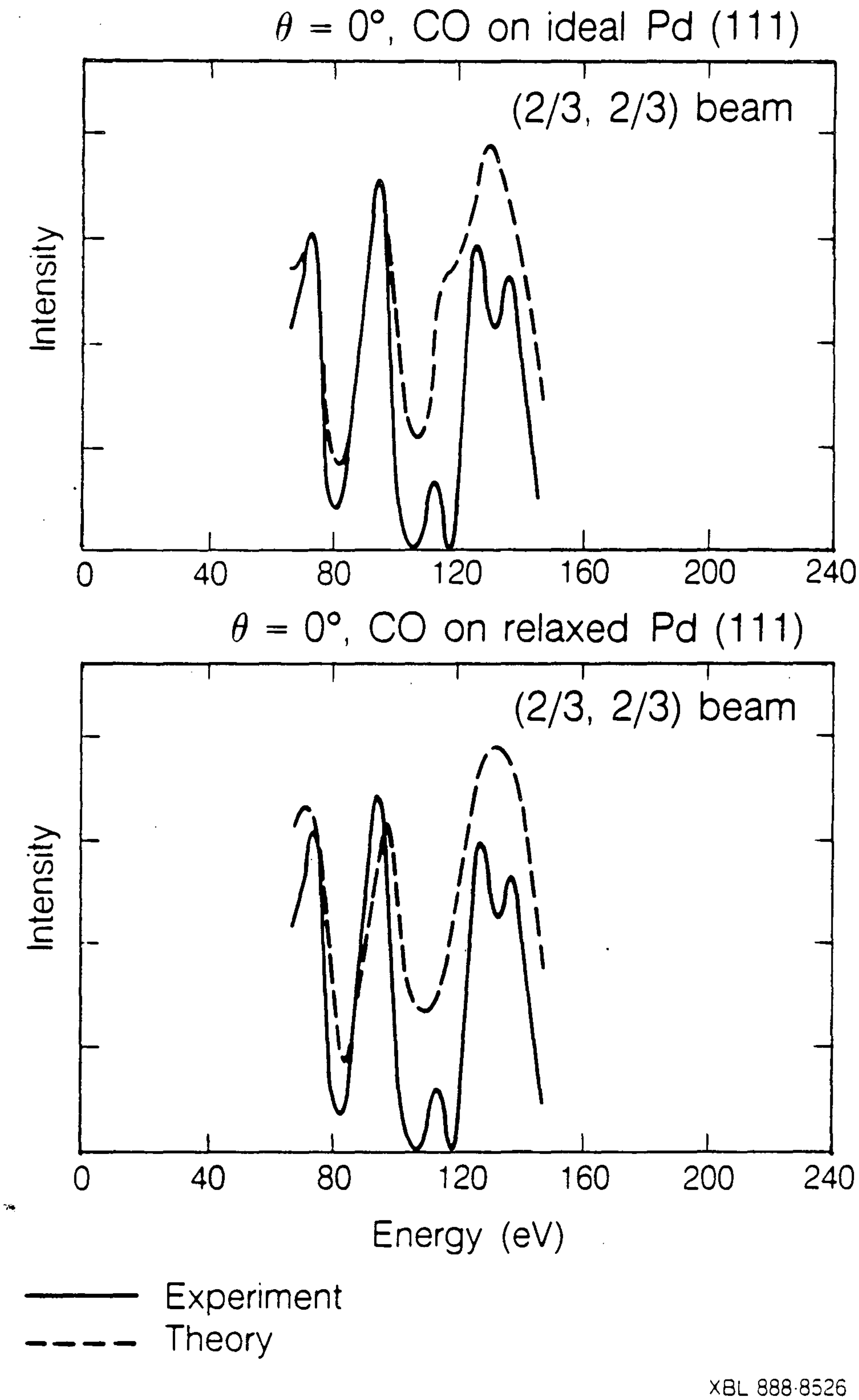

[Fig. 5-5] (continued)

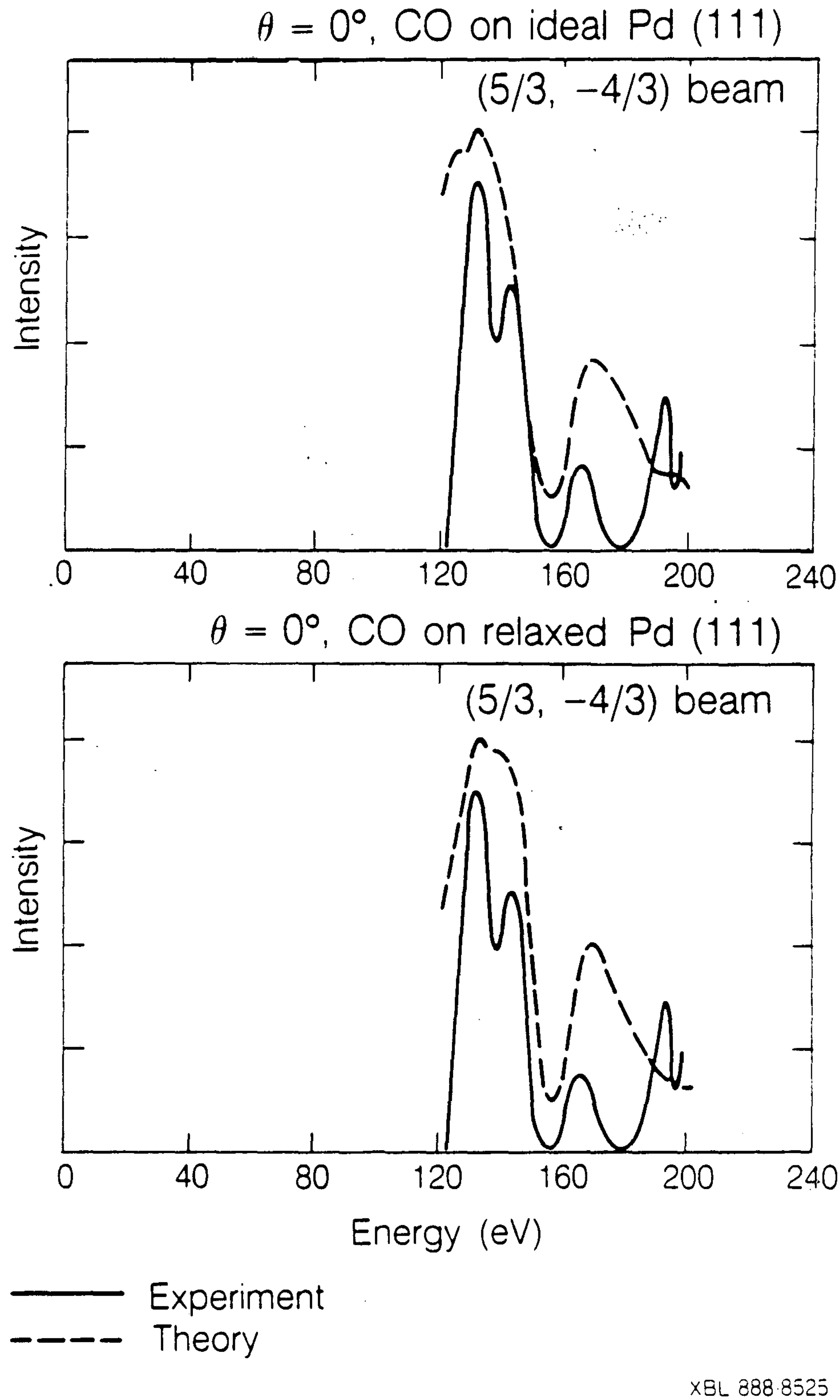

[Fig. 5-5] (continued)

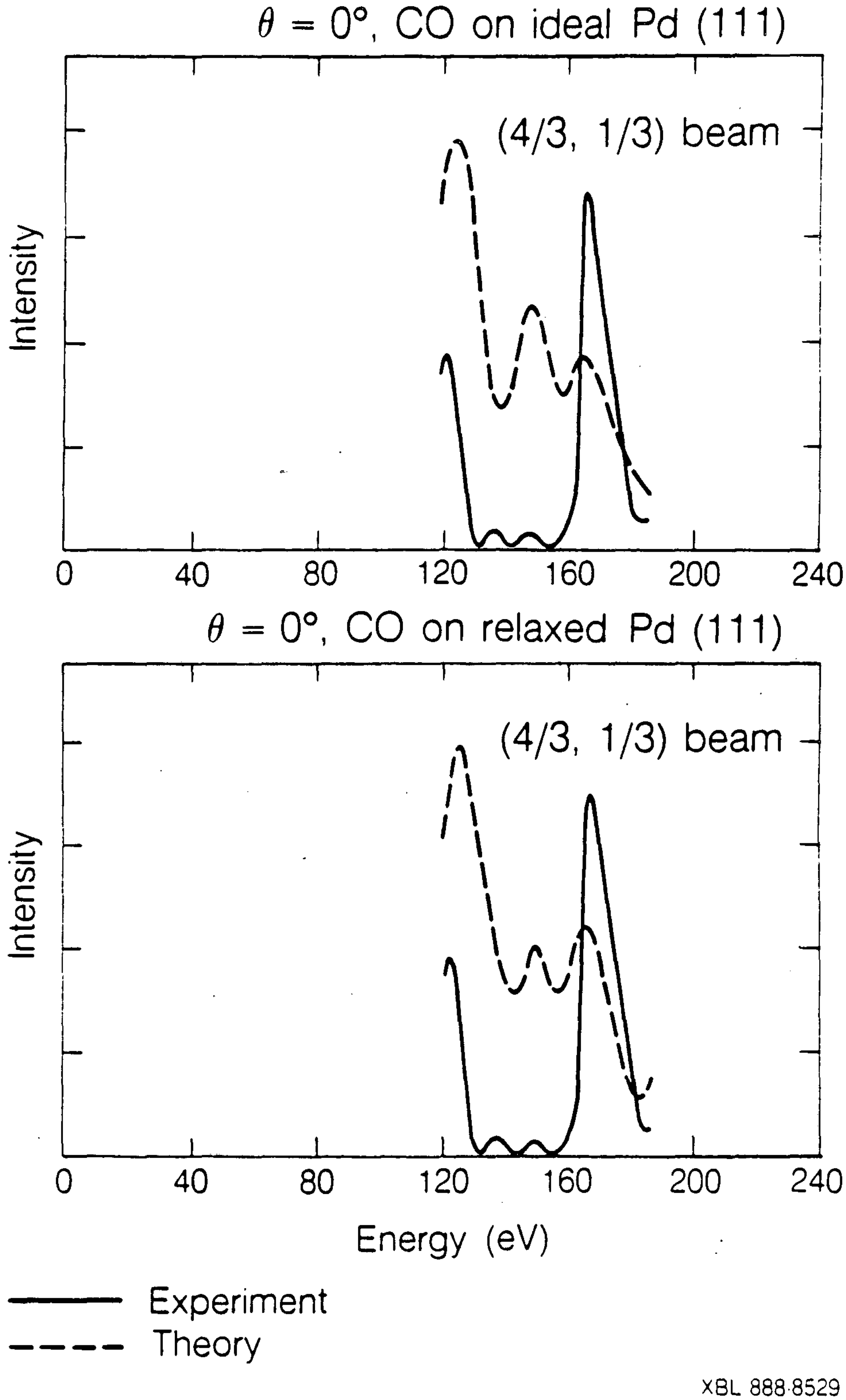

[Fig. 5-5] (continued)

[Table 5-3] Structure models corresponding to the theoretical I-V curves shown in Fig. 5-5.

	Model	Muffin-tin Zero	5-Average R-Factor
Fig. 5-5 (Upper)	fcc-hollow d_{Pd-C}=1.3Å d_{C-O}=1.1Å Ideal Pd(111)	V_0=8eV	0.3004
Fig. 5-5 (Lower)	fcc-hollow d_{Pd-C}=1.3Å d_{C-O}=1.1Å Relaxed Pd(111) (Δd_{Pd-Pd}=+0.10Å for all the layers)	V_0=6eV	0.2971

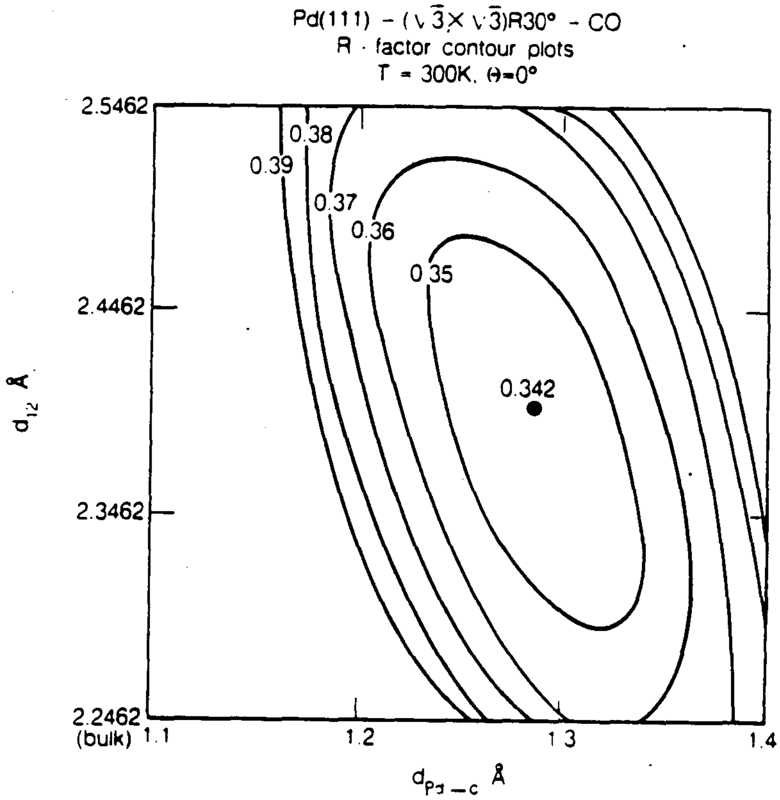

[Fig. 5-6] Contour plots for the five-R-factor average as a function of two of the structural parameters for Pd(111)-($\sqrt{3}$x$\sqrt{3}$)R30°-CO. The best R-factor value shown here is larger than the best R-factor value quoted in the text, because the contour plots are based on an approximation that allows lateral metal distortions. (a) The parameters used are the perpendicular distance between the top-layer Pd atoms and the fcc-hollow site carbon atoms (d_{Pd-C}), and the interlayer spacing between the 1st and 2nd Pd layers (d_{12}). The C-O bond length was held at 1.15Å for this plot.

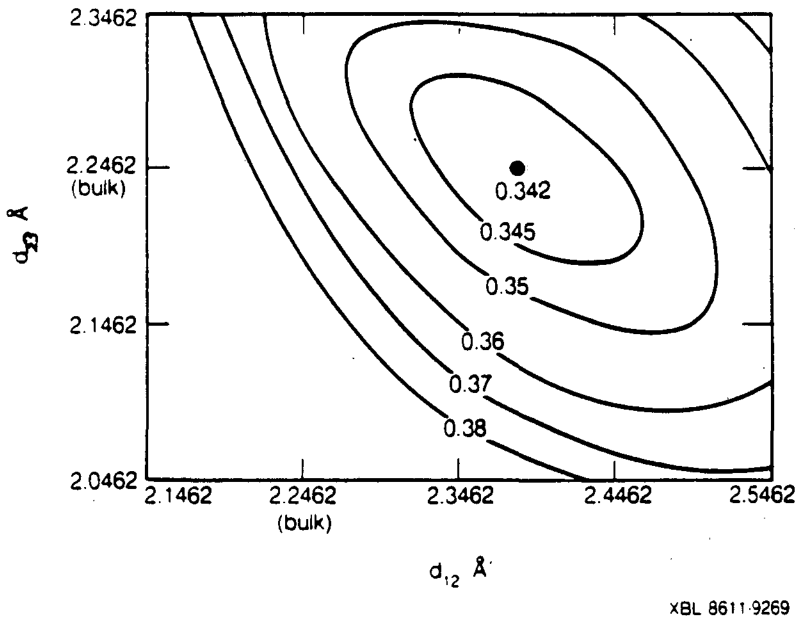

[Fig. 5-6] (continued) (b) The parameters used are the interlayer spacing between the 1st and 2nd Pd layers (d_{12}), and that between the 2nd and 3rd Pd layers (d_{23}). The perpendicular Pd-C distance d_{Pd-C} and the C-O bond length were held at 1.30Å and 1.15Å, respectively, for this plot.

Consequently, the LEED comparisons strongly favor the fcc-hollow site for CO adsorbed on an unreconstructed Pd(111) substrate. The optimal structural parameters are: C-O bond length d_{C-O} of 1.15±0.05Å, perpendicular metal-carbon distance d_{Pd-C} of 1.29±0.05Å (i.e. metal-carbon bond length b_{Pd-C} of 2.05 ± 0.04 Å), interlayer spacing between 1st and 2nd metal layers (d_{12}) of 2.3862±0.05Å (Δd_{12}= +0.14±0.05Å), and interlayer spacing between 2nd and 3rd layers (d_{23}) of 2.2462±0.05Å (Δd_{23}= 0.00±0.05Å). The optimal muffin-tin zero level, assumed layer-independent, is found to be 6±1eV below vacuum. The minimized value of the five-R-factor average is 0.30, while the corresponding Zanazzi-Jona and Pendry R-factor values are 0.56 and 0.55 (using the normal-incidence data only). Although the final R-factor values are too high to call the structure solved, they are closely comparable to values obtained for some other structures analyzed recently: for example, Pt(111)-c(4x2)-2CO[1] with R(average)=0.29, R(Zanazzi-Jona)=0.50, R(Pendry)=0.61, and Rh(111)-c($2\sqrt{3}$x4)*rect*-C_6H_6+CO[15] with R(average)=0.31, R(Zanazzi-Jona)=0.40, R(Pendry)=0.66. In view of our extensive database and the many structural models tested, we feel that we have identified the major ingredients of this structure.

5.5. Discussion

Our analysis has found the adsorption site of CO to be the fcc-hollow site. The optimal interlayer spacings and bond lengths are:

$$d_{C-O} = 1.15\AA \pm 0.05\AA$$

$$d_{Pd-C} = 1.29\AA \pm 0.05\AA$$

$$b_{Pd-C} = 2.05\AA \pm 0.04\AA$$

$$\Delta d_{12} = +0.14 \pm 0.05\AA \quad [+6.2 \pm 2.2\%]$$

$$\Delta d_{23} = 0.00 \pm 0.05\AA \quad [0.0 \pm 2.2\%]$$

5.5.1. Adsorption Site

The binding site which we obtain for a third of a monolayer of CO adsorbed on Pd(111), namely the hollow site, confirms the expectations based on vibrational spectroscopy.[12,13] We have no evidence of the mixture of domains of bridge-site CO and hollow-site CO which has been proposed based on SIMS data.[20]

The bonding of CO to transition metal surfaces can be explained by the donation-backdonation model originally proposed by Blyholder[31] : the CO 5σ orbitals donate electrons to the metal and the metal back-donates electrons to the CO $2\pi^*$ orbitals. Theoretical investigations to explain the stability of CO adsorbed at a hollow site of Pd(111) using quantum mechanical calculations have been pursued recently. Anderson *et al.*[32] have compared the chemisorption property of CO on palladium and platinum, and have proposed that the higher position of the Pd valence band compared to that of Pt, and the consequent enhancement of the backdonation, are responsible for CO on Pd(111) preferring hollow-site adsorption. More recently, Van Santen[33] has suggested that the d-band half-width is also an important factor affecting the CO adsorption site. Palladium has a d-band half-width of 2.93eV, which is narrower than that of Pt or Rh, both of which favor top-site adsorption of CO. The narrower d-band implies a decreased interaction between CO and palladium d electrons. Both the higher position of the valence band and the narrower d-band half-width for palladium seem to enhance the CO bonding in highly coordinated sites.

Total-energy calculations show little difference in binding energy between the two types of hollow sites on Pt(111)[34] ; the same holds presumably also on Pd(111). Nevertheless, the LEED result clearly shows a preference for the fcc-type hollow site. A fcc-type hollow site is located right overhead of a octahedral subsurface site where, as we mentioned before, hydrogen may sit. There may thus be a correlation between CO and hydrogen subsurface sites.

5.5.2. Bond Lengths

There is a correlation between the bond lengths of adsorbed CO and the adsorption sites, as reported by D.F. Ogletree *et al.*[1] based on LEED data: both M-C bond lengths and C-O bond lengths increase as the metal coordination number increases. Our data for CO on Pd(111) fit this scheme. Also, the Pd-C and the C-O bond lengths obtained agree well with the values found for the face-bridging CO in high-nuclearity metal carbonyl clusters[35] : the M-C and the C-O bond lengths range in such clusters from 2.00 to 2.23Å and from 1.15 to 1.21Å, respectively.

5.6. Conclusions

The structure of CO adsorbed at a coverage of 1/3 monolayer on Pd(111) has been analyzed. All CO molecules are favored to occupy fcc-type hollow sites with a $(\sqrt{3}x\sqrt{3})R30°$ surface periodicity. The C-O and Pd-C bond distances obtained agree well with the values for three-fold coordinated CO in high-nuclearity metal carbonyl clusters. The Structural result is shown in Fig. 5-7 and Table 5-4.

The Structure of Pd(111) – ($\sqrt{3}\times\sqrt{3}$)R30° – CO

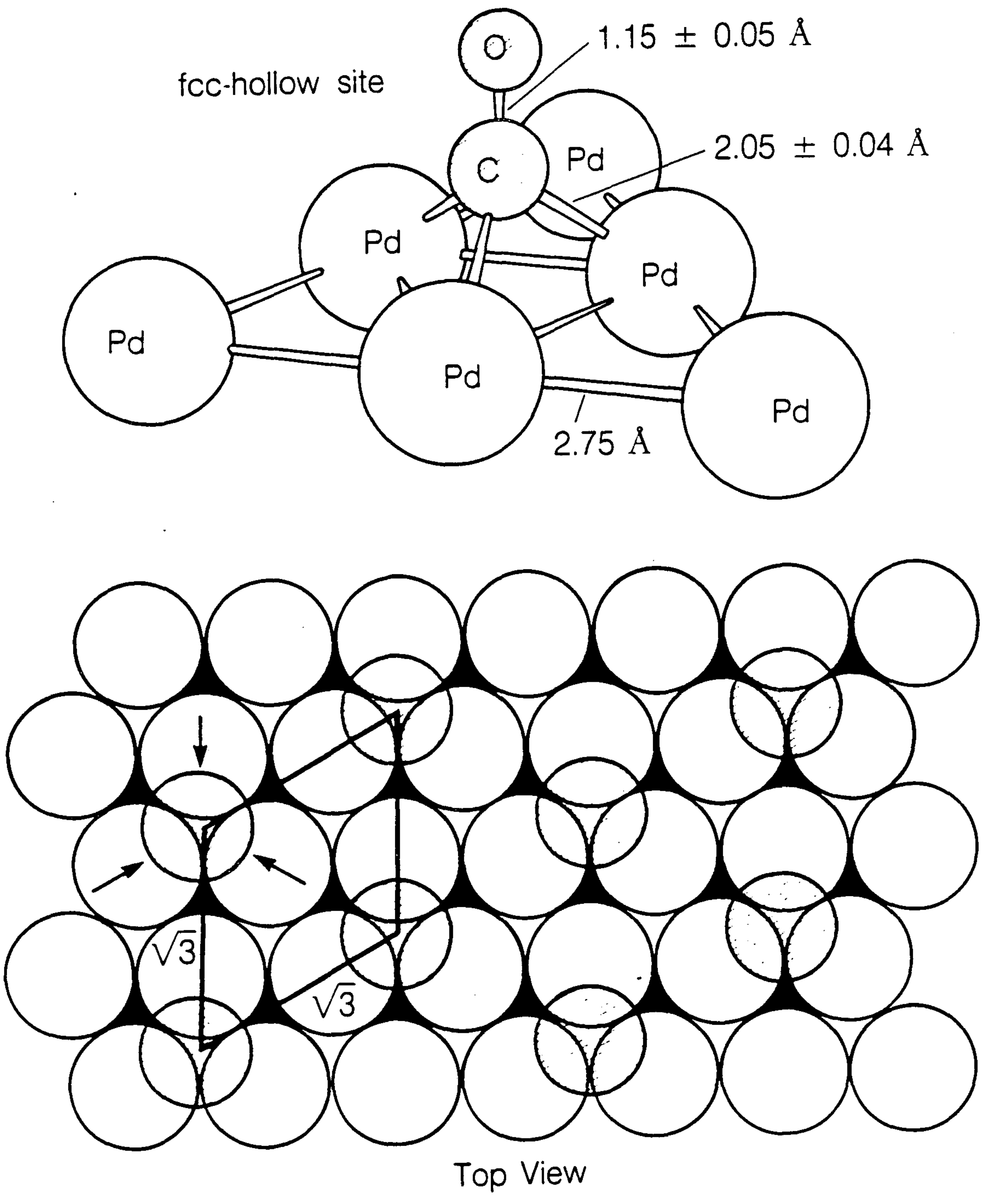

[Fig. 5-7] The optimum structure for CO in the ($\sqrt{3}\mathrm{x}\sqrt{3}$)R30° arrangement on the Pd(111) surface, as determined by dynamical LEED and R-factor analysis. The arrows in the top view indicate the lateral displacements of the Pd atoms which have been considered in the structure determination (see Table 5-1.F). The analysis showed, however, no indication of such displacement.

[Table 5-4] Structure Result in Format of Surface Crystallographic Information Service (SCIS)[36]

SURFACE: Substrate Face: Pd(111); Adsorbate CO;

Surface Pattern: $(\sqrt{3} x \sqrt{3})R30^\circ$, (2,1/1,2)

STRUCTURE: Bulk Structure: fcc; Temp: 300K; Adsorbate State: Molecular;

Coverage: 1/3 (CO/Pd)

REFERENCE UNIT CELL: a=4.76Å; b=4.76Å; A(a,b)=120°

Layer	Atom	Atom Positions		Normal Layer Spacing
A1	O	0.0	0.0	1.15
A2	C	0.0	0.0	1.29
S1	Pd	0.3333	0.0	0.0
S2	Pd	0.0	0.3333	0.0
S3	Pd	0.6667	0.6667	2.39
S4	Pd	0.6667	0.0	0.0
S5	Pd	0.0	0.6667	0.0
S6	Pd	0.3333	0.3333	2.25

2D Symmetry: p3m1

Thermal Vibrations: Debye Temp=225K with double amplitude for surface atoms;

R-factor: R_{VHT}=0.30 R_{ZJ}=0.56 R_P=0.55

References

1. D. F. Ogletree, M. A. Van Hove, and G. A. Somorjai, *Surface Science*, vol. 173, p. 351, 1986.

2. R. J. Koestner, M. A. Van Hove, and G. A. Somorjai, *Surface Science*, vol. 107, p. 439, 1981.

3. M. A. Van Hove, R. J. Koestner, J. C. Frost, and G. A. Somorjai, *Surface Science*, vol. 129, p. 482, 1983.

4. G. Michalk, W. Moritz, H. Pfnur, and D. Menzel, *Surface Science*, vol. 129, p. 92, 1983.

5. S. Andersson and J. B. Pendry, *Physical Review Letters*, vol. 43, p. 363, 1979.

6. S. Andersson and J. B. Pendry, *Journal of Physics C*, vol. 13, p. 3547, 1980.

7. M. Passler, A. Ignatiev, F. Jona, D. W. Jepsen, and P. M. Marcus, *Physical Review Letters*, vol. 43, p. 360, 1979.

8. K. Heinz, E. Lang, and K. Müller, *Surface Science*, vol. 87, p. 595, 1979.

9. S. Y. Tong, A. Maldonado, C. H. Li, and M. A. Van Hove, *Surface Science*, vol. 94, p. 73, 1980.

10. R. J. Behm, K. Christmann, G. Ertl, M. A. Van Hove, P. A. Thiel, and W. H. Weinberg, *Surface Science*, vol. 88, p. L59, 1979.

11. R. J. Behm, K. Christmann, G. Ertl, and M. A. Van Hove, *Journal of Chemical Physics*, vol. 73, p. 2984, 1980.

12. A. M. Bradshaw and F. M. Hoffmann, *Surface Science*, vol. 72, p. 513, 1978.

13. F.M. Hoffmann and A. Ortega, *Proc. Intern. Conf. on Vibrations in Adsorbed Layers*, KFA Reports, 26, p. 128, Jülich, 1978.

14. C. M. Mate and G. A. Somorjai, *Surface Science*, vol. 160, p. 542, 1985.

15. M. A. Van Hove, R. F. Lin, and G. A. Somorjai, *Journal of the American Chemical Society*, vol. 108, p. 2532, 1986.

16. M. A. Van Hove, R. F. Lin, G. A. Blackman, and G. A. Somorjai, *Acta Crystallographica*, vol. B43, p. 368, 1987.

17. G. Ertl and J. Koch, *Z. Naturforsch.*, vol. 25a, p. 1906, 1970.

18. G. Ertl and J. Koch, in *Adsorption-Desorption Phenomena*, ed. F. Ricca, p. 345, Academic Press, New York, 1972.

19. H. Conrad, G. Ertl, and J. Küppers, *Surf. Sci.*, vol. 76, p. 323, 1978.

20. A. Brown and J.C.Vickerman, *Surf. Sci.*, vol. 124, p. 267, 1983.

21. A. Noordermeer, G.A. Kok, and B.E. Nieuwenhuys, *Surf. Sci.*, vol. 165, p. 375, 1986.

22. A. Noordermeer, G.A. Kok, and B.E. Nieuwenhuys, *Surf. Sci.*, vol. 172, p. 349, 1986.

23. F.P. Netzer and M.M. El Gomati, *Surf. Sci.*, vol. 124, p. 26, 1983.

24. J. P. Bibérian and M. A. Van Hove, *Surface Science*, vol. 138, p. 361, 1984.

25. R. Miranda, K. Wandelt, D. Rieger, and R.D. Schnell, *Surf. Sci.*, vol. 139, p. 430, 1984.

26. T. Engel and J. Chem. Phys., *69*, p. 373, 1978.

27. H. Conrad, G. Ertl, J. Küppers, S. W. Wang, K. Gérard, and H. Haberland, *Phys. Rev. Letters*, vol. 42, p. 1082, 1979.

28. D.R. Lloyd, C.M. Quinn, and N.V. Richardson, *Solid State Comm.*, vol. 20, p. 409, 1976.

29. M. A. Van Hove and S. Y. Tong, *Surface Crystallography by LEED,* Springer Verlag, Berlin, 1979.

30. V.L. Moruzzi, J.F. Janak, and A.R. Williams, in *Calculated Electronic Properties of Metals*, Pergamon, New York, 1978.

31. G. Blyholder, *J. Phys. Chem.*, vol. 68, p. 2772, 1964.

32. A.B. Anderson and M.K. Awad, *J. Am. Chem. Sci.*, vol. 107, p. 7854, 1985.

33. R.A. van Santen, *Faraday Symp. Chem. Soc.*, vol. 21 (paper 1), 1986.

34. N. K. Ray and A. B. Anderson, *Surface Science*, vol. 125, p. 803, 1983.

35. P. Chini, V. Longoni, and V. G. Albrano, *Advances in Organometallic Chemistry*, vol. 14, p. 285, 1976.

36. J.M. MacLaren, J.B. Pendry, R.J. Rous, D.K. Saldin, G.A. Somorjai, M.A. Van Hove, and D.D. Vvedensky, in *Surface Crystallographic Information Services: A Handbook of Surface Structures*, Reidel, Dordrecht, 1987.

6. Structure Determination of Pd(111)-(3x3)-C_6H_6+2CO with LEED and HREELS

6.1. Introduction

In this chapter, we describe how we have determined the structure of a complex coadsorbed molecular overlayer of benzene and CO on Pd(111) crystal surface using both HREELS and LEED*. In short, HREELS has been utilized to identify the surface species and their approximate orientation followed by a dynamical LEED analysis. For the LEED analysis, we have utilized the Beam Set Neglect approximation in order to manipulate complex molecular overlayer structures with large unit cells.[1] Using this scheme, three structures of benzene coadsorbed with CO on Pt(111)[2] and Rh(111)[3,4] have been analyzed previously [Fig. 6-1]. These systems may be labeled:

I. Pt(111)-($2\sqrt{3}$x4)*rect*-2C_6H_6 + 4CO

II. Rh(111)-c($2\sqrt{3}$x4)*rect*-C_6H_6 + CO

III. Rh(111)-(3x3)-C_6H_6 + 2CO

* Some part of this chapter has been published in the following articles:
H. Ohtani, M. A. Van Hove, and G. A. Somorjai, J. Phy. Chem. **92**, 3974 (1988) (LEED structure determination).
H. Ohtani, B. E. Bent, C. M. Mate, M. A. Van Hove, and G. A. Somorjai, Applied Surface Science, **33**, 254 (1988) (HREELS).

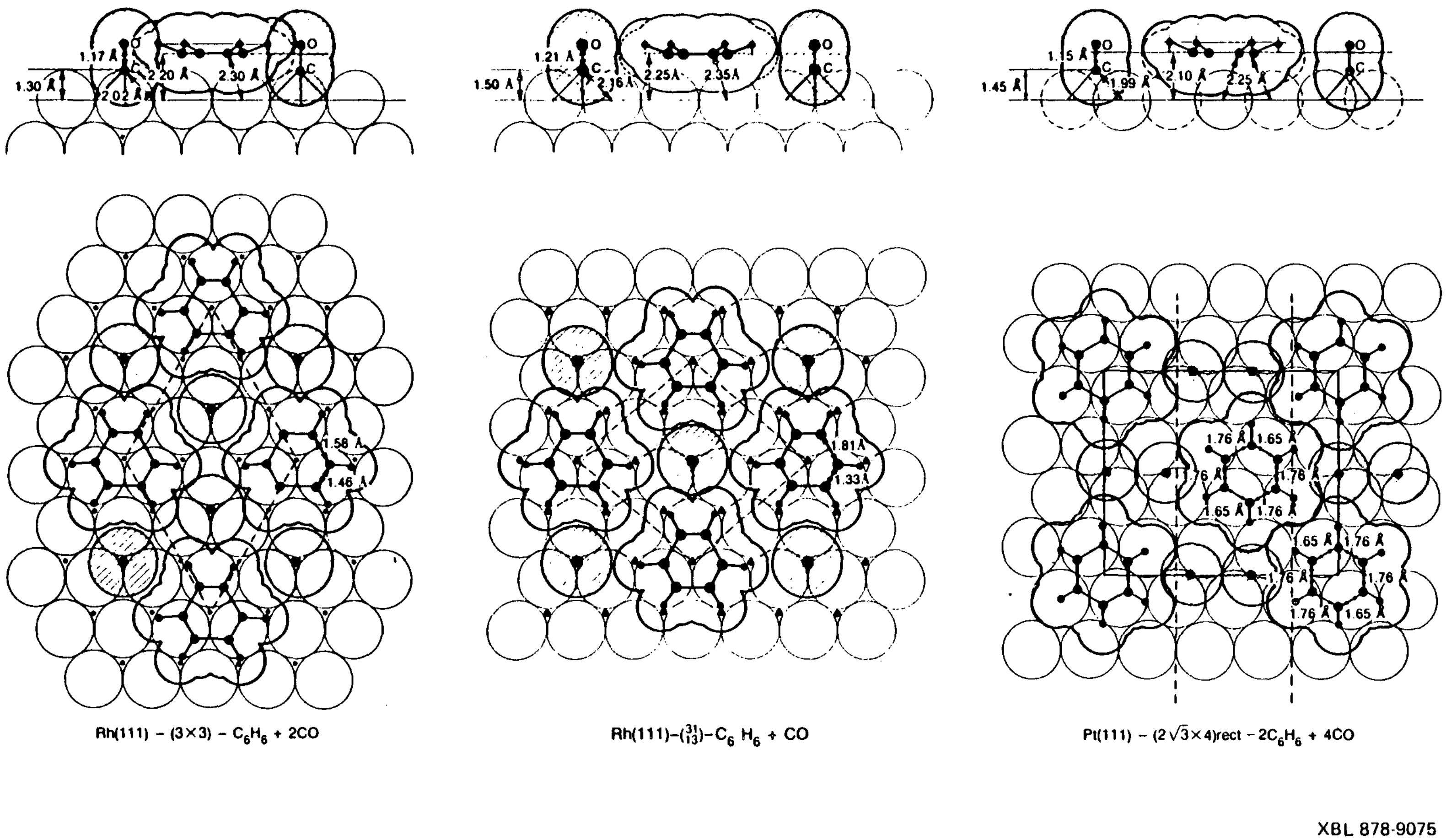

[Fig. 6-1] Coadsorption structures of benzene and CO on Rh(111) and Pt(111) determined by LEED[3,4,2]

In these cases, CO was necessary as the background gas to induce the formation of stable ordered superlattices of benzene and CO.[5] (Benzene alone forms only a disordered overlayer on Pt(111). On Rh(111) a $(\sqrt{3}x3)$-*rect*-$2C_6H_6$ ordered superstructure can be formed, but this structure is unstable under electron-beam irradiation and also easily contaminated by background CO gas to transform into the coadsorbed superstructures mentioned above.) These structure analyses[2,3,4] have confirmed that the benzene molecules are associatively adsorbed parallel to the surface. Furthermore, in all cases, significant C_6 ring expansions have been revealed compared to the gas phase benzene structure, as well as C-C bonds of unequal lengths within each C_6 ring skeleton. These results prompted us to study the structure of benzene on a third metal, Pd(111), which has the unique property to catalyze acetylene trimerization to form benzene.[6,7,8,9,10,11,12,13]

The adsorption properties of benzene on Pd(111) have been extensively studied with various surface science techniques, including Angle Resolved Ultraviolet Photoelectron Spectroscopy (ARUPS),[14,15] Angle Integrated Ultraviolet Photoemission Spectroscopy (UPS),[6] Metastable Noble Gas Deexcitation Spectroscopy (MDS),[6] Thermal Desorption Spectroscopy (TDS),[6,7,9,12,13] Electron Energy Loss Spectroscopy (EELS),[15] and High Resolution Electron Energy Loss Spectroscopy (HREELS).[11,16,17,18] These studies have indicated that benzene molecules are adsorbed parallel to the Pd(111) surface, bonding through the π electrons at room temperature, like benzene on many other transition metals. HREELS showed an increase of the γ_{CH} out-of-plane bending frequency of adsorbed benzene on

Pd(111) surface from the gas phase value. This shift is, however, much smaller than on Rh(111),[19] or Pt(111),[20] indicating that the structure of benzene on Pd(111) is closer to the gas phase structure, perhaps due to a weaker benzene-Pd(111) interaction. The ARUPS[16] data suggest that the benzene-Pd(111) complex has C_{6v} symmetry although no bond length information has been obtained.

The conversion of acetylene to benzene can proceed under UHV conditions as well as under high-pressure conditions on palladium single-crystal surfaces. This reaction is structure sensitive. The Pd(111) surface is effective under UHV conditions, while both the Pd(111) and Pd(100) are most effective under high pressure conditions[13]. Our structural LEED work on the benzene/Pd(111) system aims at understanding this reaction at a molecular level.

Ordering of the surface structure facilitates the LEED structure analysis. But at no coverage near or above room temperature could we produce an ordered superstructure of pure benzene on Pd(111). In analogy with the situation on Rh(111) and Pt(111), we coadsorbed CO and obtained one well-ordered superlattice, as described in more detail in the next section. The LEED analysis confirmed a parallel adsorption geometry of benzene centered over 3-fold fcc-type hollow site of Pd(111), with little distortion of the C_6 ring. The benzene molecules are interspersed with CO standing perpendicularly to the surface at 3-fold fcc-type hollow sites.

6.2. Sample Preparation

The Pd(111) crystal was cleaned with the same method described in Chapter 4 and 5. Spectroscopic-grade benzene was introduced into a glass and stainless-steel gas manifold. The benzene sample was degassed by freezing the sample, pumping over it and then thawing the sample. This procedure was repeated several times. Benzene was introduced into the UHV chamber through a leak valve and a stain-less doser tube 0.15mm in diameter. (The vapor pressure of benzene at room temperature is ~ 100 torr.)

When the Pd(111) sample was exposed to several Langmuirs (L) of benzene to form a saturated monolayer at room temperature, only fuzzy ring-like LEED patterns were seen around the integral order spots, indicating that the benzene overlayer was disordered. We tried different surface coverages, and also annealed below ~150C (where benzene starts to decompose), but found no ordered super-lattice.

Since CO helps to form ordered overlayers on the Rh(111) and Pt(111) surfaces, we applied the same approach to the benzene/Pd(111) system. It was difficult, however, to produce ordered surface structures on Pd(111). We have observed some LEED features by coadsorbing CO, but these were not well resolved and not fully understood [Fig. 6-2-A,B,C]. After many trials of dosing benzene and CO, we finally found a reproducible ordered (3x3) structure. The sharp (3x3) structure appeared only after a large exposure of benzene and CO. Occasional heating of the crystal up to 100C *during* the synthesis seemed to help ordering. However the final (3x3) structure was disordered by heating to 100C. Otherwise, it was stable enough to remain for weeks in the UHV chamber.

The (3x3) superstructure used in this LEED study was produced by the following procedure:

I. Exposure to 0.5L of CO at room temperature: a weak $(\sqrt{3}x\sqrt{3})R30°$-CO pattern is visible. (Exposures quoted in langmuirs have not been corrected for ion-gauge sensitivity.)

II. Exposure to 3L of benzene at room temperature: the LEED exhibits a disordered ring-like pattern.

III. Alternate dosage of benzene and CO for a total exposure of 170L and 12L, respectively, including annealing at 100C for several times: 6 spots appear around integral spots.

IV. Exposure to 120L of benzene: the (3x3) pattern starts to form.

V. Exposure to 240L of benzene: a sharp (3x3) LEED pattern is observed, as illustrated in Fig. 6-3.

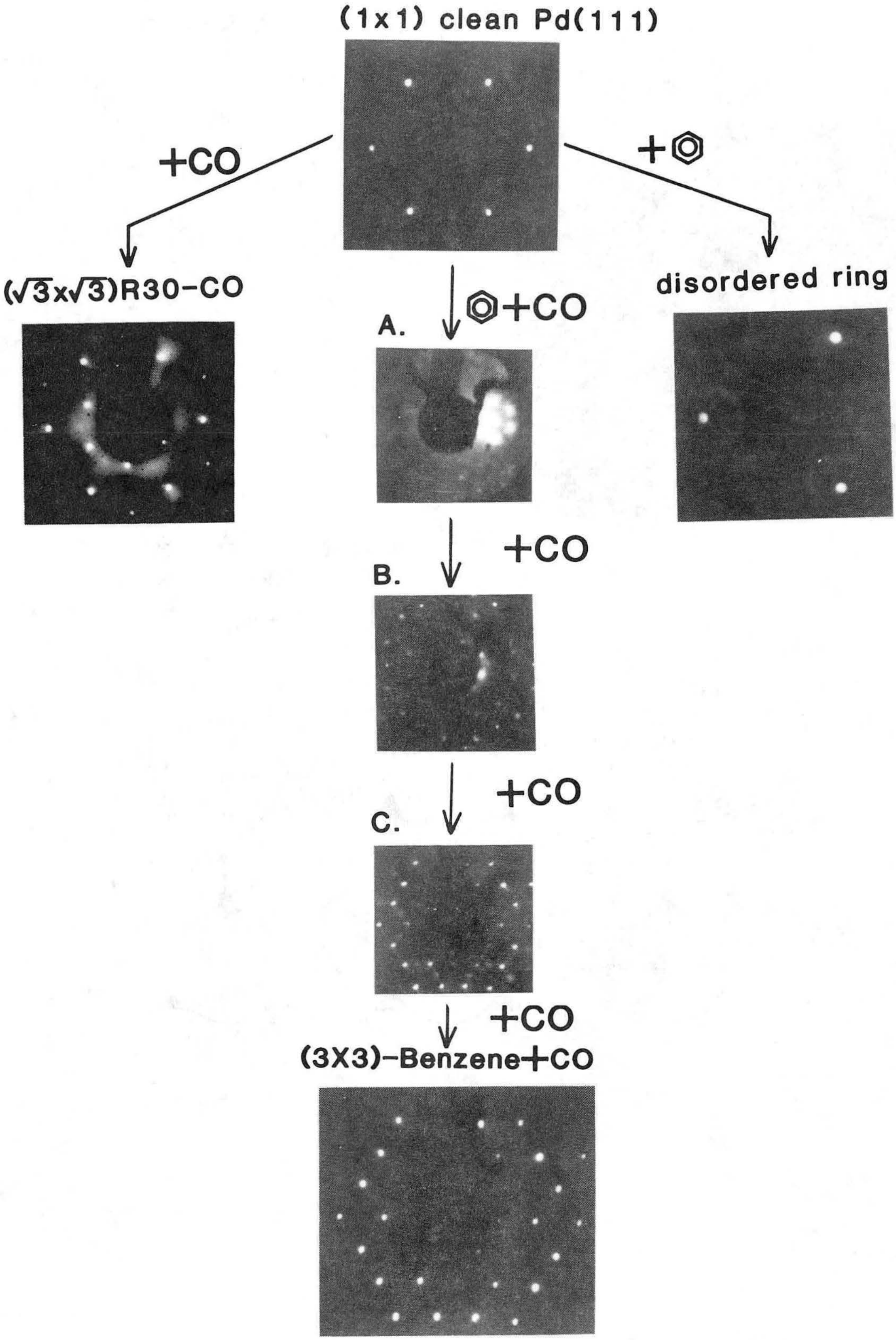

[Fig. 6-2] LEED observations of coadsorption structures of benzene and CO on Pd(111)

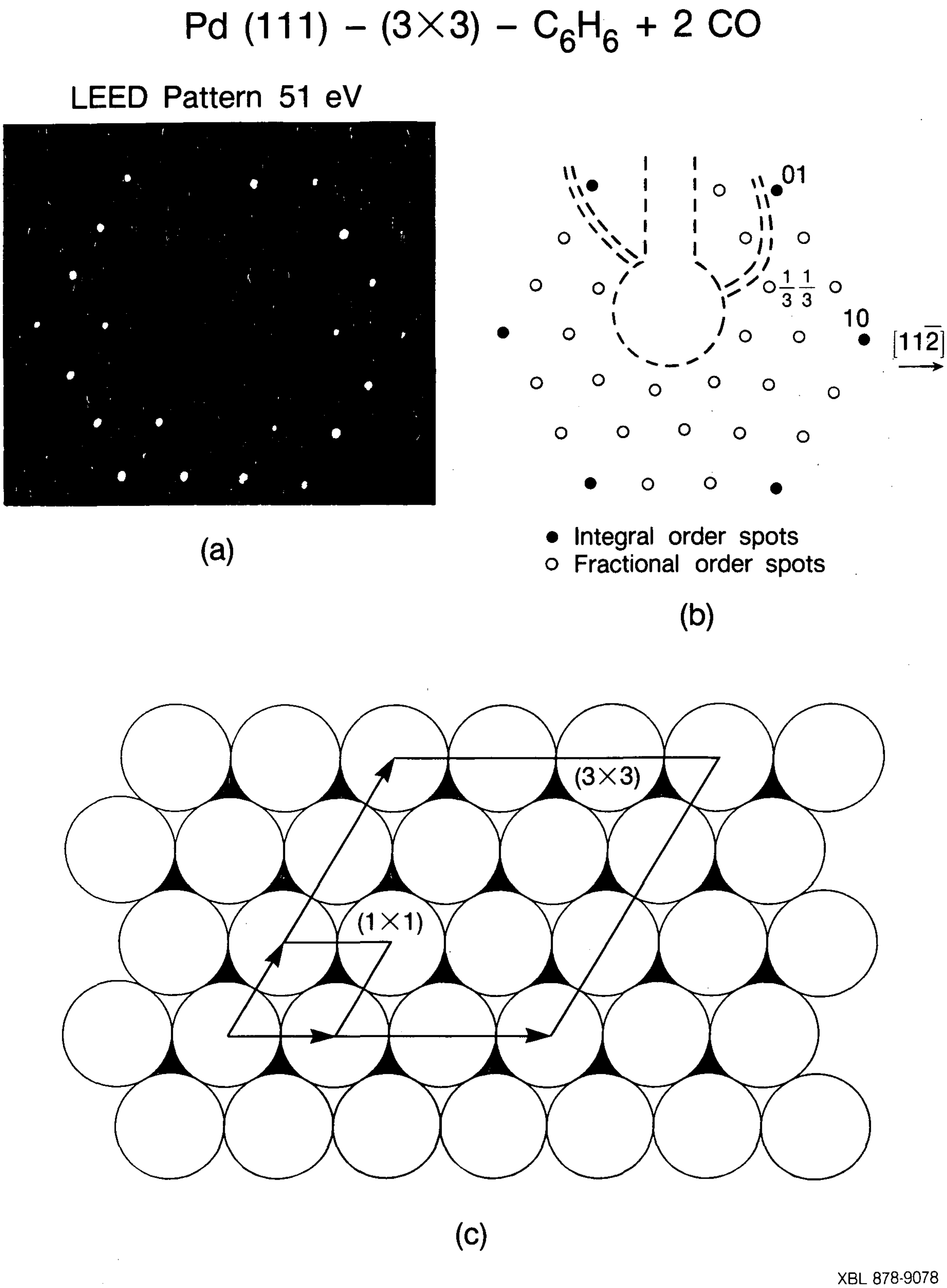

[Fig. 6-3] (a) A photograph of LEED pattern of Pd(111)-(3x3)-C_6H_6+2CO. The incident electron energy is 51eV. Near-normal incidence is used. (b) Schematic representation of the LEED pattern in (a). (c) A (3x3) surface unit cell for a (3x3) overlayer on Pd(111) in real space.

6.2.1. High Resolution Electron Energy-Loss Spectroscopy

In general, chemical information obtained with non-LEED techniques helps to narrow down the set of structure models that need to be tested by LEED analysis. HREELS[21] is one of the most powerful tools available for this purpose in the case of molecular overlayer. Figure 6-4 shows a HREEL spectra taken from the (3x3) structure of benzene and CO on Pd(111). The HREELS for pure benzene on Pd(111) is also shown for comparison. (This is essentially the same as the spectrum reported by Waddill et al)[16] The 765cm^{-1} peak is due to the γ_{C-H} mode of benzene (out of plane CH bending), and the 1735cm^{-1} peak is due to the C-O stretching mode. The spectrum for the (3x3) structure implies the following:

1. Both benzene and CO are adsorbed molecularly.
2. The very weak in-plane modes and strong γ_{CH} mode of benzene suggest that the benzene molecules lie parallel to the surface (according to the surface dipole selection rule.[21])
3. The disappearance of the 815cm^{-1} peak, which is seen in the pure benzene spectrum on Pd(111), may indicate the benzene switches to a site with different symmetry by coadsorbing with CO.(For pure benzene on Pd(111), bridge site adsorption has been proposed by Waddill et al. [9])
4. The C-O stretching frequency is such that the CO molecules are most likely bonded at three-fold hollow sites.

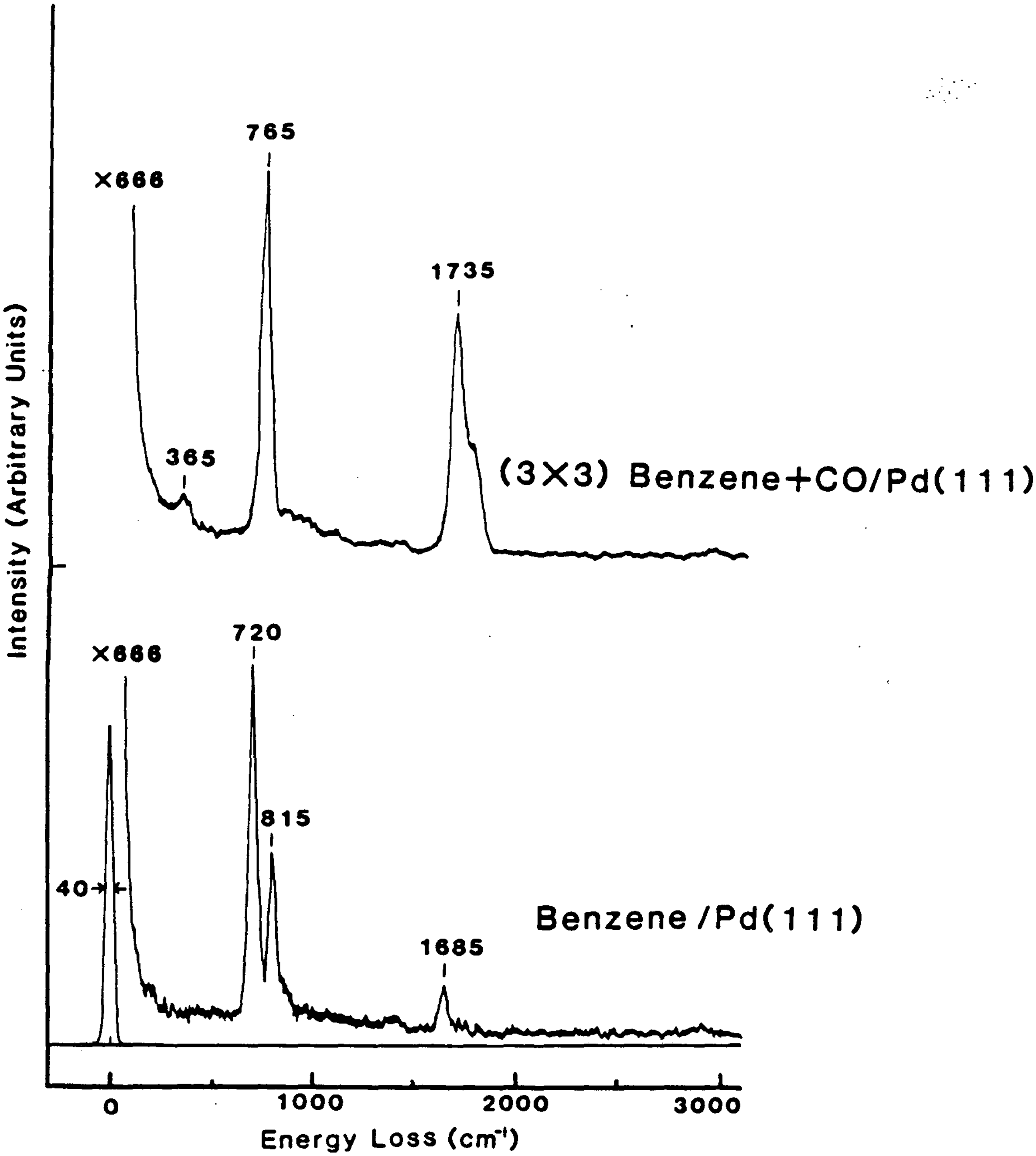

XBL 878-3560

[Fig. 6-4] Top: High Resolution Electron Energy Loss Spectrum of Pd(111)-(3x3)-C_6H_B+2CO. Bottom: HREELS of disordered C_6H_6 on Pd(111).

6.2.2. Thermal Desorption Spectroscopy

6.2.2.1. Pure Benzene Overlayer on Pd(111)

The thermal desorption spectra (TDS) of pure benzene overlayers are shown in Fig. 6-5 and Fig. 6-6. The hearing rate used was 13K/s. The benzene molecules underwent both molecular desorption and dehydrogenation evolving H_2 and left carbon on the palladium surface, consistent with the previous observation.[16,22]

6.2.2.2. Pd(111)-(3x3)-C_6H_6+2CO

The TDS was monitored at mass 2 (H_2), mass 28 (CO), and mass 78 (C_6H_6) [Table 6-1]. The heating rate used was ~15K/s. The benzene molecules underwent both molecular desorption and dehydrogenation evolving H_2 and left carbon on the palladium surface like pure benzene on the Pd(111) surface. The 78 amu desorption spectrum had two distinct peaks at 370K and 520K which contrasts with the broad TDS feature observed for pure benzene overlayer. The mass 2 (=H_2) TDS was similar to that of the pure benzene overlayer. The CO TDS peak position (~480K) was the same as for a pure CO overlayer in the ($\sqrt{3}$x$\sqrt{3}$)R30° arrangement, however the onset of the desorption starts at a lower temperature (~350K for the (3x3) structure, compared to ~380K for the pure CO overlayer). The peak area of CO TDS corresponds to about one third of a monolayer coverage.

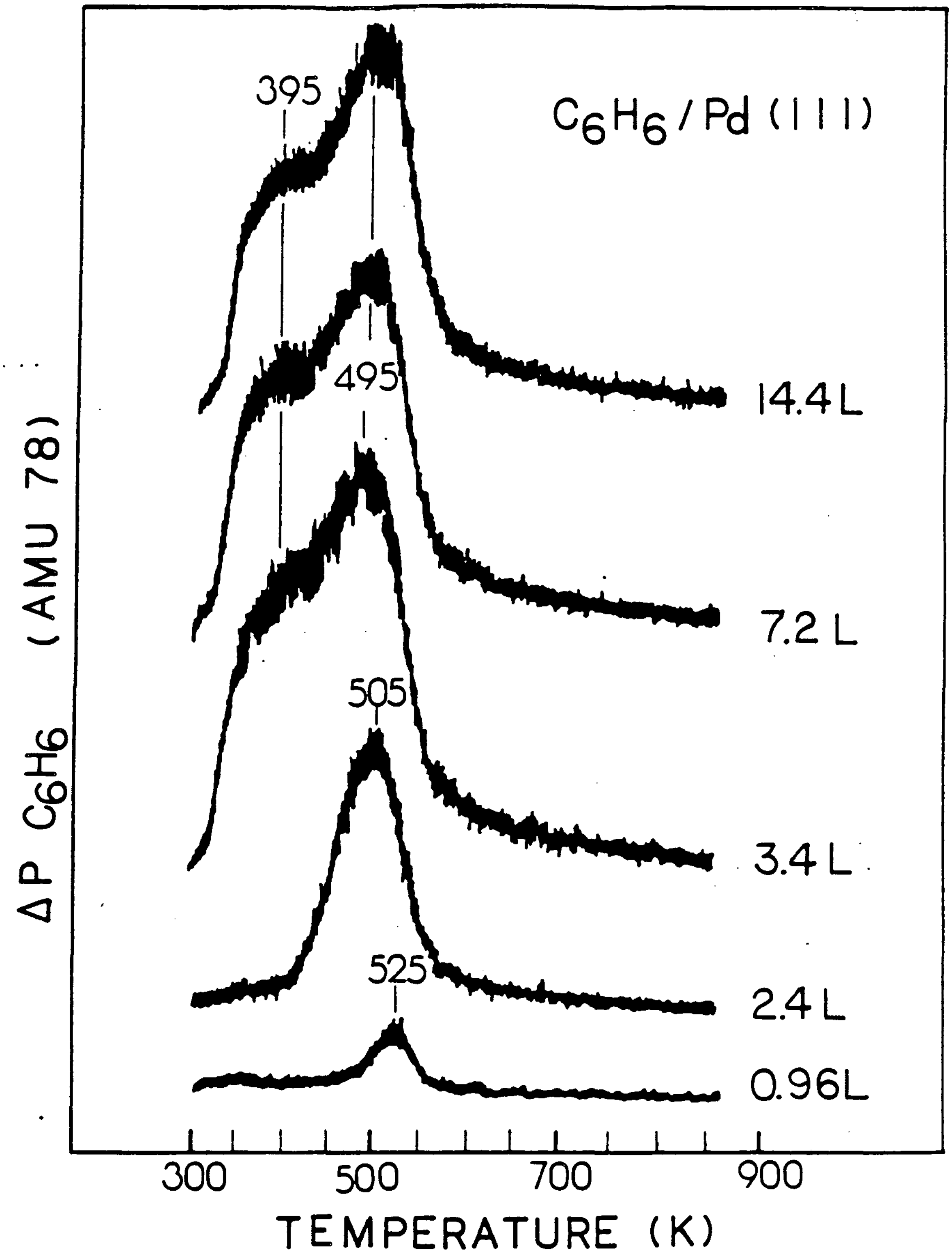

[Fig. 6-5] TDS of Benzene adsorbed on Pd(111) at room temperature. (Mass 78)

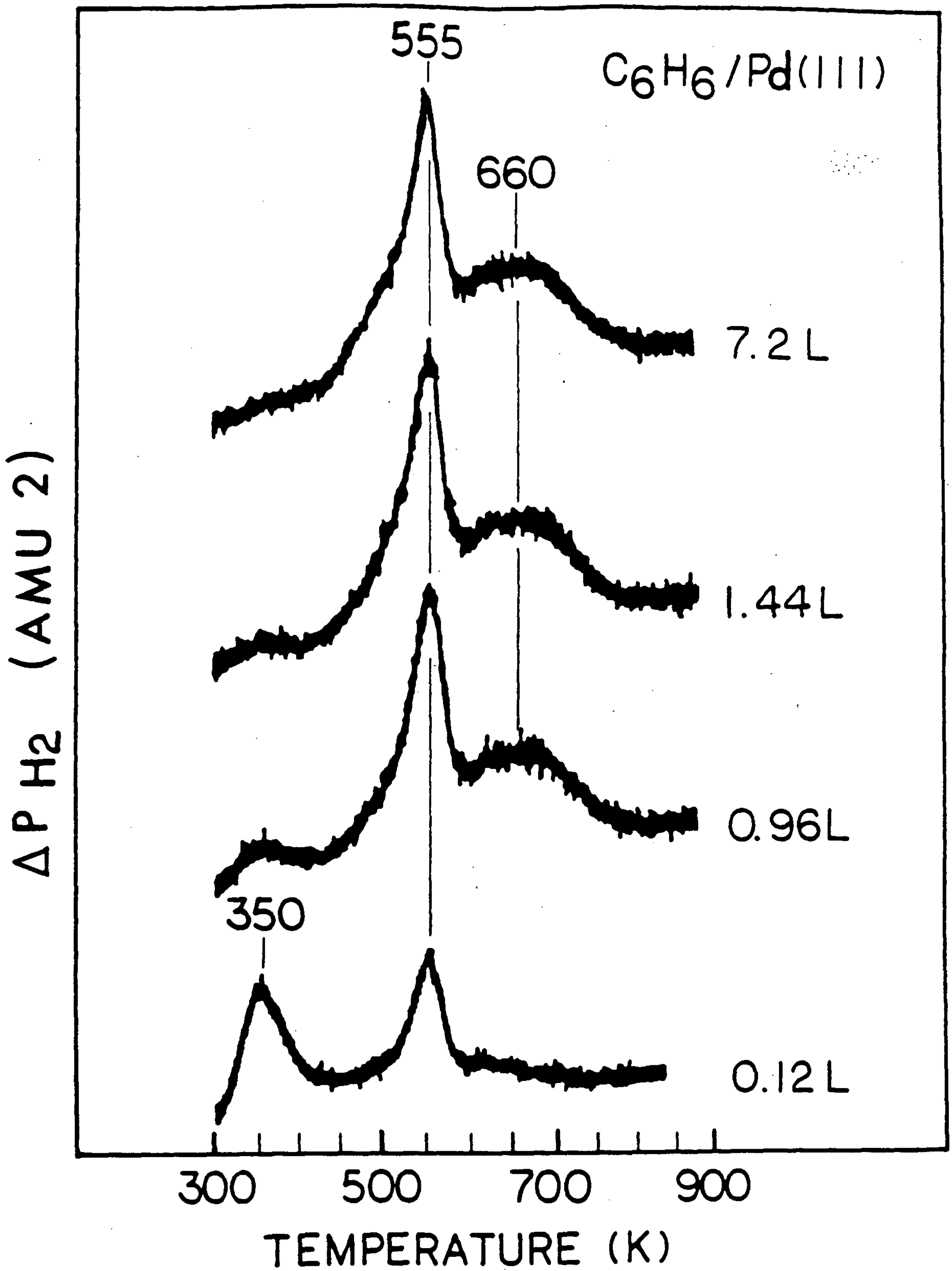

[Fig. 6-6] TDS of Benzene adsorbed on Pd(111) at room temperature. (Mass 2)

[Table 6-1] TDS from Coadsorption Structures of Benzene and CO on Pd(111)

Structure	CO peak	C_6H_6 peak	H_2 peak
Disordered C_6H_6	—	390K 505K	555K 680K
(3x3) C_6+2CO	475K	370K 520K	555K 680K
$(\sqrt{3}x\sqrt{3})R30°$-CO	480K	—	—

6.2.3. Preliminary Structure Model

HREELS indicated that benzene adsorbs molecularly parallel to the surface, whether with or without[16,17] coadsorbed CO. This orientation restricted the number of benzene molecules per (3x3) unit cell to be only one, by taking the Van der Waals sizes of benzene molecules into account. CO was molecularly adsorbed perpendicular to surface according to the HREELS data. CO TDS detected about one third of a monolayer of CO, corresponding to three CO molecules per unit cell. However the Van der Waals size consideration allows a maximum of two upright CO molecules per unit cell. Therefore, the number of CO per unit cell was set to be two, the same number found in the corresponding (3x3) structure on Rh(111). The excess CO can be at defect sites of our Pd(111) sample, or in the disordered region outside of the major (3x3) phase. (We frequently observed disordered regions, by moving the LEED electron beam across the Pd(111) sample, especially near the edge of the crystal.) Thus, our analyses are based on the model with one flat-lying benzene and two upright CO molecules at high symmetry adsorption sites in the (3x3) unit cell. Thus, the HREELS results together with thermal desorption yields of CO and knowledge of the Van der Waals sizes of each molecule, lead to the structure model as shown in Fig.6-7. The number of benzene and CO molecules within each (3x3) unit cell is thereby set to one and two, respectively.

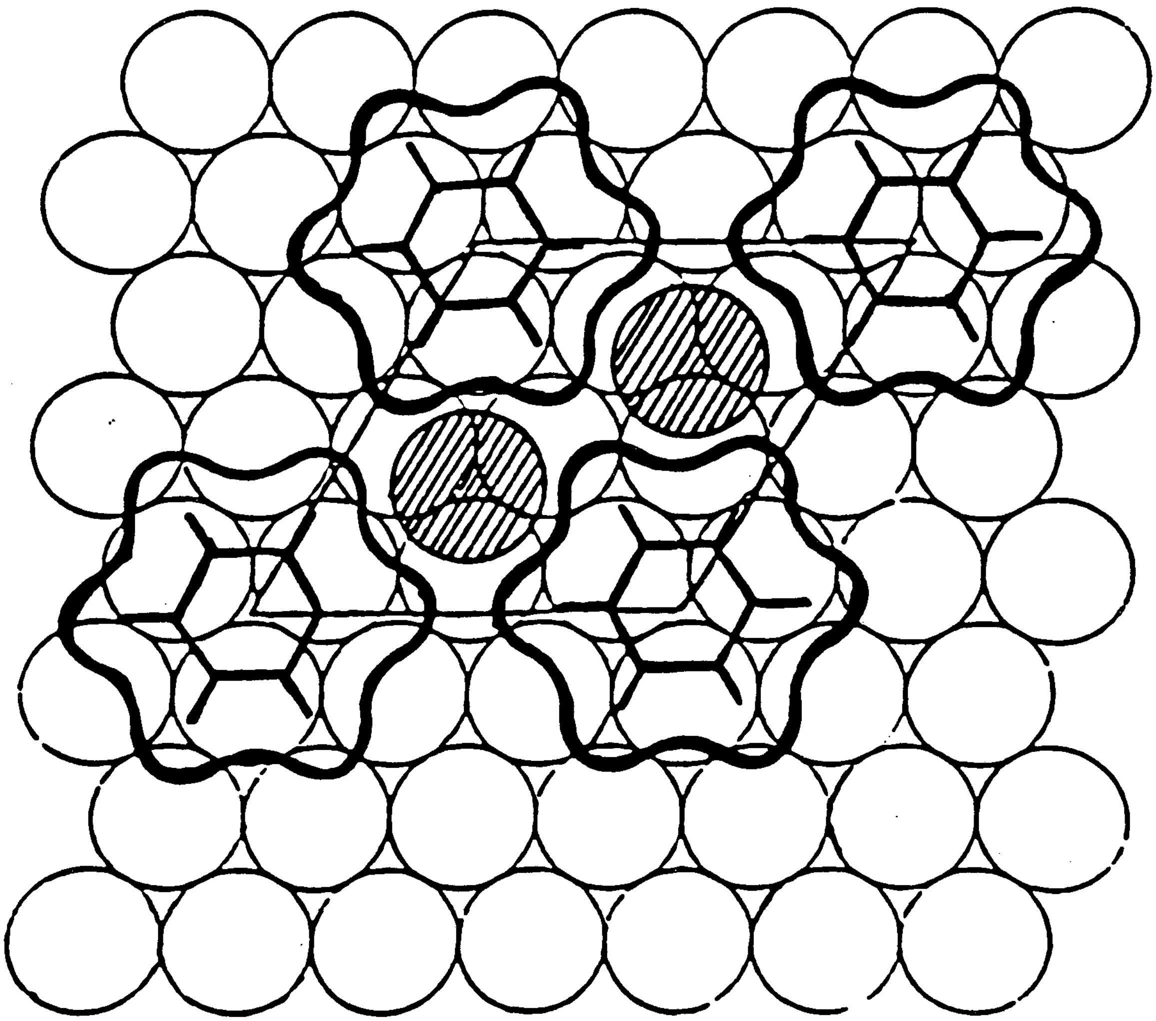

'BL 849-10795 A

[Fig. 6-7] The structure model of Pd(111)-(3x3)-C_6H_6+ 2CO obtained with HREELS and TDS. (Bond lengths, bond angles etc. are not yet determined.)

6.2.4. I-V Curve Measurement

LEED data were recorded at both room temperature and 120K. The main features of both data sets were very similar, except for the lower contrast in the LEED patterns at room temperature, due to the relatively low Debye temperature of palladium. At room temperature, the intensity of the overlayer spots was very weak especially at incident electron energies above 100eV. At 120K thermal diffuse scattering was reduced and the contrast in the diffraction pattern was improved, resulting in a larger range of useful I-V data. The following discussion refers to the 120K data.

The I-V data were collected at normal incidence and with the incident electron beam rotated 5° from normal incidence toward the $[1, 1, \bar{2}]$ direction, which can be labeled $(\theta, \phi) = (5°, 0°)$; this direction of tilt maintains one mirror plane of symmetry. The energy range used was 20-200eV. In order to confirm reproducibility several sets of experimental I-V curves were obtained from different sampling positions on the palladium crystal for both normal and off-normal incidence. After symmetrically equivalent beams were averaged together within each data set, two of such data sets from different sampling positions were further averaged together to obtain the final I-V data. The final normal-incidence data set had 16 independent beams over a cumulative energy range of 1000 eV. The (5°, 0°) data set had 29 independent beams over a cumulative energy range of 1980 eV. [Fig. 6-8, Fig. 6-9]

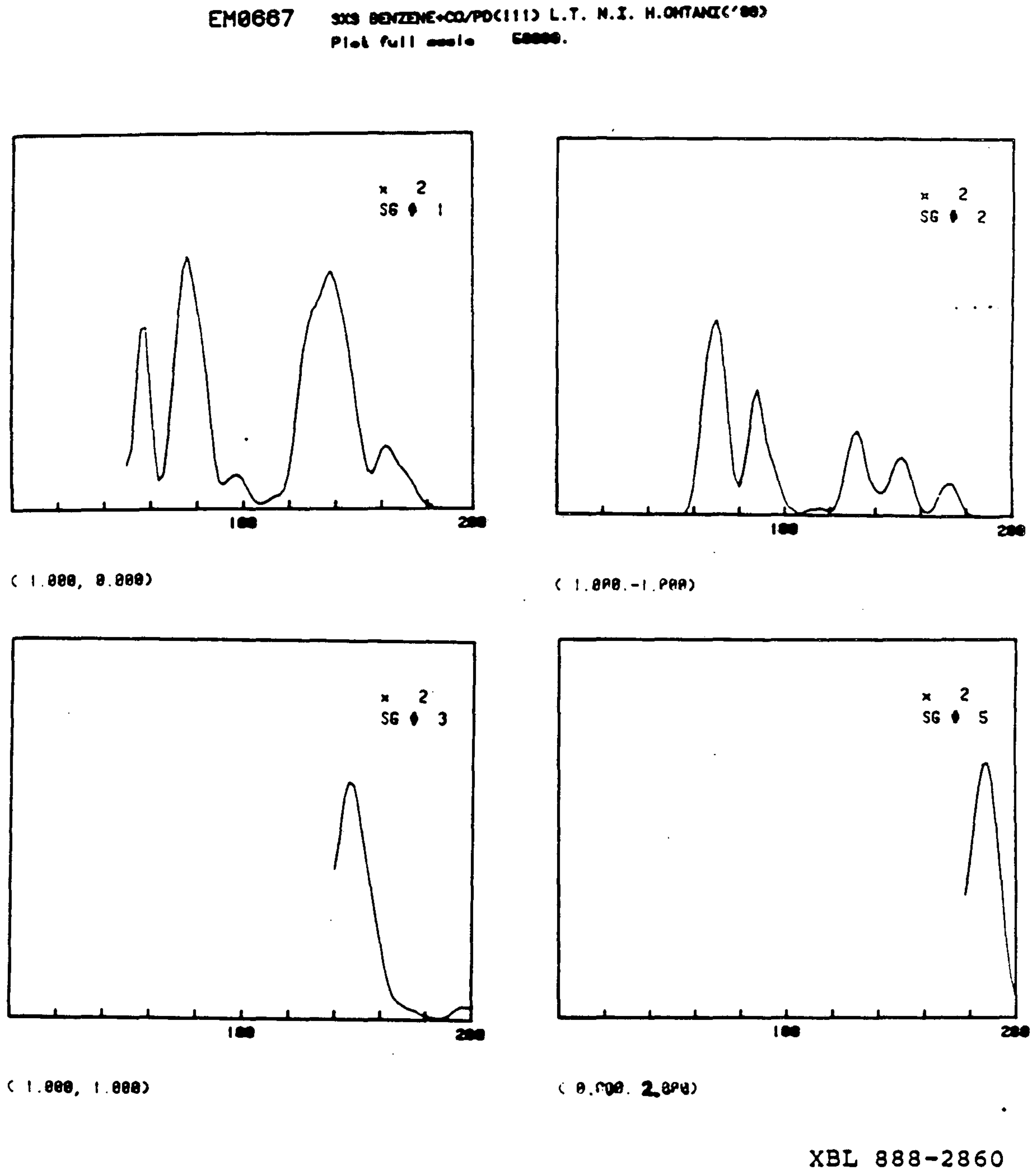

[Fig. 6-8] Experimental I-V curves for Pd(111)-(3x3)-C_6H_6+2CO obtained at 120K. (θ, ϕ)=(0°, 0°).

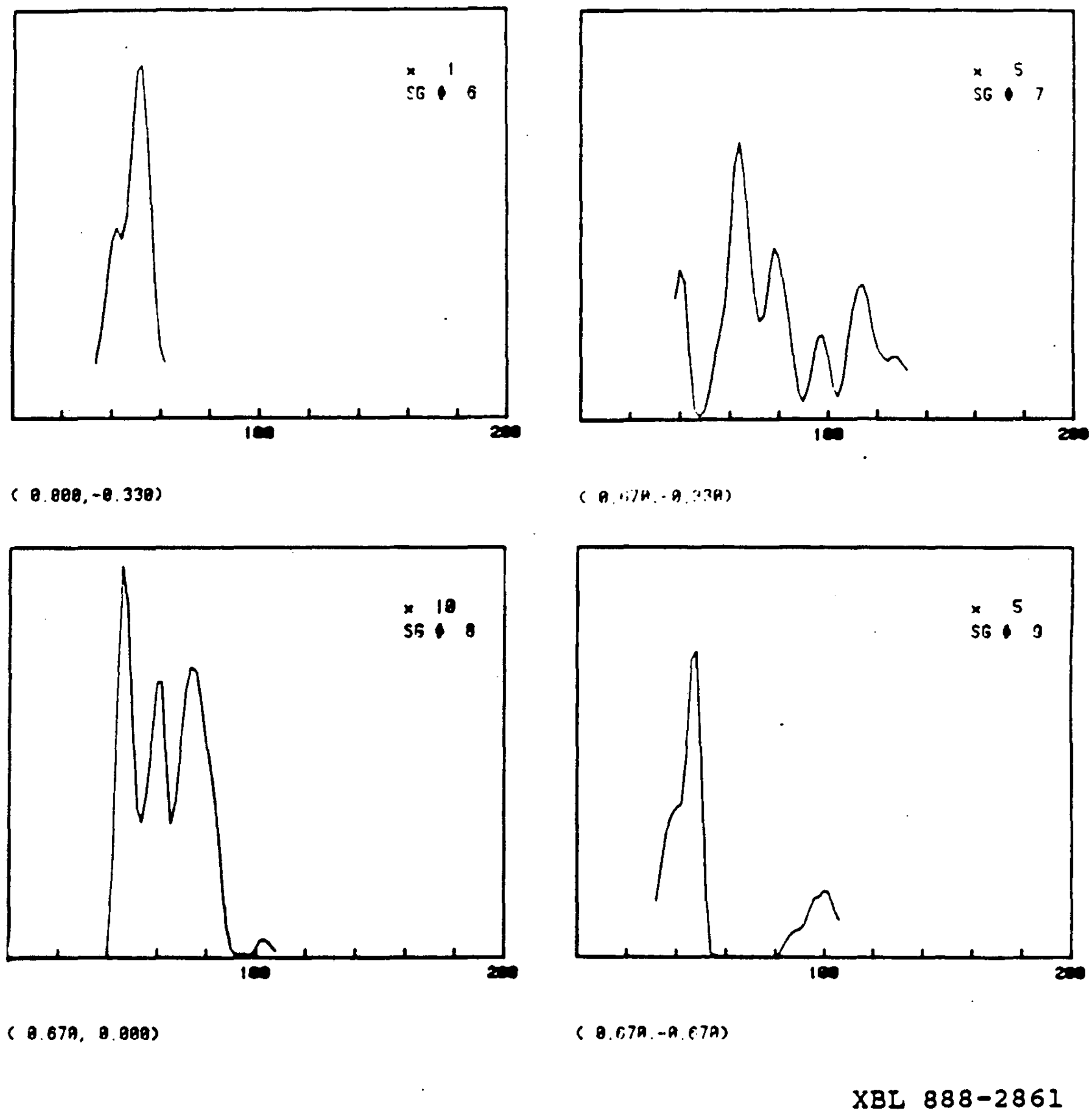

[Fig. 6-8] (continued)

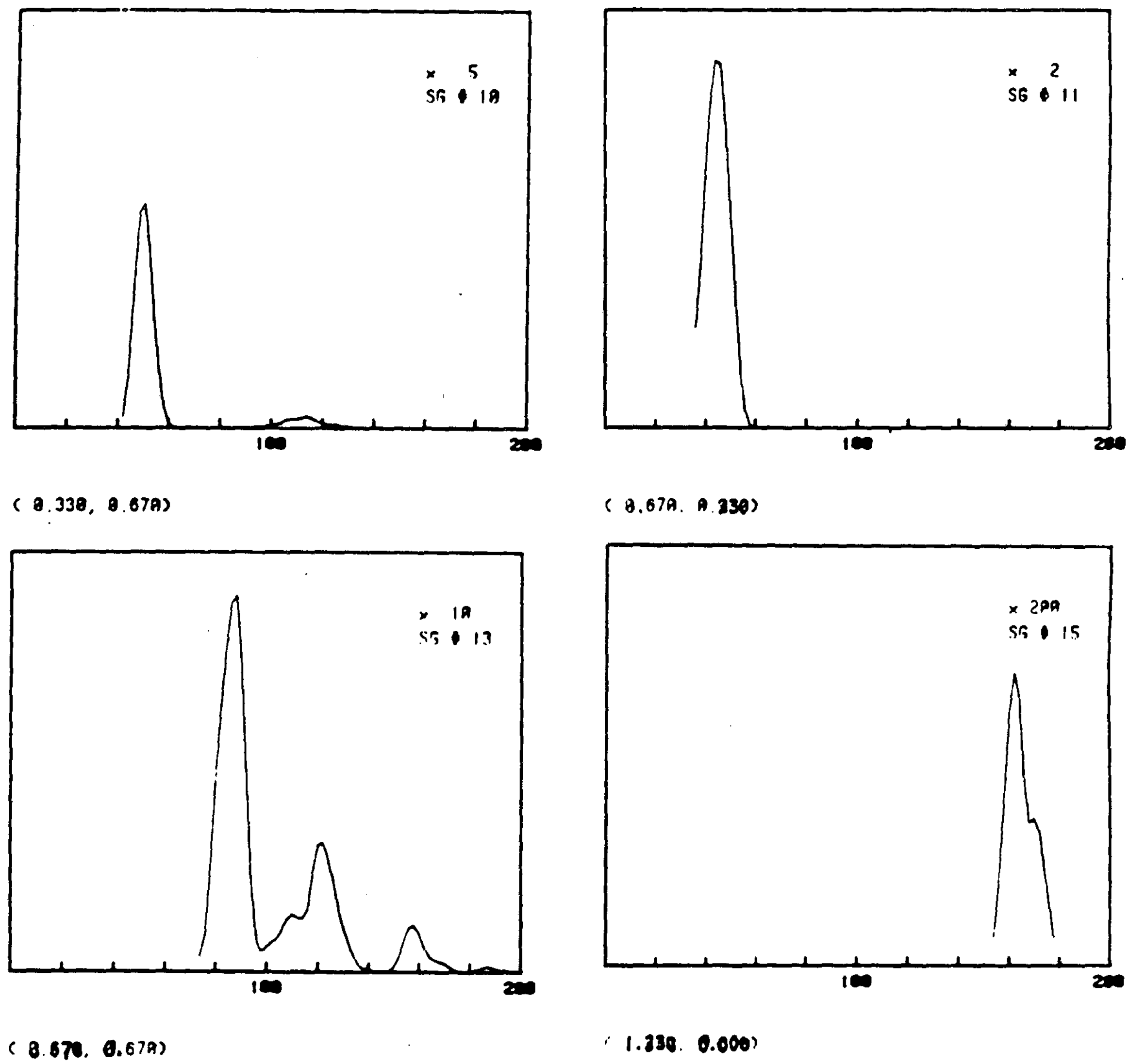

XBL 888-2862

[Fig. 6-8] (continued)

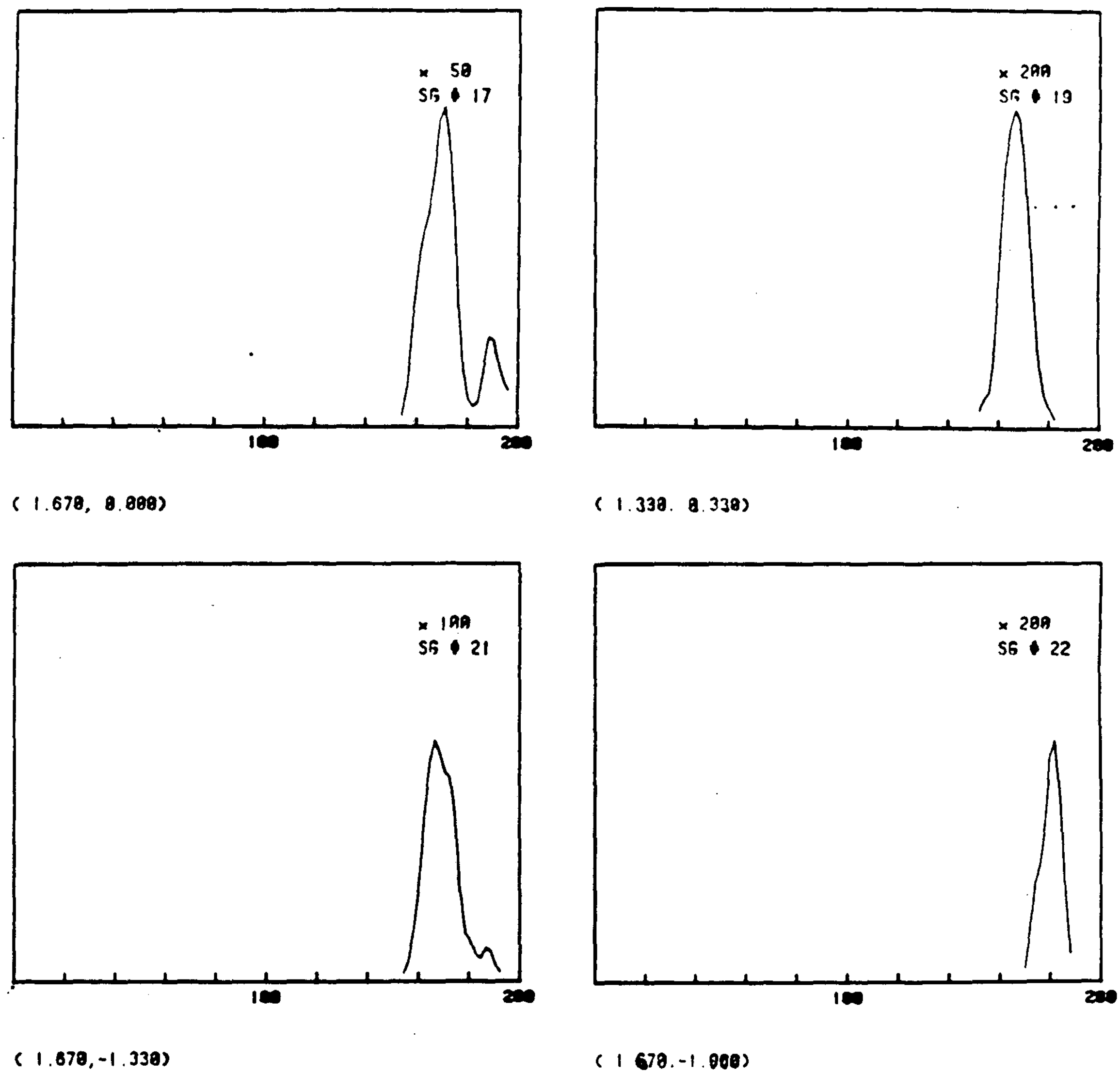

XBL 888-2863

[Fig. 6-8] (continued)

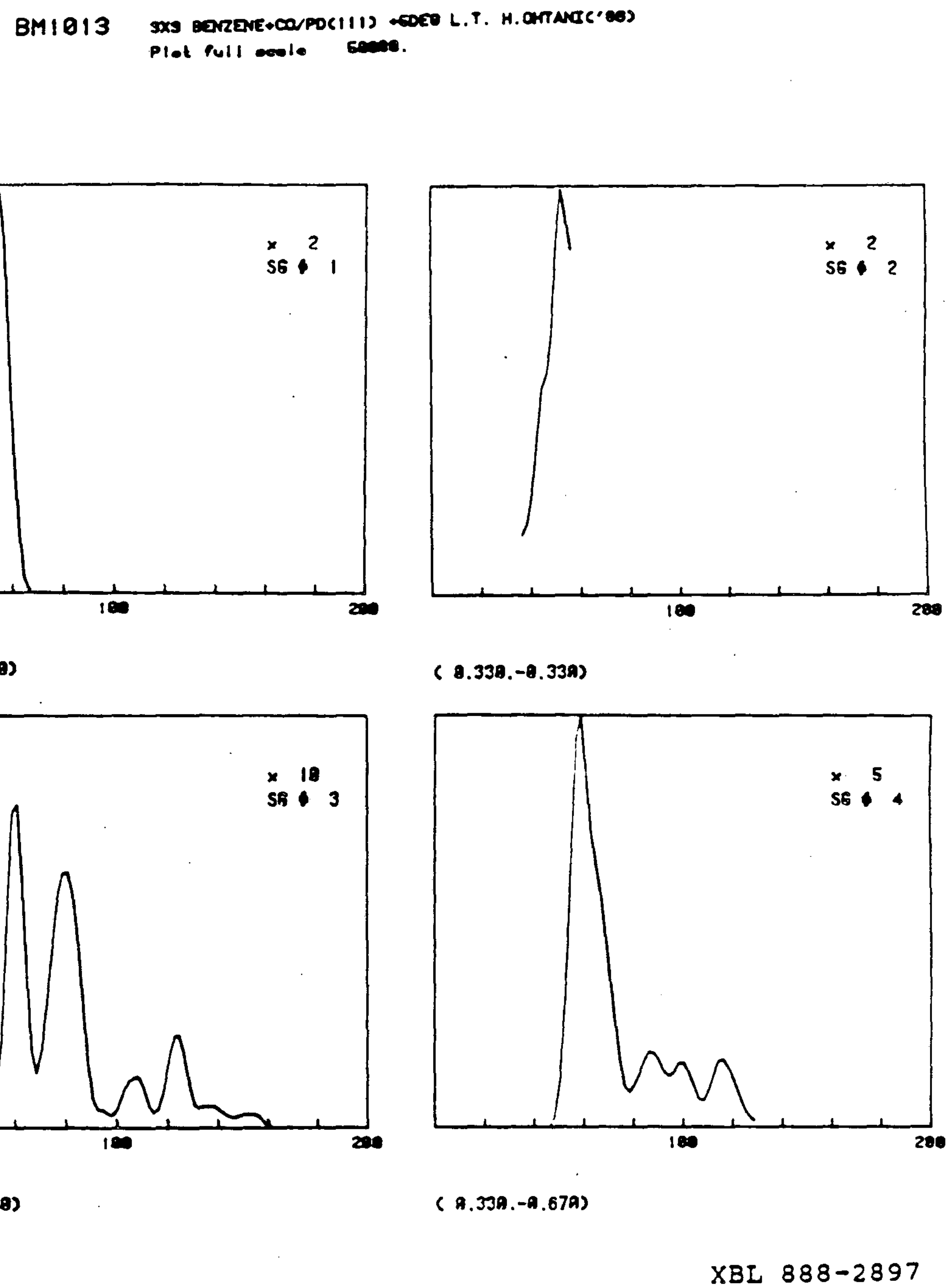

[Fig. 6-9] Experimental I-V curves for Pd(111)-(3x3)-C_6H_6+2CO obtained at 120K. (θ, ϕ)=(0°, 5°).

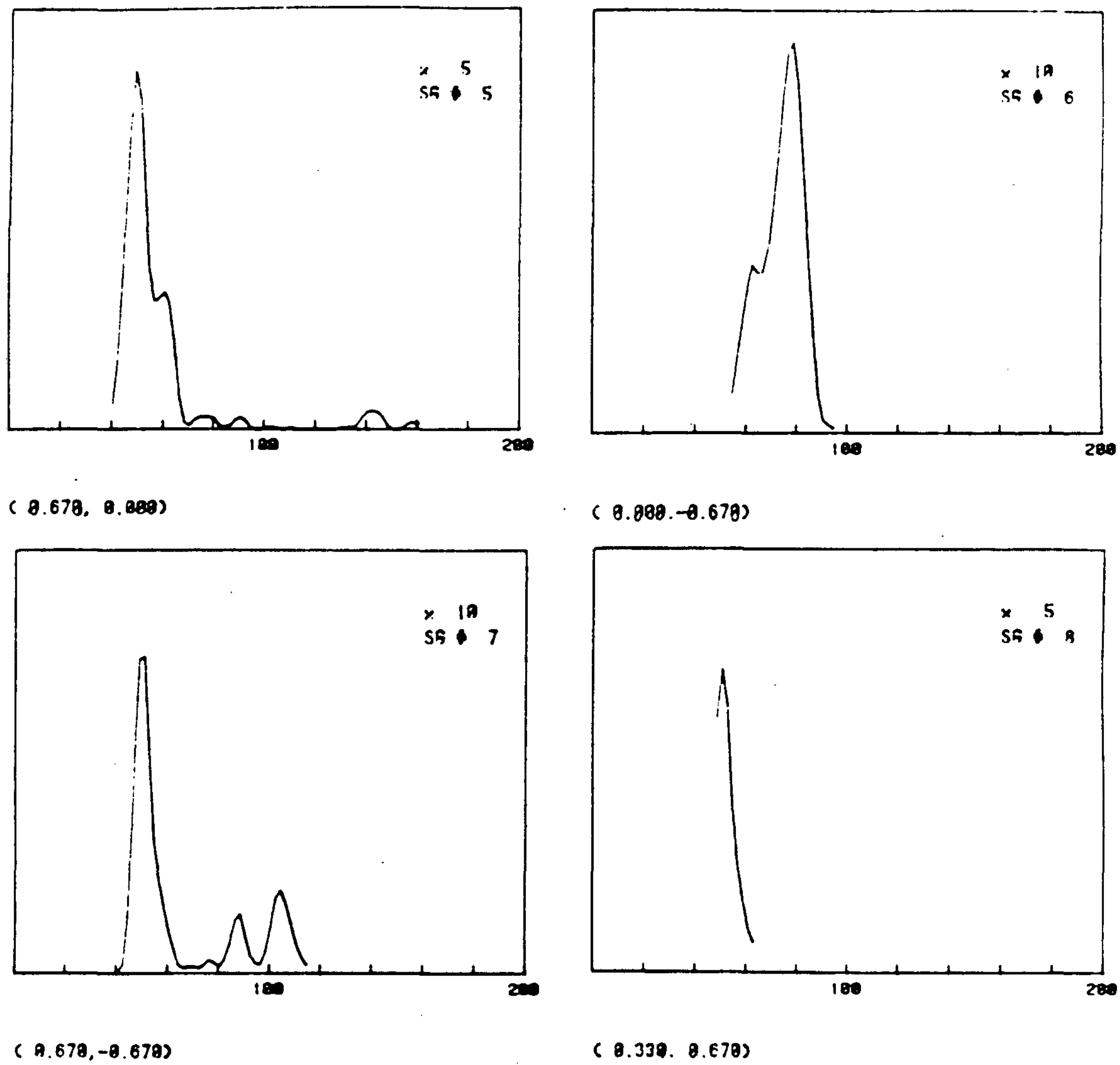

XBL 888-2898

[Fig. 6-9] (continued)

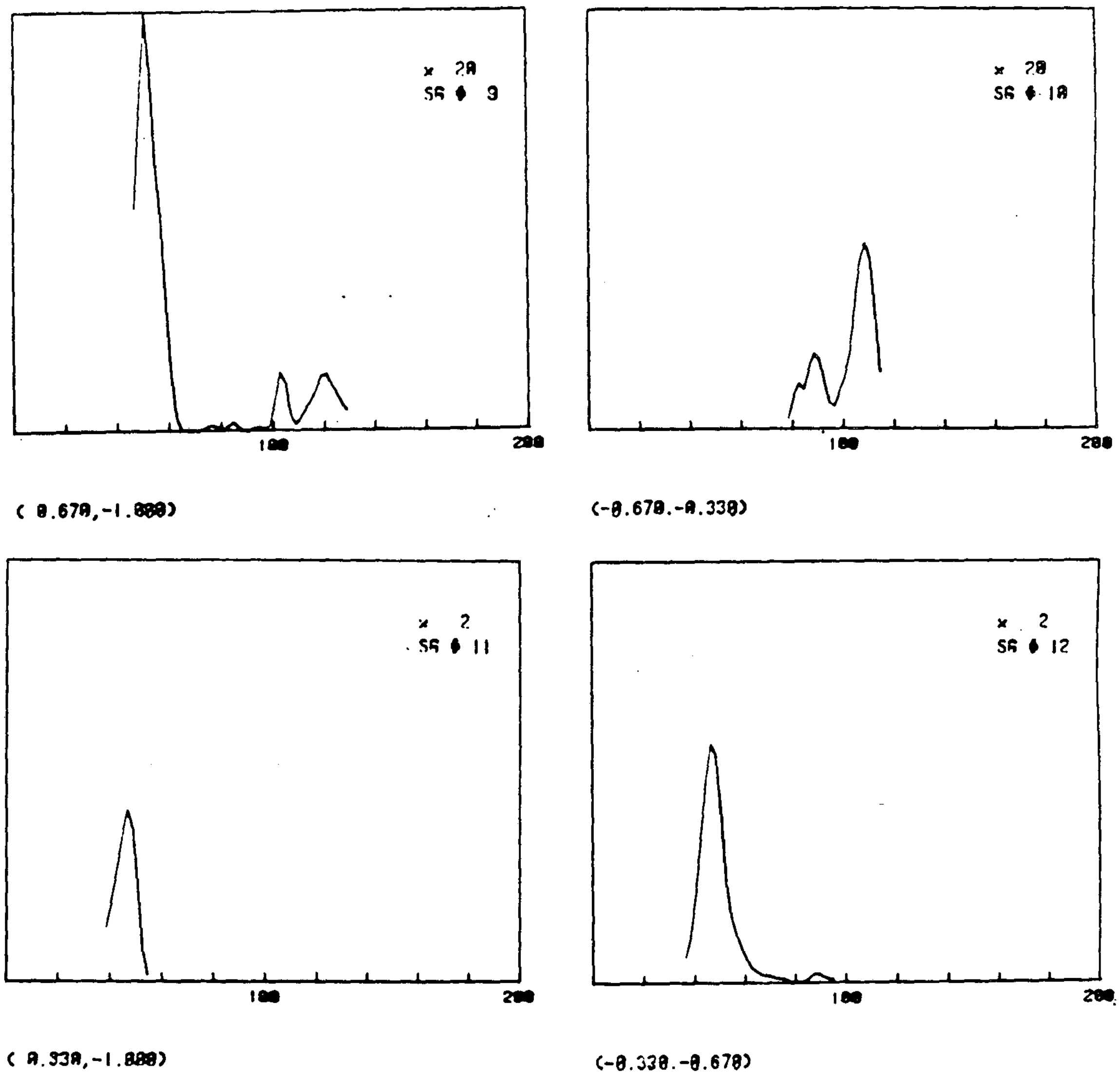

XBL 888-2899

[Fig. 6-9] (continued)

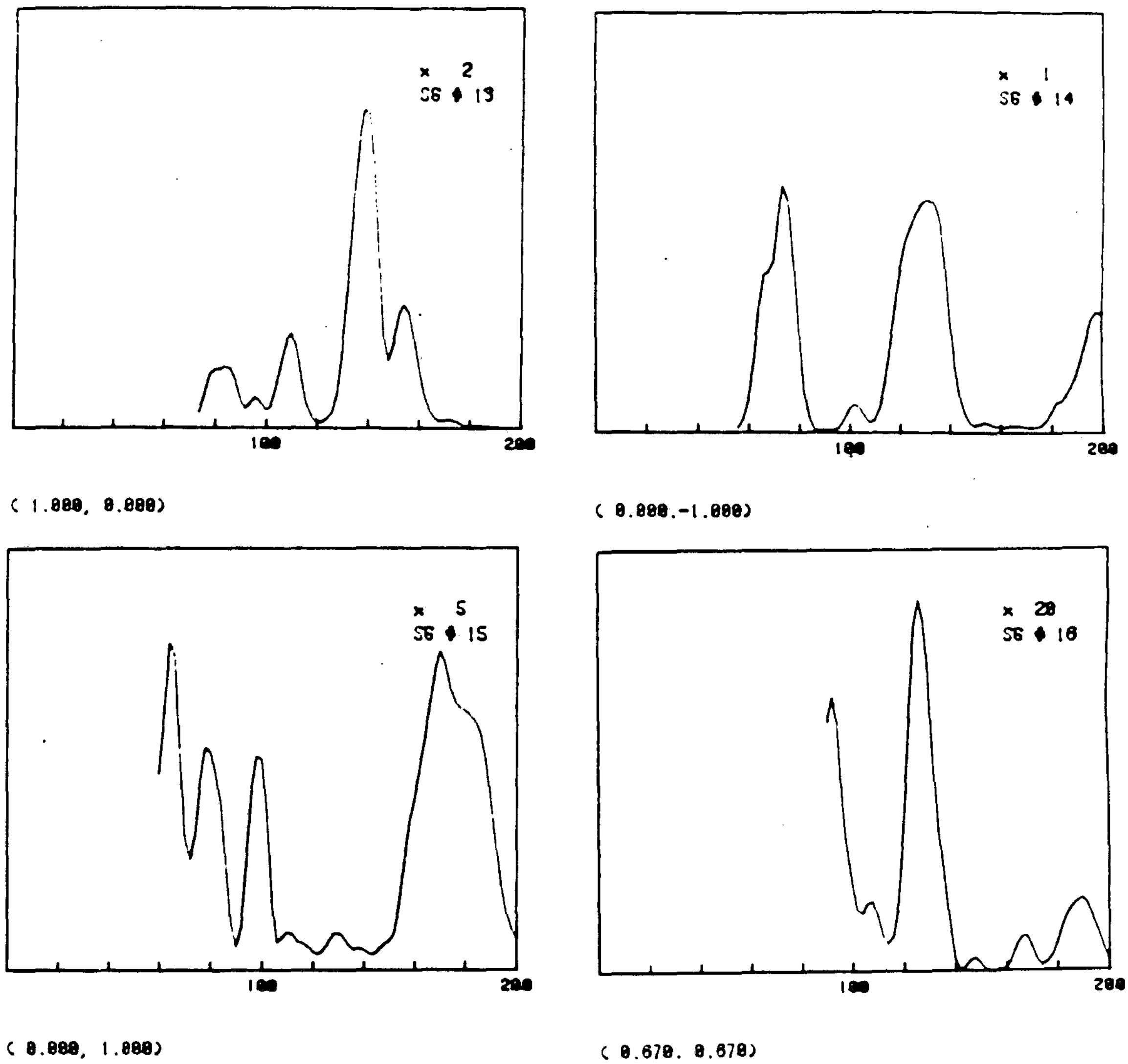

XBL 888-2900

[Fig. 6-9] (continued)

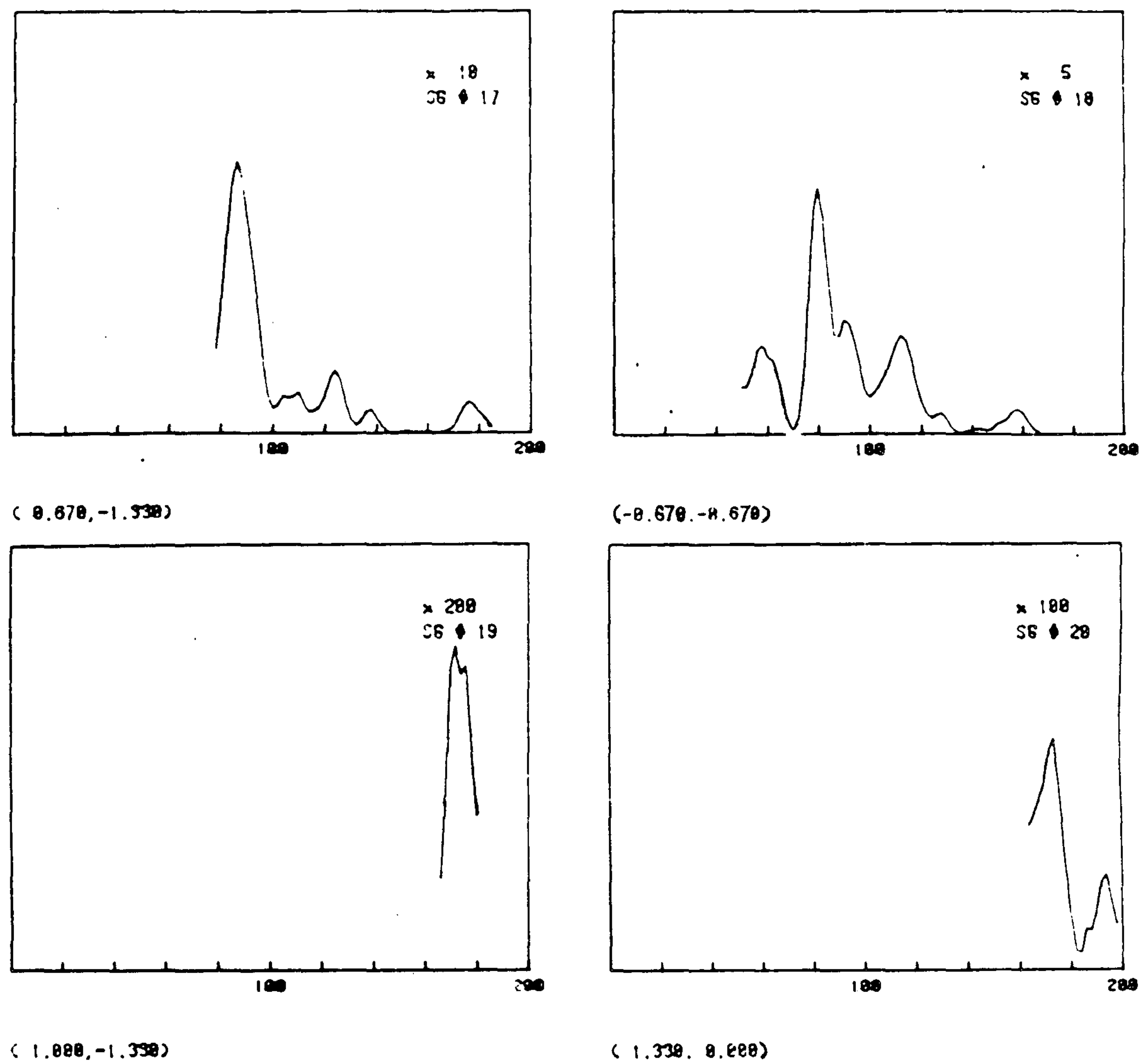

XBL 888-2901

[Fig. 6-9] (continued)

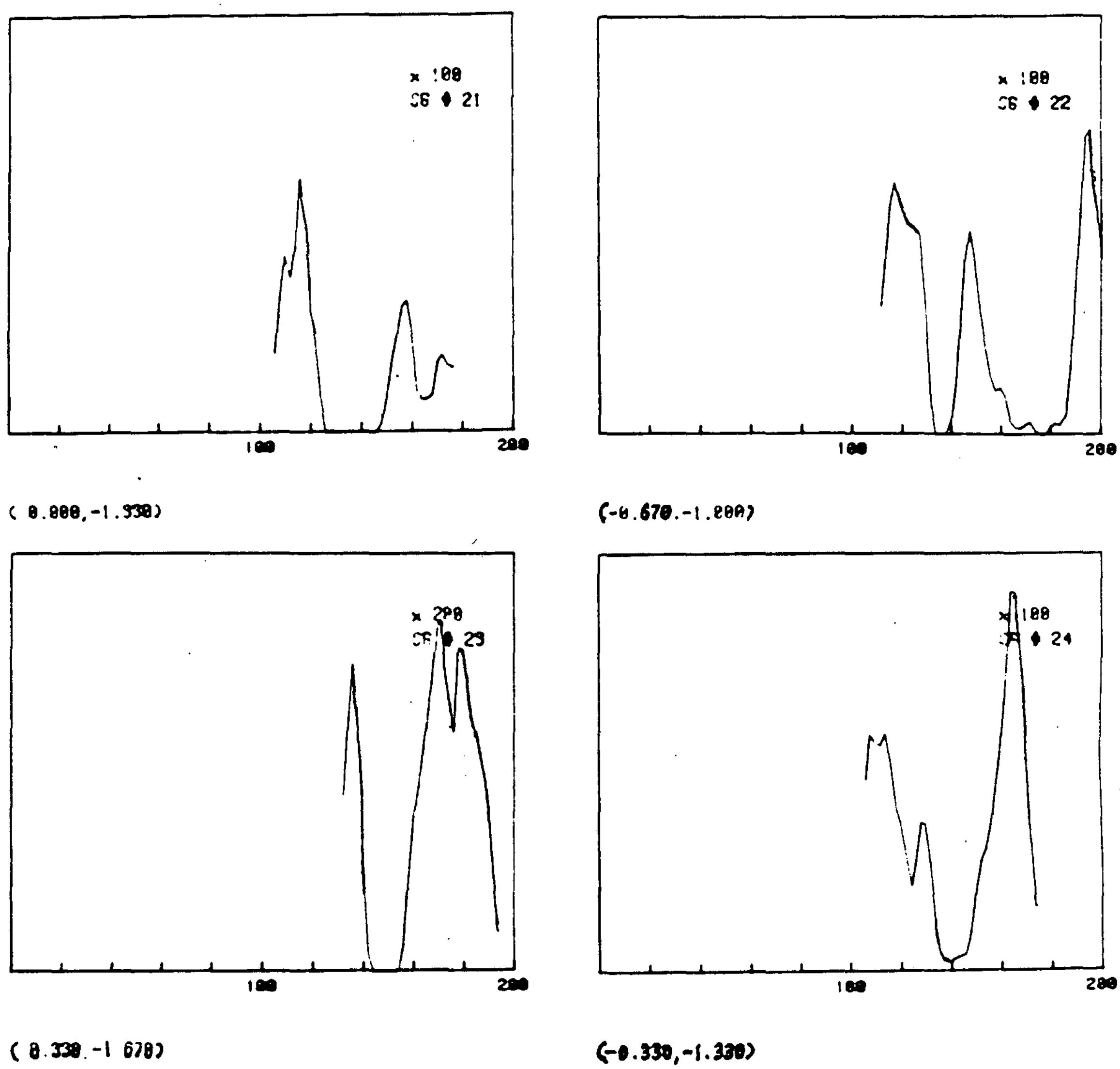

XBL 888-2902

[Fig. 6-9] (continued)

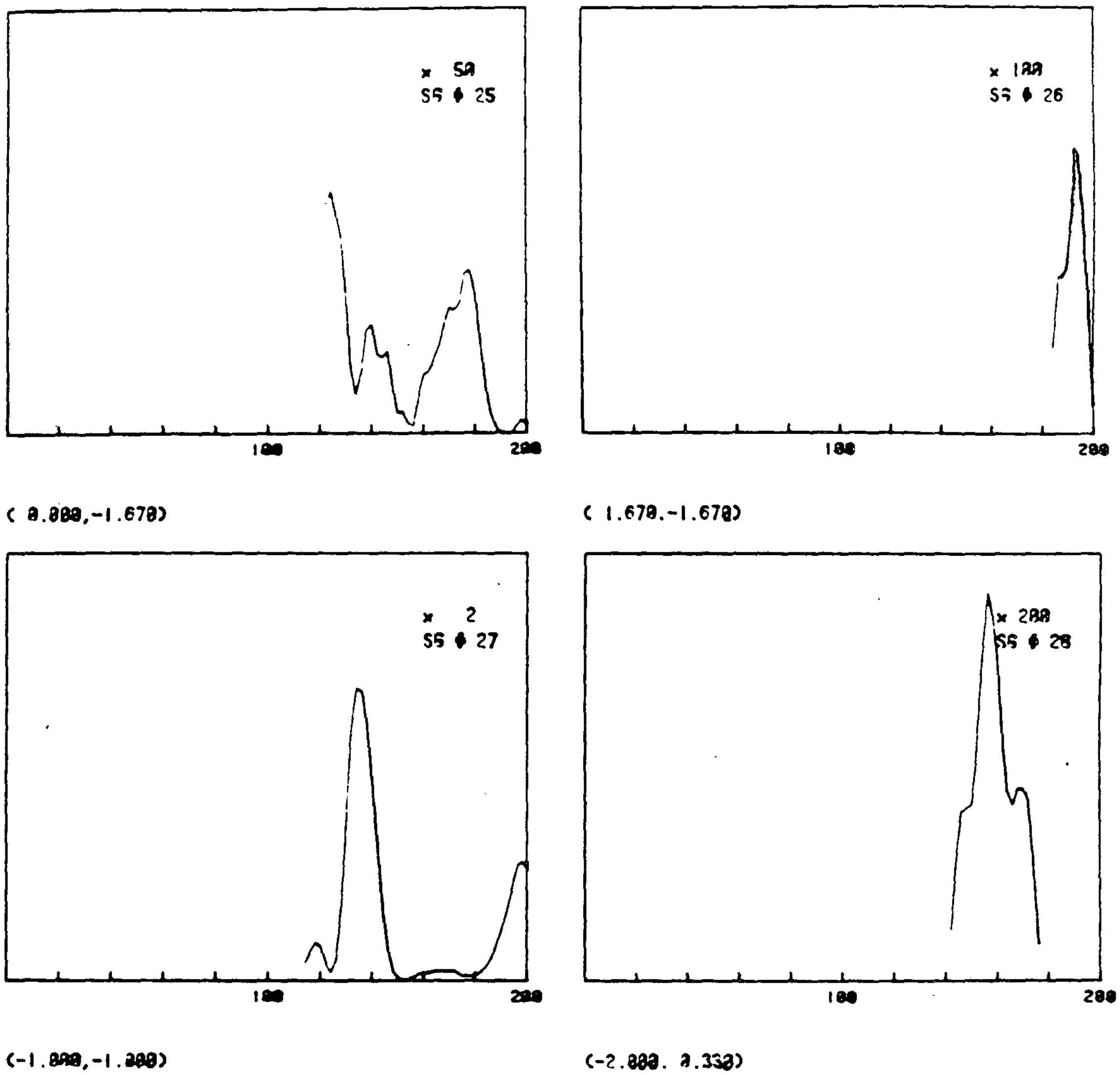

XBL 888-2903

[Fig. 6-9] (continued)

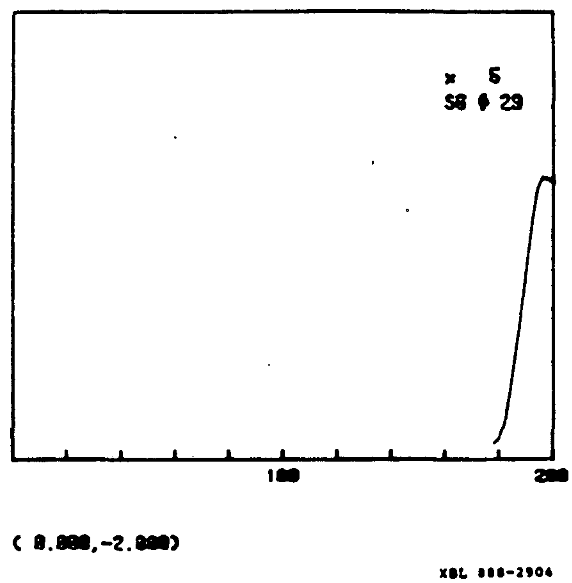

[Fig. 6-9] (continued)

6.3. Theory

The theoretical methods which we have applied in this work were very similar to those used in the structural determination of Rh(111)-(3x3)-C_6H_6 +2CO.[4]

Within the Combined Space Method[23] we have used Renormalized Forward Scattering to stack layers. The substrate layer diffraction was calculated accurately with conventional methods.[23] The overlayer diffraction matrices were obtained with Matrix Inversion within individual molecules, and Kinematic Sublayer Addition to combine the molecules. Beam Set Neglect was applied to add the overlayer to the substrate.

The non-structural parameters in our LEED calculations for the substrate were selected as described in a previous LEED study of clean and carbon monoxide-covered Pd(111).[24] For benzene, the same phase shifts as used on Rh(111)[3,4] and Pt(111)[2] were taken. Phase shifts up to $l_{max} = 5$ were used.

For the comparison between experiment and theory, a set of five R-factor formulas and their average was used, as described previously and used by us in many prior LEED analyses.[1,2,3,4,24]

6.4. Structure Analysis

Our structural search for Pd(111)-(3x3)-C_6H_6+ 2CO was very similar to that used in our analysis for Rh(111)-(3x3)-C_6H_6+2CO. We tested approximately 1500 distinct structures as shown in Table 6-2. In a first stage of the structural determination (Table 6-2 - A,B,C,D), the carbon ring was given its gas-phase geometry (hexagonal symmetry with equal C-C bond lengths of 1.397Å) and the C-O bond lengths were fixed at 1.15Å. This allowed the adsorption sites and molecular distances from the metal to be approximately determined. Here we assumed that benzene and CO are adsorbed over the same kind of high-symmetry sites, as estimated by their Van der Waals sizes (See Figure 6-10b,c). The structure where both benzene and CO adsorb over fcc-hollow sites was clearly favored by R-factor comparison as shown in Table 6-3. Two high-symmetry azimuthal (Φ) orientations of the benzene molecules were also investigated (See Table 6-2-C1, C2, Fig. 6-10a, and Fib. 6-10b). The angle Φ was confirmed to be 0°, as Van der Waals sizes would indicate (Fig. 6-10b).

Then, in the favored fcc-hollow site and with $\Phi = 0°$, we examined possible substrate relaxations (Table 6-2-E), since we had observed small relaxations for clean and CO-covered Pd(111) surfaces.[24] In the present case, the 1st and 2nd layer spacings were found to be expanded by +0.05Å with respect to the bulk value.

In trials F-J (Table 6-2), more precise analyses were conducted to determine the bond lengths and bond angles within the overlayer. In-plane Kekulé-type distortions of the C_6 ring of benzene observed on Rh(111) surface were also extensively investigated on Pd(111) surface. These consist of alternating long and short C-C bonds within the C_6 rings, with C_{3v} symmetry. Two variables can be used to describe such distortions (see Figure 6-10d): a C_6 ring radius r and an angular departure β from 6-fold symmetrical positions. Note that in the preferred benzene adsorption sites (fcc-hollow) and with $\Phi = 0$, the Kekulé distortion has the same symmetry as the metal site itself. R-factor plots as a function of r and as a function of β are shown in Figure 6-11-a and 6-11-b, respectively. They illustrate that the LEED analysis is sensitive to the distortion of the benzene molecules. The R-factor minima (C_6 radius (r) =1.43 $\pm$ 0.10 Å, and $\beta = \sim 0.75$ °) yielded the following C-C bond lengths of the C_6 ring skeleton:

$$d_1 = 2r\sin(30^\circ - \beta) = 1.40 \pm 0.10 \text{ Å}$$

$$d_2 = 2r\sin(30^\circ + \beta) = 1.46 \pm 0.10 \text{ Å}$$

(d_1 and d_2 are defined in Figure 7-4; the C-C bond with the shorter bond length d_1 is positioned over one palladium atom, whereas the C-C bonds with the longer bond length d_2 is positioned bridging two palladium atoms.)

The other three structural variables, the perpendicular metal-carbon separations for CO and benzene and the CO bond length, were determined by similar R-factor analyses in the course of trials F-J. A few theoretical I-V curves corresponding to the grid point nearest the minimum R-factor are shown in Fig. 6-12, along with experimental I-V curves.

TABLE 6-2. Test structures for Pd(111)-(3x3)-C_6H_6+2CO

	Benzene					CO			Pd(111)	Incidence Directions
				C_6 ring distortions[d]						
	site[a]	$\Phi(^\circ)$[b]	$d_{1C_{av}-C_d}(\text{Å})$[c]	$r(\text{Å})$	$\beta(^\circ)$	site	$d_{1Pd-C}(\text{Å})$[e]	$d_{C-O}(\text{Å})$[f]	$\Delta d_{1Pd-Pd}(\text{Å})$[g]	$(\theta,\phi)(^\circ)$[h]
A	top	0	−0.6(.2)0.0	1.397	0	top	1.4(.05)1.65	1.15	0	(0,0)
B	bridge	0,30	0.5(.2)1.1	1.397	0	bridge	1.5(.1)2.0	1.15	0	(0,0),(5,0),(5,180)
C1	fcc-hollow	0	0.7(.2)1.3	1.397	0	fcc-hollow	1.2(.05)1.45	1.15	0	(0,0),(4,0),(5,0),(6,0),(5,180)
C2	fcc-hollow	30	0.7(.2)1.3	1.397	0	fcc-hollow	1.2(.05)1.45	1.15	0	(0,0)
D	hcp-hollow	0	0.7(.2)1.3	1.397	0	hcp-hollow	1.2(.05)1.45	1.15	0	(0,0)
E	fcc-hollow	0	0.7(.2)1.3	1.397	0	fcc-hollow	1.2(.05)1.45	1.15	.05(.05).15	(0,0),(5,0)
F	fcc-hollow	0	0.9(.05)1.0	1.2(.17)1.71	−4(4)4	fcc-hollow	1.25(.05)1.45	1.15	.05	(0,0),(5,0)
G	fcc-hollow	0	0.9(.05)1.0	1.2(.17)1.71	−4(4)4	fcc-hollow	1.25(.05)1.45	1:1	.05	(5,0)
H	fcc-hollow	0	1.0	1.2(.17)1.71	0	fcc-hollow	1.25(.05)1.45	1.1,1.2,1.25	.05	(0,0)
I	fcc-hollow	0	0.7(.2)1.3	1.2(.17)1.71	−4(4)4	fcc-hollow	1.2(.05)1.45	1.15	.05	(0,0)
J	fcc-hollow	0	0.7(.2)1.3	1.435	−4(4)4	fcc-hollow	1.2(.05)1.45	1.15	.05	(0,0)

Notes for Table 6-2.

a The site over which the carbon ring is centered.

b The azimuthal orientation of the benzene ring, as defined in Figure 2.

c Smallest layer spacing between C of CO and C_6 carbons of C_6H_6. The first and last numbers give the range of layer spacings in Å, and the number in parentheses is the incremental step size. For example the first entry -0.6(.2)0.0 means that LEED calculations were made for carbon(CO)-carbon(C_6H_6) layer spacings of -0.6, -0.4, -0.2, and 0.0Å.

d In-plane Kekulé distortions characterized by r and β, as defined in Fig. 2.

e Perpendicular distance between topmost Pd layer and C of CO. The first and last numbers give the range of layer spacings in Å, and the number in parentheses is the incremental step size.

f C-O bond length (C-O bond always perpendicular to surface).

g Perpendiular distance between 1st and 2nd Pd layers. Positive values indicate expansions.

h Incidence directions used in theory. θ=4° and 6° correspond to checks on the accuracy of the experimental polar angle. ϕ=180° corresponds to checks on the orientation of the substrate.

[Table 6-3] R-factor comparison for CO and benzene adsorbed at different sites, keeping the substrate bulk-like.

Adsorption Sites for C_6H_6 and CO (See Fig. 6-10-c)		Minimum 5-Average R-Factor
A	aABC (top)	0.4338
B	dABC (bridge)	0.3008
C	cABC (fcc-hollow)	0.2696
D	bABC (hcp-hollow)	0.4060

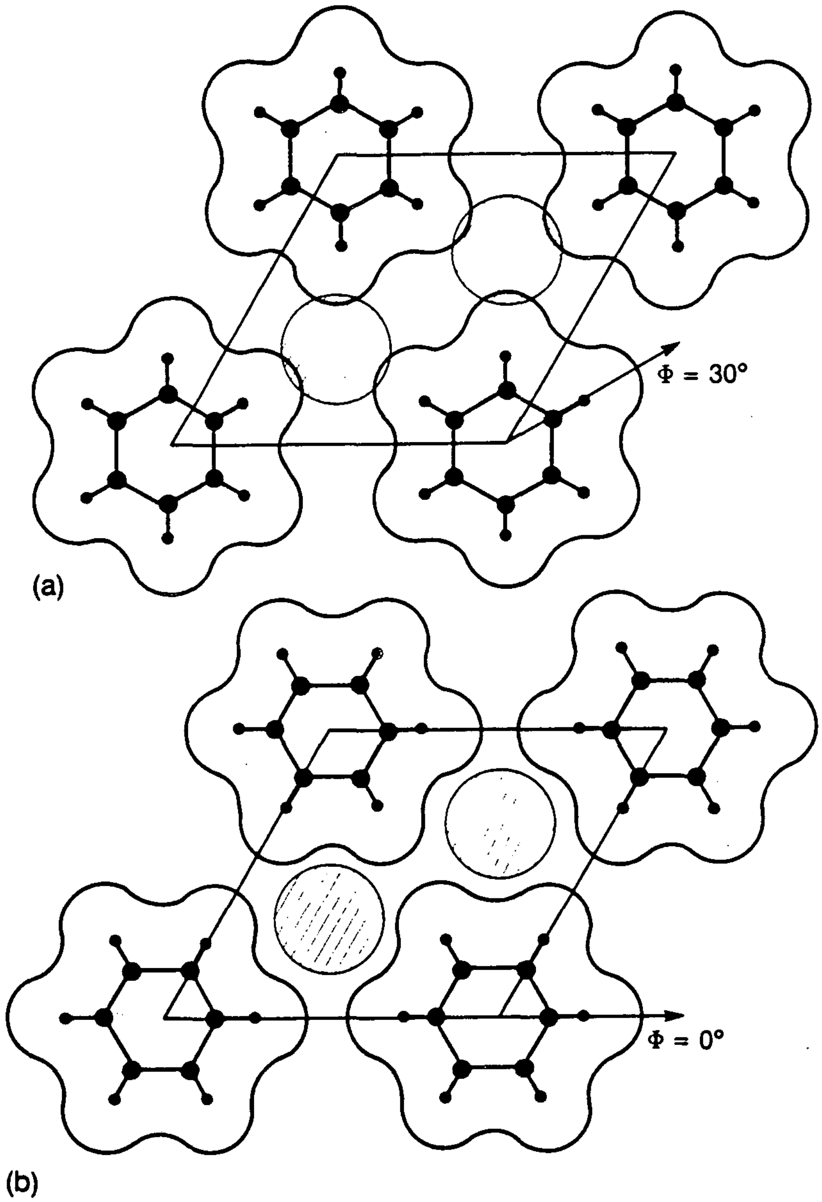

[Fig. 6-10] Panels (a) and (b) show the molecular packing within the (3x3) overlayer on Pd(111) with the help of Van der Waals contours, for two benzene orientations ($\Phi = 0^\circ$ and 30°) and two CO molecules per unit cell.

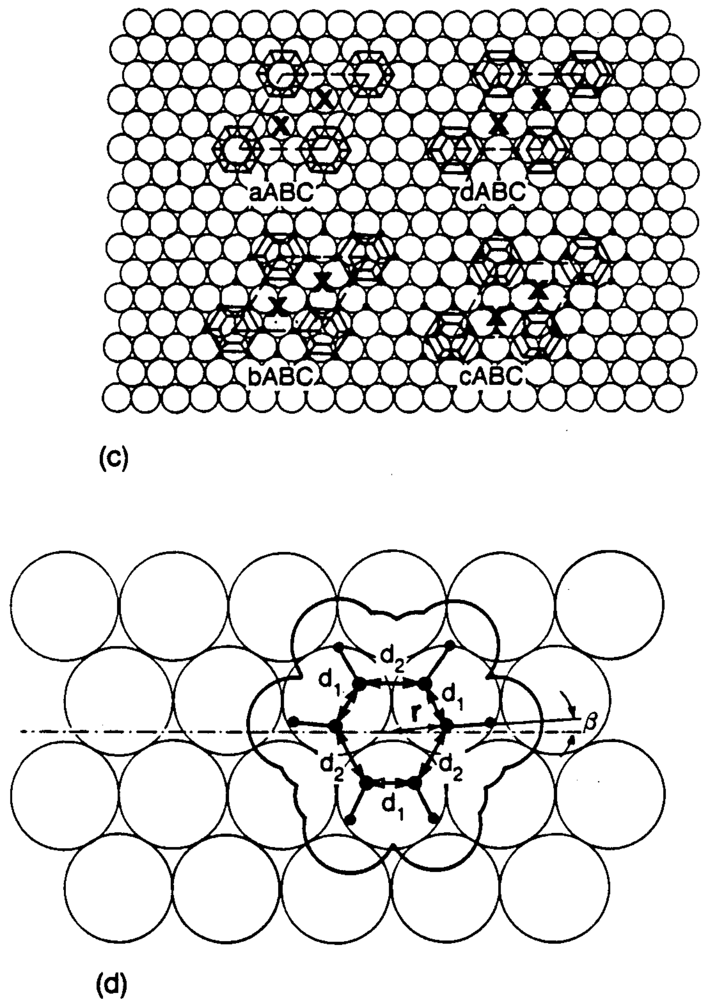

XBL 863-10703A

[Fig. 6-10] (continued) Panel (c) represents four "registries" of the (3x3) overlayer (with $\Phi = 0^\circ$) with respect to the substrate. The benzenes are represented by rings of carbons and hydrogens, the CO by crosses. Second layer palladium atoms are represented by dots in order to distinguish two kinds of hollow sites. The Kekulé distortion of benzene is defined in panel (d).

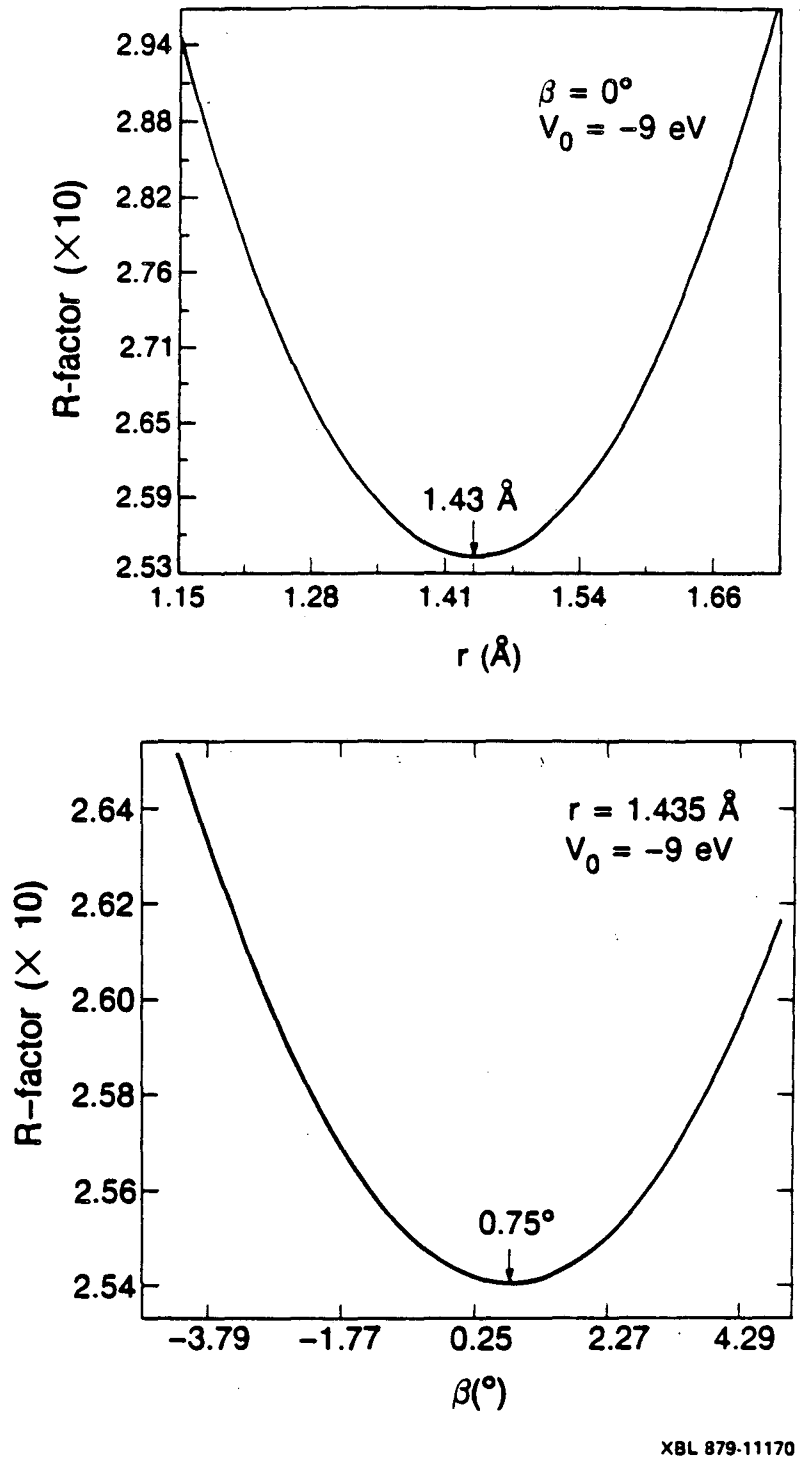

[Fig. 6-11] Five-R-factor average as a function of two of the structural parameters (r,β) describing benzene ring distortions.

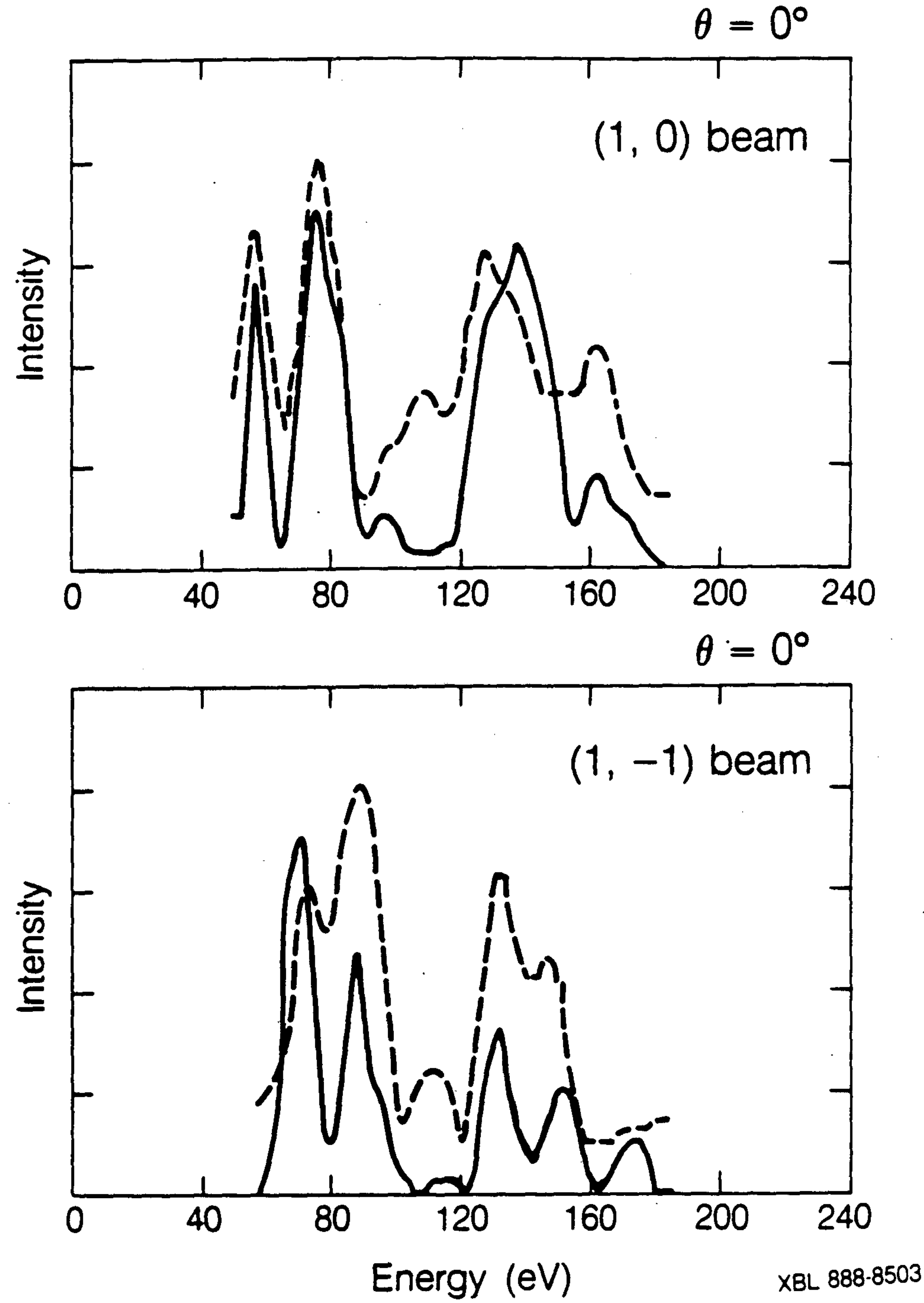

[Fig. 6-12] (Dotted line) Calculated LEED I-V curves at normal incidence for Pd(111)-(3x3)-C_6H_6 + 2CO for a structure near the minimum R-factor:

Benzene	fcc-hollow site, d_{Pd-C}=2.2Å, r=1.37Å, β=0°
CO	fcc-hollow site, d_{Pd-C}=1.3Å, d_{C-O}=1.15Å
Pd(111)	Δd_{Pd-Pd}=+0.05Å for all layers
R-factor=0.2567	

(Solid line) Experimental LEED I-V curves

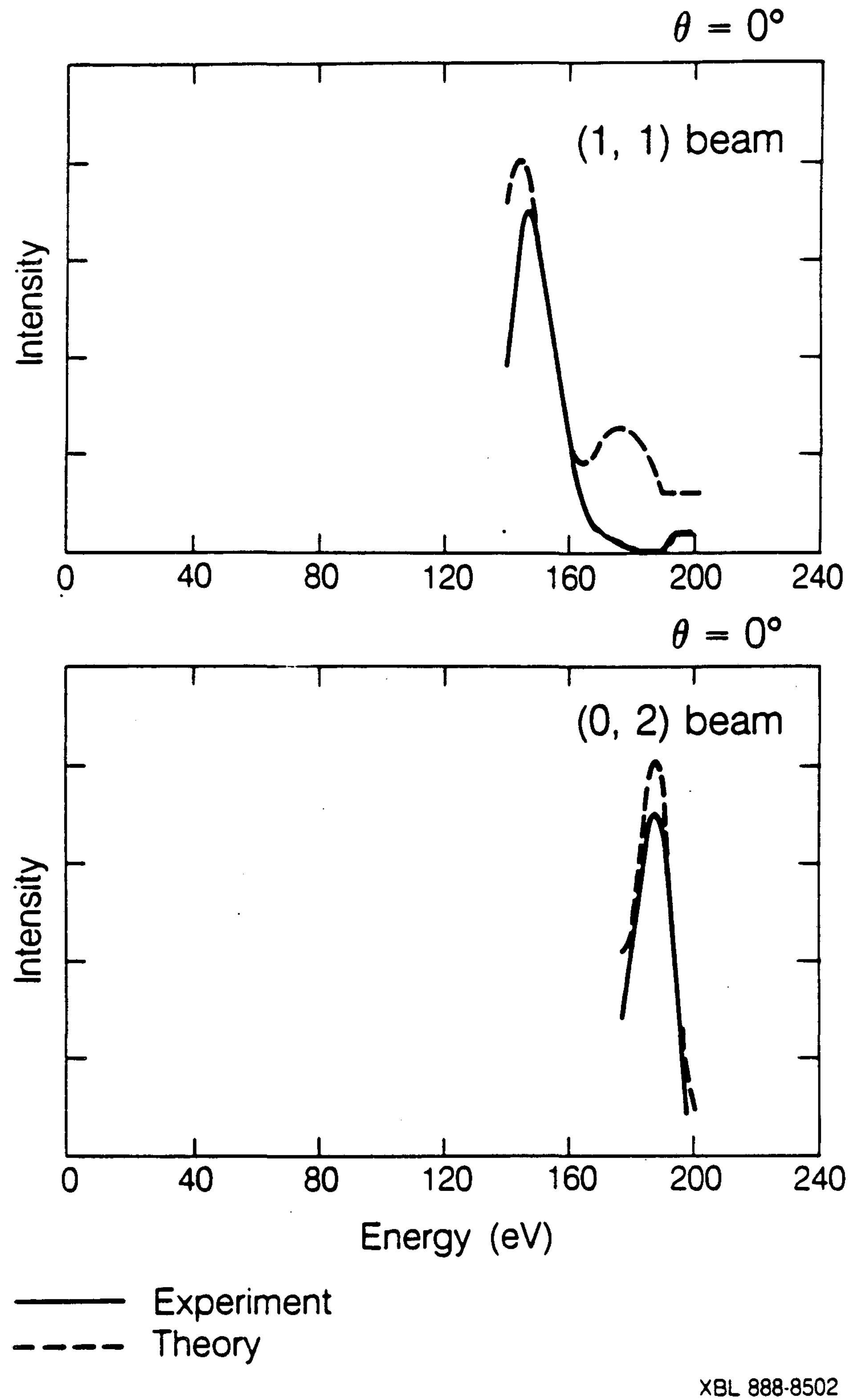

[Fig. 6-12] (continued)

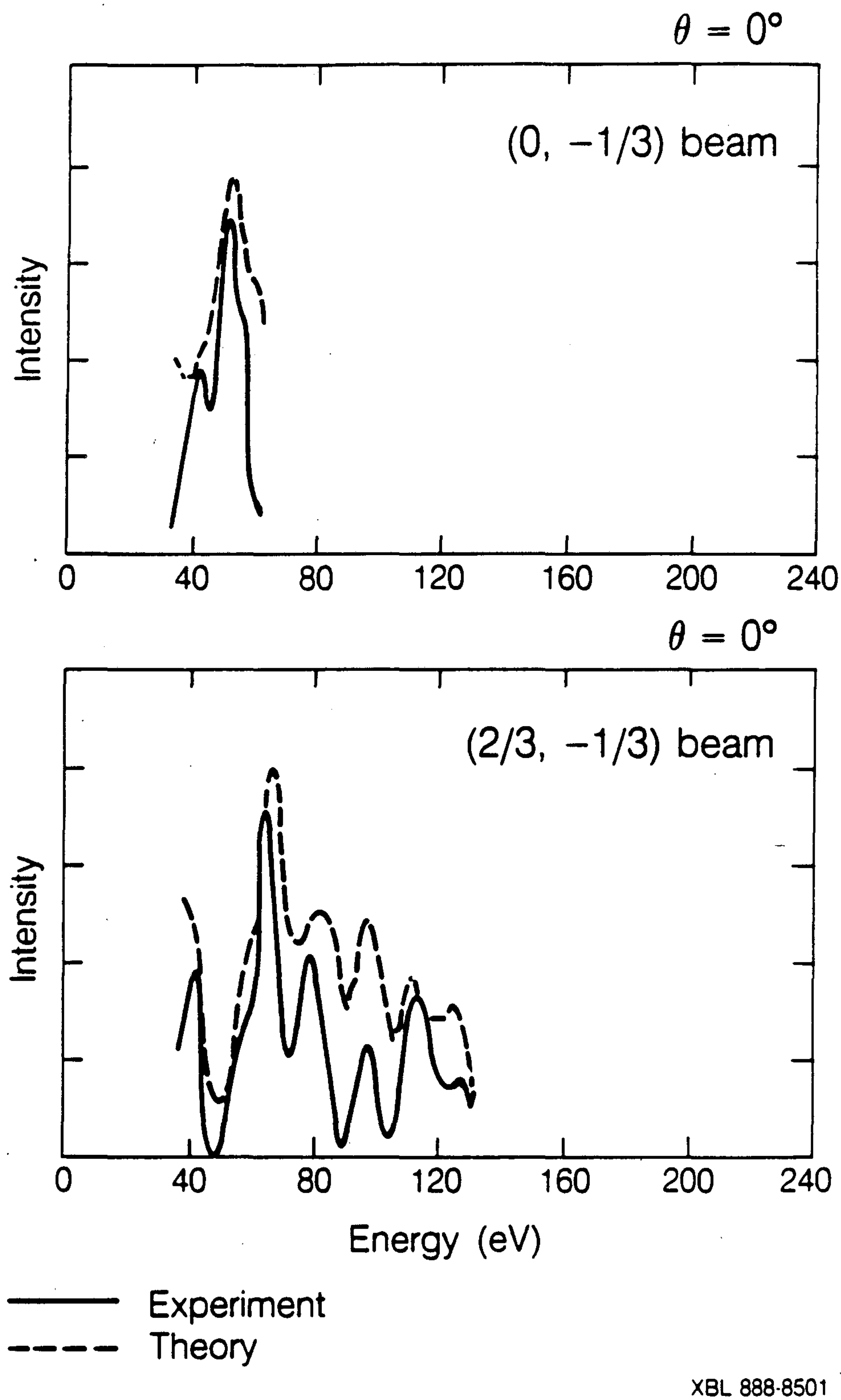

[Fig. 6-12] (continued)

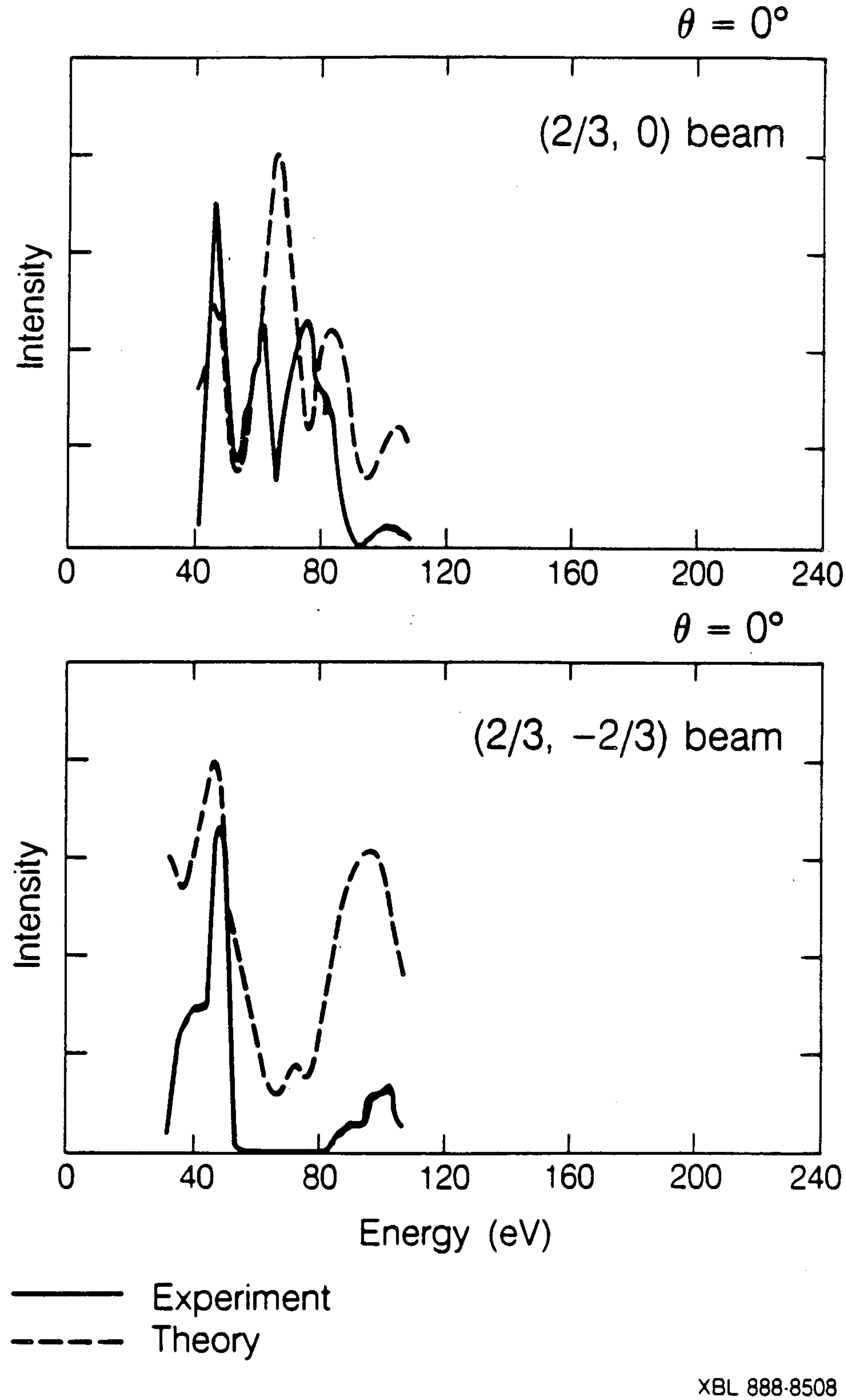

[Fig. 6-12] (continued)

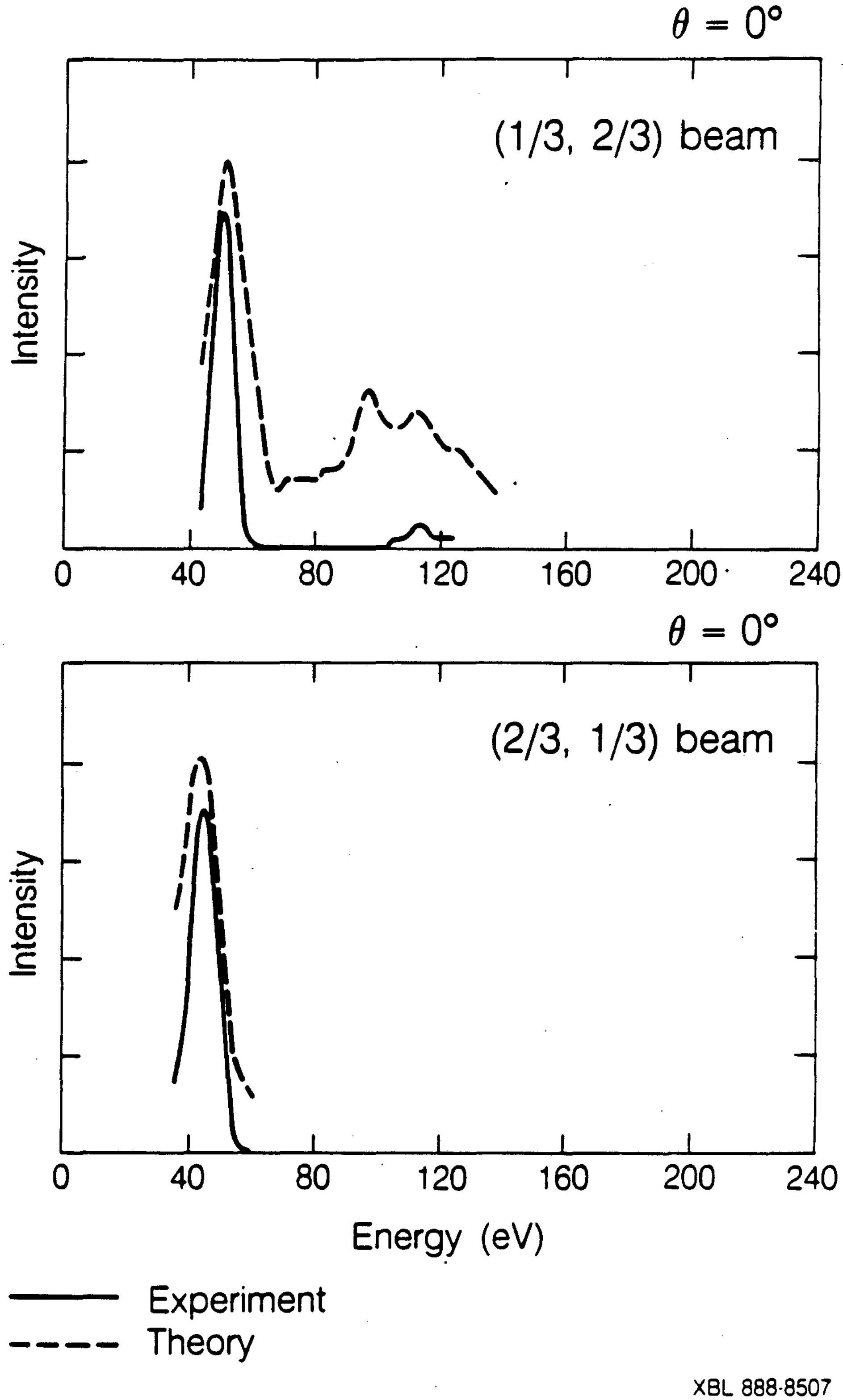

[Fig. 6-12] (continued)

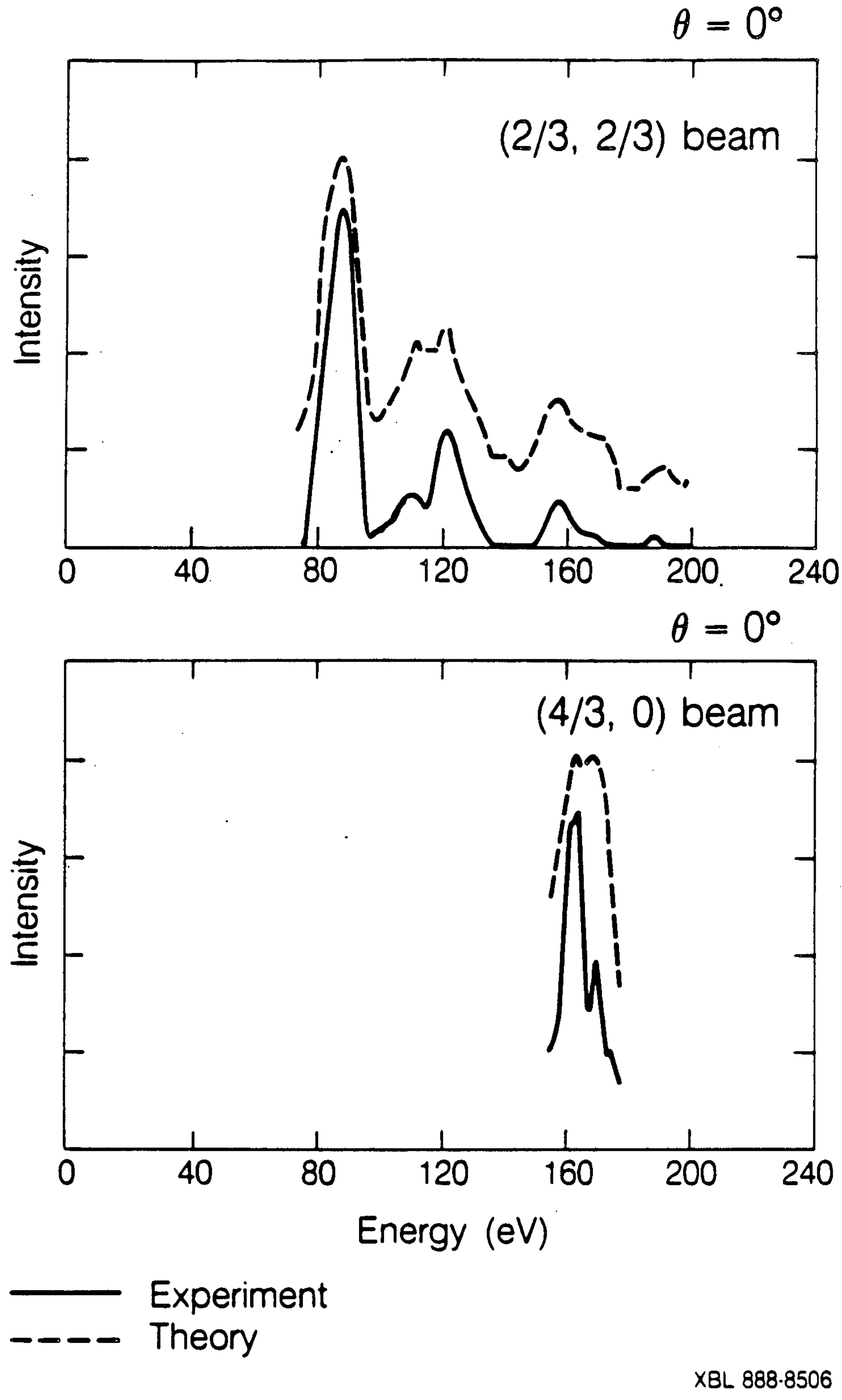

[Fig. 6-12] (continued)

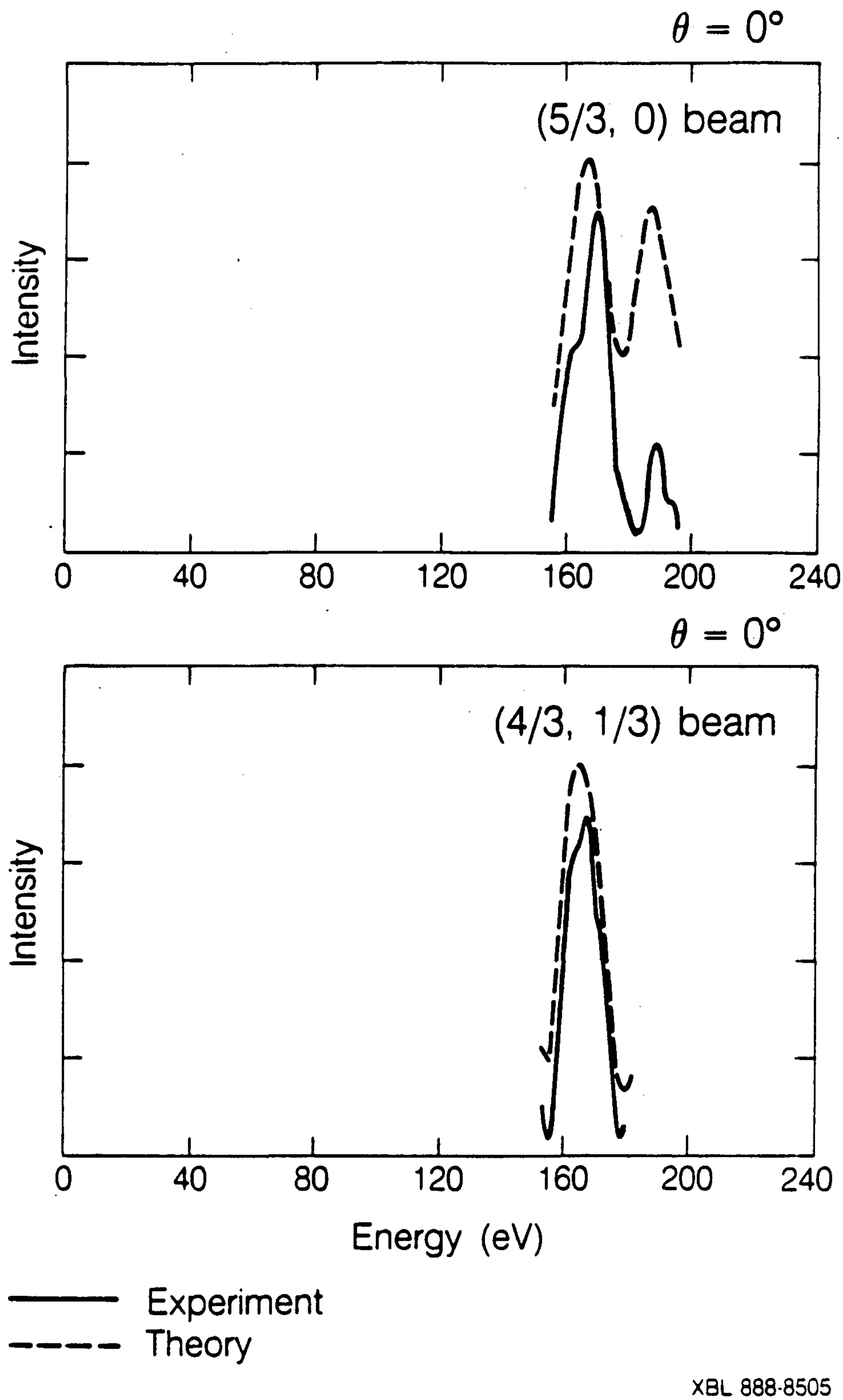

[Fig. 6-12] (continued)

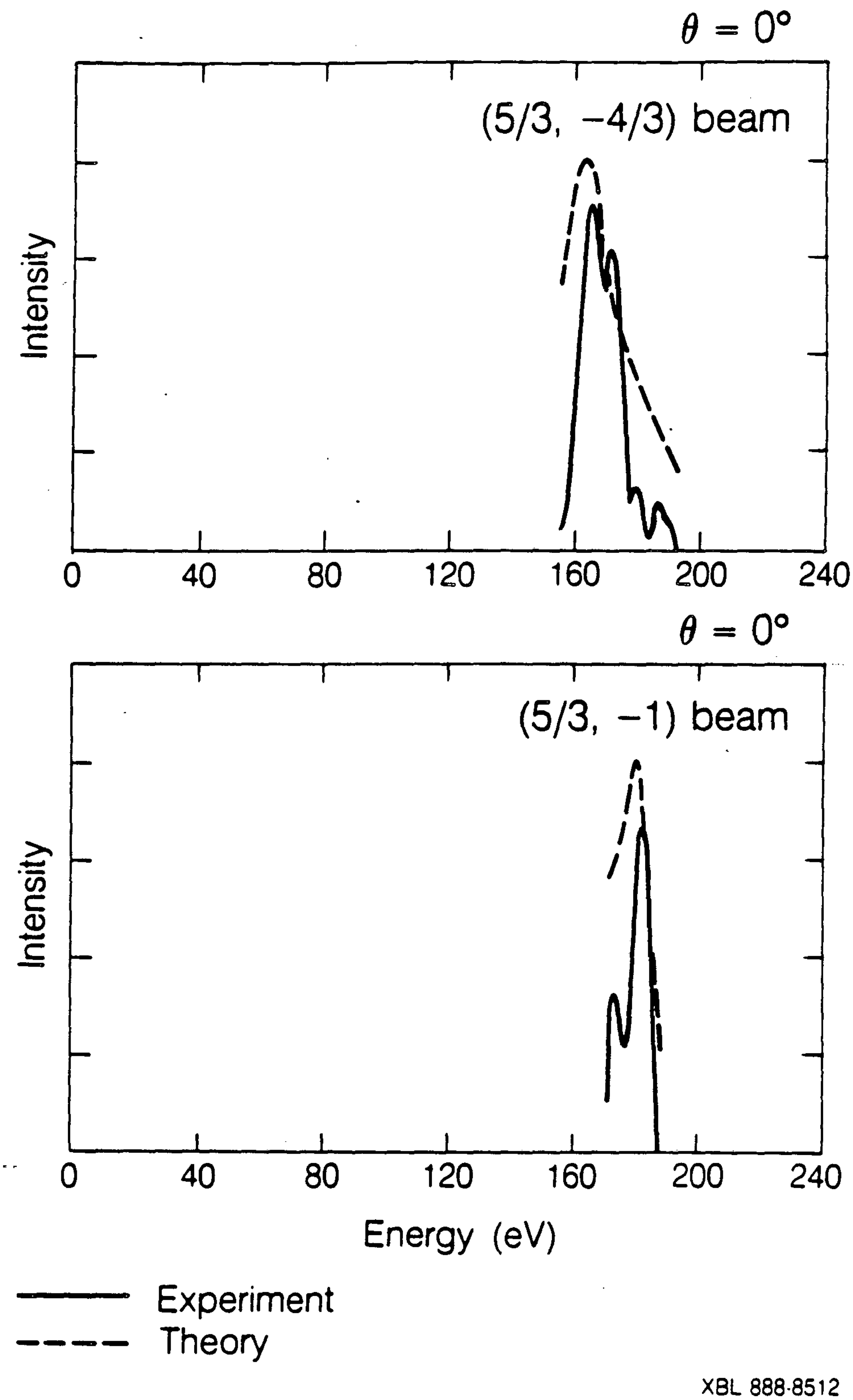

[Fig. 6-12] (continued)

6.5. Results

Our best structure for Pd(111)-(3x3)-C_6H_6 + 2CO, i.e., the structure which minimizes the R-factors, is illustrated in Fig. 6-13. The hydrogen atom positions are guessed, since they were not determined by LEED. (Some theoretical calculations indicate[25,26] that, when benzene is adsorbed on transition metals, hydrogen atoms point away from the substrate surface, perhaps due to rehybridization of the carbon atoms and/or electrostatic repulsive interactions between the hydrogen atoms and metal surfaces.) In the (3x3) structure, both benzene and CO are centered over 3-fold fcc-type hollow sites in a compact arrangement. The benzene carbon ring has a spacing of 2.25 ± 0.05 Å to the metal surface with six identical Pd-C bond lengths of 2.39 ± 0.05 Å. No significant in-plane distortion has been detected within the error bars: we find C-C distances of d_1 = 1.40 ± 0.10 Å, and d_2 = 1.46 ± 0.10 Å (d_1 and d_2 are defined in Fig. 6-10). However, the possible deviations from the gas-phase benzene structure (d_1=d_2=1.397Å) are in the same direction as those on Rh(111): shorter C-C bonds over individual metal atoms and longer C-C bonds bridging two metal atoms. The CO molecular axis is perpendicular to the surface, the C-O and Pd-C bond lengths being 1.17 ± 0.05 Å and 2.05 ± 0.04 Å, respectively.

The optimal muffin-tin zero level, assumed layer-independent, is found to be 9±1eV below vacuum. The minimized value of the five-R-factor average is 0.25, while the corresponding Zanazzi-Jona and Pendry R-factor values are 0.49 and 0.48 (using the normal-incidence data only). These R-factor values are comparable to values obtained for similar coadsorption structures: Rh(111)-c($2\sqrt{3}$x4)*rect*-C_6H_6+CO with R(average)=0.31, R(Zanazzi-Jona)=0.40, R(Pendry)=0.66, Rh(111)-(3x3)-C_6H_6 +2CO with R(average)=0.21, R(Zanazzi-Jona)=0.24, R(Pendry)=0.41, and Pt(111)-($2\sqrt{3}$x4)*rect*-2C_6H_6 + 2CO with R(average)=0.28, R(Zanazzi-Jona)=0.42, R(Pendry)=0.54. The results are summarized in the format of SCIS (Surface Crystallographic Information Service)[27] in Table 6-4.

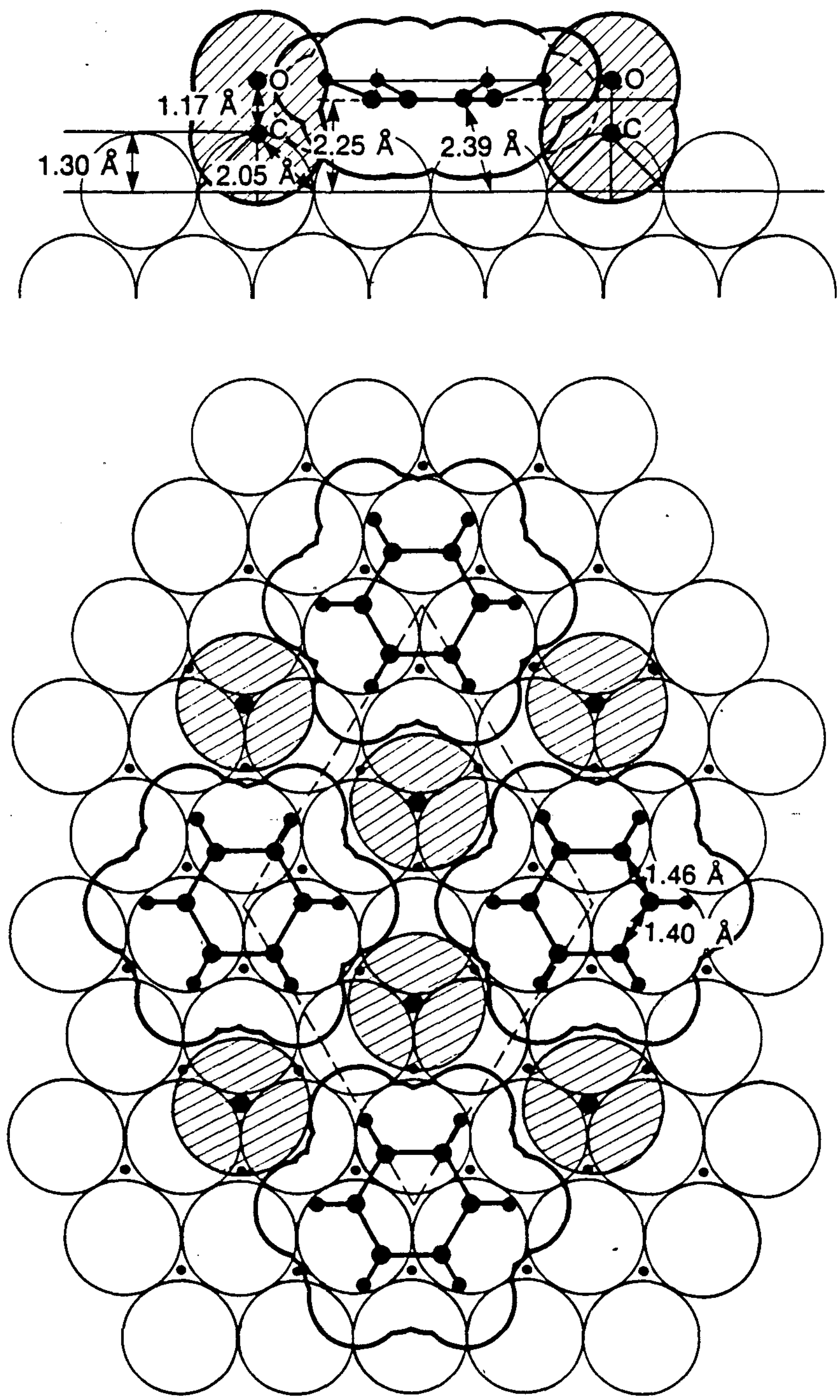

Pd (111) – (3 × 3) – C_6H_6 + 2CO

[Fig. 7-7] The optimum structure for Pd(111)-(3x3)-C_6H_6+2CO, in side view at top and top view at bottom. Van der Waals shapes are used for overlayer molecules. The CO molecules are shown shaded. The hydrogen positions are guessed. The small dots represent the second-layer metal atoms.

[Table 6-4] Structure Result in Format of Surface Crystallographic Information Service (SCIS)

SURFACE: Substrate Face: Pd(111); Adsorbate: C_6H_6, CO
Surface Pattern: (3x3), (3,0/0,3)
STRUCTURE: Bulk Structure: fcc; Temp: 150K; Adsorbate State: Molecular;
Coverage: 1/9 (C_6H_6/Pd), 2/9 (CO/Pd)
REFERENCE UNIT CELL: a=8.25Å; b=8.25Å; A(a,b)=60°

Layer	Atom	Atom Positions		Normal Layer Spacing
A1	O	0.2222	0.2222	0.00
A2	O	0.8889	0.8889	0.22
A3	C	0.5582	0.7276	0.00
A4	C	0.7276	0.5582	0.00
A5	C	0.7276	0.3809	0.00
A6	C	0.5582	0.3809	0.00
A7	C	0.3809	0.5582	0.00
A8	C	0.3809	0.7276	0.95
A9	C	0.2222	0.2222	0.00
A10	C	0.8889	0.8889	1.30
S1	Pd	0.0000	0.0000	0.00
S2	Pd	0.3333	0.0000	0.00
S3	Pd	0.6667	0.0000	0.00
S4	Pd	0.0000	0.3333	0.00
S5	Pd	0.3333	0.3333	0.00
S6	Pd	0.6667	0.3333	0.00
S7	Pd	0.0000	0.6667	0.00
S8	Pd	0.3333	0.6667	0.00
S9	Pd	0.6667	0.6667	2.30
S10	Pd	0.1111	0.1111	0.00
S11	Pd	0.4444	0.1111	0.00
S12	Pd	0.7778	0.1111	0.00
S13	Pd	0.1111	0.4444	0.00
S14	Pd	0.4444	0.4444	0.00
S15	Pd	0.7778	0.4444	0.00
S16	Pd	0.1111	0.7778	0.00
S17	Pd	0.4444	0.7778	0.00
S18	Pd	0.7778	0.7778	2.30

2D Symmetry: p3m1
Thermal Vibrations: Debye Temp=225K with double amplitude for surface atoms;
R-factor: R_{VHT}=0.25 R_{ZJ}=0.49 R_P=0.48

6.6. Discussion

The first structure analysis of coadsorbed benzene and CO on Pd(111) has been performed by LEED with a minimum R-factor of 0.25. This result gives an unique opportunity to compare similar coadsorption structures of benzene+CO on three different metal surfaces: Pd(111), Rh(111), and Pt(111). Table 6-5 gathers pertinent data for these structures, while Fig. 6-1 shows their analogies and differences.

6.6.1. Coadsorption-Induced Ordering

The present benzene/CO structure illustrates that coadsorption can produce new surface periodicities which cannot be formed by the pure component adsorbates taken separately. At room temperature, pure CO presents two ordered structures:[28] $(\sqrt{3}x\sqrt{3})R30^\circ$ at $\theta = 1/3$ and c(4x2) at $\theta = 1/2$. On the other hand, pure benzene is disordered at any surface coverage. Coadsorption of these two molecules resulted in the (3x3) structure.

Coadsorption-induced ordering of organic overlayers has already been reported on Rh(111) and Pt(111) surfaces for a variety of pairs of adsorbates. [5,29,2,30,3,4] On the Pt(111) surface, benzene by itself does not order 5,2,30,20 just as on Pd(111), but four ordered structures have been observed by coadsorbing CO.[2,5,30] On Rh(111), benzene by itself orders weakly[5,19] (electron-beam-induced disordering is rapid), while several stable ordered coadsorbed structures are observed by LEED in the presence of CO.[3,4,5]

[Table 6-5] Adsorption geometries of benzene, indicating average carbon-ring radius, C-C bond lengths (two values where long and short bond coexist), metal-carbon distances and adsorption sites of C_6H_6 ring centers

System	C_6 radius	d_{C-C} (Å)	d_{M-C} (Å)	site
benzene/surface				
Pd(111)-(3x3)-C_6H_6+2CO	1.43±0.10	1.46±0.10	2.39±0.05	fcc hollow
		1.40±0.10		
Rh(111)-(3x3)-C_6H_6+2CO[5]	1.51±0.15	1.58±0.15	2.30±0.05	hcp hollow
		1.46±0.15		
Rh(111)-c($2\sqrt{3}$x4)*rect*-C_6H_6+CO[4]	1.65±0.15	1.81±0.15	2.35±0.05	hcp hollow
		1.33±0.15		
Pt(111)-($2\sqrt{3}$x4)*rect*-2C_6H_6+4CO[3]	1.72±0.15	1.76±0.15	2.25±0.05	bridge
		1.65±0.15		
benzene/complex				
C_6H_6 on Ru_6, Os_3 clusters[48]	1.44	1.48	2.27-2.32	hollow
		1.39		
gas				
C_6H_6 molecule	1.397	1.397		
C_2H_6 molecule		1.54		
C_2H_4 molecule		1.33		
C_2H_2 molecule		1.20		

There has been no theoretical work concerning energetics of such coadsorption induced ordering, however one model for explaining this ordering behavior is that benzene and CO act like donors and acceptors, respectively, with respect to the substrate metal, and that donors are surrounded by acceptors and vice versa, in a way similar to an ionic crystal. The donor/acceptor character is suggested by work function measurements for coadsorption on Pt(111)[30,31] and Rh(111).[32]

6.6.1.1. Charge Transfer from Pd(111) to CO

It is known that, on the Pt(111) surface, CO switches its adsorption site from 1-fold to 2-fold and possibly to 3-fold as the amount of coadsorbed potassium is increased.[33] This indicates that the preferred CO adsorption site is closely related to the work function of the substrate(potassium decreases the work function by charge transfer to the metal). On the Pd(111) surface, pure CO at coverages up to 1/3 monolayers prefers to adsorb at the 3-fold site[24] since the work function of clean Pd(111) is less than that of Pt(111).[34] However, upon increasing the CO coverage, CO switches its adsorption site from 3-fold to 2-fold, and at low temperatures the 1-fold site is attainable.[31,35] The same effect has been observed on palladium crystallites supported on SiO_2, and it is interpreted in terms of charge transfer from palladium to adsorbed CO.[36] Thus CO itself seems to work as a net electron-acceptor on Pd(111). Consistent with this conclusion, the adsorption of CO increases the work function of the Pd(111) crystal surface.[37,38]

6.6.1.2. Coadsorption Effects of Benzene and CO on Pd(111)

It is believed that benzene is a net electron-donor to the Rh(111) and Pt(111) surfaces, based on work-function measurements,[30,31,32] on the reduction of the CO stretching frequency[5] when coadsorbed with benzene, and also on the fact that CO switches its adsorption site from 1-fold to 2-fold or 3-fold on these surfaces when benzene is coadsorbed.[2,3,4] Furthermore, a theoretical study on the Rh(111) surface[25] has suggested that benzene is a net electron donor to Rh(111).

Whether benzene is a net donor or acceptor toward Pd(111) is not clear. However, the large decrease in the CO stretching frequency when coadsorbed with benzene[39] might be caused by the enhanced backdonation from the palladium to the $2\pi^*$ orbital of adsorbed CO because of the coadsorbed benzene. Also, the 3-fold site of CO on Pd(111) when coadsorbed with benzene is consistent in this context.

So far the CO-induced ordering of benzene has been found on three different metal surfaces, including Pd(111), and the charge transfer between substrate and coadsorbates seems to play an important role in causing this phenomenon.

6.6.2. The Structure of Carbon Monoxide

The (3x3) unit cell contains two CO molecules, corresponding to a surface coverage of 2/9, located on 3-fold fcc-hollow sites. Pure CO is known from LEED[24] to also be adsorbed on 3-fold fcc-hollow sites at $\theta = 1/3$ (at higher coverages, a shift to bridge sites occurs).[28,35] This is consistent with the tendency known on Pt(111) and Rh(111) for CO to move to higher-coordination sites (at least when available) in the presence of donors such as benzene or alkali atoms.[2,3,4,33] Note that CO on Rh(111) is adsorbed at another kind of hollow site (hcp-hollow) in the benzene coadsorption structures.

The CO bond is perhaps slightly elongated due to coadsorbed benzene: 1.17±0.05Å in the (3x3) structure vs. 1.15±0.05Å in the pure CO overlayer[24] and 1.15Å in the gas phase. At the same time a significant reduction of the CO stretching frequency has been observed by HREELS: from about 1840 cm^{-1} to about 1750 cm^{-1}. The right part of the Fig. 6-14 shows C-O bond lengths on various metal substrates, as primarily obtained by LEED. We see that the C-O bond lengths increase as the coordination number increases; the amount of change is, however, rather small. The left part of this figure also shows metal-carbon bond lengths for CO on various metal substrates. This quantity varies appreciably, as the coordination number increases. The results on Pd(111) fit the general trend well.

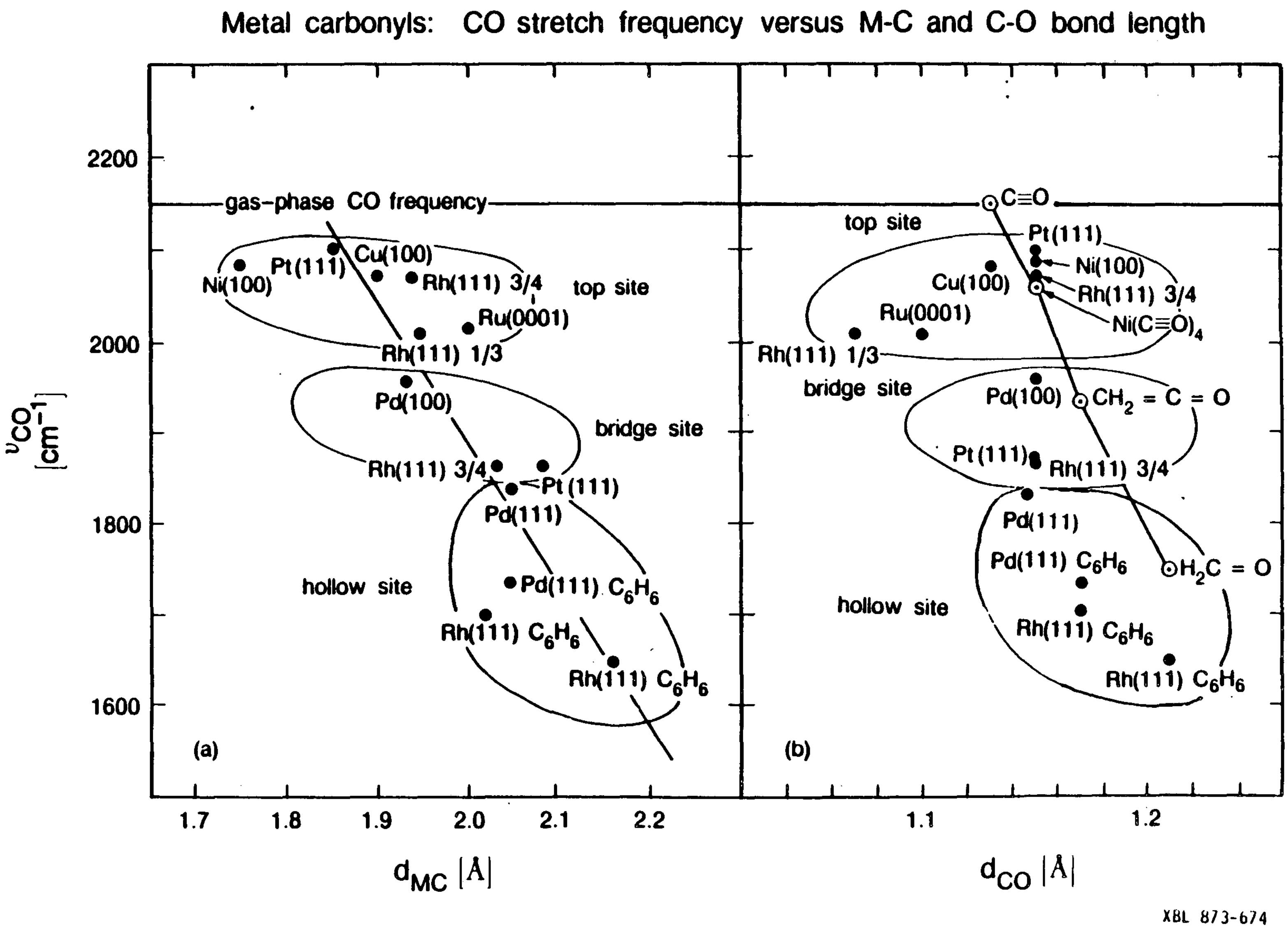

[Fig. 6-14] The correlation between the geometries of chemisorbed CO determined by LEED and CO stretching frequency observed by IR or HREELS.

6.6.3. The Structure of Benzene

6.6.3.1. Position of Benzene Relative to Pd(111)

Benzene is found to be adsorbed molecularly over a fcc-hollow site in the (3x3) structure. Pure disordered benzene is thought to adsorb over a bridge site of Pd(111), based on the similarity of HREELS for benzene on Pd(111) and Pd(100).[16] Our result implies, therefore, that the benzene molecules switch their adsorption site from bridge to fcc-hollow when coadsorbed with CO. A similar switching occurs on Rh(111), but the hcp-hollow site rather than the fcc-hollow site is found on that surface. The metal-carbon bond lengths for benzene on Pd(111) are found to be 2.39±0.05Å. This value is to be compared with 2.30±0.05Å and 2.35±0.05Å on Rh(111) and 2.25±0.05Å on Pt(111) (See Table 4). Thus there is a clear trend towards stronger metal-carbon bonding from Pd to Rh to Pt. [Table. 6-6]

Substrate	(Gas Phase)	Pd(111)	Rh(111)		Pt(111)
Surface Structure		(3x3)-C_6H_6 + 2CO	(3x3)-C_6H_6 + 2CO	c($2\sqrt{3}$x4)rect-C_6H_6 + CO	($2\sqrt{3}$x4)rect-2C_6H_6 +4CO
The Structure of Benzene	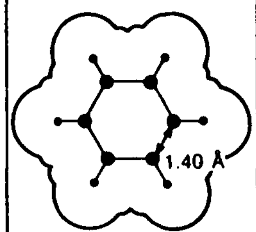	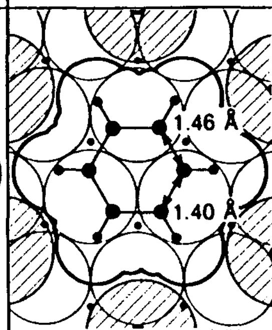	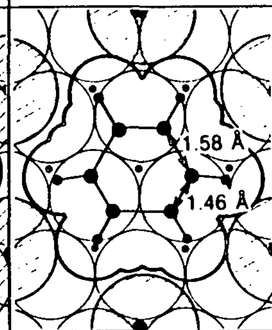	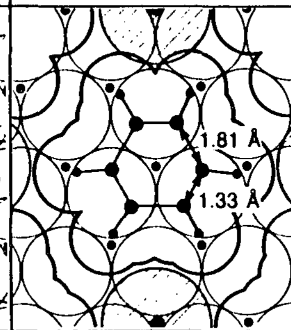	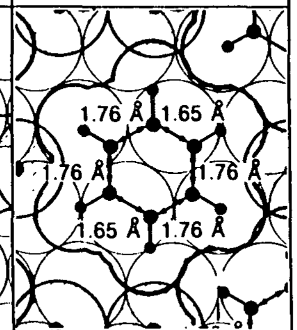
C_6 Ring Radius (Å)	1.40	1.43±0.10	1.51±0.15	1.65±0.15	1.72±0.15
d_{M-C}(Å)	-	2.39±0.05	2.30±0.05	2.35±0.05	2.25±0.05
γ_{CH}(cm^{-1})*	670	720-770	780-810		830-850

[Table 6-6] Structures of benzene on Pd(111), Rh(111), and Pt(111)
*) The out of plane CH bending frequency of benzene. For each surface, the frequency range indicated includes the values of the pure benzene overlayer and coadsorbed superlattices with CO.

XBL 878-3565

6.6.3.2. Benzene Ring Distortions

On Pd(111) (with coadsorbed CO), the benzene ring skeleton is found to be essentially indistinguishable from the gas phase structure within the error bar (±0.10Å). There may be a slight C_6 ring expansion to a radius of 1.43±0.10Å and a Kekulé distortion with a difference between C-C bonds of 0.06±0.10Å. This contrasts with benzene on Rh(111) or Pt(111) which showed significant in-plane distortions(See Table 6-6).

The benzene-transition metal interactions can be understood in the framework of d-π interaction analogous to coordination chemistry.[25,40] This interaction results in a benzene ring expansion, which increases with the metal-carbon bond strength. Table 6-6 shows such a trend from Pd(111) via Rh(111) to Pt(111). This trend parallels the decrease in benzene-metal bond length mentioned above.

On Rh(111) and Pt(111), where a strong benzene-metal interaction has been detected by LEED, the benzene rings exhibit long and short C-C bonds within the molecule. In these cases the benzene molecules adopt the same symmetry as their adsorption sites: thus, benzene adsorbed at bridge sites on Pt(111) show an in-plane distortion with C_{2v} symmetry, and benzene adsorbed at hollow sites on Rh(111) shows a Kekulé distortion with C_{3v} symmetry. It is therefore very probable that at least a weak Kekulé-type distortion exists in the case of Pd(111), although it is too small to be confirmed by LEED.

These trends are further supported by HREELS data[5,39] where the γ_{CH} mode frequency increases monotonously from the gas phase value (~670 cm^{-1})

upon adsorption of benzene on Pd(111), Rh(111), and Pt(111): the respective frequencies are 730-770cm^{-1} on Pd(111), 780-810cm^{-1} on Rh(111) and 830-850cm^{-1} on Pt(111). These frequencies include both pure benzene overlayers and coadsorbed overlayers of benzene and CO. The coadsorbed CO affects the γ_{CH} mode frequency of adsorbed benzene. However, such indirect interactions between adsorbates are less effective in changing the γ_{CH} frequency than switching substrates from Pd to Rh to Pt. Thus the trends of benzene-metal interaction obtained from benzene-CO-metal systems will presumably hold qualitatively in the case of pure benzene on Pd(111), Rh(111), and Pt(111) surfaces.

6.6.3.3. Chemical Properties

In this section, we explore the correlation between the structural bond-lengths information obtained by LEED with bond energies and catalytic properties. TDS data were gathered from various references, but because of different experimental conditions, only qualitative comparisons can be made for TDS data of different metals.

When the adsorbed benzene is heated, decomposition and molecular desorption are the competing processes on Pd(111), Rh(111), and Pt(111) surfaces. Koel et al.[41] have proposed, based on TDS and HREELS data, that benzene decomposes on Rh(111) via an acetylene-like intermediate (which however is very short-lived at the benzene decomposition temperature). Interestingly, on supported Rh particles, acetylene can be formed from benzene with coadsorbed CO.[42] This might be related to the strong benzene-metal interaction and the resulting Kekulé distortion detected by LEED.

Benzene chemisorbed on the Pt(111) crystal is less asymmetrically distorted, exhibiting a more uniform expansion of the ring. This structure may suggest a benzene intermediate on the metal surface that can desorb intact at the higher temperatures and pressures of the catalytic reaction.[2]

The benzene on Pd(111) surface was found by LEED to be weakly distorted. On this surface, a higher activation energy for decomposition is apparent: the H_2 desorption maximum due to benzene decomposition is higher on Pd(111)(~555K) than Rh(111)(~490K [41]) or Pt(111)(~545K[43,44]). This seems to correlate with the weaker benzene-palladium interaction observed by LEED. Molecular benzene desorbs from Pd(111) at the two temperature of ~430K and ~530K.[16] This indicates that benzene still exist as an intact molecule on the surface at 530K. (By contrast, Rh(111) has only a 395K desorption peak[41] and Pt(111) has 375K and 450K peaks,[43,44] indicating that decomposition is predominant at higher temperatures on these surfaces.)

It is known that acetylene can trimerize to form benzene on Pd(111) crystal surfaces,[6,7,8,9,10,11,12,13] but not on Rh(111)[45] or on Pt(111).[46] T.G. Rucker et. al. have studied[12] this reaction at high pressures(200 to 1200 Torr) in the temperature range of 273-573K, and found that benzene was the only product detected. This might be related to the weak benzene-palladium interaction and the resulting easy molecular benzene desorption at these reaction conditions.

The cyclotrimerization occurs on Pd(111) even under UHV conditions, and benzene desorbs at 250K and 490K after adsorbing acetylene at 20K and subsequent heating. The Pd(111)-(3x3)-C_6H_6+2CO structure was obtained above room temperature. Structural studies on both acetylene and benzene at low temperatures are necessary to understand such low-temperature benzene formation.

6.7. Conclusion

An ordered (3x3) benzene overlayer was formed on Pd(111) by coadsorbing benzene and CO. A dynamical LEED analysis has revealed that both benzene and CO bond over fcc-type hollow sites in a close-packed form with a 2:1 CO to C_6H_6 stoichiometry.

Weak distortions from the gas phase geometry may be present in both molecules. This contrasts with larger benzene distortion on Rh(111) and Pt(111). Clear trends emerge which indicate an increasing metal-benzene bond strength and decreasing C-C bond strength in going from Pd(111) via Rh(111) to Pt(111). These trends are consistent with vibrational spectroscopy results.

References

1. M. A. Van Hove, R. F. Lin, and G. A. Somorjai, *Physical Review Letters*, vol. 51, p. 778, 1983.

2. D. F. Ogletree, M. A. Van Hove, and G. A. Somorjai, *Surface Science*, vol. 183, p. 1, 1987.

3. M. A. Van Hove, R. F. Lin, and G. A. Somorjai, *Journal of the American Chemical Society*, vol. 108, p. 2532, 1986.

4. M. A. Van Hove, R. F. Lin, G. A. Blackman, and G. A. Somorjai, *Acta Crystallographica*, vol. B43, p. 368, 1987.

5. C. M. Mate and G. A. Somorjai, *Surface Science*, vol. 160, p. 542, 1985.

6. W. Sesselmann, B. Woratschek, G. Ertl, J. Küppers, and H. Haberland, *Surface Sci.*, vol. 130, p. 245, 1983.

7. W. T. Tysoe, G. L. Nyberg, and R. M. Lambert, *J. Chem Soc. Chem. Commun.*, p. 623, 1983.

8. W. T. Tysoe, G. L. Nyberg, and R. M. Lambert, *Surface Sci.*, vol. 135, p. 128, 1983.

9. T. M. Gentle and E. L. Mutterties, *J. Phys. Chem.*, vol. 87, p. 2469, 1983.

10. T. M. Gentle, V. H. Grassian, D. G. Klarup, and E. L. Muetterties, *J. Am. Chem. Soc.*, vol. 105, p. 6766, 1983.

11. B. Marchon, *Surface Sci.*, vol. 162, p. 382, 1985.

12. T.G. Rucker, M. A. Logan, T. M. Gentle, E. L. Muetterties, and G. A. Somorjai, *J. Phys. Chem.*, vol. 90, p. 2703, 1986.

13. M. A. Logan, T. G. Rucker, T. M. Gentle, and E. L. Muetterties, *J. Phys. Chem.*, vol. 90, p. 2709, 1986.

14. D. R. Lloyd, C. M. Quinn, and N. V. Richardson, *Solid State Comm.*, vol. 23, p. 141, 1977.

15. F. P. Netzer and J. U. Mack, *J. Chem. Phys.*, vol. 79, p. 1017, 1983.

16. G. D. Waddill and L. L. Kesmodel, *Physical Review B*, vol. 31, p. 4940, 1985.

17. G. D. Waddill and L. L. Kesmodel, *Phys. Rev. B*, vol. 32, p. 2107, 1985.

18. V. H. Grassian and E. L. Muetterties, *J. Phys. Chem.*, vol. 91, p. 389, 1987.

19. B. E. Koel, J. E. Crowell, C. M. Mate, and G. A. Somorjai, *Journal of Physical Chemistry*, vol. 88, p. 1988, 1984.

20. S. Lehwald, H. Ibach, and J. E. Demuth, *Surface Science*, vol. 78, p. 577, 1978.

21. H. Ibach and D. L. Mills, *Electron Energy Loss Spectroscopy and Surface Vibrations,* Academic Press, New York, 1982.

22. M. A. Logan, *PhD Thesis*, Chemistry Department, University of California at Berkeley, 1985.

23. M. A. Van Hove and S. Y. Tong, *Surface Crystallography by LEED,* Springer Verlag, Berlin, 1979.

24. H. Ohtani, M. A. Van Hove, and G. A. Somorjai, *Surface Sci.*, vol. 187, p. 372, 1987.

25. E. L. Garfunkel, C. Minot, A. Gavezzotti, and M. Simonetta, *Surface Sci.*, vol. 167, p. 177, 1986.

26. P. Bagus, *private communication.*

27. J.M. MacLaren, J.B. Pendry, R.J. Rous, D.K. Saldin, G.A. Somorjai, M.A. Van Hove, and D.D. Vvedensky, in *Surface Crystallographic Information Services: A Handbook of Surface Structures*, Reidel, Dordrecht, 1987.

28. A. M. Bradshaw and F. M. Hoffmann, *Surface Science*, vol. 72, p. 513, 1978.

29. C. M. Mate, B. E. Bent, and G. A. Somorjai, *J. Electron Spectroscopy and Related Phenomena*, vol. 39, p. 205, 1986.

30. D. F. Ogletree, *PhD Thesis*, Physics Department, University of California at Berkeley, 1986.

31. J. L. Gland and G. A. Somorjai, *Surface Science*, vol. 38, p. 157, 1973.

32. C. M. Mate, *PhD Thesis*, Physics Department, University of California at Berkeley, 1986.

33. E. L. Garfunkel, J. E. Crowell, and G. A. Somorjai, *J. Phys. Chem.*, vol. 86, p. 310, 1982.

34. A.B. Anderson and M.K. Awad, *J. Am. Chem. Sci.*, vol. 107, p. 7854, 1985.

35. F.M. Hoffmann and A. Ortega, *Proc. Intern. Conf. on Vibrations in Adsorbed Layers*, KFA Reports, 26, p. 128, Jülich, 1978.

36. P. Gelin, A. R. Siedle, and J. T. Yates, *J. Phys. Chem.*, vol. 88, p. 2978, 1984.

37. G. Ertl and J. Koch, *Z. Naturforsch.*, vol. 25a, p. 1906, 1970.

38. G. Ertl and J. Koch, in *Adsorption-Desorption Phenomena*, ed. F. Ricca, p. 345, Academic Press, New York, 1972.

39. H. Ohtani, B. E. Bent, C. M. Mate, and G. A. Somorjai, *Appl. Surf. Sci.*, vol. 33, p. 254, 1988.

40. I. E. Idrissi-Rachidi, C. Minot, M. A. Van Hove, and G. A. Somorjai, to be published.

41. B. E. Koel, J. E. Crowell, B. E. Bent, C. M. Mate, and G. A. Somorjai, *J. Phys. Chem.*, vol. 90, p. 2709, 1986.

42. W. L. Parker, R. M. Hexter, and A. R. Siedle, *J. Am. Chem. Soc.*, vol. 107, p. 4585, 1985.

43. M. -C. Tsai and E. L. Muetterties, *Journal of the American Chemical Society*, vol. 104, p. 2534, 1982.

44. E. L. Garfunkel, J. J. Maj, J. C. Frost, M. H. Farias, and G. A. Somorjai, *J. Phys. Chem.*, vol. 87, p. 3629, 1983.

45. C. M. Mate, *private communication.*

46. D. B. Kang and A. B. Anderson, *Surface Sci.*, vol. 155, p. 639, 1985.

7. Real Space Imaging of Molecular Overlayers with STM

7.1. Introduction

As shown in chapter 6, we have observed various distortions of chemisorbed benzene molecules. In this chapter we describe the real-space imaging of chemisorbed benzene molecules with scanning tunneling microscopy.* Scanning Tunneling Microscopy (STM) has been proved to be a very powerful tool for atomic resolution imaging of surfaces. This technique has been successfully applied to semiconductor and metal surfaces, both with and without atomic adsorbates.[1] Early results for molecular adsorbates on metal surfaces have been somewhat less encouraging. For example, CO overlayers have not been resolved on Pt(100) surfaces, even though the CO induced disappearance of the clean metal reconstruction was observed.[2,3] Other problems, including low symmetry and resolution, have been observed for images of Cu-phthalocyanine on Ag(111) surfaces.[4] The difficulties with, and the interpretation of, these measurements have led to concern about the possible role of rapid surface diffusion and to the expectation that molecules may be invisible in STM if their molecular orbitals (MO) are far from

* Some part of this chapter has been published in the following articles:
H. Ohtani, R. J. Wilson, S. Chiang, and C. M. Mate, Phys. Rev. Lett. **60**, 2398 (1988).
S. Chiang, R. J. Wilson, C. M. Mate, and H. Ohtani, J. Microscopy, in in press.
H. Ohtani, R. J. Wilson, S. Chiang, C. M. Mate, M. A. Van Hove, and G. A. Somorjai, in "Probing the Nanometer Scale Properties of Surfaces and Interfaces", American Vacuum Society (Video tape).

the Fermi level (E_f).

We have studied two ordered superlattices of coadsorbed benzene C_6H_6 and CO on a Rh(111), namely Rh(111)-(3x3)-C_6H_6+2CO and Rh(111)-c($2\sqrt{3}$x4)*rect* (or $\begin{bmatrix} 3 & 1 \\ 1 & 3 \end{bmatrix}$)-$C_6H_6$+CO. The structures of these superlattices determined with LEED have been shown in Fig. 6-1. The (3x3) unit cell contains one benzene molecule and two CO molecules, all chemisorbed over hcp-type 3-fold hollow sites which, as opposed to fcc-type hollow sites, are directly above a second layer Rh atom. The $\begin{bmatrix} 3 & 1 \\ 1 & 3 \end{bmatrix}$ primitive cell of the Rh(111)-c($2\sqrt{3}$x4)*rect* superlattice contains one benzene molecule and one CO molecule, also all chemisorbed over hcp-type 3-fold hollow sites.

7.2. Experimental

7.2.1. UHV Scanning Tunneling Microscope

We have used an UHV scanning tunneling microscope of IBM Almaden research center.[5,6] The layout of the vacuum system is shown in Fig. 7-1. The left-hand side of the figure shows the VG Escalab Mark II. This chamber (surface analysis chamber) is equipped with 500Å resolution scanning Auger and scanning electron microscopy (SAM/SEM), a dual-anode Al/Mg x-ray source for x-ray photoelectron spectroscopy (XPS), and an argon ion gun for depth profiling and ion scattering spectroscopy (ISS). The sample preparation chamber next to the analysis chamber contains an airlock, an electron beam heater, a high-energy argon ion gun for sputter cleaning samples and tips, rear view LEED, a metal evaporator for producing metallic overlayers, and leak valves for introducing gaseous reagents. The STM chamber is connected to the preparation chamber via a transfer chamber equipped with a UTI mass spectrometer for residual gas analysis.

The STM used is shown in Fig. 7-2. The vibration isolation consists of two sets of spring stages which reduce most of the vibrations to frequencies <2Hz. (This design is similar to the earlier STM models in Zurich[7,8]) Viton spacers are used to damp the high-frequency vibrations propagating along the springs. Additional damping of the low-frequency vibrations is achieved by using SmCo permanent magnets mounted on the intermediate stage to induce magnetic eddy currents in pieces of copper on the support and on the inner stage. In order to reduce the effects of thermal drift, most parts on the STM stage are made from invar or quartz. The W tip is scanned using piezoelectric tubes, 3.17mm diameter and 25.4mm long. The small wall thickness of 0.50mm gives these tubes a sensitivity of ~100Å/V.

7.2.2. Sample Preparation

7.2.2.1. Rh(111)-(3x3)-C_6H_6+2CO

The Rh single crystal sample (~1 cm diameter disk of (111) orientation within ±0.5°) was mounted on a sample holder with Ta clips. Then, the crystal was cleaned by repeated cycles of 1KeV Ar bombardment and heating at 1000°C in the presence of $4x10^{-5}$Torr Ar and $8x10^{-10}$Torr O_2. The sample was then annealed at 800°C for 10min. Cleanliness was verified by Auger spectroscopy. The Rh(111)-(3x3)-C_6eH_6+2CO structure was obtained by dosing, at room temperature, with $2x10^{-7}$ Torr.S of CO followed by saturating the surface with $3.6x10^{-6}$ Torr.s of benzene.

7.2.2.2. Rh(111)-c($2\sqrt{3}$x4)rect-C_6H_6+CO

The Rh(111) crystal was cleaned by repeated cycles of 1KeV Ar bombardment and heating at 1000°C in the presence of $1.5x10^{-5}$Torr Ar and $8x10^{-10}$Torr O_2. The sample was then annealed at 800°C for 5min and finally flashed to 1000°C for 1sec. The Rh(111)-c($2\sqrt{3}$x4)*rect*-C_6H_6+CO structure was obtained by dosing, at room temperature, with $1.1x10^{-7}$ Torr.S of CO followed by saturating the surface with $3.8x10^{-6}$ Torr.s of benzene.

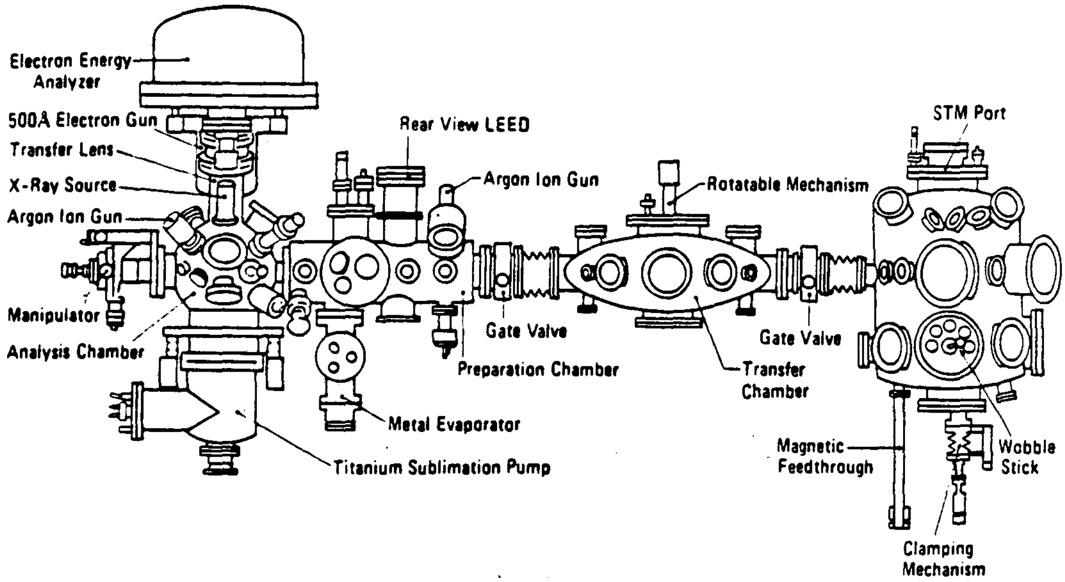

[Fig. 7-1] Layout of the UHV surface analysis and STM system.

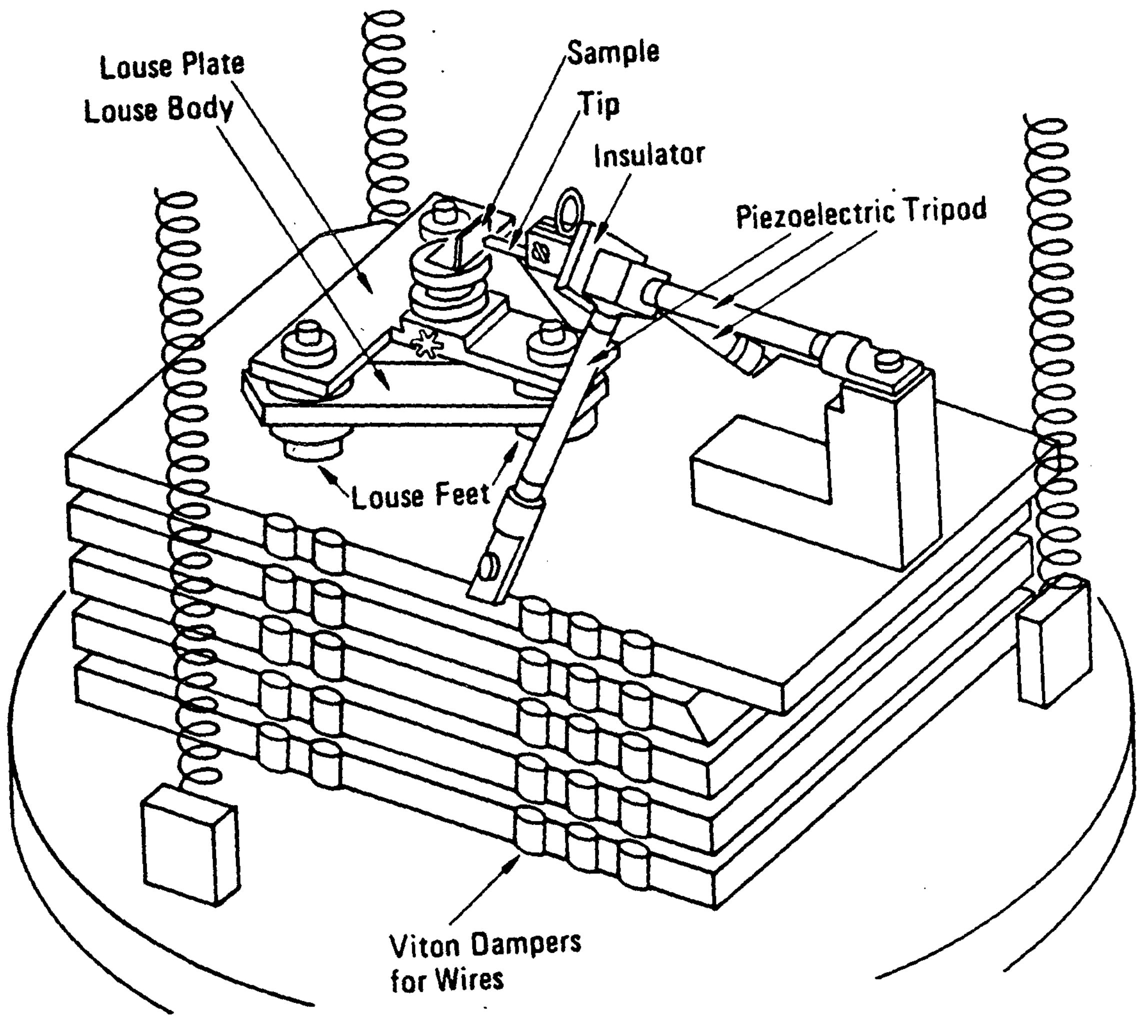

[Fig. 7-2] Schematic diagram of the STM, showing pocket STM hung on double-spring stages.

7.2.3. Determination of the Crystal Orientation with LEED

In order to interpret the STM images of the adsorbates, it is extremely important to know the location of the substrate atoms underneath the overlayers. This could be done by taking the STM image of the clean substrate with atomic resolution. For example, the binding site of Ag on Si(111) has been successfully determined by imaging both ordered Ag islands and the nearby bare Si(111) surface at the same time.[9,10] In the present case, the Rh(111) substrate was fully saturated with benzene and CO, and the bare metal atoms were not observed with STM. We have not attempted to take the STM image of clean Rh(111) since the atomic corrugation of the closed packed metal surfaces is generally very small,[11] and the Rh(111) crystal surface is too reactive towards residual gas adsorption to maintain the cleanliness for a prolonged period.

Instead, we have verified the azimuthal orientation of the Rh(111) surface with respect to the direction of the tip scanning by comparing the LEED spot intensities for the clean Rh(111) sample with data in the literature[12] as follows.

A rhodium single crystal has a fcc (face-centered cubic) structure, and the ideal (111) surface has a layer-stacking sequence that can be symbolized as ABCABC... as shown in Fig. 7-3-a. This surface has a threefold symmetry considering the 2nd layer atoms, and the corresponding LEED pattern has a threefold symmetry at normal incidence. (The (10) and (01) beams shown in Fig. 7-3-b are symmetrically inequivalent to each other.) Therefore if we find out which LEED spots of our sample correspond to the (10) or (01) beams in Fig. 7-3-b, the azimuthal orientation of our sample can be unambiguously determined using the relationship between the real space (Fig. 7-3-a) and the reciprocal space (Fig. 7-3-b).

To this end, we have calculated the Bragg peaks for each of (10) and (01) beams using kinematical approximation.[13] First, we express a general lattice vector $\vec{a_3}$ as

$$\vec{a_3} = a\vec{a_1} + b\vec{a_2} + d(0,0,1) \tag{7.1}$$

where d is the interlayer spacing and (a, b) represents the "registry shift" from one atomic plane to the next. For Rh(111),

$$a=\frac{1}{3},\ b=\frac{2}{3},\ \text{and}\ d=2.20\text{Å}=4.15\text{bohr}^{*} \tag{7.2}$$

Then, the Bragg energies E^B follow from

$$2(E^B+V_0)-|\vec{k}_{0\parallel}|^2 = 2(E^B+V_0)\cos^2\theta \tag{7.3}$$

$$= \left[(2\vec{k}_{0\parallel}\cdot\vec{g_{hk}}+|\vec{g_{hk}}|^2)\frac{d}{4\pi(n-ah-bk)}+\frac{\pi}{d}(n-ah-bk)\right]^2$$

For normal incidence (θ=0, $\vec{k}_{0\parallel}=\vec{0}$), (7.3) becomes

$$2(E^B+V_0) = \left[|\vec{g_{hk}}|^2\frac{d}{4\pi(n-ah-bk)}+\frac{\pi}{d}(n-an-bk)\right]^2 \tag{7.4}$$

where V_0 is the inner potential or muffin-tin zero level (>0), and $\vec{g_{hk}} = h\vec{g_1}+k\vec{g_2}$.

* Atomic units (bohrs for distances, 1 bohr =0.529Å; hartrees for energies, 1h=27.18eV) are used in all the equations in this section.

For the (1,0) beam,

$$(h,k)=(1,0),\quad \vec{g}_{10}=\vec{g}_1=(\frac{2\pi}{a_1},0),\quad |\vec{g}_1|^2=\frac{4\pi^2}{a_1^2} \tag{7.5}$$

For the (0,1) beam,

$$(h,k)=(0,1),\quad |\vec{g}_2|=|\vec{g}_1| \tag{7.6}$$

Since $a_1 = 2.69\text{Å} = 5.085\text{bohr}$ for Rh(111),

$$|\vec{g}_1|^2 = |\vec{g}_2|^2 = 1.527(\text{bohr}^{-2}) \tag{7.7}$$

Therefore by substituting (7.2) and (7.7) into equation (7.3), we obtained the Bragg peaks listed in Table 7-1. (We used V_0=15eV as indicated in the literature.)[14]

[Table 7-1] Expected Bragg-peak positions for Rh(111) at normal incidence.

n	(10)	(01)
1	6.6	27.5
2	18.1	11.1
3	51.0	38.2
4	99.8	81.7
5	164.3	141.0
6	244.3	215.8
7	339.8	306.2
8	450.8	412.0
9	577.4	533.4
10	719.4	670.2

These values agree very well with the theoretical and experimental I-V curves for Rh(111) in the literature.[14,12]

When we make such comparison, we have to realize that the indexing of the beams is somewhat arbitrary.[14] At the present time, there is no convention that defines which beam should be indexed as (10) or (01). In fact, our (10) beam is indexed as the (01) beam by Van Hove et al.[14,12]

Finally we have identified the (10) and (01) beams (specified in Fig. 7-1 and characterized as shown in Table 7-1) in the LEED pattern of our Rh(111) sample, so that the azimuthal orientation of our sample has been determined.

7.3. Results

The STM images were obtained in the constant current slow-scan mode (0.5 Hz/line)[1] for tip biases varying from -2V to 2V. Higher biases frequently resulted in damage to the surface and were useful primarily for tip sharpening. Images obtained by tunneling into empty states of the sample ($V_t < 0$) showed more resolution and corrugation than filled state images and are presented exclusively here.

7.3.1. Rh(111)-(3x3)-C_6H_6+2CO

7.3.1.1. The Image at $V_t = -1.25V$

Shown in Fig. 7-4 is a typical wide-scan image (300Åx90Å), which displays a variety of steps and defects. According to the kinematical LEED analysis shown in section (7.2.3), the sharp, mono-atomic step in the middle of the image has been found to lie along a $(\bar{1}01)$ direction. Therefore this step has the relatively open face of a (100)-type square lattice, as does the double step in this image. (See Fig. 2-1) The rougher step shown at the left of the image has a (111)-type close-packed face. The regularly ordered bumps on each terrace have the (3x3) periodicity (8.1Åx8.1Å), suggesting each bump corresponds to a benzene molecule.

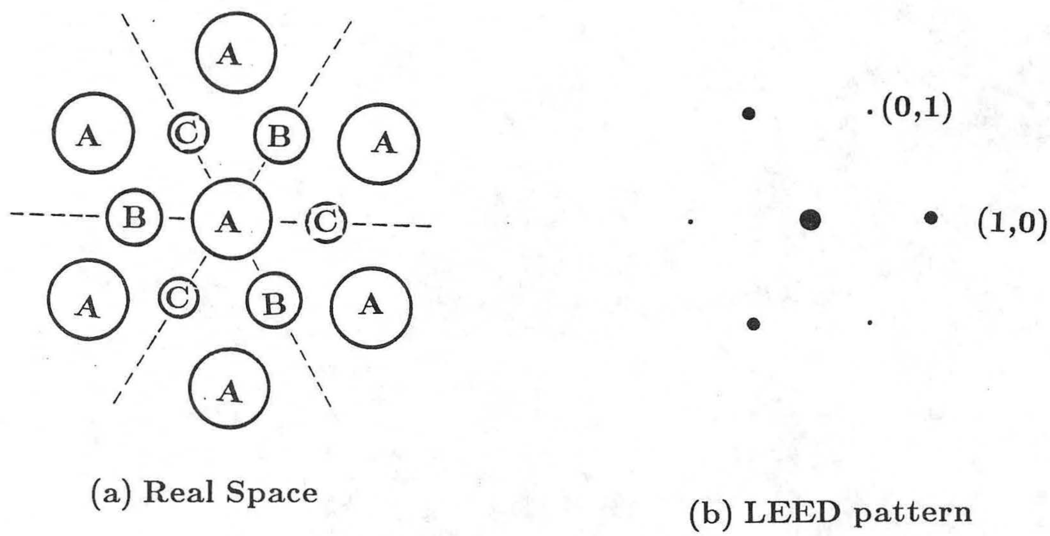

[Fig. 7-3] Sketches of the Rh(111) surface structure (a) and the corresponding LEED pattern (b). A, B, and C represents the first, second, and third layers, respectively.

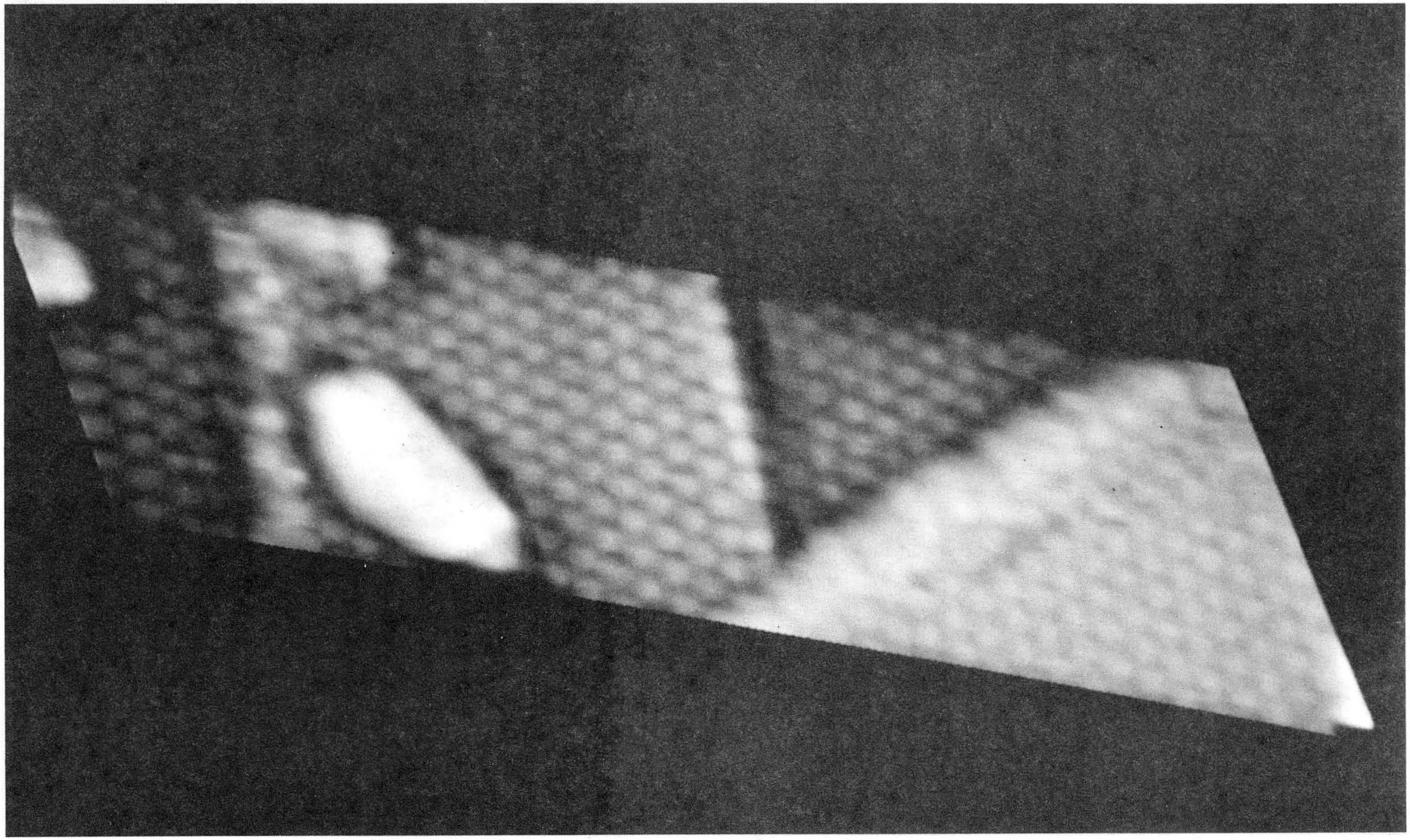

[Fig. 7-4] The 300Åx90Å image (V_t=−1.25 V, i_t=4nA), showing three steps and the (3x3) superlattice on each (111) terrace.

Fig. 7-5 shows three images in smaller area (~90Åx90Å). These images reveal a gentle 0.4Å corrugation with a (3x3) periodicity (8.1Åx8.1Å) extending over an ordered step edge (S). These images have been digitally processed by subtracting a constant height from the upper (left) terrace to improve the image contrast by reducing the step discontinuity. Using the known scan distances and the LEED assignment for the benzene binding site, we map each terrace onto a mesh representing the top two layers of Rh atoms in a fcc lattice as shown in Fig. 7-5-b. The assumption that the benzene binding site is the same on both terraces allows the unambiguous determination of the azimuthal orientation of the crystal by STM alone, which agrees with the LEED assignment in section 7.2.3.

Upon close examination, several interesting features in Fig. 7-5 become apparent. First, benzene evidently prefers to bind at sites adjacent to metal atoms which form the step edge. Second, a translational domain boundary (DB), observable on the upper terrace, preserve the hcp hollow binding site. Third, by comparison of Fig. 7-5-b and Fig. 7-5-c, which were recorded about 10 min apart, it can be seen that two benzene molecules, to the lower right of the near vertical domain boundary, have shifted in the latter image into (3x3) lattice positions. An unknown disturbance (U), which may be associated with diffusion of CO or benzene along a row in the lower terrace in Fig. 7-5-b, has disappeared in Fig 7-5-c, whereas the row of molecules just above the domain boundary on the upper terrace take on this disturbed character in Fig. 7-5-c. These disturbances probably represent a time averaged image of molecules moving between sites.

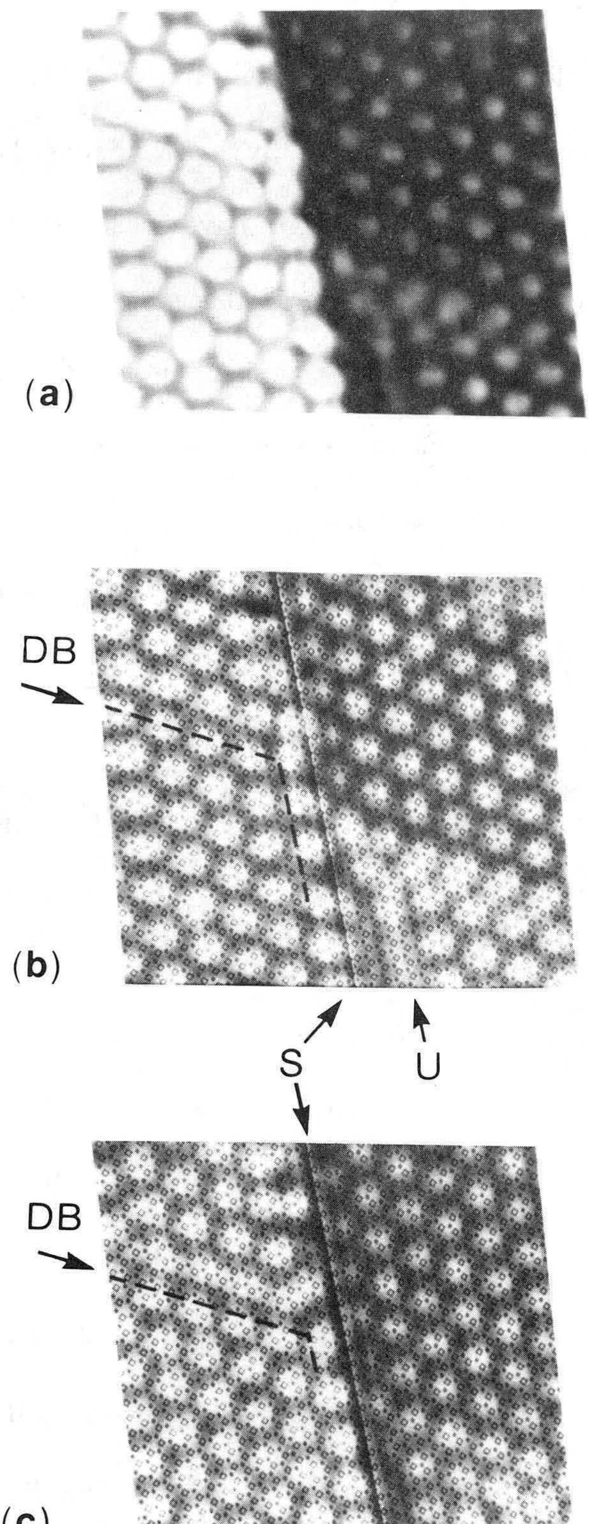

[Fig. 7-5] Three images of the (3x3) superlattice extending across an atomic step. (V_t=−1.25V, i_t=4nA). (a),(b) Images derived from the same data, (c) image recorded ~10min later.

7.3.1.2. The Image at $V_t = -1.4V$

The image taken at $V_{t=-1.4V}$ and i_t = 8nA shows flat topped, 2Å-high, nearly cylindrical benzene molecules. [Fig. 7-6] At a given bias voltage, we found that increasing the tunnel current led to an increase in the corrugation and to the appearance of a internal structure (dip at the center) of the protrusions as will be shown in Fig. 7-7. However, when the voltages were as large as those used for Fig. 7-6 (V_t=-1.4V and i_t=8nA), we could not raise the current sufficiently to observe this dip because other instabilities became apparent, as shown. The simplest explanation for the instabilities in this image involves the hopping of benzene molecules between equivalent sites, formation of benzene vacancies (V), and modifications to the tip (T). These instabilities are smaller than, but similar to, those reported for Cu phthalocyanine.[4]

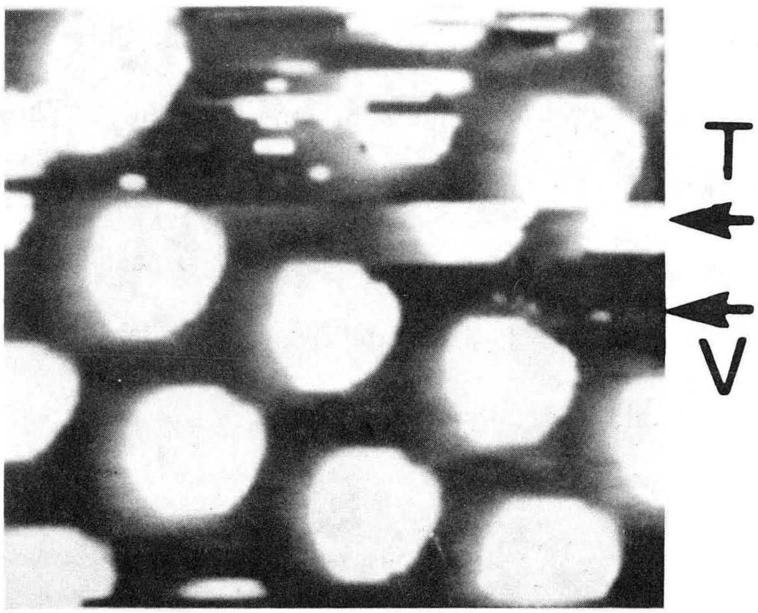

[Fig. 7-6] The STM image taken at V_t=–1.4 V and i_t=8nA

7.3.1.3. The Image at $V_t = -0.01$V

Higher-resolution images of the internal structure of the 3x3 cells were obtained by maximizing the corrugation by adjustment of the tip bias voltage (V_t), tunnel current (i_t), and tip structures. Fig. 7-7 shows a 2Å high, ring-like structure, which we observed for V_t= -0.01 V and i_t=2nA. Similar features were observed at V_t=-0.5 V with 0.5Å corrugation. The use of low bias voltages, as in previous work on Au(111),[11] appears to be advantageous for obtaining small tunnel gaps, which provide larger corrugations, while operating at reasonable tunnel currents.

The typical 3-fold character and the lateral dimensions of the protrusions corroborates the assignment of these protrusions to benzene molecules adsorbed at hollow sites but is not sufficient to determine the mesh registration uniquely. According to the superimposed mesh based on the LEED model,[15] the lobes appear to be localized between, rather than over, the underlying metal atoms. Improvements in lateral resolution will be necessary to measure the 1.5Å C-C bonds of benzene and observe proposed Kekule distortions of the benzene ring.[15]

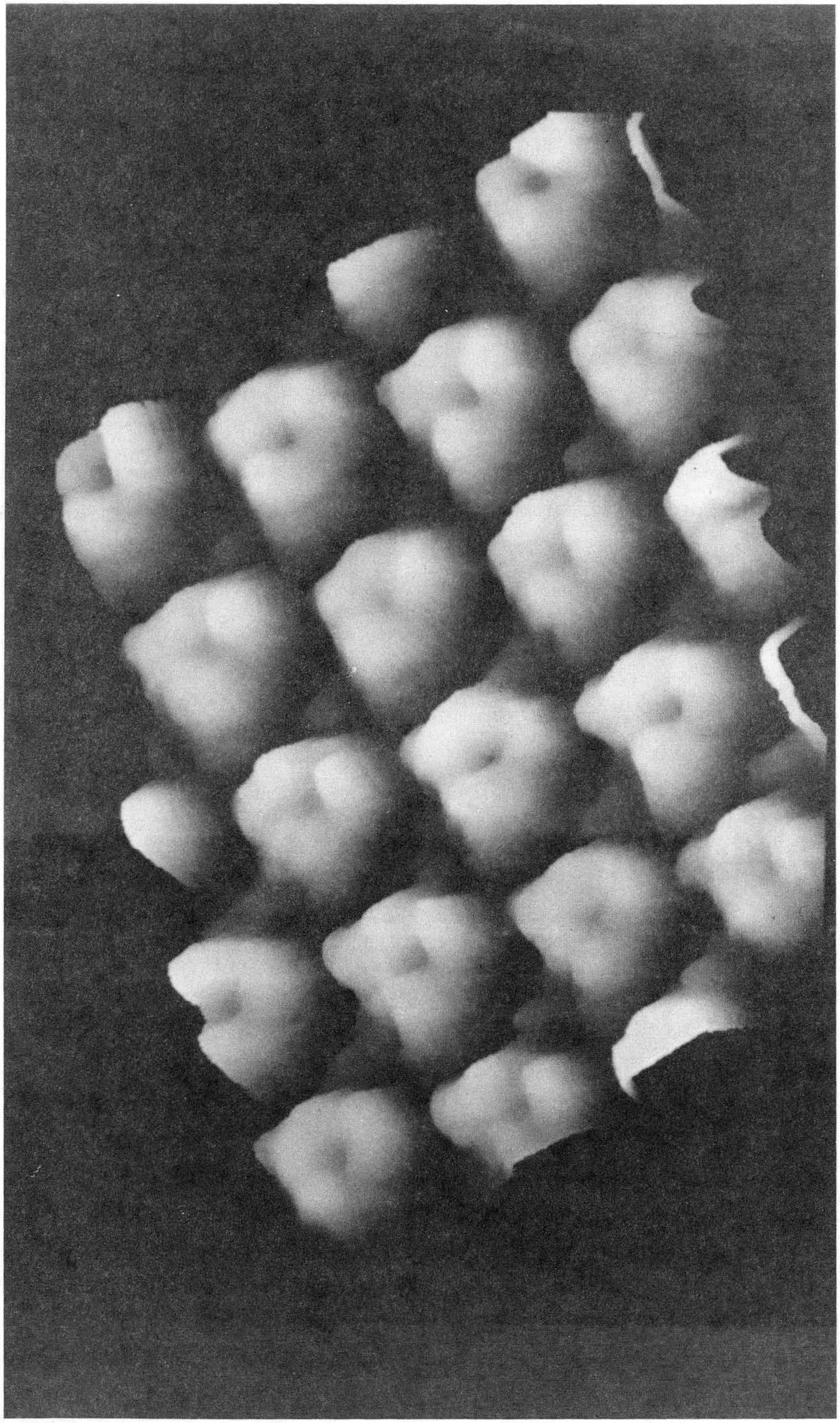

[Fig. 7-7] A three-dimensional view of the STM image (V_t=−0.01 V, i_t=2nA)

7.3.2. Rh(111)-$(2\sqrt{3}x4)$rect-C_6H_6+CO

Figure 7-8, obtained for i_t = 2nA and V_t = -0.010V, shows two views of our best STM image which shows both clearly resolved CO molecules and the hole in the benzene molecules. In Fig. 7-8-a, we show a gray scale top view of a ~ 30Åx60Å area overlaid by a mesh with the large (small) diamonds representing the top (second) layer of Rh atoms. With the mesh overlaid on the data so that the large bright rings, identified as benzene molecules from their spacing, lie on hcp-type three-fold hollow sites according to the LEED model,[16] the small protrusions in the image can be identified with CO molecules because they lie exactly at the positions expected for CO in the unit cell. The three dimensional view shown in Figure 7-8-b displays more clearly the relative heights of the benzene molecules, ~0.6Å, compared to the 0.2Å CO protrusions. Also, the benzene molecules appear as a ring composed of three protrusions ~0.1Å higher than the hole in the middle.

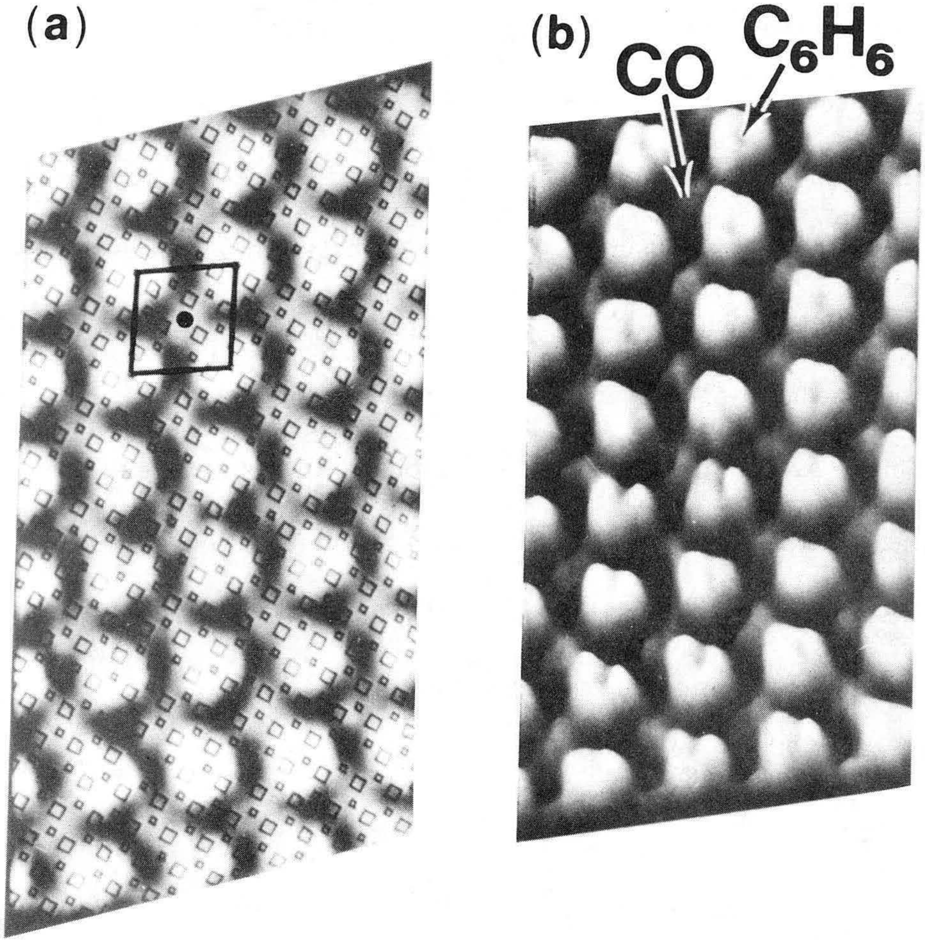

[Fig. 7-8] The STM images for Rh(111)-($2\sqrt{3}$x4)*rect*-C_6H_6, measured at V_t = -0.01V and i_t = 2nA. (a) Top view, (b) Three dimensional view of the same data shown in (a).

7.4. Discussion

We have found that the corrugation of CO is much smaller than that of benzene in the coadsorbed structures. Since, in principle, the STM images are strongly affected by the local electronic structure, any explanation for the contrast observed for benzene and CO must take account of the adsorbate electronic states. Some of the filled CO and benzene MO have been observed for Rh(111) and assigned with use of photoemission.[17] Inverse photoemission on other metal surfaces typically shows an empty 2π state[18,19] at least a few eV above E_f for CO. Empty benzene e_{2u} levels[20] are found 5 eV above E_e for Cu(111) or Ag(111), but data are not available for Rh(111). However, an extended Huckel-theory calculation[21] for benzene bonded to a threefold hollow site on a Rh(111) cluster shows that the combination of the highest filled benzene state (e_{1g}) with metal orbitals in a bonding configuration shifts these occupied states a few volts further below E_F, in agreement with Photoemission data,[17] while the same states combined in an antibonding configuration result in the existence of an empty antibonding Rh-benzene state just above E_F. In the present case, the existence of empty states near E_F which are partially localized on the π lobes of the benzene can easily account for large STM corrugations. The very small corrugation for CO molecules probably results from the lack of CO-Rh states near E_F. (Theory suggests the LUMO (lowest unoccupied molecular orbital) for CO on metal surfaces would have CO character on the order of a percent.)[22,23] In principle, it should be possible to image the $CO2\pi^*$ states more clearly by using higher bias voltages. If the STM is operated at higher voltages and lower currents, however, the corrugation is reduced. Operation at high currents, where the corrugation is larger because of the reduced tip-sample spacing, leads to instabilities, such as those evident in Fig. 7-6.

Other contributions to the image contrast between benzene and CO can be considered. Adsorbate-induced modifications to the potentials seen by tunneling electrons, which might be associated with local work function changes,[1] would change the decay lengths of electronic wave functions. These workfunction changes are known[17] for adsorbate-saturated Rh(111) surfaces ($\Delta\phi$= +0.7 for CO and $\Delta\phi$= -1.3 for benzene) and are consistent with the appearance of a protrusion for benzene. The CO, however, would be expected to appear as an array of holes in the image, contrary to observation. Other differences, such as the different spatial distribution of the CO $2\pi^*$ state as compared to the e_{1g} benzene orbitals, may also be important. Data on other systems are needed to distinguish between these alternatives.

One pleasing result of this work is that one can image certain chemisorbed molecules by examing mixed metal-adsorbate states near E_F, thereby avoiding the use of high bias voltages which often damage the surface and tip. Although we cannot give a simple rule for predicting the magnitude of the corrugation to be expected for a particular molecule on a given metal surface, it is likely that large molecules, which have many closely spaced electronic states split by strong molecule-surface interaction, will often lead to states near E_F and result in a useful STM footprint. While the origin of the image contrast is not clear, its existence and symmetry allow one to obtain many of the advantages of high resolution real-space imaging. In the present case, our STM images show nearly perfect surface order punctuated by occasional domain boundaries and defects, details of registration at steps, and a preview of surface diffusion phenomena. Our results further suggest that coadsorption techniques may be helpful in reducing surface diffusion and for moving E_F closer to molecular states. STM on carefully chosen metal-adsorbate surface appears extremely promising for observations of surface chemical processes, such as molecular diffusion, nucleation phenomena, and step- or defect- related reactivity.

References

1. G. Binnig and H. Rohrer, *IBM J. Res. Develop.*, vol. 30, p. 355, 1986.

2. R.J. Behm, W. Hosler, E. Ritter, and G. Binnig, *Phys. Rev. Lett.*, vol. 56, p. 228, 1986.

3. E. Ritter, R. J. Behm, G. Potsche, and J. Wintterlin, *Surf. Sci.*, vol. 181, p. 403, 1987.

4. J. K. Gimzewski, E. Stoll, and R. R. Schlittler, *Surf. Sci.*, vol. 181, p. 267, 1987.

5. S. Chiang and R. J. Wilson, *IBM J. Res. Develp.*, vol. 30, p. 515, 1986.

6. S. Chiang, R. J. Wilson, Ch. Gerber, and V. M. Hallmark, *J. Vac. Sci. Tech.*, vol. A6, p. 386, 1988.

7. G. Binnig and H. Rohrer, *Helv. Phys. Acta.*, vol. 55, p. 726, 1982.

8. G. Binnig and H. Rohrer, *Surface Sci.*, vol. 126, p. 236, 1983.

9. R. J. Wilson and S. Chiang, *Phys. Rev. Lett.*, vol. 59, p. 2329, 1987.

10. R. J. Wilson and S. Chiang, *J. Vac. Sci. Technol.*, vol. A6, p. 398, 1988.

11. V. M. Hallmark, S. Chiang, J. F. Rabolt, J. D. Swalen, and R. J. Wilson, *Phys. Rev. Lett.*, vol. 59, p. 2879, 1987.

12. M. A. Van Hove and R. J. Koestner, in *Determination of Surface Structure by LEED*, ed. P. M. Marcus and F. Jona, p. 357, Plenum, New York, 1984.

13. M. A. Van Hove, W. H. Weinberg, and C.-M. Chan, *Low Energy Electron Diffraction: Experiment, Theory and Structural Determination.*, p. 102,

Springer Verlag, Heidelberg, 1986.

14. M. A. Van Hove, W. H. Weinberg, and C.-M. Chan, *Low Energy Electron Diffraction: Experiment, Theory and Structural Determination.*, p. 258, Springer Verlag, Heidelberg, 1986.

15. M. A. Van Hove, R. F. Lin, G. A. Blackman, and G. A. Somorjai, *Acta Crystallographica*, vol. B43, p. 368, 1987.

16. M. A. Van Hove, R. F. Lin, and G. A. Somorjai, *Journal of the American Chemical Society*, vol. 108, p. 2532, 1986.

17. E. Bertel, G. Rosina, and F. P. Netzer, *Surf. Sci.*, vol. 172, p. L515, 1986.

18. J. Rogozik, V. Dose, K. C. Prince, A. M. Bradshaw, P. S. Bagus, K. Hermann, and P. Avouris, *Phys. Rev. B*, vol. 32, p. 4296, 1985.

19. S. Ferrer, K. H. Frank, and B. Reihl, *Surf. Sci.*, vol. 162, p. 264, 1985.

20. K. H. Frank, R. Dudde, and E. E. Koch, *Chem. Phys. Lett.*, vol. 132, p. 83, 1986.

21. E. L. Garfunkel, C. Minot, A. Gavezzotti, and M. Simonetta, *Surface Sci.*, vol. 167, p. 177, 1986.

22. I. P. Batra and P. S. Bagus, *Sol. St. Commun.*, vol. 16, p. 1097, 1975.

23. I. P. Batra, *private communication.*.

8. A Tabulation and Classification of the Surface Structures of Clean Solid Surfaces and of Adsorbed Atomic and Molecular Monolayers as Determined from Low Energy Electron Diffraction Patterns

8.1. Introduction

During the last twenty-five years low energy electron diffraction (LEED) has provided the lion's share of information on the structure of clean single-crystal surfaces and of ordered atomic or molecular adsorbates on these surfaces. In most experiments the size and the orientation of the surface unit cell was determined under well-defined conditions of temperature and exposure to ambient gases to be adsorbed. The surfaces are first cleaned in ultra high vacuum by ion sputtering or by chemical means, the composition being monitored by electron or ion spectroscopies, then the surface structure is studied by LEED. Although methods of surface structure determination have been developed to obtain interatomic distances and angles, only the size and orientation of the surface unit cell is reported in most investigations. The reason for this is that the aim of the investigations has been the study of chemical or electronic properties of surfaces with

Most of this chapter has been published in the following article:
H. Ohtani, C. -T. Kao, M.A. Van Hove, and G.A. Somorjai, Progress in Surface Science, **23**, 155 (1986).

less emphasis on the detailed atomic surface structure.

Reports of two-dimensional surface structures have rapidly accumulated in recent years. Somorjai and Szalkowski listed over 200 surface structures in 1971 and extracted certain rules of ordering.[1] In 1979 Castner and Somorjai reported over 1000 surface structures.[2] In addition, Bibérian and Somorjai reviewed the surface structures of metallic monolayers on metal crystal surfaces; these represented a rapidly growing sub-class of monolayer structures.[3]

This review updates and expands the surface structural data obtained for both clean and adsorbate-covered surfaces of single crystals: over 3000 surface structures are tabulated, most of which were studied in the last several years. These include clean and adsorbate-covered structures of single-crystal surfaces with high Miller indices and of polyatomic solids, as well as many simpler surface structures.

The available data indicate the predominance of ordering of clean solid surfaces and of adsorbed monolayers; however, these ordered surfaces only exist within a given range of temperature and coverage. It seems that there are always temperature and coverage ranges where ordered surfaces exist. There are many reconstructed surfaces and adsorbed monolayers which form both commensurate and incommensurate surface structures. A commensurate surface structure has a superlattice periodicity which is simply related to the substrate lattice periodicity, whereas an incommensurate surface structure has a superlattice periodicity independent of the substrate lattice periodicity. More accurate definitions of these terms and their physical implications are given in chapter 3.

Interesting trends of research can be identified from the data that have been reported in recent years. There is increased interest in investigations of alloy surfaces and of high Miller index (stepped) surfaces of metals. The studies of metal monolayers and organic overlayers are very rapidly growing directions of research. A large number of studies have focussed on inert gas adsorption and ordering, on the chemisorption of halogen atoms, especially chlorine, and on the coadsorption and ordering of two different adsorbates. On the other hand, there is a scarcity of surface structural information on polyatomic solids (oxides, sulfides, silicates carbonates, etc.). Also many important monatomic solids were not investigated by LEED, including boron, uranium, and manganese.

Reflecting these trends of LEED investigations, we have organized and classified the surface structural data in the following way. All the surface structures, except those formed by adsorption of organic molecules, are classified according to the rotational symmetry of the substrate surfaces when clean and unreconstructed; the surface structures formed on substrates with one-fold, two-fold, three-fold, and four-fold rotational symmetry are tabulated in Table I, II, III, and IV, respectively. The rotational symmetry of alloy surfaces is assumed to be the same as for the pure metal surfaces of the main component. This classification permits useful correlation of the various surface structures.

In addition, important subsets of the surface structures have been extracted and have been gathered in Tables V–X in order to clarify the characteristic trends in these areas. The surface structures of metallic monolayers on metal crystal surfaces and the alloy surface structures are collected in Tables V and VI, respectively. We highlight the surface structures formed by adsorption of organic molecules in Table VII. Similarly, coadsorbed overlayer structures and physisorbed overlayer structures are listed in Tables VIII and IX, respectively. The surface structures of high-Miller-index or stepped surfaces are listed in Table X. The trends and highlights in each sub-class are discussed in Section 10-2.

In recent years surface crystallography by LEED has successfully determined the precise location of the atoms within the surface unit cell (3 dimensional LEED), and the bond lengths and orientations of ordered adsorbed molecules have been also determined by this method.[4] A disordered monolayer structure has also been solved by LEED crystallography recently.[5] The surface structures that have been solved by LEED surface crystallography are marked with an asterisk "*" in the surface structure tables. The surface structures that were solved by surface science techniques other than LEED are marked with an exclamation sign "!" in the tables. These techniques include surface extended x-ray absorption fine structure (SEXAFS), medium energy ion scattering (MEIS) and high energy ion scattering (HEIS), etc.

8.2. Review of Surface Structures Studied with LEED

Tables I—X list over 3,000 surface structures, most of which have been reported within the past several years. The low-Miller-index metal surfaces and atomic adsorbates were studied predominantly in earlier years. In recent years more emphasis has been put on the polyatomic solids (compounds, alloys) surfaces, high-Miller-index stepped surfaces and the molecular overlayers with increasing complexity.

We shall in this section discuss some of the important trends that can be extracted from the surface structure tables.

8.2.1. Ordering Principles

As our Tables I—X show, a large number of ordered surface structures can be produced experimentally. Ordering can manifest itself both as commensurate and as incommensurate structures. There are also many disordered surfaces, which often are not reported in the literature. The disordered structures are usually difficult to describe accurately and are therefore difficult to reproduce exactly in other laboratories. Nevertheless, for selected surfaces, order-order and order-disorder phase transitions have been explored in considerable detail both experimentally and theoretically.

In our tables, a number of disordered surface structures are listed. However, it should be stressed that many structures reported as having a (1x1) LEED pattern may well include small or large amounts of disorder, whether in the overlayer structure or even in the substrate structure.

8.2.1.1. Adsorbate-Adsorbate and Adsorbate-Substrate Interactions

The driving force for surface ordering originates, analogous to three-dimensional crystal formation, in the interactions between atoms, ions, or molecules in the surface region. The physical origin of the forces is of various types, and the spatial dependence of these interaction forces is complex.

For adsorbates, an important distinction must be made between adsorbate-substrate and adsorbate-adsorbate interactions. The dominant adsorbate-substrate interaction is due to strong covalent or ionic chemical forces between the adsorbates and the substrate in the case of chemisorption, or to weak Van der Waals forces in the case of physisorption. Adsorbate-adsorbate interactions could be covalent bonding interactions, orbital-overlapping interactions, electrostatic interactions (ex. dipole-dipole interactions), Van der Waals interactions, etc. These are many-body interactions that could be attractive or repulsive depending on the system.

In chemisorption it is usually the case that the adsorbate-adsorbate forces are weak compared to the adsorbate-substrate binding forces (except at very close repulsive range, since atoms will not overlap). Chemisorbed species with strong unbalanced adsorbate-adsorbate forces will not be stable, and will easily undergo rearrangement or surface chemical reaction to transform into a more stable state. The adsorbate-substrate interaction includes a corrugation parallel to the surface, favoring certain adsorption sites over others and implying barriers to diffusion. This imposes the constraint that only lattice sites be occupied. With weak adsorbate-adsorbate forces the locations of the adsorbed atoms or molecules are determined by the optimum adsorbate-substrate bonding. But the adsorbate-adsorbate interactions still manage to dominate the long-range ordering of the overlayer.

A compromise is found in the formation of an adsorbate lattice that is simply related to the substrate lattice. In the ordered case this yields commensurate superlattices. The most common of these are simple superlattices with one or two adsorbates per superlattice unit cell. They occur for adsorbate coverages of 1/4, 1/3, 1/2, for example (we define the surface coverage to be unity when each (1x1) substrate cell is occupied by one adsorbate).

A special case of commensurate superlattice is the formation of periodic out-of-phase domains. They occur especially when the adsorbate coverage is not well matched to form a simple ordered lattice. Then equal domains of simple structure are mismatched to each other through dislocations (domain walls) that allow higher or lower coverages. It is not entirely straightforward to experimentally distinguish the periodic domain structures from the incommensurate structures. Therefore, many structures are found labeled as incommensurate in the literature, even though they are probably of the periodic-domain type.

An incommensurate relationship exists when there is no common periodicity between an overlayer and the substrate. This structure is dominated by adsorbate-adsorbate interaction rather than by adsorbate-substrate interactions. An example of incommensurate lattice formation occurs frequently when compounds are produced by exposure of an elemental substrate to a gas. Examples are metal oxides, nitrides, carbides and silicides. As soon as about one or two monolayers of the compound form on the surface, they frequently adopt their own lattice constant independently of the substrate lattice constant. This is because the attractive forces within the compound can be much stronger than those between the compound and the substrate.

8.2.1.2. Effects of Adsorbate Coverage

The surface coverage of an adsorbate is an important parameter in the ordering process. This is because the adsorbate-adsorbate and the adsorbate-substrate forces are strongly influenced by the surface coverage of the adsorbates. (An extreme case is alkali-metal adsorption on transition metal surfaces, where the ionicity of the adsorbate-substrate bond changes as the surface coverage increases.) At very low coverages, adsorbates may bunch together in two-dimensional islands: this occurs when there is short-range attractive adsorbate-adsorbate interactions, coupled with easy diffusion along the surface. Within each island the interactions induce an ordered arrangement of adsorbates. Other adsorbates repel each other at close adsorbate-adsorbate separations, and do not interact at the large separations: these are disordered at low coverages. But when their coverage is increased so that the mean interadsorbate distance decreases to about 5—10Å, the repulsive interactions induce and strongly influence ordering, favoring certain adsorbate configurations over others. As a result, the structure can also develop a unit cell that repeats periodically across the surface. This is most clearly evident in the low-energy electron diffraction patterns, which depend directly on the size and orientation of this unit cell.

Most adsorbates (other than some metals) will not compress into a one-monolayer overlayer on the closest-packed metal substrates. There appears to be a close-range repulsive force that keeps them apart by approximately a Van der Waals distance (this does not necessarily imply a Van der Waals interaction, since the strongest contribution to the adsorbate-adsorbate interaction is in this case mediated by the substrate). One may attempt to compress the overlayer further by increasing the coverage, which is done by exposing the surface to the corresponding gas at high pressures. The result is either no further adsorption or diffusion of the adsorbates into the substrate, forming compounds, or, if the temperature is low enough, formation of multilayers.

8.2.1.3. Physical Adsorption

When adsorbates are used which physisorb rather than chemisorb (at suitably low temperatures), one also finds that the Van der Waals distance determines the densest overlayer packing. Here it is the Van der Waals force acting directly between the adsorbates that dominates. In this case, the optimum adsorbate-substrate bonding geometry can be overridden by the lateral adsorbate-adsorbate interactions, yielding for example incommensurate structures where the overlayer and the substrate have independent lattices. Furthermore, with physisorption a larger coverage is also possible through multilayer formation.

8.2.1.4. Metallic Adsorbates

With metallic adsorbates, on the other hand, closer-packed overlayers can be formed. This is because metallic adsorbate atoms attract each other relatively strongly to form covalent bonds and cluster together with covalent interatomic distances. Thus at submonolayer coverages close-packed islands form. When the atomic sizes of the overlayer and substrate metals are nearly the same, one observes single-monolayer (1x1) structures, in which adsorbate atoms occupy every unit cell of the substrate. With less equal atomic radii, other structures are formed, dominated by the covalent closest packing distance of the adsorbate. These structures may be of the incommensurate type or, more likely, of the periodic-domain type. Beyond one close-packed overlayer, metal adsorbates frequently form multilayers or also three-dimensional crystallites. Alloy formation by interdiffusion is also observed in many cases, even in the submonolayer regime.

8.2.2. Surface Restructuring

There are many observations of deviations of a clean surface structure from the structure predicted by a simple truncation of the bulk lattice. Many LEED patterns of clean surfaces listed in Tables I—IV and X deviate from the expected

(1x1) pattern. These are relatively drastic cases where atoms may be displaced substantially from their bulk lattice sites and bonded to different atoms than the bulk structure would imply. Such cases are called reconstructions. Another cause of reconstruction is, as seen at compound surfaces, a change in elemental composition at a surface compared to the bulk composition. A different crystalline lattice may become favored as the surface composition changes due to segregation to or from the surface. Non-stoichiometric compounds often exhibit this behavior. A more subtle restructuring has also been discovered during full structural determinations. Layer spacing relaxations have been found between the first few surface layers of the less close-packed clean metal surfaces, e.g., fcc (110) and bcc(100). These relaxations correspond to deviations of the surface bond lengths from the bulk values, but do not affect the LEED pattern.

Among the clean metal surfaces, about a dozen are known to reconstruct. Over 40 clean semiconductor reconstructions are reported. Numerous reconstructions have also been found in the area of oxides and other compounds. (See the LEED patterns of clean surfaces in Tables I—IV, and X.)

Some of these reconstructions and layer spacing relaxations can be explained by the tendency for bond lengths to decrease as the bonding coordination decreases. This trend fits long-established principles, as proposed by Pauling,[6] if one relates coordination number to bond order. A good illustration is presented by the reconstructions of the clean Ir, Pt and Au(100) surfaces. In these three cases, the interatomic distance in the topmost layer shrinks by a few percent parallel to the surface. It then becomes more favorable for this layer to collapse into a nearly hexagonally close-packed layer rather than maintain the square lattice of the underlying layers. Many adsorbates on these surfaces can remove this reconstruction by cancelling the driving force towards smaller bond lengths.

In these studies surface cleanliness is monitored by various techniques including AES, XPS, HREELS, etc., and the sample is cleaned until the concentration of impurities is below the detection threshold of these techniques (a few hundredths of a monolayer). However, it is always risky to conclude that a reconstruction is a property of the clean surface, since it is very difficult to rule out the presence of at least some contaminants. Nevertheless, it is now believed that most of the nominally clean reconstructions are intrinsic properties of the clean surfaces, and are only marginally affected by small levels of impurities. This is the case of the Ir, Pt and Au(100) surfaces mentioned above.

At the same time it is also known that a fair number of reconstructions are adsorbate-induced. Even without being ordered, an adsorbate can induce a reconstruction, as happens with H on W(100). The clean W(100) crystal surface is itself already reconstructed, but hydrogen changes it further to another structure that varies smoothly with the hydrogen coverage. Often, the adsorbate fits periodically within the unit cell of the reconstructed substrate. This occurs, for example, with carbon on Ni(100) and sulfur on Fe(110), where the metal exhibits relatively minor, but interesting adsorbate-induced distortions.

Adsorbates can also restructure stepped surfaces. For example, oxygen deposited on stepped Pt surfaces has been observed to produce double-height steps. Facetting has also been observed under such circumstances.

By contrast, it is also possible, with contaminants or otherwise, to generate a metastable unreconstructed phase from a reconstructed clean surface. With suitable contaminants, such phases have been achieved with all reconstructed surfaces. In some cases, e.g., Ir(100), clean metastable structures can be obtained by appropriate heat treatments. Si(111)-(1x1) metastable unreconstructed structure can also be achieved by laser-annealing and rapid cooling processes which freeze the unreconstructed structure which is stable at high temperature.

In the case of alloys, surface segregation can lead to new ordered arrangements, through a change in the surface composition. In some cases, for instance CuAl(111) with a bulk composition of 16% of Al, the surface alloy orders while the bulk alloy has no long-range order. Such cases are reported in our tables as having a superlattice (e.g., $(\sqrt{3}x\sqrt{3})R30^\circ$ for the above-mentioned CuAl case), by reference to the (1x1) lattice of the pure majority element. One may call these alloy reordering reconstructions. They involve essentially normal lattice sites, but a different ordering at the surface compared to the bulk.

Semiconductors almost universally reconstruct when clean. This is due to the difficulty of their surface atoms to compensate for the loss of nearest neighbors, since bonding is relatively directional in semiconductors. The "dangling bonds" left by the absence of bonding partners cannot easily be used for bonding to existing surface atoms, except through more drastic rearrangements of these atoms. Therefore, most semiconductor surfaces reconstruct. Major rebonding between surface atoms occurs in this process. The associated perturbation propagates several layers into the surface until the bulk lattice is recovered. The silicon surfaces in particular have been extensively studied in their various reconstructed forms. The famous Si(111)-(7x7) structure has not yet been solved, but so much information has been gathered, including real-space topographies of this surface obtained with STM, that a good qualitative picture of its structure is becoming apparent.[7] Again with semiconductor surfaces, adsorbates can negate the need for reconstruction and induce a return to the bulk structure. This can happen by bonding of the adatoms to the "dangling bonds." Hydrogen does this particularly well and to some extent chemically passivates the resulting surface. More frequently, however, adsorbates become part of a new compound structure, by penetrating within the few topmost substrate layers.

The stoichiometry is also important in considering the reconstruction of compound semiconductors. For example a $(\sqrt{5}\times\sqrt{5})R26.6^\circ$ structure of $BaTiO_3(100)$ surface observed after high temperature annealing is considered to be due to the ordering of lattice vacancies at the surface. Another example is the GaAs(100) surface which presents various reconstructed structures as the Ga to As ratio changes. Relatively little structural knowledge has been accumulated so far on this subject, despite the great technological importance of semiconductor surfaces and the semiconductor-metal interface.

8.2.3. Simple Structures of Atomic Adsorbates at Metal Surfaces

By simple structures we mean clean unreconstructed metal surfaces with low Miller indices and atomic adsorbates thereon. These were the mainstay of the early LEED studies and constituted the bulk of earlier tabulations. In recent years this class of structures has continued to grow, mostly through new combinations of substrates and adsorbates.

The clean unreconstructed metal surfaces, by definition, have the structure expected from a simple truncation of the bulk lattice. For close-packed surfaces with low Miller indices, relaxations from the bulk atomic positions have been found to be less than about 0.02Å by various crystallographic methods, especially, LEED and MEIS or HEIS. For the more open surfaces, such as fcc(110) and bcc(100), somewhat larger relaxations have been observed, as mentioned in the previous section.

The simple atomic adsorption structures on metal surfaces are characterized by the occupancy of high-coordination sites. (Physisorption behaves differently and will be discussed in Section 10-2-8). Thus Na, S, and Cl overwhelmingly adsorb over "hollows" of the metal surface, bonding to as many metal atoms as possible. The situation is slightly more complicated with the smaller adsorbates, H, C, N, and O. Although high coordination is still preferred, the small size of these atoms often allows penetration within or even below the first metal layer. The penetration can be interstitial or substitutional. In either case the metal surface can reconstruct as a result.

8.2.4. Metallic Monolayers on Metal Crystal Surfaces

Table V lists surface structures of metal monolayers adsorbed on metal surfaces. Data on more than 400 systems have been reported so far.

At low coverages, most of the metallic adsorbates form commensurate ordered overlayers: the overlayer unit cells are closely related to the substrate unit cells. Furthermore, in many cases a (1x1) LEED pattern is observed. This suggests that adsorbed metal atoms attract each other to form 2-dimensional islands. The size of such islands can change depending on the substrate temperature, which can be detected by measuring the LEED spot size. A disordered LEED pattern is observed when the adsorbed metals repel each other. This is observed for example in the case of alkali metal adsorption on a transition metal, since the charged adatoms undergo repulsive interactions.

At higher coverages, the relative atomic sizes of the different metals becomes an important factor. When the atomic sizes of the substrate and adsorbate metals are similar, (1x1) structures are favored, whereas coincidence structures often form when the atomic sizes are much different. As the overlayer coverage increases towards saturation of a monolayer, the adsorbate-adsorbate interaction increases. Then an incommensurate hexagonal overlayer with interatomic distances close to the bulk value of the adsorbate appears to form. Another, perhaps more satisfactory interpretation of the LEED patterns yields an overlayer structure with out-of-phase domains, reflecting the remaining strength of the substrate-adatom interaction. In the case of strong adatom-adatom attraction and weak substrate-adatom attraction, one observes the independent superposition of the structures of the pure adsorbate and the pure substrate. Often such dense overlayers have a lattice that is slightly rotated with respect to the substrate lattice. This has also been experimentally observed and theoretically predicted for physisorbed films, and is called "orientational epitaxy."[8]

Under higher exposure some metals can undergo layer-by-layer growth, while several systems, such as Fe on W(110), form 3-dimensional crystallites. Most cases fall between these two extremes. Comparison of the surface tension of the adsorbate metal and of the substrate metal has failed to explain these phenomena, and up to now there is no simple rule to predict which metal film growth mechanism applies.

When a metal undergo as (1x1) epitaxial growth with a substrate lattice constant that differs from its own bulk lattice constant, the overlayer metal can be considerably strained. Therefore, the epitaxial growth must at some point be accompanied by a lattice constant change. Such a change is probably accompanied through dislocations occurring within a dozen layers from the interface.

Alloy formation is frequently observed with suitable combination of metals, usually at higher temperatures. However very little surface crystallographic data is available on such systems, and a general trend cannot be drawn at this time.

8.2.5. Alloy Surface Structures

Our Tables include about 90 surface structures of alloys, including both clean and adsorbate-covered surfaces. These are brought together in Table VI. Alloys have the special property that their surface composition can differ considerably from their bulk composition. Other compounds share this property, but the frequently easy interdiffusion in alloys stands out. Indeed, some recent studies have found substantial surface segregation. In some cases the surface composition can even oscillate from one atomic layer to the next near a surface. Furthermore, adsorbates may radically modify this surface composition. Much work is needed to clarify these issues.

The LEED pattern informs about the surface ordering. It is found that some alloys retain their bulk ordering at the surface. For instance, Ni_3Al, as well as other Cu_3Au-type alloys, have a (100) face which exhibits the periodicity expected from the alternating bulk stacking of 50—50 mixed NiAl layers and of pure Ni layers. (Some authors refer to these surface structures as c(2×2): we prefer the notation (1x1) since the bulk periodicity is not changed.)

Other alloys, exemplified by Cu-rich CuAl, are disordered in the bulk, but order at some faces. Thus the (111) face of αCu-16at%Al exhibits a $(\sqrt{3}\times\sqrt{3})R30^\circ$ surface periodicity (relative to the (1x1) surface lattice of pure Cu(111)). The other low-Miller-index faces of this alloy do not order.

8.2.6. Organic Adsorbates

Around 390 LEED structures are reported in Table VII, dealing with the adsorption of organic molecules. By far the most frequently studied substrates are metals, with only a dozen cases of semiconductors or insulators. Platinum substrates have been most extensively used, due no doubt to their importance in both heterogeneous catalysis and electrochemistry. The most common adsorbates in this table are C_2H_2 (acetylene), C_2H_4 (ethylene), C_6H_6 (benzene), C_2H_6 (ethane), HCOOH (formic acid), and CH_3OH (methanol), reflecting the same technological applications.

Most organic adsorption studies have been carried out near room temperature, with frequent cursory explorations of the higher-temperature behavior. Especially with organics, temperature is a crucial variable, given the frequently diverse reaction mechanisms that can occur when molecules interact with surfaces. A number of studies have explored the lower temperatures, especially with the relatively reactive metal surfaces to the left of the Periodic Table, such as Fe, Mo, and W. At higher temperatures, decomposition of molecules is the rule. With hydrocarbons sequential decomposition has been studied in greatest detail with the help of HREELS vibrational analysis.

The LEED patterns generally reflect disorder at high temperatures. Exceptions occur especially with carbon layers resulting from the decomposition of organic adsorbates: these may form either carbidic chemisorbed layers that are ordered or graphitic layers that have characteristic diffraction patterns.

Ordered LEED patterns for organic adsorption are frequent at lower temperatures. They can often be interpreted in terms of close-packed layers of molecules, consistent with known Van der Waals sizes and shapes. These ordered structures usually are commensurate with the substrate lattice, indicating strong chemisorption in preferred sites. It appears that many hydrocarbons lie flat on the surface, using unsaturated π-orbitals to bond to the surface. By contrast, non-hydrocarbon molecules form patterns that indicate a variety of bonding orientations. Thus CO is found to strongly prefer an upright orientation. However, upon heating unsaturated-hydrocarbon adsorbates evolve hydrogen and new species may be formed which bond through the missing hydrogen positions. An example is ethylidyne, CCH_3, which can be formed from ethylene, C_2H_4, upon heating. Ethylidyne has the ethane geometry, but three hydrogens at one end are replaced by three substrate atoms.

8.2.7. Coadsorbed Surface Structures

Table VIII brings together surface structures formed upon coadsorption of two or more different species. Listed are ~150 structures. In general, coadsorbed surface structures may be classified in two categories: cooperative adsorption and competitive adsorption. In cooperative adsorption, the two kinds of adsorbate mix well together and interpenetrate. In competitive adsorption the adsorbates segregate to form separate non-mixed domains. For example, addition of CO to a preadsorbed (2x2) oxygen layer on Pd(111) eventually forms a mixed CO+O phase (cooperative adsorption). On the other hand, addition of O_2 to a preadsorbed CO layer (at low coverages: $\theta < 0.33$) on Pd(111) forms separate domains of O and of CO (competitive adsorption). Therefore, in this instance the order of adsorption affects the reactivity towards CO_2 formation.

Coadsorption structures have been extensively examined on Rh(111), Pt(111), and Pd(111) using various pairs of adsorbates from the set C_2H_2, C_2H_3 (ethylidyne), C_6H_6, Na, CO, and NO. Among these, the hydrocarbons and Na transfer electrons to Rh(111) when adsorbed: they are donors. CO and NO have the opposite electron-transfer character, and are therefore acceptors. It has been observed that long-range ordering of the mixed layer requires the coadsorption of an electron donor with an acceptor. Donor-donor and acceptor-acceptor combinations are either disordered or segregate into separate regions. The combination of donor and acceptor seems to stabilize the mixed cooperative phase. Then each donor adsorbate surrounds itself with acceptors, while each acceptor surrounds itself with donors. This is analogous to the three-dimensional ionic lattices which also exhibit great stability.

As an illustration, on Pd(111) and Pt(111), benzene molecules adsorb in a disordered manner at room temperature. However, addition of CO to these disordered overlayers produces ordered surface structures.

8.2.8. Physisorbed Surface Structures

At low enough temperatures most gas-phase species will physisorb on many surfaces. In many instances, the physisorbed state is short-lived (lifetime well below a second), because of a low barrier to a chemisorbed state. With inert gases and with saturated hydrocarbons, however, physisorption is commonplace and stable on many types of substrate. These substrates include metals as well as inert surfaces such as the graphite basal plane. Also, more reactive species such as O_2, CO and NO physisorb stably on the graphite basal plane. We shall focus our discussion on this type of relatively stable physisorption. Over 60 such structures are listed in Table IX. Little is known about the structure of the less stable short-lived physisorbed species, despite their obvious importance as precursors to chemisorbed species.

In physisorption the adsorbate-adsorbate interactions are usually comparable in strength to the adsorbate-substrate interactions, all of which are dominated by the Van der Waals forces. With stable physisorption, there is no chemistry to perturb the adsorbates over large ranges of temperature and coverage. One can therefore examine large parts of the phase diagrams of these adsorption systems.

Many phases have been observed in physisorption, and new classes of phases continue to be discovered. There are commensurate and incommensurate phases, disordered lattice-gas and fluid or liquid phases. There are out-of-phase domain structures, including striped-domain phases, pinwheel and herringbone structures, and modulated hexatic reentrant fluid phases, among others.[4] Relative to chemisorption and its more complex interactions, physisorption has the advantage that simpler theories can be set up to describe the phase diagrams. The two-dimensional nature of the problem has especially helped the general theory of phase transitions, because many models can only be solved in two dimensions.

From the point of view of physisorption phases, one should distinguish between the ordering of the positions and the orientations of the adsorbed species. With spherically symmetrical species like inert gases this is not an issue, but all molecules do offer the additional degrees of orientational freedom, which freeze in at different temperatures than does the positional ordering. This adds considerable richness to the phase diagrams.

The simpler among the observed LEED patterns for physisorbed species can often be easily interpreted in terms of structural models. The known Van der Waals sizes of the species leads to satisfactory structures which are more or less close-packed. This is especially straightforward with inert gases. With molecules, the best structural models usually involve flat-lying species, which are arranged in a closest-packed superlattice. The flat geometry provides the greatest attractive Van der Waals interaction with the substrate.

8.2.9. High-Miller-Index (Stepped) Surface Structures

Over 380 surface structures have been observed on the high-Miller-index surfaces, see Table X. About 250 of these were reported during the past six years, which clearly indicates a fast growing interest in this field. In this period, much work has focussed on the clean and chemisorbed structure of high-Miller-index semiconductor surfaces. In particular, very interesting reconstructions of the various high-Miller-index Si, Ge and GaAs surfaces have been observed.

Most of the stepped surfaces reported in Table V have close-packed terraces separated by steps of one atomic height. Many ordered overlayer structures on these one-atomic-height stepped surfaces have been reported. The observed LEED patterns indicate a strong dependence on the width of the terraces. With wide terraces, adsorbates often order as if no steps were present, i.e., as on the low-Miller-index surface. When the terraces become narrow, the adsorbates are strongly affected by the steps. For instance, carbon monoxide adsorbs with (2x2) and $(\sqrt{3}x\sqrt{3})R30^\circ$ patterns on Rh(S)-[6(111)X(100)], which has (111) terraces six atoms wide separated by (100) oriented steps. These two patterns are also observed on Rh(111). But for the case of Rh(331) with (111) terraces three atoms wide, quite different structures for chemisorbed CO have been observed.

Another important observation is that reconstructions of the high-Miller-index surfaces are frequently induced by the adsorption of O_2, H_2, etc. Examples include: ReO_3 compound formation on the oxygen covered Re(S)-[6(0001)x(16$\bar{7}$6)] surface; new facet formation on the Ni(210) surface after the adsorption of O_2; facet formation due to the decomposition of hydrocarbons on various Pt and Rh high-Miller-index surfaces; and graphite formation or faceting on Pt(S)-[4(111)x(100)] after the total dehydrogenation of ethylene or benzene on this surface. These restructuring phenomena can often be ascribed to the formation of a stable new phase like oxide, carbide, and nitride. The study of the surfaces of oxide-, carbide- and nitride- solids will help understand the restructuring phenomena observed on the stepped surfaces.

A comment about the superlattice notation for stepped surfaces: an adsorbate superlattice designation like (2x2) is meant to imply a superlattice relative to the close-packed lattice within a terrace, rather than relative to the step-to-step repetition distance.

8.3. Future Directions

The solid surface presents a two-dimensional world where molecules may order and interact differently from that in three dimensions. Surface restructuring of many solids when clean either by relaxation or by reconstruction clearly indicates this. When investigating polyatomic solids, compounds or alloys, the surface composition will also be different than the bulk composition to provide on additional important variable that alters the surface structure; non-stoichiometry.

We should mention several monoatomic solids including boron, manganese and uranium that escaped the attention of surface scientists. However, future studies clearly will focus on surfaces of increasing chemical complexity. These include high-Miller-index (stepped) surfaces, and the surface structures of diatomic and polyatomic solids, the oxides, sulfides, carbides, nitrides, silicates, carbonates, as well as alloys. Many more adsorption structures will also be explored on semiconductor surfaces. Organic molecules of increasing size will be investigated and it is very likely that the surfaces of organic solids will be the subjects of structural studies as they are most important in the biosciences and chemical technologies. Coadsorption will continue to expand as an area of interest for the study of chemical reactions including the effects of promoters and inhibitors. Underexplored adsorbates include inorganic molecules (with the exception of CO and NO). Also semiconducting materials are rarely deposited on metals, while metals are currently very much studied on semiconducting substrates.

One interesting observation recently has been the ordering of adsorbed monolayers at low temperatures as low as 30 K for CO and 60 K for C_2H_2 on close-packed metal surfaces.[9] This finding indicates the low activation energy for surface diffusion as compared to desorption of these molecules. It is likely that adsorbate surface structures will be studied increasingly at low temperatures as a consequence.

Rapid dynamical surface structure calculations have become possible due to recent developments of simplified computational techniques.[10,11] This way the precise locations of atoms and molecules in the surface unit cells can be determined. The surface structures listed in Tables I–X are excellent candidates for surface crystallography investigations. It is hoped that a large number of them will be scrutinized by LEED crystallography in the near future so that we can improve our understanding of the surface chemical bonds in atomic and molecular monolayers.

References

1. G. A. Somorjai and F. J. Szalk wski, *J. Chem. Phys.*, vol. 54, p. 389, 1971.
2. D. G. Castner and G. A. Somorjai, *Chem. Rev.*, vol. 79, p. 233, 1979.
3. J. P. Bibérian and G. A. Somorjai, *J. Vac. Sci. and Tech.*, vol. 16, p. 2073, 1979.
4. M. A. Van Hove, W. H. Weinberg, and C.-M. Chan, *Low Energy Electron Diffraction: Experiment, Theory and Structural Determination.*, Springer Verlag, Heidelberg, 1986.
5. P. R. Rous, J. B. Pendry, D. K. Saldin, K. Heinz, K. Müller, and N. Bickel, *Physical Review Letters*, vol. 57, p. 2951, 1986.
6. L. Pauling, *The Nature of the Chemical Bond,* p. 93, Cornell University Press, Ithaca, New York, 1960.
7. K. Takayanagi, Y. Tanishiro, S. Takahashi, and M. Takahashi, *Surf. Sci.*, vol. 164, p. 367, 1985.
8. G. C. Shaw, S. C. Fain, Jr., and M. D. Chinn, *Phys. Rev. Lett.*, vol. 41, p. 955, 1978.
9. G. S. Blackman, *PhD Thesis*, Chemistry Department, University of California at Berkeley, 1988.
10. M. A. Van Hove, R. J. Koestner, J. C. Frost, and G. A. Somorjai, *Surface Science*, vol. 129, p. 482, 1983.

11. M. A. Van Hove, R. F. Lin, and G. A. Somorjai, *Physical Review Letters*, vol. 51, p. 778, 1983.

TABLE I. Surface Structures on Substrates with One-fold Rotational Symmetry[†]

Substrate	Adsorbate	Surface Structure	Reference
(Al,Ga)As(110)	[clean]	(1×1)	1375
AlP(110)	[clean]	*(1×1)	1521,1863*
CdTe(110)	[clean]	*(1×1)	1367,1382*,1495 1504,1620
CoSi(100)	[clean]	(2×1)	1312
$CoSi_2$(100)	[clean]	(1×1)	1312
GaAs(110)	[clean]	*!(1×1)	896,949,1008,1090,1124,1182 1449,1480,1519 1524,1567,1572 1575,1576,1702* 1764*,1765!
		(2×2)	1567
	Ag	(1×1)	1575
		[001] Streaks	1575
		c(4×4) [Multilayer]	1344
	Al	(1×1)	1375,1432,1607
	Al (low coverage)	*(1×1)–Al	1871*
	Al (medium coverage)	*(1×1)–Al	1871*
	Al (high coverage)	*(1×1)–Al	1871*
		(1×4) [Multilayer]	1344
	As	(1×1)	579,1375
	Au	Disordered	1008
	Cu	Polycrystalline	1182
	Ga	Polycrystalline	1305
		(1×1) [Multilayer]	1432
	Ge	(1×1)–Ge	1089,1520,1572
		(3×1)–Ge	588
		(2×1)–Ge	588
		(3×1)+(1×4) with Streaks	1089
		(1×1)+Blurred (8×10)	1089
	H_2O	(1×1)	1006
	In	(1×1)	1432
	$Fe(CO)_5$	Facet{100}	1377
	O_2	Disordered	744
	Pd	Disordered	1008
	Sb	*(1×1)–Sb	1320,1367,1383 1424,1442*
	ZnSe	(1×1)	1444
		(1×2)	1444
GaP(110)	[clean]	*(1×1)	819,1445*,1495 1521,1619
	Al	AlP(110)	1426
		(1×1)	1521
GaSb(110)	[clean]	*!(1×1)	1378*,1420*,1766!
InAs(110)	[clean]	*(1×1)	1423*
InP(110)	[clean]	*(1×1)	1495,1521,1568 1570,1573,1618* 1784*
	Al	(1×1)	1521
		(1×1) Diffuse	1570
	Cl_2	Disordered	1660

TABLE I. Surface Structures on Substrates with One-fold Rotational Symmetry (Continued)

Substrate	Adsorbate	Surface Structure	Reference
	Cu	(1×1)	1568
	H_2O	Ordered	1573
		Disordered	1573
	Ni	Disordered	1568
InSb(110)	[clean]	*(1×1)	1181,1420,1888*
	Sn	Amorphous	1181
Te(10$\bar{1}$0)	[clean]	*(1×1)	1801*
ZnO(10$\bar{1}$0)	[clean]	*(1×1)	1104,1239,1612 1772*
	H_2O	Disordered	1104
	O_2	(1×1)–O	392
	Xe	Hexagonal	1026
		Disordered	1026
ZnO(11$\bar{2}$0)	[clean]	*(1×1)	1772*
ZnS(110)	[clean]	*(1×1)	1445*
ZnSe(110)	[clean]	*(1×1)	1478*
	O_2	ZnO(000$\bar{1}$)	642
ZnTe(110)	[clean]	*(1×1)	1378*,1495,1504

†Organic overlayer structures and high-Miller-index surface structures are not included. See Table VII and Table X, respectively, for these structures.

TABLE II. Surface Structures on Substrates with Two-fold Rotational Symmetry†

Substrate	Adsorbate	Surface Structure	Reference
Ag(110)	[clean]	*!(1×1)	707,888,1522,1534
			1750!,1751,1872*
	Br_2	(2×1)–Br	888
		c(4×2)–Br	888
		AgBr	888
	C_2N_2	Disordered	407
	Cl_2	Adsorbed	732
	Cs	(1×2)	859,1534
		(1×3)	859,1534
	HCN	Disordered	407
	H_2O	Disordered	878
	H_2O+Li^+	Complex	1557
	H_2S	(3×2)–S	627
		c(10×2)–S	627
		(3×4)–S	627
	I_2	Pseudohexagonal–I	1145
		c(2×2)–I	1145
	K	(1×2)	1534
		(1×3)	1534
	Li	(1×2)	1534
	Na	(1×1)	489
	NO	Disordered	345
	O_2	!(2×1)–O	146,341,342,343
			344,695,878,943
			974,1027,1047
			1140,1143,1160
			1300,1690,1751!
		(1×2)–O	1376
		(3×1)–O	146,341,342,343
			695,878,974,1143
			1160,1300,1690
		(4×1)–O	146,341,342,878
			974,1143,1300
			1690
		(5×1)–O	146,341,695,1300
		(6×1)–O	146,341,1300
		(7×1)–O	146
		c(6×2)–O	974
	$O(a)+CO_2$	(2×2)	1143
	$O(a)+SO_2$	c(6×2)–SO_3	1027,1371
		(1×2)–SO_4 etc.	1371
	O_2+H_2O	(1×2)–OH	878
		(1×3)–OH	878
	SO_2	(1×2)–SO_2	1027,1371
		c(4×2)–SO_2	1027,1371
		(1×1)	1371

TABLE II. Surface Structures on Substrates with Two-fold Rotational Symmetry (Continued)

Substrate	Adsorbate	Surface Structure	Reference
		$\begin{bmatrix} \frac{2}{3} & 1 \\ \frac{4}{3} & 0 \end{bmatrix}-SO_2$	1027
	Xe	Hexagonal Overlayer	159
Al(110)	[clean]	(1×1)+(1×2)	965
		*(1×1)	1354,1409*,1464 1498,1566*,1721*
	CO	Not Adsorbed	1273
	O_2	(331) facets	123
		(111) facets	122
		Disordered	709
Au(110)	[clean]	*(1×2)	754,1009,1098,1166 1752*
		(1×2)+(1×1)	965
		(1×3)	754,1098
	Bi	$\begin{bmatrix} 1 & 1 \\ 1 & -1 \end{bmatrix}$	498
		$\begin{bmatrix} 2 & 1 \\ -1 & 1 \end{bmatrix}$	498
		(2×1)	498
	H_2S	(1×2)–S	251
		c(4×2)–S	251
	Pb	(1×3)	444,495,683
		(1×1)	444,495,683
		(7×1)	444,495,683
		(7×3)	444,495,683
		(4×4)	444,495,683
C(10$\bar{1}$0)	[clean]	c(2×2/3)	1033
C(110),diamond	O_2	Not Adsorbed	164
	N_2	Not Adsorbed	164
	NH_3	Not Adsorbed	164
	H_2S	Not Adsorbed	164
CdTe(100)	[clean]	(3×1),(1×1),{110}f	1393
Co(10$\bar{1}$0)	O_2	(2×1)–O	1070
Co(11$\bar{2}$0)	[clean]	*(1×1)	1197,1768,1848*
	CO	(3×1)–CO	902
		Disordered	902
	H_2O	Disordered	1310
		(4×1)–O	1310
		Complicated	1310

TABLE II. Surface Structures on Substrates with Two-fold Rotational Symmetry (Continued)

Substrate	Adsorbate	Surface Structure	Reference
Cr(110)	[clean]	(1×1)	1343
	CO	Disordered	1343
	Br_2	$\begin{bmatrix} 1 & 1 \\ -1 & 2 \end{bmatrix}$	1016
		$\begin{bmatrix} 1 & \frac{1}{1+X} \\ -1 & \frac{2}{1+X} \end{bmatrix}$–Br (0<X<1/3)	1016
		$\begin{bmatrix} 1 & 1 \\ -2 & 2 \end{bmatrix}$–Br	1016
	O_2	(3×1)–O	140
		(100) facets	140,256
		Cr_2O_3(0001)	140,256
		Cr_2O_3	1261
		Disordered	1261
Cu(110)	[clean]	*!(1×1)	725*,925,995,1023,1131 1135!,1136*,1436 1498,1723*
	Au	$\begin{bmatrix} 1 & 0 \\ \frac{-1}{2} & \frac{3}{2} \end{bmatrix}$	479
		(1×2)	479
		(2×2)	479
		Complex Structures	479
	Br_2	c(2×2)	1557
	Br(a)+H_2O	(3×2)	1557
	C	Disordered	1695
	C+O_2	(2×1)	1695
	CO	Ordered 1D	26
		(2×3)–CO	26
		(2×1)–CO	255,876,1234
		c(5/4×2)	876
		c(1.3×2)–CO	1234
		Hexagonal Overlayer	255
	H_2	Not Adsorbed	7
	H_2O	Disordered	26
		Not Specified	1131
		c(2×2)–H_2O	1023,1178,1270
		c(2×2)	1557
		(2×1)–OH	1270

TABLE II. Surface Structures on Substrates with Two-fold Rotational Symmetry (Continued)

Substrate	Adsorbate	Surface Structure	Reference
		(1×1)–H_2O	1178
	H_2S	c(2×3)–S	35
		Adsorbed	35
	I_2	!c(2×2)–I	572,1915!
		!c(2×2) Compressed	1915!
	Kr	c(2×8)–Kr	1304,1331
		Quasiperfect Hex.	1331
	N_2O	(2×1)–O	879
	$Ni(CO_4)$+CO	(1×1)+Disordered	1048
	O_2	!(2×1)–O	7,8,9,45,46,246
			656,750,879,885
			920,953,982,1053
			1066,1076,1095
			1257,1285,1695
			1916!,1917!,1918!
		c(2×1)–O	1270
		Streaks along <110>	1023
		(1×1)–O	656,885
		(3×1)–O_2	885
		c(6×2)–O	8,9,45,46,246,656
			885,920,1066,1076
			1095,1257,750,953
			1285,1695
		(5×3)–O	8,115
		c(14×7)–O	1332
	O(a)+CO	Disordered	1066
	O(a)+H_2O	(2×1)–O,H_2O	1023
		c(2×2)–O,H_2O	1023
		(2×1)–H_2O	1270
		(1×1)–H_2O,OH	1270
		(2×1)–OH,O	1270
	Pb	$\begin{bmatrix} 1 & 1 \\ -1 & 1 \end{bmatrix}$	481,482
		(5×1)	481,482
		(4×1)	482
	Pd	(2×1)–Pd	726
		(1×1)–Pd	726
	Xe	c(2×2)–Xe	159,1331,1611
		Hexagonal Overlayer	159,1611
		Pseudo-Hexagonal	1331

TABLE II. Surface Structures on Substrates with Two-fold Rotational Symmetry (Continued)

Substrate	Adsorbate	Surface Structure	Reference
Cu/Au(110)	[clean]	Streak	737
		(1×2)	737
		Complex Pattern	737
		c(3×1)	737
		(2×2)	737
Cu/Ni(110)	CO	(2×1)–CO	134
		(2×2)–CO	134
		(1×2)–CO	787
	H_2	(1×3)–H	787
	H_2S	c(2×2)–S	134
	O_2	(2×1)–O	134,872
		(2×2)–O	872
Cu(110)–Ni(1°)	O_2	(2×1)–O	1311
		c(6×2)–O	1311
Cu/Pd(110)	[clean]	(2×1)	737
Cu–25% Zn(110)	[clean]	(1×1)	1152
	O_2	Disordered	1152

TABLE II. Surface Structures on Substrates with Two-fold Rotational Symmetry (Continued)

Substrate	Adsorbate	Surface Structure	Reference
Fe(110)	[clean]	*(1×1)	1015,1639*
	CO	$\begin{bmatrix} 3 & -2 \\ 0 & 4 \end{bmatrix}$–CO	346
		c(2×4)	810
		(1×2)	810
		c(2×2)	687
		(1×4)	687
		$\begin{bmatrix} 4 & 0 \\ -1 & 3 \end{bmatrix}$	687
	CO_2	c(2×2)	687
		(1×4)	687
		$\begin{bmatrix} 4 & 0 \\ -1 & 3 \end{bmatrix}$	687
	Fe_3O_4	Not Well Ordered	1189
	H_2	*(2×1)–H	177,1753*
		*(3×1)–2H	177,1753*
		(1×1)–H	177
		c(2×2)–H	687,1298
		(3×3)–6H	1298
		$\begin{bmatrix} 1 & -1 \\ 1 & 2 \end{bmatrix}$	687
	H_2S or S	(2×4)–S	114
		(1×2)–S	114
		*(2×2)–S	836,1000,1015,1608*
		c(3×1)–S	836
		c(18×3)–S	836
	K	Hexagonal Array	728
	K+O_2	c(4×2)	786
	N_2	$\begin{bmatrix} 3 & -2 \\ 0 & 4 \end{bmatrix}$–$N_2$	346
	NH_3	(2×2)	687
		Disordered	1686
		$\begin{bmatrix} 4 & 1 \\ -3 & 3 \end{bmatrix}$	687
		(2×2)–NH	1686

TABLE II. Surface Structures on Substrates with Two-fold Rotational Symmetry (Continued)

Substrate	Adsorbate	Surface Structure	Reference
	O_2	c(2×2)–O	87,88,99
		(2×2)–O	1015
		c(3×1)–O	87,88,99
		(2×8)–O	98
		FeO(111)	87,88,99,269
		(2×1)–O	141
		(5×12)–O	1664
Fe/Cr(110)	O_2	Cr_2O_3(0001)	280
		Amorphous Oxide	279
Ge(110)	[clean]	c(8×10)	804,1683
		Ge(17,15,1)–(2×1)	804,1683
	H_2S	(10×5)–S	178
	O_2	Disordered	17,18
		(1×1)–O	17,18
GaAs(100)	[clean]	(2×4)	1085,1090,1274,1387
		(4×2)	1274
		c(4×4)	697,1085,1240 1387,1541
		(4×6)	697,1090,1213,1240 1377,1448,1541
		c(6×4)	697
		(1×1)	1213,1519
		(2×8)	1449
		c(2×8)	697,1090,1213,1240 1541
		c(8×2)	697,1090,1213,1448 1541
		(8×2)–Ga	1519
		(1×2)	1448
		(1×6)	697,1541
	[laser process]	(1×1)+steps	1446
	Ag	c(8×2)	710
		c(2×8)	710
		c(4×4)	710
		c(6×6) [Multilayer]	1344
	Al	c(8×2)	710
		c(2×8)	710
		c(2×2) [Multilayer]	1344
	As_4	c(4×4)	1422
	As_4,Ga	(2×4)	1365
		(4×6)	1365
		c(8×2)	1365
		(4×1)	1365
		(3×1)	1365

TABLE II. Surface Structures on Substrates with Two-fold Rotational Symmetry (Continued)

Substrate	Adsorbate	Surface Structure	Reference
	$Fe(CO)_5$	$(1/\sqrt{2}\times1/\sqrt{2})R45°$ [Multilayer]	1377
	Bi	(1×1)–Bi	1491
		(1×2)–Bi	1491
		(3×1)–Bi	1491
		(8×2)–Bi	1491
	Ge	(1×2)–Ge	1213
		(1×2)+(2×1)	1213
	H_2	(1×1)	1541
	H_2S	c(2×8)–H_2S	589
		(2×1)	589
	HCl,H_2O	(1×1)	1518
	Pb	(1×4)–Pb	1387
	Pb,As_4	(1×2)–Pb	1387
	Sn	(1×3)–Sn	1387
	Sn	(1×2)–Sn	1387
GaAs(100)–As rich	[clean]	c(4×4)	1214,1524
GaAs(100)–Ga rich	[clean]	(4×6)	1214,1524
GaP(100)	[clean]	(4×2)	694
	Cs	(1×4)–Cs	694
		(7×1)–Cs	694
		(1×4)–Cs	694
	PH_3	(1×2)	694
	Si	(2×1)	1554
Ge(110)	H_2S	(10×5)–S	178
	O_2	Disordered	17,18
		(1×1)–0	17,18
InP(100)	[clean]	(4×2)	1170,1384
	[laser annealed]	(1×1)	1170,1384
	[laser annealed]	(1×1)+steps	1446
	Sb	*(1×1)	1919*,1920*
InSb(001)	[clean]	c(2×8)	1159,1421
	Sn	α–Sn(001)–(2×1)	1159
Ir(110)	[clean]	*(1×2)	701*,1321,1665 1787,1875*
		*(1×1)	1786*
	CO	(2×2)–CO	347,348
		(4×2)–CO	348
	H_2	(1×2)	830
		Adsorbed	347
	H_2O	Adsorbed	615
	H_2S	*(2×2)–2S	715,1875*
		(1×2)–S	715
		c(2×4)–S	715
	N_2	(1×2)	678
		(2×2)–N_2	678
		Not Adsorbed	347
	NO	Disordered	677
		Streaks	677

TABLE II. Surface Structures on Substrates with Two-fold Rotational Symmetry (Continued)

Substrate	Adsorbate	Surface Structure	Reference
	O_2	(1×2)–O	347,1687
		(1×4)–Oxide	571,706
		Disordered	571
		(2×2)–O	571,706
		*c(2×2)–O	571,706,1788*
		(3×2)	706
		(1×1)–O	1676,1687
LaB_6(110)	[clean]	c(2×2)	775,1328
	O_2	(1×1)–O	349,1328
Mo(110)	[clean]	*(1×1)	1634*
	Al	Hexagonal	515
	Au	Disordered	1681
	C	(4×6)–C	1250
	Cl_2	(2×1)–Cl	1250
		(1×1)–Cl	1250
		(1×2)–Cl	1250
		(1×3)–Cl	1250
	CO	(1×1)–CO	62,100
		c(2×2)–CO	94
		Disordered	406
	CO_2	Disordered	94
	Cs	Hexagonal	512
	H_2	Adsorbed	100
	H_2S	(2×2)–S	351
		c(2×2)–S	351
		(1×1)–S	351
		c(1×3)–S	351
		c(1×5)–S	351
		(1×3)–S	351
		c(1×7)–S	351
		(1×4)–S	351
		(1×5)–S	351
		c(1×11)–S	351
		$\begin{bmatrix} 2 & 2 \\ -1 & 1 \end{bmatrix}$–S	351
	K	Hexagonal	512
	KCl	Disordered	781
	N_2	(1×1)–N	62
	Na	No Ordered Structure	512
	O_2	(2×2)–O	62,63,100,1154
		(2×1)–O	62,63,100
		(1×1)–O	62,63
		Disordered	350
		Complex	1154
	Rb	Hexagonal	512

TABLE II. Surface Structures on Substrates with Two-fold Rotational Symmetry (Continued)

Substrate	Adsorbate	Surface Structure	Reference
$MoO_3(010)$	[clean]	(1×1)	922,1128
	H_2	3D–MoO_2	922
Na(110)	[clean]	*(1×1)	1754*,1755*
	O_2	$Na_2O(111)$	352*
$Na_{2/3}WO_3(110)$	[clean]	(3×1)	906
Nb(110)	CO	Disordered	101
		(3×1)–O	101
	H_2	(1×1)–H	111
	O_2	(3×1)–O	101
		NbO(111)	192
		NbO(110)	192
		NbO(220)	192
		Oxide	101
		Complex Pattern	1688
	Sn	Disordered	505
		(3×1)	505
Ni(110)	[clean]	(2×1)	882
		*!(1×1)	890,1061!,1459*
			1468,1469,1470
			1756*,1757*,1758!,1853!
	C	c(4×5)–C	1198
	Cl_2	c(2×2)–Cl	1341
		(10×2)–Cl Diffuse	1341
	CO	(1×1)–CO	2,94
		Adsorbed	198
		c(2×1)–CO	353,356,359,645
		(2×1)–CO	356,357,358
		c(2×2)–CO	359,645
		(4×2)–CO	359,645
	CO+O_2	(3×1)–CO+O_2	91
	Cs	Disordered	455
	D_2	(2×1)–D	869,944,1097
		(1×2)–D	869,944,1097
	H_2	(1×2)–H	59,81,94,110,198
			203,353,360,867
			941,927,1031,1074,1527,1673
		(2×1)–2H	867
		(2×1)–H	941,890,1031,1074
			1527
		c(2×6)–H	890,1031
		(2×6)–H	1074
		(2×3) with streaks	1031
		c(2×4)–H	1031

TABLE II. Surface Structures on Substrates with Two-fold Rotational Symmetry (Continued)

Substrate	Adsorbate	Surface Structure	Reference
	H_2O	$(2\times1)-H_2O$	110
	H_2S (or S)	*!c(2×2)–S	36,198,205,294 1079,1142!,1370 1759*,1853!
		*(2×2)–S	1079,1867*
		(3×2)–S	36
		(1×1)–S	1142
	H_2Se	!c(2×2)–Se	137,1708!
	K	Disordered	455
	N_2	$(2\times1)-N_2$	1074,1309
		$(2/3\times1/3)-N_2$	1074
		(2×3)–N	759
		$c(2\times4)-N_2$	759
	N_2^+	Disordered	1290
		(2×3)–N	1290
	Na	Disordered	455,458,460
		Hexagonal	455,458,460
	NH_3	$(1\times1)-NH_3$	840,880,1560
		$(4\times2)-NH_3$	840
		$c(6\times2)-NH_3$	840
		$c(4\times2)-NH_3$	840,880
		(3×2)–NH	1107
	NH_3+e^-	$c(2\times2)-NH_2$	840
		(2×3)–N	840
	NO	(2×3)–N	361
		(2×1)–O	361
	O_2	!(2×1)–O	2,3,51,57,83,89 91,92,99,198,353 354,355,729!,912,968 1069,1074,1140 1164,1168,1290 1292,1370,1437
		(3×1)–O	2,51,83,89,91,92 94,198,353,354 355,912,1011,1041 1437
		(2×1)+(3×1)–O	968
		(5×1)–O	2,89
		(9×4)–O	51,354,355,1437
		Disordered	1437
		NiO(100)	6,51,83,91,198, 354,355
		Disordered Oxide	1437
	O_2+H_2O	(2×1)–OH	1011

TABLE II. Surface Structures on Substrates with Two-fold Rotational Symmetry (Continued)

Substrate	Adsorbate	Surface Structure	Reference
	Pb	$\begin{pmatrix} 1 & 1 \\ 1 & -1 \end{pmatrix}$	471
		(3×1)	471
		(4×1)	471
		(5×1)	471
	Se	c(2×2)–Se	1370
	Te	c(2×2)–Te	1370
	Yb	(2×1)–Yb	844
NiAl(110)	[clean]	*(1×1)	1771*
Ni–25% Fe(110)	H_2S,H_2	(2×3)–S	1121
$Ni_4Mo(101)$	[clean]	Ordered	1115
Pd(110)	[clean]	*(1×1)	1760*
	Cl_2	c(16×2)–Cl	1341
	CO	(5×2)–CO	95
		(2×1)–CO	95,209
		(4×2)–CO	209
		c(2×2)–CO	209
		c(4×2)–CO	1359
		(4×1)–CO	1359
		c(4×2)–CO Imperfect	1251
	Cs	*(1×2)+Disordered Cs	1760*
	H_2	(1×2)–H	212,1173
		(2×1)–H	1173
	H_2S	(2×3)	625
		c(2×2)	625
		c(8×2)	625
		(3×2)	625
	Na	*(1×2)+Disordered Na	1760*
	O_2	(1×3)–O	95
		(1×2)–O	95
		c(2×4)–O	95
	Xe	Hexagonal	743
Pt(110)	[clean]	!(1×2)	960,1062,1080,1166,1187 1271,1279,1297 1761!,1890
		(1×1)	1279
	C_2N_2	(1×1)	407,435
	C_3O_2	(1×1)–C_3O_2	365
	Cl_2	(1×2)–Cl	1341
		(1×1)–Cl	1341
		(2×1)–Cl Diffuse	1341
	CO	(2×1)–CO	366,981,1271 1279,1297,1360
		(1×1)–CO	139,364,763,1271 1279,1297,1360
		(1×2)–CO	1360
		(1×1)+(1×2)	1297,1360
		c(8×4)–CO	1271,1279,1360

TABLE II. Surface Structures on Substrates with Two-fold Rotational Symmetry (Continued)

Substrate	Adsorbate	Surface Structure	Reference
	CO+NO	(1×1)–CO+NO	364
	H_2	(1×1)	1279
		(1×2)	1279
	H_2S	c(2×6)–S	247,367,368,1114
		(2×3)–S	247,367,368,1114
		(4×3)–S	247,367,368,1114
			1116
		c(2×4)–S	247,367,368,1114
		(4×4)–S	247,367,1114
	HCN	$\begin{bmatrix} 1 & \frac{2}{3} \\ -1 & \frac{2}{3} \end{bmatrix}$	434
		c(2×4)	434
		(1×1)	434
	HNCO	(2×2)–NCO	657
		(1×2)–NCO	657
	NO	(1×1)–NO	222,364
		(2×1)–NO	614
		c(4×8)–NO	614
		Disordered	614
	O_2	(2×1)–O	11,363
		(4×2)–O	11
		Adsorbed	362
		c(2×2)–O	363
		PtO(100)	363
		(1×1)–CO	139,364
		(1×3)	763
		(1×5)	763
		(1×7)	763
		Satellite Spots	1279
Pt–2% Cu(110)	[clean]	(1×3)	1062
	CO	(1×1)–CO	1063
Re($10\bar{1}0$)	[clean]	*(1×1)	584*
	Ba	c(2×2)	1591
	Mg	(1×3)	1675
Re($11\bar{2}0$)	after NH_3 synthesis	(1×1)	977
Rh(110)	[clean]	*(1×1)	1800*
	CO	(2×1)–CO	369
		c(2×2)–C	369
		Disordered	569
	H_2S	*c(2×2)–S	769*
	NO	Disordered	569,791
		(2×2)–N,O	569,791
		(2×1)–N,O	569,791

TABLE II. Surface Structures on Substrates with Two-fold Rotational Symmetry (Continued)

Substrate	Adsorbate	Surface Structure	Reference
	O_2	Disordered	96,97
		c(2×4)–O	96,97
		c(2×8)–O	96,97
		(2×2)–O	96,97
		(2×3)–O	96,97
		(1×2)–O	96,97
		(1×3)–O	96,97
	S or H_2S	*c(2×2)–S	769*,1473
Ru(101)	CO	$\begin{bmatrix}1 & 1\\3 & 0\end{bmatrix}$–CO	372
		$\begin{bmatrix}0 & 1\\2 & 0\end{bmatrix}$–C	372
	NO	Disordered	373
	O_2	$\begin{bmatrix}1 & 1\\3 & 0\end{bmatrix}$–O	374
		$\begin{bmatrix}2 & 1\\5 & 0\end{bmatrix}$–O	374
		$\begin{bmatrix}4 & 1\\9 & 0\end{bmatrix}$–O	374
Ru(10$\bar{1}$0)	Cl_2	(1×1)–Cl	1052
		(2×3)–Cl	1052
		$\begin{bmatrix}2 & 0\\-1 & 3\end{bmatrix}$–Cl	1052
		$\begin{bmatrix}2 & 0\\-1 & 4\end{bmatrix}$–Cl	1052
		(2×1)–Cl	1052
	CO	Disordered	371
	H_2	Not Adsorbed	371
	N_2	Not Adsorbed	371
	NO	c(4×2)–N+O	370,371
		(2×1)–N+O	370,371
		(2×1)–O	371
		c(4×2)–O	371
		c(2×6)–O	370
		(7×1)–O	370
		c(4×8)–O	370
		(2×1)–N	371
		c(4×2)–N	371
	O_2	c(4×2)–O	370,371
		(2×1)–O	370,371
		c(2×6)–O	370
		(7×1)–O	370
		c(4×8)–O	370

TABLE II. Surface Structures on Substrates with Two-fold Rotational Symmetry (Continued)

Substrate	Adsorbate	Surface Structure	Reference
Si(110)	[clean]	(4×5)	803,1685
		(2×1)	803,1685
		(5×1)	803,1685
	Bi	(2×3)–Bi	659
		Disordered	659
	H_2	(1×1)–H	375
	H_2O	Adsorbed	903
	Si,laser	(1×2)	1392
SnO_2(101)	[clean]	(1×1)	1183
$SrTiO_3$(110)	[clean]	(3×2)	1490
Ta(110)	Al	Hexagonal	508,509
		Square	508,509
	Cl_2	(1×1)–Cl.	1180
		(1×2)–Cl	1180
		c(1×5)–Cl	1180
		c(1×7)–Cl	1180
		Streak <001>	1180
		Complicated	1180
	CO	Disordered	101,102
		(3×1)–O	101,102
	H_2	(1×1)–H	102
	I_2	$\begin{bmatrix} 3 & 0 \\ -1 & 1 \end{bmatrix}$–I	1180
		(1×1)+c(1×3)–I	1180
		(1×1) with ring	1180
		c(4×4)–I	1180
	N_2	Not Adsorbed	101
	O_2	(3×1)–O	101,102
		Oxide	101,102
TiO_2(100)	[clean]	(011)–(2×1) facet	1318,1615
		(114)facet	1318
	H_2O	Disordered	376
	O_2	Disordered	376
TiO_2(110)	[clean]	(1×1)	1615
V(110)	[clean]	*(1×1)	649*,1498,1762*
	CO	Disordered	101
		(3×1)–O	101
	O_2	(3×1)–O	101
V_6O_{13}(001)	K	No Superstructure	1186
W(110)	[clean]	*(1×1)	1123,1247,1763*
	Ag	Hexagonal Structures	546,547
		Ag(111)	1151
	Au	Hexagonal Structures	546,548

TABLE II. Surface Structures on Substrates with Two-fold Rotational Symmetry (Continued)

Substrate	Adsorbate	Surface Structure	Reference
	Ba	Disordered Hexagonal	533–535
		Hexagonal	533–535
		$\begin{bmatrix} 2 & 2 \\ 0 & 6 \end{bmatrix}$	533–535
		$\begin{bmatrix} 2 & 2 \\ 0 & 5 \end{bmatrix}$	533–535
		$\begin{bmatrix} 3 & 3 \\ 1 & 5 \end{bmatrix}$	533–535
		Hexagonal Compact	533–535
	Be	(1×9)	529
		(1×1)	529
		$\begin{bmatrix} 9 & 0 \\ -1 & 1 \end{bmatrix}$	529
	Cl_2	(5×2)–Cl	796
	CO	Disordered	109
		c(9×5)–CO	109
		(1×1)–CO	379
		c(2×2)–CO	379
		(2×7)–CO	389
		c(4×1)–CO	389
		(3×1)–CO	389
		(4×1)–CO	389
		(5×1)–CO	389,390
		(2×1)–C+O	389,390
		c(9×5)–C+O	389
	CO+O_2	c(11×5)–CO+O_2	93
	Cs	Disordered Hexagonal	523,527,528
		Hexagonal	523,527,528,1677
	Cu	Hexagonal	543–545
		Cu(111)	1151
	Fe	3-Dimensional Crystals	451
		Fe(110)	1325
		(1×1)	1325
	H_2 or D_2	(2×1)–H	136,1516,1674
		(1×2)–H	672
		(2×2)–H	1516,1674
		(1×1)–H	1516
		Ordered	1438
		(2×2)–H_2	1516
		(2×1)–H_2	1516
	I_2	(2×2)–I	391
		(2×1)–I	391

TABLE II. Surface Structures on Substrates with Two-fold Rotational Symmetry (Continued)

Substrate	Adsorbate	Surface Structure	Reference
	Li	$\begin{bmatrix} 1 & 5 \\ -2 & 2 \end{bmatrix}$	517–519
		(2×2)	517–519
		$\begin{bmatrix} 1 & 1 \\ -1 & 2 \end{bmatrix}$	517–519
		(2×3)–Li	1269
		c(2×2)–Li	1269
		c(3×1)–Li	1269
		c(1×1)–Li	1269
	N_2	(2×2)–N	758
	Na	$\begin{bmatrix} 1 & 5 \\ -2 & 2 \end{bmatrix}$	445,446
		(2×2)	445,446
		$\begin{bmatrix} 1 & 1 \\ -1 & 2 \end{bmatrix}$	445,446
		$\begin{bmatrix} 1 & 1 \\ 0 & 8 \end{bmatrix}$	445,446
		$\begin{bmatrix} 1 & 1 \\ 0 & 5 \end{bmatrix}$	445,446
		Hexagonal	445,446
	Ni	(1×1)–Ni	970
		(8×2)–Ni	970
		(7×2)–Ni	970
	NO	(1×1) streaked	661
		c(11×5)	661,799
		(2×2)	661,799
	O_2	*(2×1)–O	57,103,377–385,386*,387 599,699,1277,1418 1587,1651
		c(2×2)–O	104
		(2×2)–O	104,387,599,699
		(1×1)–O	104
		c(14×7)–O	57,103,104,628
		c(21×7)–O	104
		c(48×16)–O	104
		WO_3(100)	388
		WO_3(111)	388
	Pd	(1×3)	542
		Hexagonal	542
	Pd(1ML)+CO	Not Adsorbed	1218
	Pd(2.2ML)+O_2	(2×2)–O	1218

TABLE II. Surface Structures on Substrates with Two-fold Rotational Symmetry (Continued)

Substrate	Adsorbate	Surface Structure	Reference
	Pb	Split $\begin{bmatrix} 3 & 0 \\ -1 & 1 \end{bmatrix}$	551,552
		$\begin{bmatrix} 3 & 0 \\ -1 & 1 \end{bmatrix}$	551,552
	S_2	(2×2)–S	1246
		(7×2)–S	1246
		Rotated Structure	1246
		(1×N)–S (N>=3)	1246
	Sb	$\begin{bmatrix} 1 & 1 \\ 0 & 4 \end{bmatrix}$	553,555
		$\begin{bmatrix} 2 & 0 \\ -1 & 1 \end{bmatrix}$	553,555
		$\begin{bmatrix} 3 & 0 \\ -1 & 1 \end{bmatrix}$	553,555
		$\begin{bmatrix} 4 & 0 \\ -1 & 1 \end{bmatrix}$	553,555
	Sc	$\begin{bmatrix} 1 & 1 \\ 0 & 3 \end{bmatrix}$	536–538
		$\begin{bmatrix} 2 & 2 \\ 0 & 8 \end{bmatrix}$	536–538
	Se	(5×2)–Se	1228
		(1×3)–Se	1228
		Complex	1228
	Sr	$\begin{bmatrix} 3 & 3 \\ -2 & 5 \end{bmatrix}$	530
		$\begin{bmatrix} 2 & 2 \\ 0 & 6 \end{bmatrix}$	530
		$\begin{bmatrix} 2 & 2 \\ 1 & 6 \end{bmatrix}$	530
		$\begin{bmatrix} 1 & 0 \\ 0 & 3 \end{bmatrix}$	530
		Hexagonal	530

TABLE II. Surface Structures on Substrates with Two-fold Rotational Symmetry (Continued)

Substrate	Adsorbate	Surface Structure	Reference
	Te	(4×2)–Te	1280
		(20×2)–Te	1280
		(17×2)–Te	1280
		(5×2)–Te	1280
		(22×2)–Te	1280
	W	Ring Pattern	1623
	WO_2	(2×2)	1501
	Xe	(2×2)–Xe	713
		Disordered	713
	Y	Hexagonal	539,540
ZnSe(100)	[clean]	$(\sqrt{2}\times\sqrt{2})R45°$	1393
		(5×1)	1393
ZnTe(100)	[clean]	(1×3),(1×1)+{110}f	1393
	Au	(1×1)–Au	1188

†Organic overlayer structures are not included. See Table VII for these structures.

TABLE III. Surface Structures on Substrates with Three-fold Rotational Symmetry†

Substrate	Adsorbate	Surface Structure	Reference
Ag(111)	[clean]	*(1×1)	975,1894*,1895*,1896*
	Al	Disordered	491
	Au	*(1×1)	491,1355,1825* 1826
	Bi	Disordered	491
	Br_2	$(\sqrt{3}\times\sqrt{3})R30°$–Br	155
		(3×3)–Br	155
	Cd	No Condensation	491
	Cl_2	(1×1)+Disordered	1050
		$(\sqrt{3}\times\sqrt{3})R30°$–Cl	151,1050
		(10×10)–Cl	151
		AgCl(111)	152,732,1050
	Co	Disordered	491
	$CO+O_2$	$(2\times\sqrt{3})$–$(CO+O_2)$	27
	Cr	Disordered	491
	Cu	Hexagonal Overlayer	1822–1824
	H_2O	Disordered	1034
	H_2S	(4×4)–S	627
		$\begin{bmatrix} 3 & 2 \\ -2 & 1 \end{bmatrix}$–S	627
	I_2	*$(\sqrt{3}\times\sqrt{3})R30°$–I	145,149,150,1145 1225*,1259,1440
		Hexagonal Overlayer	1145
	K	Hexagonal Overlayer	1345
	Kr	Hexagonal Overlayer	156
	Mg	Disordered	491
	Na	(1×1)	488
	Ni	Hexagonal Overlayer	491,1821
	NO	Disordered	163
	O_2	(2×2)–O	1
		$(\sqrt{3}\times\sqrt{3})R30°$–O	1
		Not Adsorbed	146
		(4×4)–O	147,148
	Pb	$(\sqrt{3}\times\sqrt{3})R30°$–Pb	975
		Pb(111)	975
		Hexagonal Overlayer	491,1827
	Pd	(1×1)	1463
		Disordered	491
	Rb	(1×1)–Rb	490,705
		(9×9)	705
	S_2	$(\sqrt{39}\times\sqrt{39})R16.1°$–S	714
		$(\sqrt{7}\times\sqrt{7})R10.9°$ of γ–$Ag_2S(111)$	714
	Sb	Disordered	491
	Sn	Disordered	491
	Tl	Hexagonal Overlayer	491
	Xe	Hexagonal Overlayer	156,157,158,159 160
		*Incommensurate	1599*,1845*
	Zn	No Condensation	491

TABLE III. Surface Structures on Substrates with Three-fold Rotational Symmetry (Continued)

Substrate	Adsorbate	Surface Structure	Reference
Ag(111)–Rb dosed	O_2	$(2\sqrt{3}\times2\sqrt{3})R30°$–Rb/O	653
		(4×4)–Rb/O	653
		Complex Structures	653
		(9×9)–Rb/O	653
Al(111)	[clean]	*(1×1)	863,951,1141*,1354,1467* 1472*,1498,1640
	Ag	Ag–Al(0001)	1161
	CO	Disordered	1175
		Not Adsorbed	1273
	Cu	(1×1)	863
		Disordered [Multilayer]	863
		Cu(111) [Multilayer]	863
	H_2O	Disordered	1157
	Mn	$\begin{bmatrix} 6 & 0 \\ -1 & 2 \end{bmatrix}$	502
		Hexagonal rotated±9°	502
	Na	$\begin{bmatrix} 1 & 1 \\ -1 & 2 \end{bmatrix}$	500
		(2×1)	500
	Ni	(1×1)	1680
		$\begin{bmatrix} 1 & 1 \\ -1 & 2 \end{bmatrix}$	1839
	O_2	(4×4)–O	123
		*!(1×1)–O	638,709,756,951,1141* 1397,1467*,1621 1637,1774!,1775!
		Oxide-like	1141
	Pb	Hexagonal rotated±9°	504
		Hexagonal Overlayer	1060
	Pd	Hexagonal Overlayer	1682
		$(\sqrt{3}\times\sqrt{3})R30°$–Pd	1661
	Sn	Hexagonal Rotated±9°	504
		Hexagonal Overlayer	1060,1682
	Tl	$(\sqrt{3}\times\sqrt{3})R30°$–Tl	1661
Au(111)	[clean]	(23×1)	861,1146,1558,1889
		(5×1)	1146
	Ag	(1×1)	491,1825
		fcc(111)	1689
	Ag,Air	$Ag_2O(110)$–(2×1)	997
	Bi	$\begin{bmatrix} 10 & 10 \\ -10 & 20 \end{bmatrix}$	498
		(2×2)	924

TABLE III. Surface Structures on Substrates with Three-fold Rotational Symmetry (Continued)

Substrate	Adsorbate	Surface Structure	Reference
	Cl_2	(1×1)–Cl	647
	Cr	Hexagonal	493
	Cu	($\sqrt{3}\times\sqrt{3}$)R30°–Cu	861,1558,1582
		(1×1)	1558
		Extra Lines(RHEED)	1836,1837
	Fe	(1×1)	1828,1830–1832
	O_2	Oxide	161
		Not Adsorbed	162
		Adsorbed	162
	Pb	Hexagonal Rotated±5°	444,495
		($\sqrt{3}\times\sqrt{3}$)R30°	924
		(1×1)	683
	Pd	(1×1)	1807,1834
	Pt	(1×1)	1835
	Si	(2×2)–AuSi	1622
		(3×3)–AuSi	1622
		Hexagonal Silicide	1622
Be(0001)	[clean]	*(1×1)	911,1900*,1901*
	CO	Disordered	22
	H_2	Not Adsorbed	22
	N_2	Not Adsorbed	22
	O_2	Disordered	22
		BeO(0001)–(1×1)	911
		BeO(0001)–(2×2)	911
Bi(0001)	O_2	($\sqrt{3}\times\sqrt{3}$)R30°	576,1065,1288
		(1×1)	576
		Coincidence Lattice	576,1065
		BiO	1288
	O_2+K	($\sqrt{3}\times\sqrt{3}$)R30°+BiO(0001)layer	1288
	Cl_2	(1×1)–Cl	1242
		($2\sqrt{3}\times2\sqrt{3}$)R30°–$BiCl_3$	1242
		(4×4)	1242
C(111), diamond	[clean]	(2×2)	820
		(2×1)	820
		*(1×1)	1551*
	H_2 (or D_2)	(1×1)–H(or D)	30,1386,1697
	H_2S	Not Adsorbed	164
	N_2	Not Adsorbed	164
	NH_3	Not Adsorbed	164
	O_2	Adsorbed	16
		Not Adsorbed	164
	P	($\sqrt{3}\times\sqrt{3}$)R30°–P	30
C(0001), graphite	[clean]	(2×2)	1190
		*(1×1)	1373,1439*,1846*
	Ar	($\sqrt{3}\times\sqrt{3}$)R30°–Ar	720,960
		*Incommensurate	1882,1903*
	Ar+Xe	($\sqrt{3}\times\sqrt{3}$)R30°–Ar,Xe	1193
	CF_4	(2×2)–CF_4	1192,1194
		Close to (2×2)	1404

TABLE III. Surface Structures on Substrates with Three-fold Rotational Symmetry (Continued)

Substrate	Adsorbate	Surface Structure	Reference
	CO	$(\sqrt{3}\times\sqrt{3})R30°$–CO	884
		$(2\sqrt{3}\times2\sqrt{3})R30°$–CO	889
		$(2\sqrt{3}\times\sqrt{3})R30°$ [Herringbone]	884
		Triangular Incommensurate (2×2)	884
	H_2	$(\sqrt{3}\times\sqrt{3})R30°$–$H_2$	1283
		(2×2)	1373
		$(\sqrt{3}\times\sqrt{3})R30°$	1373
	K (intercalated)	*Disordered	1847*
	KOH	Disordered	1083
	Kr	!$(\sqrt{3}\times\sqrt{3})R30°$–Kr	166,167,174,721 828,960,1616,1904!
		Incommensurate	1413,1616
		Disordered	1413
	N_2	$(2\sqrt{3}\times2\sqrt{3})R30°$–$N_2$	889
		$(\sqrt{3}\times\sqrt{3})R30°$	1064,1190,1512
		$(\sqrt{3}\times\sqrt{3})R30°$+(2×1)	1435
		Commensurate	1190,1883
		Incommensurate	1443,1883
	NaOH	1/2 Order Ring	1083
	Ne	Incommensurate	629
		$(\sqrt{3}\times\sqrt{3})R30°$ rotated by ±17°	629,960
		Ordered	1338
	NO	Incommensurate	1602
	O_2	Triangular	1883
		Centered-Parallelogram–O_2	1425,1883
		$(\sqrt{3}\times\sqrt{3})R30°$–$O_2$	1200
		Physisorbed	1411
	Xe	$(\sqrt{3}\times\sqrt{3})R30°$–Xe	165,618,960,1038,1201
Cd(0001)	[clean]	(1×1)	1902
CdS(0001)	O_2	Disordered	25
CdTe($\overline{111}$)	[clean]	(2×2)	1393
CdTe(111)	[clean]	(1×1),(1×1)+{110}f	1393
Co(0001)	[clean]	*(1×1)	1130,1580,1613*
	CO	$(\sqrt{3}\times\sqrt{3})R30°$–CO	168,1130,1362
		$(2\sqrt{3}\times2\sqrt{3})R30°$–CO	1130,1362
		c(4×2)–CO	1362,1581
		$(\sqrt{7}/2\times\sqrt{7}/2)R19.10°$–CO	1362
		Hexagonal Overlayer	168
		$(\sqrt{7/3}\times\sqrt{7/3})R10.9°$–CO	1130
	H_2O	Disordered	1310
	NO	$(\sqrt{39}\times\sqrt{39})R16.1°$–N,O	788
	O_2	No Superstructure	1235
Co(111)	[clean]	*(1×1)	1613*
CoO(111)	[clean]	*(1×1)	1769*
Cr(111)	Ag	(8×8)	46

TABLE III. Surface Structures on Substrates with Three-fold Rotational Symmetry (Continued)

Substrate	Adsorbate	Surface Structure	Reference
	Au	$\begin{bmatrix} \frac{2}{3} & 3 \\ \frac{-2}{3} & \frac{4}{3} \end{bmatrix}$	52
	Bi	$\begin{bmatrix} 1 & 1 \\ -1 & 2 \end{bmatrix}$	61
		$\begin{bmatrix} 2 & -1 \\ 0 & 2 \end{bmatrix}$	61
		$\begin{bmatrix} 2 & 3 \\ 1 & 2 \end{bmatrix}$	61
	Fe	(1×1)	39
	Ni	(1×1)	43,44
	O_2	$(\sqrt{3}\times\sqrt{3})R30°$–O	169
	Pb	(4×4)	55,58
	Sn	$\begin{bmatrix} 1 & 1 \\ -1 & 2 \end{bmatrix}$	54
Cu(111)	[clean]	*(1×1)	1101,1408*,1419 1462,1510,1538 1635
	Ag	(8×8)	477
		3 Dimensional Crystals	1813,1815–1818
		(1×1)	1526
	Au	$\begin{bmatrix} \frac{2}{3} & \frac{2}{3} \\ -\frac{2}{3} & \frac{4}{3} \end{bmatrix}$	479
		(2×2)	479
		3 Dimensional crystals	1815,1819
	Bi	$\begin{bmatrix} 1 & 1 \\ -1 & 2 \end{bmatrix}$	487
		$\begin{bmatrix} 2 & -1 \\ 0 & 2 \end{bmatrix}$	487
		$\begin{bmatrix} 2 & 3 \\ 1 & 2 \end{bmatrix}$	487
	C_2N_2	Disordered	666
	C	Disordered	840,1695
	Cl_2	$(\sqrt{3}\times\sqrt{3})R30°$–Cl	151,1102
		$(6\sqrt{3}\times6\sqrt{3})R30°$–Cl	151
		$(12\sqrt{3}\times12\sqrt{3})R30°$–Cl	151
		$(4\sqrt{7}\times4\sqrt{7})R19.2°$–Cl	151

TABLE III. Surface Structures on Substrates with Three-fold Rotational Symmetry (Continued)

Substrate	Adsorbate	Surface Structure	Reference
	CO	Not Adsorbed	26
		$(\sqrt{3}\times\sqrt{3})R30°$	172,173,590,1306
		$(1.5\times1.5)R18°$	590
		(1.39×1.39)	591,592,593
		$(\sqrt{7/3}\times\sqrt{7/3})R49.1°$	172,173
		$(3/2\times3/2)$	173
	Co	(1×1)–Co	1299
	Fe	(1×1)	474
	H_2	Not Adsorbed	7
	H_2S	$(\sqrt{3}\times\sqrt{3})R30°$–S	35
		Adsorbed	35
	HNCO	Disordered	624
	I_2.	!$(\sqrt{3}\times\sqrt{3})R30°$–I	574,1259,1779!
	Na	(2×2)–Na	1571
	Ni	*(1×1)–Ni	475,476,1466* 1813
	$Ni(CO)_4$+CO	(1×1)+Disordered	1048
	O_2	Disordered	7,170,171,1095 1244
		(7×7)–O	7,8
		$(\sqrt{3}\times\sqrt{3})R30°$–O	7,8,1286
		(2×2)–O	7,8,115
		(3×3)–O	8
		(11×5)R5°–O	9
		(2×2)R30°–O	115,119
		$\begin{bmatrix} 3 & 2 \\ -1 & 2 \end{bmatrix}$–O	1066
		Hexagonal	246
	O_2+HCN	Disordered	1244
	O(a)+CO	Disordered	1066
	Pb	(4×4)	481,484
	Pd	(1×1)	726,11441538
	Sn	$\begin{bmatrix} 1 & 1 \\ -1 & 2 \end{bmatrix}$	480
	Te	!$(2\sqrt{3}\times\sqrt{3})R30°$	1905!
	Xe	$(\sqrt{3}\times\sqrt{3})R30°$–Xe	159
Cu/Al(111)	[clean]	(1×1)	813
		$(\sqrt{3}\times\sqrt{3})R30°$	813
Cu–5.7% Al(111)	[clean]	(1×1)	813
Cu–10% Al(111)	[clean]	(1×1)	1303
		$(\sqrt{3}\times\sqrt{3})R30°$–Al	1303
Cu–11% Al(111)	[clean]	(1×1)	1506
Cu–12.5% Al(111)	[clean]	$(\sqrt{3}\times\sqrt{3})R30°$	813
Cu–16% Al(111)	[clean]	*$(\sqrt{3}\times\sqrt{3})R30°$	1699*

TABLE III. Surface Structures on Substrates with Three-fold Rotational Symmetry (Continued)

Substrate	Adsorbate	Surface Structure	Reference
Cu/Au(1$\bar{1}$1)	[clean]	$(2/3\sqrt{3}\times 2/3\sqrt{3})$R30°	737
		(2×2)	737
Cu/Ni(111)	CO	Disordered	173,734
Cu/Pd(1$\bar{1}$1)	[clean]	(1×1)	737
Cu–25% Zn(111)	[clean]	(1×1)	1152
	O_2	Disordered	1152
Fe(111)	[clean]	*(1×1)	1700*,1701*
	CO	Disordered	1004
		(1×1)	687
		(5×5)	687
		(3×3)	687
	CO_2	(1×1)	687
		(5×5)	687
		(3×3)	687
	H_2	Adsorbed	177
		(1×1)	687
	H_2O	(1×1)–H_2O	1588
	K	(3×3)–K	665,1350
	N_2	c(2×2)–N	1350
		(3×3)–N	1350
	N(a)+K	(3×3)–K,N	1350
	NH_3	Disordered	176,687
		(3×3)–N	176,687
		(5×5)	687
		$(\sqrt{19}\times\sqrt{19})$R23.4°–N	176
		$(\sqrt{21}\times\sqrt{21})$R10.9°–N	176,687
	O_2	(6×6)–O	175
		(5×5)–O	175
		(4×4)–O	175
		$(2\sqrt{7}\times 2\sqrt{7})$R19.1°–O	175
		$(2\sqrt{3}\times 2\sqrt{3})$R30°–O	175
	S	(1×1)–S	1577,1655
Fe–18% Cr–12% Ni(111)	[clean]	(1×1)	1249
	I_2	$(\sqrt{3}\times\sqrt{3})$R30°–I	1249
	H_2O	Ordered	1249
	O_2	Ordered	1249
	I(a)+H_2O	Oxide Not Formed	1249
	H_2O(a)+I_2	Adsorbed	1249
α–Fe_2O_3(001)	[clean]	(2×2)	1118
		Incommensurate	1118
		$(\sqrt{3}\times\sqrt{3})$R30°	1118
FeTi(111)	[clean]	(1×1)	1241
GaAs(111)	[clean]	c(8×2)	1170
	Laser-annealed	(1×1)	1170
		*(2×2)	1090,1702*
GaAs($\overline{111}$)	[clean]	(1×1)	1090
GaAs($\overline{111}$)	$Fe(CO)_5$	Facet{100}	1377

TABLE III. Surface Structures on Substrates with Three-fold Rotational Symmetry (Continued)

Substrate	Adsorbate	Surface Structure	Reference
GaAs($\overline{111}$)–As rich	[clean]	(2×2)	1524,1541
	H_2	(1×1)	1541
GaAs($\overline{111}$)–Ga rich	[clean]	($\sqrt{19}\times\sqrt{19}$)R23.4°	1541
		(1×1)	1541
GaP(111)	[clean]	*(2×2)	819,1703*
Ge(111)	[clean]	(2×8)	804,996,1046,1075
		(2×1)	1046,1075,1086 1296,1374,1683
		(1×1)	1075,1296,1374
		c(2×8)	1550
	laser process	(1×1)	1492
	Al	(2×1)	1550
	Au	($\sqrt{3}\times\sqrt{3}$)R30°–Au	1223
	Cl_2 or Cl	(7×7)–Cl	1088
		!(1×1)–Cl	1704!
	H_2O	(1×1)–H_2O	121,179,1662
	H_2S	(2×2)–S	37
		(2×1)–S	178
	H_2Se	(2×2)–Se	37
	I_2 or I	(1×1)–I	19,1088
	In	(n×2$\sqrt{3}$)–In,n=10–13	802
		(4$\sqrt{3}$×4$\sqrt{3}$)R30°–In	802
		($\sqrt{31}\times\sqrt{31}$)R(±9°)–In	802
		($\sqrt{61}\times\sqrt{61}$)R(30±4°)–In	802
		(4.3×4.3)–In	802
		(4×4)–In	802
	O_2	Disordered	17,18
		(1×1)	19,21
	P	(1×1)–P	19
	Pb	($\sqrt{3}\times\sqrt{3}$)R30°–Pb	1075,1400,1474
		(1×1)–Pb	1075,1474
	S	($\sqrt{3}\times\sqrt{3}$)R30°	1589
		(3×3)	1589
		(2×8)–Ge_2S	1589
	Si	(1×1) with streaks	1029
	Sn	(2×8)–Sn	639
		($\sqrt{3}\times\sqrt{3}$)R30°–Sn	639,1049
		(7×7)–Sn	639,1049
		(5×5)–Sn	639,1049
		(3×2$\sqrt{3}$)–Sn	996
		($\sqrt{91}\times\sqrt{3}$)–Sn	996
		(1×1)–Sn	996
	Te	(2×2)–Te	1088
InSb(111)	[clean]	!(2×2)	849,852,1906!
	a–Sn	a–Sn(111) (1×1) [Multi Layer]	849
InSb($\overline{111}$)	[clean]	(3×3)	849,852
	a–Sn	a–Sn(111) (1×1) [Multi Layer]	849

TABLE III. Surface Structures on Substrates with Three-fold Rotational Symmetry (Continued)

Substrate	Adsorbate	Surface Structure	Reference
Ir(111)	[clean]	*(1×1)	1705*
	Au	(1×1)	453
	CO	($\sqrt{3}\times\sqrt{3}$)R30°–CO	124,180,182,183 185,186
		($2\sqrt{3}\times2\sqrt{3}$)R30°–CO	180,182,183,185 186
	Cr	Hexagonal	453
	H_2	Adsorbed	187
	H_2O	Not Adsorbed	182
	H_2S	*($\sqrt{3}\times\sqrt{3}$)R30°–S	822*
	NO	(2×2)–NO	188
	O_2	*(2×2)–O or (2×1)–O	124,180,181,182 183,184,827*
		Ir oxide	181
LaB_6(111)	[clean]	(1×1)	775,1328
	O_2	(1×1)	1328
Mg(0001)	[clean]	(1×1)	1289
	O_2	(1×1)R30°–MgO(111)	655
		($\sqrt{7}\times\sqrt{7}/2$)R19°	655
		Disordered	1289
		(1×1)	797,1289
		MgO(111)	1671
Mo(111)	[clean]	(1×1)	1203
	H_2S	c(4×2)–H_2S	191
		MoS_2(0001)	191
	KCl	disordered	781
	N_2+NH_3	Disordered	1203
	N_2+NH_3	(433)facet	1203
		c(3×2)–N/Mo(433)	1203
	O_2	(211) facets	14,189
		(110) facets	189
		(4×2)–O	190
		(4×4)	898
		(1×3)	898
		(112)–(1×2) Facets	898
		(112)–(1×3) Facets	898
		MoO_2(100)	898
MoS_2(0001)	[clean]	*(1×1)	1706*
	Cs	Amorphous Layer	686,855
MoSe(0001)	[clean]	(1×1)	1035
	H_2O	Not Adsorbed	1035
	$HClO_4$	Not Adsorbed	1035
	I_2	Slightly Adsorbed	1035
	NaI_3	Slightly Adsorbed	1035
Na(0001)	[clean]	*(1×1)	1731*
Na_2O(111)	[clean]	*(1×1)	1755*

TABLE III. Surface Structures on Substrates with Three-fold Rotational Symmetry (Continued)

Substrate	Adsorbate	Surface Structure	Reference
Nb(111)	O_2	(2×2)–O	192
		(1×1)–O	192
$NbSe_2(0001)$	[clean]	*(1×1)	1706*
Ni(111)	[clean]	*!(1×1)	1707*,1794!
	Ag	(6×6)	465,466
	Au	(6×6)	467,468,469,470
		(13×13)	467,468,469
	Bi	$(\sqrt{3}\times\sqrt{3})R30°$–Bi	864
		(7×7)–Bi	864
		$(\sqrt{7}/4\times\sqrt{7}/4)R19°$–Bi	864
	Cl_2	$(\sqrt{3}\times\sqrt{3})R30°$–Cl	206
		$\begin{bmatrix}2 & 1\\ 4 & 7\end{bmatrix}$–Cl	206
	CO	!$(\sqrt{3}\times\sqrt{3})R30°$–CO	195,196,199,200,1314 1795!
		Hexagonal Overlayer	200
		(2×2)–CO	3
		$(\sqrt{3}\times\sqrt{3})R30°$–O	5
		$(2\times\sqrt{3})$–CO	5
		$(\sqrt{39}\times\sqrt{39})$–C	5,27
		!(1×1)–C (graphite)	1907
		Disordered	198,1402
		$(\sqrt{7}\times\sqrt{7})R19.1°$	195,196
		$(\sqrt{7}/2\times\sqrt{7}/2)R19°$–CO	957,1402
		c(4×2)–CO	195,196,957,1402
		c(2×2)–CO	1314
		Complex Pattern	1402
	CO_2	(2×2)–CO_2	5
		$(\sqrt{3}\times\sqrt{3})R30°$–O	5
		$(2\times\sqrt{3})$–CO_2	5
		$(\sqrt{39}\times\sqrt{39})$–C	5,27
	GeH_4	$(\sqrt{3}\times2\sqrt{3})R30°$	907
		$(\sqrt{3}\times\sqrt{3})R30°$–Ge	907
		(1×1)–Ge	907
	H_2	(1×1)–H	3
		(2×2)–(2)H	29,201,202,204 823*,1585,1666
		(2×1)	1667
		Disordered	203
	H_2S or S_2	*(2×2)–S	36,118,197,198 205*,294,577,990 992,1264,1493
		$(\sqrt{3}\times\sqrt{3})R30°$–S	36,118,577,1264
		(5×5)–S	36
		Adsorbed	36
		$(5\sqrt{3}\times2)$	606,992
		$(8\sqrt{3}\times2)$–S	607,608,609
		Complex	1493

TABLE III. Surface Structures on Substrates with Three-fold Rotational Symmetry (Continued)

Substrate	Adsorbate	Surface Structure	Reference
	H_2Se	!(2×2)–Se	137,577,1708!
		(4×4)–Se	577
		$(\sqrt{3}\times\sqrt{3})$R30°–Se	137,577
	H_2O	$(\sqrt{3}\times\sqrt{3})$R30°	1308
	Mo	(5×5)	447,448
		(4×4)	447,448
		$\begin{bmatrix} 2 & 0 \\ 5 & 10 \end{bmatrix}$	447,448
	. . .	$\begin{bmatrix} 1 & 0 \\ 5 & 10 \end{bmatrix}$	447,448
	N_2	Not Adsorbed	131
	Na	Hexagonal	455,458,460
	NH_3	(2×2)–NH	778
		(6×2)–N	778
		$(\sqrt{7}\times\sqrt{7})$R19°	811,818
		Disordered	811
		$(\sqrt{7}/2\times\sqrt{7}/2)$R19°	1282
	$Ni(CO)_4$,CO	$(\sqrt{7}/2\times\sqrt{7}/2)$R19°–CO	1150
		c(4×2)–CO	1150
	NO	c(4×2)–NO	193
		Hexagonal Overlayer	193
		(2×2)–O	193
		(6×2)–N	193
		(1×1)–NO	676
		c(4×2)–NO	676
		Complex	676
		(2×2)–O	676
		$\begin{bmatrix} 2 & 1 \\ 4 & 7 \end{bmatrix}$–Cl	206
	O_2	*(2×2)–O	2,3,4,116,193,194 195,196,197*,198 577,883,990,1282 1308,1346,1351 1652
		!$(\sqrt{3}\times\sqrt{3})$R30°–O	2,5,195,577,1346 1351,1652,1796!
		$(\sqrt{3}\times\sqrt{21})$–O	116
		NiO(111)	4,6,116,193,194
		NiO	1351
	O(a)+H_2O	No New Features	1308
	O(a)+NO	(2×2)	676
	Pb	$\begin{bmatrix} 1 & 1 \\ -1 & 2 \end{bmatrix}$	471,472
		(7×7)	471,864
		(13×13)	471,472

TABLE III. Surface Structures on Substrates with Three-fold Rotational Symmetry (Continued)

Substrate	Adsorbate	Surface Structure	Reference
		(3×3)	471,864,1060
		(4×4)–Pb	864,1060
		Hexagonal Rotated±3°	472
		($\sqrt{3}\times\sqrt{3}$)R30°–Pb	864,1060
	PF_3	(2×2)	833
	SiH_4	(2×2)	907
		($\sqrt{3}\times\sqrt{3}$)R30°–Si	907
		(2×2)–Si	907
	Sn	(2×2)–Sn	1060
		($\sqrt{3}\times\sqrt{3}$)R30°–Sn	1060
	Te	($2\sqrt{3}\times2\sqrt{3}$)R30°–Te	577
		($\sqrt{3}\times\sqrt{3}$)R30°–Te	577
Ni–17% Cu(111)	[clean]	(1×1)	868
	H_2	(2×2)–H	868
Ni–25% Fe(111)	H_2S,H_2	(3×3)–S	1121
NiI_2(0001)	[clean]	!(1×1)	1908!
NiO(111)	Si	($\sqrt{3}\times\sqrt{3}$)R30°–Si	1185
$NiSi_2$(111)	[clean]	*(1×1)	1770*
Os(0001)	CO	($\sqrt{3}\times\sqrt{3}$)R30°–CO	1169
		($2\sqrt{3}\times2\sqrt{3}$)R30°–CO	1169
		($3\sqrt{3}\times3\sqrt{3}$)R30°–CO	1169
Pd(111)	[clean]	*!(1×1)	1208,1509,1709! 1710*,1861*
	Au	!(1×1)–Au	1709!,1807
	Br_2	($\sqrt{3}\times\sqrt{3}$)R30°–Br	1103,1208,1327
		Ring pattern	1327
	C	Ring pattern	762
	Cl_2	($\sqrt{3}\times\sqrt{3}$)R30°–Cl	785
		(3×3)–Cl	785
	CO	*($\sqrt{3}\times\sqrt{3}$)R30°–CO	209,210,691,1042,1861*
		Hexagonal Overlayer	209
		c(4×2)–CO	210
		c(4×2)	691
		Disordered	1208
		(1×1)	1509
	CO_2	Not Adsorbed	691
	Fe	(1×1)	1546
	H_2	(1×1)–H	211,212
	H_2S	*($\sqrt{3}\times\sqrt{3}$)R30°–S	1710*
	NO	c(4×2)–NO	208
		(2×2)–NO	208
	O_2	(2×2)–O	207,691,1670
		($\sqrt{3}\times\sqrt{3}$)R30°–O	207
		(2×2)–PdO	207
		(1×1)	1509,1670
	O_2+CO	($\sqrt{3}\times\sqrt{3}$)R30°	691
		(2×1)	691
	PF_3	(2×2)	833

TABLE III. Surface Structures on Substrates with Three-fold Rotational Symmetry (Continued)

Substrate	Adsorbate	Surface Structure	Reference
Pd–33% Ag(111)	[clean]	(1×1)	877
	CO	(1×1)	877
Pd–25% Cu(111)	[clean]	(1×1)	877
	CO	(1×1)	877
$Pd_2Si(0001)$	[clean]	(3×3)	1555
		(1×1)	1555
Pt(111)	[clean]	*!(1×1)	1226,1556,1614*,1711*,1712* 1799*,1874!
	Ag	Disorderd	1254
	Au	Disorderd	1254
	Br_2	(3×3)–Br	724
	Cu	(12×12)–Cu	1054
		(2×2)–Cu	1054
	C_2N_2	Disorderd	1002
	Cl_2+Br_2	c(2×4)–Cl,Br	610
		$(\sqrt{3}\times\sqrt{3})R30°$–Cl,Br	610
		(3×3)–Cl,Br	610
		$(\sqrt{7}\times\sqrt{7})R19.1°$	610
	CO	$(\sqrt{3}\times\sqrt{3})R30°$–CO	218,696,1205,1452
		*c(4×2)–2CO	28,107,120,218 219,696,981,1196 1205,1232,1237 1452,1711*
		Hexagonal Overlayer	218
		(2×2)–CO	120
		$(\sqrt{2/3}\times\sqrt{2/3})R15°$–CO	1232
		Ordered	1232
	$CO+O_2$	$(\sqrt{3}\times\sqrt{3})R30°$(Misfit)	909
	Cu	(1×1)–Cu	842
		Cu(111) Multilayers	842
		Alloy Formation	842
	F	Streak Pattern	1694
	H_2	Not Adsorbed	120
		Adsorbed	220,221
		(1×1)–H	1110
	$H_2+C_2N_2$	Disorderd	1002
	H_2+O_2	$(\sqrt{3}\times\sqrt{3})R30°$	11
	H_2O	$(\sqrt{3}\times\sqrt{3})R30°$–$H_2O$	223,224,929
		$H_2O(111)$	224
		Not Adsorbed	580
	H_2S or S_2	(2×2)–S	225,226,227,247,933,1114,1248
		*$(\sqrt{3}\times\sqrt{3})R30°$–S	225,226,227,247,874,933,1114,1712*,1248
		Complex Structure	1114
		$\begin{bmatrix} 4 & -1 \\ -1 & 2 \end{bmatrix}$–S	225,226
		Hexagonal	227
	HBr	c(3×3)–3Br,HBr	806,1258
		(3×3)	806

TABLE III. Surface Structures on Substrates with Three-fold Rotational Symmetry (Continued)

Substrate	Adsorbate	Surface Structure	Reference
	HCl	Disordered	806
	HI	$(\sqrt{3}\times\sqrt{3})R30°$–I	774
		$(\sqrt{7}\times\sqrt{7})R19.1°$–I	580,774
	I_2	$(\sqrt{7}\times\sqrt{7})R19.1°$–I	580,937,1106,1258 1391,1556
		$(3\sqrt{3}\times9\sqrt{3})R30°$–I	937
		$(\sqrt{3}\times\sqrt{3})R30°$–I	937,1258,1391
		(3×3)–I	937
	I_2(a)+HBr	HBr Not Adsorbed	1258
	I(a)+Cu	(3×3)–I,Cu	1556
		(10×10)–I,Cu	1556
	I(a)+Ag	(3×3)–Ag+I	937,1106,1391
		(5×5)–Ag+I	937
		(12×12)–Ag+I	1106
		(17×17)–Ag+I	937
		(18×18)–Ag+I	1106
		(18×18)+(10×10)–Ag+I	1106
		$(\sqrt{7}\times\sqrt{7})$+(3×3)	1391
		$(\sqrt{3}\times\sqrt{3})R30°$–Ag,I	1391
	K	$(\sqrt{3}\times\sqrt{3})R30°$–K	1071,1238,1337
		$\begin{bmatrix}1.66 & 0\\ 0 & 1.66\end{bmatrix}$–K	1337
		Ring Pattern	1337
	K+CO	Disorderd	1255
	K+O_2	(4×4)–K,O	1238,1337
		(8×2)	1337
		(10×2)	1337
		K_2O	1337
	N	Disordered	228
	NH_3	Disordered	599
		Adsorbed	626
		Not Adsorbed	580
	NO	Disordered	222
		(2×2)–NO	690,1030,1096
	NO_2	Disorderd	1227
		(2×2)–O,NO,(NO_2)	1227
	O_2	(2×2)–O	10,11,213,214,215 216,217,581,952 1221,1237,1248 1301
		(2×2)–O,(O_2)	1221
		$(\sqrt{3}\times\sqrt{3})R30°$–O	214,215,217,708
		(1×1)–O	708,1171
		Not Adsorbed	120
		$(4\sqrt{3}\times4\sqrt{3})R30°$–O	214,215
		PtO_2(0001)	214,215
		(3×15)–O	217
		disordered	581
		(3/2×3/2)R15°–O_2	1221

TABLE III. Surface Structures on Substrates with Three-fold Rotational Symmetry (Continued)

Substrate	Adsorbate	Surface Structure	Reference
	SO_2	Disorderd	1179
	$S+O_2$	(2×2)–O	1040
	O_2	Not Adsorbed	1248
	Xe	($\sqrt{3}\times\sqrt{3}$)R30°–Xe	846
		Hexagonal	846
PtNi(111)	[clean]	*(1×1)	1909
Pt–22% Ni(111)	[clean]	(1×1)	1162
Pt–50% Ni(111)	[clean]	(1×1)	1162
Pt_3Ti(111)	[clean]	(2×2)	935
Re(0001)	Ba	(2×2)	565,566
		Hexagonal	565,566
	CO	Not Adsorbed	24
		(2×2)–CO	23
		Disordered	230,1132
		($\sqrt{3}$×4)	1176
		(2×$\sqrt{3}$)	230
	H_2	Not Adsorbed	24
		Disordered	664
	H_2O	($\sqrt{3}\times\sqrt{3}$)R30°–H_2O	1003
		(2×2)–H_2O	1003
	N_2	Not Adsorbed	24
	O_2	(2×2)–O	23,24,229,723
		Ordered	1515
		(2×1)–O	972,1654
Re(0001) on Pt(111)	CO	($\sqrt{3}$×4)rect	843
		(2×2)	843
	O_2	(2×1)–O	843
Rh(111)	[clean]	*(1×1)	1648,1713*,1800*
	C	($2\sqrt{3}\times2\sqrt{3}$)R30°–C	1012
	C_2N_2	Adsorbed	926
	Cl_2	($\sqrt{3}\times\sqrt{3}$)R30°–Cl	654
		(4×4)–Cl	654
	CO	*($\sqrt{3}\times\sqrt{3}$)R30°–CO	231,652*,727,931
		*(2×2)–3CO	12,231,727,931 1122*
		($\sqrt{3}$×7)rect	1844
	CO+Na	c(4×2)–CO+Na	1844
	CO+NO	Disordered	1876
	CO_2	($\sqrt{3}\times\sqrt{3}$)R30°–CO	231
		(2×2)–CO	231
	H_2	Adsorbed	231
	H_2+CO	(2×2)	829
		($\sqrt{3}\times\sqrt{3}$)R30°	829
		(2×2)	829
	H_2O	($\sqrt{3}\times\sqrt{3}$)R30°–H_2O	583
	H_2S or S_2	c(2×4)–S	875
		*($\sqrt{3}\times\sqrt{3}$)R30°–S	1768*
	NO	c(4×2)–NO	231
		(2×2)–NO	231

TABLE III. Surface Structures on Substrates with Three-fold Rotational Symmetry (Continued)

Substrate	Adsorbate	Surface Structure	Reference
	O_2	(2×2)–O	12,231
		Disordered	570,583
		(2×2)	570
		(2×1)–O	1692
		(8×8)–Rh_2O_3(0001)	1692
Ru(0001)	[clean]	*(1×1)	914,1127*,1233,1380
	C_2N_2	c(2×2)–CN	1217
		(3×3)–CN	1217
		c(4×8)–CN	1217
		(1×2)	1217
		(1×3)	1217
		(1×1)	1217
		Graphite	1217
	CO	*($\sqrt{3}$×$\sqrt{3}$)R30°–CO	12,233,248,716 825,914,1127* 1357
		(2×2)–CO	12,248
		(2$\sqrt{3}$×2$\sqrt{3}$)R30°–CO	716,825
		(5$\sqrt{3}$×5$\sqrt{3}$)R30°–CO	825
	CO+O_2	(2×2)	768
	CO_2	($\sqrt{3}$×$\sqrt{3}$)R30°–CO_2	12
		(2×2)–CO_2	12
	Cu	Disordered	1679
	H_2	(1×1)–H	234,870
	H_2O	($\sqrt{3}$×$\sqrt{3}$)R30° + halo	1233,1380
		($\sqrt{3}$×$\sqrt{3}$)R30°	835,1380
		($\sqrt{3}$×$\sqrt{3}$)R30°–H_2O	1082
		Hexagon	1233,1380
		(2×2)–O_2	1233
		Complex	1233
	H_2S	(2×2)	740
		($\sqrt{3}$×$\sqrt{3}$)R30°	740
		c(4×2)	740
	Na	(3/2×3/2)–Na	1129,1406
		Ring Pattern	1129
		(2×2)–Na	1082,1129
		($\sqrt{3}$×$\sqrt{3}$)R30°–Na	1082,1129,1406
		Hexagonal Overlayer	1406
	Na+CO	(2$\sqrt{3}$×2$\sqrt{3}$)R30°	976
	Na+H_2O	(2$\sqrt{3}$×2$\sqrt{3}$)R30°	1082
		Complex	1082
	N_2	Adsorbed	234
		($\sqrt{3}$×$\sqrt{3}$)R30°–N_2	1455
	N_2O	(2×2)	832
	NH_3	(2×2)–NH_3	234,235,1045
		($\sqrt{3}$×$\sqrt{3}$)R30°–NH_3	235
		(2$\sqrt{3}$×2$\sqrt{3}$)R30°–NH_3	1045
	NO	(2×2)–NO	598
		(2$\sqrt{3}$×2$\sqrt{3}$)R30°–NH_3	1045
		(2×1)–NO	963

TABLE III. Surface Structures on Substrates with Three-fold Rotational Symmetry (Continued)

Substrate	Adsorbate	Surface Structure	Reference
	O_2	(2×2)–O	12,232,248,832
			1233
		(2×1)–O	963,1233
		(1×2)–O	619,631
	O(a)+NO	Disordered	963
Sb(0001)	Fe	(1×1)	567
	Th	$\begin{pmatrix} 1 & 1 \\ 1 & -1 \end{pmatrix}$	510,511
Sc(0001)	[clean]	*(1×1)	1333*
Si(111)	[clean]	*!(2×1)	847,856,947,954
			956,1019,1028
			1086,1087,1361
			1374,1412*,1427,1428
			1457,1477,1528,1533
			1542,1543,1563
			1646*,1714!
		(7×7)	851,857,921,934,954
			996,1019,1021,1022
			1056,1073
			1158,1170,1206,1207
			1210,1342,1457
			1475,1477,1483,1486
			1499,1507,1517
			1525,1529,1533
			1536,1537,1543
			1685
		(1×1)	568,954,1366,1427
			1457,1492,1543
			1544
		$(\sqrt{19}\times\sqrt{19})$	1653
	Laser-annealed	*(1×1)	1170,1492,1517,1716*
		(1×1)+Steps	1446
	Ag	(6×1)–Ag	795,807,948,1158
			1342,1696
		$(\sqrt{7}\times\sqrt{7})$R19.1°–Ag	1696
		*!$(\sqrt{3}\times\sqrt{3})$R30°–Ag	807,923,1037,1073
			1108,1158,1206
			1322,1342*,1536
			1650,1696,1910!,1911!
		*(3×1)–Ag	807,948,1037,1158
			1342*,1536,1696
		$\sqrt{3}$(3×1)	1536
		(1×1)–Ag	1022,1206
		!Ag Island	1911!
	Ag(a)+H	$(\sqrt{3}\times\sqrt{3})$R30°	1536
	Al	$(\sqrt{7}\times\sqrt{7})$R19.1°–Al	816
		(1×1)	1563
		$(\sqrt{3}\times\sqrt{3})$R30°	816,1563

TABLE III. Surface Structures on Substrates with Three-fold Rotational Symmetry (Continued)

Substrate	Adsorbate	Surface Structure	Reference
	Au	(5×1)–Au	792,1091,1628 1669
		$(\sqrt{3}\times\sqrt{3})$R30°–Au	792,1091,1215 1322,1499,1628 1669
		(6×6)–Au	792,1091,1215
		(1×1)–Au	956,1091
	Bi	$(\sqrt{3}\times\sqrt{3})$R30°–Bi	736
		Bi(0001)–(1×1)	736
	Br	!Not Specified	1858!,1859!
	Cl	(7×7)	1088
		$(\sqrt{19}\times\sqrt{19})$–Cl	1088,1385
	Cl_2	Disordered	138
		!(7×7)–Cl	138,236,1715!
		!(1×1)–Cl	138,236,1715!
	Co	(1×1)	851
		(1×1)–$CoSi_2$	851,1414
		$(\sqrt{7}\times\sqrt{7})$–2d Silicide	851
		(2×2) or (2×1)–2d Silicide	851
	Cr	(1×1)	1500
		$(\sqrt{3}\times\sqrt{3})$R30°	1500
		(7×7)	1500
	Cu	(1×1)–Cu	841
		Cu(111) or Cu-Si(111) [Multi Layers]	841
		5×5–Cu	841,857,858
		(4×1)	856
		(4×2) [Multi Layer]	856
		Cu(111)–$\sqrt{3}\times\sqrt{3}$ [Multi Layer]	856
		Cu(111)–(1×1) [Multi Layer]	856
	Cu(a)+O_2	5×5	856
	D_2	(7×7)	1369
	Ga	$(\sqrt{3}\times\sqrt{3})$R30°–Ga	1028
		(1×1)–Ga	1028
		(7×7)–Ge	1029,1537
		(1×1)–Ge	1029,1486,1544
		(5×5)	1475,1483,1486
		(5×5)–Ge	1029
		(5×5)–SiGe(111)	934,1010
		Ordered	1507
		$(\sqrt{3}\times\sqrt{3})$R30°	1544
	H_2	(1×1)–H	237,1216,1477
		(7×7)–H	237,904,1610
		(2×1)	1477
	H_2O	(1×1)	1477
		Adsorbed	903
	I	*(7×7)–I	1088*
	I_2	(1×1)–I	133
		!(7×7)–I	1857!
	In	$(\sqrt{3}\times\sqrt{3})$R30°–In	1028
		(2×2)–In	1028
		Complicated	1028

TABLE III. Surface Structures on Substrates with Three-fold Rotational Symmetry (Continued)

Substrate	Adsorbate	Surface Structure	Reference
	Kr	(7×7)	1125
	N_2	(8×8)–N	34,586,1229
		Doublet	586
		Diffuse	586
		Si(1×1)	1229
		Quadruplet	1229
	N	(1×1)	798
	NH_3	(8×8)–N	238
		(7×7)+quadruplet	1479
		(7×7)+(8×8)	1479
	Ni	!(1×1)–$NiSi_2$	838,1434,1659,1860!
		(1×1)–Ni	850,1366,1434
		Disordered	964
		(1×1)–Ni w.streaks	964
		($\sqrt{3}$×$\sqrt{3}$)R30°	964,969
		($\sqrt{19}$×$\sqrt{19}$)R±23.5°–Ni	964,1366
		Si(111)–(7×7)	964
	NO	Disorderd	1021
		(8×8)–N	1021
		Complex	1021
	O_2	Disordered	17,20,21
		(1×1)	847
	P	(6$\sqrt{3}$×6$\sqrt{3}$)–P	132,133
		(1×1)–P	132
		(2$\sqrt{3}$×2$\sqrt{3}$)–P	132
		(4×4)–P	133
	Pd	Disordered	964,1207
		(5×1)	964
		($\sqrt{3}$×$\sqrt{3}$)R30°-Pd	964,1456,1484 1487,1496
		(3×1)–Pd	1456
		(1×1)+Streaks	964,1456
		(2$\sqrt{3}$×2$\sqrt{3}$)R30°–Pd	964,1456
		Pd_2Si (Epitaxial)	1134
	PH_3	(7×7)–P	239
		(1×1)–P	239
		(6$\sqrt{3}$×6$\sqrt{3}$)–P	239
		(2$\sqrt{3}$×2$\sqrt{3}$)–P	239
	Si	(1×1)	1517
	Si+laser	(1×1)	1392
	Sb	(1×1)–Sb	1019
	Sn	(1×1)–Sn	996
		($\sqrt{3}$×$\sqrt{3}$)R30°–Sn	996
		(2$\sqrt{3}$×2$\sqrt{3}$)R30°–Sn	996
		($\sqrt{133}$×4$\sqrt{3}$)–Sn	996
		(3$\sqrt{7}$×3$\sqrt{7}$)R(30±10.9)°–Sn	996
		(2$\sqrt{91}$×2$\sqrt{91}$)R(30±3.0)°–Sn	996
	Te	!(7×7)–Te	1088,1857!
		(1×1)–Te	1617
	Yb	(2×1)–Yb	844,1525
		(3×1)–Yb	844,1525

TABLE III. Surface Structures on Substrates with Three-fold Rotational Symmetry (Continued)

Substrate	Adsorbate	Surface Structure	Reference
		(2×1)+(7×7)	844
		(5×1)–Yb	1525
	Xe	(7×7)	1125
Ti(0001)	[clean]	*(1×1)	1007,1717*
	Cd	*(1×1)	562*,563,564
	CO	(1×1)–CO	18,240
		(2×2)–CO	240
		$(\sqrt{3}\times\sqrt{3})R30°$–N	241,242
	Cu	Extra Spots	561
	N_2	*(1×1)–N	241,242*
		$(\sqrt{3}\times\sqrt{3})R30°$–N	241,242
	O_2	(1×1)–O	18
TiC(111)	[clean]	(1×1)	1631
Th(111)	CO	Disordered	243
		$ThO_2(111)$	243
	O_2	Disordered	243
		$ThO_2(111)$	243
$UO_2(111)$	O_2	(3×3)–O	13
		$(2\sqrt{3}\times2\sqrt{3})R30°$–O	13
W(111)	Cl_2	Facet Surface	796
	CO	Disordered	746
		{211} facets	746
	O_2	Disordered	244,746
		{211} facets	15,746
		(4×4)–O	746
Y(0001)	[clean]	(1×1)	1120
Xe(111)	[clean]	*(1×1)	1912*
Zn(0001)	[clean]	*(1×1)	1267,1870*
	Cu	(1×1)	449,450
	O_2	(1×1)–O	122
		ZnO(0001)	245
	SO_2	No LEED Pattern	1569
		Oxide	1569
$Zn(000\bar{1})$	O_2	$(\sqrt{3}\times\sqrt{3})R30°$–O	122
ZnO(0001)	[clean]	*(1×1)	1104,1239,1773*
	H_2O	Disordered	1104
$ZnO(000\bar{1})$	[clean]	(1×1)	1104
	H_2O	Disordered	1104
	K	$(2\sqrt{3}\times2\sqrt{3})R30°$–K	1629
	Xe	Disordered	1026
ZnSe(111)	[clean]	(2×2)	1393
		(1×1)+{110}facet+(2×2)	1393
$ZnSe(\overline{111})$	[clean]	(1×1)	1393
		(1×1)+{331}f+{110}f,{110}f	1393
ZnTe(111)	[clean]	(2×2)	1393
		(1×1)	1393
$ZnTe(\overline{111})$	[clean]	(1×1)+{331}f+{110}f	1393
Zr(0001)	[clean]	*(1×1)	1473,1642*
	O_2	*(2×2)–O	1718*

†Organic overlayer structures are not included. See Table VII for these structures.

TABLE IV. Surface Structures on Substrates with Four-fold Rotational Symmetry[†]

Substrate	Adsorbate	Surface Structure	Reference
Ag(100)	[clean]	*(1×1)	1272,1562,1897*,1898*,1899*
	Au	(1×1)	1806
	Cl_2	!c(2×2)–Cl	572,605,732,962
			1719!
	Cl_2+K	c(2×2)–K/Cl	673
	Cu	Epitaxial	1167
		Cu(100)	1476
		(1×1)	1820
	Fe	(1×1)	1272
	H_2O	Disordered	1034
	H_2S	(2×2)–S	627
		$\begin{bmatrix} 4 & -1 \\ 1 & 4 \end{bmatrix}$–S	627
		$\begin{bmatrix} 4 & 4 \\ -4 & 4 \end{bmatrix}$–S	627
		Partially Disordered	1117
	I_2	c(2×2)–I	1145
	K+O_2	$\begin{bmatrix} 1 & 1 \\ -5 & 4 \end{bmatrix}$	658
		Hexagonal Overlayer	658
	Ni	(1×1)	1820
	O_2	Disordered	146
	O(ad.)+H_2O	c(2×2)–OH	1034
	Pd	Epitaxial	1167
		(1×1)	1463
	Se	*c(2×2)–Se	250*
Al(100)	[clean]	*!(1×1)	1077!,1354,1532
			1720*,1721*
	Ag	(5×1)–Ag	1363
		(1×1) [Multilayer]	1363
	Au	Disordered	1363
	CO	Not Adsorbed	1273
		Disordered	1368
	Cu	Disordered	1363
	Fe	Poor Epitaxy	452
	H_2	(1×1)	1693
	Na	*c(2×2)	499*,500,501,1720*
		Hexagonal Overlayer	500
	O_2	Disordered	42,43,44,709

TABLE IV. Surface Structures on Substrates with Four-fold Rotational Symmetry (Continued)

Substrate	Adsorbate	Surface Structure	Reference
	Pb	$\begin{bmatrix} 2 & 0 \\ -1 & 2 \end{bmatrix}$	503
		c(2×2)–Pb	704
		$\begin{bmatrix} 2 & 0 \\ 1 & n \end{bmatrix}$–Pb	704
		$2<n<3$	
	Sm	(1×1) Disorder	1532
		Complicated	1532
	Sn	$\begin{bmatrix} 2 & 0 \\ -1 & 3 \end{bmatrix}$	503
		c(2×6)–Sn	704
		$\begin{bmatrix} 2 & 0 \\ 1 & n \end{bmatrix}$–Sn, $2<n<3$	704
Au(100)	[clean]	(1×5)	1153
		c(26×68)	1153
		(5×20)	1170,1361
		$\begin{bmatrix} X & 0 \\ Z & Y \end{bmatrix}$	967
		$X=24\pm3, Y=43$ or $48, -5\leq Z\leq 0$	
	Laser-annealed	*(1×1)	1170,1293,1361
			1722*
	Ag	(1×1)	473,474,494,1838
	Bi	$\begin{bmatrix} 2 & 0 \\ -1 & 2 \end{bmatrix}$	498
	Br_2	(1×1)–Br	793
		c(2×2)–Br	793
		$(\sqrt{2}\times4\sqrt{2})R45°$	793
		c(4×2)	793
	CO	Disordered	252
	Cu	(1×1)	473
	Fe	(1×1)	1828–1830
	H_2S	(2×2)–S	251
		c(2×2)–S	251
		(6×6)–S	251
		c(4×4)–S	251
	Na	Hexagonal	492
		Ordered	492

TABLE IV. Surface Structures on Substrates with Four-fold Rotational Symmetry (Continued)

Substrate	Adsorbate	Surface Structure	Reference
	Pb	$\begin{bmatrix}1 & 1\\ 1 & -1\end{bmatrix}$	441–444
		$\begin{bmatrix}1 & 1\\ -3 & 4\end{bmatrix}$	441–444
		$\begin{bmatrix}1 & 1\\ -1 & 2\end{bmatrix}$	441–444
	...	$\begin{bmatrix}2 & 0\\ -1 & 3\end{bmatrix}$	441–444
		(1×1)	683
	Pd	(1×1)	473,1833
		c(2×2)	683
		c($7\sqrt{2}\times\sqrt{2}$)R45°	683
		c($3\sqrt{2}\times\sqrt{2}$)R45°	683
		c(6×2)	683
	Pt	(1×1)	438,439,440
	Xe	Disordered	252
$BaTiO_3$(100)	[clean]	(2×2)	853,1490
		(3×3)	1490
		(1×1)	853,1490
	O_2	Disordered	853
C(100),diamond	H_2S	Not Adsorbed	164
	N_2	Not Adsorbed	164
	NH_3	Not Adsorbed	164
	O_2	Disordered	16
		Not Adsorbed	164
CaO(100)	[clean]	*(1×1)	755*,1641*
Ce(100)	[clean]	$\begin{bmatrix}\frac{3}{5} & \pm\frac{1}{5}\\ \frac{1}{5} & \pm\frac{2}{5}\end{bmatrix}$	845
Co(100)	[clean]	*(1×1)	1539,1776*
	C	(2×2)–C	1539
	CO	c(2×2)–CO	253,1553
		(2×2)–C	253
	H_2S or S	(2×2)–S	1539
		*c(2×2)–S	1539,1548,1698*
	H_2S+C	(2×2)–S,C	1539
	O_2	(2×2)–O	254
		*c(2×2)–O	254,1777*
	S	*c(2×2)–S	1698*
CoO(100)	[clean]	*(1×1)	1778*

TABLE IV. Surface Structures on Substrates with Four-fold Rotational Symmetry (Continued)

Substrate	Adsorbate	Surface Structure	Reference
Cr(100)	[clean]	(1×1)	1126,1330,1606
	C,O,N	c(2×2)	1126
	Br_2	c(2×2)–Br	1051
		c(2×4)–Br	1051
		Pseudohexagonal $CrBr_2$	1051
	Cl_2	c(2×2)–Cl	1330
		(2×5)–Cl	1330
		c(2×4)–Cl	1330
	H_2S	c(2×2)–S	1245
	N	(1×1)–N	1330
		($\sqrt{2}$R45°×$\sqrt{5}$R27°)–N	1330
		c(2×2)–N	1330
	N_2	c(2×2)–N	1245
		c($\sqrt{2}$×3$\sqrt{2}$)R±45°–N	1245
		(1×1)–N	1245
	O_2	c(2×2)–O	255,634,1245
		Cr_2O_3(310)	256
		(1×1)–O	1245
		c(2×4)–O	1245
	Br_2	c(2×2)–Br	1051
		c(2×4)–Br	1051
		CrB_2	1051
Cu(100)	[clean]	*(1×1)	585,1101,1419 1723*
	Ag	$\begin{bmatrix} 2 & 0 \\ -1 & 5 \end{bmatrix}$	473,477
	Au	$\begin{bmatrix} 1 & 1 \\ 1 & -1 \end{bmatrix}$	473,478
		$\begin{bmatrix} 2 & 0 \\ -1 & 7 \end{bmatrix}$	473,478
	Bi	(2×2)	483,486
		$\begin{bmatrix} 1 & 1 \\ 1 & -1 \end{bmatrix}$	483,486
		$\begin{bmatrix} 1 & 1 \\ -4 & 5 \end{bmatrix}$	483,486
		$\begin{bmatrix} 5 & 4 \\ -4 & 5 \end{bmatrix}$	483,486
		(1×1)	703
		c(2×2)	703

TABLE IV. Surface Structures on Substrates with Four-fold Rotational Symmetry (Continued)

Substrate	Adsorbate	Surface Structure	Reference
	Cl_2	*!c(2×2)–Cl	1081,1102,1461
			1545,1724*,1869!
	Co	(1×1)–Co	983,1105,1810
			1811
	Co (Multilayer)+CO	c(2×2)–CO	983
	CO	*c(2×2)–CO	125,126,265,1005
			1353,1407,1605
			1663,1780*
		$(7\sqrt{2}\times\sqrt{2})R45°$–CO	1407
		$(\sqrt{2}\times\sqrt{2})R45°$	1626
		Hexagonal Overlayer	126,127,265
		(2×2)–C	26,125
	Cs	Disordered	865
	Cs	Hexagonal Overlayer	865
		Quasi-Hexagonal	865
	Fe	(1×1)	452,1808,1809
	H_2S	Adsorbed	35
		!(2×2)–S	35,260,262,1211
			1725!
		(2×1)–S	128
		Partially Disordered	1117
	I_2	!(2×2)–I	1779!
	K	$\begin{bmatrix} 2 & 3 \\ 0 & 5 \end{bmatrix}$	1405
		$\begin{bmatrix} 2 & 2 \\ 0 & 3 \end{bmatrix}$	1405
		Incommensurate	1405
	Mn	c(2×2)–Mn	1319
	N_2	(1×1)–N	49
		c(2×2)–N	47,132,258,261
			266
	Nb	Incommensurate	667
	Ni	(1×1)	1812
	O_2	(1×1)–O	9,45
		(2×1)–O	9,45,46
		(2×4)R45°–O	7,47,246,261
		(2×3)–O	119
		c(4×4)–O	119
		*!c(2×2)–O	171,246,257,258
			259,260,263,264
			1417,1726!,1727!
			1781*
		(2×2)	171
		$(2\times2\sqrt{2})R45°$	259,262,263,264
		Hexagonal	259
		(410) facets	259

TABLE IV. Surface Structures on Substrates with Four-fold Rotational Symmetry (Continued)

Substrate	Adsorbate	Surface Structure	Reference
		$(\sqrt{2}\times\sqrt{2})R45°$–O	641,1095,1285 1598,1633
		*$(\sqrt{2}\times2\sqrt{2})R45°$–O	1095,1781*
		$(2\sqrt{2}\times2\sqrt{2})R45°$–O	1633
		$(\sqrt{2}\times0.46nm)R45°$–O [Coincidence]	1691
	Pb	$\begin{bmatrix}2 & 2\\ -2 & 2\end{bmatrix}$	481–485
		$\begin{bmatrix}1 & 1\\ -2 & 3\end{bmatrix}$	481–485
		*c$(5\sqrt{2}\times\sqrt{2})R45°$–Pb	703,1295*
		*c(2×2)–Pb	1295*
		$(2\sqrt{2}\times2\sqrt{2})R45°$–Pb	1295
	Sn(θ>1)+Pb	Disordered	1041
	Pd	c(2×1)–Pd	726
		(1×1)–Pd	726,1649
		c(2×2)–Cu_3Pd	1649
	Sn	(2×2)	480
	Te	*!(2×2)–Te	267*,1119,1728!
	Tl	$\begin{bmatrix}2 & 2\\ 2 & -2\end{bmatrix}$	1167,1564
		$\begin{bmatrix}4 & 0\\ 2 & 7\end{bmatrix}$–Tl	1167,1336,1564
		$\begin{bmatrix}4 & 0\\ 2 & 6\end{bmatrix}$–Tl	1336,1564
		$\begin{bmatrix}6 & 6\\ 2 & -2\end{bmatrix}$	1564
		c(4×4)–Tl	1336
	Xe	Hexagonal Overlayer	159
		Disordered	741
Cu–3% Al(100)	O_2	c(2×2)–O	1632
		Disordered	1632
Cu–5.7% Al(100)	[clean]	(1×1)	813
Cu–12.5% Al(100)	[clean]	(1×1)	813
$Cu_3Au(100)$	[clean]	c(2×2)	916
Cu/Au(100)	[clean]	c(2×2)	737
Cu/Pd(100)	[clean]	Streak	737
		c(2×2)	737
CuSn(100)	[clean]	c(2×2)	1481
		$(3\sqrt{2}\times\sqrt{2})R45°$	1481
		c(3×2)+(2×2)	1481
Cu–25% Zn(100)	[clean]	(1×1)	1152
	O_2	Disordered	1152
EuO(100)	[clean]	(1×1)	1502

TABLE IV. Surface Structures on Substrates with Four-fold Rotational Symmetry (Continued)

Substrate	Adsorbate	Surface Structure	Reference
Fe(100)	[clean]	*(1×1)	989,1078,1729*
	Br_2	c(2×2)	752
		(2 sin α'×2 sin α')Rα'	752
		α'=26.57°,37.49°,40.5°	
		$\begin{bmatrix} 1 & \frac{1}{\tan\alpha} \\ -1 & \frac{1}{\tan\alpha} \end{bmatrix}$	752
		α=53.13°,53.47°,56.31°	
		(√41/5×√41/5)R38.7°	752
		c(2×4)	752
	CBr_4	c(2×2)	757
		(2 sin α'×2 sin α')Rα'	757
	CCl_4	(2 sin α' × 2 sin α')Rα'	753
		(√13×√13))R $\tan^{-1}(2/3)$	753
		(6×6)–Cl	753
		$\begin{bmatrix} 1 & \frac{1}{\tan\alpha} \\ -1 & \frac{1}{\tan\alpha} \end{bmatrix}$	753
		c(2×2)	753
	CO	*c(2×2)–CO	275*,1596
		*c(2×2)–C,O–Disordered	783,893,1601*
		Disordered	783
	Fe_3O_4	(1×1)–like	1189
	H_2	Adsorbed	177
	H_2O	c(2×2)	278
	H_2S or S	*c(2×2)–S	276,277*,1552,1630
		Complex	1552
		c(6×2)	1552
	I_2	c(2×2)–I	751
		(2sin40.5×2sin40.5)R40.5°–I	751
		(√85×√85)R40.6°–I	751
	K	Disordered	665
		(2×2)–K	784
		Hexagonal Close Pack	784
	N	c(2×2)–N	893
	NH_3	Disordered	176
		*c(2×2)–N	176,1224*

TABLE IV. Surface Structures on Substrates with Four-fold Rotational Symmetry (Continued)

Substrate	Adsorbate	Surface Structure	Reference
	O_2	c(2×2)–O	60,269,270,271 274,635,893,1596
		*(1×1)–O	144,268*,271,272 1596
		FeO(100)	60,269,270,272 273,635
		FeO(111)	270,635
		FeO(110)	272
		Disordered	273,276
	Se	c(2×2)–Se	1078
	Si	c(2×2)–Si	985,986
	Te	(2×2)–Te	1204
		c(2×2)–Te	1204
Fe/Cr(100)	O_2	c(2×2)–O	279,636
		c(4×4)–O	279
		Oxide	280
FeTi(100)	[clean]	(1×1)	1241
	S	c(2×2)–S	1241
Ge(100)	[clean]	!(2×1)	1094,1213,1522,1636 1645,1783!
		(2×2)	1449
		(4×2)	804
	Ag	(1×1)–Ag	1522
	Bi	(1×1)–Bi	1449
	I_2	(3×3)–I	19
	O_2	Disordered	17,18
		(1×1)	1094
Ir(100)	[clean]	*(1×1)	866,1199*,1293 1361,1381
		*(5×1)	866,1156*,1361 1381,1785*
	Ba	(2×1)–Ba	1399
	CO	c(2×2)–CO	48
		(2×2)–CO	48
		(1×1)–CO	282
	CO_2	c(2×2)–CO_2	48
		(2×2)–CO_2	48
		(7×20)–CO_2	48
	Cs	c(4×2)–Cs w.Streak	1395
		Close Packed Layer	1395
		Compressed Layer	1395
		(5×5)–Cs	1395
	H_2	Adsorbed	281
	K	c($2\sqrt{2}$×$4\sqrt{2}$)R45°	866
		$\begin{bmatrix} 2 & 1 \\ -1 & 2 \end{bmatrix}$	866
		c(4×2)	866
		(3×2)	866
		c(2×2)	866

TABLE IV. Surface Structures on Substrates with Four-fold Rotational Symmetry (Continued)

Substrate	Adsorbate	Surface Structure	Reference
		$\begin{bmatrix} \frac{5}{2} & 0 \\ \frac{-5}{4} & \frac{5}{3} \end{bmatrix}$	866
		$\begin{bmatrix} 2 & 0 \\ -1 & \frac{5}{3} \end{bmatrix}$	866
		$\begin{bmatrix} \frac{10}{7} & 0 \\ \frac{-5}{7} & \frac{5}{3} \end{bmatrix}$	866
	Kr	(3×5)–Kr	283
		Kr(111)	283
	NO	(1×1)–NO	188
	O_2	(2×1)–O	48,281
		(5×1)–O	48
	O_2	(1×1)–O	797
KBr(100)	[clean]	(1×1)	1592
KCl(100)	[clean]	(1×1)	1592
LaB_6(001)	[clean]	(1×1)	738,1625
	O_2	(1×1)	770
MgO(100)	[clean]	*(1×1)	755,908,918,1067*,1139,1284 1574*
	Ag	(1×1)	1559
Mo(100)	[clean]	*(1×1)	761*,1379
	Ag	Ag(100)	513,514
		Ag(110)	513,514
	CO	Disordered	62,693
		(1×1)–CO	62,64,285,286 1379
		c(2×2)–CO	64,285,286
		(4×1)–CO	64
	Cs	($\sqrt{2}$×$\sqrt{2}$)R45°	932
		(2×2)	932
		c(2×2)	932
		Rectangular Centered Mesh	932
		Quasi Hexagonal	932
		Hexagonal Overlayer	932
	Cs(a)+O_2	c(2×2)+(4×1)	932
		(4×1)	932
		Disordered	932

TABLE IV. Surface Structures on Substrates with Four-fold Rotational Symmetry (Continued)

Substrate	Adsorbate	Surface Structure	Reference
	O(a)+Cs	c(2×2)–Cs+O	932
		(110) Microfacets	932
		Disordered	932
	Ga	(1×1)–Ga	789
	H_2	c(4×2)–H	77
		(3×2)–H	780
		($\sqrt{2}\times\sqrt{2}$)–H	780,814
		(1×1)–H	77
	H_2S, S, or S_2	(1×1)–S	130,1149
		(1×1)–S Diffuse	1174
		($\sqrt{5}\times\sqrt{5}$)–S	130,288
		*c(2×2)–S	130,578,917,998, 1039,1149,1174,1913*
		MoS_2(100)	288
		(2×1)–S	578,612,917,998,1039,1149,1174
		($\sqrt{5}\times\sqrt{5}$)R26.6°	578,613
		c(4×4)–S	578,613,998
		c(4×2)–S	578,917,998,1039,1149 1174
		$\begin{pmatrix}1 & 1\\ 2 & -1\end{pmatrix}$–S	578,917,998,1039,1174,1149
	H_2S+O_2	($\sqrt{5}\times\sqrt{5}$)R26.6°–S,O	917
	N_2	(1×1)–N	62
		*c(2×2)–N	287*
	O_2	Disordered	61,62
		c(2×2)–O	61,62,63,64,284 660,898
		($\sqrt{5}\times\sqrt{5}$)R26°–O	61,62,189,190,284 660,898,1155,1379
		(2×2)–O	61,189,190,660 1379
		c(4×4)–O	62,189,284,660 898
		*(2×1)–O	189*,190,660,748 898
		(5×5)–O	748
		(4×1)	898
		(6×1)–O	748
		(6×2)–O	284,660,7484
		(3×1)–O	284,748
		(1×1)–O	284,660,898,1155
		c(4×4)+(2×1)–O	748
		(2×1)+c(2×2)	748
		Microfacet	660
		streak(1×1)–O	660
		diffuse(1×1)–O	660
		Facet	748
		(110),(112) Facets	898
		MoO_2(110)	898

TABLE IV. Surface Structures on Substrates with Four-fold Rotational Symmetry (Continued)

Substrate	Adsorbate	Surface Structure	Reference
	O(a)+CO	(2×1)–O	817
	O(a)+CO_2	(2×1)–O	817
	Si	*(1×1)–Si	1730*
	Sn	$\begin{bmatrix} 1 & 1 \\ 1 & -1 \end{bmatrix}$	516
		(1×2)	516
		(1×1)–Sn	789
		c(2×2)–Sn	789
NaCl(100)	Ag	Ag(111)	1678
	Xe	Hexagonal Overlayer	289
$Na_{0.47}$ WO_3(100)	[clean]	(3×1)	808
$Na_{0.72}$ WO_3(100)	[clean]	(2×1)	808
		c(2×2)	808
$Na_{0.79}$ WO_3(100)	[clean]	(2×1)	1485
Nb(100)	N_2	(5×1)–N	290
	O_2	c(2×2)–O	192,290
		(1×1)–O	192,290
		(3×10)–NbO_2	290
Ni(100)	[clean]	*!(1×1)	973,1092,1231 1458,1561,1565,1739!,1864*
	Ba	Disordered	454
	C	*(2×2)–C	640,745*,1231,1673
	C(a)+O_2	c(2×2)–O	1177
	Cl_2	(2×2)–Cl	662
		c(2×2)–Cl	662
	Co	(1×1)	1803
	CO	*!c(2×2)–CO	54,55,68,129,198 300,301,302,747* 782,950,981,993 1202,1604*,1605 1789*,1790*,1791!,1795!
		c(2×2)	1281
		(2×2)–CO	69
		c($\sqrt{2}$×3$\sqrt{2}$)R45°–CO	1202
		Hexagonal Overlayer	129,301,302
		(2×2)–C	198
		Disordered	1291
	CO+H_2	c(3×3)	301
	CO_2	(2×2)–O+c(2×2)–CO	76
	Cr	(1×1)	463,464
	Cs	(2×2)	454
		Hexagonal	463,464
	Cu	*(1×1)–Cu	1113,1458*,1804
	e beam	(2×2)	1401
	Fe	c(2×2)–Fe	973
		(2×2) (Multilayer)	973
		c(2×2) (Multilayer)	973
		Fe(110) (Multilayer)	452,973

TABLE IV. Surface Structures on Substrates with Four-fold Rotational Symmetry (Continued)

Substrate	Adsorbate	Surface Structure	Reference
	H_2	Disordered	198,203,211
		c(2×2)–H	301
		(1×1)–H	1092,1202,1658
		(1×1)–H streaked	663
	H_2+CO	c(2×2)–CO,H	1202
		c($\sqrt{2}$×2$\sqrt{2}$)R45°–CO,H	1202
	H_2S, S, or S_2	*(2×2)–S	36,118,197,198 621,622,623 637,979,1329,1508 1732*
		*!c(2×2)–S	36,118,197!,198 293,294,303,304 340,621–623 681,979,1121,1329 1482,1725!,1734!,1735!,1736!,1792* 1793!,1852!
		(2×1)–S	198
		c(2×2)–H_2S	304
		Ni_3S_2 Island	681
	H_2S,H_2	c(2×2)–S	1121
	H_2S+Na	*c(2×2)Na+c(2×2)S	1887*
		*(2×2)Na+c(2×2)S	1887*
		*(2×2)Na+(2×2)S	1887*
	H_2Se	*(2×2)–Se	197,198,1732*,1866!
		*c(2×2)–Se	142,197,198,293 294,305,340*,1733!
		(2×1)–Se	198
		c(4×2)–Se	305
	H_3P	Disordered	662
	HCl	c(2×2)–HCl	1644
		c(2×2)–Cl	1644
	I_2	c(2×2)–I	1036,1148
		NiI_2	1148
		$\begin{pmatrix} 1-\frac{1}{\tan\theta} & -1-\frac{1}{\tan\theta} \\ \frac{2}{\tan\theta} & \frac{2}{\tan\theta} \end{pmatrix},\theta\text{–}61^\circ$	1148
		$\begin{pmatrix} 5 & -3 \\ 3 & -5 \end{pmatrix}$	1148
		$\begin{pmatrix} 7 & -5 \\ 3 & \frac{3}{5} \end{pmatrix}$	1148
		(2×4)–I_2	1148
	K	(4×2)	454
		Hexagonal	457,461,462

TABLE IV. Surface Structures on Substrates with Four-fold Rotational Symmetry (Continued)

Substrate	Adsorbate	Surface Structure	Reference
	N_2	Not Adsorbed	80,81
		(2×2)–N	772,1578
		c(2×2)–N_2	984,987
	N_2H_2	(2×2)–N	690
	Na	*c(2×2)–Na	452,454–459,1737*,1865*
	NH_3	c(2×2)–N	1137
		c(2×2)–Na	
	NO	(1×1)	767,663,812
		*c(2×2)–N+O	767,812*
		c(2×2) streaked	663
		(2×2)	767,812
		Disordered	779
	O_2	*!(2×2)–O	2,49,50,51,198 296–299,310,766 978,1095,1138 1168,1195,1356 1358,1364,1417 1732*,1738!,1743!
		*!c(2×2)–O	2,6,52–57,197*,198 290–299,310,340,640 766,978,1044,1095 1138,1168,1195 1220,1356,1358 1417,1441,1565 1738!,1739!,1740!,1741!,1742!,1743!,1793!
		(2×1)–O	198
		NiO(100)	6,297,298,299,310
		NiO(1$\bar{1}$1)	298,299
		Disordered	1291
	O(a)+CO	c(2×2)–C,O	1356
	P	($\sqrt{5}$×$\sqrt{5}$)R26.7°–P	773,1644
		$\begin{bmatrix} 1 & -1 \\ 2 & 3 \end{bmatrix}$–P	773
		$\begin{bmatrix} 1 & -1 \\ 2 & 1 \end{bmatrix}$–P	773

TABLE IV. Surface Structures on Substrates with Four-fold Rotational Symmetry (Continued)

Substrate	Adsorbate	Surface Structure	Reference
	Pb	$\begin{bmatrix} 1 & 1 \\ 1 & -1 \end{bmatrix}$	471
		$\begin{bmatrix} 1 & 1 \\ -2 & 3 \end{bmatrix}$	471
		$(5\sqrt{2}\times\sqrt{2})R45°$–Pb	773
	Si	c(2×2)–Si	1644
		$(2\sqrt{2}\times\sqrt{2})R45°$–Si	1644
	Sn	c(2×2)–Sn	773
	SO_2	c(2×2)–SO_2	86
		(2×2)–SO_2	86
	S,C	(1×1)	1561
	Te	*(2×2)–Te	197,198,306,1119 1732*
		*c(2×2)–Te	197,198,294,305 340,1119,1231 1597,1744*
		(2×1)–Te	198
		c(4×2)–Te	305,306
	Xe	Partially Ordered	1268
$Ni_3Al(001)$	[clean]	*(1×1)	1868*
NiCu(100) (Ni<50%)	S	c(2×2)–S	905
Ni–24% Fe(100)	O_2	c(2×2)–O	573
Ni–25% Fe(100)	H_2S,H_2	c(2×2)–S	1121
Ni–41% Fe(100)	[clean]	(1×1)	1263
	O_2	c(2×2)–O	1263
		Oxide	1263
NiO(100)	[clean]	*(1×1)	755,894,1638*
	Cl_2	Disordered	309
	H_2	Adsorbed	307
		Ni(100)	307
		(1×1)	894
		Coincidence	894
		(2×2)	894
	H_2S	Ni(100)–c(2×2)–S	308
	S	c(2×2)–S	1185
	SO_2	Disordered	1583
Pb(100)	O_2	PbO(100)	1691
Pd(100)	[clean]	*(1×1)	1797*
	Ag	(1×1)	473,1797*
	Au	(1×1)	473,1806,1807
	C	c(4×2)–C	762
	CO	Disordered	70
		c(4×2)–CO	70
		c(2×2)–CO	210
		(2×4)R45°–CO	71,209,210
		$c(2\sqrt{2}\times\sqrt{2})R45°$–CO	1276,1294
		$*(2\sqrt{2}\times\sqrt{2})R45°$–2CO	910,1797*
		Incommensurate	1276

TABLE IV. Surface Structures on Substrates with Four-fold Rotational Symmetry (Continued)

Substrate	Adsorbate	Surface Structure	Reference
		Hexagonal Overlayer	209,210
	Cu	(1×1)	862
	Fe	Fe(100) and Fe(110)	452
	H_2	c(2×2)–H	595,919,1163,1454
		(1×1)–H	919
	H(a)+O_2	Adsorbed	1163,1454
	H_2+O_2	Disordered	1163
		(2×2)–O,H	1163
	H_2S	(2×2)–S	1294
		*c(2×2)–S	1294*
	Kr	Liquid-like	913
	Ni	(1×1)	1805
	NO	(2×2)	910
	O_2	(2×2)–O	596,597,891,939 1163,1334,1454
		c(2×2)–O	596,682,939,1334
		(2×2)+(7×7)–O	682
		(5×5)–O	596,1334
		($\sqrt{5}\times\sqrt{5}$)R27°	596,1334
		Oxide	1334
		Hexagonal	1334
		Disordered O_2	1454
	O(a)+CO	Disorderd	939
	O(a)+H_2O	(2×1)–OH	940
	O(a)+H_2	Not Adsorbed	1163,1454
		(2×2)	1454
	Xe	Hexagonal Overlayer	311
		Liquid-like	913
		Island	913
Pt(100)	[clean]	(5×20) or hex	862,946,1265,1394
		*!(1×1)	1265,1293*,1394 1745*,1798!
		(1×5)	1265,1394,1171
	Au	$\begin{bmatrix} 14 & 1 \\ -1 & 5 \end{bmatrix}$	671
		(1×1)–Au	671
		(1×5)–Au	671
		(1×7)–Au	671
	C	Ring Pattern	762
	C_2N_2	(1×1)	433
	CO	c(4×2)–CO	28,72,73,120,314 316,663,952,1307
		($3\sqrt{2}\times\sqrt{2}$)R45°–CO	28,72,73,316
		($\sqrt{2}\times\sqrt{5}$)R45°–CO	72,73

TABLE IV. Surface Structures on Substrates with Four-fold Rotational Symmetry (Continued)

Substrate	Adsorbate	Surface Structure	Reference
		(2×4)–CO	10
		(1×3)–CO	10
		(1×1)–CO	120,312,314,316 663
		c(2×2)–CO	312,316,928,1059 1252,663
		Reconstructed hex (or 5×20)	1059
	$CO+H_2$	c(2×2)–$CO+H_2$	72,74
	$CO+O_2$	(1×1) Diffuse	909
		c(2×2)–CO+(3×1)–O	928
	Cu	(1×1)	862
	F_2	(1×1)–F	886
	H_2	Adsorbed	312,317
		(2×2)–H	72,74
		Not Adsorbed	312
		(1×1)–H	582
	H_2O	Not Adsorbed	1258
	H_2O+HBr	c($2\sqrt{2}\times\sqrt{2}$)R45°–Br,HBr	1258
	H_2S or S_2	(2×2)–S	225,226,247,320
		c(2×2)–S	225,226,247,320,321
	HBr	c($2\sqrt{2}\times\sqrt{2}$)R45°–(Br+HBr)	806,1258
	Br,HBr(a)+H_2O	Not Adsorbed	1258
	Br,HBr(a)+NH_3	No Affinity	1258
	HCl	(2×2)–(Cl+HCl)	806
	HI	c($\sqrt{2}\times\sqrt{2}$)R45°–I	580
		c(2×4)–I	774
		Ring Pattern	774
		c($2\sqrt{2}\times n\sqrt{2}$)R45°, n≥7	774
		c($2\sqrt{2}\times\sqrt{2}$)R45°–I	774
	I_2	c($\sqrt{2}\times\sqrt{2}$)R45°–I	580
		Incommensurate–I	1390
		c($\sqrt{2}\times 5\sqrt{2}$)R45°–I	1390
		c($\sqrt{2}\times 2\sqrt{2}$)R45°–I	1390
		Hexagonal Overlayer	1390
		c(2×4)	1390
		($\sqrt{7}\times\sqrt{7}$)R19.1°–I	1390
	I(a)+Ag	($\sqrt{2}\times\sqrt{2}$)R45°–I,Ag	1390
		($10\sqrt{2}\times 10\sqrt{2}$)R45°–I,Ag	1390
		($\sqrt{34}\times\sqrt{34}$)R31°–I,Ag	1390
	N	Disordered	228
	NH_3	Poorly Ordered	1258
	NO	(1×1)–NO	318
		c(4×2)–NO	319
		(5×1)–NO	826
		c(2×4)–NO	826
		(1×1)+c(2×4)	946
	NO_2	(1×1)–N,NO	881
		(5×20)–NO_2	881

TABLE IV. Surface Structures on Substrates with Four-fold Rotational Symmetry (Continued)

Substrate	Adsorbate	Surface Structure	Reference
	O_2	Not Adsorbed	120,312
		Adsorbed	312,315
		$(2\sqrt{2}\times2\sqrt{2})R45°$–O	215,313
		$PtO_2(0001)$	215
		(5×1)–O	315
		(5×1)+(1×1)–O	708,1171
		$(2\sqrt{2}\times\sqrt{2})R45°$–O	708
		(2×1)–O	315
		(3×1)–O	928,1014
		Complex	1014
	SO_2	(1×1) Diffuse	1258
	$SO_2(a)+NH_3$	(1×1) Diffuse	1258
$Pt_3Ti(100)$	[clean]	c(2×2)	935
Rh(100)	[clean]	*(1×1)	895,1024,1348 1800*
		(2×2)	1147
	Ag	(1×1)–Ag	895
		Complex [Multilayer]	895
	CO	Hexagonal Overlayer	231
		(4×1)–CO	58
		c(2×2)–CO	231,1348
	$CO(a)+D_2$	Compressed (CO)	1348
	CO_2	c(2×2)–CO	231
		Hexagonal Overlayer	231
	D_2	(1×1)–D	1348
	D(a)+CO	c(2×2)	1348
	Fe	Fe(100) and Fe(110)	452
	H_2	Adsorbed	231
	H_2S or S	c(2×2)–S	1403
		*(2×2)–S	742*,1403,1473
	N_2O	(2×2)	801
	NO	c(2×2)–NO	231
		Disordered	1024
	$NO+D_2$	Disordered	1025
	O_2	(2×2)–O	231,1403
		c(2×2)–O	231
		c(2×2)	801
		c(2×8)–O	58
		(3×1)	1403
Si(100)	[clean]	*!(2×1)	848,980,1017 1019,1084!,1207 1222,1428,1451,1477 1494,1483,1505 1514,1517,1523 1535,1547,1549 1645,1746*
		(2×2)	1579
		c(4×2)	1600

TABLE IV. Surface Structures on Substrates with Four-fold Rotational Symmetry (Continued)

Substrate	Adsorbate	Surface Structure	Reference
	Ag	(2×1)	923
		Ag(111)	1352
	Au	Au(111)	Si(100)
	Ga	(3×2)–Ga	800
		(5×2)–Ga	800
		(2×2)–Ga	800
		(8×1)–Ga	800,809
	Ge	(2×1)	1483
	H	(1×1)–H	325
		(2×1)–H	325
	H_2	(1×1)–H	322,323,324
			633,680
			1494
		(1×1)–2H	848,999,1222,1477,1488,1535
		(2×1)–H	237,848,999
			1222,1477,1488,1489
			1494,1535
	H_2O	(2×1)	1477
		Adsorbed	903
	I_2	(3×3)–I	326
	In	(2×1)–In	971
		(4×3)–In	971
		(1×1)–In	971
	K	(2×1)–K	1184
	N	Not Ordered	1230
	NH_3	(111) facets	238
	Ni	$NiSi_2(100)$	854,1659
	O_2	(1×1)–O	17,18,20
	Pd	Pd_2Si (Not Epitaxial)	1134
		(2×1)	1207
		(111) facets	17,18,20
	PH_3	(2×1)	1451
	Sb	(1×1)–Sb	1019
	Si	(1×1)	1517
	Si+laser	(2×1)	1392
	Sn	c(4×4)–Sn	959
		(6×2)–S	959
		c(8×4)–Sn	959,971
		(5×1)–Sn	959,971
		(2×1)–Sn	959
		(1×1)–Sn	959
SiC(100)	[clean]	(1×1)	1450
$SmB_6(001)$	[clean]	(2×2)	738
		(3×3)	738
Sn(100)	[clean]	(2×1)	1421,1497,1513
	H_2	(2×1)	1497,1513
Sr(100)	O_2	SrO(100)	327
$SrTiO_3(100)$	O_2	(1×1)	1672
		(2×2)	1672
		(2×1)	1672

TABLE IV. Surface Structures on Substrates with Four-fold Rotational Symmetry (Continued)

Substrate	Adsorbate	Surface Structure	Reference
Ta(100)	[clean]	*(1×1)	966,1219*
	Au	Split $\begin{bmatrix} 1 & 1 \\ -1 & 2 \end{bmatrix}$	506,507
	CO	c(3×1)–O	328
	CO_2	c(3×1)–O	328
	H_2	(1×1)	1219
	I_2	Amorphous	1180
		c(2×10)	1180
		c(2×2)	1180
	N_2	Adsorbed	328
	NO	c(3×1)–O	328
	O_2	(2×8/9)–O	328
		c(3×1)–O	328
		(4×1)–O	328
		(3×3)–O	873
		(1×2)–O	873
		*(1×3)–O	873*
	Th	$\begin{bmatrix} 1 & 1 \\ 1 & -1 \end{bmatrix}$	510,511
		(1×1)	510,511
Th(100)	CO	Disordered	329
	O_2	Disordered	329
		ThO_2	329
TiC(001)	[clean]	(1×1)	1631
	O_2	Disordered	611
UO_2(100)	[clean]	c(2×2)	648
V(100)	[clean]	*(1×1)	1126,1315*,1498
	Br_2	(1×1)–Br	651
		(5×1)–Br	1126
		c(2×2)–Br	1126
		(6×4)–Br	1126
		Ring Pattern	1126
	CO	(5×1)–O	1315
	H_2	Disordered	65
	O_2	(1×1)–O	65,651
		(2×2)–O	65
		(5×1)–O	1315
	O	(5×1)	1126
	S	c(2×2)–S	650,1315
		(1×1)–S	650
		(5×1)	650
		$(\sqrt{2}\times\sqrt{5})R27°$–S	1315

TABLE IV. Surface Structures on Substrates with Four-fold Rotational Symmetry (Continued)

Substrate	Adsorbate	Surface Structure	Reference
W(100)	[clean]	*c(2×2)	749,1147,1340 1347,1388,1396 1503,1668*
		(2×2)	1340
		*(1×1)	1340,1347,1396 1471,1656,1763*,1802*
	Ag	(2×1)	546
		$\begin{bmatrix}1 & 1\\ 1 & -1\end{bmatrix}$	546
		(1×1)	546
	Au	(2×1)	546
		$\begin{bmatrix}2 & 0\\ -1 & 2\end{bmatrix}$	546
		(1×1)	546
	Ba	$\begin{bmatrix}2 & 0\\ -8 & 2\end{bmatrix}$	531,532
		split $\begin{bmatrix}1 & 1\\ -2 & 2\end{bmatrix}$	531,532
		$\begin{bmatrix}1 & 1\\ -2 & 2\end{bmatrix}$	531,532
		$\begin{bmatrix}1 & 1\\ 1 & -1\end{bmatrix}$	531,532
		c(4×2)–Ba	735
		$c(2\sqrt{2}\times\sqrt{2})$–Ba	735
		$c(\sqrt{6}\times\sqrt{2})R45°$–Ba	735
		$c(2\sqrt{2}\times 2/3\sqrt{6})R45°$–Ba	735
		(2×12)–Ba	994
		(2×10)–Ba	994
		(3×2)–Ba	994
		(3×2)+c(2×2)	994
		c(2×1.86)	994
		(10×21)–Ba	994
		c(2×2)–Ba	1399
		$c(2\times k)$ $(1.86 \leq k \leq 2\sqrt{2/3})$	994
		Hexagonal	994
	Bi	c(2×2)	1260
		(2×2)	1260
		(1×1)	1260

TABLE IV. Surface Structures on Substrates with Four-fold Rotational Symmetry (Continued)

Substrate	Adsorbate	Surface Structure	Reference
	Br_2	c(2×2)	604
		$(0.75\sqrt{2}\times\sqrt{2})R45°$	604
		c(4×2)	604
		(5×2)	604
		c(6×2)	604
		(7×2)	604
		c(8×2)	604
	C	(5×1)–C	821
	Cl_2	c(2×2)	643
		c(4×1)	644
		(1×1)	644
		$\begin{bmatrix} -7 & 1 \\ 1 & 1 \end{bmatrix}$–Cl	733
		$\begin{bmatrix} -5 & 1 \\ 1 & 1 \end{bmatrix}$–Cl	733
		$(3\sqrt{2}\times\sqrt{2})R45°$–Cl	733
	CO+N_2	(4×1)–CO+N_2	82
	CO	Disordered	75
		*c(2×2)–CO	66,75,1465*
		c(2×2)–C+O	777
	CO_2	Disordered	338
		(2×1)–O	338
		c(2×2)–CO	338
	Cs	$\begin{bmatrix} 1 & 1 \\ 1 & -1 \end{bmatrix}$	523,524,525,526
		(2×2)	523,524,525,526
		Split (2×2)	523,524
		Hexagonal	525,526
	Cu	(2×2)	543
		$\begin{bmatrix} 1 & 1 \\ 1 & -1 \end{bmatrix}$	543
	Ga	(1×1)–Ga	789
	H_2	c(2×2)–H	66,78,79,337,411 712,771,1275,1347 1361,1388,1603 1668
		$(\sqrt{2}\times\sqrt{2})$–H	834,1032,1511
		Incommensurate $(\sqrt{2}\times\sqrt{2})$–H	1032
		1 dim order	1032
		(2×5)–H	79
		(4×1)–H	79
		(1×1)–(2)H	411,771,897*,1032,1165 1347,1388,1747*
		(2×2)–H	1361

TABLE IV. Surface Structures on Substrates with Four-fold Rotational Symmetry (Continued)

Substrate	Adsorbate	Surface Structure	Reference
		Incommensurate	834,1511
		Disordered	771,834
	H_2S	(2×1)	821
		c(2×2)–S	887
	Hg	(1×1)	549
	K	$\begin{pmatrix} 1 & 1 \\ 1 & 1 \end{pmatrix}$	1841
	N_2	*c(2×2)–N	68,82,131,776 1099,1465*,1748*
		Contracted Domain	1609
	N_2O	(1×1)–N_2O	143
		(4×1)–N_2O	143
	Na	$\begin{pmatrix} 1 & 1 \\ 1 & -1 \end{pmatrix}$	1840
	NH_3	Disordered	84
		c(2×2)–NH_2	84
		c(2×2)–N	1099
		(1×1)–NH_2	84
	NO	(2×2)–NO	339
		(4×1)–NO	339
		(2×2)–O	339
		(4×1)–O	339
		(2×1)–O	339
	O_2	*Disordered	330,1749*
		(4×1)–O	66,330–333,336,821 1058
		(2×2)–O	330–334
		(2×1)–O	66,67,330–336,821,1058
		(3×3)–O	331,333,335
		c(2×2)–O	333
		c(8×2)–O	333
		(3×1)–O	333
		(1×1)–O	333
		(8×1)–O	333
		(4×4)–O	333,335
		(110) facets	333
	O_2+H_2	($\sqrt{2}$×$\sqrt{2}$)+(4×1)–O,H	815

TABLE IV. Surface Structures on Substrates with Four-fold Rotational Symmetry (Continued)

Substrate	Adsorbate	Surface Structure	Reference
	Pb	Disordered (2×2)	550
		Split $\begin{bmatrix}1 & 1\\1 & -1\end{bmatrix}$	550
		$\begin{bmatrix}1 & 1\\1 & -1\end{bmatrix}$	550,551
		$\begin{bmatrix}1 & 1\\-2 & 2\end{bmatrix}$	550
		Hexagonal	550
		(2×2)	551
		$\begin{bmatrix}2 & 0\\-1 & 2\end{bmatrix}$	551
		(1×1)	551,702
		c(4×2)–Pb	702
		c(2×2)–Pb	702
	Pd	$(2\sqrt{2}\times\sqrt{2})R45°$–Pd	646
		(2×1)–Pd	646
		c(2×2)–Pd	646
	Rb	$\begin{bmatrix}1 & 1\\1 & -1\end{bmatrix}$	522
		(2×2)	522
		Hexagonal	522
	S	(2×2)–S	1324
		(3×3)–S	1324
		(4×2)–S	1324
		(2×1)–S	1324
		(5×5)–S	1324
	Sb	(2×2)	553,554
		$\begin{bmatrix}1 & 1\\1 & -1\end{bmatrix}$	553,554
		(1×1)	553,554
	Se	(2×1)	1326
		(8×1)	1326
		(6×1)	1326
		(3×1)	1326
		c(2×2)	1326
	Sn	(1×1)–Sn	789
		c(2×2)–Sn	789

TABLE IV. Surface Structures on Substrates with Four-fold Rotational Symmetry (Continued)

Substrate	Adsorbate	Surface Structure	Reference
	Te	(3×3)–Te	1323
		(2×2)–Te	1323
		Complex	1323
		(2×1)–Te	1323
	Th	$\begin{pmatrix} 1 & 1 \\ 1 & -1 \end{pmatrix}$	556–560
		(1×1)	556–560
		$\begin{pmatrix} 2 & 0 \\ -1 & 3 \end{pmatrix}$	559,560
		Hexagonal	559,560
	Rb	$\begin{pmatrix} 1 & 1 \\ 1 & -1 \end{pmatrix}$	522
		(2×2)	522
		Hexagonal	522
	Zr	(1×1)	541,764,789
		$\begin{pmatrix} 2 & 0 \\ -1 & 2 \end{pmatrix}$	541
		c(2×2)	764,789
WO_3(100)	[clean]	split (1×1)	991
		(5×1)	1393
		$(\sqrt{2}\times\sqrt{2})R45°$,(5×1)	1393
Xe(100)	[clean]	*(1×1)	1914*

†Organic overlayer structures are not included. See Table VII for these structures.

TABLE V. Surface Structures of Metallic Monolayers on Metal Crystal Surfaces

Substrate	Adsorbate	Surface Structure	Reference
Ag(100)	Au	(1×1)	1806
	Cu	Epitaxial	1167
		Cu(100)	1476
		(1×1)	1820
	Fe	(1×1)	1272
	Ni	(1×1)	1820
	Pd	Epitaxial	1167
		(1×1)	1463
Ag(110)	Cs	(1×2)	859,1534
		(1×3)	859,1534
	K	(1×2)	1534
		(1×3)	1534
	Li	(1×2)	1534
	Na	(1×1)	489
Ag(111)	Al	Disordered	491
	Au	(1×1)	491,1355,1825 1826
	Bi	Disordered	491
	Cd	No Condensation	491
	Co	Disordered	491
	Cr	Disordered	491
	Cu	Hexagonal Overlayer	1822–1824
	K	Hexagonal Overlayer	1345
	Mg	Disordered	491
	Na	(1×1)	488
	Ni	Hexagonal Overlayer	491,1821
	Pb	$(\sqrt{3}\times\sqrt{3})R30°$–Pb	975
		Pb(111)	975
		Hexagonal Overlayer	491,1827
	Pd	(1×1)	1463
		Disordered	491
	Rb	(1×1)–Rb	490,705
		(9×9)	705
	Sb	Disordered	491
	Sn	Disordered	491
	Tl	Hexagonal Overlayer	491
	Zn	No Condensation	491
Al(100)	Ag	(5×1)–Ag	1363
		(1×1) [Multilayer]	1363
	Au	Disordered	1363
	Cu	Disordered	1363
	Fe	Poor Epitaxy	452
	Na	*c(2×2)	499,500,501*,1926*
		Hexagonal Overlayer	500
	Pb	$\begin{bmatrix} 2 & 0 \\ -1 & 2 \end{bmatrix}$	503
		c(2×2)–Pb	704

TABLE V. Surface Structures of Metallic Monolayers on Metal Crystal Surfaces (Continued)

Substrate	Adsorbate	Surface Structure	Reference
		$\begin{bmatrix} 2 & 0 \\ 1 & n \end{bmatrix}$–Pb 2<n<3	704
	Sm	(1×1) Disorder	1532
		Complicated	1532
	Sn	$\begin{bmatrix} 2 & 0 \\ -1 & 3 \end{bmatrix}$	503
		c(2×6)–Sn	704
		$\begin{bmatrix} 2 & 0 \\ 1 & n \end{bmatrix}$ 2<n<3	704
Au(100)	Ag	(1×1)	473,474,494,1838
	Bi	$\begin{bmatrix} 2 & 0 \\ -1 & 2 \end{bmatrix}$	498
	Cu	(1×1)	473
	Fe	(1×1)	1828–1830
	Na	Hexagonal	492
		Ordered	492
	Pb	$\begin{bmatrix} 1 & 1 \\ 1 & -1 \end{bmatrix}$	441–444
		$\begin{bmatrix} 1 & 1 \\ -3 & 4 \end{bmatrix}$	441–444
		$\begin{bmatrix} 1 & 1 \\ -1 & 2 \end{bmatrix}$	441–444
		$\begin{bmatrix} 2 & 0 \\ -1 & 3 \end{bmatrix}$	441–444
		(1×1)	683
	Pd	(1×1)	473,1833
		c(2×2)	683
		c($7\sqrt{2}\times\sqrt{2}$)R45°	683
		c($3\sqrt{2}\times\sqrt{2}$)R45°	683
		c(6×2)	683
	Pt	(1×1)	438,439,440
Au(110)	Bi	$\begin{bmatrix} 1 & 1 \\ 1 & -1 \end{bmatrix}$	498
		$\begin{bmatrix} 2 & 1 \\ -1 & 1 \end{bmatrix}$	498
		(2×1)	498

TABLE V. Surface Structures of Metallic Monolayers on Metal Crystal Surfaces (Continued)

Substrate	Adsorbate	Surface Structure	Reference
	Pb	(1×3)	444,495,683
		(1×1)	444,495,683
		(7×1)	444,495,683
		(7×3)	444,495,683
		(4×4)	444,495,683
Au(111)	Ag	(1×1)	491,1825
		fcc(111)	1689
	Ag,Air	$Ag_2O(110)$–(2×1)	997
	Bi	$\begin{bmatrix} 10 & 10 \\ -10 & 20 \end{bmatrix}$	498
		(2×2)	924
	Cr	Hexagonal	493
	Cu	$(\sqrt{3}\times\sqrt{3})R30°$–Cu	861,1558,1582
		(1×1)	1558
		Extra Lines(RHEED)	1836,1837
	Fe	(1×1)	1828,1830–1832
	Pb	Hexagonal Rotated±5°	444,495
		$(\sqrt{3}\times\sqrt{3})R30°$	924
		(1×1)	683
	Pd	(1×1)	1807,1834
	Pt	(1×1)	1835
Au(311)	Pb	(5×3)	496
		(3×3)–Pb	730
		(3×4)–Pb	730
Au(511)	Pb	$\begin{bmatrix} 1 & 1 \\ 1 & 1 \end{bmatrix}$	444
		$\begin{bmatrix} 2 & 0 \\ 1 & 3 \end{bmatrix}$	444
	Pd	c(2×2)	683
		$c(7\sqrt{2}\times\sqrt{2})R45°$	683
		$c(3\sqrt{2}\times\sqrt{2})R45°$	683
		c(6×2)	683
Au(711)	Pb	$\begin{bmatrix} 1 & 1 \\ 1 & -1 \end{bmatrix}$	444
		$\begin{bmatrix} 2 & 0 \\ -1 & 3 \end{bmatrix}$	444
	Pd	c(2×2)	683
		$c(7\sqrt{2}\times\sqrt{2})R45°$	683
		$c(3\sqrt{2}\times\sqrt{2})R45°$	683
		c(6×2)	683
Au(911)	Pb	$\begin{bmatrix} 1 & 1 \\ 1 & -1 \end{bmatrix}$	444

TABLE V. Surface Structures of Metallic Monolayers on Metal Crystal Surfaces (Continued)

Substrate	Adsorbate	Surface Structure	Reference
		$\begin{pmatrix} 2 & 0 \\ -1 & 3 \end{pmatrix}$	444
	Pd	c(2×2)	683
		c(7$\sqrt{2}$×$\sqrt{2}$)R45°	683
		c(3$\sqrt{2}$×$\sqrt{2}$)R45°	683
		c(6×2)	683
Au(11,1,1)	Pb	$\begin{pmatrix} 1 & 1 \\ 1 & -1 \end{pmatrix}$	444
		$\begin{pmatrix} 2 & 0 \\ -1 & 3 \end{pmatrix}$	444
Au(210)	Pb	(1×1)	497
Au(320)	Pb	(3×3)	496
		(1×1)–Pb	730
Cr(111)	Ag	(8×8)	46
	Au	$\begin{pmatrix} \frac{2}{3} & \frac{3}{3} \\ \frac{-2}{3} & \frac{4}{3} \end{pmatrix}$	52
	Bi	$\begin{pmatrix} 1 & 1 \\ -1 & 2 \end{pmatrix}$	61
		$\begin{pmatrix} 2 & -1 \\ 0 & 2 \end{pmatrix}$	61
		$\begin{pmatrix} 2 & 3 \\ 1 & 2 \end{pmatrix}$	61
	Fe	(1×1)	39
	Ni	(1×1)	43,44
	Pb	(4×4)	55,58
	Sn	$\begin{pmatrix} 1 & 1 \\ -1 & 2 \end{pmatrix}$	54
Cu(100)	Ag	$\begin{pmatrix} 2 & 0 \\ -1 & 5 \end{pmatrix}$	473,477
	Au	$\begin{pmatrix} 1 & 1 \\ 1 & -1 \end{pmatrix}$	473,478
		$\begin{pmatrix} 2 & 0 \\ -1 & 7 \end{pmatrix}$	473,478

TABLE V. Surface Structures of Metallic Monolayers on Metal Crystal Surfaces (Continued)

Substrate	Adsorbate	Surface Structure	Reference
	Bi	(2×2)	483,486
		$\begin{pmatrix}1 & 1\\1 & -1\end{pmatrix}$	483,486
		$\begin{pmatrix}1 & 1\\-4 & 5\end{pmatrix}$	483,486
		$\begin{pmatrix}5 & 4\\-4 & 5\end{pmatrix}$	483,486
		(1×1)	703
		c(2×2)	703
	Co	(1×1)–Co	983,1105,1810 1811
	Cs	Hexagonal Overlayer	865
		Quasi-Hexagonal	865
		Disordered	865
	Fe	(1×1)	452,1808,1809
	K	$\begin{pmatrix}2 & 3\\0 & 5\end{pmatrix}$	1405
		$\begin{pmatrix}2 & 2\\0 & 3\end{pmatrix}$	1405
		Incommensurate	1405
	Mn	c(2×2)–Mn	1319
	Nb	Incommensurate	667
	Ni	(1×1)	1812
	Pb	$\begin{pmatrix}2 & 2\\-2 & 2\end{pmatrix}$	481–485
		$\begin{pmatrix}1 & 1\\-2 & 3\end{pmatrix}$	481–485
		*c($5\sqrt{2}\times\sqrt{2}$)R45°–Pb	703,1295*
		*c(2×2)–Pb	1295*
		($2\sqrt{2}\times2\sqrt{2}$)R45°–Pb	1295
	Pd	c(2×1)–Pd	726
		(1×1)–Pd	726,1649
		c(2×2)–Cu_3Pd	1649
	Sn	(2×2)	480
	Te	*!(2×2)–Te	267*,1119,1728!

TABLE V. Surface Structures of Metallic Monolayers on Metal Crystal Surfaces (Continued)

Substrate	Adsorbate	Surface Structure	Reference
	Tl	$\begin{pmatrix} 2 & 2 \\ 2 & -2 \end{pmatrix}$	1167,1564
		$\begin{pmatrix} 4 & 0 \\ 2 & 7 \end{pmatrix}$–Tl	1167,1336,1564
		$\begin{pmatrix} 4 & 0 \\ 2 & 6 \end{pmatrix}$–Tl	1336,1564
		$\begin{pmatrix} 6 & 6 \\ 2 & -2 \end{pmatrix}$	1564
		c(4×4)–Tl	1336
Cu(110)	Au	$\begin{pmatrix} 1 & 0 \\ \frac{-1}{2} & \frac{3}{2} \end{pmatrix}$	479
		(1×2)	479
		(2×2)	479
	Pb	$\begin{pmatrix} 1 & 1 \\ -1 & 1 \end{pmatrix}$	481,482
		(5×1)	481,482
		(4×1)	482
	Pd	(2×1)–Pd	726
		(1×1)–Pd	726
Cu(111)	Ag	(8×8)	477
		3 Dimensional Crystals	1813,1815–1818
		(1×1)	1526
	Au	$\begin{pmatrix} \frac{2}{3} & \frac{2}{3} \\ -\frac{2}{3} & \frac{4}{3} \end{pmatrix}$	479
		(2×2)	479
		3 Dimensional Crystals	1815,1819
	Bi	$\begin{pmatrix} 1 & 1 \\ -1 & 2 \end{pmatrix}$	487
		$\begin{pmatrix} 2 & -1 \\ 0 & 2 \end{pmatrix}$	487
		$\begin{pmatrix} 2 & 3 \\ 1 & 2 \end{pmatrix}$	487

TABLE V. Surface Structures of Metallic Monolayers on Metal Crystal Surfaces (Continued)

Substrate	Adsorbate	Surface Structure	Reference
	Co	(1×1)–Co	1299
	Cs	*(2×2)–Cs	711,1430*
	Fe	(1×1)	474
	Na	(2×2)–Na	1571
	Ni	*(1×1)–Ni	475,476,1466* 1813
	Pb	(4×4)	481,484
	Pd	(1×1)	726,1538
	Sn	$\begin{bmatrix} 1 & 1 \\ -1 & 2 \end{bmatrix}$	480
Cu(211)	Pb	(4×1)	484
Cu(311)	Pb	$\begin{bmatrix} 3 & 1 \\ -2 & 1 \end{bmatrix}$	484
		(4×2)	484
Cu(511)	Pb	(4×1)	482
Cu(711)	Pb	(4×1)	482,484
Fe(100)	K	Disordered	665
		(2×2)–K	784
		Hexagonal Close Pack	784
Fe(110)	K	Hexagonal Array	728
Fe(111)	K	(3×3)–K	665,1350
Ge(111)	Al	(2×1)	1550
	Au	$(\sqrt{3}\times\sqrt{3})R30°$–Au	1223
Ir(100)	Ba	(2×1)–Ba	1399
	Cs	c(4×2)–Cs w.Streak	1395
		Close Packed Layer	1395
		Compressed Layer	1395
		(5×5)–Cs	1395
	K	$c(2\sqrt{2}\times4\sqrt{2})R45°$	866
		$\begin{bmatrix} 2 & 1 \\ -1 & 2 \end{bmatrix}$	866
		c(4×2)	866
		(3×2)	866
		c(2×2)	866
		$\begin{bmatrix} \frac{5}{2} & 0 \\ \frac{-5}{4} & \frac{5}{3} \end{bmatrix}$	866
		$\begin{bmatrix} 2 & 0 \\ -1 & \frac{5}{3} \end{bmatrix}$	866

TABLE V. Surface Structures of Metallic Monolayers on Metal Crystal Surfaces (Continued)

Substrate	Adsorbate	Surface Structure	Reference
		$\begin{bmatrix} \frac{10}{7} & \underline{0} \\ \frac{-5}{7} & \frac{5}{3} \end{bmatrix}$	866
Ir(111)	Au	(1×1)	453
	Cr	Hexagonal	453
Mo(100)	Ag	Ag(100)	513,514
		Ag(110)	513,514
	Cs	$(\sqrt{2}\times\sqrt{2})R45°$	932
		(2×2)	932
		c(2×2)	932
		Rectangular Centered Mesh	932
		Quasi Hexagonal	932
		Hexagonal Overlayer	932
	Ga	(1×1)–Ga	789
	Sn	$\begin{bmatrix} 1 & 1 \\ 1 & -1 \end{bmatrix}$	516
		(1×2)	516
		(1×1)–Sn	789
		c(2×2)–Sn	789
Mo(110)	Al	Hexagonal	515
	Au	Disordered	1681
	Cs	Hexagonal	512
	K	Hexagonal	512
	Na	No Ordered Structure	512
	Rb	Hexagonal	512
Mo(211)	Ba	(1×5)	1591,1675
		(4×2)	1591
	Cs	c(2×1/J),0.15<J<0.64	1590
		c(2×2)	1590
	La	Linear Chains	1447
		c(2×2)	1447
		c(2×4/3)	1447
	Li	(1×4)–Li	1593
		(1×2)–Li	1593
		(1×1)–Li	1593
	Na	(1×4)–Na	1684
		(1×3)–Na	1684
		(1×2)–Na	1684
		(1×3/2)–Na	1684
	Sr	(1×9)–Sr	1594
		(1×5)–Sr	1594
		(4×2)–Sr	1594
Nb(110)	Sn	Disordered	505
		(3×1)	505

TABLE V. Surface Structures of Metallic Monolayers on Metal Crystal Surfaces (Continued)

Substrate	Adsorbate	Surface Structure	Reference
Ni(100)	Ba	Disordered	454
	Co	(1×1)	1803
	Cr	(1×1)	463,464
	Cs	(2×2)	454
		Hexagonal	463,464
	Cu	*(1×1)–Cu	1113,1458*,1804
	Fe	c(2×2)–Fe	973
		Fe(110)	452,973
	K	(4×2)	454
	Na	$\begin{pmatrix} 1 & 1 \\ 1 & -1 \end{pmatrix}$	452,454–459
		*c(2×2)–Na	1737*,1865*
	Pb	$\begin{pmatrix} 1 & 1 \\ 1 & -1 \end{pmatrix}$	471
		$\begin{pmatrix} 1 & 1 \\ -2 & 3 \end{pmatrix}$	471
		$(5\sqrt{2}\times\sqrt{2})R45°$–Pb	773
	Sn	c(2×2)–Sn	773
Ni(110)	Cs	Disordered	455
	K	Disordered	455
	Na	Disordered	455,458,460
		Hexagonal	455,458,460
	Pb	$\begin{pmatrix} 1 & 1 \\ 1 & -1 \end{pmatrix}$	471
		(3×1)	471
		(4×1)	471
		(5×1)	471
	Yb	(2×1)–Yb	844
Ni(111)	Ag	(6×6)	465,466
	Au	(6×6)	467,468,469,470
		(13×13)	467,468,469
	Bi	$(\sqrt{3}\times\sqrt{3})R30°$–Bi	864
		(7×7)–Bi	864
		$(\sqrt{7}/4\times\sqrt{7}/4)R19°$–Bi	864
	Mo	(5×5)	447,448
		(4×4)	447,448
		$\begin{pmatrix} 2 & 0 \\ 5 & 10 \end{pmatrix}$	447,448
		$\begin{pmatrix} 1 & 0 \\ 5 & 10 \end{pmatrix}$	447,448
	Na	Hexagonal	455,458,460

TABLE V. Surface Structures of Metallic Monolayers on Metal Crystal Surfaces (Continued)

Substrate	Adsorbate	Surface Structure	Reference
	Pb	$\begin{bmatrix} 1 & 1 \\ -1 & 2 \end{bmatrix}$	471,472
		(7×7)	471,864
		(13×13)	471,472
		(3×3)	471,864,1060
		(4×4)–Pb	864,1060
		Hexagonal Rotated±3°	472
		$(\sqrt{3}\times\sqrt{3})$R30°–Pb	864,1060
	Sn	(2×2)–Sn	1060
		$(\sqrt{3}\times\sqrt{3})$R30°–Sn	1060
	Te	$(2\sqrt{3}\times2\sqrt{3})$R30°–Te	577
Pd(100)	Ag	*(1×1)	473,1797*
	Au	(1×1)	473,1806,1807
	Cs	*(1×2)+Disordered C_s	1760*
	Cu	(1×1)	862
	Fe	Fe(100) and Fe(110)	452
	Na	*(1×2)+Disordered Na	1760*
	Ni	(1×1)	1805
Pd(111)	Au	!(1×1)–Au	1709!
	Fe	(1×1)	1546
Pt(100)	Au	$\begin{bmatrix} 14 & 1 \\ -1 & 5 \end{bmatrix}$	671
		(1×1)–Au	671
		(1×5)–Au	671
		(1×7)–Au	671
Pt(111)	Ag	Disordered	1254
	Au	Disordered	1254
	Cu	(1×1)–Cu	842
		Cu(111) Multilayers	842
		Alloy Formation	842
	K	$(\sqrt{3}\times\sqrt{3})$R30°–K	1071,1238,1337
		$\begin{bmatrix} 1.66 & 0 \\ 0 & 1.66 \end{bmatrix}$–K	1337
		Ring Pattern	1337
Re(0001)	Ba	(2×2)	565,566
		Hexagonal	565,566
Re($10\bar{1}0$)	Ba	c(2×2)	1591
	Mg	(1×3)	1675

TABLE V. Surface Structures of Metallic Monolayers on Metal Crystal Surfaces (Continued)

Substrate	Adsorbate	Surface Structure	Reference
Rh(100)	Ag	(1×1)	895
		Complex	895
	Fe	Fe(100) and Fe(110)	452
Ru(0001)	Cu	Disordered	1679
	Na	(3/2×3/2)–Na	1129,1406
		Ring Pattern	1129
		(2×2)–Na	1082,1129
		$(\sqrt{3}\times\sqrt{3})R30°$–Na	1082,1129,1406
		Hexagonal Overlayer	1406
Sb(0001)	Fe	(1×1)	567
	Th	$\begin{bmatrix}1 & 1\\ 1 & -1\end{bmatrix}$	510,511
		(1×1)	510,511
Ta(110)	Al	Hexagonal	508,509
		Square	508,509
Ti(0001)	Cd	*(1×1)	562*,563,564
	Cu	Extra Spots	561
W(100)	Ag	(2×1)	546
		$\begin{bmatrix}1 & 1\\ 1 & -1\end{bmatrix}$	546
		(1×1)	546
	Au	(2×1)	546
		$\begin{bmatrix}2 & 0\\ -1 & 2\end{bmatrix}$	546
		(1×1)	546
	Ba	$\begin{bmatrix}2 & 0\\ -8 & 2\end{bmatrix}$	531,532
		split $\begin{bmatrix}1 & 1\\ -2 & 2\end{bmatrix}$	531,532
		$\begin{bmatrix}1 & 1\\ -2 & 2\end{bmatrix}$	531,532
		$\begin{bmatrix}1 & 1\\ 1 & -1\end{bmatrix}$	531,532
		c(4×2)–Ba	735
		$c(2\sqrt{2}\times\sqrt{2})$–Ba	735
		$c(\sqrt{6}\times\sqrt{2})R45°$–Ba	735
		$c(2\sqrt{2}\times 2/3\sqrt{6})R45°$–Ba	735
		(2×12)–Ba	994
		(2×10)–Ba	994

TABLE V. Surface Structures of Metallic Monolayers on Metal Crystal Surfaces (Continued)

Substrate	Adsorbate	Surface Structure	Reference
		(3×2)–Ba	994
		(3×2)+c(2×2)	994
		c(2×1.86)	994
		(10×21)–Ba	994
		c(2×2)–Ba	1399
		$c(2\times K),(1.86\leq K\leq 2\sqrt{2/3})$	994
		Hexagonal	994
	Bi	c(2×2)	1260
		(2×2)	1260
		(1×1)	1260
	Cs	$\begin{pmatrix}1 & 1\\1 & -1\end{pmatrix}$	523,524,525,526
		(2×2)	523,524,525,526
		Split (2×2)	523,524
		Hexagonal	525,526
	Cu	(2×2)	543
		$\begin{pmatrix}1 & 1\\1 & -1\end{pmatrix}$	543
	Ga	(1×1)–Ga	789
	Hg	(1×1)	549
	K	$\begin{pmatrix}1 & 1\\1 & 1\end{pmatrix}$	1841
	Na	$\begin{pmatrix}1 & 1\\1 & -1\end{pmatrix}$	1840
	Pb	Disordered (2×2)	550
		Split $\begin{pmatrix}1 & 1\\1 & -1\end{pmatrix}$	550
		$\begin{pmatrix}1 & 1\\1 & -1\end{pmatrix}$	550,551
		$\begin{pmatrix}1 & 1\\-2 & 2\end{pmatrix}$	550
		Hexagonal	550
		(2×2)	551
		$\begin{pmatrix}2 & 0\\-1 & 2\end{pmatrix}$	551
		(1×1)	551,702
		c(4×2)–Pb	702
		c(2×2)–Pb	702

TABLE V. Surface Structures of Metallic Monolayers on Metal Crystal Surfaces (Continued)

Substrate	Adsorbate	Surface Structure	Reference
	Pd	$(2\sqrt{2}\times\sqrt{2})R45°$–Pd	646
		(2×1)–Pd	646
		c(2×2)–Pd	646
	Rb	$\begin{bmatrix} 1 & 1 \\ 1 & -1 \end{bmatrix}$	522
		(2×2)	522
		Hexagonal	522
	Sb	(2×2)	553,554
		$\begin{bmatrix} 1 & 1 \\ 1 & -1 \end{bmatrix}$	553,554
		(1×1)	553,554
	Sn	(1×1)–Sn	789
		c(2×2)–Sn	789
	Th	$\begin{bmatrix} 1 & 1 \\ 1 & -1 \end{bmatrix}$	556–560
		(1×1)	556–560
		$\begin{bmatrix} 2 & 0 \\ -1 & 3 \end{bmatrix}$	559,560
		Hexagonal	559,560
	Rb	$\begin{bmatrix} 1 & 1 \\ 1 & -1 \end{bmatrix}$	522
		(2×2)	522
		Hexagonal	522
	Zr	(1×1)	541,764,789
		$\begin{bmatrix} 2 & 0 \\ -1 & 2 \end{bmatrix}$	541
		c(2×2)	764,789
W(110)	Ag	Hexagonal Structures	546,547
		Ag(111)	1151
	Au	Hexagonal Structures	546,548
	Ba	Disordered Hexagonal	533–535
		Hexagonal	533–535
		$\begin{bmatrix} 2 & 2 \\ 0 & 6 \end{bmatrix}$	533–535
		$\begin{bmatrix} 2 & 2 \\ 0 & 5 \end{bmatrix}$	533–535

TABLE V. Surface Structures of Metallic Monolayers on Metal Crystal Surfaces (Continued)

Substrate	Adsorbate	Surface Structure	Reference
		$\begin{pmatrix}3 & 3\\1 & 5\end{pmatrix}$	533–535
		Hexagonal Compact	533–535
	Be	(1×9)	529
		(1×1)	529
		$\begin{pmatrix}9 & 0\\-1 & 1\end{pmatrix}$	529
	Cs	Disordered Hexagonal	523,527,528
		Hexagonal	523,527,528,1677
	Cu	Hexagonal	543–545
		Cu(111)	1151
	Fe	3-Dimensional Crystals	451
		Fe(110)	1325
		(1×1)	1325
	Li	$\begin{pmatrix}1 & 5\\-2 & 2\end{pmatrix}$	517–519
		(2×2)	517–519
		$\begin{pmatrix}1 & 1\\-1 & 2\end{pmatrix}$	517–519
		(2×3)–Li	1269
		c(2×2)–Li	1269
		c(3×1)–Li	1269
		c(1×1)–Li	1269
	Na	$\begin{pmatrix}1 & 5\\-2 & 2\end{pmatrix}$	445,446
		(2×2)	445,446
		$\begin{pmatrix}1 & 1\\-1 & 2\end{pmatrix}$	445,446
		$\begin{pmatrix}1 & 1\\0 & 8\end{pmatrix}$	445,446
		$\begin{pmatrix}1 & 1\\0 & 5\end{pmatrix}$	445,446
		Hexagonal	445,446
	Ni	(1×1)–Ni	970
		(8×2)–Ni	970
		(7×2)–Ni	970
	Pd	(1×3)	542
		Hexagonal	542

TABLE V. Surface Structures of Metallic Monolayers on Metal Crystal Surfaces (Continued)

Substrate	Adsorbate	Surface Structure	Reference
	Pb	Split $\begin{bmatrix} 3 & 0 \\ -1 & 1 \end{bmatrix}$	551,552
		$\begin{bmatrix} 3 & 0 \\ -1 & 1 \end{bmatrix}$	551,552
	Sb	$\begin{bmatrix} 1 & 1 \\ 0 & 4 \end{bmatrix}$	553,555
		$\begin{bmatrix} 2 & 0 \\ -1 & 1 \end{bmatrix}$	553,555
		$\begin{bmatrix} 3 & 0 \\ -1 & 1 \end{bmatrix}$	553,555
		$\begin{bmatrix} 4 & 0 \\ -1 & 1 \end{bmatrix}$	553,555
	Sc	$\begin{bmatrix} 1 & 1 \\ 0 & 3 \end{bmatrix}$	536–538
		$\begin{bmatrix} 2 & 2 \\ 0 & 8 \end{bmatrix}$	536–538
	Sr	$\begin{bmatrix} 3 & 3 \\ -2 & 5 \end{bmatrix}$	530
		$\begin{bmatrix} 2 & 2 \\ 0 & 6 \end{bmatrix}$	530
		$\begin{bmatrix} 2 & 2 \\ 1 & 6 \end{bmatrix}$	530
		$\begin{bmatrix} 1 & 0 \\ 0 & 3 \end{bmatrix}$	530
	W	Ring Pattern	1623
	Y	Hexagonal	539,540

TABLE V. Surface Structures of Metallic Monolayers on Metal Crystal Surfaces (Continued)

Substrate	Adsorbate	Surface Structure	Reference
W(211)	Ag	(1×1)–Ag	969
	Au	(1×1)–Au	969
		(1×2)–Au	969
		(1×3)–Au	969
		(1×4)–Au	969
	Li	(4×1)	518,520
		(3×1)	518,520
		(2×1)	518,520
		Incoherent	518,520
		(1×1)	518,520
		[clean]	(2×2)
	Mg	(1×7)–Mg	1657
		(3×3)–Mg	1657
	Na	(2×1)	521
		Compressed(2×1)	521
	Sb	(2×1)	553
		(1×1)	553
W(221)	Na	Compressed(2×1)	521
		(2×1)	521
	Ni	(1×1)–Ni	970
		(6×1)–Ni	970
Zn(0001)	Cu	(1×1)	449,450

TABLE VI. Surface Structures of Alloys

Substrate	Adsorbate	Surface Structure	Reference
Ag(111)–Rb dosed	O_2	$(2\sqrt{3}\times2\sqrt{3})R30°$–Rb/O	653
		(4×4)–Rb/O	653
		Complex Structures	653
		(9×9)–Rb/O	653
Cu–3% Al(100)	O_2	c(2×2)–O	1632
		Disordered	1632
Cu–5.7% Al(100)	[clean]	(1×1)	813
Cu–12.5% Al(100)	[clean]	(1×1)	813
Cu_3Al(100)	[clean]	c(2×2)	916
Cu/Al(111)	[clean]	(1×1)	835
		$(\sqrt{3}\times\sqrt{3})R30°$	835
Cu–5.7% Al(111)	[clean]	(1×1)	813
Cu–10% Al(111)	[clean]	(1×1)	1303
		$(\sqrt{3}\times\sqrt{3})R30°$–Al	1303
Cu–11% Al(111)	[clean]	*(1×1)	1506*
Cu–12.5% Al(111)	[clean]	$(\sqrt{3}\times\sqrt{3})R30°$	813
Cu–16% Al(111)	[clean]	*$(\sqrt{3}\times\sqrt{3})R30°$	1699*
Cu/Au(100)	[clean]	c(2×2)	737
Cu/Au(110)	[clean]	Streak	737
		(1×2)	737
		Complex Pattern	737
		c(3×1)	737
		c(2×2)	737
Cu/Au(111)	[clean]	$(2/3\sqrt{3}\times2/3\sqrt{3})R30°$	737
		(2×2)	737
Cu/Au($1\bar{1}1$)	[clean]	$(2/3\sqrt{3}\times2/3\sqrt{3})R30°$	737
		(2×2)	737
Cu(110)–Ni(1°)	O_2	(2×1)–O	1311
		c(6×2)–O	1311
Cu/Ni(110)	CO	(2×1)–CO	134
		(2×2)–CO	134
		(1×2)–CO	787
	H_2	(1×3)–H	787
	H_2S	c(2×2)–S	134
	O_2	(2×1)–O	134,872
		(2×2)–O	872
Cu/Ni(111)	CO	Disordered	173,734
Cu/Pd(100)	[clean]	Streak	737
		c(2×2)	737
Cu/Pd(110)	[clean]	(2×1)	737
Cu/Pd(111)	[clean]	(1×1)	737
Cu/Pd($1\bar{1}1$)	[clean]	(1×1)	737
CuSn(100)	[clean]	c(2×2)	1481
		$(3\sqrt{2}\times\sqrt{2})R45°$	1481
		c(3×2)+(2×2)	1481
Cu–25% Zn(100)	[clean]	(1×1)	1152
	O_2	Disordered	1152
Cu–25% Zn(110)	[clean]	(1×1)	1152
	O_2	Disordered	1152

TABLE VI. Surface Structures of Alloys (Continued)

Substrate	Adsorbate	Surface Structure	Reference
Cu–25% Zn(111)	[clean]	(1×1)	1152
	O_2	Disordered	1152
Fe/Cr(100)	O_2	c(2×2)–O	279,636
		c(4×4)–O	279
		Oxide	280
Fe/Cr(110)	O_2	Cr_2O_3(0001)	280
		Amorphous Oxide	279
Fe–18% Cr–12% Ni(111)	[clean]	(1×1)	1249
	I_2	($\sqrt{3}\times\sqrt{3}$)R30°–I	1249
	H_2O	Ordered	1249
	O_2	Ordered	1249
	I(a)+H_2O	Oxide Not Formed	1249
	H_2O(a)+I_2	Adsorbed	1249
FeTi(100)	[clean]	(1×1)	1241
	S	c(2×2)–S	1241
FeTi(111)	[clean]	(1×1)	1241
Ni_3Al(001)	[clean]	*(1×1)	1868*
NiAl(110)	[clean]	*(1×1)	1771*
NiCu(100) (Ni<50%)	S	c(2×2)–S	905
Ni–17% Cu(111)	[clean]	(1×1)	868
	H_2	(2×2)–H	868
Ni–24% Fe(100)	O_2	c(2×2)–O	573
Ni–25% Fe(100)	H_2S,H_2	c(2×2)–S	1121
Ni–25% Fe(110)	H_2S,H_2	(2×3)–S	1121
Ni–25% Fe(111)	H_2S,H_2	(3×3)–S	1121
Ni–41% Fe(100)	[clean]	(1×1)	1263
	O_2	c(2×2)–O	1263
		Oxide	1263
Ni_4Mo(211)	[clean]	Ordered	1115
Pd–33% Ag(111)	[clean]	(1×1)	877
	CO	(1×1)	877
Pd–25% Cu(111)	[clean]	(1×1)	877
	CO	(1×1)	877
Pt–2% Cu(110)	[clean]	(1×3)	1062
	CO	(1×1)–CO	1063
Pt–22% Ni(111)	[clean]	(1×1)	1162
Pt–50% Ni(111)	[clean]	(1×1)	1162
Pt_3Ti(100)	[clean]	c(2×2)	935
Pt_3Ti(111)	[clean]	(2×2)	935

TABLE VII. Surface Structure Formed by Adsorption of Organic Molecules

Substrate	Adsorbate	Surface Structure	Reference
Ag(100)	$C_2H_4Cl_2$	*c(2×2)–Cl	154,249*,1873*
Ag(110)	C_2H_2	Not Adsorbed	812
	C_2H_4	Not Adsorbed	1690
	$C_2H_4+O_2$	(2×1)–O	1001
	$C_2H_4Cl_2$	(2×1)–Cl	154
		c(4×2)–Cl	154
	$O(a)+C_2H_2$	c(2×6)–acetylide	1335,1398
		(2×2)–acetylide	1335,1398
		(2×3)–acetylide	1335,1398
		(1×1)–C	1335
Ag(111)	CH_2Br_2	(1×1)	594
	CH_3I	$(\sqrt{3}\times\sqrt{3})R30°$–I	594
	$CHCl_3$	(1×1)	594
	$C_2H_4CL_2$	$(\sqrt{3}\times\sqrt{3})R30°$–Cl	153,154
		(3×3)–Cl	153,154
	Acetic Acid	$\begin{bmatrix}2 & -0.7\\ 2 & 2.7\end{bmatrix} + \begin{bmatrix}2.8 & 1.4\\ 0 & 2.5\end{bmatrix}$	587
		Ring Pattern	587
	Propanoic Acid	$\begin{bmatrix}4 & 2\\ 0 & 4.3\end{bmatrix} + \begin{bmatrix}3.9 & 1.3\\ 1 & 4.6\end{bmatrix}$	587
		$\begin{bmatrix}4 & 2\\ 0 & 4.3\end{bmatrix}$	587
Ag[3(111)×(100)]	CH_2Br_2	(1×1)	594
	CH_3I	$(\sqrt{3}\times\sqrt{3})R30°$–I	594
	$CHCl_3$	(1×1)	594
Al(100)	C_2H_4	(1×1)	1693
Au(111)	C_2H_4	Not Adsorbed	161
	benzene	Not Adsorbed	161
	cyclohexene	Not Adsorbed	161
	naphthalene	Disordered	161
	n-heptane	Not Adsorbed	161
Au(S)–[6(111)×(100)]	C_2H_4	Not Adsorbed	161
	benzene	Not Adsorbed	161
	cyclohexene	Not Adsorbed	161
	naphthalene	Disordered	161
	n-heptane	Not Adsorbed	161
C(0001), graphite	CH_4	$(\sqrt{3}\times\sqrt{3})R30°$	1018
	C_2H_6	$(4\times\sqrt{3})$–C_2H_6	1191
		(2×2)–C_2H_6	1191
		$(10\times2\sqrt{3})$–C_2H_6	1191
		$(\sqrt{3}\times\sqrt{3})$–C_2H_6	1191

TABLE VII. Surface Structure Formed by Adsorption of Organic Molecules (Continued)

Substrate	Adsorbate	Surface Structure	Reference
Cr(100)	C_2H_4	c(2×2)–C	1245
		$(\sqrt{2}\times3\sqrt{2})R\pm45°$–C	1245
Cu(100)	C_2H_4	(2×2)	26
	O(a)+HCOOH	!Disordered–HCO_2	1921!,1922!
	O(a)+CH_3OH	!Disordered–CH_3O	1922!
	Cu-phtalocyanine	$\begin{bmatrix}5 & -2\\ 2 & 5\end{bmatrix}$	408
	D-tryptophan	(4×4)	409
	Fe-phtalocyanine	$\begin{bmatrix}5 & -2\\ 2 & 5\end{bmatrix}$	408
	glycine	(4×2)	409
		$\begin{bmatrix}8 & -4\\ 0.8 & 1.6\end{bmatrix}$	409
	H-phtalocyanine	$\begin{bmatrix}5 & -2\\ 2 & 5\end{bmatrix}$	408
	L-alanine	$\begin{bmatrix}2 & 1\\ 2 & -1\end{bmatrix}$	409
	L-tryptophan	(4×4)	409
	D-tryptophan	(4×4)	409
Cu(110)	C_2H_4	Ord. 1D	26
	HCOOH	!HCO_2–Disordered	1849!
Cu(111)	C_2H_4	Not Adsorbed	26
	Cu-phtalocyanine	Adsorbed	408
	D-tryptophan	$\begin{bmatrix}-8 & 1\\ -2 & 4\end{bmatrix}$	409
	Fe-phtalocyanine	Adsorbed	408
	glycine	(8×8)	409
	H-phtalocyanine	Adsorbed	408
	L-alanine	$(2\sqrt{13}\times2\sqrt{13})R13°40°$	409
	L-tryptophan	$\begin{bmatrix}7 & 1\\ -2 & 4\end{bmatrix}$	409
Cu(S)–[3(100)×(100)]	CH_4	Not Adsorbed	132
	C_2H_4	Not Adsorbed	132
Cu(S)–[4(100)×(100)]	CH_4	Not Adsorbed	132
	C_2H_4	Not Adsorbed	132

TABLE VII. Surface Structure Formed by Adsorption of Organic Molecules (Continued)

Substrate	Adsorbate	Surface Structure	Reference
Fe(100)	C_2H_4	c(2×2)–C	274,893
Fe(110)	C_2H_2	(2×2)	687
		(2×3)	687
		Coincidence	687
		$\begin{bmatrix} 4 & 0 \\ -1 & 3 \end{bmatrix}$	687
Fe(111)	C_2H_2	(1×1)	687
		(5×5)	687
		(3×3)	687
	C_2H_4	(1×1)	687
		(5×5)	687
		(3×3)	687
GaAs(110)	HCOOH	c(2×2)–H+HCOO	1124,1302
Ir(100)	C_2H_2	Disordered	281,410
		c(2×2)–C	281,410
	C_2H_4	Disordered	410
		c(2×2)–C	410
	benzene	Disordered	410
Ir(110)	C_2H_4	Disordered	347
		(1×1)–C	347
	benzene	Disordered	347
		(1×1)–C	347
Ir(111)	C_2H_2	$(\sqrt{3}\times\sqrt{3})R30°$	187
		(9×9)–C	187
	C_2H_4	$(\sqrt{3}\times\sqrt{3})R30°$	187
		(9×9)–C	187
	benzene	(3×3)	187
		(9×9)–C	187
	cyclohexane	Disordered	187
		(9×9)–C	187
Ir(S)–[6(111)×(100)]	C_2H_2	(2×2)	187
	C_2H_4	(2×2)	187
	benzene	Disordered	187
	cyclohexane	(2×2)	187
Mo(100)	CH_4	c(4×4)–C	286
		c(2×2)–C	286
		$c(6\sqrt{2}\times2\sqrt{2})R45°$–C	286
		(1×1)–C	286
	C_2H_4	c(2×2)–carbide	602,603,659
		$\begin{bmatrix} 3 & 0 \\ 1 & -1 \end{bmatrix}$	602,603,660
		(1×1)	602,603,660
		(1×1) w. Streaks	1379
		c(2×2)–C	660
	HCOOH	Disordered	1155
	O(a)+C_2H_4	(2×1)–O	817
	O(a)+HCOOH	(2×1)–O,C	1155

TABLE VII. Surface Structure Formed by Adsorption of Organic Molecules (Continued)

Substrate	Adsorbate	Surface Structure	Reference
Ni(100)	CH_4	c(2×2)	117
		(2×2)	117
	C_2H_2	*c(2×2)	416,1923*
		(2×2)	416
		c(4×2)	417
		(2×2)–C	417
	C_2H_4	c(2×2)	88,416
		Quasi-c(2×2)	1561
		(2×2)	416
		*(2×2)–C(p4g)	417,670,745*, 1092,1177
		c(4×2)	417
		$(\sqrt{7}\times\sqrt{7})R19°$–C	88
	C_2H_6	c(2×2)	117
		(2×2)	117
	CH_3OH	Disordered	601
		c(2×2)	601
	benzene	c(4×4)	415
Ni(110)	CH_4	(2×2)	117
		(4×3)	117
		(4×5)–C	117,418
		(2×3)–C	418,679
	C_2H_2	c(2×2)–C_2H_2	915
	C_2H_4	(2×1)–C	419,420,421
		(4×5)–C	419,420,915
		c(2×4)–C_2H_4	915
		c(2×2)–CCH	915
		Graphite Overlayer	420
	C_2H_6	(2×2)	117
	CH_3OH	c(2×4)–CH_3O	890
		c(2×6)–CH_3O	890
		c(2×2)–CO	890
	C_5H_{12}	(4×3)	422
		(4×5)	422

TABLE VII. Surface Structure Formed by Adsorption of Organic Molecules (Continued)

Substrate	Adsorbate	Surface Structure	Reference
Ni(111)	CH_4	(2×2)	117
		(2×2)–C	990
		Graphite	990
		(2×√3)	117
		(16√3×16√3)–R30°–C	739
		(4×5)	739
	C_2H_2	*!(2×2)–C_2H_2	412,413,719,1262*,1925!
		(√3×√3)R30°+(2×2)	719
		Disordered	1627
	C_2H_4	(2×2)	29,39,412
	C_2H_6	(2×2)	39,117
		(2×√3)	117
		(√7×√7)R19°–C	29
		(2×2)–C	990
		Disordered Graphite	990
	benzene	(2√3×2√3)R30°	414,415
	cyclohexane	(2√3×2√3)R30°	414
Pb(100)	HCOOH	Not Adsorbed	1691
Pd(100)	benzene	c(4×4)	616,617
		(2×2)R45°–C_6H_6	616,617,630
Pd(111)	C_2H_2	(√3×√3)R30°–C_2H_2	1043,1209
	C_2H_4	(√3×√3)R30° Diffuse	1209
		Disordered	1266
		(√3×√3)R30°–C_2H_3	1266
	CH_3OH	(√3×√3)R30°–CO,H_2	1042
		Complex	1042
	Benzene	Disordered	961
	Benzene + CO	(2√3×2√3)R30°	961
		Complex	961
		*(3×3)–C_6H_6+2CO	961,1862*
Pt(100)	C_2H_2	c(2×2)	28,72,321,431,432
	C_2H_4	c(2×2)	28,72,313,321,431
		Graphite Overlayer	313,426
		(511),(311)facets	426
	acrylic acid	(1×1) Diffuse	1258
	acrylic acid(a)+NH_3	(1×1) Diffuse	1258
	aniline	Disordered	430
	benzene	Disordered	432
		2(1 dimensional order)	429
	cyanobenzene	Disordered	430
	mesitylene	3(1 dimensional order)	430
	M-xylene	3(1 dimensional order)	430
	naphthalene	(1×1)	429
	nitrobenzene	Disordered	430
	N-butylbenzene	Disordered	430
	pyridine	(1×1)	429
		c(2×2)	429

TABLE VII. Surface Structure Formed by Adsorption of Organic Molecules (Continued)

Substrate	Adsorbate	Surface Structure	Reference
	toluene	3(1 dimensional order)	430
	T-butylbenzene	Disordered	430
Pt(110)	HCOOH	1–D Disordered	1080
	CH_3NCO	(1×2)	938
	benzene	Disordered	1172
Pt(111)	C_2H_2	(2×1)	28
		(2×2)	423,424,425,1316 1196
	C_2H_2+H_2	*(2×2)–C_2H_3	824*,1316,1587
	C_2H_4	(2×2)	40,424,425,1196 1313
		*(2×2)–C_2H_3	824*,1316,1586
		(2×1)	28
		2(1 dimensional order)–C	221
		Disordered	1316
		Complex	1313
		Graphite Overlayer	221,426,1093
	(O)+C_2H_4	(2×2)	1313
		Ordered	1313
	C_3H_4	(2×2)	1316
	C_3H_4+H_2	(2×2)	1316
	C_3H_6	Disordered	1316
		(2×2)	1316
	cis-2-C_4H_8	$(2\sqrt{3}\times2\sqrt{3})R30°$	1316
	trans-2-C_4H_8	(8×8)	1316
	$C_{10}H_8$	(6×3)–$C_{10}H_8$	668
	acetic acid	(2×2)	580,1287
		Disordered	587,1287
	acetnitrile	(1×1) Diffuse	1258
		(2×2)	580,1287
		Disordered	1287
	acetnitrile+I_2	I_2 Adsorbed	1258
	aniline	3(1 dimensional order)	430
	azulene	Disorderd	1349
		(3×3)	1349
		(3×3)+(3×3)R30°	1349
		(10×10)	1349
	benzene	Disordered	429,1854,1891
		*Graphite	1924*
	benzene+CO	$\begin{pmatrix}-2 & 2\\ 5 & 5\end{pmatrix}=\begin{pmatrix}4 & -2\\ 0 & 4\end{pmatrix}$	221,428,429
		*$\begin{pmatrix}4 & -2\\ 0 & 5\end{pmatrix}=\begin{pmatrix}-2 & 2\\ 4 & 4\end{pmatrix}$ $=(2\sqrt{3}\times4)rect-2C_6H_6+4CO$	428,429,1854*
	cyanobenzene	3(1 dimensional order)	430

TABLE VII. Surface Structure Formed by Adsorption of Organic Molecules (Continued)

Substrate	Adsorbate	Surface Structure	Reference
	cyclohexane	$\begin{bmatrix} 4 & -1 \\ 1 & 5 \end{bmatrix}$	427
		Disordered	221
		(2×2)	221
		Graphite Overlayer	221
	dichloromethane	Not Adsorbed	580
	dimethylsulfoxide	(2×2)	580,1287
		$(\sqrt{3}\times\sqrt{3})R30°$	1287
		(1×1)	1287
	dimethylformamide	(2×2) Diffuse	580,1258
		Disordered	1287
	DMSO	(1×1)–DMSO	1258
	DMSO(a)+I_2	Ordered	1258
	DMSO(a)+pyridine	Not Adsorbed	1258
	I(a)+pyridine	Not Adsorbed	1258
	I(a)+acetnitrile	Not Adsorbed	1258
	I(a)+DMSO	DMSO Not Adsorbed	1258
	I_2+DMSO	$c(2\times4\sqrt{3}/3)$–I,DMSO	1258
	mesitylene	3.4(1 dimensional order)	430
	m-xylene	2.6(1 dimensional order)	430
	naphthalene	(6×6)	224,429
		napthalene (001)	224
		(6×3)	1349
		Disordered	1349
	nitrobenzene	3(1 dimensional order)	430
	n-butane	$\begin{bmatrix} 2 & 1 \\ -1 & 2 \end{bmatrix}$	427
		$\begin{bmatrix} 2 & 2 \\ -5 & 5 \end{bmatrix}$	427
		$\begin{bmatrix} 3 & -2 \\ 2 & 5 \end{bmatrix}$	427
	N-butylbenzene	Disordered	430
	n-heptane	$\begin{bmatrix} 2 & 1 \\ 0 & 8 \end{bmatrix}$	427
		(2×2)	221
	n-hexane	$\begin{bmatrix} 2 & 1 \\ -1 & 3 \end{bmatrix}$	427
	n-octane	$\begin{bmatrix} 2 & 1 \\ -1 & 4 \end{bmatrix}$	427

TABLE VII. Surface Structure Formed by Adsorption of Organic Molecules (Continued)

Substrate	Adsorbate	Surface Structure	Reference
	n-pentane	$\begin{bmatrix} 2 & 1 \\ 0 & 6 \end{bmatrix}$	427
	propylene-carbonate	(2×2)	580,1287
		Disordered	1287
	propanoic Acid	Disordered	587
	pyridine	(2×2)	429,580,1287
		(1×1) Diffuse	1258
		Disordered	1287
	pyridine(a)+DMSO	Not Adsorbed	1258
	pyridine(a)+H_2O	Not Adsorbed	1258
	pyridine(a)+I_2	I_2 Adsorbed	1258
	p-dioxane	(2×2)	580,1287
		Disordered	1287
	sulfolane	(2×2)	580,1287
		$(\sqrt{3}\times\sqrt{3})R30°$	580,1287
		(1×1)	580,1287
	toluene	3(1 dimensional order)	221,430
		(4×2)	430
		Graphite Overlayer	430
	T-butylbenzene	Disordered	430
Pt(S)–[7(111)×(100)]	azulene	1/3 order ring	1057
	naphthalene	1/3 order spots	1057
Pt(S)–[4(111)×(100)]	C_2H_4	Disordered	221
		Graphite Overlayer	221
		Facets	221
	benzene	Disordered	221
		Graphite Overlayer	221
		Facets	221
	cyclohexane	Disordered	221
		(4×2)–C	221
	n-heptane	(4×2)	221
		(4×2)–C	221
	toluene	Disordered	221
		2(1 dimensional order)–C	221
Pt(S)–[6(111)×(100)]	C_2H_4	(2×2)	120,221
		$\begin{bmatrix} 3 & 2 \\ -2 & 5 \end{bmatrix}$–C	221
		$\begin{bmatrix} 6 & 1 \\ -1 & 7 \end{bmatrix}$–C	221
		$(\sqrt{19}\times\sqrt{19})R23.4°$–C	426
		Graphite Overlayer	426

TABLE VII. Surface Structure Formed by Adsorption of Organic Molecules (Continued)

Substrate	Adsorbate	Surface Structure	Reference
	benzene	3(1 dimensional order)	221
		(9×9)–C	221
	cyclohexane	2(1 dimensional order)	221
	n-heptane	(2×2)	221
		$\begin{bmatrix}1 & 1\\ -1 & 2\end{bmatrix}$	221
		(9×9)–C	221
	toluene	Disordered	221
		(9×9)–C	221
Pt(S)–[7(111)×(310)]	C_2H_4	Disordered	221
		Graphite Overlayer	221
	benzene	Disordered	221
	cyclohexane	Disordered	221
	n-heptane	Disordered	221
	toluene	Disordered	221
		Graphite Overlayer	221
Pt(S)–[9(111)×(100)]	C_2H_4	Adsorbed	221
	benzene	Disordered	221
		$\begin{bmatrix}1 & 1\\ -1 & 2\end{bmatrix}$–C	221
		Graphite Overlayer	221
	cyclohexane	Disordered	221
	n-heptane	(2×2)	221
		$\begin{bmatrix}1 & 1\\ -1 & 2\end{bmatrix}$	221
		(5×5)–C	221
		(2×2)–C	221
		$\begin{bmatrix}1 & 1\\ -1 & 2\end{bmatrix}$–C	221
		2(1 dimensional order)–C	221
	toluene	3(1 dimensional order)	221
		Graphite Overlayer	221
Pt(S)–[9(111)×(111)]	C_2H_4	Disordered	120
		Graphite Overlayer	398,399
		(2×2)	685
Pt(S)–[5(100)×(111)]	C_2H_4	Graphite Overlayer	426
		(511),(311) and (731) facets	426
Re(0001)	C_2H_2	Disordered	436,664
		(2×$\sqrt{3}$)R30°–C	436
	C_2H_4	Disordered	436,664
		(2×$\sqrt{3}$)R30°–C	436

TABLE VII. Surface Structure Formed by Adsorption of Organic Molecules (Continued)

Substrate	Adsorbate	Surface Structure	Reference
Re(S)–[14(0001)×(10$\bar{1}$1)]	C_2H_2	Disordered	664
	C_2H_4	(2×√3)R30°	664
Re(S)–[6(0001)×(16$\bar{7}$1)]	C_2H_2	Disordered	664
	C_2H_4	Disordered	664
Rh(100)	C_2H_2	c(2×2)	231
		c(2×2)–C_2H+C_2H_3	1880
	C_2H_4	c(2×2)	231
		c(2×2)–C_2H+C_2H_3	1878
		(2×2)–C_2H	1878
		c(2×2)–C	231,1403
		Graphite Overlayer	231,1403
	CO+C_2H_4	c(4×2)–CO+C_2H_3	1878
		split c(2×2)–CO+C_2H_3	1878
	C_6H_6	c(4×4)	1879
	C_6H_6+CO	c(2√2×4√2)R45°–CO+C_6H_6	1879
		c(2×2)	1879
Rh(111)	C_2H_2	c(4×2)	231,831
		(2×2)	831
	C_2H_2+CO	c(4×2)–CO+C_2H_2	1844,1881
	C_2H_2+Na	Disordered	1876
	C_2H_4	c(4×2)	231,831,1256,1372
		*(2×2)–C_2H_3(ethylidyne)	831,1256*,1372
		Partially Ordered	955
		(8×8)–C	231
		(2×2)R30°–C	231
		(√19×√19)R23.4°–C	231
		(2√3×2√3)R30°–C	231
		(12×12)–C	231
	C_2H_4+CO	c(4×2)–CO+C_2H_3	1881
	C_2H_4+NO	*c(4×2)–NO+C_2H_3	1877*
	C_2H_4+H_2	c(4×2)–CCH_3	955
		c(4×2)	1372
		(2×2)+c(4×2)	1256
	C_3H_6+CO	(2√3×2√3)R30°–CO+C_3H_5	1884
	CH_3OH	Disordered	988
	benzene	(2√3×3)rect	1842,1892
		(√7×√7)R19.1°	1892
	benzene+CO	*c(2√3×4)rect	1068,1416,1453,1842,1856*,1892
		$=\begin{pmatrix}3 & 1\\1 & 3\end{pmatrix}$–$C_6H_6$+CO	
		*(3×3)–C_6H_6+2CO	1068,1842,1855*,1892
	benzene+Na	(√3×√3)R30°+(2√3×3)rect	1876
	C_6H_5F+CO	(3×3)	1844
	methylacetylene	c(4×2)	1372
	naphthalene	(3√3×3√3)R30°	1068
		(3×3)	1068
	propylene	(2×2)+(2√3×2√3)R30°	1372

TABLE VII. Surface Structure Formed by Adsorption of Organic Molecules (Continued)

Substrate	Adsorbate	Surface Structure	Reference
		$(2\sqrt{3}\times2\sqrt{3})R30°$	1372
Rh(331)	C_2H_2	$\begin{bmatrix}-1 & 1\\ 3 & 0\end{bmatrix}$	402
	C_2H_4	$\begin{bmatrix}-1 & 1\\ 3 & 0\end{bmatrix}$	402,722
		Graphite Overlayer	402,722
Rh(S)–[6(111)×(100)]	C_2H_2	Disordered	402
	C_2H_4	Disordered	402,722
		(111),(100) facets	402,722
Ru(0001)	C_2H_6	Disordered	692
	cycropropane	Disordered	692,1111
	cyclohexane	Disordered	692,1112
		(1×1)	692
	cyclooctane	(1×1)	692
Si(111)	C_2H_2	Disorderd	437
	CH_3OH	(7×7)–CH_3O+H+CH_3OH	837
		Disordered	988
		Disorderd CH_3O+H	942
Si(311)	C_2H_2	c(1×1)	135
		(2×1)	135
		(3×1)	135
	C_2H_4	c(1×1)	135
		(2×1)	135
		(3×1)	135
Ta(100)	C_2H_4	Adsorbed	328
W(100)	CH_4	(5×1)–C	41
	C_2H_2	Disordered	700
		(5×1)–C	700,901
		c(3×2)–C	700
		c(2×2)–C	700
	propylene	$\begin{bmatrix}3 & 0\\ 1 & -1\end{bmatrix}$–C	887
		(5×1)–C	887
W(110)	C_2H_2	(2×2)–C_2H_2	1072
		c(2×2)–C_2H_2	1072
		(15×3)R14°–C	1072
	C_2H_4	(15×3)Rα–C	41
		(15×12)Rα–C	41
W(111)	CH_4	(6×6)–C	41
	C_2H_4	(1×1)	1595
	C_2H_6	(1×1)	1595
W(211)	propylene	c(6×4)–C	887
ZnO($10\bar{1}0$)	C_6H_6	c(2×2)–C_6H_6	632,620
		c(4×3)–C_6H_6	632,620

TABLE VIII. Coadsorbed Overlayer Structures

Substrate	Adsorbate	Surface Structure	Reference
Ag(100)	Cl_2+K	c(2×2)–K/Cl	673
	K+O_2	$\begin{bmatrix} 1 & 1 \\ -5 & 4 \end{bmatrix}$	658
		Hexagonal Overlayer	658
	O(ad.)+H_2O	c(2×2)–OH	1034
Ag(110)	C_2H_4+O_2	(2×1)–O	1001
	H_2O+Li^+	Complex	1557
	O(a)+C_2H_2	c(2×6)–acetylide	1335,1398
		(2×2)–acetylide	1335,1398
		(2×3)–acetylide	1335,1398
		(1×1)–C	1335
	O(a)+SO_2	c(6×2)–SO_3	1027,1371
		(1×2)–SO_4	1371
	O_2+H_2O	(1×2)–OH	878
		(1×3)–OH	878
Ag(111)	CO+O_2	(2×$\sqrt{3}$)–(CO+O_2)	27
Bi(0001)	O_2+K	$\sqrt{3}$+BiO(0001)layer	1288
C(0001), graphite	Ar+Xe	($\sqrt{3}\times\sqrt{3}$)R30°–Ar,Xe	1193
Co(100)	H_2S+C	(2×2)–S,C	1539
Cr(100)	C,O,N	c(2×2)	1126
Cu(110)	Br(a)+H_2O	(3×2)	1557
	C+O_2	(2×1)	1695
	Ni(CO_4)+CO	(1×1)	1048
	O(a)+CO	Disordered	1066
	O(a)+H_2O	(2×1)–O,H_2O	1023
		c(2×2)–O,H_2O	1023
		(2×1)–H_2O	1270
		(1×1)–H_2O,OH	1270
		(2×1)–OH,O	1270
Cu(111)	$Ni(CO)_4$+CO	(1×1)	1048
	O_2+HCN	Disordered	1244
	O(a)+CO	Disordered	1066
	O(a)+CO_2	(2×2)	1142
Fe(110)	K+O_2	c(4×2)	786
Fe(111)	N(a)+K	(3×3)–K,N	1350
Fe–18% Cr–12% Ni(111)	I(a)+H_2O	Oxide Not Formed	1249
	H_2O(a)+I_2	Adsorbed	1249
GaAs(100)	As_4,Ga	(2×4)	1365
		(4×6)	1365
		c(8×2)	1365
		(4×1)	1365
		(3×1)	1365
	HCl,H_2O	(1×1)	1518
	Pb,As_4	(1×2)–Pb	1387

TABLE VIII. Coadsorbed Overlayer Structures (Continued)

Substrate	Adsorbate	Surface Structure	Reference
Hg(110)	O(ad)+SO_2	c(6×2)–SO_3	1027,1371
		(1×2)–SO_4 etc.	1371
	O_2+H_2O	(1×2)–OH	878
		(1×3)–OH	878
Mo(100)	Cs+O_2	c(2×2)+(4×1)	932
		(4×1)	932
		c(2×2)	932
	H_2S+O_2	($\sqrt{5}$×$\sqrt{5}$)R26.6°–S,O	917
	O(a)+CO	(2×1)–O	817
	O(a)+CO_2	(2×1)–O	817
	O(a)+C_2H_4	(2×1)–O	817
	O(a)+HCOOH	(2×1)–O,C	1155
Mo(111)	N_2+NH_3	Disordered	1203
	N_2+NH_3	(433)facet	1203
		c(3×2)–N/Mo(433)	1203
Ni(100)	C(a)+O_2	c(2×2)–O	1177
	CO+H_2	c(3×3)	301
	H_2+CO	c(2×2)–CO,H	1202
		c($\sqrt{2}$×2$\sqrt{2}$)R45°–CO,H	1202
	H_2S,H_2	c(2×2)–S	1121
	H_2S+Na	*c(2×2)Na+c(2×2)S	1887*
		*(2×2)Na+c(2×2)S	1887*
		*(2×2)Na+(2×2)S	1887*
	O(a)+CO	c(2×2)–C,O	1356
	S,C	(1×1)	1561
Ni(110)	CO+O_2	(3×1)–(CO+O_2)	91
	O_2+H_2O	(2×1)–OH	1011
Ni(111)	NI$(CO)_4$,CO	($\sqrt{7}$/2×$\sqrt{7}$/2)R19°–CO	1150
		c(4×2)–CO	1150
Ni(111)	O(a)+H_2O	No New Features	1308
	O(a)+NO	(2×2)	676
Ni(331)	O,CO	(2×3)	1318
Pd(100)	H(a)+O_2	Adsorbed	1163,1454
	H_2,O_2	Disordered	1163
		(2×2)–O,H	1163
	O_2+CO	Disorderd	939
	O_2+H_2O	(2×1)–OH	940
	O(a)+H_2	Not Adsorbed	1163,1454
Pd(111)	O_2+CO	($\sqrt{3}$×$\sqrt{3}$)R30°	691
		(2×1)	691

TABLE VIII. Coadsorbed Overlayer Structures (Continued)

Substrate	Adsorbate	Surface Structure	Reference
Pt(100)	$CO+H_2$	$c(2\times2)$–$(CO+H_2)$	72,74
	$CO+O_2$	(1×1) diffuse	909
		$c(2\times2)$–$CO+(3\times1)$–O	928
	H_2O+HBr	$c(2\sqrt{2}\times\sqrt{2})R45°$–Br,HBr	1258
	Br,HBr(a)+H_2O	Not Adsorbed	1258
	Br,HBr(a)+NH_3	No Affinity	1258
	I(a)+Ag	$(\sqrt{2}\times\sqrt{2})R45°$–I,Ag	1390
		$(10\sqrt{2}\times10\sqrt{2})R45°$–I,Ag	1390
		$(\sqrt{34}\times\sqrt{34})R31°$–I,Ag	1390
	SO_2(a)+NH_3	(1×1) Diffuse	1258
Pt(110)	CO+NO	(1×1)–CO+NO	364
Pt(111)	$C_2H_2+H_2$	*(2×2)–C_2H_3	824,1316,1587
	(O)+C_2H_4	(2×2)	1313
		Ordered	1313
	benzene+CO	$\begin{bmatrix}-2 & 2\\ 5 & 5\end{bmatrix} = \begin{bmatrix}4 & -2\\ 0 & 4\end{bmatrix}$	221,428,429
		*$\begin{bmatrix}4 & -2\\ 0 & 5\end{bmatrix} = \begin{bmatrix}-2 & 2\\ 4 & 4\end{bmatrix}$	428,429,1854*
		$= (2\sqrt{3}\times4)$rect-$2C_6H_6+4CO$	
	DMSO(a)+I_2	Ordered	1258
	DMSO(a)+pyridine	Not Adsorbed	1258
	I(a)+pyridine	Not Adsorbed	1258
		Pyridine Adsorbed	1258
	I(a)+acetnitrile	Acetnitrile Not Adsorbed	1258
	I(a)+DMSO	DMSO Not Adsorbed	1258
	I_2+DMSO	$c(2\times4\sqrt{3}/3)$–I,DMSO	1258
	pyridine(a)+DMSO	Adsorbed	1258
	pyridine(a)+H_2O	Adsorbed	1258
	pyridine(a)+I_2	I_2 Adsorbed	1258
	$H_2+C_2N_2$	Disorderd	1002
	Cl_2+Br_2	$c(2\times4)$–Cl,Br	610
		$(\sqrt{3}\times\sqrt{3})R30°$–Cl,Br	610
		(3×3)–Cl,Br	610
		$(\sqrt{7}\times\sqrt{7})R19.1°$	610
	$CO+O_2$	$(\sqrt{3}\times\sqrt{3})R30°$(misfit)	909
	H_2+O_2	$(\sqrt{3}\times\sqrt{3})R30°$	11
	I_2(a)+HBr	HBr Not Adsorbed	1258
	I(a)+Cu	(3×3)–I,Cu	1556
		(10×10)–I,Cu	1556
	I_2+Ag	(3×3)–Ag,I	937,1106,1391
		(5×5)–Ag,I	937
		(17×17)–Ag,I	937
		$(\sqrt{7}\times\sqrt{7})+(3\times3)$	1391
		$(\sqrt{3}\times\sqrt{3})R30°$–Ag,I	1391

TABLE VIII. Coadsorbed Overlayer Structures (Continued)

Substrate	Adsorbate	Surface Structure	Reference
	K+CO	Disorderd	1255
	$K+O_2$	(4×4)–K,O	1238,1337
		(8×2)	1337
		(10×2)	1337
		K_2O	1337
	$S+O_2$	(2×2)–O	1040
Pt(S)–[6(111)×(100)]	$K(a)+O_2$	(4×4) Potassium Oxide	1337
		(8×2) Potassium Oxide	1337
		(10×2) Potassium Oxide	1337
Rh(100)	$CO(a)+D_2$	Compressed (CO)	1348
	$CO+CH_4$	$c(4\times2)–CO+C_2H_3$	1878
		split $c(2\times2)–CO+C_2H_3$	1878
	C_6H_6+CO	$c(2\sqrt{2}\times4\sqrt{2})R45°–CO+C_6H_6$	1879
	D(a)+CO	c(2×2)	1348
	$NO+D_2$	Disordered	1025
	$Na+H_2O$	$(2\sqrt{3}\times\sqrt{3})R30$	1082
		Complex	1082
Rh(111)		$(\sqrt{3}\times7)$rect	1844
	CO+Na	c(4×2)–CO+Na	1844
	H_2+CO	(2×2)	829
		$(\sqrt{3}\times\sqrt{3})R30°$	829
	$C_2H_2+H_2$	c(4×2)	231,831
	C_2H_2+CO	$c(4\times2)–CO+C_2H_2$	1844,1881
	C_2H_2+Na	Disordered	1876
	$C_2H_4+H_2$	$c(4\times2)–CCH_3$	955
		c(4×2)	1372
		(2×2)+c(4×2)	1256
	C_3H_6+CO	$(2\sqrt{3}\times2\sqrt{3})R30°–CO+C_3H_5$	1884
	Benzene+CO	*c(2√3×4)rect $=\begin{pmatrix}3 & 1\\ 1 & 3\end{pmatrix}–C_6H_6+CO$	1068,1416,1453,1842,1856*
		$*(3\times3)–C_6H_6+2CO$	1068,1842,1855*
	Benzene+Na	$(\sqrt{3}\times\sqrt{3})R30°+(2\sqrt{3}\times3)$rect	1876
	C_6H_5F+CO	(3×3)	1844
	NO+CO	Disordered	1876
Ru(0001)	$CO+O_2$	(2×2)	768
	Na+CO	$(2\sqrt{3}\times2\sqrt{3})R30°$	976
Si(111)	Ag(a)+H	$(\sqrt{3}\times\sqrt{3})R30°$	1536
W(100)	$CO+N_2$	$(4\times1)–(CO+N_2)$	82
	O_2+H_2	$(\sqrt{2}\times\sqrt{2})+(4\times1)$–O,H	815
W(110)	$CO+O_2$	$c(11\times5)–(CO+O_2)$	93
	Pd(1 ML)+CO	Not Adsorbed	1218
	$Pd(2.2\ ML)+O_2$	(2×2)–O	1218
W(221)	$CO+O_2$	$(1\times1)–(CO+O_2)$	108
		$(1\times2)–(CO+O_2)$	108

TABLE IX. Physisorbed Overlayer Structures

Substrate	Adsorbate	Surface Structure	Reference
Ag(110)	Xe	Hexagonal Overlayer	159
Ag(111)	Kr	Hexagonal Overlayer	156
	Xe	Hexagonal Overlayer	156,157,158,159 160
Ag(211)	Xe	Hexagonal Overlayer	159
Au(100)	Xe	Disordered	252
C(0001), graphite	Ar	$(\sqrt{3}\times\sqrt{3})R30°$–Ar	720,960
	Ar	Incommensurate	1882
	Ar+Xe	$(\sqrt{3}\times\sqrt{3})R30°$–Ar,Xe	1193
	CF_4	(2×2)–CF_4	1194
		Close to (2×2)	1404
	CH_4	$(\sqrt{3}\times\sqrt{3})R30°$	1018
	C_2H_6	$(4\times\sqrt{3})$–C_2H_6	1191
		(2×2)–C_2H_6	1191
		$(10\times2\sqrt{3})$–C_2H_6	1191
		$(\sqrt{3}\times\sqrt{3})$–C_2H_6	1191
	CO	$(\sqrt{3}\times\sqrt{3})R30°$–CO	884
		$(2\sqrt{3}\times2\sqrt{3})R30°$–CO	889
		$(2\sqrt{3}\times\sqrt{3})R30°$	884
		Incommensurate(2×2)	884
	H_2	$(\sqrt{3}\times\sqrt{3})R30°$–$H_2$	1283
	Kr	$(\sqrt{3}\times\sqrt{3})R30°$–Kr	166,167,174,721 828,960,1616
		Incommensurate	1616
	N_2	$(2\sqrt{3}\times2\sqrt{3})R30°$–$N_2$	889
		$(\sqrt{3}\times\sqrt{3})R30°$	1064
		$(\sqrt{3}\times\sqrt{3})R30°+(2\times1)$	1435
		Commensurate	1190,1512,1883
		Incommensurate	1443,1190,1512,1883
	Ne	Incommensurate	629
		$(\sqrt{3}\times\sqrt{3})R30°$ rotated by 17°	629
		Layer+Island	960
		Ordered	1338
	NO	Incommensurate	1602
	O_2	Triangular	1883
		Centered-Parallelogram–O_2	1200,1425,1883
		Physisorbed	1411
	Xe	$(\sqrt{3}\times\sqrt{3})R30°$–Xe	165,618,960,1038,1201
Cu(100)	Xe	Hexagonal Overlayer	159
		Disordered	741
Cu(110)	Kr	$c(2\times8)$–Kr	1304,1331
	Xe	$c(2\times2)$–Xe	159,1331,1611
		Hexagonal Overlayer	159,1611
Cu(111)	Xe	$(\sqrt{3}\times\sqrt{3})R30°$–Xe	159
Cu(211)	Kr	Hexagonal Overlayer	156
	Xe	Hexagonal Overlayer	156

TABLE IX. Physisorbed Overlayer Structures (Continued)

Substrate	Adsorbate	Surface Structure	Reference
Cu(311)	Xe	Hexagonal Overlayer	394
Cu(610)	Xe	(2×6)–Xe	790
Ir(100)	Kr	(3×5)–Kr	283
		Kr(111)	283
NaCl(100)	Xe	Hexagonal Overlayer	289
Ni(100)	Xe	Partially Ordered	1268
Pd(100)	Kr	Liquid-like	913
	Xe	Hexagonal Overlayer	311
		Liquid-like	913
Pd(110)	Xe	Hexagonal	743
Pd(S)–[8(100)×(110)]	Xe	1–D Periodicity	1100
Pt(111)	Xe	($\sqrt{3}\times\sqrt{3}$)R30°–Xe	846
		Hexagonal Overlayer	846
Si(111)	Kr	(1×1)	1125
	Xe	(1×1)	1125
W(110)	Xe	(2×2)–Xe	713
		Disordered	713
ZnO(000$\bar{1}$)	Xe	Disordered	1026
ZnO(10$\bar{1}$0)	Xe	Hexagonal	1026

TABLE X. Surface Structures on High-Miller-Index (Stepped) Substrates†

Substrate	Adsorbate	Surface Structure	Reference
Ag(211)	Xe	Hexagonal Overlayer	159
Ag(331)	Cl_2	(6×1)–Cl	393
	O_2	Disordered	393
		Ag(110)–(2×1)–O	393
Al(311)	[clean]	*(1×1)	860*
Au(210)	Pb	(1×1)	497
Au(311)	Pb	(5×3)	496
		(3×3)–Pb	730
		(3×4)–Pb	730
Au(320)	Pb	(3×3)	496
		(1×1)	730
Au(511)	Pb	$\begin{bmatrix}1 & 1\\ 1 & 1\end{bmatrix}$	444
		$\begin{bmatrix}2 & 0\\ 1 & 3\end{bmatrix}$	444
	Pd	c(2×2)	683
		c(7√2×√2)R45°	683
		c(3√2×√2)R45°	683
		c(6×2)	683
Au(711)	Pb	$\begin{bmatrix}1 & 1\\ 1 & -1\end{bmatrix}$	444
		$\begin{bmatrix}2 & 0\\ -1 & 3\end{bmatrix}$	444
	Pd	c(2×2)	683
		c(7√2×√2)R45°	683
		c(3√2×√2)R45°	683
		c(6×2)	683
Au(911)	Pb	$\begin{bmatrix}1 & 1\\ 1 & -1\end{bmatrix}$	444
		$\begin{bmatrix}2 & 0\\ -1 & 3\end{bmatrix}$	444
	Pd	c(2×2)	683
		c(7√2×√2)R45°	683
		c(3√2×√2)R45°	683
		c(6×2)	683
Au(11,1,1)	Pb	$\begin{bmatrix}1 & 1\\ 1 & -1\end{bmatrix}$	444
		$\begin{bmatrix}2 & 0\\ -1 & 3\end{bmatrix}$	444
Au(S)–[6(111)×(100)]	O_2	Oxide	161
Bi(1,0,$\bar{1}$,16)	[clean]	(1×1)	1109

TABLE X. Surface Structures on High-Miller-Index (Stepped) Substrates (Continued)

Substrate	Adsorbate	Surface Structure	Reference
C(0001) [stepped]	K	(1×1)–K	1433
	K	(2×2)–K	1433
	K	No LEED Superstructure	1540
Co(10$\bar{1}$2)	[clean]	(1×1)	698,1584
	CO	Co_3C(001)–(2×3)	698
		(3×1)–CO	698
Cu(210)	O_2	(410),(530)facets	259
		Streak pattern	688
		(2×1)–O	688
		(3×1)–O	688
	N	c(11$\sqrt{2}$×$\sqrt{2}$)R45°–N	794
		(2×3)–N	794
Cu(211)	Kr	Hexagonal Overlayer	156
	O_2	Cu(S)[5(111)×2(100)]	958
	Facet		958
	Pb	(4×1)	484
	Xe	Hexagonal Overlayer	156
Cu(311)	[clean]	*(1×1)	925,1473,1782*
	CO	Adsorbed	394
	Pb	$\begin{pmatrix} 3 & 1 \\ -2 & 1 \end{pmatrix}$	484
		(4×2)	484
	Xe	Hexagonal Overlayer	394
Cu(322)	O_2	(1×1)–O	1257
Cu(410)	O_2	(1×1) Streaked	958
		!(1×1)–O [c(2×2)–O on a terrace]	958!,1133,1257
		!(1×1)–2O	958!
Cu(511)	[clean]	(1×1)	925
	Pb	(4×1)	482
Cu(530)	O_2	(1×1)–O	1257
Cu(610)	Xe	(2×6)–Xe	790
Cu(711)	[clean]	(1×1)	925
	Pb	(4×1)	482,484
Cu(841)	O_2	(410),(100)facets	259
Cu(S)–[3(100)×(100)]	CO	Not Adsorbed	132
	N_2	(1×2)–N	132
Cu(S)–[4(100)×(100)]	CO	Not Adsorbed	132
	N_2	(1×3)–N	132
	O_2	(1×1)–O	132
Cu(S)–[4(100)×(111)]	H_2S	8(1d)–S	35

TABLE X. Surface Structures on High-Miller-Index (Stepped) Substrates (Continued)

Substrate	Adsorbate	Surface Structure	Reference
Fe(210)	[clean]	*(1×1)	1530,1767*
Fe(211)	[clean]	*(1×1)	1460*,1531
Fe(310)	[clean]	*(1×1)	1410*,1530
Fe(12,1,0)	N_2	Reconstruction by Nitride Formation	669
GaAs(211)	[clean]	(110)facets	936
Ge(210)	[clean]	(2×2)	804,1683
Ge(211)	[clean]	(3×1) (311)facets	936
		(1×2)	804,1683
Ge(311)	[clean]	(3×1)	804,1683
Ge(331)	[clean]	(5×1)	804,1683
Ge(510)	[clean]	(1×2)	804,1683
Ge(511)	[clean]	(3×1)	804,1683
Ge(551)	[clean]	(5×2)	804,1683
Ir(S)–[6(111)×(100)]	CO	Disordered	182
	H_2	Adsorbed	187
	H_2O	Not Adsorbed	182
	O_2	(2×1)–O	182
LaB_6(210)	O_2	Disordered	1624
Mo(100)[Stepped]	Cs	(2×2)	932
		c(2×2)	932
	Cs(a)+O_2	c(2×2)	932
		Disordered	932
Mo(211)	Ba	(1×5)	1591,1675
		(4×2)	1591
	Cs	c(2×1/J),0.15<J<0.64	1590
		c(2×2)	1590
	CO	Disordered	105
	H_2	(1×2)–H	105
	La	Linear Chains	1447
		c(2×2)	1447
		c(2×4/3)	1447
	Li	(1×4)–Li	1593
		(1×2)–Li	1593
		(1×1)–Li	1593
	N_2	Not Adsorbed	105
	Na	(1×4)–Na	1684
		(1×3)–Na	1684
		(1×2)–Na	1684
		(1×3/2)–Na	1684
	O_2	(2×1)–O	105
		(1×2)–O	105
		(1×3)–O	105
		c(4×2)–O	105
	Sr	(1×9)–Sr	1594
		(1×5)–Sr	1594
		(4×2)–Sr	1594
Nb(750)	O_2	(110)Terrace+(310)Step	1688

TABLE X. Surface Structures on High-Miller-Index (Stepped) Substrates (Continued)

Substrate	Adsorbate	Surface Structure	Reference
Ni(210)	N_2	Ni(100)–$(6\sqrt{2}\times\sqrt{2})R45°$–N	395
		$c(11\sqrt{2}\times\sqrt{2})R45°$–N	794
		(2×3)–N	794
		Ni(110)–(2×3)–N	395
	O_2	Facets	395,794
Ni(211)	O_2	NiO	1351
Ni(311)	[clean]	*(1×1)	900*,1473,1885*,1886*
Ni(331)	[clean]	(1×1)	1247,1893
	S	(1×2)–S	1893
		(2×5)–S	1893
		(2×1)–S	1893
	O,CO	(2×3)	1893
Ni(hk0)[(210)to(410)]	[clean]	Ordered	871
	O_2	Facets	871
Ni(S)–[3(100)×(111)]	H_2S	(2×2)	1055
Ni(S)–[5(100)×(111)]	[clean]	Streaks	1055
	CO	Streaks Disappear	1055
	H_2S	Streaks Disappear	1055
$Ni_4Mo(211)$	[clean]	Ordered	1115
Pd(111)[Stepped]	NO	c(4×2)–NO	1236
		(2×2)–NO	1236
Pd(210)	CO	(1×1)–CO	209,210
		(1×2)–CO	209,210
Pd(311)	CO	(2×1)–CO	209
		3(1 dimensional order)–CO	209
Pd(331)	O_2	Disordered	675
		2(1 dimensional order)	675
		$\begin{bmatrix}1 & 2\\2 & 0\end{bmatrix}$–O	675
	NO	Disordered	675
Pd(S)–[8(100)×(110)]	Xe	1-D Periodicity	1100
Pd(S)–[9(111)×(111)]	CO	$(\sqrt{3}\times\sqrt{3})R30°$–CO	209
		Hexagonal Overlayer	209
Pt(321)	[clean]	Ordered	1212
	O_2	Disordered	760
Pt(654)	O_2	$(\sqrt{3}\times\sqrt{3})R30°$–O	760
Pt(997)	[clean]	(1×1)	1226,1278
	O_2	Pt(S)–[(17(111)×2(11$\bar{1}$)]–O	1226,1278
Pt(12,9,8)	O_2	$(\sqrt{3}\times\sqrt{3})R30°$–O	760
Pt(12,11,9)	[clean]	(1×1)	1226
Pt(62,62,60)	[clean]	(1×1)	1226
		(2×2)–O	760
Pt(S)–[4(111)×(100)]	CO	Disordered	899
	H_2	Facets	221
Pt(S)–[5(100)×(111)]	O_2	(1×1)–O	708,1171
		$(2\sqrt{2}\times\sqrt{2})R45°$–O	708,1171
		Terrace Broadening and Diffused Background	1171

TABLE X. Surface Structures on High-Miller-Index (Stepped) Substrates (Continued)

Substrate	Adsorbate	Surface Structure	Reference
Pt(S)–[6(111)×(111)]	I_2	(3×3)or($\sqrt{3}\times\sqrt{3}$)R30° Domains	930
	NH_3	Adsorbed	626
	O_2	($\sqrt{3}\times\sqrt{3}$)R30°–PtO_2(0001)	805
		($4\sqrt{3}\times2\sqrt{3}$)R30°–PtO_2(0001)	805
Pt(S)–[6(111)×(100)]	CO	Disordered	120
	H_2	2(1 dimensional order)–H	120,221
		Adsorbed	396
		Pt(S)–[11(111)×2(100)]	396
	K(a)+O_2	(4×4) Potassium Oxide	1337
		(8×2) Potassium Oxide	1337
		(10×2) Potassium Oxide	1337
	O_2	2(1 dimensional order)–O	120
		Pt(111)–(2×2)–O	215,708,1171
		Pt(111)–($\sqrt{3}\times\sqrt{3}$)R30°–O	215
		Pt(111)–($\sqrt{79}\times\sqrt{79}$)–R18°7′–O	215
		Pt(111)–($4\times2\sqrt{3}$)–R30°–O	215
		Pt(111)–3(1 dimensional order)–O	215
		Reconstructed (2×2)	1171
		Terrace Broadening	
Pt(S)–[7(111)×(310)]	O_2	($\sqrt{3}\times\sqrt{3}$)–R30°–O	760
		(2×2)–O	760
Pt(S)–[9(111)×(100)]	H_2	2(1 dimensional order)–H	221
	H_2S	(2×2)–S	1339
		($\sqrt{3}\times\sqrt{3}$)–R30°–S	1339
Pt(S)–[9(111)×(111)]	C_2N_2	Disordered	685
	CO	Disordered	120,685
		($\sqrt{3}\times\sqrt{3}$)R30°–CO	685
		c(4×2)–CO	685
	H_2	(2×2)–H	120
		Adsorbed	400
	N	Disordered	228
	O_2	(2×2)–O	397,398,399,685
		Not Adsorbed	120
Pt(S)–[12(111)×(111)]	NH_3	Disordered	401
	NO	(2×2)–NO	401
	O_2	(2×2)–O	689
Pt(S)–[13(111)×(310)]	O_2	(2×2)–O	708,1171
		($\sqrt{3}\times\sqrt{3}$)R30°–O	708
		Reconstructed (2×2)	1171
		Terrace Broadening	
Pt(S)–[20(111)×(111)]	O_2	(2×2)–O	1013
Re(S)–[6(0001)×(16$\bar{7}$6)]	O_2	ReO_3 Reconstruction	1654
Re(S)–[14(0001)×(10$\bar{1}$1)]	CO	(2×2)–CO	230
		(2×1)–C	230
	H_2	Disordered	663
Re(S)–[(14(0001)×(16$\bar{7}$1)]	H_2	Disordered	664
Re(S)[16(0001)×2(10$\bar{1}$1)]	O_2	(2×2)	1515

TABLE X. Surface Structures on High-Miller-Index (Stepped) Substrates (Continued)

Substrate	Adsorbate	Surface Structure	Reference
Rh(331)	[clean]	(1×1)	839
	CO	$\begin{bmatrix}1 & 2\\ 5 & -1\end{bmatrix}$–CO	402,722
		$\begin{bmatrix}1 & 2\\ 2 & 0\end{bmatrix}$–CO	402
		Hexagonal Overlayer	402
	CO_2	$\begin{bmatrix}1 & 2\\ 5 & -1\end{bmatrix}$–CO	402
		$\begin{bmatrix}1 & 2\\ 2 & 0\end{bmatrix}$–CO	402,722
		Hexagonal Overlayer	402,722
	H_2	Adsorbed	402
		(1×1)	722
	NO	Disordered	402
		$\begin{bmatrix}-1 & 1\\ 3 & 0\end{bmatrix}$	402
	O_2	2(1 dimensional order)–O	402,722
		$\begin{bmatrix}1 & 2\\ 2 & 0\end{bmatrix}$–O	402,722
		$\begin{bmatrix}1 & 2\\ 7 & -1\end{bmatrix}$–O	402,722
		Facets	402
Rh(S)–[6(111)×(100)]	CO	$(\sqrt{3}\times\sqrt{3})$–R30°–CO	402,722
		(2×2)–CO	402
	CO_2	$(\sqrt{3}\times\sqrt{3})$–R30°–CO	402
		(2×2)–CO	402,722
	H_2	Adsorbed	402
		(1×1)	722
	NO	(2×2)–NO	402,722
	O_2	(2×2)–O	402,722
		Rh(S)–[12(111)×2(100)]–(2×2)–O	402
		Rh(111)–(2×2)–O	402
Si(111)[Stepped]	Ni	Si(221)–(2×2)	964
	Pd	Si(221)–(2×2)	964
	Si+laser	Unchanged	1392
Si(210)	[clean]	(2×2)	803,1685
Si(211)	[clean]	Complex	1317
		(4×2)	803,936,1685
	Ga	Ordered	1317
	H_2	Ordered (facet)	1317
Si(311)	[clean]	(3×2)	803,1685
	NH_3	Adsorbed	238

TABLE X. Surface Structures on High-Miller-Index (Stepped) Substrates (Continued)

Substrate	Adsorbate	Surface Structure	Reference
Si(320)	[clean]	(1×2)	803,1685
		(1×1)	803
		Facet	803
Si(331)	[clean]	(13×1)	803
		(13×2)	1685
Si(510)	[clean]	(1×2)	803,1685
Si(511)	[clean]	(3×1)	803,1685
Si(S)–[14(111)×($\bar{1}\bar{1}$2)]	Si	(1×1)	1517
Si(hkl)([001]zone)	[clean]	Facets	892
	Au	Diffuse	892
		Facets	892
		3d–Au clusters	892
Ta(211)	CO	Disordered	101,102
		(3×1)–O	102
	H_2	(1×1)–H	102
	N_2	Disordered	102
		(311) facets	102
	O_2	(3×1)–O	101,102
Ti_2O_3 (047)	[clean]	(1×1)	1020
		Oxide	101,102
W(100)[Stepped]	[clean]	($\sqrt{2}$×$\sqrt{2}$)R45°	1243
W(210)	CO	(2×1)–CO	138,575,1647
		(1×1)–CO	138
	N_2	(2×1)–N	131,575,887,1647
W(211)	[clean]	(1×1)	887
		(1×2)	1147
		(2×2)	1147
	Ag	(1×1)–Ag	969
	Au	(1×1)	969
		(1×2)	969
		(1×3)	969
		(1×4)	969
	C	c(10×4)–C	887
		c(6×4)–C	887
	CO	c(2×4)–C,O	887
	H_2S	c(2×6)–S	887
		c(2×2)–S	887
	Li	(4×1)	518,520
		(3×1)	518,520
		(2×1)	518,520
		Incoherent	518,520
		(1×1)	518,520
	Mg	(1×7)–Mg	1657
		(3×3)–Mg	1657
	Na	(2×1)	521
		Compressed(2×1)	521

TABLE X. Surface Structures on High-Miller-Index (Stepped) Substrates (Continued)

Substrate	Adsorbate	Surface Structure	Reference
	O_2	(2×1)–O	15,106,107,108,403, 404,887,1415,1431
		(1×1)–O	106,107,403,404,887
		(1×2)–O	15,106,404,887
		(1×3)–O	106
		(1×4)–O	106,404
		(1×n)–O (n=3–7)	887
	Sb	(2×1)	553
		(1×1)	553
W(221)	CO	Disordered	108
		c(6×4)–CO	108
		(2×1)–CO	108
		c(2×4)–CO	108
	$CO+O_2$	(1×1)–$CO+O_2$	108
		(1×2)–$CO+O_2$	108
	H_2	(1×1)–H	112
	Na	Compressed(2×1)	521
		(2×1)	521
	Ni	(1×1)–Ni	970
		(6×1)–Ni	970
	NH_3	c(4×2)–NH_2	113
	O_2	(2×1)–O	15,106,107,108 403,404
		(1×2)–O	15,106,404
		(1×1)–O	106,107,403,404
		(1×3)–k	106
		(1×4)–O	106,404
W(310)	N_2	(2×1)–N	131
		c(2×2)–N	131
	O_2	(2×1)–O	1389
W(S)–[6(110)×(1$\bar{1}$0)]	O_2	(2×1)–O	382
W(S)–[8(110)×(112)]	O_2	(2×1)–O	382
W(S)–[10(110)×(0$\bar{1}$1)]	O_2	(2×1)–O	405
W(S)–[12(110)×(1$\bar{1}$0)]	O_2	(2×1)–O	382
W(S)–[13(001)×(1$\bar{1}$0)]	H_2	$(\sqrt{2}\times\sqrt{2})R45°$–H	945
		Incommensurate	945
		(1×1)–H	945
W(S)–[16(110)×(112)]	O_2	(2×1)–O	382
W(S)–[24(110)×(011)]	O_2	(2×1)–O	405
ZnO(40$\bar{4}$1)	[clean]	Similar to 1×1	1239
ZnO(50$\bar{5}$1)	[clean]	Similar to 1×1	1239

†Organic overlayer structures are not included. See Table VII for these structures.

References for Tables I—X

1. K. Muller, *Zeits. Naturforschung 20A*, 153 (1965).
2. A. U. MacRae, *Surface Sci. 1*, 319 (1964).
3. L. H. Germer, E. J. Schneiber and C. D. Hartman, *Phil. Mag. 5*, 222 (1960).
4. R. L. Park and H. E. Farnsworth, *Appl. Phys. Letters 3*, 167 (1963).
5. T. Edmonds and R. C. Pitkethly, *Surface Sci. 15*, 137 (1969).
6. A. U. MacRae, *Science 139*, 379 (1963).
7. G. Ertl, *Surface Sci. 6*, 208 (1967).
8. N. Takahashi et al., *C. R. Acad. Sci. 269 B*, 618 (1969).
9. G. W. Simmons, D. F. Mitchell and K. R. Lawless, *Surface Sci. 8*, 130 (1967).
10. C. W. Tucker, Jr., *Surface Sci. 2*, 516 (1964).
11. C. W. Tucker, Jr., *J. Appl. Phys. 35*, 1897 (1964).
12. J. T. Grant and T. W. Haas, *Surface Sci. 21*, 76 (1970)
13. W. P. Ellis, *J. Chem. Phys. 48*, 5695 (1968).
14. J. Ferrante and G. C. Barton, NASA Tech. Note D-4735 (1968).
15. N. J. Taylor, *Surface Sci. 2*, 544 (1964).
16. J. B. Marsh and H. E. Farnsworth, *Surface Sci. 1*, 3 (1964)
17. R. E. Schlier and H. E. Farnsworth, *J. Chem. Phys. 30*, 917 (1959).
18. H. E. Farnsworth, R. E. Schlier, T. H. George and R. M. Buerger, *J. Appl. Phys. 29*, 1150 (1958).
19. J. J. Lander and J. Morrison, *J. Appl. Phys. 34*, 1411 (1963).
20. J. J. Lander and J. Morrison, *J. Appl. Phys. 33*, 2089 (1962).
21. G. Rovida et al., *Surface Sci. 14*, 93 (1969).
22. R. O. Adams, *The Structure and Chemistry of Solid Surfaces*, ed. G. A. Somorjai, John Wiley and Sons, Inc., New York (1969).
23. H. E. Farnsworth and D. M. Zehner, *Surface Sci. 17*, 7 (1969).
24. G. J. Dooley and T. W. Haas, *Surface Sci. 19*, 1 (1970).
25. B. D. Campbell, C. A. Haque and H. E. Farnsworth, *The Structure and Chemistry of Solid Surfaces*, ed. G. A. Somorjai, John Wiley and Sons, Inc., New York, 1969.
26. G. Ertl, *Surface Sci. 7*, 309 (1977).
27. T. Edmonds and R. C. Pitkethly, *Surface Sci. 17*, 450 (1969).
28. A. E. Morgan and G. A. Somorjai, *J. Chem. Phys. 51*, 3309 (1969).
29. J. C. Bertolini and G. Dalmai-Imelik, Coll. Intern. CNRS, Paris, 7–11 July 1969.
30. J. J. Lander and J. Morrison, *Surface Sci. 4*, 241 (1966).
31. L. H. Germer and A. U. MacRae, *J. Chem. Phys. 36*, 1555 (1962).
32. A. J. van Bommel and F. Meyer, *Surface Sci. 8*, 381 (1967).
33. J. J. Lander and J. Morrison, *J. Chem. Phys. 37*, 729 (1962).
34. R. Heckingbottom, *The Structure and Chemistry of Solid Surfaces*, ed. G. A. Somorjai, John Wiley and Sons, Inc., New York (1969).
35. J. L. Domange and J. Oudar, *Surface Sci. 11*, 124 (1968).
36. M. Perdereau and J. Oudar, *Surface Sci. 20*, 80 (1970).
37. A. J. van Bommel and F. Meyer, *Surface Sci. 6*, 391 (1967).
38. J. V. Florio and W. D. Robertson, *Surface Sci. 18*, 398 (1969).
39. J. C. Bertolini and G. Dalmai-Imelik, Rapport Inst. de Rech. sur la Catalyse, Villeurbanne (1969).
40. D. L. Smith and R. F. Merrill, *J. Chem. Phys. 52*, 5861 (1970).
41. M. Boudart and D. F. Ollis, *The Structure and Chemistry of Solid Surfaces*, ed., G. A. Somorjai, John Wiley and Sons, Inc., New York (1969).
42. F. Jona, *J. Phys. Chem. Solids 28*, 2155 (1967).
43. S. M. Bedair, F. Hoffmann and H. P. Smith, Jr., *J. Appl. Phys. 39*, 4026 (1968).
44. H. H. Farrell, Ph.D. Dissertation, University of California, Berkeley (1969).
45. L. K. Jordan and E. J. Scheibner, *Surface Sci. 10*, 373 (1968).
46. L. Trepte, C. Menzel-Kopp and E. Mensel, *Surface Sci. 8*, 223 (1967).
47. R. N. Lee and H. E. Farnsworth, *Surface Sci. 3*, 461 (1965).
48. J. T. Grant, *Surface Sci. 18*, 228 (1969).
49. R. E. Schlier and H. E. Farnsworth, *J. Appl. Phys. 25*, 1333 (1954).
50. H. E. Farnsworth and J. Tuul, *J. Phys. Chem. Solids 9*, 48 (1958).
51. J. W. May and L. H. Germer, *Surface Sci. 11*, 443 (1968).
52. R. E. Schlier and H. E. Farnsworth, *Advances Catalysis 9*, 434 (1957).

53. L. H. Germer and C. D. Hartman, *J. Appl. Phys. 31*, 2085 (1960).
54. H. E. Farnsworth and H. H. Madden, Jr., *J. Appl. Phys. 32*, 1933 (1961).
55. R. L. Park and H. E. Farnsworth, *J. Chem. Phys. 43*, 2351 (1965).
56. L. H. Germer, *Advances Catalysis 13*, 191 (1962).
57. L. H. Germer, R. Stern and A. U. MacRae, Metal Surfaces ASM, Metals Park, Ohio, 1963, p. 287.
58. C. W. Tucker, Jr., *J. Appl. Phys. 37*, 3013 (1966).
59. C. A. Haque and H. E. Farnsworth, *Surface Sci. 1*, 378 (1964).
60. A. J. Pignocco and G. E. Pellissier, *J. Electrochem. Soc. 112*, 1188 (1965).
61. H. K. A. Kann and S. Feuerstein, *J. Chem. Phys. 50*, 3618 (1969).
62. K. Hayek and H. E. Farnsworth, *Surface Sci. 10*, 429 (1968).
63. H. E. Farnsworth and K. Hayek, Suppl. Nuovo Cimento 5, 2 (1967).
64. G. J. Dooley and T. W. Haas, *J. Chem. Phys. 52*, 461 (1970).
65. K. K. Vijai and P. F. Packman, *J. Chem. Phys. 50*, 1343 (1969).
66. P. J. Estrup, *The Structure and Chemistry of Solid Surfaces*, ed. G.A. Somorjai, John Wiley and Sons, Inc., New York, 1969.
67. J. Anderson and W. E. Danforth, J. Franklin Inst. 279, 160 (1965).
68. M. Onchi and H. E. Farnsworth, *Surface Sci. 11*, 203 (1968).
69. R. A. Armstrong, *The Structure and Chemistry of Solid Surfaces*, ed. G. A. Somorjai, John Wiley and Sons, Inc., New York (1969).
70. J. C. Tracy and P. W. Palmberg, *J. Chem. Phys. 51*, 4852 (1969).
71. R. L. Park and H. H. Madden, *Surface Sci. 11*, 188 (1968).
72. A. E. Morgan and G. A. Somorjai, *Surface Sci. 12*, 405 (1968).
73. C. Burggraf and A. Mosser, C. R. Acad. Sci. 268 B, 1167 (1969).
74. A. E. Morgan and G. A. Somorjai, *Trans. Am. Cryst. Assoc. 4*, 59, (1968).
75. J. Anderson and P. J. Estrup, *J. Chem. Phys. 46*, 563 (1967).
76. M. Onchi and H. E. Farnsworth, *Surface Sci. 13*, 425 (1969).
77. G. J. Dooley and T. W. Haas, *J. Chem. Phys. 52*, 993 (1970).
78. P. W. Tamm and L. D. Schmidt, *J. Chem. Phys. 51*, 5352 (1969).
79. P. J. Estrup and J. Anderson, *J. Chem. Phys. 45*, 2254 (1966).
80. H. H. Madden and H. E. Farnsworth, *J. Chem. Phys. 34*, 1186 (1961).
81. J. W. May and L. H. Germer, *The Structure and Chemistry of Surface*, ed. G. A. Somorjai, John Wiley and Sons, Inc., New York (1969).
82. P. J. Estrup and J. Anderson, *J. Chem. Phys. 46*, 567 (1967).
83. T. L. Park and H. E. Farnsworth, *J. Appl. Phys. 35*, 2220 (1964).
84. P. J. Estrup and J. Anderson, *J. Chem. Phys. 49*, 523 (1968).
85. E. Margot et al., *C. R. Acad. Sci. 270 C*, 1261 (1970).
86. N, W. Wideswell and J. M. Ballingal, *J. Vac. Sci. Techn. 7*, 496 (1970).
87. F. Portele, *Zeits. Naturforschung 24A*, 1268 (1969).
88. G. Dalmai-Imelik and J. C. Bertolini, *C. R. Acad. Sci. 270*, 1079 (1970).
89. L. H. Germer and A. U. MacRae, *J. Appl. Phys. 33*, 2923 (1962).
90. L. H. Germer, A. U. MacRae and A. Robert, Welch Foundation Research Bull. No. 11, 1961, p. 5.
91. R. L. Park and H. E. Farnsworth, *J. Chem. Phys. 40*, 2354 (1964).
92. L. H. Germer, J. W. May and R. J. Szostak, *Surface Sci. 7*, 430 (1967).
93. J. W. May, L. H. Germer and C. C. Chang, *J. Chem. Phys. 45*, 2383 (1966).
94. A. G. Jackson and M. P. Hooker, *Surface Sci. 6*, 297 (1967).
95. G. Ertl and P. Rau, *Surface Sci. 15*, 443 (1969).
96. C. W. Tucker, Jr., *J. Appl. Phys. 38*, 2696 (1967).
97. C. W. Tucker, Jr., *J. Appl. Phys. 37*, 4147 (1966).
98. A. J. Pignocco and G. E. Pellisier, *Surface Sci. 7*, 261 (1967).
99. K. Moliere and F. Portele, *The Structure and Chemistry of Solid Surfaces*, ed. G. A. Somorjai, John Wiley and Sons, Inc., N. Y. (1969).
100. T. W. Haas and A. G. Jackson, *J. Chem. Phys. 44*, 2921 (1966).
101. T. W. Haas, A. G. Jackson and M. P. Hooker, *J. Chem. Phys. 46*, 3025 (1967).
102. T. W. Haas, *The Structure and Chemistry of Solid Surfaces*, ed. G. A. Somorjai, John Wiley and Sons, Inc., N. Y. 1969.
103. L. H. Germer, *Physics Today*, July 1964, p. 19.
104. L. H. Germer and J. W. May, *Surface Sci. 4*, 452 (1966).
105. G. J. Dooley and T. W. Haas, *J. Vac. Sci. Techn. 7*, 49 (1970).
106. C. C. Chang and L. H. Germer, *Surface Sci. 8*, 115 (1967).
107. T. C. Tracy and J. M. Blakeley, *The Structure and Chemistry of Solid Surfaces*, ed. G. A. Somorjai, John Wiley and Sons, Inc., N. Y. (1969).

108. C. C. Chang, *J. Electrochem. Soc. 115*, 354 (1968).
109. J. W. May and L. H. Germer, *J. Chem. Phys. 44*, 2895 (1966).
110. L. H. Germer and A. U. MacRae, Proc. Natl. Acad. Sci. U.S. 48, 997 (1962).
111. T. W. Haas, *J. Appl. Phys. 39*, 5854 (1968).
112. D. L. Adams et al., *Surface Sci. 22*, 45 (1970).
113. J. W. May, R. J. Szostak and L. H. Germer, *Surface Sci. 15*, 37 (1969)
114. D. H. Buckley, NASA Techn. Note D-5689, 1970.
115. I. Marklund, S. Andersson and J. Martinsson, *Arkiv for Fysik 37*, 127 (1968).
116. P. Legare and G. Marie, *J. Chim. Phys. Physsichim. Biol. 68*(7–8), 120 (1971).
117. G. Marie, J. R. Anderson, and B. B. Johnson, *Proc. Roy. Soc. Lond. A*, 320, 227 (1970).
118. T. Edmonds, J. J. McCarrol and R. C. Pitkethly, *J. Vac. Sci. Tech. 8*(1) 68 (1971).
119. K. Okado, T. Halsushika, H. Tomita, S. Motov and N. Takalashi, *Shinku 13* (11), 371 (1970).
120. B. Lang, R. W. Joyner, and G. A. Somorjai, *Surf. Sci. 30*, 454 (1972).
121. M. Henzler, and J. Topler, *Surf. Sci. 40*, 388 (1973).
122. H. Van Hove, R. Leysen, *Phys. Status Solidi A 9*(1), 361 (1972).
123. S. M. Bedair and H. P. Smith, Jr., *J. Appl. Phys. 42*, 3616 (1971).
124. J. T. Grant, *Surface Sci. 25*, 451 (1971).
125. R. W. Joyner, C. S. McKee and M. W. Roberts, *Surface Sci. 26*, 303 (1971).
126. J. C. Tracy, *J. Chem. Phys. 56*(6), 2748 (1971).
127. M. A. Chester, and J. Pritchard, *Surface Sci. 28*, 460 (1971).
128. R. W. Joyner, C. S. McKee and M. W. Roberts, *Surface Sci. 27*, 279 (1971).
129. J. C. Tracy, *J. Chem. Phys. 56*(6), 2736 (1971).
130. D. Tabor and J. M. Wilson, *J. Cryst. Growth 9*, 60 (1971).
131. D. L. Adams and L. H. Germer, *Surface Sci. 27*, 21 (1971).
132. J. Perdereau and G. E. Rhead, *Surface Sci. 24*, 555 (1971).
133. P. W. Palmberg, *Surface Sci. 25*, 104 (1971).
134. G. Ertl and J. Kuppers, *Surface Sci. 24*, 104 (1971).
135. R. Heckingbottom and P. R. Wood, *Surface Sci. 23*, 437 (1970).
136. K. J. Matysik, *Surface Sci. 29*, 324 (1972).
137. G. E. Becker and H. D. Hagstrum, *Surface Sci. 30*, 505 (1972).
138. D. L. Adams and L. H. Germer, *Surface Sci. 32*, 205 (1972).
139. H. P. Bonzel and R. Ku, *Surface Sci. 33*, 91 (1972).
140. P. Michel and Ch. Jardin, *Surface Sci. 36*, 478 (1973).
141. A. Melmed and J. J. Carroll, *J. Vac. Sci. Technol. 10*, 164 (1973).
142. H. D. Hagstrum and G. E. Becker, *Phys. Rev. Lett. 22*, 1054 (1969); *J. Chem. Phys. 54*, 1015 (1971).
143. W. H. Weinberg and R. P. Merrill, *Surface Sci. 32*, 317 (1972).
144. P. B. Sewell, D. F. Mitchell and M. Cohen, *Surface Sci. 33*, 535 (1972).
145. F. Forstmann, W. Berndt and P. Buttner, *Phys. Rev. Lett. 30*, 17 (1973).
146. H.A. Engelhardt and D. Menzel, *Surface Sci. 57*, 591 (1976).
147. H. Albers, W. J. J. VanderWal and G. A. Bootsma, *Surface Sci. 68*, 47 (1977).
148. G. Rovida, F. Pratesi, M. Maglietta and E. Ferroni, *Surface Sci. 43*, 230 (1974).
149. W. Berndt, Proc 2nd International Conference on Solid Surfaces 653 (1974).
150. F. Forstmann, Proc 2nd International Conference on Solid Surfaces 657 (1974).
151. P. J. Goddard and R. M. Lambert, *Surface Sci. 67*, 180 (1977).
152. Y. Tu and J. M. Blakely, *Journal of Vacuum Science Technology 15*, 563 (1978).
153. G. Rovida, F. Pratesi, M. Maglietta and E. Ferroni Proc 2nd International Conference on Solid Surfaces, 117 (1974).
154. G. Rovida and F. Pratesi, *Surface Sci. 51*, 270 (1975).
155. P. J. Goddard, K. Schwaha and R. M. Lambart, *Surface Sci. 71*, 351 (1978).
156. R. H. Roberts and J. Pritchard, *Surface Sci. 54*, 687 (1976).
157. N. Stone, M. A. VanHove, S. Y. Tong and M. B. Webb, *Physical Review Letter 40*, 273 (1978).
158. G. McElhiney, H. Papp and J. Pritchard, *Surface Sci. 54*, 617 (1976).
159. M. A. Chesters, M. Hussain and J. Pritchard, *Surface Sci. 35*, 161 (1973).
160. P. I. Cohen, J. Unguris and M. B. Webb, *Surface Sci. 58*, 429 (1976).
161. M. A. Chesters and G. A. Somorjai, *Surface Sci. 52*, 21 (1975).
162. D. M. Zehner and J. F. Wendelken, Proc. 7th Internal Vacuum Congress and 3rd International Conference on Solid Surfaces 517 (1977).
163. P. J. Goddard, J. West and R. M. Lambert, *Surface Sci. 71*, 447 (1978).
164. P. G. Lurie and J. M. Wilson, *Surface Sci. 65*, 453 (1977).
165. J. Suzanne, J. P. Coulomb and M. Bienfait, *Surface Sci. 40*, 414 (1973).

166. M. D. Chinn and S. C. Fain, Jr., *Journal of Vacuum Science Technology 14*, 314 (1977).
167. H. M. Kramer and J. Suzanne, *Surface Sci. 54*, 659 (1976).
168. M. E. Bridge, C. M. Comrie and R. M. Lambert, *Surface Sci. 67*, 393 (1977).
169. C. Jardin and P. Michel, *Surface Sci. 71*, 575 (1978).
170. F. H. P. M. Habraken, E. P. Kieffer and G. A. Bootsma, Proc 7th International Vacuum Congress and 3rd International Conference on Solid Surfaces 877 (1977).
171. L. McDonnel and D. P. Woodruff, *Surface Sci. 46*, 505 (1974).
172. J. Kessler and F. Thieme, *Surface Sci. 67*, 405 (1977).
173. C. Benndorf, K. H. Gressman and F. Thieme, *Surface Sci. 61*, 646, (1976).
174. M. D. Chinn and S. C. Fain, Jr., *Physical Review Letters 39*, 146 (1977).
175. S. Nakanishi and T. Horiguchi, Proc. 7th International Vacuum Congress and 3rd International Conference on Solid Surfaces, A2727 (1977).
176. M. Grunze, F. Bozso, G. Ertl and M. Weiss, *Applications of Surface Science 1*, 241 (1978).
177. F. Bozso, G. Ertl, M. Grunze and M. Weiss, *Applications of Surface Science 1*, 103 (1978).
178. B. Z. Olshanetsky, S. M. Repinsky and A. A. Shklyaev, *Surface Sci. 64*, 224 (1977).
179. S. Sinharoy and M. Henzler, *Surface Sci. 51*, 75 (1975).
180. V. P. Ivanov, G. K. Boreshov, V. I. Savchenko, W. F. Egelhoff, Jr. and W. H. Weinberg, *Journal of Catalysis 48*, 269 (1977).
181. H. Conrad, J. Kuppers, F. Nitschke and A. Plagge, *Surface Sci. 69*, 668 (1977).
182. D. I. Hagen, B. E. Nieuwenhuys, G. Rovida and G. A. Somorjai, *Surface Sci. 57*, 632 (1976).
183. J. Kuppers and A. Plagge, *Journal of Vacuum Science Technology 13*, 259 (1976).
184. V. P. Ivanov, G. K. Boreskov, V. I. Savchenko, W. F. Egelhoff, Jr. and W. H. Weinberg, *Surface Sci. 61*, 207 (1976).
185. C. M. Comrie and W. H. Weinberg, *Journal of Vacuum Science Technology 13*, 264 (1976).
186. C. M. Comrie and W. H. Weinberg, *J. Chem. Phys. 64*, 250 (1976).
187. B. E. Nieuwenhuys, D. I. Hagen, G. Rovida and G. A. Somorjai, *Surface Sci. 59*, 155 (1976).
188. J. Kanski and T. N. Rhodin, *Surface Sci. 65*, 63 (1977).
189. L. J. Clark, Proc 7th International Vacuum Congress and 3rd International Conference on Solid Surfaces, A2725 (1977).
190. H. M. Kennett and A. E. Lee, *Surface Sci. 48*, 606 (1975).
191. J. M. Wilson, *Surface Sci. 59*, 315 (1976).
192. R. Pantel, M. Bujor and J. Bardolle, *Surface Sci. 62*, 739 (1977).
193. H. Conrad, G. Ertl, J. Kuppers and E. E. Latta, *Surface Sci. 50*, 296 (1975).
194. P. H. Holloway and J. B. Hudson, *Surface Sci. 43*, 141 (1974).
195. H. Conrad, G. Ertl, J. Kuppers and E. E. Latta, *Surface Sci. 57*, 475 (1976).
196. W. Erley, K. Besoche and H. Wagner, *J. Chem. Phys. 66*, 5269 (1977).
197. P.M. Marcus, J.E. Demuth and D.W. Jepsen, *Surface Sci. 53*, 501 (1975).
198. J. E. Demuth, and T. N. Rhodin, *Surface Sci. 45*, 249 (1974).
199. G. Ertl, *Surface Sci. 47*, 86 (1975).
200. K. Christmann, O. Schober and G. Ertl, *J. Chem. Phys. 60*, 4719 (1974).
201. M. A. Van Hove, G. Ertl, W. H. Weinberg, K. Christmann and H.J. Behm, Proc 7th International Vacuum Congress and 3rd International Conference on Solid Surfaces, 2415 (1977).
202. H. Conrad, G. Ertl, J. Kuppers and E. E. Latta, *Surface Sci. 58*, 578 (1976).
203. K. Christmann, O. Schober, G. Ertl and M. Neumann, *J. Chem. Phys. 60*, 4528 (1974).
204. G. Casalone, M. G. Cattania, M. Simonetta and M. Tescari, *Surface Sci. 72*, 739 (1978).
205. J. E. Demuth, D. W. Jepsen and P. M. Marcus, *Phys. Rev. Lett. 32*, 1182 (1974).
206. W. Erley and H. Wagner, *Surface Sci. 66*, 371 (1977).
207. H. Conrad, G. Ertl, J. Kuppers and E. E. Latta, *Surface Sci. 65*, 245 (1977).
208. H. Conrad, G. Ertl, J. Kuppers and E. E. Latta, *Surface Sci. 65*, 235 (1977).
209. H. Conrad, G. Ertl, J. Koch and E. E. Latta, *Surface Sci. 43*, 462 (1974).
210. A. M. Bradshaw and F. M. Hoffman, *Surface Sci. 72*, 513 (1978).
211. K. Christmann, G. Ertl and O. Schober, *Surface Sci. 40*, 61 (1973).
212. H. Conrad, G. Ertl and E. E. Latta, *Surface Sci. 41*, 435 (1974).
213. H. P. Bonzel and R. Ku, *Surface Sci. 40*, 85 (1973).
214. B. Carriere, J. P. Deville, G. Maire and P. Legare, *Sci. 58*, 578 (1976).
215. P. Legare, G. Maire, B. Cariere and J. P. Deville, *Surface Sci. 68*, 348 (1977).
216. J. A. Joebstl, *Journal of Vacuum Science Technology 12*, 347 (1975).
217. W. H. Weinberg, D. R. Monroe, V. Lampton and R. P. Merrill, *Journal of Vacuum Science Technology 14*, 444 (1977).
218. G. Ertl, M. Neumann and K. M. Streit, *Surface Sci. 64*, 393 (1977).

219. S. L. Bernasek and G. A. Somorjai, *J. Chem. Phys. 60*, 4552 (1974).
220. K. Christmann, G. Ertl and T. Pignet, *Surface Sci. 54*, 365 (1976).
221. K. Baron, D. W. Blakely and G. A. Somorjai, *Surface Sci. 41*, 45 (1974).
222. C. M. Comrie, W. H. Weinberg and R. M. Lambert, *Surface Sci. 57*, 619 (1976).
223. L. E. Firment and G. A. Somorjai, *J. Chem. Phys. 63*, 1037 (1975).
224. L. E. Firment and G. A. Somorjai, *Surface Sci. 55*, 413 (1976).
225. W. Heegemann, E. Bechtold and K. Hayek, Proc 2nd International Conference on Solid Surfaces, 185 (1974).
226. W. Heegemann, K. H. Meister, E. Bechtold and K. Hayek, *Surface Sci. 49*, 161 (1975).
227. Y. Berthier, M. Perdereau. and J. Oudar, *Surface Sci. 44*, 281 (1974).
228. K. Schwaka and E. Bechtold, *Surface Sci. 66*, 383 (1977).
229. D. A. Gorodetsky and A. N. Knysh, *Surface Sci. 40*, 651 (1973).
230. M. Housley, R. Ducros, G. Piquard and A. Cassuto, *Surface Sci. 68*, 277 (1977).
231. D. G. Castner, B. A. Sexton and G. A. Somorjai, *Surface Sci. 71*, 519 (1978).
232. T. E. Madey, H. A. Engelhardt and D. Menzel, *Surface Sci. 48*, 304 (1975).
233. T. E. Madey and D. Menzel, Proc 2nd International Conference on Solid Surfaces, 229 (1974).
234. L. R. Danielson, M. J. Dresser, E. E. Donaldson and J. T. Dickinson, *Surface Sci. 71*, 599 (1978).
235. L. R. Danielson, M. J. Dresser, E. E. Donaldson and D. R. Sandstrom, *Surface Sci. 71*, 615 (1978).
236. K. C. Pandey, T. Sakurai and H. D. Hagstrum, *Phys. Rev. B. 16*, 3648 (1977).
237. H. Ibach and J. E. Rowe, *Surface Sci. 43*, 481 (1974).
238. R. Heckingbottom and P. R. Wood, *Surface Sci. 36*, 594 (1973).
239. A. J. van Bommel and J. E. Crombeen, *Surface Sci. 36*, 773 (1973).
240. H. D. Shih, F. Jona, D. W. Jepsen and P. M. Marcus, *Journal of Vacuum Science Technology 15*, 596 (1978).
241. H. D. Shih, F. Jona, D. W. Jepsen and P. M. Marcus, *Physical Review Letters 36*, 798 (1976).
242. H. D. Shih, F. Jona, D. W. Jepsen and P. M. Marcus, *Surface Sci. 60*, 445 (1976).
243. R. Bastasz, C. A. Colmenares, R. L. Smith and G. A. Somorjai, *Surface Sci. 67*, 45 (1977).
244. T. E. Madey, J. J. Czyzewski and J. T. Yates, Jr., *Surface Sci. 57*, 580 (1976).
245. W. N. Unertl and J. M. Blakely, *Surface Sci. 69*, 23 (1977).
246. A. Oustry, L. Lafourcade and A. Escaut, *Surface Sci. 40*, 545 (1973).
247. Y. Berthier, M. Perdereau and J. Oudar, *Surface Sci. 36*, 225 (1973).
248. J. C. Fuggle, E. Umbach, P. Feulner and D. Menzel, *Surface Sci. 64*, 69 (1977).
249. E. Zanazzi, F. Jona, D. W. Jepsen and P. M. Marcus, *Phys. Rev. B 14*, 432 (1976).
250. A. Ignatiev, F. Jonà, D. W. Jepsen and P. M. Marcus, *Surface Sci. 40*, 439 (1973).
251. M. Kostelitz, J. L. Domange and J. Oudar, *Surface Sci. 34*, 431 (1973).
252. G. McElhiney and J. Pritchard, *Surface Sci. 60*, 397 (1976).
253. M. Maglietta and G. Rovida, *Surface Sci. 71*, 495 (1978).
254. G. Rovida and M. Maglietta, Proc. 7th International Vacuum Congress and 3rd International Conference on Solid Surfaces 963 (1977).
255. K. Horn, M. Hussain and J. Pritchard, *Surface Sci. 63*, 244 (1977).
256. S. Ekelund and C. Leygraf, *Surface Sci. 40*, 179 (1973).
257. L. McDonnell, D. P. Woodruff and K. A. R. Mitchell, *Surface Sci. 45*, 1 (1974).
258. G. G. Tibbetts, J. M. Burkstrand and J. C. Tracy, *Phys. Rev. B 15*, 3652 (1977).
259. E. Legrand-Bonnyns and A. Ponslet, *Surface Sci. 53*, 675 (1975).
260. G. G. Tibbetts, J. M. Burkstrand and J. C. Tracy, *Journal of Vacuum Science Technology 13*, 362 (1976).
261. E. G. McRae and C. W. Caldwell, *Surface Sci. 57*, 77 (1976).
262. J. R. Noonan, D. M. Zehner and L. H. Jenkins, *Surface Sci. 69*, 731 (1977).
263. P. Hoffmann, R. Unwin, W. Wyrobisch and A. M. Bradshaw, *Surface Sci. 72*, 635 (1978).
264. U. Gerhardt and G. Franz-Moller, Proc. 7th International Vacuum Congress and 3rd International Conference on Solid Surfaces 897 (1977).
265. C. R. Brundle and K. Wandelt, Proc. 7th International Vacuum Congress and 3rd International Conference on Solid Surfaces, 1171 (1977).
266. J. M. Burkstrand, G. G. Kleiman, G. G. Tibbetts and J. C. Tracy, *Journal of Vacuum Science Technology 13*, 291 (1976).
267. A. Salwen and J. Rundgren, *Surface Sci. 53*, 523 (1975).
268. K. O. Legg, F. Jona, D. W. Jepsen and P. M. Marcus, *Physical Review B 16*, 5271 (1977).
269. C. Leygraf and S. Ekelund, *Surface Sci. 40*, 609 (1973).
270. G. W. Simmons and D. J. Dwyer, *Surface Sci. 48*, 373 (1975).
271. C. F. Brucker and T. N. Rhodin, *Surface Sci. 57*, 523 (1976).
272. T. Horiguchi and S. Nakanishi, Proc. 2nd International Conference on Solid Surfaces, 89 (1974).
273. M. Watanabe, M. Miyarmura, T. Matsudaira and M. Onchi, Proc. 2nd International Conference on Solid Surfaces, 501 (1974).

274. C. Brucker and T. Rhodin, *Journal of Catalysis 47*, 214 (1977).
275. F. Jona, K. O. Legg, H. D. Shih, D. W. Jepsen and P. M. Marcus, *Physical Revlew Letters 40*, 1466 (1978).
276. T. Matsudaira, M. Watanabe and M. Onchi, Proc. 2nd International Conference on Solid Surfaces, 181 (1974).
277. K. O. Legg, F. Jona, D. W. Jepsen and P. M. Marcus, *Surface Sci. 66*, 25 (1977).
278. D. J. Dwyer and G. W. Simmons, *Surface Sci. 64*, 617 (1977).
279. C. Leygraf, G. Hultquist and S. Ekelund, *Surface Sci. 51*, 409 (1975).
280. C. Leygraf and G. Hultquist, *Surface Sci. 61*, 69 (1976).
281. T. N. Rhodin and G. Broden, *Surface Sci. 60*, 466 (1976).
282. G. Broden and T. N. Rhodin, *S. S. Comm 18*, 105 (1976).
283. A. Ignatiev, T.N. Rhodin and S.Y. Tong, *Surface Sci. 42*, 37 (1974).
284. R. Riwan, C. Guillot and J. Paigne, *Surface Sci. 47*, 183 (1975).
285. J. Lecante, R. Riwan and G. Guillot, *Surface Sci. 35*, 271 (1973).
286. C. Guillot, R. Riwan and J. Lecante, *Surface Sci. 59*, 581 (1976).
287. A. Ignatiev, F. Jona, D. W. Jepsen and P. M. Marcus, *Surface Sci. 49*, 189 (1975).
288. J. M. Wilson, *Surface Sci. 53*, 330 (1975).
289. A. Glachant, J. P. Coulomb and J. P. Biberian, *Surface Sci. 59*, 619 (1976).
290. H. H. Farrell and M. Strongin, *Surface Sci. 38*, 18 (1973).
291. H. H. Brongersma and J. B. Theeten, *Surface Sci. 54*, 519 (1976).
292. Y. Murata, S. Ohtani and K. Terada, Proc 2nd International Conference on Solid Surfaces, 837 (1974).
293. J. E. Demuth, D. W. Jepsen and P. M. Marcus, *Journal of Vacuum Science Technology 11*, 190 (1974).
294. T. N. Rhodin and J. E. Demuth, Proc. 2nd International Conference on Solid Surfaces, 167 (1974).
295. S. Andersson, B. Kasemo, J. B. Pendry and M. A. VanHove, *Phys. Rev. Lett. 31*, 595 (1973).
296. E. G. McRae and C. W. Caldwell, *Surface Sci. 57*, 63 (1976).
297. P. H. Holloway and J. B. Hudson, *Surface Sci. 43*, 123 (1974).
298. G. Dalmai-Imelik, J. C. Bertolini and J. Rousseau, *Surface Sci. 63*, 67 (1977).
299. D. F. Mitchell, P. B. Sewell and M. Cohen, *Surface Sci. 61*, 355 (1976).
300. S. Andersson and J. B. Pendry, *Surface Sci. 71*, 75 (1978).
301. S. Andersson, Proc. 3rd International Vacuum Congress and 7th International Conference on Solid Surfaces, 1019 (1977).
302. K. Horn, A. M. Bradshaw and K. Jacobi, *Surface Sci. 72*, 719 (1978).
303. J. E. Demuth, D. W. Jepsen and P. M. Marcus, *Surface Sci. 45*, 733 (1974).
304. T. Matsudaira, M. Nishijima and M. Onchi, *Surface Sci. 61*, 651 (1976).
305. H. Froitzheim and H. D. Hagstrum, *Journal of Vacuum Science Technology 15*, 485 (1978).
306. G. E. Becker and H. D. Hagstrum, *Journal of Vacuum Science Technology 11*, 234 (1974).
307. J. M. Rickard, M. Perdereau and L. G. Dufour, Proc. 7th International Vacuum Congress and 3rd International Conference on Solid Surfaces, 847 (1977).
308. A. Steinbrunn, P. Dumas and J. C. Colson, *Surface Sci. 74*, 201 (1978).
309. F. P. Netzer and M. Prutton, *Surface Sci. 52*, 505 (1975).
310. C. A. Pagageorgopoulos and J. M. Chen, *Surface Sci. 52*, 40 (1975).
311. P. W. Palmberg, *Surface Sci. 25*, 104 (1971).
312. C. R. Helms, H. P. Bonzel and S. Kelemen, *J. Chem. Phys. 65*, 1773 (1976).
313. B. Lang, P. Legare and G. Maire, *Surface Sci. 47*, 89 (1975).
314. G. Kneringer and F. P. Netzer, *Surface Sci. 49*, 125 (1975).
315. G. Pirug, G. Broden and H. P. Bonzel, Proc. 7th International Vacuum Congress and 3rd International Conference on Solid Surfaces 907 (1977).
316. G. Broden, G. Pirug and H. P. Bonzel, *Surface Sci. 72*, 45 (1978).
317. F. P. Netzer and G. Kneringer, *Surface Sci. 51*, 526 (1975).
318. H. P. Bonzel and G. Pirug, *Surface Sci. 62*, 45 (1977).
319. H. P. Bonzel, G. Broden and G. Pirug, *Journal of Catalysis 53*, 96 (1978).
320. T. E. Fischer and S. R. Kelemen, *Surface Sci. 69*, 1 (1977).
321. T. E. Fischer and S. R. Kelemen, *Journal of Vacuum Science Technology 15*, 607 (1978).
322. S. J. White and D. P. Woodruff, *Surface Sci. 63*, 254 (1977).
323. S. J. White, D. P. Woodruff, B. W. Holland and R. S. Zimmer, *Surface Sci. 74*, 34 (1978).
324. S. J. White, D. P. Woodruff, B. W. Holland and R. S. Zimmer, *Surface Sci. 68*, 457 (1977).
325. T. Sakurai and H. D. Hagstrum, *Phys. Rev. B 14*, 1593 (1976).
326. J. J. Lander and J. Morrison, *J. Chem. Phys. 37*, 729 (1962).
327. A. P. Janssen and R. C. Schoonmaker, *Surface Sci. 55*, 109 (1976).
328. M. A. Chesters, B. J. Hopkins and M. R. Leggett, *Surface Sci. 43*, 1 (1974).
329. T. N. Taylor, C. A. Colmenares, R. L. Smith and G. A. Somorjai, *Surface Sci. 54*, 317 (1976).
330. B. J. Hopkins, G. D. Watts and A. R. Jones, *Surface Sci. 52*, 715 (1975).

331. C. A. Papageorgopoulous and J. M. Chen, *Surface Sci. 39*, 313 (1973).
332. A. M. Bradshaw, D. Menzel and M. Steinkilberg, Proc. 2nd International Conference on Solid Surfaces, 841 (1974).
333. E. Bauer, H. Poppa and Y. Viswanath, *Surface Sci. 58*, 578 (1976).
334. S. Prigge, H. Niehus and E. Bauer, *Surface Sci. 65*, 141 (1977).
335. J. L. Desplat, Proc. 2nd International Conference on Solid Surfaces 177 (1974).
336. P. E. Luscher and F. M. Propst, *Journal of Vacuum Science Technology 14*, 400 (1977).
337. R. Jaeger and D. Menzel, *Surface Sci. 63*, 232 (1977).
338. B. J. Hopkins, A. R. Jones and R. I. Winton, *Surface Sci. 57*, 266 (1976).
339. S. Usami and T. Nakagima, Proc. 2nd International Conference on Solid Surfaces, 237 (1974).
340. J. E. Demuth, D. W. Jepsen and P. M. Marcus, *Phys. Rev. Lett 31*, 540 (1973).
341. H. A. Engelhardt, A. M. Bradshaw and D. Menzel, *Surface Sci. 40*, 410 (1973).
342. G. Rovida and F. Pratesi, *Surface Sci. 52*, 542 (1975).
343. W. Heiland, F. Iberl, E. Taglauer and D. Menzel, *Surface Sci. 53*, 383 (1975).
344. E. Zanazzi, M. Maglietta, U. Bardi, F. Jona, D. W. Jepsen and P. M. Marcus, Proc. 7th International Vacuum Congress and 3rd International Conference on Solid Surfaces, 2447 (1977)
345. R. A. Marbrow and R. M. Lambert, *Surface Sci. 61*, 317 (1976).
346. G. Gafner and R. Feder, *Surface Sci. 57*, 37 (1976).
347. B. E. Nieuwenhuys and G. A. Somorjai, *Surface Sci. 72*, 8 (1978).
348. J. L. Taylor and W. H. Weinberg, *Journal of Vacuum Science Technology 15*, 590 (1978).
349. E.B . Bas, P. Hafner and S. Klauser, Proc. 7th International Vacuum Congress and 3rd International Conference on Solid Surfaces 881 (1977).
350. T. Miura and Y. Tuzi, Proc. 2nd International Conference on Solid Surfaces, 85 (1974).
351. L. Peralta, Y. Berthier and J. Oudar, *Surface Sci. 55*, 199 (1976)
352. S. Andersson, J. B. Pendry and P. M. Echenique, *Surface Sci. 65*, 539 (1977).
353. J. Kuppers, *Surface Sci. 36*, 53 (1973).
354. D. F. Mitchell, P. B. Sewell, Proc. 7th International Vacuum Congress and 3rd International Conference on Solid Surfaces 963 (1977).
355. D. F. Mitchell, P. B. Sewell and M. Cohen, *Surface Sci. 69*, 310 (1977).
356. H. H. Madden, J. Kuppers and G. Ertl, *J. Chem. Phys. 58*, 3401 (1973).
357. H. H. Madden and G. Ertl, *Surface Sci. 35*, 211 (1973).
358. H. H. Madden, J. Kuppers and G. Ertl, *Journal of Vacuum Science Technology 11*, 190 (1974).
359. T. N. Taylor and P. J. Estrup, *Journal of Vacuum Science Technology 10*, 26 (1973).
360. T. N. Taylor and P. J. Estrup, *Journal of Vacuum Science Technology 11*, 244 (1974).
361. G. L. Price, B. A. Sexton and B. G. Baker, *Surface Science 60*, 506 (1976).
362. M. Wilf and P. T. Dawson, *Surface Sci. 65*, 399 (1977).
363. R. Ducros and R. P. Merrill, *Surface Sci. 55*, 227 (1976).
364. R. M. Lambert and C. M. Comrie, *Surface Sci. 46*, 61 (1974).
365. P. D. Reed and R. M. Lambert, *Surface Sci. 57*, 485 (1976).
366. R. M. Lambert, *Surface Sci. 49*, 325 (1975).
367. Y. Berthier, J. Oudar and M. Huber, *Surface Sci. 65*, 361 (1977).
368. H. P. Bonzel and R. Ku, *J. Chem. Phys. 58*, 4617 (1973).
369. R. A. Marbrow and R. M. Lambert, *Surface Sci. 67*, 489 (1977).
370. T. W. Orent and R.S. Hansen, *Surface Sci. 67*, 325 (1977).
371. R. Ku, N. A. Gjostein and H. P. Bonzel, *Surface Sci. 64*, 465 (1977).
372. P. D. Reed, C. M. Comrie and R. M. Lambert, *Surface Sci. 59*, 33 (1976).
373. P. D. Reed, C. M. Comrie and R. M. Lambert, *Surface Sci. 72*, 423 (1978).
374. P. D. Reed, C. M. Comrie and R. M. Lambert, *Surface Sci. 64*, 603 (1977).
375. T. Sakurai and H. D. Hagstrum, *Journal of Vacuum Science Technology 13*, 807 (1976).
376. W. J. Lo, Y. W. Chung and G. A. Somorjai, *Surface Sci. 71*, 199 (1978) .
377. M. A. VanHove, S. Y. Tong and M. H. Elconin, *Surface Sci. 64*, 85 (1977).
378. G. C. Wang, T. M. Lu and M. G. Lagally, Proc. 7th International Vacuum Congress and 3rd International Conference on Solid Surfaces, A2726 (1974).
379. J. M. Baker and D. E. Eastman, *Journal of Vacuum Science Technology 10*, 223 (1973).
380. J. C. Buchholz and M. G. Lagally, *Journal of Vacuum Science Technology 11*, 194 (1974).
381. J. C. Buchholz and M. G. Lagally, *Physical Rev. Lett. 35*, 442 (1975).
382. K. Besocke and S. Berger, Proc. 7th International Vacuum Congress and 3rd International Conference on Solid Surfaces 893 (1977).
383. T. E. Madey and J. T. Yates, *Surface Sci. 63*, 203 (1977).
384. T. Engel, H. Niehus and E. Bauer, *Surface Sci. 52*, 237 (1975).

385. J. C. Buchholz, G. C. Wang and M. G. Lagally, *Surface Sci. 49*, 508 (1975).
386. M. A. VanHove and S. Y. Tong, *Physical Review Letters 35*, 1092 (1975).
387. E. Bauer and T. Engel, *Surface Sci. 71*, 695 (1978).
388. N. R. Avery, *Surface Sci. 41*, 533 (1974).
389. Ch. Steinbruchel and R. Gomer, *Surface Sci. 67*, 21 (1977).
390. Ch. Steinbruchel and R. Gomer, *Journal of Vacuum Science Technology 14*, 484 (1977).
391. N. R. Avery, *Surface Sci. 43*, 101 (1974).
392. W. Gopel, *Surface Sci. 62*, 165 (1977).
393. R. A. Marbrow and R. M. Lambert, *Surface Sci. 71*, 107 (1978).
394. H. Papp and J. Pritchard, *Surface Sci. 53*, 371 (1975).
395. R. E. Kirby, C. S. McKee and M. W. Roberts, *Surface Sci. 55*, 725 (1976).
396. G. Maire, P. Bernhardt, P. Legare and G. Lindauer, Proc. 7th International Vacuum Congress and 3rd International Conference on Solid Surfaces, 861 (1977).
397. K. Schwaha and E. Bechtold, *Surface Sci. 65*, 277 (1977).
398. F. P. Netzer and R. A. Wille, *Journal of Catalysis 51*, 18 (1978).
399. F. P. Netzer and R. A. Wille, Proc. 7th International Vacuum Congress and 3rd International Conference on Solid Surfaces, 927 (1977).
400. K. Christmann and G. Ertl, *Surface Sci. 60*, 365 (1976).
401. J. Gland, *Surface Sci. 71*, 327 (1978).
402. D. G. Castner and G. A. Somorjai, *Surface Sci. 83*, 60 (1979).
403. G. Ertl and M. Plancher, *Surface Sci. 48*, 364 (1975).
404. B. J. Hopkins and G. D. Watts, *Surface Sci. 44*, 237 (1974).
405. T. Engel, T. von dem Hagen and E. Bauer, *Surface Sci. 62*, 361 (1977).
406. E. Gillet, J. C. Chiarena and M. Gillet, *Surface Sci. 67*, 393 (1977)
407. M. E. Bridge, R. A. Marbrow and R. M. Lambert, *Surface Sci. 57*, 415 (1976).
408. J. C. Buchholz and G. A. Somorjai, *J. Chem Phys. 66*, 573 (1977).
409. L. L. Atanasoska, J. C. Buchholz and G. A. Somorjai, *Surface Sci. 72*, 189 (1978).
410. G. Broden, T. Rhodin and W. Capehart, *Surface Sci. 61*, 143 (1976).
411. C. A. Papageorgopoulos and J. M. Chen, *Surface Sci. 39*, 283 (1973).
412. D. E. Eastman and J. E. Denuth, Proc. 2nd International Conference on Solid Surfaces, 827 (1974).
413. J. E. Demuth, *Surface Sci. 69*, 365 (1977).
414. G. Dalmai-Imelik, J. C. Bertolini, J. Massardier, J. Rousseau and B. Imelik, Proc. 7th International Vacuum Congress and 3rd International Conference on Solid Surfaces, 1179 (1977).
415. J. C. Bertolini, G.Dalmai-Imelik and J. Rousseau, *Surface Sci. 67*, 478 (1977).
416. C. Casalone, M. G. Cattania, M. Simonetta and M. Tescari, *Surface Sci. 62*, 321 (1977).
417. K. Horn, A. M. Bradshaw and K. Jacobi, *Journal of Vacuum Science Technology 15*, 575 (1978).
418. F. C. Schouter, E. W. Kaleveld and G. A. Bootsma, *Surface Science 63*, 460 (1977).
419. J. McCarty and R. J. Madix, *Journal of Catalysis 38*, 402 (1975).
420. J. G. McCarty and R. J. Madix, *Journal of Catalysis 48*, 422 (1977).
421. N. M. Abbas and R. J. Madix, *Surface Science 62*, 739 (1977).
422. G. Maire, J. R. Anderson and B. B. Johnson, *Proc. Roy. Soc. (London) A 320*, 227 (1970).
423. L. L. Kesmodel, R. C. Baetzold and G. A. Somorjai, *Surface Sci. 66*, 299 (1977).
424. P. C. Stair and G. A. Somorjai, *J. Chem. Phys. 66*, 573 (1977).
425. W. H. Weinberg, H. A. Deans and R. P. Merrill, *Surface Sci. 41*, 312 (1974).
426. B. Lang, *Surface Sci. 53*, 317 (1975).
427. L. E. Firmet and G. A. Somorjai, *J. Chem. Phys. 66*, 2901 (1977).
428. P. C. Stair and G. A. Somorjai, *J. Chem. Phys. 67*, 4361 (1977).
429. J. L. Gland and G. A. Somorjai, *Surface Sci. 38*, 157 (1973).
430. J. L. Gland and G. A. Somorjai, *Surface Sci. 41*, 387 (1974).
431. T. E. Fischer and S. R. Kelemen, *Surface Sci. 69*, 485 (1977).
432. T. E. Fischer, S. R. Kelemen and H. P. Bonzel, *Surface Sci. 64*, 85 (1977).
433. F. P. Netzer, *Surface Sci. 52*, 709 (1975)
434. M. E. Bridge and R. M. Lambert, *Journal of Catalysis 46*, 143 (1977).
435. M. E. Bridge and R. M. Lambert, *Surface Sci. 63*, 315 (1977).
436. R. Ducros, M. Housley, M. Alnot and A. Cassuot, *Surface Sci. 71*, 433 (1978).
437. Y. W. Chung, W. Siekhaus and G. A. Somorjai, *Surface Sci. 58*, 341 (1976).
438. J. P. Biberian and G. A. Somorjai, *J. Vac. Sci. and Techn. 16*, 2073 (1979).
439. J. W. Matthews and W. A. Jesser, *Acta Metal. 15*, 595 (1967).
440. J. W. Matthews, *Phil. Mag. 13*, 1207 (1966).
441. J. P. Biberian and G. E. Rhead, *J. Phys. F 3*, 675 (1973).

442. J. P. Biberian and M. Huber, *Surface Sci. 55*, 259 (1976).
443. A. K. Green, S. Prigge and E. Bauer, *Thin Solid Films 52*, 163 (1978).
444. J. P. Biberian, *Surface Sci. 74*, 437 (1978).
445. V. K. Medvedev, A. G. Nauvomets and A. G. Fedorus, *Sov. Phys. Solid State 12*, 301 (1970).
446. A. G. Naumovets and A. G. Fedorus, *JETP Lett. 10*, 6 (1969).
447. L. G. Feinstein and E. Blanc, *Surface Sci. 18*, 350 (1969).
448. T. Edmonds and J. J. McCarroll, *Surface Sci. 24*, 353 (1971).
449. I. Abbati, L. Braicovich, C. M. Bertoni, C. Calandra and F. Manghi, *Phys. Rev. Lett. 40*, 469 (1978).
450. J. Abbati and L. Braicovich, Proc. 7th Vac. Congr. and 3rd Intern. Conf. Solid Surfaces, 1117 (Vienna 1977).
451. A. J. Melmed and J. J. McCarroll, *Surface Sci. 19*, 243 (1970).
452. D. C. Hothersall, *Phil. Mag. 15*, 1023 (1967).
453. R. E. Thomas and G. A. Haas, *J. Appl. Phys. 43*, 4900 (1972).
454. S. Anderson and B. Kasemo, *Surface Sci. 32*, 78 (1972).
455. R. L. Gerlach and T. N. Rhodin, *Surface Sci. 17*, 32 (1969).
456. S. Anderson and J. B. Pendry, *J. Phys. C. 6*, 601 (1973).
457. S. Anderson and U. Jostell, *Surface Sci. 46*, 625 (1974).
458. R. L. Gerlach and T. N. Rhodin, *The Structure and Chemistry of Solid Surfaces*, G. A. Somorjai (1968), p. 55.
459. S. Anderson and J. B. Pendry, *J. Phys. C. 5*, L41 (1972).
460. R. L. Gerlach and T. N. Rhodin, *Surface Sci. 10*, 446 (1968).
461. S. Anderson and U. Jostell, *Solid State Comm. 13*, 829 (1973).
462. S. Anderson and U. Jostell, *Solid State Comm. 13*, 833 (1973).
463. C. A. Papageorgopoulos and J. M. Chen, *Surface Sci. 52*, 40 (1975).
464. C. A. Papageorgopoulos and J. M. Chen, *Surface Sci. 52*, 53 (1975).
465. L. G. Beinstein, E. Blanc and D. Dufayard, *Surface Sci. 19*, 269 (1970).
466. D. C. Jackson, T. E. Gallon and A. Chambers, *Surface Sci. 36*, 381 (1973).
467. J. J. Burton, C. R. Helms and R. S. Polizzotti, *Surface Sci. 57*, 425 (1976).
468. J. J. Burton, C. R. Helms and R. S. Polizzotti, *J. Chem. Phys. 65*, 1089 (1976).
469. J. J. Burton, C. R. Helms and R. S. Polizzotti, *J. Vac. Sci. Technol. 13*, 204 (1976).
470. J. R. Wolfe and H. W. Weart, *The Structure and Chemistry of Solid Surfaces*, G. A. Somorjai (1968), p. 32.
471. J. Perdereau and I. Szymerska, *Surface Sci. 32*, 247 (1972).
472. E. Alkhoury Nemen, R. C. Cinti and T. T. A. Nguyen, *Surface Sci. 30*, 697 (1972).
473. P. W. Palmberg and T. N. Rhodin, *J. Chem. Phys. 49*, 134 (1968).
474. U. Gradmann, W. Kummerle and P. Tillmanns, *Thin Solid Films 34*, 249 (1976).
475. C. A. Haque and H. E. Farnsworth, *Surface Sci. 4*, 195 (1966).
476. U. Gradmann, *Surface Sci. 13*, 498 (1969).
477. E. Bauer, *Surface Sci. 7*, 351 (1967).
478. P. W. Palmberg and T. N. Rhodin, *J. of Appl. Phys. 39*, 2425 (1968).
479. Y. Fujinaga, *Surface Sci. 64*, 751 (1977).
480. J. Erlewein and S. Hofmann, *Surface Sci. 68*, 71 (1977).
481. J. Henrion and G. E. Rhead, *Surface Sci. 29*, 20 (1972).
482. A. Sepulveda and G. E. Rhead, *Surface Sci. 66*, 436 (1977).
483. C. Argile and G. E. Rhead, *Surface Sci. 78*, 115 (1978).
484. M. G. Barthes and G. E. Rhead, *Surface Sci. 80*, 421 (1979).
485. K. Reichelt and F. Muller, *J. of Crystal Growth 21*, 323 (1974).
486. F. Delamare and G. E. Rhead, *Surface Sci. 35*, 172 (1973).
487. F. Delamare and G. E. Rhead, *Surface Sci. 35*, 185 (1973).
488. P. J. Goddard, J. West and R. M. Lambert, *Surface Sci. 71*, 447 (1978).
489. R. A. Marbrow and R. M. Lambert, *Surface Sci. 61*, 329 (1976).
490. P. J. Goddard and R. M. Lambert, *Surface Sci. 79*, 93 (1979).
491. R. C. Newman, *Phil. Mag. 2*, 750 (1957).
492. E. Bauer, Structure et Proprietes des Solides, CNRS, Paris (1969).
493. R. E. Thomas and G. A. Haas, *J. Appl. Phys. 43*, 4900 (1972).
494. H. E. Farnsworth, *Phys. Rev. 40*, 684 (1932).
495. J. Perdereau, J. P. Biberian and G. E. Rhead, *J. Phys. F 4*, 798 (1974).
496. M. G. Barthes and G. E. Rhead, *Surface Sci. 85*, L211 (1979).
497. M. G. Barthes, Theis University of Paris, 1978.
498. A. Sepulveda and G. E. Rhead, *Surface Sci. 49*, 669 (1975).
499. B. A. Hutchins, T. N. Rhodin and J. E. Demuth, *Surface Sci. 54*, 419 (1976).
500. J. O. Porteus, *Surface Sci. 41*, 515 (1974).
501. M. A. Van Hove, S. Y. Tong and N. Stoner, *Surface Sci. 54*, 259 (1976).

502. I. A. S. Edwards and H. R. Thirsk, *Surface Sci. 39*, 245 (1973).
503. C. Argile and G. E. Rhead, *Surface Sci. 78*, 125 (1978).
504. C. Argile, Thesis University of Paris, 1978.
505. A. G. Jackson and M. P. Hooker, *The Structure and Chemistry of Solid Surfaces*, G. A. Somorjai (1968), p. 73.
506. A. G. Elliot, *Surface Sci. 51*, 489 (1975).
507. J. P. Biberian, *Surface Sci. 59*, 307 (1976).
508. T. W. Haas, A. G. Jackson and M. P. Hooker, *J. Appl. Phys. 38*, 4998 (1967).
509. A. G. Jackson, M. P. Hooker and T. W. Haas, *Surface Sci. 10*, 308 (1968).
510. J. H. Pollard and W. E. Danforth, *The Structure and Chemistry of Solid Surfaces*, G. A. Somorjai (1968), p. 71.
511. J. H. Pollard and W. E. Danforth, *J. Appl. Phys. 39*, 4019 (1968).
512. S. Thomas and T. W. Haas, *J. Vac. Sci. Technol. 9*, 840 (1972).
513. K. Hartig, A. P. Janssen and J. A. Venables, *Surface Sci. 74*,, 69 (1978).
514. K. Hartig, Thesis Ruhr-Universitat, Bochum.
515. A. G. Jackson and M. P. Hooker, *Surface Sci. 28*,, 373 (1971).
516. A. G. Jackson and M. P. Hooker, *Surface Sci. 27*,, 197 (1971).
517. D. A. Gorodetsky, Yu. P. Melnik and A. A. Yasko, *Ukr. Fiz. Zhurn. 12*, 649 (1967).
518. V. K. Medvedev and T. P. Smereka, *Sov. Phys. Solid State 16*, 1046 (1974).
519. A. G. Naumovets and A. G. Fedorus, *Sov. Phys. JETP 41*, 587 (1975).
520. V. K. Medvedev, A. G. Naumovets and T. P. Smereka, *Surface Sci. 34*, 368 (1973).
521. J. M. Chen and C. A. Papageorgopoulos, *Surface Sci. 21*, 377 (1970).
522. S. Thomas and T. W. Haas, *J. Vac. Sci. Technol. 10*, 218 (1973).
523. A. U. MacRae, K. Muller, J. J. Lander and J. Morrison, *Surface Sci. 15*, 483 (1969).
524. C. A. Papageorgopoulos and J. M. Chen, *Surface Sci. 39*, 283 (1973).
525. V. B. Voronin, A. G. Nauvomets and A. G. Fedorus, *JETP Lett. 15*, 370 (1972).
526. C. S. Wang, *J. Appl. Phys. 48*, 1477 (1977).
527. A. G. Fedorus and A. G. Naumovets, *Surface Sci. 21*, 426 (1970).
528. A. G. Fedorus and A. G. Naumovets, *Sov. Phys. Solid State 12*, 301 (1970).
529. H. Niehus, Thesis Clausthal, 1975.
530. O. V. Kanash, A. G. Neumovets and A. G. Fedorus, *Sov. Phys. JETP 40*, 903 (1974).
531. D. A. Gorodetskii and Yu. P. Mel'nik, *Akad. Nauk SSSR 33*, 430 (1969).
532. D. A. Gorodetskii, Yu. P. Mel'nik, V. K. Sklyar and V. A. Usenko, *Surface Sci. 85*, L503 (1979).
533. D. A. Gorodetskii and Yu. P. Mel'nik, *Surface Sci. 62*, 647 (1977).
534. D. A. Gorodetskii, A. D. Gorchinskii, V. I. Maksimenko and Yu. P. Mel'nik, *Sov. Phys. Solid State 18*, 691 (1976).
535. D. A. Gorodetskii, A. M. Komev and Yu. P. Mel'nik, *Izv. Akad. Nauk SSSR Ser. Fiz. 28*, 1337 (1964).
536. V. B. Voronin and A. G. Naumovets, *Ukr. Fiz. Zhurn. 13*, 1389 (1968).
537. V. B. Voronin, *Soviet Phys. Solid State 9*, 1758 (1968).
538. D. A. Gorodetskii, A. A. Yas'ko, *Sov. Phys. Solid State 10*, 1812 (1969).
539. D. A. Gorodetskii, A. A. Yas'ko and S. A. Shevlyakov, *Izv. Akad. Nauk SSSR, Ser. Fiz. 35*, 436 (1971).
540. V. B. Voronin and A. G. Naumovets, *Izv. Akad. Nauk SSSR Ser. Fiz. 35*, 325 (1971).
541. G. E. Hill, J. Marklund and J. Martinson, *Surface Sci. 24*, 435 (1971).
542. D. Paraschkevov, W. Schlenk, R. P. Bajpai and E. Bauer, Proc. 7th Intern. Vac. Congr. and 3rd Intern. Conf. Solid Surfaces, Vienna 1737 (1977).
543. E. Bauer, H. Poppa, G. Todd and F. Bonczek, *J. Appl. Physics 45*, 5164 (1974).
544. N. J. Taylor, *Surface Sci. 4*, 161 (1966).
545. A. R. Moss and B. H. Blott, *Surface Sci. 17*, 240 (1969).
546. E. Bauer, H. Poppa, G. Todd and P. R. Davis, *J. Appl. Physics 48*, 3773 (1977).
547. J. B. Hudson and C. M. Lo, *Surface Sci. 36*, 141 (1973).
548. P. D. Augustus and J. P. Jones, *Surface Sci. 64*, 713 (1977).
549. R. G. Jones and D. L. Perry, *Surface Sci. 71*, 59 (1978).
550. D. A. Gorodetskii and A. A. Yas'ko, *Sov. Phys. Solid State 14*, 636 (1972).
551. E. Bauer, H. Poppa and G. Todd, *Thin Solid Films 28*, 19 (1975).
552. D. A. Gorodetskii and A. A. Yas'ko, *Sov. Phys. Solid State 11*, 640 (1969).
553. B. J. Hopkins, G. D. Watts, *Surface Sci. 47*, 195 (1975).
554. B. J. Hopkins, G. D. Watts, *Surface Sci. 45*, 77 (1974).
555. D. A. Gorodetskii, A. A. Yas'ko, *Sov. Phys. Solid State 13*, 1085 (1971).
556. P. J. Estrup, J. Anderson and W. E. Danforth, *Surface Sci. 4*, 286 (1966).
557. P. J. Estrup and J. Anderson, *Surface Sci. 7*, 255 (1967).
558. P. J. Estrup and J. Anderson, *Surface Sci. 8*, 101 (1967).
559. J. H. Pollard, *Surface Sci. 20*, 269 (1970).

560. J. Anderson, P. J. Estrup and W. E. Danforth, *Appl. Phys. Lett. 7*, 122 (1965).
561. R. E. Schlier and H. E. Farnsworth, *J. Phys. Chem. Solids 6*, 271 (1958).
562. H. D. Shih, F. Jona, D. W. Jepsen and P. M. Marcus, *Phys. Rev. B 15*, 5550 (1977).
563. H. D. Shih, F. Jona, D. W. Jepsen and P. M. Marcus, *Phys. Rev. B 15*, 5561 (1971).
564. H. D. Shih, F. Jona, D. W. Jepsen and P. M. Marcus, *Comm. on Physics 1*, 25 (1976).
565. D. A. Gorodetskii and A. N. Knysh, *Surface Sci. 40*, 636 (1973).
566. D. A. Gorodetskii and A. N. Knysh, *Surface Sci. 40*, 651 (1973).
567. T. Shigematsu, S. Hine and T. Takada, *J. Crystal Growth 43*, 531 (1978).
568. T. Narusawa, S. Shimizu and S. Komiya, *J. Vac. Sci. Technol. 16*, 366 (1979).
569. R. J. Baird, R. C. Ku and P. Wynblatt, *J. Vac. Sci. Technol. 16*, 435 (1979).
570. P. A. Thiel, J. T. Yates and W. H. Weinberg, *J. Vac. Sci. Technol. 16*, 438 (1979).
571. D. E. Ibbotson, J. C. Taylor and W. H. Weinberg, *J. Vac. Sci. Technol. 16*, 439 (1979).
572. S. P. Weeks and J. E. Rowe, *J. Vac. Sci. Technol. 16*, 470 (1979).
573. C. R. Brundle, E. Silverman and R. J. Madix, *J. Vac. Sci. Technol. 16*, 474 (1979).
574. P. H. Citrin, P. Eisenberger, R. C. Hewitt and H. H. Farrell, *J. Vac. Sci. Technol. 16*, 537 (1979).
575. A. Ignatiev, H. B. Nielsen and D. L. Adams, *J. Vac. Sci. Technol. 16*, 552 (1979).
576. T. N. Taylor, J. W. Rogers and W. P. Ellis, *J. Vac. Sci. Technol. 16*, 581 (1979).
577. T. W. Capehart and T. N. Rhodin, *J. Vac. Sci. Technol. 16*, 594 (1979).
578. L. J. Clarke, *J. Vac. Sci. Technol. 16*, 651 (1979).
579. B. J. Mrstik, S. Y. Tong, M. A. Van Hove, *J. Vac. Sci. Technol. 16*, 1258 (1979).
580. A. T. Hubbard, *J. Vac. Sci. Technol. 17*, 49 (1980).
581. G. B. Fischer, B. A. Sexton and J. L. Gland, *J. Vac. Sci. Technol. 17*, 144 (1980).
582. P. R. Norton, D. K. Creber and J. A. Davies, *J. Vac. Sci. Technol. 17*, 149 (1980).
583. J. J. Zinck and W. H. Weinberg, *J. Vac. Sci. Technol. 17*, 188 (1980).
584. H. L. Davis and D. M. Zehner, *J. Vac. Sci. Technol. 17*, 190 (1980).
585. J. R. Noonan and H. L. Davis, *J. Vac. Sci. Technol. 17*, 194 (1980).
586. J. F. Delord, A. G. Schrott and S. C. Fain, Jr., *J. Vac. Sci. Technol. 17*, 517 (1980).
587. L. E. Firment and G. A. Somorjai, *J. Vac. Sci. Technol. 17*, 574 (1980).
588. W. Monch and H. Gant, *J. Vac. Sci. Technol. 17*, 1094 (1980).
589. J. Massies, F. Dezaly and N. T. Linh, *J. Vac. Sci. Technol. 17*, 1134 (1980).
590. P. Hollins and T. Pritchard, *Surface Sci. 99*, L389-394 (1980).
591. M. A. Chesters, Ph.D. Thesis, London University (1972).
592. J. Pritchard, *J. Vac. Sci. Technol. 89*, 486 (1979).
593. P. Hollins and J. Pritchard, *Surface Sci. 89*, 486 (1979)
594. L. J. Gerenser and R. C. Baetzold, *Surface Sci. 99*, 259 (1980).
595. R. J. Behm, K. Christmann and G. Ertl, *Surface Sci. 99*, 320 (1980).
596. S. D. Bader, T. W. Orent and L. Richter, *Bull. Am. Phy. Soc. 24*, 468 (1979).
597. S. D. Bader, *Surface Sci. 99*, 392 (1980).
598. P. Feulner, S. Kulkarni, E. Umbach and D. Menzel, *Surface Sci. 99*, 489 (1980).
599. K. J. Rawlings, *Surface Sci. 99*, 507 (1980).
600. B. A. Sexton and G. E. Mitchell, *Surface Sci. 99*, 523 (1980).
601. F. L. Baudais, H. J. Borschke, J. D. Fedyk and M. J. Digna *Surface Sci. 100*, 210 (1980).
602. G. Guillot, R. Riwan and J. Lecante, *Surface Sci. 59*, 581 (1976).
603. E. J. Ko and R. J. Madix, *100*, L449 (1980).
604. K. J. Rawlings, G. G. Price and B. J. Hopkins, *Surface Sci. 100*, 289 (1980).
605. M. Kitson and R. M. Lambert, *Surface Sci. 100*, 368 (1980).
606. P. Delescluse and A. Masson, *Surface Sci. 100*, 423 (1980).
607. M. Perdereau and J. Oudar, *Surface Sci. 20*, 80 (1970).
608. T. Edmonds, J. J. McCarroll and R. C. Pitkethly, *J. Vac. Sci. Technol. 8*, 68 (1971).
609. P. H. Holloway, and J. B. Hudson, *Surface Sci. 33*, 56 (1972).
610. H. H. Farrell, *Surface Sci. 100*, 613 (1980).
611. C. Oshima, M. Aono, T. Tanaka, S. Kawai, S. Zaima and Y. Shimbata, *Surface Sci. 102*, 312 (1981).
612. L. J. Clarke, *Surface Sci. 102*, 331 (1981).
613. L. J. Clarke, Ph.D. Thesis, Cambridge, U.K. (1978).
614. R. J. Gorte and J. L. Gland, *Surface Sci. 102*, 348 (1981).
615. T. S. Wittrig, D. E. Ibbotson and W. H. Weinberg, *Surface Sci. 102*, 506 (1981).
616. P. Hofmann, K. Horn and A. M. Bradshaw, *Surface Sci. 105*, L260 (1981).
617. G. L. Nyberg and N. V. Richardson, *Surface Sci. 85*, 335 (1979).
618. S. Calisti and J. Suzanne, *Surface Sci. 105*, L255 (1981).
619. S. K. Shi, J. A. Schreifels and J. M. White, *Surface Sci. 105*, 1 (1981).

620. D. Poso, W. Ranke and K. Jacobi, *Surface Sci. 105*, 77 (1981).
621. D. W. Goodman, and M. Kiskinova, *Surface Sci. 105*, L265 (1981).
622. H. D. Hagstrum and G. E. Becker, *Proc. Roy. Soc. (London) A331*, 395 (1971).
623. G. B. Fisher, *Surface Sci. 62*, 31 (1977).
624. F. Solymosi and J. Kiss, *Surface Sci. 104*, 181 (1981).
625. L. Peralta, Y. Berthier and M. Huber, *Surface Sci. 104*, 435 (1981).
626. J. L. Gland and E. B. Kollin, *Surface Sci. 104*, 478 (1981).
627. G. Rouida and F. Pratesi, *Surface Sci. 104*, 609 (1981).
628. E. Bauer and T. Engel, *Surface Sci. 71*, 695 (1978).
629. S. Calisti and J. Suzanne, *Surface Sci. 105*, L255 (1981).
630. P. Hofmann, K. Horn and A. M. Bradshaw, *Surface Sci. 105*, L260 (1981).
631. S. K. Shi, J. A. Schreifels and J. M. White, *Surface Sci. 105*, 1 (1981).
632. D. Poss, W. Ranke and K. Jacobi, *Surface Sci. 105*, 77 (1981).
633. H. H. Madden, *Surface Science 105*, 129 (1981).
634. P. Michel and C. Jardin, *Surface Sci. 36*, 478 (1973).
635. G. W. Simmons and D. J. Dwyer, *Surface Sci. 48*, 373 (1975).
636. C. Leygraf and G. Hultquist, *Surface Sci. 61*, 61 (1976).
637. D. W. Goodman and M. Kiskinova, *Surface Sci. 105*, L265 (1981).
638. S. A. Flodstrom, C. W. B. Martinson, R. Z. Bockrach, S. B. M. Hagstrm and R. S. Bauer, *Phys. Rev. Lett. 40*, 907 (1978).
639. T. Ichikawa and S. Ino, *Surface Sci. 105*, 395 (1981).
640. D. J. Godfrey and D. P. Woodruff, *Surface Sci. 105*, 438 (1981).
641. D. J. Godfrey and D. P. Woodruff, *Surface Sci. 105*, 459 (1981).
642. T. Takahashi, H. Takiguchi and A. Ebina, *Surface Sci. 105*, 475 (1981).
643. M. K. Debe and D. A. King, *Surface Sci. 81*, 193 (1978).
644. H. M. Kramer and E. Bauer, *Surface Sci. 107*, 1 (1981).
645. T. N. Taylor and P. J. Estrup, *J. Vac. Sci. Technol. 10*, 26 (1973).
646. S. Prigge, H. Roux and E. Bauer, *Surface Sci. 107*, 101 (1981).
647. N. D. Spencer and R. M. Lambert, *Surface Sci. 107*, 237 (1981).
648. T. N. Taylor and W. P. Ellis, *Surface Sci. 107*, 249 (1981).
649. D. L. Adams and H. B. Nielsen, *Surface Sci. 107*, 305 (1981).
650. P. W. Davies and R. M. Lambert, *Surface Sci. 107*, 391 (1981).
651. P. W. Davies and R. M. Lambert, *Surface Sci. 95*, 571 (1980).
652. R. J. Koestner, M. A. Van Hove and G. A. Somorjai, *Surface Sci. 107*, 439 (1981).
653. P. J. Goddard and R. M. Lambert, *Surface Sci. 107*, 519 (1981).
654. M. P. Cox and R. M. Lambert, *Surface Sci. 107*, 547 (1981).
655. H. Namba, J. Dennille and J. M. Gilles, *Surface Sci. 108*, 446 (1981).
656. J. F. Wendelken, *Surface Sci. 108*, 605 (1981).
657. F. Solymosi and J. Kiss, *Surface Sci. 108*, 641 (1981).
658. M. Kitson and K. M. Lambert, *Surface Sci. 109*, 60 (1981).
659. T. Oyama, S. Ohi, A. Kawazu and G. Tominaga, *Surface Sci. 109*, 82 (1981).
660. E. I. Ko and R. J. Madix, *Surface Sci. 109*, 221 (1981).
661. K. J. Rawlings, S. D. Foulias and B. J. Hopkins, *Surface Sci. 108*, 49 (1981).
662. M. Kiskinova and D. W. Goodman, *Surface Sci. 108*, 64 (1981).
663. P. R. Norton, J. A. Davies, D. K. Creber, C. W. Sitter and T. E. Jackman, *Surface Sci. 108*, 205 (1981).
664. R. Ducros, M. Housley, G. Piquard and M. Alnot, *Surface Sci. 108*, 235 (1981).
665. S. B. Lee, M. Weiss and G. Ertl, *Surface Sci. 108*, 357 (1981).
666. F. Solymosi and J. Kiss, *Surface Sci. 108*, 368 (1981).
667. W. S. Yang and F. Jona, *Surface Sci. 109*, L505 (1981).
668. D. Dahlgren and J. C. Hemminger, *Surface Sci. 109*, L513 (1981).
669. P. A. Dowben, M. Grunze and R. G. Jones, *Surface Sci. 109*, L519 (1981).
670. M. Kiskinova and D. W. Goodman, *Surface Sci. 109*, L555 (1981).
671. J. W. A. Sachtler, M. A. Van Hove, J. P. Biberian and G. A. Somorjai, *Surface Sci. 110*, 19 (1981).
672. M. W. Holmes and D. A. King, *Surface Sci. 110*, 120 (1981).
673. M. Kitson and R. M. Lambert, *Surface Sci. 110*, 205 (1981).
674. C. J. Schramn, Jr., M. A. Langell and S. L. Bernasek, *Surface Sci. 110*, 217 (1981).
675. P. W. Davies and R. M. Lambert, *Surface Sci. 110*, 227 (1981).
676. F. P. Netzer and T. E. Madey, *Surface Sci. 110*, 251 (1981).
677. D. E. Ibbotson, T. S. Wittrig and W. H. Weinberg, *Surface Sci. 110*, 294 (1981).
678. D. E. Ibbotson, T. S. Wittrig and W. H. Weinberg, *Surface Sci. 110*, 313 (1981).

679. F. C. Schouten, E. T. Brake, O. L. J. Gijzeman and G. A. Bootsma, *Surface Sci. 74*, 1 (1978).
680. S. J. White, D. P. Woodruff, B. W. Holland and R. S. Zimmer, *Surface Sci. 74*, 34 (1978).
681. A. Steinbrunn, P. Dumas and J. C. Colson, *Surface Sci. 74*, 201 (1978).
682. S. D. Bader, J. M. Blakely, M. B. Brodsky, R. J. Friddle and R. L. Panosh, *Surface Sci. 74*, 405 (1978).
683. J. P. Biberian, *Surface Sci. 74*, 437 (1978).
684. B. Goldstein and D. J. Szostak, *Surface Sci. 74*, 461 (1978).
685. F. P. Netzer and R. A. Wille, *Surface Sci. 74*, 547 (1978).
686. C. A. Papageargopoulos, *Surface Sci. 75*, 17 (1978).
687. K. Yoshida and G. A. Somorjai, *Surface Sci. 75*, 46 (1978).
688. C. S. Mckee, L. V. Remny and M. W. Roberts, *Surface Sci. 75*, 92 (1978).
689. J. L. Gland and V. L. Korehak, *Surface Sci. 75*, 733 (1978).
690. H. Ibach and S. Lehwald, *Surface Sci. 76*, 1 (1978).
691. H. Conrad, G. Ertl and J. Kuppers, *Surface Sci. 76*, 323 (1978).
692. T. E. Madey and J. T. Yates, Jr., *Surface Sci. 76*, 397 (1978).
693. T. E. Felter and P. J. Estrup, *Surface Sci. 76*, 464 (1978).
694. A. J. Van Boommel and J. E. Crombeen, *Surface Sci. 76*, 499 (1978).
695. H. Albers, W. J. J. Van Der Wal, O. L. J. Gijzemann and G. A. Bootsma, *Surface Sci. 77*, 1 (1978).
696. H. Hopster and H. Ibach, *Surface Sci. 77*, 109 (1978).
697. P. Drathen, W. Ranke and K. Jacobi, *Surface Sci. 77*, L162 (1978).
698. K. A. Prior, K. Schwaha and R. M. Lambert, *Surface Sci. 77*, 193 (1978).
699. W. Y. Ching, D. L. Huber, M. G. Lagally and G. C. Wang, *Surface Sci. 77*, 550 (1978).
700. K. J. Rawlings, B. J. Hopkins and S. D. Foulias, *Surface Sci. 77*, 561 (1978).
701. C. M. Chan, S. L. Cunningham, K. L. Luke, W. H. Weinberg and S. P. Withrow, *Surface Sci. 78*, 15 (1978).
702. J. P. Jones and E. W. Roberts, *Surface Sci. 78*, 37 (1978).
703. C. Argile and G. E. Rhead, *Surface Sci. 78*, 115 (1978).
704. C. Argile and G. E. Rhead, *Surface Sci. 78*, 125 (1978).
705. P. J. Goddard and R. M. Lambert, *Surface Sci. 79*, 93 (1979).
706. J. L. Taylor, D. E. Ibbotson and W. H. Weinberg, *Surface Sci. 79*, 349 (1979).
707. M. Alff and W. Moritz, *Surface Sci. 80*, 24 (1979).
708. G. Maire, P. Legare and Lindauer, *Surface Sci. 80*, 238 (1979).
709. C. W. B. Martinson and S. A. Flodstrom, *Surface Sci. 80*, 306 (1979).
710. J. Massies, P. Elienne, N. T. Linh, *Surface Sci. 80*, 550 (1979).
711. S. A. Lindgren and L. Wallden, *Surface Sci. 80*, 620 (1979).
712. M. K. Debe and D. A. King, *Surface Sci. 81*, 193 (1979).
713. T. Engel, P. Bornemann and E. Bauer, *Surface Sci. 81*, 252 (1979).
714. K. Schwaha, N. D. Spencer and R. M. Lambert, *Surface Sci. 81*, 273 (1979).
715. E. D. Williams, C. M. Chan and W. H. Weinberg, *Surface Sci. 81*, L309 (1979).
716. E. D. Williams and W. H. Weinberg, *Surface Sci. 82*, 93 (1979).
717. K. Oura and T. Hamawa, *Surface Sci. 82*, 202 (1979).
718. J. F. Van Der Veen, R. M. Tromp, R. G. Smeenk and F. W. Saris, *Surface Sci. 82*, 468 (1979).
719. M. G. Cattania, M. Simonetta and M. Tescari, *Surface Sci. 82*, L615 (1979).
720. C. G. Shaw and S. C. Fain, Jr., *Surface Sci. 83*, 1 (1979).
721. M. D. Chim and S. C. Fain, Jr., *Phys. Rev. Lett. 39*, 146 (1977).
722. D. G. Castner and G. A. Somorjai, *Surface Sci. 83*, 60 (1979).
723. R. Pantel, M. Bujor and J. Bardolle, *Surface Sci. 83*, 228 (1979).
724. E. Bertel, K. Schwaha and F. P. Netzer, *Surface Sci. 83*, 439 (1979).
725. H. L. Danis, J. R. Noonan and L. H. Jenkins, *Surface Sci. 83*, 559 (1979).
726. Y. Fujunaga, *Surface Sci. 84*, 1 (1979).
727. P. A. Thiel, E. D. Williams, J. T. Yates, Jr. and W. H. Weiberg, *Surface Sci. 84*, 54 (1979).
728. G. Broden and H. P. Bonzel, *Surface Sci. 84*, 106 (1979).
729. L. K. Verheij, J. A. Van Den Berg and D. G. Armour, *Surface Sci. 84*, 408 (1979).
730. M. G. Barthes and G. E. Rhead, *Surface Sci. 85*, L211 (1979).
731. P. R. Novtom, J. A. Davies, D. P. Jackson and N. Matsunami, *Surface Sci. 85*, 269 (1979).
732. Y. Y. Tu, J. M. Blakely, *Surface Sci. 85*, 276 (1979).
733. G. G. Price, K. J. Rawlings and B. J. Hopkins, *Surface Sci. 85*, 379 (1979).
734. C. Benndorf, K. H. Gressmann, J. Kessler, W. Kirstein and F. Thieme, *Surface Sci. 85*, 389 (1979).
735. D. A. Gorodetsky, Y. P. Melnik, V. K. Sklyar and V. A. Usenko, *Surface Sci. 85*, L503 (1979).
736. A. Kawazu, Y. Saito, N. Ogiwara, T. Otsuki and G. Tominaga, *Surface Sci. 86*, 108 (1979).
737. Y. Fujinaga, *Surface Sci. 86*, 581 (1979).
738. M. Aono, R. Nishitani, C. Oshima, T. Tanaka, E. Bannai and S. Kawai, *Surface Sci. 86*, 631 (1979).

739. F. C. Schouten, O. L. J. Gijzeman and G. A. Bootsma, *Surface Sci. 87*, 1 (1979).
740. S. R. Kelemen and T. E. Fischer, *Surface Sci. 87*, 53 (1979).
741. A. Glachant and U. Bardi, *Surface Sci. 87*, 187 (1979).
742. S. Hengrasmee, P. R. Watson, D. C. Frost and K. A. R. Mitchell, *Surface Sci. 87*, L249 (1979).
743. J. Kuppers, F. Nitschke, K. Wandelt and G. Ertl, *Surface Sci. 87*, 295 (1979).
744. A. Kahn, D. Kanani, P. Mark, P. W. Chye, C. Y. Su, I. Lindau and W. E. Spicer, *Surface Sci. 87*, 325 (1979).
745. J. H. Onuferko, D. P. Woodruff and B. W. Holland, *Surface Sci. 87*, 357 (1979).
746. H. Nilhus, *Surface Sci. 87*, 561 (1979).
747. K. Heinz, E. Lang and K. Muller, *Surface Sci. 87*, 595 (1979).
748. E. Bauer and H. Poppa, *Surface Sci. 88*, 31 (1979).
749. M. N. Read and G. J. Russell, *Surface Sci. 88*, 95 (1979).
750. F. H. P. M. Habraken, G. A. Bootsma, P. Hofmann, S. Hachicha and A. M. Bradshaw, *Surface Sci. 88*, 285 (1979).
751. R. G. Jones and D. L. Perry, *Surface Sci. 88*, 331 (1979).
752. P. A. Dowben and R. G. Jones, *Surface Sci. 88*, 348 (1979).
753. R. G. Jones, *Surface Sci. 88*, 367 (1979).
754. W. Moritz and D. Wolf, *Surface Sci. 88*, L29 (1979).
755. M. Prutton, J. A. Walker, M. R. Welton-Cook, R. C. Felton and J. A. Ramsey, *Surface Sci. 89*, 95 (1979).
756. C. W. B. Madinson, S. A. Flodstrom, J. Rundgren and P. Westrin, *Surface Sci. 89*, 102 (1979).
757. P. A. Dowben and R. G. Jones, *Surface Sci. 89*, 114 (1979).
758. C. Somerton and D. A. King, *Surface Sci. 89*, 391 (1979).
759. M. Grunze, R. K. Driscoll, G. N. Burland, J. C. L. Cornish and J. Pritchard, *Surface Sci. 89*, 381 (1979).
760. S. M. Davis and G. A. Somorjai, *Surface Sci. 91*, 73 (1980).
761. L. J. Clarke, *Surface Sci. 91*, 131 (1980).
762. J. C. Hamilton and J. M. Blakely, *Surface Sci. 91*, 199 (1980).
763. M. Salmeron and G. A. Somorjai, *Surface Sci. 91*, 373 (1980).
764. P. R. Davis, *Surface Sci. 91*, 385 (1980).
765. C. M. Chan, M. A. Van Hove, W. H. Weiberg and E. D. Williams. *Surface Sci. 91*, 440 (1980).
766. G. Hanke, E. Lang, K. Heinz and K. Muller, *Surface Sci. 91*, 551 (1980).
767. G. L. Price and B. G. Baker, *Surface Sci. 91*, 571 (1980).
768. H. I. Lee, G. Praline and J. M. White, *Surface Sci. 91*, 581 (1980).
769. S. Hengrasmee, P. R. Watson, D. C. Frost and K. A. R. Mitchell, *Surface Sci. 92*, 71 (1980).
770. P. Nishitani, S. Kawai, H. Iwasaki, S. Nakamura, M. Aono and T. Tanaka, *Surface Sci. 92*, 191 (1980).
771. D. A. King and G. Thomas, *Surface Sci. 92*, 201 (1980).
772. R. S. Li and L. X. Tu, *Surface Sci. 92*, L71 (1980).
773. O. Oda and G. E. Rhead, *Surface Sci. 92*, 617 (1980).
774. G. A. Garwood, Jr. and A. T. Hubbard, *Surface Sci. 92*, 467 (1980).
775. R. Nishitani, M. Aono, T. Tanaka, C. Oshima, S. Kawai, H. Iwasaki and S. Nakamura, *Surface Sci. 93*, 535 (1980).
776. A. H. Mahan, T. W. Riddle, F. B. Duming and G. K. Walters, *Surface Sci. 93*, 550 (1980).
777. J. Anderson and P. J. Estrup, *J. Chem. Phys. 46*, 563 (1967).
778. C. W. Seabury, T. N. Rhodin, R. J. Purtell and R. P. Merrill, *Surface Sci. 93*, 117 (1980).
779. Y. Sakisaka, M. Miyamura, J. Tamaki, M. Nishijima and M. Onchi, *Surface Sci. 93*, 327 (1980).
780. R. A. Barker, S. Semancik, P. J. Estrup, *Surface Sci. 94*, L162 (1980).
781. F. Bonczek, T. Engel and E. Bauer, *Surface Sci. 94*, 57 (1980).
782. S. Y. Tong, A. Maldonado, C. H. Li, and M. A. Van Hove, *Surface Sci. 94*, 73 (1980).
783. J. Benziger, and R. J. Madix, *Surface Sci. 94*, 119 (1980).
784. M. Textor, I. D. Gay and R. Mason, FRS, *Proc. Roy. Soc. (London) A356*, 37 (1977).
785. W. Erley, *Surface Sci. 94*, 281 (1980).
786. G. Pirug, G. Broden and H. P. Bonzel, *Surface Sci. 94*, 323 (1980).
787. D. T. Ling and W. E. Spicer, *Surface Sci. 94*, 403 (1980).
788. M. E. Bridge and R. M. Lambert, *Surface Sci. 94*, 469 (1980).
789. O. Nishikawa, M. Wada and M. Konishi, *Surface Sci. 97*, 16 (1980).
790. U. Bardi, A. Glachant and M. Bienfait, *Surface Sci. 97*, 137 (1980).
791. R. J. Baird, R. C. Ku and P. Wynblatt, *Surface Sci. 97*, 346 (1980).
792. N. Osakahe, Y. Tamishiro, K. K. Yagi and G. Honjo, *Surface Sci. 97*, 393 (1980).
793. E. Bertel and F. P. Netzer, *Surface Sci. 97*, 409 (1980).
794. R. G. Kirby, C. S. McKee and L. V. Renny, *Surface Sci. 97*, 457 (1980).
795. T. Ichikawa and S. Ino, *Surface Sci. 97*, 489 (1980).
796. F. Bonczek, T. Engel and E. Bauer, *Surface Sci. 97*, 595 (1980).

797. B. E. Hayden, E. Schweizer, R. Kotz and A. M. Bradshaw, *Surface Sci. 111*, 26 (1981).
798. A. G. Schrott and S. C. Fain, Jr., *Surface Sci. 111*, 39 (1981).
799. K. J. Rawlings, S. D. Foulias and B. J. Hopkins, *Surface Sci. 111*, L690 (1981).
800. T. Sakamoto and H. Kawanami, *Surface Sci. 111*, 177 (1981).
801. W. M. Daniel, Y. Kim, H. C. Peebles and J. M. White, *Surface Sci. 111*, 189 (1981).
802. T. Ichikawa, *Surface Sci. 111*, 227 (1981).
803. B. Z. Olshanetsky and V. I. Mashanov, *Surface Sci. 111*, 414 (1981).
804. B. Z. Olshanetsky, V. I. Mashanov and A. I. Nikiforov, *Surface Sci. 111*, 429 (1981).
805. M. Salmeron, L. Brewer and G. A. Somorjai, *Surface Sci. 112*, 207 (1981).
806. G. A. Garwood, Jr. and A. T. Hubbard, *Surface Sci. 112*, 281 (1981).
807. M. Saitoh, F. Shoji, K. Oura and T. Hanawa, *Surface Sci. 112*, 306 (1981).
808. M. A. Langell and S. L. Bernasek, *J. Vac. Sci. Technol. 17*, 1287 (1980).
809. S. Shimizu and S. Komiya, *J. Vac. Sci. Technol. 18*, 765 (1981).
810. W. Erley, *J. Vac. Sci. Technol. 18*, 472 (1981).
811. T. E. Madey, J. G. Houston, C. W. Seabury and T. N. Rhodin, *J. Vac. Sci. Technol. 18*, 476 (1981).
812. M. A. Passler, T. H. Lin and A. Ignatiev, *J. Vac. Sci. Technol. 18*, 481 (1981).
813. R. J. Baird and W. Eberhardt, *J. Vac. Sci. Technol. 18*, 538 (1981).
814. S. Semancik and P. J. Estrup, *J. Vac. Sci. Technol. 18*, 541 (1981).
815. R. A. Barker and P. J. Estrup, *J. Vac. Sci. Technol. 18*, 546 (1981).
816. G. V. Hansson, R. Z. Bachrach, R. S. Bauer and P. Chiaradia, *J. Vac. Sci. Technol. 18*, 550 (1981).
817. B. W. Walker and P. C. Stair, *J. Vac. Sci. Technol. 18*, 591 (1981).
818. C. W. Seabury, T. N. Rhodin, R. J. Purtell and R. P. Merrill, *J. Vac. Sci. Technol. 18*, 602 (1981).
819. B. W. Lee, R. K. Ni, N. Masud, X. R. Wang, D. C. Wang and M. Rowe, *J. Vac. Sci. Technol. 19*, 294 (1981).
820. B. B. Pate, P. M. Stefan, C. Binns, P. J. Jupiter, M. L. Shek, I. Lindau and W. E. Spicer, *J. Vac. Sci. Technol. 19*, 349 (1981).
821. E. I. Ko and R. J. Madix, *J. Phys. Chem. 85*, 4019 (1981).
822. C. M. Chan and W. H. Weinberg, *J. Chem. Phys. 71*, 3988 (1979).
823. K. Christmann, R. J. Behm, G. Ertl, M. A. Van Hove and W. H. Weinberg, *J. Chem. Phys. 70*, 4168 (1979).
824. L. L. Kesmodel, L. H. Dubois and G. A. Somorjai, *J. Chem. Phys. 70*, 2180 (1979).
825. G. E. Thomas and W. H. Weinberg, *J. Chem. Phys. 70*, 1437 (1979).
826. G. Pirug, H. P. Bonzel, H. Hopster and H. Ibach, *J. Chem. Phys. 71*, 593 (1979).
827. C. M. Chan and W. H. Weinberg, *J. Chem. Phys. 71*, 2788 (1979).
828. Y. Larher and A. Terlain, *J. Chem. Phys. 72*, 1052 (1980).
829. E. D. Williams, P. A. Thiel, W. H. Weinberg and J. T. Yates, Jr., *J. Chem. Phys. 72*, 3496 (1980).
830. D. E. Ibbostson, T. S. Wittrig and W. H. Weinberg, *J. Chem. Phys. 72*, 4885 (1980).
831. L. H. Dubois, D. G. Castner and G. A. Somorjai, *J. Chem. Phys. 72*, 5234 (1980).
832. S. K. Shi and J. M. White, *J. Chem. Phys. 73*, 5889 (1980).
833. F. Nitschke, G. Ertl and J. Kuppers, *J. Chem. Phys. 74*, 5911 (1981).
834. R. A. Barker and P. J. Estrup, *J. Chem. Phys. 74*, 1442 (1981).
835. P. A. Thiel, F. M. Hoffmann and W. H. Weinberg, *J. Chem. Phys. 75*, 5556 (1981).
836. S. R. Kelemen and A. Kaldor, *J. Chem. Phys. 75*, 1530 (1981).
837. J. A. Stroscio, S. R. Bare and W. Ho, *Surface Sci. 154*, 35 (1985).
838. E. J. Van Loenen, A. E. M. J. Fischer, J. F. van der Veen and F. Legoues, *Surface Sci. 154*, 52 (1985).
839. L. A. DeLouise and N. Winograd, *Surface Sci. 154*, 79 (1985).
840. C. Klauber, M. D. Alvey and J. T. Yates, Jr., *Surface Sci. 154*, 139 (1985).
841. E. Daugy, P. Mathiez, F. Salvan and J. M. Layet, *Surface Sci. 154*, 267 (1985).
842. M. T. Paffeit, C. T. Campbell, T. N. Taylor and S. Srinivasan, *Surface Sci. 154*, 284 (1985).
843. F. Zaera and G. A. Somorjai, *Surface Sci. 154*, 303 (1985).
844. I. Chorkendorff, J. Kofoed and J. Onsgaard, *Surface Sci. 152/153*,, 749 (1985).
845. G. Strasser, G. Rosina, E. Bertel and F. P. Netzer, *Surface Sci. 152/153*, 765 (1985).
846. B. Poelsema, L. K. Verheij and G. Comsa, *Surface Sci. 152/153*, 851 (1985).
847. Y. Canivez, M. Wautelet, L. D. Laude and R. Andrew, *Surface Sci. 152/153*, 995 (1985).
848. P. Koke, A. Goldmann, W. Monch, G. Wolfgarten and J. Pollmann, *Surface Sci. 152/153*, 1001 (1985).
849. I. Hernandes-Calderon and H. HLchst, *Surface Sci. 152/153*, 1035 (1985).
850. P. Morgen, W. Wurth and E. Umbach, *Surface Sci. 152/153*, 1086 (1985).
851. C. Pirri, J. C. Peruchetti, G. Gewinner and J. Derrien, *Surface Sci. 152/153*, 1106 (1985).
852. I. Hernandez-Calderon, *Surface Sci. 152/153*, 1130 (1985).
853. B. Cord and R. Courths, *Surface Sci. 152/153*, 1141 (1985).
854. P. C. Pond and D. Cherns, *Surface Sci. 152/153*, 1197 (1985).
855. S. Kennov, S. Ladas and C. Papageorgopoulos, *Surface Sci. 152/153*, 1213 (1985).

856. A. Taleb-Ibrahimi, V. Mercier, C. A. Sebenne, D. Bolmont and P. Chen, *Surface Sci. 152/153*, 1228 (1985).
857. E. Daugy, P. Mathiez, F. Salvan, J. M. Layet and J. Derrien, *Surface Sci. 152/153*, 1239 (1985).
858. J. T. Grant and T. W. Haas, *Surf. Sci. 19*, 347 (1970). (1985).
859. S. M. Francis and N. V. Richardson, *Surface Sci. 152/153*, 63 (1985).
860. J. R. Noonan, H. L. Davis and W. Erley, *Surface Sci. 152/153*, 142 (1985).
861. M. S. Zei, Y. Nakai, D. Weick and G. Lehmpfuhl, *Surface Sci. 152/153*, 254 (1985).
862. C. J. Barnes, M. Lindroos and M. Pessa, *Surface Sci. 152/153*, 260 (1985).
863. H. Asonen, C. J. Barnes, A. Salokatve and M. Pessa, *Surface Sci. 152/153*, 262 (1985).
864. K. Gurtler and K. Jacobi, *Surface Sci. 152/153*, 272 (1985).
865. J. Cousty, R. Riwan and P. Soukiassian, *Surface Sci. 152/153*, 297 (1985).
866. K. Heinz, H. Hertrich, L. Hammar and K. Muller, *Surface Sci. 152/153*, 303 (1985).
867. K. Christmann, F. Chehab, V. Penka and G. Ertl, *Surface Sci. 152/153*, 356 (1985).
868. F. Chehab, W. Krstein and F. Thieme, *Surface Sci. 152/153*, 367 (1985).
869. K. Griffiths, P. R. Norton, J. A. Davies, W. N. Unertl and T. E. Jackman, *Surface Sci. 152/153*, 374 (1985).
870. P. Hofmann and D. Menzel, *Surface Sci. 152/153*, 382 (1985).
871. J. C. Boulliard and M. Sotto, *Surface Sci. 152/153*, 392 (1985).
872. C. Benndorf, G. Klatte and F. Thieme, *Surface Sci. 152/153*, 399 (1985).
873. A. V. Titov and H. Jagodzinski, *Surface Sci. 152/153*, 409 (1985)..
874. K. Hayek, H. Glassl, A. Gutmann, H. Leonhard, M. Prutton, S. P. Tear and M. R. Welton-Cook, *Surface Sci. 152/153*, 419 (1985).
875. J. S. Foord and A. E. Reynolds, *Surface Sci. 152/153*, 426 (1985).
876. C. Harendt, J. Goschnick and W. Hirschwald, *Surface Sci. 152/153*, 453 (1985).
877. G. A. Kok, A. Noordermeer and B. F. Nieuwenhuys, *Surface Sci. 152/153*, 505 (1985).
878. K. Bange, T. E. Madey and J. K. Sass, *Surface Sci. 152/153*, 550 (1985).
879. U. Dobler, K. Baberschke, J. Haase and A. Puschmann, *Surface Sci. 152/153*, 569 (1985).
880. T. E. Madey and C. Benndorf, *Surface Sci. 152/153*, 587 (1985).
881. U. Schwalke, H. Niehus and G. Comsa, *Surface Sci. 152/153*, 596 (1985).
882. H. Hiehus and G. Comsa, *Surface Sci. 151*, L171 (1985).
883. W. Altmann, K. Desinger, M. Donath, V. Dose, A. Goldmann and H. Scheidt, *Surface Sci. 151*, L185 (1985).
884. H. You and S. C. Fain, Jr., *Surface Sci. 151*, 361 (1985).
885. G. R. Gruzalski, D. M. Zehner, J. F. Wendelken and R. S. Hathcock, *Surface Sci. 151*, 430 (1985).
886. E. Bechtold and H. Leonhard, *Surface Sci. 151*, 521 (1985).
887. J. B. Benziger and R. E. Preston, *Surface Sci. 151*, 183 (1985).
888. C. Benndorf and B. Kruger, *Surface Sci. 151*, 271 (1985).
889. K. Morishige, C. Mowforth and R. K. Thomas, *Surface Sci. 151*, 289 (1985).
890. S. R. Bare, J. A. Stroscio and W. Ho, *Surface Sci. 150*, 399 (1985).
891. K. H. Rieder and W. Stocker, *Surface Sci. 150*, L66 (1985).
892. A. G. Schrott and J. M. Blakely, *Surface Sci. 150*, L77 (1985).
893. T. J. Vink, O. L. J. Gijzeman and J. W. Geus, *Surface Sci. 150*, 14 (1985).
894. R. P. Furstenau, G. McDougall and M. A. Langell, *Surface Sci. 150*, 55 (1985).
895. H. C. Peebles, D. D. Beck, J. M. White and C. T. Campbell, *Surface Sci. 150*, 120 (1985).
896. L. Smit, T. E. Derry and J. F. van der Veen, *Surface Sci. 150*, 245 (1985).
897. M. A. Passler, B. W. Lee and A. Ignatiev, *Surface Sci. 150*, 263 (1985).
898. C. Zhang, M. A. Van Hove and G. A. Somorjai, *Surface Sci. 149*, 326 (1985).
899. B. E. Hayden, K. Kretzschmar and A. M. Bradshaw, *Surface Sci. 149*, 394 (1985).
900. D. L. Adams, W. T. Moore and K. A. R. Mitchell, *Surface Sci. 149*, 407 (1985).
901. P. M. Stefan, M. L. Shek and W. E. Spicer, *Surface Sci. 149*, 423 (1985).
902. H. Papp, *Surface Sci. 149*, 460 (1985).
903. W. Ranke and D. Schmeisser, *Surface Sci. 149*, 485 (1985).
904. H. Froitzheim, U. Kohler and H. Lammering, *Surface Sci. 149*, 537 (1985).
905. M. L. Shek, *Surface Sci. 149*, L39 (1985).
906. R. G. Egdell, H. Innes and M. D. Hill, *Surface Sci. 149*, 33 (1985).
907. L. H. Dubois and R. G. Nuzzo, *Surface Sci. 149*, 133 (1985).
908. P. A. Maksym, *Surface Sci. 149*, 157 (1985).
909. R. C. Yeates, J. E. Turner, A. J. Gellman and G. A. Somorjai, *Surface Sci. 149*, 175 (1985).
910. J. Rogozik, J. Kuppers and V. Dose, *Surface Sci. 148*, L653 (1984).
911. D. E. Fowler and J. M. Blakely, *Surface Sci. 148*, 265 and 283 (1984).
912. T. Engel, K. H. Rieder and I. P. Batra, *Surface Sci. 148*, 321 (1984).
913. E. R. Moog and M. B. Webb, *Surface Sci. 148*, 338 (1984).
914. H. Pfnur and D. Menzel, *Surface Sci. 148*, 411 (1984).

915. J. A. Stroscio, S. R. Bare and W. Ho, *Surface Sci. 148*, 499 (1984).
916. E. G. McRae and R. A. Malic, *Surface Sci. 148*, 551 (1984).
917. V. Maurice, L. Peralta, Y. Berthier and J. Oudar, *Surface Sci. 148*, 623 (1984).
918. P. Cantini and E. Cevasco, *Surface Sci. 148*, 37 (1984).
919. K. H. Rieder and W. Stocker, *Surface Sci. 148*, 139 (1984).
920. G. R. Gruzalski, D. M. Zehner and J. F. Wendelken, *Surface Sci. 147*, L623 (1984).
921. E. G. McRae and P. M. Petroff, *Surface Sci. 147*, 385 (1984).
922. L. C. Dufour, O. Bertrand and N. Floquet, *Surface Sci. 147*, 396
923. M. Hanbucken, M. Fukamoto and J. A. Venables, *Surface Sci. 147*, 433 (1984).
924. J. P. Ganon and J. Clavilier, *Surface Sci. 147*, 583 (1984).
925. D. Gorse, B. Salanon, F. Fabre, A. Kara, J. Perreau, G. Armand and J. Lapujoulade, *Surface Sci. 148*, 611, (1984).
926. F. Solymosi and L. Bugyi, *Surface Sci. 147*, 685 (1984).
927. G. J. R. Jones, J. H. Onuferko, D. P. Woodruff and B. W. Holland, *Surface Sci. 147*, 1 (1984).
928. R. J. Behm, P. A. Thiel, P. R. Norton and P. E. Bindner, *Surface Sci. 147*, 143 (1984).
929. E. Langenbach, A. Spitzer and H. Luth, *Surface Sci. 147*, 179 (1984).
930. T. Solomun, A. Wieckowski, S. D. Rosasco and A. T. Hubbard, *Surface Sci. 147*, 241 (1984).
931. L. A. DeLouise, E. J. White and N. Winograd, *Surface Sci. 147*, 252 (1984).
932. R. Riwan, P. Soukiassian, S. Zuber and J. Cousty, *Surface Sci. 146*, 382 (1984).
933. J. Billy and M. Abon, *Surface Sci. 146*, L525 (1984).
934. E. G. McRae, H.-J. Gossmann and L. C. Feldman, *Surface Sci. 146*, L540 (1984).
935. U. Bardi and P. N. Ross, *Surface Sci. 146*, L555 (1984).
936. P. Hren, D. W. Tu and A. Kahn, *Surface Sci. 146*, 69 (1984).
937. A. Wieckowski, B. C. Schardt, S. D. Rosasco, J. L. Stickney and A. T. Hubbard, *Surface Sci. 146*, 115 (1984).
938. M. Surman, F. Solymosi, R. D. Diehl, P. Hofmann and D. A. King, *Surface Sci. 146*, 135 (1984).
939. E. M. Stuve, R. J. Madix and C. R. Brundle, *Surface Sci. 146*, 155 (1984).
940. E. M. Stuve, S. W. Jorgensen and R. J. Madix, *Surface Sci. 146*, 179 (1984).
941. M. Nishijima, M. Jo and M. Onchi, *Surf. Sci. 151*, L179 (1985).
942. K. Edamoto, Y. Kubota, M. Onchi and M. Nishijima, *Surf. Sci. 146*, L533 (1984).
943. A. Puschmann and J. Haase, *Surf. Sci. 144*, 559 (1984).
944. T. E. Jackman, J. A. Davies, P. R. Norton, W. N. Unertl and K. Griffiths, *Surf. Sci. 141*, L313 (1984).
945. J. F. Wendelken and G.-C. Wang, *Surf. Sci. 140*, 425 (1984).
946. U. Schwalke, H. Niehus and G. Comsa, *Surf. Sci. 137*, 23 (1984).
947. V. Y. Aristov, I. E. Batov and V. A. Grazhulis, *Surf. Sci. 132*, 73 (1983).
948. S. Kono, H. Sakurai, K. Higashiyama and T. Sagawa, *Surf. Sci. 130*, L299 (1983).
949. C. B. Duke, S. L. Richardson, A. Paton and A. Kahn, *Surf. Sci. L135*, 127 (1983).
950. K. E. Foley and N. Winograd, *Surf. Sci. 122*, 541 (1982).
951. C. B. Bargeron, B. H. Nall and A. N. Jette, *Surf. Sci. 120*, L483 (1982).
952. P. R. Norton, J. W. Goodale and D. K. Creber, *Surf. Sci. 119*, 411 (1982).
953. J. Lapujoulade, Y. L. Cruer, M. Lefort, Y. Lejay and E. Maurel, *Surf. Sci. 118*, 103 (1982).
954. R. I. G. Uhrberg, G. V. Hansson, J. M. Nicholls and S. A. Flodstrom, *Surf. Sci. 117*, 394 (1982).
955. B. E. Koel, B. E. Bent and G. A. Somorjai, *Surface Sci. 146*, 211 (1984).
956. A. Taleb-Ibrahimi, C. A. Sebenne, D. Bolmont and P. Chen, *Surface Sci. 146*, 229 (1984).
957. M. Trenary, K. J. Uram, F. Bozso and J. T. Yates, Jr., *Surface Sci. 146*, 269 (1984).
958. K. A. Thompson and C. S. Fadley, *Surface Sci. 146*, 281 (1984).
959. K. Ueda, K. Kinoshita and M. Mannami, *Surface Sci. 145*, 261 (1984).
960. J. A. Venables, J. L. Seguin, J. Suzanne and M. Bienfait, *Surface Sci. 145*, 345 (1984).
961. H. Ohtani, B. E. Bent, C. M. Mate and G. A. Somorjai, unpublished results.
962. W. R. Lambert, M. J. Cardillo, P. L. Trevor and R. B. Doak, *Surface Sci. 145*, 519 (1984).
963. H. Conrad, R. Scala, W. Stenzel and R. Unwin, *Surface Sci. 145*, 1 (1984).
964. J. G. Clabes, *Surface Sci. 145*, 87 (1984).
965. M. J. Yacaman and P. Schabes-Retchkiman, *Surface Sci. 144*, L439 (1984).
966. S. T. Ceyer, A. J. Melmed, J. J. Carroll and W. R. Graham, *Surface Sci. 144*, L444 (1984).
967. G. K. Binnig, H. Rohrer, C. Gerber and E. Stoll, *Surface Sci. 144*, 321 (1984).
968. J. S. Villarrubia and W. Ho, *Surface Sci. 144*, 370 (1984).
969. J. Kolaczkiewicz and E. Bauer, *Surface Sci. 144*, 477 (1984).
970. J. Kolaczkiewicz and E. Bauer, *Surface Sci. 144*, 495 (1984).
971. N. Kuwata, T. Asai, K. Kimura and M. Mannami, *Surface Sci. 144*, L393 (1984).
972. J. Jupille, J. Fusy and P. Pareja, *Surface Sci. 144*, L433 (1984).
973. Y. C. Lee, M. Abu-Joudeh and P. A. Montano, *Surface Sci. 144*, 469 (1984).

974. C. T. Campbell and M. T. Paffett, *Surface Sci. 144*, 517 (1984).
975. A. Rolland, J. Bernardini and M. G. Barthes-Labrousse, *Surface Sci. 143*, 579 (1984).
976. F. P. Netzer, D. L. Doering and T. E. Madey, *Surface Sci. 143*, L363 (1984).
977. M. Asscher and G. A. Somorjai, *Surface Sci. 143*, L389 (1984).
978. J. Szeftel and S. Lehwald, *Surface Sci. 143*, 11 (1984).
979. J. L. Gland, R. J. Madix, R. W. McCabe and C. DeMaggio, *Surface Sci. 143*, 46 (1984).
980. F. Stucki, J. Anderson, G. J. Lapeyre and H. H. Farrell, *Surface Sci. 143*, 84 (1984).
981. D. Rieger, R. D. Schnell and W. Steinmann, *Surface Sci. 143*, 157 (1984).
982. T. M. Hupkens and J. M. Fluit, *Surface Sci. 143*, 267 (1984).
983. F. Falo, I. Cano and M. Salmeron, *Surface Sci. 143*, 303 (1984).
984. W. F. Egelhoff, *Surface Sci. 141*, L324 (1984).
985. H. Viefhaus and W. Rossow, *Surface Sci. 141*, 341 (1984).
986. B. Egert, H. J. Grabke, Y. Sakisaka and T. N. Rhodin, *Surface Sci. 141*, 397 (1984).
987. M. Grunze, P. A. Dowben and R. G. Jones, *Surface Sci. 141*, 455 (1984).
988. F. Solymosi, A. Berko and T. I. Tarnoczi, *Surface Sci. 141*, 533 (1984).
989. L. Marchut, T. M. Buck, G. H. Wheatley and C. J. McMahon, Jr., *Surface Sci. 141*, 549 (1984).
990. J. B. Benziger and R. E. Preston, *Surface Sci. 141*, 567 (1984).
991. P. A. Cox, M. D. Hill, F. Peplinskii and R. G. Egdell, *Surface Sci. 141*, 13 (1984).
992. D. A. Andrews and D. P. Woodruff, *Surface Sci. 141*, 31 (1984).
993. R. G. Tobin, S. Chiang, P. A. Thiel and P. L. Richards, *Surface Sci. 140*, 393 (1984).
994. A. G. Fedorus and V. V. Gonchar, *Surface Sci. 140*, 499 (1984).
995. H. Niehus and G. Comsa, *Surface Sci. 140*, 18 (1984).
996. T. Ichikawa, *Surface Sci. 140*, 37 (1984).
997. W. Krakow, *Surface Sci. 140*, 137 (1984).
998. M. H. Farias, A. J. Gellman, G. A. Somorjai, R. R. Chianelli and K. S. Liang, *Surface Sci. 140*, 181 (1984).
999. J. A. Schaefer, F. Stucki, J. A. Anderson, G. J. Lapeyre and W. Gopel, *Surface Sci. 140*, 207 (1984).
1000. E. Tamura and R. Feder, *Surface Sci. 139*, L191 (1984).
1001. C. T. Campbell and M. T. Paffett, *Surface Sci. 139*, 396 (1984).
1002. J. R. Kingsley, D. Dahlgren and J. C. Hemminger, *Surface Sci. 139*, 417 (1984).
1003. J. Jupille, P. Pareja and J. Fusy, *Surface Sci. 139*, 505 (1984).
1004. U. Seip, M.-C. Tsai Christmann, J. Kuppers and G. Ertl, *Surface Sci. 139*, 29 (1984).
1005. C. F. McConville, C. Somerton and D. P. Woodruff, *Surface Sci. 139*, 75 (1984).
1006. W. Mokwa, P. Kohl and G. Heiland, *Surface Sci. 139*, 98 (1984).
1007. C. B. Bargeron, B. H. Nall and A. N. Jette, *Surface Sci. 139*, 219 (1984).
1008. H.-J. Gossmann and W. M. Gibson, *Surface Sci. 139*, 239 (1984).
1009. Y. Kuk, L. C. Feldman and I. K. Robinson, *Surface Sci. 138*, L168 (1984).
1010. H.-J. Gossmann, J. C. Bean, L. C. Feldman and W. M. Gibson, *Surface Sci. 138*, L175 (1984).
1011. C. Benndorf, C. Nobl and T. E. Madey, *Surface Sci. 138*, 292 (1984).
1012. L. A. DeLouise and N. Winograd, *Surface Sci. 138*, 417 (1984).
1013. J. Segner, C. T. Campbell, G. Doyen and G. Ertl, *Surface Sci. 138*, 505 (1984).
1014. K. Griffiths, T. E. Jackman, J. A. Davies and P. R. Norton, *Surface Sci. 138*, 113 (1984)
1015. J. Kirschner, *Surface Sci. 138*, 191 (1984).
1016. J. S. Foord and R. M. Lambert, *Surface Sci. 138*, 258 (1984).
1017. M. Hanbucken, H. Neddermeyer and J. A. Venables, *Surface Sci. 137*, L92 (1984).
1018. R. Beaume, J. Suzanne, J. P. Coulomb, A. Glachant and G. Bomchil, *Surface Sci. 137*, L117 (1984).
1019. R. A. Metzger and F. G. Allen, *Surface Sci. 137*, 397 (1984).
1020. J. M. McKay and V. E. Henrich, *Surface Sci. 137*, 463 (1984).
1021. M. Nishijima, H. Kobayashi, K. Edamoto and M. Onchi, *Surface Sci. 137*, 473 (1984).
1022. E. J. van Loenen, M. Iwami, R. M. Tromp and J. F. van der Veen, *Surface Sci. 137*, 1 (1984).
1023. K. Bange, D. E. Grider, T. E. Madey and J. K. Sass, *Surface Sci. 137*, 38 (1984).
1024. P. Ho and J. M. White, *Surface Sci. 137*, 103 (1984).
1025. P. Ho and J. M. White, *Surface Sci. 137*, 117 (1984).
1026. A. Gutmann, G. Zwicker, D. Schmeisser and K. Jacobi, *Surface Sci. 137*, 211 (1984).
1027. D. A. Outka and R. J. Madix, *Surface Sci. 137*, 242 (1984).
1028. D. Bolmont, P. Chen, C. A. Sebenne and F. Proix, *Surface Sci. 137*, 280 (1984).
1029. T. Ichikawa and S. Ino, *Surface Sci. 136*, 267 (1984).
1030. M. Kiskinova, G. Pirug and H. P. Bonzel, *Surface Sci. 136*, 285 (1984).
1031. V. Penka, K. Christmann and G. Ertl, *Surface Sci. 136*, 307 (1984).
1032. A. H. Smith, R. A. Barker and P. J. Estrup, *Surface Sci. 136*, 327 (1984).
1033. S. R. Kelemen and C. A. Mims, *Surface Sci. 136*, L35 (1984).

1034. M. Klaua and T. E. Madey, *Surface Sci. 136*, L42 (1984).
1035. J. L. Stickney, S. D. Rosasco, B. C. Schardt, T. Solomun, A. T. Hubbard and B. A. Parkinson, *Surface Sci. 136*, 15 (1984).
1036. C. Somerton, C. F. McConville, D. P. Woodruff and R. G. Jones, *Surface Sci. 136*, 23 (1984).
1037. K. Horioka, H. Iwasaki, S. Maruno, S. T. Li and S. Nakamura, *Surface Sci. 136*, 121 (1984).
1038. G. Bracco, P. Cantini, E. Cavanna, R. Tatarek and A. Glachant, *Surface Sci. 136*, 169 (1984).
1039. A. J. Gellman, M. H. Farias, M. Salmeron and G. A. Somorjai, *Surface Sci. 136*, 217 (1984).
1040. U. Kohler, M. Alavi and H.-W. Wassmuth, *Surface Sci. 136*, 243 (1984).
1041. C. Argile and G. E. Rhead, *Surface Sci. 135*, 18 (1983).
1042. G. A. Kok, A. Noordermeer and B. E. Nieuwenhuys, *Surface Sci. 135*, 65 (1983).
1043. W. T. Tysoe, G. L. Nyberg and R. M. Lambert, *Surface Sci. 135*, 128 (1983).
1044. J. W. M. Frenken, R. G. Smeenk and J. F. van der Veen, *Surface Sci. 135*, 147 (1983).
1045. C. Benndorf and T. E. Madey, *Surface Sci. 135*, 164 (1983).
1046. G. Quentel and R. Kern, *Surface Sci. 135*, 325 (1983).
1047. R. Kotz and B. E. Hayden, *Surface Sci. 135*, 374 (1983).
1048. C. M. A. M. Mesters, G. Wermer, O. L. J. Gijzeman and J. W. Geus, *Surface Sci. 135*, 396 (1983).
1049. H. Sakurai, K. Higashiyama, S. Kono and T. Sagawa, *Surface Sci. 134*, L550 (1983).
1050. M. Bowker and K. C. Waugh, *Surface Sci. 134*, 639 (1983).
1051. A. P. C. Reed, R. M. Lambert and J. S. Foord, *Surface Sci. 134*, 689 (1983).
1052. N. J. Gudde and R. M. Lambert, *Surface Sci. 134*, 703 (1983).
1053. P. S. Uy, J. Bardolle and M. Bujor, *Surface Sci. 134*, 713 (1983).
1054. R. C. Yeates and G. A. Somorjai, *Surface Sci. 134*, 729 (1983).
1055. R. C. Cinti, T. T. A. Nguyen, Y. Capiomont and S. Kennou, *Surface Sci. 134*, 755 (1983).
1056. J. StLor, R. Jaeger, G. Rossi, T. Kendelewiczx and I. Lindau, *Surface Sci. 134*, 813 (1983).
1057. D. Dahlgren and J. C. Hemminger, *Surface Sci. 134*, 836 (1983).
1058. J.-M. Baribeau and J.-D. Carette, *Surface Sci. 134*, 886 (1983).
1059. M. P. Cox, G. Ertl, R. Imbihl and J. Rhstig, *Surface Sci. 134*, L517 (1983).
1060. K. Gurtler and K. Jacobi, *Surface Sci. 134*, 309 (1983).
1061. R. Feidenhans'l, J. E. Sorensen and I. Stensgaard, *Surface Sci. 134*, 329 (1983).
1062. M. L. Shek, P. M. Stefan, I. Lindau and W. E. Spicer, *Surface Sci. 134*, 399 (1983).
1063. M. L. Shek, P. M. Stefan, I. Lindau and W. E. Spicer, *Surface Sci. 134*, 427 (1983).
1064. Y. Larher, *Surface Sci. 134*, 469 (1983).
1065. T. N. Tayler, C. T. Campbell, J. W. Rogers, Jr., W. P. Ellis and J. M. White, *Surface Sci. 134*, 529 (1983).
1066. P. Hollins and J. Pritchard, *Surface Sci. 134*, 91 (1983).
1067. T. Urao, T. Kanaji and M. Kaburagi, *Surface Sci. 134*, 109 (1983).
1068. R. F. Lin, R. J. Koestner, M. A. Van Hove and G. A. Somorjai, *Surface Sci. 134*, 161 (1983).
1069. M. Schuster and C. Varelas, *Surface Sci. 134*, 195 (1983).
1070. A. Bogen and J. Kuppers, *Surface Sci. 134*, 223 (1983).
1071. M. Kiskinova, G. Pirug and H. P. Bonzel, *Surface Sci. 133*, 321 (1983).
1072. S. D. Foulias, K. J. Rawlings and B. J. Hopkins, *Surface Sci. 133*, 377 (1983).
1073. Y. Horio and A. Ichimiya, *Surface Sci. 133*, 393 (1983).
1074. K. Jacobi and H. H. Rotermund, *Surface Sci. 133*, 401 (1983).
1075. J. J. Metois and G. L. Lay, *Surface Sci. 133*, 422 (1983).
1076. R. Feidenhans'l and I. Stensgaard, *Surface Sci. 133*, 453 (1983).
1077. N. Masud, R. Baudoing, D. Aberdam and C. Gaubert, *Surface Sci. 133*, 580 (1983).
1078. S. Nakanishi and T. Horiguchi, *Surface Sci. 133*, 605 (1983).
1079. R. J. Madix, M. Thornburg and S.-B. Lee, *Surface Sci. 133*, L477 (1983).
1080. P. Hofmann, S. R. Bare, N. V. Richardson and D. A. King, Surface Sci. 133, L459 (1983).
1081. K. K. Kleinherbers and A. Goldmann, *Surface Sci. 133*, 38 (1983).
1082. D. L. Doering, S. Semancik and T. E. Madey, *Surface Sci. 133*, 49 (1983).
1083. S. R. Kelemen and C. A. Mims, *Surface Sci. 133*, 71 (1983).
1084. R. M. Tromp, R. G. Smeenk, F. W. Saris and D. J. Chadi, *Surface Sci. 133*, 137 (1983).
1085. J. H. Neave, P. K. Larsen, J. F. van der Veen, P. J. Dobson and B. A. Joyce, *Surface Sci. 133*, 267 (1983).
1086. G. V. Hansson, R. I. G. Uhrberg and J. M. Nicholls, *Surface Sci. 132*, 31 (1983).
1087. F. Houzay, G. Guichar, R. Pinchaux, G. Jezequel, F. Solal, A. Barsky, P. Steiner and Y. Petroff, *Surface Sci. 132*, 40 (1983).
1088. P. H. Citrin and J. F. Rowe, *Surface Sci. 132*, 205 (1983).
1089. P. Chen, D. Bolmont and C. A. Sebenne, *Surface Sci. 132*, 505 (1983).
1090. J. R. Waldrop, E. A. Kraut, S. P. Kowalczyk and R. W. Grant, *Surface Sci. 132*, 513 (1983).
1091. Y. Yabuuchi, F. Shoji, K. Oura and T. Hanawa, *Surface Sci. 131*, L412 (1983).

1092. K. H. Rieder and H. Wilsch, *Surface Sci. 131*, 245 (1983).
1093. J. Segner, H. Robota, W. Vielhaber, G. Ertl, F. Frenkel, J. Hager, W. Krieger and H. Walther, *Surface Sci. 131*, 273 (1983).
1094. J. G. Nelson, W. J. Gignac, R. S. Williams, S. W. Robey, J. G. Tobin and D. A. Shirley, *Surface Sci. 131*, 290 (1983).
1095. S. M. Thurgate and P. J. Jennings, *Surface Sci. 131*, 309 (1983).
1096. B. E. Hayden, *Surface Sci. 131*, 419 (1983).
1097. I. Stensgaard and R. Feidenhans'l, *Surface Sci. 131*, L373 (1983).
1098. G. Binning, H, Rohrer, C. Gerber and E. Weibel, *Surface Sci. 131*, L379 (1983).
1099. C. Egawa, S. Naito and K. Tamaru, *Surface Sci. 131*, 49 (1983).
1100. R. Miranda, S. Daiser, K. Wandelt and G. Ertl, *Surface Sci. 131*, 61 (1983).
1101. D. Westphal and A. Goldmann, *Surface Sci. 131*, 92 (1983).
1102. D. Westphal and A. Goldmann, *Surface Sci. 131*, 113 (1983).
1103. D. R. Lloyd and F. P. Netzer, *Surface Sci. 131*, 139 (1983).
1104. G. Zwicker and K. Jacobi, *Surface Sci. 131*, 179 (1983).
1105. R. Miranda, D. Chandesris and J. Lecante, *Surface Sci. 130*, 269 (1983).
1106. J. L. Stickney, S. D. Rosasco, D. Song, M. P. Soriaga and A. T. Hubbard, *Surface Sci. 130*, 326 (1983).
1107. M. Huttinger and J. Kuppers, *Surface Sci. 130*, L277 (1983).
1108. S. Kono, H. Sakurai, K. Higashiyama and T. Sagawa, *Surface Sci. 130*, L299 (1983).
1109. W. P. Ellis, K. A. Thompson and N. S. Nogar, *Surface Sci. 130*, L317 (1983).
1110. J. Lee, J. P. Cowin and L. Wharton, *Surface Sci. 130*, 1 (1983).
1111. T. E. Felter, F. N. Hoffmann, P. A. Thiel and W. H. Weinberg, *Surface Sci. 130*, 163 (1983).
1112. F. M. Hoffmann, T. E. Felter, P. A. Thiel and W. H. Weinberg, *Surface Sci. 130*, 173 (1983).
1113. P. A. Montano, P. P. Vaishnava and E. Boling, *Surface Sci. 130*, 191 (1983).
1114. C. M. Pradier, Y. Berthier and J. Oudar, *Surface Sci. 130*, 229 (1983).
1115. M. Yamamoto and D. N. Seidman, *Surface Sci. 129*, 281 (1983).
1116. V. Maurice, J. J. Legendre and M. Huber, *Surface Sci. 129*, 301 (1983).
1117. V. Maurice, J. J. Legendre and M. Huber, *Surface Sci. 129*, 312 (1983).
1118. R. L. Kurtz and V. E. Henrich, *Surface Sci. 129*, 345 (1983).
1119. P. D. Johnson, D. P. Woodruff, H. H. Farrell, N. V. Smith and M. M. Traum, *Surface Sci. 129*, 366 (1983).
1120. M. P. Cox, J. S. Foord, R. M. Lambert and R. H. Prince, *Surface Sci. 129*, 375 (1983).
1121. P. Marcus, A. Teissier and J. Oudar, *Surface Sci. 129*, 432 (1983).
1122. M. A. Van Hove, R. J. Koestner, J. C. Frost and G. A. Somorjai, *Surface Sci. 129*, 482 (1983).
1123. R. Opila and R. Gomer, *Surface Sci. 129*, 563 (1983).
1124. M. Mattern-Klosson, X. M. Ding, H. Luth and A. Spitzer, *Surface Sci. 129*, 1 (1983).
1125. E. Conrad and M. B. Webb, *Surface Sci. 129*, 37 (1983).
1126. J. S. Foord, A. P. C. Reed and R. M. Lambert, *Surface Sci. 129*, 79 (1983).
1127. G. Michalk, W. Moritz, H. Pfnur and D. Menzel, *Surface Sci. 129*, 92 (1983).
1128. L. E. Firment and A. Ferretti, *Surface Sci. 129*, 155 (1983).
1129. D. L. Doering and S. Semancik, *Surface Sci. 129*, 177 (1983).
1130. H. Papp, *Surface Sci. 129*, 205 (1983).
1131. P. S. Uy, J. Bardolle and M. Bujor, *Surface Sci. 129*, 219 (1983).
1132. R. Ducros, B. Tardy and J. C. Bertolini, *Surface Sci. 128*, L219 (1983).
1133. A. J. Algra, E. P. T. M. Suurmeijer and A. L. Boers, *Surface Sci. 128*, 207 (1983).
1134. R. M. Tromp, E. J. Van Loenen, M. Iwami, R. G. Smeenk, F. W. Saris, F. Nava and G. Ottaviani, *Surface Sci. 128*, 224 (1983).
1135. I. Stensgaard, R. Feidenhans'l and J. E. Sϕrensen, *Surface Sci. 128*, 281 (1983).
1136. D. L. Adams, H. E. Nielsen and J. N. Andersen, *Surface Sci. 128*, 294 (1983).
1137. M. Grunze, P. A. Dowben and C. R. Brundle, *Surface Sci. 128*, 311 (1983).
1138. K. H. Rieder, *Surface Sci. 128*, 325 (1983).
1139. A. Ichimiya and Y. Takeuchi, *Surface Sci. 128*, 343 (1983).
1140. C. Benndorf, M. Frank and F. Thieme, *Surface Sci. 128*, 417 (1983).
1141. V. Martines, F. Soria, M. C. Munoz and J. L. Sacedon, *Surface Sci. 128*, 424 (1983).
1142. R. Baudoing, E. Blanc, C. Gaubert, Y. Gauthier and N. Gnuchev, *Surface Sci. 128*, 22 (1983).
1143. C. Backx, C. P. M. de Groot, P. Biloen and W. M. H. Sachtler, *Surface Sci. 128*, 81 (1983).
1144. B. C. De Cooman, V. D. Vankar and R. W. Vook, *Surface Sci. 128*, 128 (1983).
1145. U. Bardi and G. Rovida, *Surface Sci. 128*, 145 (1983).
1146. K. Truszkowska and M. J. Yacaman, *Surface Sci. 127*, L159 (1983).
1147. C.-F. Ai and T. T. Tsong, *Surface Sci. 127*, L165 (1983).
1148. R. G. Jones, C. F. McConville and D. P. Woodruff, *Surface Sci. 127*, 424 (1983).

1149. M. Salmeron, G. A. Somorjai and R. R. Chianelli, *Surface Sci. 127*, 526 (1983).
1150. J. L. Gland, R. W. McCabe and G. E. Mitchell, *Surface Sci. 127*, L123 (1983).
1151. B. T. Jonker, N. C. Bartelt and R. L. Park, *Surface Sci. 127*, 183 (1983).
1152. S. Maroie, P. A. Thiry, R. Caudano and J. J. Verbist, *Surface Sci. 127*, 200 (1983).
1153. K. H. Rieder, T. Engel, R. H. Swendsen and M. Manninen, *Surface Sci. 127*, 223 (1983).
1154. E. Bauer and H. Poppa, *Surface Sci. 127*, 243 (1983).
1155. S. L. Miles, S. L. Bernasek and J. L. Gland, *Surface Sci. 127*, 271 (1983).
1156. E. Lang, K. Muller, K. Heinz, M. A. Van Hove, R. J. Koestner and G. A. Somorjai, *Surface Sci. 127*, 347 (1983).
1157. F. P. Netzer and T. E. Madey, *Surface Sci. 127*, L102 (1983).
1158. T. Yokotsuka, S. Kono, S. Suzuki and T. Sagawa, *Surface Sci. 127*, (1983).
1159. H. Hochst and I. Hernandez-Calderon, *Surface Sci. 126*, 25 (1983).
1160. K. C. Prince and A. M. Bradshaw, *Surface Sci. 126*, 49 (1983).
1161. U. O. Karlsson, G. V. Hansson and S. A. Flodstrom, *Surface Sci. 126*, 58 (1983).
1162. J. Massardier, B. Tardy, M. Abon and J. C. Bertolini, *Surface Sci. 126*, 154 (1983).
1163. C. Nyberg and C. G. Tengstal, *Surface Sci. 126*, 163 (1983).
1164. A. M. Baro and L. Olle, *Surface Sci. 126*, 170 (1983).
1165. E. F. J. Didham, W. Allison and R. F. Willis, *Surface Sci. 126*, 219 (1983).
1166. D. P. Jackson, T. E. Jackman, J. A. Davies, W. N. Unertl and P. R. Norton, *Surface Sci. 126*, 226 (1983).
1167. C. Binns, C. Norris, G. C. Smith, H. A. Padmore, M. G. Barthes-Labrousse, *Surface Sci. 126*, 258 (1983).
1168. C. Benndorf, C. Nobl and F. Thieme, *Surface Sci. 126*, 265 (1983).
1169. N. Vennemann, E. W. Schwarz and M. Neumann, *Surface Sci. 126*, 273 (1983).
1170. J. M. Moison and M. Bensoussan, *Surface Sci. 126*, 294 (1983).
1171. G. Lindauer, P. Legare and G. Maire, *Surface Sci. 126*, 301 (1983).
1172. M. Surman, S. R. Bare, P. Hofmann and D. A. King, *Surface Sci. 126*, 349 (1983).
1173. M. G. Cattania, V. Penka, R. J. Behm, K. Christmann and G. Ertl, *Surface Sci. 126*, 382 (1983).
1174. M. Salmeron and G. A. Somorjai, *Surface Sci. 126*, 410 (1983).
1175. K. Khonde, J. Darville and J. M. Gilles, *Surface Sci. 126*, 414 (1983).
1176. S. Tatarenko, R. Ducros and M. Alnot, *Surface Sci. 126*, 422 (1983).
1177. F. Labohm, C. W. R. Engelen, O. L. J. Gijzeman, J. W. Geus and G.A. Bootsma, *Surface Sci. 126*, 429 (1983).
1178. K. Bange, D. Grider and J. K. Sass, *Surface Sci. 126*, 437 (1983).
1179. U. Kohler and H.-W. Wassmuth, *Surface Sci. 126*, 448 (1983).
1180. Z. T. Stott and H. P. Hughes, *Surface Sci. 126*, 455 (1983).
1181. M. Mattern and H. Luth, *Surface Sci. 126*, 502 (1983).
1182. D. Bolmont, V. Mercier, P. Chen, H. Lhth and C. A. Sebenne, *Surface Sci. 126*, 509 (1983).
1183. E. De Fresart, J. Darville and J. M. Gilles, *Surface Sci. 126*, 518 (1983).
1184. H. Tochihara, *Surface Sci. 126*, 523 (1983).
1185. N. Floquet and L.-C. Dufour, *Surface Sci. 126*, 543 (1983).
1186. J. P. Landuyt, L. Vandenbroucke, R. D. Gryse and J. Vennik, *Surface Sci. 126*, 598 (1983).
1187. A. M. Lahee, W. Allison, R. F. Willis and K. H. Rieder, *Surface Sci. 126*, 654 (1983).
1188. M. Shiojiri, N. Nakamura, C. Kaito and T. Miyano, *Surface Sci. 126*, 719 (1983).
1189. M. Domke, B. Kyvelos and G. Kaindl, *Surface Sci. 126*, 727 (1983).
1190. R. D. Diehl and S. C. Fain, Jr., *Surface Sci. 125*, 116 (1983).
1191. J. Suzanne, J. L. Seguin, H. Taub and J. P. Biberian, *Surface Sci. 125*, 153 (1983).
1192. K. Kjaer, M. Nielsen, J. Bohr, H. J. Lauter and J. P. McTague, *Surface Sci. 125*, 171 (1983).
1193. J. Bohr, M. Nielsen, J. Als-Nielsen, K. Kjaer and J. P. McTague, *Surface Sci. 125*, 181 (1983)
1194. P. Bak and T. Bohr, *Surface Sci. 125*, 279 (1983).
1195. D. E. Taylor and R. L. Park, *Surface Sci. 125*, L73 (1983).
1196. N. Freyer, G. Pirug and H. P. Bonzel, *Surface Sci. 125*, 327 (1983).
1197. M. Welz, W. Moritz and D. Wolf, *Surface Sci. 125*, 473 (1983).
1198. R. J. Madix, J. L. Gland, G. E. Mitchell and B. A. Sexton, Surface Sci. 125, 481 (1983).
1199. K. Heinz and G. Besold, *Surface Sci. 125*, 515 (1983).
1200. P. A. Heiney, P. W. Stephens, S. G. J. Mochrie, J. Akimitsu, R. J. Birgeneau and P. M. Horn, *Surface Sci. 125*, 539 (1983).
1201. G. Bracco, P. Cantini, A. Glachant and R. Tatarek, *Surface Sci. 125*, L81 (1983).
1202. H. C. Peebles, D. E. Peebles and J. M. White, *Surface Sci. 125*, L87 (1983).
1203. C. Egawa, S. Naito and K. Tamaru, *Surface Sci. 125*, 605 (1983).
1204. S. Nakanishi and T. Horiguchi, *Surface Sci. 125*, 635 (1983).
1205. B. E. Hayden and A. M. Bradshaw, *Surface Sci. 125*, 787 (1983).
1206. F. Houzay, G. M. Guichar, A. Cros, F. Salvan, P. Pinchaux and J. Derrien, *Surface Sci. 124*, L1 (1983).
1207. R. M. Tromp, E. J. van Loenen, M. Iwami, R. G. Smeenk, F. W. Saris, F. Nava and G. Ottaviani, *Surface Sci. 124*, 1 (1983).

1208. F. P. Netzer and M. M. El Gomati, *Surface Sci. 124*, 26 (1983).
1209. J. A. Gates and L. L. Kesmodel, *Surface Sci. 124*, 68 (1983).
1210. E. G. McRae, *Surface Sci. 124*, 106 (1983).
1211. D. T. Ling, J. N. Miller, D. L. Weissman, P. Pianetta, P. M. Stefan, I. Lindau and W. E. Spicer, *Surface Sci. 124*, 175 (1983).
1212. M. R. McClellan, F. R. McFeely and J. L. Gland, *Surface Sci. 124*, 188 (1983).
1213. B. J. Mrstik, *Surface Sci. 124*, 253 (1983).
1214. S. P. Svensson, J. Kanski, T. G. Andersson and P. O. Nilsson, *Surface Sci. 124*, L31 (1983).
1215. J. Derrien and F. Ringeisen, *Surface Sci. 124*, L35 (1983).
1216. G. Schulze and M. Henzler, *Surface Sci. 124*, 336 (1983).
1217. N. J. Gudde and R. M. Lambert, *Surface Sci. 124*, 372 (1983).
1218. D. Prigge, W. Schlenk and E. Bauer, *Surface Sci. 123*, L698 (1982).
1219. A. Titov and W. Moritz, *Surface Sci. 123*, L709 (1982).
1220. H. Scheidt, M. Globl and V. Dose, *Surface Sci. 123*, L728 (1982).
1221. H. Steininger, S. Lehwald and H. Ibach, *Surface Sci. 123*, 1 (1982).
1222. S. Maruno, H. Iwasaki, K. Horioka, S.-T. Li and S. Nakamura, *Surface Sci. 123*, 18 (1982).
1223. G. Le Lay, M. Manneville and J. J. Metois, *Surface Sci. 123*, 117 (1982).
1224. R. Imbihl, R. J. Behm, G. Ertl and W. Moritz, *Surface Sci. 123*, 129 (1982).
1225. M. Maglietta, E. Zanazzi, U. Bardi, D. Sondericker, F. Jona and P. M. Marcus, *Surface Sci. 123*, 141 (1982).
1226. B. Poelsema, R. L. Palmer and G. Comsa, *Surface Sci. 123*, 152 (1982).
1227. D. Dahlgren and J. C. Hemminger, *Surface Sci. 123*, L739 (1982).
1228. G. Popov and E. Bauer, *Surface Sci. 123*, 165 (1982).
1229. A. G. Schrott and S. C. Fain, Jr., *Surface Sci. 123*, 204 (1982).
1230. A. G. Schrott, Q. X. Su and S. C. Fain, Jr., *Surface Sci. 123*, 223 (1982).
1231. J. K. Lang, K. D. Jamison, F. B. Dunning, G. K. Walters, M. A. Passler, A. Ignatiev, E. Tamura and R. Feder, *Surface Sci. 123*, 247 (1982).
1232. H. Steininger, S. Lehwald and H. Ibach, *Surface Sci. 123*, 264 (1982).
1233. D. L. Doering and T. E. Madey, *Surface Sci. 123*, 305 (1982).
1234. D. P. Woodruff, B. E. Hayden, K. Prince and A. M. Bradshaw, *Surface Sci. 123*, 397 (1982).
1235. G. R. Castro and J. Kuppers, *Surface Sci. 123*, 456 (1982).
1236. H.-D. Schmick and H.-W. Wassmuth, *Surface Sci. 123*, 471 (1982).
1237. P. R. Norton, J. A. Davies and T. E. Jackmon, *Surface Sci. 122*, L593 (1982).
1238. G. Pirug, H. P. Bonzel and G. Broden, *Surface Sci. 122*, 1 (1982).
1239. W. H. Cheng and H. H. Kung, *Surface Sci. 122*, 21 (1982).
1240. G. Landgren, S. P. Svensson and T. G. Andersson, *Surface Sci. 122*, 55 (1982).
1241. T. E. Felter, S. A. Steward and F. S. Uribe, *Surface Sci. 122*, 69 (1982).
1242. C. T. Campbell and T. N. Taylor, *Surface Sci. 122*, 119 (1982).
1243. G.-C. Wang and T.-M. Lu, *Surface Sci. 122*, L635 (1982).
1244. F. Solymosi and A. Berko, *Surface Sci. 122*, 275 (1982).
1245. G. Gewinner, J. C. Peruchetti and A. Jaegle, *Surface Sci. 122*, 383 (1982).
1246. G. Popov and E. Bauer, *Surface Sci. 122*, 433 (1982).
1247. W. T. Moore, S. J. White, D. C. Frost, and K. A. R. Mitchell, *Surf. Sci. 116*, 261 (1982).
1248. S. Astegger and E. Bechtold, *Surface Sci. 122*, 491 (1982).
1249. G. A. Garwood Jr., A. T. Hubbard and J. B. Lumsden, *Surface Sci. 121*, L524 (1982).
1250. L. J. Clarke and L. Morales de la Garza, *Surface Sci. 121*, 32 (1982).
1251. H. Conrad, G. Ertl, J. Kuppers, W. Sesselmann and H. Haberland, *Surface Sci. 121*, 161 (1982).
1252. P. A. Thiel, R. J. Behm, P. R. Norton and G. Ertl, *Surface Sci. 121*, L553 (1982).
1253. A. Fujimori, F. Minami and N. Tsuda, *Surface Sci. 121*, 199 (1982).
1254. P. W. Davies, M. A. Quinlan and G. A. Somorjai, *Surface Sci. 121*, 290 (1982).
1255. J. E. Crowell, E. L. Garfunkel and G. A. Somorjai, *Surface Sci. 121*, 303 (1982).
1256. R. J. Koestner, M. A. Van Hove and G. A. Somorjai, *Surface Sci. 121*, 321 (1982).
1257. R. H. Milne, *Surface Sci. 121*, 347 (1982).
1258. J. Y. Katekaru, G. A. Garwood, Jr., J. F. Hershberger and A. T. Hubbard, *Surface Sci. 121*, 396 (1982).
1259. S. B. DiCenzo, G. K. Wertheim and D. N. E. Buchanan, *Surface Sci. 121*, 411 (1982).
1260. J. P. Jones, *Surface Sci. 121*, 487 (1982).
1261. Y. Sakisaka, H. Kato and M. Onchi, *Surface Sci. 120*, 150 (1982).
1262. G. Casalone, M. G. Cattania, F. Merati and M. Simonetta, *Surface Sci. 120*, 171 (1982).
1263. S. E. Greco, J. P. Roux and J. M. Blakely, *Surface Sci. 120*, 203 (1982).
1264. T. W. Capehart, C. W. Seabury, G. W. Graham and T. N. Rhodin, *Surface Sci. 120*, L441 (1982).
1265. K. Heinz, E. Lang, K. Strauss and K. Muller, *Surface Sci. 120*, L401 (1982).

1266. J. A. Gates and L. L. Kesmodel, *Surface Sci. 120*, L461 (1982).
1267. A. Fasana and L. Braicovich, *Surface Sci. 120*, 239 (1982).
1268. K. Christmann and J. E. Demuth, *Surface Sci. 120*, 291 (1982).
1269. A. G. Naumovets and A. G. Fedorus, *Zh. Eksperim Teor. Fiz. 68*, 1183 (1975) [*Soviet Phys.-JETP 41*, 587 (1976)].
1270. A. Spitzer and H. Luth, *Surface Sci. 120*, 376 (1982).
1271. T. E. Jackman, J. A. Davies, D. P. Jackson, W. N. Unertl and P. R. Norton, *Surface Sci. 120*, 389 (1982).
1272. G. C. Smith, H. A. Padmore and C. Norris, *Surface Sci. 119*, L287 (1982).
1273. C. B. Bargeron and B. H. Nall, *Surface Sci. 119*, L319 (1982).
1274. P. J. Dobson, J. H. Neave and B. A. Joyce, *Surface Sci. 119*, L339 (1982).
1275. T. N. Gardiner and E. Bauer, *Surface Sci. 119*, L353 (1982).
1276. A. Ortega, F. M. Hoffman and A. M. Bradshaw, *Surface Sci. 119*, 79 (1982).
1277. M. Grunze, C. R. Brundle, and D. Tomanek, *Surface Sci. 119*, 133 (1982).
1278. G. Comsa, G. Mechtersheimer and B. Poelsema, *Surface Sci. 119*, 159 (1982).
1279. S. Ferrer and H. R. Bonzel, *Surface Sci. 119*, 234 (1982).
1280. C. Park, E. Bauer and H. M. Kramer, *Surface Sci. 119*, 251 (1982).
1281. P. J. Orders, S. Kono, C. S. Fadley, R. Trehan and J. T. Lloyd, *Surface Sci.119*, 371 (1982).
1282. F. P. Netzer and T. E. Madey, *Surface Sci. 119*, 422 (1982).
1283. J. L. Seguin and J. Suzanne, *Surface Sci. 118*, L241 (1982).
1284. K. H. Rieder, *Surface Sci. 118*, 57 (1982).
1285. A. Spitzer and H. Luth, *Surface Sci. 118*, 121 (1982).
1286. A. Spitzer and H. Lth, *Surface Sci. 118*, 136 (1982).
1287. G. A. Garwood, Jr. and A. T. Hubbard, *Surface Sci. 118*, 223 (1982).
1288. C. T. Campbell and T. N. Taylor, *Surface Sci. 118*, 401 (1982).
1289. S. A. Flodstrom and C. W. B. Martinsson, *Surface Sci. 118*, 513 (1982).
1290. E. Roman and R. Riwan, *Surface Sci. 118*, 682 (1982).
1291. J. Ibanez, N. Garcia, J. M. Rojo and N. Cabrera, *Surface Sci. 117*, 23 (1982).
1292. W. Englert, E. Taglauer and W. Heiland, *Surface Sci. 117*, 124 (1982).
1293. E. Lang, W. Grimm and K. Heinz, *Surface Sci. 117*, 169 (1982).
1294. W. Berndt, R. Hora and M. Scheffler, *Surface Sci. 117*, 188 (1982).
1295. W. Hoesler and W. Moritz, *Surface Sci. 117*, 196 (1982).
1296. Y. Y. Aristov, N. I. Golovko, V. A. Grazhulis, Y. A. Ossipyan and V. I. Talyanskii, *Surface Sci. 117*, 204 (1982).
1297. P. Hofmann, S. R. Bare and D. A. King, *Surface Sci. 117*, 245 (1982).
1298. R. Imbihl, R. J. Behm, K. Christmann, G. Ertl and T. Matsushima, *Surface Sci. 117*, 257 (1982).
1299. R. Miranda, F. Yndurain, D. Chandesris, J. Lecante and Y. Petroff, *Surface Sci. 117*, 319 (1982).
1300. R. Kotz, B. E. Hayden, E. Schweizer and A. M. Bradshaw, *Surface Sci. 117*, 331 (1982).
1301. S. Lehwald, H. Ibach and H. Steininger, *Surface Sci. 117*, 342 (1982).
1302. R. Matz and H. Luth, *Surface Sci. 117*, 362 (1982).
1303. M. Pessa, H. Asonen, R. S. Rao, R. Prasad and A. Bansil, *Surface Sci. 117*, 371 (1982).
1304. K. Horn, C. Mariani and L. Cramer, *Surface Sci. 117*, 376 (1982).
1305. D. Bolmont, P. Chen and C. A. Sebenne, *Surface Sci. 117*, 417 (1982).
1306. S. . Lindgren, J. Paul and L. Wallden, *Surface Sci. 117*, 426 (1982).
1307. R. Brooks, N. V. Richardson and D. A. King, *Surface Sci. 117*, 434 (1982).
1308. T. E. Madey and F. P. Netzer, *Surface Sci. 117*, 549 (1982).
1309. Ya-Po Hsu, K. Jacobi and H. H. Rotermund, *Surface Sci. 117*, 581 (1982).
1310. J. M. Heras, H. Papp and W. Spiess, *Surface Sci. 117*, 590 (1982).
1311. C. M. A. M. Mesters, A. F. H. Wielers, O. L. J. Gijzeman, G. A. Bootsma and J. W. Geus, *Surface Sci. 117*, 605 (1982).
1312. G. Castro, J. E. Hulse, J. Kuppers and A. Rodriguez Gonzalez-Elipe, *Surface Sci. 117*, 621 (1982).
1313. H. Steininger, H. Ibach and S. Lehwald, *Surface Sci. 117*, 685 (1982).
1314. K. E. Foley and N. Winograd, *Surface Sci. 116*, 1 (1982).
1315. V. Jensen, J. N. Andersen, H. B. Nielsen and D. L. Adams, *Surface Sci. 116*, 66 (1982).
1316. R. J. Koestner, J. C. Frost, P. C. Stair, M. A. Van Hove and G. A. Somorjai, *Surface Sci. 116*, 85 (1982).
1317. P. Kaplan, *Surface Sci. 116*, 104 (1982).
1318. L. E. Firment, *Surface Sci. 116*, 205 (1982).
1319. C. Binns and C. Norris, *Surface Sci. 116*, 338 (1982).
1320. J. Carelli and A. Kahn, *Surface Sci. 116*, 380 (1982).
1321. T. S. Wittrig, P. D. Szuromi and W. H. Weinberg, *Surface Sci. 116*, 414 (1982).
1322. A. Cros, F. Houzay, G. M. Guichar and R. Pinchaux, *Surface Sci. 116*, L232 (1982).
1323. C. Park, H. M. Kramer and E. Bauer, *Surface Sci. 116*, 456 (1982).

1324. C. Park, H. M. Kramer and E. Bauer, *Surface Sci. 116*, 467 (1982).
1325. U. Gradmann and G. Waller, *Surface Sci. 116*, 539 (1982).
1326. C. Park, H. M. Kramer and E. Bauer, *Surface Sci. 115*, 1 (1982).
1327. W. T. Tysoe and P. M. Lambert, *Surface Sci. 115*, 37 (1982).
1328. R. Nishitani, C. Oshima, M. Aono, T. Tanaka, S. Kawai, H. Iwasaki and S. Nakamura, *Surface Sci. 115*, 48 (1982).
1329. S. W. Johnson and R. J. Madix, *Surface Sci. 115*, 61 (1982).
1330. J. S. Foord and R. M. Lambert, *Surface Sci. 115*, 141 (1982).
1331. A. Glachant, M. Jaubert, M. Bienfait and G. Boato, *Surface Sci. 115*, 219 (1982).
1332. H. Poppa and F. Soria, *Surface Sci. 115*, L105 (1982).
1333. S. Tougaard and A. Ignatiev, *Surface Sci. 115*, 270 (1982).
1334. T. W. Orent and S. D. Bader, *Surface Sci. 115*, 323 (1982).
1335. M. A. Barteau and R. J. Madix, *Surface Sci. 115*, 355 (1982).
1336. C. Binns and C. Norris, *Surface Sci. 115*, 395 (1982).
1337. E. L. Garfunkel and G. A. Somorjai, *Surface Sci. 115*, 441 (1982).
1338. S. Calisti, J. Suzanne and J. A. Venables, *Surface Sci. 115*, 455 (1982).
1339. G. E. Gdowski and R. J. Madix, *Surface Sci. 115*, 524 (1982).
1340. R. T. Tung, W. R. Graham and A. J. Melmed, *Surface Sci. 115*, 576 (1982).
1341. W. Erley, *Surface Sci. 114*, 47 (1982).
1342. Y. Terada, T. Yoshizuka, K. Oura and T. Hanawa, *Surface Sci. 114*, 65 (1982).
1343. H. Kato, Y. Sakisaka, T. Miyano, K. Kamei, M. Nishijima and M. Onchi, *Surface Sci. 114*, 96 (1982).
1344. J. Massies and N. T. Linh, *Surface Sci. 114*, 147 (1982).
1345.
1346. T. Narusawa, W. M. Gibson and E. Tornqvist, *Surface Sci. 114*, 331 (1982).
1347. G.-C. Wang, J. Unguris, D. T. Pierce and R. J. Celotta, *Surface Sci. 114*, L35 (1982).
1348. Y. Kim, H. C. Peebles and J. M. White, *Surface Sci. 114*, 363 (1982).
1349. D. Dahlgren and J. C. Hemminger, *Surface Sci. 114*, 459 (1982).
1350. G. Ertl, S. B. Lee and M. Weiss, *Surface Sci. 114*, 527 (1982).
1351. D. F. Mitchell and M. J. Graham, *Surface Sci. 114*, 546 (1982).
1352. M. Hanbucken and H. Neddermeyer, *Surface Sci. 114*, 563 (1982).
1353. R. Ryberg, *Surface Sci. 114*, 627 (1982).
1354. P. E. Viljoen, B. J. Wessels, G. L. P. Berning and J. P. Roux, *J. Vac. Sci. Technol. 20*, 204 (1982).
1355. L. C. Feldman, R. J. Culbertson and P. J. Silverman, *J. Vac. Sci. Technol. 20*, 368 (1982).
1356. M. Oku and C. R. Brundle, *J. Vac. Sci. Technol. 20*, 532 (1982).
1357. E. D. Williams and W. H. Weinberg, *J. Vac. Sci. Technol. 20*, 534 (1982).
1358. J. E. Black, T. S. Rahman and D. L. Mills, *J. Vac. Sci. Technol. 20*, 567 (1982).
1359. S.-W. Wang, *J. Vac. Sci. Technol. 20*, 600 (1982).
1360. W. N. Unertl, T. E. Jackman, P. R. Norton, D. P. Jackson and J. A. Davies, *J. Vac. Sci. Technol. 20*, 607 (1982).
1361. D. E. Eastman, F. J. Himpsel and J. F. van der Veen, *J. Vac. Sci. Technol. 20*, 609 (1982).
1363. D. Heskett, F. Greuter, H.-J. Freund and E. W. Plummer, *J. Vac. Sci. Technol. 20*, 623 (1982).
1363. W. F. Egelhoff, Jr., *J. Vac. Sci. Technol. 20*, 668 (1982).
1364. P. H. Holloway and R. A. Outlaw, *J. Vac. Sci. Technol. 20*, 671 (1982).
1365. J. M. Van Hove and P. I. Cohen, *J. Vac. Sci. Technol. 20*, 726 (1982).
1366. Y. J. Chabal, J. E. Rowe and S. B. Christman, *J. Vac. Sci. Technol. 20*, 763 (1982).
1367. A. Kahn, J. Carelli, C. B. Duke, A. Paton and W. K. Ford, *J. Vac. Sci. Technol. 20*, 775 (1982).
1368. K. Khonde, J. Darville and J. M. Gilles, *J. Vac. Sci. Technol. 20*, 834 (1982).
1369. R. J. Culbertson, L. C. Feldman, P. J. Silverman and R. Haight, *J. Vac. Sci. Technol. 20*, 868 (1982).
1370. K. Jacobi, G. W. Graham and T. N. Rhodin, *J. Vac. Sci. Technol. 20*, 878 (1982).
1371. D. A. Outka and R. J. Madix, *J. Vac. Sci. Technol. 20*, 882 (1982).
1372. M. A. Van Hove, R. J. Koestner and G. A. Somorjai, *J. Vac. Sci. Technol. 20*, 886 (1982).
1373. N. J. Wu and A. Ignatiev, *J. Vac. Sci. Technol. 20*, 896 (1982).
1374. D. Haneman and R. Z. Bachrach, *J. Vac. Sci. Technol. 21*, 337 (1982).
1375. A. Kahn, J. Carelli, D. L. Miller and S. P. Kowalczyk, *J. Vac. Sci. Technol. 21*, 380 (1982).
1376. E. Zanazzi, M. Maglietta, U. Bardi, F. Jona and P. M. Marcus, *J. Vac. Sci. Technol. A 1*, 7 (1983).
1377. R. Kaplan, *J. Vac. Sci. Technol. A 1*, 551 (1983).
1378. C. B. Duke, A. Paton and A. Kahn, *J. Vac. Sci. Technol. A 1*, 672 (1983).
1379. S. H. Overbury and P. C. Stair, *J. Vac. Sci. Technol. A 1*, 1055 (1982).
1380. E. D. Williams and D. L. Doering, *J. Vac. Sci. Technol. A 1*, 1188 (1983).
1381. G. Besold, K. Heinz, E. Lang and K. Muller, *J. Vac. Sci. Technol. A 1*, 1473 (1983).
1382. C. B. Duke, A. Paton, W. K. Ford, A. Kahn and G. Scott, *J. Vac. Sci. Technol. 20*, 778 (1982).

1383. P. Skeath, C. Y. Su, I. Lindau and W. E. Spicer, *J. Vac. Sci. Technol. 20*, 779 (1982).
1384. J. M. Moison and M. Bensoussan, *J. Vac. Sci. Technol. 21*, 315 (1982).
1385. J. E. Rowe and P. H. Citrin, *J. Vac. Sci. Technol. 21*, 338 (1982).
1386. B. J. Waclawski, D. T. Pierce, N. Swanson and R. J. Celotta, *J. Vac. Sci. Technol. 21*, 368 (1982).
1387. J. F. van der Veen, L. Smit, P. K. Larsen, J. H. Neave and B. A. Joyce, *J. Vac. Sci. Technol. 21*, 375 (1982).
1388. J. F. Wendelken and G.-C. Wang, *J. Vac. Sci. Technol. A 2*, 888 (1984).
1389. G.-C. Wang and T.-M. Lu, *J. Vac. Sci. Technol. A 2*, 1048 (1984).
1390. J. L. Stickney, S. D. Rosasco, B. C. Schardt and A. T. Hubbard, *J. Phys. Chem. 88*, 251 (1984).
1391. A. T. Hubbard, J. L. Stickney, S. D. Rosasco, M. P. Soriaga and D. Song, *J. Electroanal. Chem. Interfac. Electrochem. 150*, 165 (1983).
1392. T. De Jong, L. Smit, V. V. Korablev, R. M. Tromp and F. W. Saris, *Appl. Surf. Sci. 10*, 10 (1982).
1393. T. Takahashi and A. Ebina, *Appl. Surf. Sci. 11/12*, 268 (1982).
1394. K. Heinz, E. Lang, K. Strauss and K. Muller, *Appl. Surf. Sci. 11/12*, 611 (1982).
1395. K. Muller, E. Lang, H. Endriss and K. Heinz, *Appl. Surf. Sci. 11/12*, 625 (1982).
1396. M. A. Stevens-Kalceff and C. J. Russel, *Appl. Surf. Sci. 13*, 94 (1982).
1397. J. A. Ramsey, *Appl. Surf. Sci. 13*, 159 (1982).
1398. R. Madix, *Appl. Surf. Sci. 14*, 41 (1982).
1399. A. Shih, G. A. Haas and C. R. K. Marrian, *Appl. Surf. Sci. 16*, 93 (1982).
1400. G. Le Lay and J. J. Metois, *Appl. Surf. Sci. 17*, 131 (1982).
1401. W. Wen-Hao and J. Verhoeven, *Appl. Surf. Sci. 17*, 331 (1982).
1402. F. P. Netzer and T. E. Madey, *J. Chem. Phys. 76*, 710 (1982).
1403. L. H. Dubois, *J. Chem. Phys. 77*, 5228 (1982).
1404. J. Suzanne, J. L. Seguin, M. Bienfait and E. Lerner, *Phys. Rev. Lett. 52*, 632 (1984).
1405. T. Aruga, H. Tochihara and Y. Murata, *Phys. Rev. Lett. 52*, 1794 (1984).
1406. D. L. Doering and S. Semancik, *Phys. Rev. Lett. 53*, 66 (1984).
1407. R. Ryberg, *Phys. Rev. Lett. 53*, 945 (1984).
1408. S. . Lindgren, L. Wallden, J. Rundgren and P. Westrin, *Phys. Rev. B 29*, 576 (1984).
1409. J. R. Noonan and H. L. Davis, *Phys. Rev. B 29*, 4349 (1984).
1410. J. Sokolov, F. Jona and P. M. Marcus, *Phys. Rev. B 29*, 5402 (1984).
1411. M. F. Toney and S. C. Fain, Jr., *Phys. Rev. B 30*, 1115 (1984).
1412. F. J. Himpsel, P. M. Marcus, R. Tromp, I. P. Batra, M. R. Cook, F. Jona and H. Liu, *Phys. Rev. B 30*, 2257 (1984).
1413. Z. P. Hu and A. Ignatiev, *Phys. Rev. B 30*, 4856 (1984).
1414. C. Pirri, J. C. Peruchetti, G. Gewinner and J. Derrien, *Phys. Rev. B 30*, 6227 (1984).
1415. G.-C. Wang and T.-M. Lu, *Phys. Rev. Lett. 50*, 2014 (1983).
1416. M. A. Van Hove, R. Lin and G. A. Somorjai, *Phys. Rev. Lett. 51*, 778 (1983).
1417. H. Richter and U. Gerhardt, *Phys. Rev. Lett. 51*, 1570 (1983).
1418. P. K. Wu, J. H. Perepezko, J. T. McKinney and M. G. Lagally, *Phys. Rev. Lett. 51*, 1577 (1983).
1419. A. H. Weiss, I. J. Rosenberg, K. F. Canter, C. B. Duke and A. Paton, *Phys. Rev. B 27*, 867 (1983).
1420. C. B. Duke, A. Paton and A. Kahn, *Phys. Rev. B 27*, 3436 (1983).
1421. I. Hernandez-Calderon and H. Hochst, *Phys. Rev. B 27*, 4961 (1983).
1422. P. K. Larsen, J. H. Neave, J. F. van der Veen, P. J. Dobson and B. A. Joyce, *Phys. Rev. B 27*, 4966 (1983).
1423. C. B. Duke, A. Paton, A. Kahn and C. R. Bonapace, *Phys. Rev. B 27*, 6189 (1983).
1424. P. Skeath, C. Y. Su, W. A. Harrison, I. Lindau and W. E. Spicer, *Phys. Rev. B 27*, 6246 (1983).
1425. M. F. Toney, R. D. Diehl and S. C. Fain, Jr., *Phys. Rev. B 27*, 6413 (1983).
1426. C. B. Duke, A. Paton, A. Kahn and C. R. Bonapace, *Phys. Rev. B 28*, 852 (1983).
1427. W. S. Yang and F. Jona, *Phys. Rev. B 28*, 1178 (1983).
1428. W. S. Yang, F. Jona and P. M. Marcus, *Phys. Rev. B 28*, 2049 (1983).
1429. H. Liu, M. R. Cook, F. Jona and P. M. Marcus, *Phys. Rev. B 28*, 6137 (1983).
1430. S. . Lindgren, L. Wallden, J. Rundgren, P. Westrin and J. Neve, *Phys. Rev. B 28*, 6707 (1983).
1431. G.-C. Wang and T.-M. Lu, *Phys. Rev. B 28*, 6795 (1983).
1432. P. Skeath, I. Lindau, C. Y. Su and W. E. Spicer, *Phys. Rev. B 28*, 7051 (1983).
1433. N. J. Wu and A. Ignatiev, *Phys. Rev. B 28*, 7288 (1983).
1434. W. S. Yang, F. Jona and P. M. Marcus, *Phys. Rev. B 28*, 7377 (1983).
1435. R. D. Diehl, M. F. Toney and S. C. Fain, Jr., *Phys. Rev. Lett. 48*, 177 (1982).
1436. D. L. Adams, H. B. Nielsen, J. N. Andersen, I. Stensgaard, R. Feidenhans'l and J. E. Sorensen, *Phys. Rev. Lett. 49*, 669 (1982).
1437. S. Masuda, M. Nishijima, Y. Sakisaka and M. Onchi, *Phys. Rev. B 25*, 863 (1982).
1438. J. M. Baribeau and J. D. Carette, *Phys. Rev. B 25*, 2962 (1982).
1439. N. J. Wu and A. Ignatiev, *Phys. Rev. B 25*, 2983 (1982).

1440. G. K. Wertheim, S. B. DiCenzo and D. N. E. Buchanan, *Phys. Rev. B 25*, 3020 (1982).
1441. S. Y. Tong and K. H. Lau, *Phys. Rev. B 25*, 7382 (1982).
1442. C. B. Duke, A. Paton, W. K. Ford, A. Kahn and J. Carelli, *Phys. Rev. B 26*, 803 (1982).
1443. R. D. Diehl and S. C. Fain, Jr., *Phys. Rev. B 26*, 4785 (1982).
1444. D.-W. Tu and A. Kahn, *J. Vac. Sci. Technol. A* 2, 511 (1984).
1445. C. B. Duke, A. Paton, and A. Kahn, *J. Vac. Sci. Technol. A* 2, 515 (1984).
1446. J. M. Moison and M. Bensoussan, *Appl. Surf. Sci. 20*, 84 (1984).
1447. Y. B. Lozovyi, V. K. Medvedev, T. P. Smereka, B. M. Palyukh and G. V. Babkin, *Fiz. Tverdogo Tela. 24*, 2130 (1982).
1448. L. G. Salmon and T. N. Rhodin, Tenth International Symposium on Gallium Arsenide and Related Compounds, 561 (1983).
1449. V. F. Dvoryankin, A. A. Komarov, V. V. Panteleev, *Izv. Akad. Nauk SSSR Neorg. Mater. 19*, 186 (1983).
1450. R. Kaplan, *J. Appl. Phys. 56*, 1636 (1984).
1451. B. S. Meyerson and M. L. Yu, *J. Electrochem. Soc. 131*, 2366 (1984).
1452. B. E. Hayden and A. M. Bradshaw, *J. Electron Spectrosc. and Relat. Phenom. 30*, 51 (1983).
1453. B. E. Koel and G. A. Somorjai, *J. Electron Spectrosc. and Relat. Phenom. 29*, 287 (1983).
1454. C. Nyberg and C. G. Tengstal, *J. Electron Spectrosc. and Relat. Phenom. 29*, 191 (1983).
1455. A. B. Anton, N. R. Avery, B. H. Toby and W. H. Weinberg, *J. Electron Spectrosc. and Relat. Phenom. 29*, 181 (1983).
1456. A. Oustry, J. Berty, M. Caumont, and M. J. David, *J. Microsc. and Spectrosc. Electron. 9*, 49 (1984).
1457. N. P. Lieske, *J. Phys. and Chem. Solids 45*, 821 (1984).
1458. M. Abu-Joudeh, P. P. Vaishnava, and P. A. Montano, *J. Phys. C 17*, 6899 (1984).
1459. Y. Gauthier, R. Baudoing, Y. Joly, C. Gaubert, and J. Rundgren, *J. Phys. C. 17*, 4547 (1984).
1460. J. Sokolov, H. D. Shih, U. Bardi, F. Jona, and P.M. Marcus, *J. Phys. C. 17*, 371 (1984).
1461. F. Jona, D. Westphal, A. Goldmann and P.M. Marcus, *J. Phys. C 16*, 3001 (1983).
1462. J. Neve, P. Westrin, J. Rundgren, *J. Phys. C 16*, 1291 (1983).
1463. G. C. Smith, C. Nooris, C. Binns, and H. A. Padmore, *J. Phys. C 15*, 6481 (1982).
1464. H. B. Nielsen, J. N. Andersen, L. Petersen, and D. L. Adams, *J. Phys. C 15*, L1113 (1982).
1465. K. Griffiths, D. A. King, G. C. Aers and J. B. Pendry, *J. Phys. C. 15*, 4921 (1982).
1466. S. P. Tear and K. Roll, *J. Phys. C 15*, 5521 (1982).
1467. J. Neve, J. Rundgren and P. Westrin, *J. Phys. C. 15*, 4391 (1982).
1468. L. J. Clarke, R. Baudoing and Y. Gauthier, *J. Phys. C. 15*, 3249 (1982).
1469. Y. Gauthier, R. Baudoing and L. Clarke, *J. Phys. C. 15*, 3231 (1982).
1470. Y. Gauthier, R. Baudoing, C. Gaubert and L. Clarke, *J. Phys. C. 15*, 3223 (1982).
1471. M. K. Debe and D. A. King, *J. Phys. C 15*, 2257 (1982).
1472. H. B. Nielsen and D. L. Adams, *J. Phys. C 15*, 615 (1982).
1473. W. T. Moore, D. C. Frost and K. A. R. Mitchell, *J. Phys. C 15*, L5 (1982).
1474. G. Le Lay and J. J. Metois, *J. Phys. Colloq. 45*, No. C5, C5-427-33 (1984).
1475. K. Shoji, H. Ueba, and C. Tatsuyama, *J. Vac. Soc. Jpn. 26*, 778 (1983).
1476. H. -J. Gossmann, L. C. Feldman and W. M. Gibson, *J. Vac. Sci. and Technol. B* 2, 407 (1984).
1477. J. A. Schaefer, F. Stucki, D. J. Frankel, W. Gopel and G. J. Lapeyre, *J. Vac. Sci. and Technol. B* 2, 359 (1984).
1478. C. B. Duke, A. Paton, A. Kahn and D. W. Tu, *J. Vac. Sci. and Technol. B* 2, 366 (1984).
1479. C. Maillot, H. Roulet and G. Dufour, *J. Vac. Sci. and Technol. B* 2, 316 (1984).
1480. C. B. Duke and A. Paton, *J. Vac. Sci. and Technol. B* 2, 327 (1984).
1481. Y. Fujinaga, *J. Vac. Soc. Jpn. 25*, 468 (1982).
1482. J. Tang, *J. Zhejiang Univ. 18* 81 (1984).
1483. K. Shoji, M. Hyodo, H. Ueba and C. Tatsuyama, *Jpn. J. Appl. Phys. Part 1, 22*, 1482 (1983).
1484. Y. Yabuuchi, F. Shoji, K. Oura, T. Hanawa, Y. Kishikawa and S. Okada, *Jpn. J. Appl. Phys. Part 1, 21*, L752 (1982).
1485. H. Nakamatsu, Y. Yamamoto, S. Kawai, K. Oura and T. Hanawa, *Jpn. J. Appl. Phys. Part 2, 22*, L461 (1983).
1486. K. Shoji, M. Hyodo, H. Ueba and C. Tatsuyama, *Jpn. J. Appl. Phys. Part 2, 22*, L200 (1983).
1487. Y. Yabuuchi, F. Shoji, K. Oura, T. Hanawa, Y. Kishikawa and S. Okada, *Jpn. J. Appl. Phys. Part 2, 21*, L752 (1982).
1488. S. Maruno, H. Iwasaki, K. Horioka, Sung-te Li, S. Nakamura, *Jpn. J. Appl. Phys. Part 2, 21*, L263 (1982).
1489. K. Horioka, H. Iwasaki, A. Ichimiya, S. Maruno, S. Te Li and S. Nakamura, *Jpn. J. Appl. Phys. Part 2, 21*, L189 (1982).
1490. Y. Y. Tomashpol'skii, E. N. Lubnin, M. A. Sevost'yanov and V. I. Kukuev, *Kristallografiya 27*, 1152 (1982).
1491. V. F. Dvoryankin, A. Y. Mityagin and V. V. Panteleev, *Kristallografiya 27*, 349 (1982).
1492. D. M. Zehner and C. W. White, Laser Annealing of Semiconductors, 281 (1982).
1493. R. Ramanathan and J. M. Blakeley, *Mater. Lett.* 2, 12 (1983).

1494. H. Iwasaki, S. Maruno, K. Horioka, S. -T. Li and S. Nakamura, Molecular Beam Epitaxy and Clean Surface Techniques. Collected Papers of 2nd International Symposium, 305 (1982).
1495. H. Sato, A. Ebina and T. Takahashi, Molecular Beam Epitaxy and Clean Surface Techniques. Collected Papers of 2nd International Symposium, 309 (1982).
1496. K. Oura, Y. Yabuuchi, F. Shoji, T. Hanawa and S. Okada. Proceedings of the 6th International Conference on Ion Beam Analysis 23 (1983).
1497. D. P. Woodruff and K. Horn, *Philos. Mag. A 47*, L5 (1983).
1498. D. L. Adams, H. B. Nielsen and J. N. Andersen, *Phys. Scr. T4*, 22 (1983).
1499. F. Houzay, G. M. Guichar, A. Cros, F. Salvan, R. Pinchaux and J. Derrien, *Physica B and C 117*, 840 (1983).
1500. V. G. Lifshits, V. G. Zavodinskii and N. I. Plyusnin, *Phys. Chem. and Mech. Surf. 2*, 784 (1984).
1501. P. P. Lutsishin and T. N. Nakhodkin, *Phys. Chem. and Mech. Surf. 1*, 3596 (1984).
1502. V. A. Grazhulis, A. M. Ionov, V. F. Kuleshov, *Phys. Chem. and Mech. Surf. 2*, 540 (1984).
1503. T. Matsubara, *Prog. Theor. Phys. 71*, 399 (1984).
1504. H. Sato, A. Ebina and T. Takahashi, *Rec. Electr. and Commun. Eng., Conversazione Tohoku Univ. 51*, 9 (1982).
1505. J. C. Dupuy, B. Vilotitch and A. Sibai, *Rev. Phys. Appl. 19*, 965 (1984).
1506. G. L. P. Berning and W. J. Coleman, S. Afr. *J. Phys. 7 (1984)*.
1507. P. Chen, D. Bolmont and C. A. Sebenne, *Thin Solid Films 111*, 367 (1984).
1508. P. Godowski and S. Mroz, *Thin Solid Films 111*, 129 (1984).
1509. V. D. Vankar, R. W. Vook and B. C. De Cooman, *Thin Solid Films 102*, 313 (1983).
1510. V. E. de Carvalho, M. W. Cook, P. G. Cowell, O. S. Heavens, M. Prutton and S. P. Tear, *Vacuum 34*, 893 (1984).
1511. B. J. Hinch, M. S. Foster, G. Jennings and R. F. Willis, *Vacuum 33*, 864 (1983).
1512. R. D. Diehl, S. C. Fain, Jr., J. Talbot, D. J. Tildesley and W. A. Steele, *Vacuum 33*, 857 (1983).
1513. D. P. Woodruff and K. Horn, *Vacuum 33*, 633 (1983).
1514. G. J. R. Jones and B. W. Holland, *Vacuum 33*, 627 (1983).
1515. S. Tatarenko and R. Ducros, *Vide Les Couches Minces 38*, 121 (1983).
1516. V. V. Gonchar, Y. M. Kagan, O. V. Kanash, A. G. Naumovets and A. G. Fedorus, *Zh. Eksp. and Teor. Fiz. 84*, 249 (1983).
1517. T. De Yong, W. A. S. Douma, L. Smit, V. V. Korablev and F. W. Saris, *J. Vac. Sci. and Technol. B 1*, 888 (1983).
1518. J. M. Woodall, P. Oelhafen, T. N. Jackson, J. L. Freeouf and G. D. Pettit, *J. Vac. Sci. and Technol. B 1*, 795 (1983).
1519. P. Oelhafen, J. L. Freeouf, G. D. Pettit and J. M. Woodall, *J. Vac. Sci. and Technol. B 1*, 787 (1983).
1520. P. Zurcher, J. Anderson, D. Frankel and G. J. Lapeyre, *J. Vac. Sci. and Technol. B 1*, 682 (1983).
1521. A. Kahn, C. R. Bonapace, C. B. Duke and A. Paton, *J. Vac. Sci. and Technol. B 1*, 613 (1983).
1522. J. R. Lince, J. G. Nelson and R. S. Williams, *J. Vac. Sci. and Technol. B. 1*, 553(1983).
1523. W. S. Yang, F. Jona and P. M. Marcus, *J. Vac. Sci. and Technol. B 1*, 718 (1983).
1524. R. S. Bauer, *J. Vac. Sci. and Technol. B 1*, 314 (1983).
1525. J. Kofoed, I. Chorkendorff and J. Onsgaard, *Solid State Commun. 52*, 283 (1984).
1526. B. T. Jonker and R. L. Park, *Solid State Commun. 51*, 871 (1984).
1527. K. Christemann, V. Penka, R. J. Behm, F. Chehab and G. Ertl, *Solid State Commun. 51*, 487 (1984).
1528. R. Feder and W. Monch, *Solid State Commun. 50*, 311 (1984).
1529. J. Derrien and F. Ringeisen, *Solid State Commun. 50*, 627 (1984).
1530. J. Sokolov, F. Jona and P. M. Marcus, *Solid State Commun. 49*, 307 (1984).
1531. J. Sokolov, H. D. Shih, U. Bardi, F. Jona and P. M. Marcus, *Solid State Commun. 48*, 739 (1983).
1532. A. Faldt and H. P. Myers, *Solid State Commun. 48*, 253 (1983).
1533. W. S. Yang and F. Jona, *Solid State Commun. 48*, 377 (1983).
1534. B. E. Hayden, K. C. Prince, P. J. Davie, G. Paolucci and A. M. Bradshaw, *Solid State Commun. 48*, 325 (1983).
1535. F. Stucki, J. A. Schaefer, J. R. Anderson, G. J. Lapeyre and W. Gopel, *Solid State Commun. 47*, 795 (1983).
1536. K. Horioka, H. Iwasaki, S. Maruno, S. Te Li and S. Nakamura, *Solid State Commun. 47*, 55 (1983).
1537. P. Chen, D. Bolmond and C. A. Sebenne, *Solid State Commun. 46*, 689 (1983).
1538. M. Pessa and O. Jylha, *Solid State Commun. 46*, 419 (1983).
1539. M. Maglietta, A. Fallavollita and G. Rovida, *Solid State Commun. 46*, 273 (1983).
1540. N. J. Wu and A. Ignatiev, *Solid State Commun. 46*, 59 (1983).
1541. R. D. Bringans and B. Z. Bachrach, *Solid State Commun. 45*, 83 (1983).
1542. R. Feder, *Solid State Commun. 45*, 51 (1983).
1543. H. Kobayashi, K. Edamoto, M. Onchi and M. Nishijima, *Solid State Commun. 44*, 1449 (1982).
1544. P. Chen, D. Bolmont and C. Sebenne, *Solid State Commun. 44*, 1191 (1982).
1545. D. Westphal, A. Goldmann, F. Jona and P. M. Marcus, *Solid State Commun. 44*, 685 (1982).
1546. C. Binns, C. Norris, I. Lindau, M. L. Shek, B. Pate, P. M. Stefan and W. E. Spicer, *Solid State Commun. 43*, 853 (1982).

1547. W. S. Yang, F. Jona and P. M. Marcus, *Solid State Commun. 43*, 847 (1982).
1548. M. Maglietta, *Solid State Commun. 43*, 395 (1982).
1549. S. J. White, D. C. Frost, K. A. R. Mitchell, *Solid State Commun. 42*, 763 (1982).
1550. W. S. Yang and F. Jona, *Solid State Commun. 42*, 49 (1982).
1551. W. S. Yang, J. Sokolov, F. Jona and P. M. Marcus, *Solid State Commun. 41*, 191 (1982).
1552. T. Weir and G. W. Simmons, *AIP Conf. Proc. No. 84*, 113 (1982).
1553. M. Maglietta, *Appl. Phys. A. 31*, 165 (1983).
1554. T. D. Jong, W. A. S. Douma, J. F. Van der Veen, F. W. Saris and J. Haisma, *Appl. Phys. Lett. 42*, 1037 (1983).
1555. K. Oura, S. Okada, Y. Kishikawa and T. Hanawa, *Appl. Phys. Lett. 40*, 138 (1982).
1556. J. L. Stickney, S. D. Rosasco and A. T. Hubbard, *J. Electrochem. Soc. 131*, 260 (1984).
1557. J. K. Sass, K. Bange, R. Dohl, E. Piltz, and R. Unwin, *Ber. Bunsenges, Phys. Chem. 88*, 354 (1984).
1558. Y. Nakai, M. S. Zei, D. M. Kolb and G. Lehmpfuhl, *Ber. Bunsenges, Phys. Chem. 88*, 340 (1984).
1559. M. Ohno, Y. Nakanishi and G. Shimaoka, *Bull. Res. Inst. Electron Shizuoka Univ. 19*, 19 (1984).
1560. C. Klauber, M. D. Alvey and J. T. Yates, *Chem. Phys. Lett. 106*, 477 (1984).
1561. R. Ramanathan, M. Quinlan and H. Wise, *Chem. Phys. Lett. 106*, 87 (1984).
1562. G. C. Smith, C. Norris and C. Binns, *J. Phys. C. 17*, 4389 (1984).
1563. C. Ping, D. Bolmont and C. A. Sebenne, *J. Phys. C. 17*, 4897 (1984).
1564. C. Binns, M. G. Barthes-Labrousse and C. Norris, *J. Phys. C. 17*, 1465 (1984).
1565. M. Maglietta, *J. Phys. C. 17*, 363 (1984).
1566. J. N. Andersen, H. B. Nielsen, L. Petersen and D. L. Adams, *J. Phys. C 17*, 173 (1984).
1567. F. Proix, A. Akremi and Z. T. Zhong, *J. Phys. C 16*, 5449 (1983).
1568. G. J. Hughes, A. Mckinley and R. H. Williams, *J. Phys. C 16*, 2391 (1983).
1569. T. C. Gainey and B. J. Hopkins, *J. Phys. C 16*, 975 (1983).
1570. A. Mckinley, G. J. Hughes and R. H. Williams, *J. Phys. C 15*, 7049 (1982).
1571. S. A. Lindgren, J. Paul, L. Wallden and P. Westrin, *J. Phys. C 15*, 6285 (1982).
1572. P. Chen, D. Bolmont and C. A. Sebenne, *J. Phys. C 15*, 6101 (1982).
1573. V. Montgomery, R. H. Williams, *J. Phys. C 15*, 5887 (1982).
1574. M. R. Welton-Cook and W. Berndt, *J. Phys. C 15*, 5691 (1982).
1575. D. Bolmont, P. Chen, F. Proix and C. A. Sebenne, *J. Phys. C 15*, 3639 (1982).
1576. N. Masud, *J. Phys. C. 15*, 3209 (1982).
1577. F. Storbeck, *Acta. Phys. Acad. Sci. Hung 49*, 75 (1980).
1578. L. R. Sheng, L.-X. Tu, *Acta Phys. Sin. (China) 29*, 524 (1980).
1579. D. J. Chadi, *Appl. Opt. 19*, 3971 (1980).
1580. M. Maglietta, E. Zanazzi, F. Jona, D. W. Jepsen, P. M. Marcus, *Appl. Phys. 15*, 409 (1978).
1581. M. Maglietta, *Appl. Phys. A31*, 165 (1983).
1582. Y. Nakai, M. S. Zei, D. M. Kolb, G. Lehmpfuhl, *Ber. Bunsenges, Phys. Chem. 88*, 340 (1984).
1583. A. Steinbrum, P. Dumas, J. C. Colson, C. R. Hebd, *Seances. Acad. Sci. Ser. C 290*, 329 (1980).
1584. K. A. Prior, K. Schwaha, M. E. Bridge, R. M. Lambert, *Chem. Phys. Lett. 65*, 472 (1979).
1585. G. Casalone, M. G. Cattania, M. Simonetta and M. Tescari, *Chem. Phys. Lett. 61*, 36 (1979).
1586. I. L. Kesmodel, L. H. Dubois, G. A. Somorjai, *Chem. Phys. Lett. 56*, 267 (1978).
1587. M. G. Lagally, Wang Gwo-Ching and Lu Toh-Ming, *CRC Crit. Rev. Solid State and Mater. Sci. 7*, 233 (1978).
1588. H. J. Mussig and W. Arabczyk, *Cryst. Res. and Technol. 16*, 827 (1981).
1589. M. Klaua, K. Meinel, O. P. Pchelyakov, V. A. Ivanchenko and S. I. Stenin, *Sov. Phys. Solid State 23*, 1501 (1981).
1590. M. S. Gupalo, V. K. Medvedev, B. M. Palyukh and T. P. Smereka, *Sov. Phys. Solid State 23*, 1211 (1981).
1591. V. K. Medvedev and I. N. Yakovkin, *Sov. Phys. Solid State 23, 379 (1981).*
1592. S. A. Knyazev and G. K. Zyryanov, *Sov. Phys. Solid State, 22, 1554 (1980).*
1593. M. S. Gupalo, V. K. Medvedev, B. M. Palyukh and T. P. Smereka, *Sov. Phys. Solid State 21*, 568 (1979).
1594. V. K. Medvedev and I. N. Yakovkin, *Sov. Phys. Solid State, 21*, 187 (1979).
1595. H. F. Winters, *IBM, J. Res. and Dev.* 22, 260 (1978).
1596. C. R. Brundle, *IBM, J. Res. and Dev.*, 22, 235 (1978).
1597. A. Ignatiev, *IEEE Trans. Nucl. Sci. NS-26*, 1824 (1979).
1598. S. A. Isa, *Iraqi J. Sci. 20*, 225 (1979).
1599. N. Stoner, M. A. Van Hove, S. Y. Tong, and M.B. Webb, *Phys. Rev. Lett., 40, 243 (1978).*
1600. Mark J. Cardillo and G. E. Becker, *Phys. Rev. Lett., 40, 1148 (1978).*
1601. F. Jona, K. O. Legg, H. D. Shih D. W. Jepsen, and P. M. Marcus, *Phys. Rev. Lett. 40, 1466 (1978).*
1602. J. Suzanne, J. P. Coulomb, M. Bienfait, M. Matecki, A. Thomy, B. Croset and C. Marti, *Phys. Rev. Lett. 41, 760 (1978).*
1603. R. A. Barker and P. J. Estrup, *Phys. Rev. Lett., 41, 1307 (1978).*
1604. M. Passler, A. Ignatiev, F. Jona, D. W. Jepsen and P. M. Marcus, *Phys. Rev. Lett. 43, 360 (1979).*

1605. S. Andersson and J. B. Pendry, *Phys. Rev. Lett., 43, 363 (1979).*
1606. G. Gewinner, J. C. Peruchetti, A. Jaegle and R. Riedinger, *Phys. Rev. Lett. 43*, 935 (1979).
1607. R. J. Meyer, L. J. Brillson, A. Kahn, D. Kanani, J. Carelli, J. L. Yeh, G. Margaritondo and A. D. Katnani, *Phys. Rev. Lett. 46, 440 (1979).*
1608. H. D. Shih, F. Jona, D. W. Jepsen and P. M. Marcus, *Phys. Rev. Lett. 46, 731 (1979).*
1609. K. Griffiths, C. Kendon, D. A. King and J. B. Pendry, *Phys. Rev. Lett. 46*, 1584 (1981).
1610. E. G. McRae and C. W. Caldwell, *Phys. Rev. Lett. 46, 1632 (1981).*
1611. M. Jaubert, A. Glachant, M. Bienfait and G. Boato, *Phys. Rev. Lett. 46, 1679 (1981).*
1612. C. B. Duke, R. J. Meyer, A. Paton and P. Marck, *Phy. Rev. B 18*, 4225 (1978).
1613. B. W. Lee, R. Alsenz, A. Ignatiev and M. A. Van Hove, *Phys. Rev. B 17*, 1510 (1978).
1614. D. L. Adams, H. B. Nielsen and M. A. Van Hove, *Phys. Rev. B 20*, 4789 (1979).
1615. R. H. Tait and R. V. Kasowski, *Phys. Rev. B 20*, 5178 (1979).
1616. S. C. Fain, Jr., M. D. Chinn and R. D. Diehl, *Phys. Rev. B 21*, 4170 (1980).
1617. D. W. Jepsen, H. D. Shih, F. Jona and P. M. Marcus, *Phys. Rev. B 22*, 814 (1980).
1618. R. J. Meyer, C. B. Duke, A. Paton, J. C. Tsang, J. L. Yeh, A. Kahn and P. Mark, *Phys. Rev. B 22*, 6171 (1980).
1619. C. B. Duke, A. Paton, W. K. Ford, A. Kahn and J. Carelli, *Phys. Rev. B 24*, 562 (1981).
1620. C. B. Duke, A. Paton, W. K. Ford, A. Kahn and G. Scott, *Phys. Rev. B 24*, 3310 (1981).
1621. F. Soria, V. Martinez, M. C. Munoz and J. L. Sacedon, *Phys. Rev. B 24*, 6926 (1981).
1622. A. K. Green and E. Bauer, *J. Appl. Phys. 52*, 5098 (1981).
1623. P. Hahn, J. Clabes and M. Henzler, *J. Appl. Phys. 51*, 2079 (1980).
1624. C. Oshima, M. Aono, T. Tanaka, R. Nishitani and S. Kawai, *J. Appl. Phys. 51*, 997 (1980).
1625. M. Aono, C. Oshima, T. Tanoka, E. Bannai and S. Kawai, *J. Appl. Phys. 49*, 2761 (1978).
1626. S. A. Isa, R. W. Joyner and M. W. Roberts, *J. Chem. Soc. Faraday Trans. I 74*, 546 (1978).
1627. J. C. Bertolini, J. Massardier and G. Dalmai-Imelik, *J. Chem. Soc. Faraday Trans. I 74*, 1720 (1978).
1628. G. Le Lay, *J. Crystal Growth 54*, 501 (1981).
1629. M. Grunze, W. Hirschwald and D. Hofmann, *J. Cryst. Growth 52*, 241 (1981).
1630. K. Nii, K. Yoshihara, *J. Jpn. Inst. Met. 44*, 100 (1980).
1631. C. Oshima, M. Oano, S. Zaima, Y. Shibata and S. Kawai, *J. Less-Common Met. 82*, 69 (1981).
1632. A. Landet, M. Jardinier-Offergeld and F. Bouillon, *J. Microsc. and Spectrosc. Electron 30*, 101 (1978).
1633. C. Benndorf, B. Egert, G. Keller, H. Seidel and F. Thieme, *J. Phys. Chem. Solids 40*, 877 (1979).
1634. L. Morales, D. O. Garza and L. J. Clarke, *J. Phys. C. 14*, 5391 (1981).
1635. S. P. Tear, K. Roll and M. Prutton, *J. Phys. C. 14*, 3297 (1981).
1636. J. C. Fernandez, W. S. Yang, H. D. Shih, F. Jona, P. W. Jepsen and P. M. Marcus, *J. Phys. C. 14*, L55 (1981).
1637. F. Jona and P. M. Marcus, *J. Phys. C 13*, L477 (1980).
1638. M. R. Welton-Cook and M. Prutton, *J. Phys. C 13*, 3993 (1980).
1639. H. D. Shih, F. Jona, U. Bardi and P. M. Marcus, *J. Phys. C 13*, 3801 (1980).
1640. F. Jona, D. Sondericker and P. M. Marcus, *J. Phys. C 13*, L155 (1980).
1641. M. Prutton, J. A. Ramsey, J. A. Walker and M. R. Welton-Cook, *J. Phys. C 12*, 5271 (1979).
1642. W. T. Moore, P. R. Watson, D. C. Frost and K. A. R. Mitchell, *J. Phys. C 12*, L887 (1979).
1643. K. Griffiths and D. A. King, *J. Phys. C 12*, L755 (1979).
1644. T. Matsudaira and M. Onchi, *J. Phys. C 12*, 3381 (1979).
1645. F. Jona, H. D. Shih, D. W. Jepsen and P. M. Marcus, *J. Phys. C 12*, L455 (1979).
1646. R. Feder, W. Monch and P. P. Auer, *J. Phys. C 12*, L179 (1979).
1647. A. Ignatiev, H. B. Nielsen and D. L. Adams, *J. Phys. C 11*, L837 (1978).
1648. F. R. Shepherd, P. R. Watson, D. C. Frost and K. A. R. Mitchell, *J. Phys. C. 11*, 4591 (1978).
1649. Y. Fujinaga, *J. Vac. Soc. JPN 23*, 253 (1980).
1650. Y. Terada, T. Yoshizuka, K. Oura and T. Hanawa, *JPN, J. Appl. Phys. 20*, L333 (1981).
1651. M. G. Lagally, T. M. Lu and G. C. Wang, "Ordering in Two Dimensions," Proceedings of an International Conference on Ordering in Two Dimensions, P 113 (1981).
1652. R. L. Park, T. L. Einstein, A. R. Kortan and L. D. Roelofs, "Ordering in Two Dimensions," Proceedings of an International Conference on Ordering in Two Dimensions, P17 (1981).
1653. Y. J. Chabal and J. E. Rowe, *Ibid*, P251 (1981).
1654. R. Ducros, M. Housley and G. Piquard, *Phys. Status Solidi A. 56*, 187 (1979).
1655. W. Arabczyk, H. J. Mussig and F. Storbeck, *Phys. Status Solidi A 55*, 437 (1979).
1656. R. Feder and J. Kirschner, *Phys. Status Solidi A 45*, K117 (1978).
1657. V. K. Medvedev and V. N. Pogoreli, *UKR Fiz. Zh. 25*, 1524 (1980).
1658. K. Chritmann, Z. *Naturforsch. A. 34A*, 22 (1979).
1659. K. C. R. Chiu, J. M. Paate, J. E. Rowe, T. T. Sheng and A. G. Cullis, *Appl. Phys. Lett. 38*, 988 (1981).
1660. V. Montgomery, R. H. Williams and R. R. Varma, *J. Phys. C 11*, 1989 (1978).
1661. K. J. Rawlings, M. J. Gibson and P. J. Dobson, *J. Phys. D 11*, 2059 (1978).

1662. A. A. Galaev, L. V. Gamosov, Yu N. Parkhomenko and A. V. Shirkov, *Sov. Phys. Crystallogr. 24*, 72 (1979).
1663. S. Ferrer, L. Gonzalez, M. Salmeron, J. A. Verges and F. Ndurain, *Solid State Commun. 38*, 317 (1981).
1664. W. Erley and H. Ibach, *Solid State Commun. 37*, 937 (1981).
1665. C. M. Chan, M. A. Van Hove, W. H. Weinberg and E. D. Williams, *Solid State Commun. 30*, 47 (1979).
1666. M. A. Van Hove, G. Ertl, K. Christmann, R. J. Behm and W. H. Weinberg, *Solid State Commun. 28*, 373 (1978).
1667. J. Behm, K. Christmann and G. Ertl, *Solid State Commun. 25*, 763 (1978).
1668. R. A. Barker, P. J. Estrup, F. Jona, and P. M. Marcus, *Solid State Commun. 25*, 375 (1978).
1669. V. G. Lifshits, V. B. Akilov and Y. L. Gavriljuk, *Solid State Commun. 40*, 429 (1981).
1670. P. Legare, Y. Holl and G. Maire, *Solid State Commun. 31*, 307 (1979).
1671. H. Namba, J. Darville, J. M. Gilles, *Solid State Commun. 34*, 287 (1980).
1672. R. Courths, *Phys. Status Solidi B 100*, 135 (1980).
1673. J. H. Onuferko, PHD Thesis, Univ. Warwick Coventry, England.
1674. I. F. Lyuksyutov and A. G. Fedorus, *Zh. Eksp and Teor. Fiz. 80*, 2511 (1981).
1675 F. Lyuksyutov, V. K. Medvedev and I. N. Yakovkin, *Zh. Eksp. and Teor. Fiz. 80*, 2452 (1981).
1676. V. P. Ivanov, V. I. Savchenko and V. L. Tataurov, *Sov. Phys. Tech. Phys. 26*, 237 (1981).
1677. B. M. Zykov, V. K. Tskhakaya, *Sov. Phys. Tech. Phys. 24*, 948 (1979).
1678. A. Gutmann and K. Hayek, *Thin Solid Films 58*, 145 (1979).
1679. K. Christmann, G. Ertl and H. Shimizu, *Thin Solid Films 57*, 247 (1979).
1680. M. G. Barthes and A. Rolland, *Thin Solid Films 76*, 45 (1981).
1681. B. Gruzza and E. Gillet, *Thin Solid Films 68*, 345 (1980).
1682. C. Argile and G. E. Rhead, *Thin Solid Films 67*, 299 (1980).
1683. B. Z. Olshanetskii, V. I. Mashanov and A. I. Nikiforov, *Sov. Phys. Solid State 23*, 1505 (1981).
1684. M. S. Gupalo, V. K. Medvedev, B. M. Palyukh and T. P. Smereka, *Sov. Phys. Solid State 22*, 1873 (1980).
1685. B. Z. Olshanetskii and V. I. Mashanov, *Sov. Phys. Solid State 22*, 1705 (1980).
1686. M. Weiss, G. Ertl and F. Nitschke, *Appl. Surf. Sci. 2*, 614 (1979).
1687. J. Kuppers and H. Mitchel, *Appl. Surf. Sci. 3*, 179 (1979).
1688. K. H. Rieder, *Appl. Surf. Sci. 4*, 183-9 (1980).
1689. H. Geiger and P. Wissmann, *Appl. Surf. Sci. 5*, 153 (1980).
1690. G. Ronida, F. Pratesi and E. Ferroni, *Appl. Surf. Sci. 5*, 121 (1980).
1691. S. A. Isa, R. W. Joyner, M. H. Matloob and M. Wyn Roberts, *Appl. Surf. Sci. 5*, 345 (1980).
1692. D. G. Castner and G. A. Somorjai, *Appl. Surf. Sci. 6*, 29 (1980).
1693. K. Khonde, J. Darville, S. E. Donnelly and J. M. Gilles, *Appl. Surf. Sci. 6*, 297 (1980).
1694. E. Bechtold, *Appl. Surf. Sci. 7*, 231 (1981).
1695. O. Oda, L. J. Harrekamp and G. A. Bootsma, *Appl. Surf. Sci. 7*, 206 (1981).
1696. G. Le Lay A. Chauvet, M. Manneville and R. Kern, *Appl. Surf. Sci. 9*, 190 (1981).
1697. G. Vidali, M. W. Cole, W. H. Weinberg, and W. A. Steele, *Phys. Rev. Lett. 51*, 118 (1983).
1698. M. Maglietta, *Solid State Comm. 43*, 395 (1982).
1699. R. J. Baird, D. F. Ogletree, M. A. Van Hove, and G. A. Somorjai *Surface Sci. 165*, 345 (1986).
1700. J. Sokolov, F. Jona, and P. M. Marcus, *Phys. Rev. B*, 1397 (1986).
1701. H. D. Shih, F. Jona, and P. M. Marcus, *Surface Sci. 104*, 39 (1981).
1702. S. Y. Tong, W. M. Mei, and G. Xu, *J. Vac. Sci. Tech. B 2*, 393 (1984).
1703. G. Xu, W. Y. Hu, M. W. Puga, S. Y. Tong. J. L. Yeh, S. R. Wang and B. W. Lee. *Phys. Rev. B 32*, 8473 (1985).
1704. P. H. Citrin, J. E. Rowe and P. Eisenberger, *Phys. Rev. B 28*, 2299 (1983).
1705. C. M. Chan, S. L. Cunningman, M. A. Van Hove, W. H. Weinberg, and S. P. Withrow, *Surface Sci. 66*, 394 (1977).
1706. B. J. Mrstik, R. Kaplan, T. L. Reinecke, M.A. Van Hove, and S. Y. Tong, *Phys. Rev. B 15*, 897 (1977).
1707. J. E. Demuth, P.M. Marcus, and D. W. Jepsen, *Phys. Rev. B 11*, 1460 (1975).
1708. D. H. Rosenblatt, S. D. Kevan. J. G. Tobin, R. F. Davis, M. G. Mason, D. R. Denley, D. A. Shirley, Y. Huang, and S. Y. Tong, *Phys. Rev. B26*, 1812 (1982).
1709. Y. Kuk, L. C. Feldman. and P.J. Silverman, *Phys. Rev. Lett. 50*, 511 (1983).
1710. F. Maca, M. Scheffler, and W. Berndt, *Surface Sci. 160*, 467 (1985).
1711. D. F. Ogletree, M. A. Van Hove, and G. A. Somorjai, *Surface Sci. 173*, 351 (1986).
1712. K. Hayek, H. Glassl, A. Gutmann, H. Leonhard, P. Prutton, S. P. Tear, and M.R. Welton-Cook, *Surface Sci. 152*, 419 (1985).
1713. M. A. Van Hove, R. J. Koestner, in Surface Structure by LEED, ed. P. M. Marcus and F. Jona, Plenum, New York (1984).
1714. L. Smit, R. M. Tromp, and J. F. Van der Veen, *Surface Sci. 163*, 315 (1985).
1715. P. H. Citrin, J. E. Rowe, and P. Eisenberger, *Phys. Rev. B 28* 2299 (1983).
1716. G. J. Jones, and B. W. Holland, *Solid State Comm. 53*, 45 (1985).
1717. H. D. Shih, F. Jona, D. W. Jepsen, and P. M. Marcus, *J. Phys. C 9*, 1405 (1976).

1718. K. C. Hui, R. H. Milne, K. A. R. Mitchell, W. T. Moore, and M. Y. Zhou, *Solid State Comm. 56*, 83 (1985).
1719. M. J. Cardillo, G. E. Becker, D. R. Hamann, J. A. Serri, L. Whitman, and L. F. Mattheiss, *Phys. Rev. B 28*, 494 (1983).
1720. M. A. Van Hove, S. Y. Tong. and N. Stoner, *Surface Sci. 54*, 259 (1976).
1721. Groupe d'Etude des Surfaces, *Surface Sci. 62*, 567 (1977).
1722. E. Lang, W. Grimm, and K. Heinz, *Surface Sci. 117*, 169 (1982).
1723. H. L. Davis, R. J. Noonan, *Surface Sci. 126*, 245 (1983).
1724. F. Jona, D. Westphal, A. Goldman, and P. M. Marcus, *J. Phys. C 16*, 3001 (1983).
1725. E. L. Bullock, C. S. Fadley, and P. J. Orders. *Phys. Rev. B 28*, 4867 (1983).
1726. J. G. Tobin, L. E. Klebanoff, D. H. Rosenblatt, R. F. Davis E. Umbach, A. G. Baca, D. A. Shirley, Y. Huang, W. M. Kang, and S. Y. Tong, *Phys. Rev. B 26*, 7076 (1982).
1727. U. Dobler, K. Baberschke, J. Stor, and D. A. Outka, *Phys. Rev. B 31*, 2532 (1985).
1728. F. Comin, P. H. Citrin, P. Eisenberger, and J. E. Rowe, *Phys. Rev. B 26*, 7060 (1982).
1729. K. O. Legg, F. Jona, D. W. Jepsen, and P. M. Marcus, *J. Phys. C 10*, 937, (1977).
1730. A. Ignatiev, F. Jona, D. W. Jepsen, and P. M. Marcus, *Phys. Rev. B 11*, 4780 (1975).
1731. S. A. Lindgren, J. Paul, L. Wallden, and P. Westrin, *J. Phys. C 15*, 6285 (1982).
1732. M. A. Van Hove, and S. Y. Tong, *J. Vac. Sci. Tec. 12*, 230 (1975).
1733. D. H. Rosenblatt, S. D. Kevan, J. G. Tobin, R. F. Davis, M. G. Mason, D. A. Shirley, J. C. Tang, and S. Y. Tong, *Phys. Rev. B 26*, 3181 (1982).
1734. J. J. Barton, C. C. Bahr, Z. Hussain, S. W. Robey, L. E. Klebanoff and D. A. Shirley, *J. Vac. Sc. Tech. A 2*, 847 (1984).
1735. P. J. Orders, B. Sinkovic, C. S. Fadley, R. Trehan, Z. Hussain, and J. Lecante, *Phys. Rev. B 30*, 1838 (1984).
1736. J. Stohr, R. Jaeger, and S. Brennan, *Surf. Sci. 117*, 503 (1982).
1737. J. E. Demuth, D. W. Jepsen, and P. M. Marcus, *J. Phys. C 8*, L25 (1975).
1738. J. Stohr, R. Jaeger, and T. Kendelewicz, *Phys. Rev. Lett. 49*, 142 (1982).
1739. J. W. M. Frenken, J. F. Van der Veen, and G. Allan, *Phys. Rev. Lett. 51*, 1876 (1983).
1740. M. de Crescenzi, F. Antonangeli, C. Bellini, and R. Rosei, *Phys. Rev. Lett. 50*, 1949 (1983).
1741. S. Y. Tong, W. M. Kang, D. H. Rosenblatt, J. G. Tobin, and D. A. Shirley, *Phys. Rev. B 27*, 4632 (1983).
1742. T. S. Rahman, D. L. Mills, J. E. Black, J. M. Szeftel, S. Lehwald and H. Ibach, *Phys. Rev. B 30*, 589 (1984).
1743. D. Norman, J. Sthr, R. Jaeger, P. J. Durham, and J. B. Pendry, *Phys. Rev. Lett. 51*, 2052 (1983).
1744. J. E. Demuth. D. W. Jepsen, and P. M. Marcus, *J. Phys. C 6*, L307 (1973).
1745. R. Feder, *Surface Sci. 68*, 229 (1977).
1746. B. W. Holland, C. D. Duke, and A. Paton, *Surface Sci. 140*, L269 (1984).
1747. M. A. Passler, A. Ignatiev, B. W. Lee, D. Adams, M. A. Van Hove, in Determination of Surface Structure by LEED, Plenum, New York (1984).
1748. K. Griffiths. D. A. King, G. C. Aers, and J. B. Pendry, *J. Phys. C 15*, 4921 (1982).
1749. K. Heinz, D. K. Saldin, and J. B. Pendry, *Phys. Rev. Lett. 55*, 2312 (1985).
1750. Y, Kuk, and L. C. Feldman, *Phys. Rev. B 30*, 5811 (1984).
1751. A. Puschmann, and J. Haasse, *Surface Sci. 144*, 559 (1984).
1752. W. Moritz, and D. Wolf, *Surface Sci. 163*, L655 (1985).
1753. W. Moritz, R. Imbihl, R. J. Behm, G. Ertl, and T. Matsushima, *J. Chem. Phys 83*, 1959 (1985).
1754. P. M. Echenique, *J. Phys. C 9*, 3193 (1976).
1755. S. Andersson, J. B. Pendry, and P. M. Echenique, *Surface Sci. 65*, 539 (1977).
1756. D. L. Adams, L. E. Peterson, and C. S. Sorenson, *J. Phys. C 18*, 1753 (1985).
1757. M. L. Xu, and S. Y. Tong, *Phys. Rev. B 31*, 6332 (1985).
1758. E. Tornquist, E. D. Adams, M. Copel, T. Gustafsson, and W. R. Graham, *J. Vac. Sci. Tech. A 2*, 939 (1984).
1759. R, Baudoing, Y. Gauthier, and Y. Joly, *J. Phys. C 18*, 4061 (1985).
1760. C. J. Barnes, M. Q. Ding, M. Lindroos, R. D. Diehl, and D. A. King, *Surface Sci. 162*, 59 (1985).
1761. H. Niehus, *Surface Sci. 145*, 407 (1984).
1762. D. L. Adams, and H. B. Nielsen, *Surface Sci. 116*, 598 (1982).
1763. M. A. Van Hove, and S. Y. Tong, *Surface Sci. 54*, 91 (1976).
1764. C. B. Duke, and A. Paton, *J. Vac. Sci. Tech. B 2*, 327 (1984).
1765. H. J. Grossman, and M. W. Gibson, *J. Vac. Sci. Tech. B 2*, 343 (1984).
1766. L. Smit, R. M. Tromp, and J. F. Van der Veen, *Phys. Rev. B 29*, 4814 (1984).
1767. J. Sokolov, F. Jona, and P. M. Marcus, *Phys. Rev. B 31*, 1929 (1985).
1768. P. C. Wong, M. Y. Zhou, K. C. Hui, and K. A. R. Mitchell, *Surface Sci. 163*, 172 (1985).
1769. A. Ignatiev, B. W. Lee, M. A. Van Hove, in Proceedings of the 7th International Vacuum Congress and 3rd International Conference on Solid Surfaces, Vienna (1977).
1770. W. S. Yang, F. Jona, and P. M. Marcus, *Phys. Rev. B 28*, 7377 (1983).
1771. H. L. Davis and J. R. Noonan, *Phys. Rev. Lett. 54*, 566 (1985).

1772. C. B. Duke, A. R. Lubinsky, B. W. Lee, and P. Mark, *J. Vac. Sci. Tech. 13*, 761 (1976).
1773. A. R. Lubinsky, C. B. Duke, S. C. Chang, B. W. Lee, and P. Mark *J. Vac. Sci. Tech. 13*, 189 (1976).
1774. D. Norman, S. Brennan, R. Jaeger and J. Stohr, *Surface Sci. 105*, L297 (1981).
1775. R. Z. Bachrach, G. V. Hansson and R. S. Bauer, *Surface Sci. 109*, L560 (1981).
1776. M. Maglietta, E. Zanazzi, F. Jona, D. W. Jepsen and P. M. Marcus, *Applied Physics 15*, 409 (1978).
1777. M. Maglietta, E. Zanazzi, U. Bardi and F. Jona, *Surface Sci. 77*, 101 (1978).
1778. R. C. Felton, M. Prutton, S. P. Tear and M. R. Welton-Cook, *Surface Science 88*, 474 (1979).
1779. P. H. Citrin, P. Eisenberger and R. C. Hewitt, *Physical Revier Letters 45*, 1948 (1980).
1780. S. Andersson and J. B. Pendry, *Journal of Physics C 13*, 2547 (1980).
1781. J. Onuferko and D. P. Woodruff, *Surface Science 95*, 555 (1980).
1782. R. W. Streater, W. T. Moore, P. R. Watson, D. C. Frost and K. A. R. Mitchell, *Surface Sci. 72*, 744 (1978).
1783. P. Eisenberger and W. C. Marra, *Physical Review Letters 46*, 1081 (1981).
1784. S. P. Tear, M. R. Welton-Cook, M. Prutton and J. A. Walker, *Surface Science 99*, 598 (1980).
1785. M. A. Van Hove, R. J. Koestner, P. C. Stair, J. P. Biberian, L. L. Kesmodel, I. Bartos and G. A. Somorjai, *Surface Sci. 103*, 218 (1981).
1786. C. M. Chan, S. M. Cunningham, K. L. Luke, W. H. Weinberg and S. P. Withrow, *Surface Sci. 78*, 15 (1978).
1787. C. M. Chan, M. A. Van Hove, W. H. Weinberg and E. D. Williams, *Journal of Vacuum Science and Technology 16*, 642 (1979).
1788. C. M. Chan, K. L. Luke, M. A. Van Hove, W. H. Weinberg and S. P. Withrow, *Surface Sci. 78*, 386 (1978).
1789. S. Y. Tong, A. Maldonado, C. H. Li and M. A. Van Hove, *Surface Sci. 94*, 73 (1980).
1790. S. Andersson and J. B. Pendry, *Journal of Physics C 13*, 3547 (1980).
1791. L. G. Petersson, S. Kono, N. F. T. Hall, C. S. Fadley and J. B. Pendry, *Physical Review Letters 42*, 1545 (1979).
1792. Y. Gauthier, D. Aberdam and R. Baudoing, *Surface Sci. 78*, 339 (1978).
1793. D. H. Rosenblatt, J. G. Tobin, M. G. Mason, R. F. Davis, S. D. Kevan, D. A. Shirley, C. H. Li and S. Y. Tong, *Physical Review B 23*, 3828 (1981).
1794. T. Narasawa, W. M. Gibson and E. Tornquist, *Physical Review Letters 47*, 417 (1981).
1795. S. D. Kevan, R. F. Davis, D. H. Rosenblatt, J. G. Tobin, M. G. Mason, D. A. Shirley, C. H. Li and S. Y. Tong, *Physical Review Letters 46*, 1629 (1981).
1796. T. Narasawa and W. M. Gibson, *Surface Science 114*, 331 (1981).
1797. R. J. Behm, K. Christmann, G. Ertl and M. A. Van Hove, *Journal of Chemical Phisics 73*, 2984 (1980).
1798. J. A. Davies, T. E. Jackman, D. P. Jackson and P. R. Norton, *Surface Science 109*, 20 (1981).
1799. R. Feder, H. Pleyer, P. Bauer and N. Muller, *Surface Sci. 109*, 419 (1981).
1800. S. Hengrasmee, A. R. Mitchell, P. R. Watson and S. J. White, *Canadian Journal of Physics 58*, 200 (1980).
1801. R. J. Meyer, W. R. Salaneck, C. B. Duke, A. Paton, C. H. Griffiths, L. Kovnat and L. E. Meyer, *Physical Review B 21*, 4542 (1980).
1802. F. S. Marsh, M. K. Debe and D. A. King, *Journal of Physics C 13*, 2799 (1980).
1803. W. A. Jesser and J. W. Matthews, *Acta Mett. 16*, 1307 (1968).
1804. A. Chambers and D. C. Jackson, *Phil. Mag. 31*, 1357 (1975).
1805. J. W. Matthews, *Thin Solid Films 12*, 243 (1972).
1806. J. W. Matthews, *Phil. Mag. 13*, 1207 (1966).
1807. K. Yagi, K. Takanayagi, K. Kobayashi and G. Honjo, *J. Crystal. Growth 9*, 84 (1971).
1808. W. A. Jesser and J. W. Matthews, *Phil. Mag. 17*, 595 (1968).
1809. W. A. Jesser and J. W. Matthews, *Phil. Mag. 15*, 1097 (1967).
1810. W. A. Jesser and J. W. Matthews, *Phil. Mag. 17*, 461 (1968).
1811. A. I. Fedorenko and R. Vincent, *Phil. Mag. 24*, 55 (1971).
1812. R. Kuntze, A. Chambers and M. Prutton, *Thin Solid Films 4*, 47 (1969).
1813. U. Gradmann, *Ann. Physik. 13*, 213 (1964).
1814. U. Gradmann, *Ann. Physik. 17*, 91 (1966).
1815. R. W. Vook, C. T. Horng and J. E. Macur, *J. of Crystal Growth 31*, 353 (1975).
1816. R. W. Vook and C. T. Horng, *Phil. Mag. 33*, 843 (1976).
1817. C. T. Horng and R. W. Vook, *Surface Sci. 54*, 309 (1976).
1818. U. Gradmann, *Phys. Kondens. Materie 3*, 91 (1964).
1819. R. W. Vook and J. E. Macur, *Thin Solid Films 32*, 199 (1976).
1820. L. A. Bruce, H. Jaeger, *Phil. Mag. 36*, 1331 (1977).
1821. C. Gonzalez, *Acta Met. 15*, 1373 (1967).
1822. C. T. Horng and R. W. Vook, *J. Vac. Sci. Technol. 11*, 140 (1974).
1823. E. Grhnbaum, G. Kremer and C. Reymond, *J. Vac. Sci. Technol. 6*, 475 (1969).
1824. R. C. Newman and D. W. Pashley, *Phil. Mag. 46*, 927 (1955).
1825. F. Soria, J. L. Sacedon, P. M. Echenique and D. Titterington, *Surface Sci. 68*, 448 (1977).
1826. M. Klaua and H. Bethce, *J. of Crystal Growth 3,4* 188 (1968).

1827. E. Grunbaum, Proc. *Phys. Soc. (London) 72*, 459 (1958).
1828. E. F. Wassermann and H. P. Jablonski, *Surface Sci. 22*, 69 (1970).
1829. D. C. Hothersall, *Phil. Mag. 15*, 1023 (1967).
1830. P. Gueguen, C. Camoin and M. Gillet, *Thin Solid Films 26*, 107 (1975).
1831. G. Honjo, K. Takayanagi, K. Kobayashi and K. Yagi, *J. of Crystal Growth 42*, 98 (1977).
1832. P. Gueguen, M. Cahareau and M. Gillet, *Thin Solid Films 16*, 27 (1973).
1833. D. Cherns and M. J. Stowell, *Thin Solid Films 29*, 107 (1975).
1834. D. Cherns and M. J. Stowell, *Thin Solid Films 29*, 127 (1975).
1835. W. A. Jesser, J. W. Matthews and D. Kuhlmann-Wilsdorf, *Appl. Phys. Lett. 9*, 176 (1966).
1836. J. E. Macur and R. W. Vook, 32nd Ann. Proc. Electron Microscopy Soc. Amer., St. Louis, Missouri, 1974, C. J. Arceneaux (ed.).
1837. J. E. Macur, 33rd Ann. Proc. Electron Microscopy Soc. Amer., Las Vegas, Nevada, 1975, B. W. Bailey (ed.), p. 98.
1838. J. W. Matthews, *Phys. Thin Films 4*, 137 (1967).
1839. G. Dorey, *Thin Solid Films 5*, 69 (1970).
1840. A. Mlynczak and R. Niedermayer, *Thin Solid Films 28*, 37 (1975).
1841. P. W. Steinhage and H. Mayer, *Thin Solid Films 28*, 131 (1975).
1842. C. M. Mate and G. A. Somorjai, *Surface Sci. 160*, 542 (1985).
1843. S. Thomas and T. W. Haas, *Surface Sci. 28*, 632 (1971).
1844. C. M. Mate, B. E. Bent and G. A. Somorjai, *J. of Electron. Spectrosc. Related Phenom. 39*, 205 (1986).
1845. P. I. Cohen, J. Unguris, and M. B. Webb, *Surface Sci. 58*, 429 (1976).
1846. N. J. Wu and A. Ignatiev, *Phys. Rev. B 25*, 2983 (1982).
1847. N. J. Wu and A. Ignatiev, *Phys. Rev. B28*, 7288 (1983).
1848. M. Weltz, W. Moritz, and D. Wolf, *Surface. Sci. 125*, 473 (1983).
1849. D. A. Outka, R. J. Madix, and J. Stohr, *Surface Sci. 164*, 235 (1985).
1850. A. Puschman, J. Hasse, M. D. Crapper, C. E. Riley, and D. P. Woodruff, *Phys. Rev. Lett. 54*, 2250 (1985).
1851. D. Sondericker, F. Jona, and P. M. Marcus, *Phys. Rev. B33*, 900 (1986).
1852. J. Stohr, E. B. Kollin, D. A. Fischer, J. B. Hasting, F. Zaera, and F. Sette, *Phys. Rev. Lett. 55*, 1468 (1985).
1853. J. F. Van der Veen, R. M. Tromp, R. G. Smeenk, and F. W. Saris, *Surface Sci. 82*, 468 (1979).
1854. D. F. Ogletree, M. A. Van Hove, and G. A. Somorjai, *Surface Sci. 183*, 1 (1987).
1855. R. F. Lin, G. S. Blackman, A. M. Van Hove, and G. A. Somorjai, *Acta Crystallographica B*, in press (1987).
1856. M. A. Van Hove, R. F. Lin, and G. A. Somorjai, *J. Am. Chem. Soc. 108*, 2532 (1986).
1857. P. H. Citrin, P. Eisenberger, and J. E. Rowe, *Phys. Rev. Lett. 48*, 802 (1982).
1858. G. Materlik, A. Frohm, and M. J. Bedzyk, *Phys. Rev. Lett. 52*, 441 (1984).
1859. J. A. Golovchenko, J. R. Patel, D. R. Kaplan, P. L. Cowan, and M. J. Bedzyk, *Phys. Rev. Lett. 49*, 1560 (1982).
1860. E. J. Van Loenen, J. W. M. Frenken, J. F. Van der Veen, and S. Valeri, *Phys. Rev. Lett. 54*, 827 (1985).
1861. H. Ohtani, M. A. Van Hove, and G. A. Somorjai, *Surface Sci.* in press (1987).
1862. H. Ohtani, M. A. Van Hove, and G. A. Somorjai, unpublished results.
1863. C. B. Duke, A. Paton, A. Kahn, and C. R. Bonapace, *Phys. Rev. B28*, 852 (1983).
1864. J. E. Demuth, P. M. Marcus, and D. W. Jepsen, *Phys. Rev. B11*, 1460 (1975).
1865. S. Anderson and J. B. Pendry, *Sol. St. Comm. 16*, 563 (1975).
1866. D. H. Rosenblatt, S. D. Kevan, J. G. Tobin, R. F. Davis, M. G. Mason, D. R. Denley, D. A. Shirley, Y. Huang, and S. Y. Tong, *Phys. Rev. B26*, 1812 (1982).
1867. M. A. Van Hove and S. Y. Tong, *J. Vac. Sci. Tech. 12*, 230 (1975).
1868. D. Sondericker, F. Jona, and P. M. Marcus, *Phys. Rev. B33*, 900 (1986).
1869. P. H. Citrin, D. R. Hamann, L. F. Mattheiss, and J. E. Rowe, *Phys. Rev. Lett. 49*, 1712 (1982).
1870. W. N. Unertl and H. V. Thapliyal, *J. Vac. Sci. Technol. 12*, 263 (1975).
1871. A. Kahn, J. Carelli, D. Kanani, C. B. Duke, A. Paton, L. Brillson, *J. Vac. Sci. Tech. 19*, 331 (1981).
1872. J. R. Noonan and H. R. Davis, *Vacuum 31*, 107 (1982).
1873. E. Zanazzi and F. Jana, *Surf. Sci. 62*, 61 (1977).
1874. J. F. Van der Veen, R. G. Smeenk, R. M. Tromp, and F. M. Saris, *Surf. Sci. 79*, 219 (1979).
1875. C. M. Chan and M. A. Van Hove, unpublished results.
1876. C. M. Mate, C.-T. Kao and G. A. Somorjai, unpublished results.
1877. G. S. Blackman, C.-T. Kao, R. J. Koestner, B. E. Bent, C. M. Mate, M. A. Van Hove, and G. A. Somorjai, unpublished results.
1878. A. L. Slavin, B. E. Bent, C.-T. Kao and G. A. Somorjai, unpublished results.
1879. B. E. Bent, C.-T. Kao and G. A. Somorjai, unpublished results.
1880. C.-T. Kao, B. E. Bent and G. A. Somorjai, unpublished results.
1881. C.-T. Kao, C. M. Mate, B. E. Bent and G. A. Somorjai, unpublished results.
1882. C. G. Shaw, S. C. Fain, Jr., and M. D. Chinn, *Phys. Rev. Lett. 41*, 955 (1978).

1883. S. C. Fain, Jr., M. F. Torey, R. D. Diehl, Proc. 9th Intern. Vacuum Congr. & 5th Int. Conf. Solid Surfaces (Madrid, 1983), ed. by J. L. de Segovia, p. 129.
1884. B. E. Koel, J. E. Crowell, C. M. Mate, and G. A. Somorjai, *J. Phys. Chem. 88*, 1988 (1984).
1885. W. T. Moore, S. J. White, D. C. Frost, and K. A. R. Mitchell, *Surface. Sci. 116*, 253 (1982).
1886. W. T. Moore, S. J. White, D. C. Frost, and K. A. R. Mitchell, *Surface. Sci. 116*, 261 (1982).
1887. S. Andersson and J. B. Pendry, *J. Phys. C. 9*, 2721 (1976).
1888. R. J. Meyer, C. B. Duke, A. Paton, J. L. Yeh, J. C. Tsung, A. Kahn, and P. Mark, *Phys. Rev. B 21*, 4740 (1980).
1889. H. Melle and E. Menzel, *Z. Naturforsch. 33a*, 282 (1978).
1890. H. Niehus, *Surf. Sci. 145*, 407 (1984).
1891. S. Lehwald, H. Ibach, and J. E. Demuth, *Surf. Sci. 78*, 577 (1978).
1892. B. E. Koel, J. E. Crowell, C. M. Mate, and G. A. Somorjai, *J. Phys. Chem. 88*, 1988 (1984).
1893. W. T. Moore, S. J. White, D. C. Frost, and K. A. R. Mitchell, *Surface Sci. 116*, 253 (1982).
1894. F. Frostmann, *Japn. J. Appl. Phys.*, Suppl. 2 Part 2, 657 (1974).
1895. N. Stoner, Ph.D. Thesis, University of Wisconsin, Milwaukee (1976).
1896. F. Soria, J. L. Sacedon, P. M. Echenique, D. Titterington, *Surf. Sci. 68*, 448 (1977).
1897. D. W. Jepsen, P. M. Marcus, F. Jona, *Phys. Rev. B 5*, 3933 (1972).
1898. D. W. Jepsen, P. M. Marcus, F. Jona, *Phys. Rev. B 8*, 5523 (1973).
1899. W. Moritz, Ph.D. Thesis, University of Munich (1976).
1900. J. A. Strozier, R. O. Jones, *Phys. Rev. B. 3*, 3228 (1971).
1901. J. A. Strozier, R. O. Jones, *Phys. Rev. Lett. 25*, 516 (1970).
1902. H. D. Shih, F. Jona, D. W. Jepsen, P. M. Marcus, *Commun. Phys. 1*, 25 (1976).
1903. C. G. Shaw, S. C. Fain, M. D. Chinn, M. F. Toney, *Surface Sci. 97*, 128 (1980).
1904. C. Bouldin, E. A. Stern, *Phys. Rev. B 25*, 3462 (1982).
1905. F. Comin, P. H. Citrin, P. Eisenberger, J. E. Rowe, *Phys. Rev. B 26*, 7060 (1982).
1906. J. Bohr, R. Feidenhansl, M. Nielsen, M. Toney, R. L. Johnson, and I. K. Robinson, *Phys. Rev. Lett. 54*, 1275 (1985).
1907. R. Rosei, M. de Crescenzi, F. Sette, C. Quaresima, A. Savoia, P. Perfetti, *Phys. Rev. B 28*, 1161 (1983).
1908. R. G. Jones, S. Ainsworth, M. D. Crapper, C. Somerton, D. P. Woodruff, R. S. Brooks, J. C. Campuzano, D. A. King, G. M. Lamble, *Surf. Sci. 152/153*, 443 (1985).
1909. Y. Gauthier, R. Baudoing, Y. Joly, J. Rundgren, J. C. Bertolini, and J. Massardier, *Surf. Sci. 162*, 342 (1985).
1910. M. Saitoh, F. Shoji, K. Oura, T. Hanawa, *Jap. J. Appl. Phys. 19*, L421 (1980).
1911. J. Stohr, R. Jaeger, G. Rossi, T. Kendelewicz, I. Lindau, *Surf. Sci. 134*, 813 (1983).
1912. A. Ignatiev, T. N. Rhodin, S. Y. Tong, B. I. Lundqvist, J. B. Pendry, *Solid State Commun. 9*, 1851 (1971).
1913. L. J. Clarke, *Surf. Sci. 102*, 331 (1981).
1914. A. Ignatiev, J. B. Pendry, T. N. Rhodin, *Phys. Rev. Lett. 26*, 189 (1971).
1915. P. H. Citrin, *Bull. Am. Phys. Soc. 25*, 383 (1980).
1916. A. G. J. de Wit, R. P. N. Bronckers, Th. M. Hupkens, J. M. Fluit, *Surf. Sci. 90*, 676 (1979).
1917. R. Feidenhansl, I. Stensgaard, *Surf. Sci. 133*, 453 (1983).
1918. U. Dobler, K. Baberschke, J. Haase, A. Puschmann, *Phys. Rev. Lett. 52*, 1437 (1984).
1919. C. B. Duke, A. Paton, A. Kahn, K. Li, *Bull. Am. Phys. Soc. 30*, 313 (1985).
1920. C. B. Duke, C. Mailhiot, A. Paton, K. Li, C. Bonapace, A. Kahn, *Surf. Sci. 163*, 391 (1985).
1921. J. Stohr, D. A. Outka, R. J. Madix, and U. Dobler, *Phys. Ref. Lett., 54*, 1256 (1985).
1922. D. A. Outka, R. J. Madix, and J. Stohr, *Surf. Sci. 164*, 235 (1985).
1923. G. Casalone, M. G. Cattania, M. Simonetta, *Surf. Sci. 103*, L121 (1981).
1924. Z. P. Hu, D. F. Ogletree, M. A. Van Hove, and G. A. Somorjai, *Surf. Sci. 180*, 433 (1987).
1925. H. Kobayashi, H. Teramae, T. Yamabe, M. Yamaguchi, *Surf. Sci. 141*, 580 (1984).
1926. B. A. Hutchins, T. N. Rhodin, J. E. Demuth, *Surf. Sci. 54*, 419 (1976).

LAWRENCE BERKELEY LABORATORY
CENTER FOR ADVANCED MATERIALS
1 CYCLOTRON ROAD
BERKELEY, CALIFORNIA 94720